Analyse et Simulation Numérique par Relaxation d'Ecoulements Diphasiques Compressibles. Contribution au Traitement des Phases Evanescentes.

Khaled Saleh

Université Pierre et Marie Curie
Paris 6

Laboratoire Jacques-Louis Lions
UMR 7598

Thèse de Doctorat de
l'Université Pierre et Marie Curie

Présentée et soutenue publiquement le 26 novembre 2012

pour l'obtention du grade de
Docteur de l'Université Pierre et Marie Curie
Spécialité : Mathématiques Appliquées

par
Khaled Saleh

Analyse et Simulation Numérique par Relaxation d'Écoulements Diphasiques Compressibles

Contribution au Traitement des Phases Évanescentes

Après avis des rapporteurs

M. Thierry Gallouët
M. Roberto Natalini

Devant le jury composé de

M.	Grégoire Allaire	Examinateur
M.	François Bouchut	Examinateur
M.	Frédéric Coquel	Directeur de Thèse
M.	Thierry Gallouët	Rapporteur
M^{me}	Edwige Godlewski	Examinateur
M.	Jean-Marc Hérard	Directeur de Thèse
M.	Nicolas Seguin	Co-Encadrant

École Doctorale de Sciences Mathématiques de Paris Centre
ED 386

Faculté de Mathématiques
UFR 929

Khaled Saleh :

UPMC, Université Paris 06, UMR 7598, Laboratoire Jacques-Louis Lions, F-75005, Paris, France.
CNRS, UMR 7598, Laboratoire Jacques-Louis Lions, F-75005, Paris, France.

EDF R&D, Département Mécanique des Fluides, Energies, Environnement,
6 quai Watier BP 49, 78401 Chatou Cedex, France.

Adresse électronique: saleh@ann.jussieu.fr

Remerciements

Je tiens en premier lieu à remercier mes deux directeurs de thèse, Frédéric Coquel et Jean-Marc Hérard, ainsi que Nicolas Seguin, mon troisième (et non le moindre) encadrant. Comme je le dis souvent, j'ai été, durant ces trois années de thèse, extrêmement bien entouré, puisque j'ai eu la chance de bénéficier du soutien, de l'expérience et des conseils de trois remarquables chercheurs. Ils ont été, tout au long de ces trois années, toujours disponibles et je les salue tous les trois pour leurs remarquables qualités pédagogiques. Il est rare, je pense, d'être entouré d'aussi bons professeurs, qui ont toujours su répondre avec clarté et précision à mes interrogations. Je salue aussi leur grande gentillesse et leurs conseils avisés, qui m'ont aidé à orienter mon choix de carrière. Merci à Frédéric pour sa persévérance et son optimisme à toute épreuve, me poussant toujours à aller jusqu'au bout des résultats, même ceux qui étaient difficiles à démontrer. Je le remercie aussi pour sa minutie dans la relecture, qui a grandement contribué à améliorer mes écrits ! D'ailleurs, je crois que cela a été contagieux, puisque je suis moi même devenu très (trop ?) perfectionniste... Merci à Jean-Marc, qui a toujours su replacer mes recherches dans leur contexte industriel. J'ai appris grâce à lui qu'il était possible de concilier mon goût pour les mathématiques et les préoccupations industrielles comme celles d'un grand groupe comme EDF. Merci enfin à Nicolas pour sa disponibilité, sa pédagogie et sa rigueur. Merci pour toutes les fois où je n'arrivais pas à débugger mon code! Par ailleurs, je serai toujours admiratif de son impressionnant sens physique.

Je remercie Thierry Gallouët et Roberto Natalini d'avoir accepté de rapporter sur ce manuscrit. Je remercie en particulier Thierry pour les échanges très intéressants que nous avons pu avoir, concernant mes travaux. Je remercie également Grégoire Allaire d'avoir accepté de faire partie de mon jury de soutenance, et de l'avoir présidé. J'ai été également très heureux de compter parmi les membres de mon jury François Bouchut et Edwige Godlewski. Merci aussi à Sergey Gavrilyuk d'avoir accepté de participer à mon jury, même s'il n'a pas pu être présent pour des raisons indépendantes de sa volonté.

Ce travail a été réalisé en grande partie au sein du département Mécanique des Fluides, Energies, Environnement, de la division Recherche et Développement d'EDF. Je souhaite à ce titre remercier EDF et l'ANRT pour le financement du contrat CIFRE, dont j'ai bénéficié durant ces trois années de recherche. A EDF, j'ai eu le plaisir de faire partie du groupe I81 au département MFEE. Je voudrais remercier Isabelle Flour, chef du groupe I81 pendant mon séjour à EDF. Elle est à mes yeux l'exemple même du chef rigoureux et proche à la fois. Je la remercie de s'être toujours assurée du bon déroulement de ma thèse au sein du groupe. Merci aux thésards du groupe qui contribuent grandement à l'excellente ambiance qui règne à Chatou. Merci aux anciens : Laetitia, Bertrand et Arnaud (ton accent te perdra). Merci à Clara et Sana pour votre constante bonne humeur

(et aussi pour la douce musique de vos talons hauts que j'ai appris à reconnaître à des dizaines de mètres !). Je pense également à Avner et Romain, toujours partants pour résoudre un exo de maths, à Christophe (tes pâtisseries me manquent déjà), ainsi qu'à Franck. Merci enfin à ma grande sœur de thèse Kateryna pour ces trois années de bonne humeur. Merci à toi pour ta gentillesse incommensurable et un grand merci d'avoir été mon agent et d'avoir fait ma pub auprès de qui tu sais ! Je n'oublie pas non plus les stagiaires que j'ai croisés au département : Marie l'antiboise, Erwan (pro du ping-pong), Vincent (toujours dernier à sortir de table) et aussi une jeune stagiaire prénommée Haïfa, dont je me demande ce qu'elle est devenue. Je souhaite aussi remercier les ingénieurs d'EDF avec qui j'ai pu échanger, voire travailler lors de cette thèse : Olivier Hurisse, Bruno Audebert, Jérôme Lavieville, Frédéric Archambeau, Martin Ferrand, Mathieu Guingo. Merci enfin à Marie-Line, Chantal et Eliane pour leur accueil chaleureux à l'antenne de gestion du groupe.

Une autre grande chance pour moi a été de faire partie intégrante des doctorants du laboratoire Jacques-Louis Lions, ce qui n'était pas *a priori* évident pour un doctorant en entreprise. J'y ai développé de nombreux contacts à la fois sur le plan professionnel et sur le plan humain. Je souhaite exprimer ma gratitude à Edwige Godlewski, directrice adjointe du laboratoire et Yvon Maday, directeur du laboratoire, qui se sont assurés que mon séjour au laboratoire se déroule dans les meilleures conditions, notamment après la fin de mon contrat avec EDF. Merci aussi au secrétariat du laboratoire : Mesdames Boulic et Ruprecht, Madame Lendo et Madame Foucart et bien sûr Madame Salima Lounici. Je voudrais aussi remercier Khashayar Dadras et saluer l'excellent travail qu'il accomplit pour le bon fontionnement de l'informatique au laboratoire. Merci également à Christian David, grâce à qui j'ai toujours eu le matériel dont j'avais besoin. Merci enfin à Antoine Le Hyaric pour l'aide qu'il m'a apportée sur mes videos de simulations numériques. Passer du temps au laboratoire a toujours été pour moi un plaisir, grâce notamment aux doctorants du bureau 15-25 302 : Kamel, un ami valeureux et mon témoin de mariage, Imen, Etienne, Kirill, Pierre, Pierre-Henri, et enfin Simona, Luis-Miguel et Abdellah, avec qui nous aurions pu ouvrir une petite cafétéria dans le bureau ! Il y a aussi les autres doctorants du laboratoire : Lise-Marie, Charles (j'aurais aimé lire ce que tu fais mais c'est écrit trop petit), Hassan, Haidar, Magali, les « contrôleurs » Malik et Vincent. Merci aux organisateurs du GTT, qui ont toujours su m'avoir par les sentiments. Ayant chaque semaine la ferme intention de faire le pique-assiette au goûter du GTT avant de directement repartir travailler, je suis toujours (ok presque toujours) resté pour l'exposé, et j'ai pu y voir des exposés de très grande qualité, dont certains, je l'avoue, me faisaient un peu complexer... Merci donc à Alexis, Nicole, Juliette et Jean-Paul. Jean-Paul, qui même après huit heures de vol et un décalage horaire, a réussi à débloquer une difficulté sur laquelle je bloquais depuis pas mal de temps. Merci encore pour cela ! Je pense également à Benjamin, mon grand frère de thèse, que je remercie pour ses conseils avisés. Je me souviendrai toujours de l'ambiance exceptionnelle qui régnait dans le voisinage du bureau 16-26 301, grâce aux jeunes chercheurs permanents ou de passage : Nicolas et Nicolas (qui se départageront), Laurent et Jean-François bien sûr, mais aussi Fred (Lagoutière) et Fred (Charles), Clément, Franck et l'autre membre de l' « Egyptian connection » : Ayman. Merci aussi à Christophe Chalons avec qui j'ai toujours eu plaisir de discuter Baer-Nunziato et à Emmanuel Audusse avec qui j'ai apprécié travailler (d'ailleurs ce n'est pas fini, il faut vraiment qu'on termine ce papier, n'est-ce pas Nicolas ?).

Le CEMRACS 2011 a été pour moi une très agréable expérience. Il m'a permis d'avancer sur ma thèse, en particulier sur le quatrième chapitre, tout en ayant l'impression d'être en vacances (mais j'ai quand même bossé hein !). J'ai d'excellents souvenirs avec Anne-Céline (« pourquoi, y'a deux Célines ? »), Anne-Claire, Guilhem et Benoit, mais aussi avec la « team ramadan » : Tassadit

(à qui je souhaite une excellente fin de thèse sur Baer-Nunziato !), El Hassan, Mohamed Abaidi (« pourquoi, y'a deux Célines ? ») et Mohamed Ghattassi. Merci aussi à Nina, Mathieu, Rémi, David et Fabien, pour n'avoir jamais voulu m'apprendre la Coinche... Merci enfin aux strasbourgeois, Anaïs, Hélène, et les garçons : Jonathan et Ahmed. Ahmed, qui m'a appris, à moi l'Egyptien, comment préparer une chicha.

Merci à Mohamed Jaoua de m'avoir permis d'enseigner à l'Université Française d'Egypte. Merci aussi à Manuel pour ses excellents plans resto au Caire !

Avant de commencer cette thèse, j'ai eu le plaisir de suivre les cours du master ANEDP de Paris 6, où j'ai fait la connaissance de jeunes chercheurs d'horizons très différents, devenus pour certains des amis. Je pense à Nafi, Maxime, Cécile, Manu, Morgan et Aurore, et je souhaite bon courage à ceux d'entre eux qui finissent bientôt leur thèse.

Je remercie également mes meilleurs amis, Wassef, Ali et Sullym (dans l'ordre chronologique de rencontre). Je crois que je ne compte plus les fous rires qu'on a pu avoir ensemble ! Merci à vous trois d'avoir été là et de m'avoir permis, chacun à sa façon, de sortir un petit peu de mon univers de matheux.

Un grand MERCI à ma famille, en France et en Egypte, pour m'avoir soutenu durant toutes mes années d'études. Merci à mes frères Nouredine et Nassim (les lascars, experts de la vanne) d'avoir manqué vos cours pour assister à ma soutenance. Bon courage pour vos études, et si jamais vous avez des questions, *on va voir ce qu'on peut faire*. Merci à ma sœur Ghadah ainsi qu'à son époux Mohamed, et bienvenue à mon petit neveu Adam (plus tard, tu pourras dire que j'ai parlé de toi dans ma thèse). Et surtout, surtout, merci à mes parents, que j'aime tendrement. Merci pour tous les sacrifices que vous avez faits et continuez de faire pour nous. Que Dieu vous garde à nos côtés.

Enfin, je dédie ce travail à ma très chère femme Haïfa. Merci pour ton amour, ta tendresse, ton amitié, ton soutien dans les moments difficiles. Toi qui as toujours su m'encourager et me donner confiance en moi, merci d'être là. Tout ceci n'est rien sans toi.

Résumé

Dans le cadre du nucléaire civil, la modélisation des écoulements diphasiques est nécessaire à la représentation de nombreuses configurations d'écoulements fluides dans les circuits primaire et secondaire des centrales s'appuyant sur des réacteurs à eau pressurisée (REP). Les applications visées concernent non seulement le fonctionnement nominal, mais aussi et surtout les configurations incidentelles, parmi lesquelles on peut citer l'accident par perte de réfrigérant primaire (APRP), les phénomènes de crise d'ébullition, mais aussi le renoyage des coeurs. En régime nominal dans le circuit primaire, le fonctionnement est très proche du fonctionnement monophasique pur, la vapeur étant a priori absente. En revanche, le taux de présence de vapeur peut devenir de faible à conséquent dans les situations incidentelles.

Cette thèse s'intéresse plus particulièrement au modèle diphasique de Baer-Nunziato qui entre dans la classe des modèles bifluides hyperboliques. L'objectif de ce travail est de proposer quelques techniques de prise en compte de la disparition de phase, régime qui occasionne d'importantes instabilités tant au niveau du modèle qu'au niveau de sa simulation numérique.

L'enseignement principal de la thèse est que dans ces régimes, il est possible des stabiliser les solutions en introduisant une dissipation de l'entropie totale de mélange. D'un point de vue numérique, cette dissipation d'entropie supplémentaire permet en effet d'obtenir des approximations stables dans ces régimes. Les méthodes d'analyse et d'approximation proposées reposent de façon intensive sur les techniques d'approximation par relaxation de type Suliciu, et les méthodes numériques qui en découlent. Deux approches sont principalement étudiées.

Dans une première approche dite *approche Eulerienne directe*, la résolution exacte du problème de Riemann pour le système relaxé permet de définir un schéma numérique extrêmement précis pour le modèle de Baer-Nunziato. Nous montrons que dans les régimes de fonctionnement normal (i.e. sans disparition de phase), la méthode numérique ainsi obtenue est bien plus économique en terme de coût CPU (à précision donnée) que le schéma classique très simple de Rusanov. De plus, nous montrons que ce nouveau schéma est très robuste puisqu'il permet la simulation des régimes de disparition de phase. Les travaux furent initialement développés sur la version 1D du modèle, pour laquelle une inégalité d'entropie discrète vérifiée par le schéma fut démontrée. Ils furent ensuite étendus en 3D et intégrés à un prototype de code industriel développé par EDF.

La deuxième approche, dite *approche par splitting acoustique*, propose à travers un opérateur de splitting temporel, de séparer les phénomènes de propagation d'ondes acoustiques et les phénomènes associés au transport matériel. Cette approche a le double objectif d'éviter la résonance due à

l'interaction entre ces deux types d'ondes, mais surtout de permettre à long terme un traitement implicite des phénomènes acoustiques, tout en explicitant la discrétisation des phénomènes de transport. On parle alors de méthodes semi-implicites. Le schéma que nous proposons admet une mise en oeuvre remarquablement simple. De plus, nous montrons qu'il permet la prise en compte simple de la disparition de phase. Une des principales nouveautés de ce travail est d'exploiter des fermetures dissipatives du couple vitesse et pression d'interface, et de montrer que ces fermetures permettent le contrôle de la taille des solutions du problème de Riemann associé à l'étape acoustique.

Abstract

This thesis deals with the Baer-Nunziato two-phase flow model. The main objective of this work is to propose some techniques to cope with phase vanishing regimes which produce important instabilities in the model and its numerical simulations. Through analysis and simulation methods using Suliciu relaxation approximations, we prove that in these regimes, the solutions can be stabilised by introducing some extra dissipation of the total mixture entropy.

In a first approach, called the Eulerian approach, the exact resolution of the relaxation Riemann problem provides an accurate entropy-satisfying numerical scheme, which turns out to be much more efficient in terms of CPU-cost than the classical and very simple Rusanov's scheme. Moreover, the scheme is proved to handle the vanishing phase regimes with great stability. The scheme, first developed in 1D, is then extended in 3D and implemented in an industrial code developed by EDF.

The second approach, called the acoustic splitting approach, considers a separation of fast acoustic waves from slow material waves. The objective is to avoid the resonance due to the interaction between these two types of waves, and to allow an implicit treatment of the acoustics, while material waves are explicitly discretized. The resulting scheme is very simple and allows to deal simply with phase vanishing. The originality of this work is to use new dissipative closure laws for the interfacial velocity and pressure, in order to control the solutions of the Riemann problem associated with the acoustic step, in the phase vanishing regimes.

Table des matières

Introduction générale

0.1 Contexte général

La modélisation des écoulements diphasiques est nécessaire à la représentation de nombreuses configurations d'écoulements fluides et, si l'on se restreint au cadre nucléaire civil, devient essentielle dans le contexte des écoulements dans les circuits primaire et secondaire des centrales s'appuyant sur des réacteurs à eau pressurisée (REP) (pour une représentation schématique d'une centrale de type REP, voir la figure 0.1). Ceci justifie l'intérêt constant porté par EDF, le CEA et l'IRSN depuis de nombreuses années à ce domaine. Les applications visées concernent non seulement le fonctionnement nominal, mais aussi et surtout les configurations incidentelles, parmi lesquelles on peut citer l'accident par perte de réfrigérant primaire (APRP), les phénomènes de crise d'ébullition, mais aussi le renoyage des cœurs. Le fonctionnement des générateurs de vapeur et des condenseurs constitue un autre champ d'application de cette classe de modèles fluides.

Dans cette optique, les acteurs mentionnés précédemment mais aussi AREVA développent conjointement, au sein du projet NEPTUNE, une plateforme de codes de simulation des écoulements diphasiques, ayant pour objectif de fournir des approximations discrètes des solutions de plusieurs modèles diphasiques, et autorisant le couplage de ces codes ([26]). En régime nominal dans le circuit primaire, le fonctionnement est très proche du fonctionnement monophasique pur, la vapeur étant *a priori* absente. En revanche, le taux de présence de vapeur peut devenir de faible à conséquent dans les situations incidentelles. Dans ce cas, les inhomogénéités spatiales et temporelles deviennent importantes, et il convient alors, si l'on souhaite associer un caractère prédictif aux simulations, disposer de modèles conduisant *a minima* à des problèmes de Cauchy bien posés.

Deux grandes classes de modèles moyennés, (*i.e.* proposant des équations d'évolution pour les moments statistiques d'ordre un au moins) ont été proposées dans la littérature depuis les années 1970 (voir parmi d'autres références les ouvrages [29, 21]). Une première classe correspond à une représentation homogène monofluide, décrivant essentiellement les propriétés moyennes du mélange eau-vapeur (masse, débit, énergie), et éventuellement le déséquilibre de titre masse. Les codes français THYC (EDF), FLICA et GENEPI (CEA), sont basés sur de tels modèles d'écoulements diphasiques. Une autre approche possible repose sur l'utilisation de l'approche à deux fluides, c'est le cas pour les codes CATHARE et NEPTUNE_CFD (France) et RELAP (USA). Dans cette dernière formulation, les moments d'ordre un associés à la densité, au débit, et à l'énergie sont prédits par des lois d'évolution pour chaque phase, le taux de présence statistique de phase étant fourni par une équation d'évolution ou une fermeture algébrique. L'approche monofluide permet d'éviter le recours à de nombreuses lois de fermeture, hormis sur le plan des lois d'état thermodynamique et des transferts de masse interfaciaux. Les systèmes fermés associés ont en général une structure convective assez proche de celle des équations d'Euler, et l'on peut dans certains cas (les plus simples) s'appuyer sur des résultats de caractérisation des solutions de ces équations. Un inconvénient évident est qu'ils ne fournissent pas d'information précise et pertinente sur les déséquilibres de vitesse/pression/température entre phases. Enfin, dans les cas optimaux, l'obtention de solutions numériques raisonnablement proches de la convergence ne requiert pas obligatoirement des maillages très fins. Inversement, l'approche à deux fluides fournit *a priori* une représentation plus fine de la réalité en prenant en compte les déséquilibres entre phases, mais elle nécessite de fournir des lois de fermeture cohérentes (notamment par rapport à la caractérisation entropique) et suf-

fisamment renseignées (pour ce qui concerne les échelles de temps de relaxation par exemple). En outre, il n'existe pas de consensus actuellement concernant la forme optimale des lois de fermeture des termes de transfert interfacial, ou des échelles de temps de relaxation. Selon que l'on considère telle ou telle loi de fermeture, les propriétés des modèles peuvent clairement différer. Au-delà de la difficulté du traitement des phases évanescentes, problème sur lequel tout le monde s'accorde, des discussions perdurent sur la nature hyperbolique du système au premier ordre. Ce système s'écrivant sous forme non conservative, l'analyse des fermetures des produits non conservatifs a fait l'objet de peu d'études jusqu'alors.

On s'attachera dans cette thèse plus particulièrement à proposer quelques techniques de prise en compte des phases évanescentes, en caractérisant au mieux les solutions discontinues des modèles diphasiques considérés, ainsi que leur caractérisation entropique.

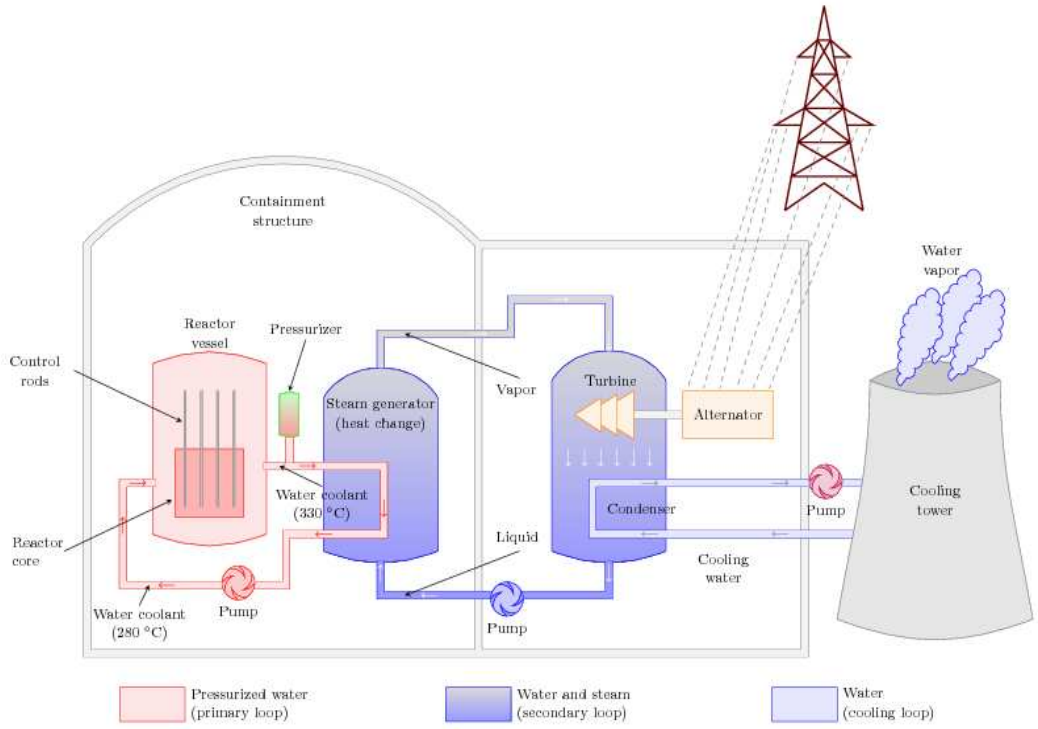

Figure 1: Schéma d'une centrale nucléaire de type REP.

0.2 Les modèles diphasiques de type Baer-Nunziato

Les modèles que nous considérons dans ce mémoire s'inscrivent dans la classe des modèles bifluides à deux pressions qui permettent de prendre en compte le cas plus général de déséquilibre entre les pressions phasiques. Ce type de modèle fut par exemple étudié par Ransom et Hicks [36] ainsi que Stewart et Wendroff [41]. L'évolution de l'interface, identifiée à l'évolution des fractions statistiques est alors décrite par une équation aux dérivées partielles supplémentaire. Cette loi est généralement une équation de transport avec terme source où la vitesse de transport est appelée *vitesse interfaciale*. Intervient également dans ces modèles une *pression interfaciale* qui est possiblement différente des deux pressions phasiques. L'existence d'une équation de transport sur les taux de présence donne à ces modèles à deux pressions la propriété d'avoir une structure convective faiblement hyperbolique. Ils ne sont donc pas susceptibles *a priori* de développer de fortes instabilités non physiques liés à l'existence d'une zone elliptique.

Le modèle considéré ici est une généralisation du modèle introduit par Baer et Nunziato [7] pour l'étude de matériaux granulaires réactifs. Ce premier modèle visait à modéliser des mélanges de deux phases compressibles où l'une des deux phases est présente en petite quantité devant l'autre. On parle de phase diluée et de phase dominante. Dans ce contexte, la vitesse interfaciale est identifiée à la vitesse de la phase diluée et la pression interfaciale à la pression de la phase dominante. Ce modèle fut généralisé par Coquel *et al.* [16] puis Gallouët *et al.* [23] à d'autres fermetures pour le couple pression-vitesse interfaciales, tandis que d'autres fermetures sont proposées par Saurel *et al.* [39], Abgrall-Saurel [2] et Papin-Abgrall [35]. Dans ce cadre citons également les travaux de Gallouët *et al.* [22], Gavrilyuk-Saurel [24], Kapila *et al.* [30, 31].

Le modèle homogène de Baer-Nunziato fait l'objet d'un nombre croissant de contributions à la simulation numérique. Des solveurs basés sur le problème de Riemann exact ou approché ont été notamment proposés par Schwedeman *et al.* [40], Deledicque-Papalexandris [20], Saurel-Abgrall [38], Ambroso *et al.* [6], Kröner *et al.* [42], Karni–Hernàndez-Dueñas [32], Tokareva-Toro [43].

Dans tout ce mémoire, nous désignerons le modèle étudié par *modèle de Baer-Nunziato*, même s'il résulte de diverses extensions du modèle initial introduit dans [7].

0.2.1 Le modèle avec énergie en plusieurs variables d'espace

Le modèle a pour inconnues physiques une masse volumique $\rho_k(\mathbf{x},t)$, une vitesse $\mathbf{u}_k(\mathbf{x},t)$, et une pression $p_k(\mathbf{x},t)$ pour chaque phase $k \in \{1,2\}$ ainsi que le taux de présence statistique $\alpha_1(\mathbf{x},t)$ qui indique la probabilité de présence de la phase 1 en $\mathbf{x}$ à la date t (avec $\alpha_2 = 1-\alpha_1$). On se donne par ailleurs une loi d'état thermodynamique pour chaque phase k sous la forme $(\rho_k, p_k) \mapsto e_k(\rho_k, p_k)$, où e_k est l'énergie interne spécifique de la phase k. On note E_k l'énergie massique totale de la phase k, définie par

$$E_k = \frac{|\mathbf{u}_k|^2}{2} + e_k(\rho_k, p_k), \quad k \in \{1,2\}. \tag{0.2.1}$$

En l'absence de diffusion visqueuse, le modèle de Baer-Nunziato s'écrit alors en dimension d sous la forme d'un système de $5+2d$ équations aux dérivées partielles: pour $\mathbf{x}\in\mathbb{R}^d, d\geq 1$ et $t>0$,

$$\begin{aligned}
&\partial_t\alpha_1 + \mathbf{V_I}\cdot\nabla\alpha_1 = \Phi,\\
&\partial_t(\alpha_1\rho_1) + \nabla\cdot(\alpha_1\rho_1\mathbf{u}_1) = 0,\\
&\partial_t(\alpha_1\rho_1\mathbf{u}_1) + \nabla\cdot(\alpha_1\rho_1\mathbf{u}_1\otimes\mathbf{u}_1) + \nabla(\alpha_1 p_1) - P_I\nabla\alpha_1 = \mathbf{D}_1,\\
&\partial_t(\alpha_1\rho_1 E_1) + \nabla\cdot(\alpha_1\rho_1 E_1\mathbf{u}_1 + \alpha_1 p_1\mathbf{u}_1) - P_I\mathbf{V_I}\cdot\nabla\alpha_1 = \Psi_1,\\
&\partial_t(\alpha_2\rho_2) + \nabla\cdot(\alpha_2\rho_2\mathbf{u}_2) = 0,\\
&\partial_t(\alpha_2\rho_2\mathbf{u}_2) + \nabla\cdot(\alpha_2\rho_2\mathbf{u}_2\otimes\mathbf{u}_2) + \nabla(\alpha_2 p_2) - P_I\nabla\alpha_2 = \mathbf{D}_2,\\
&\partial_t(\alpha_2\rho_2 E_2) + \nabla\cdot(\alpha_2\rho_2 E_2\mathbf{u}_2 + \alpha_2 p_2\mathbf{u}_2) - P_I\mathbf{V_I}\cdot\nabla\alpha_2 = \Psi_2.
\end{aligned} \tag{0.2.2}$$

Les lois de fermeture retenues pour le couple vitesse-pression d'interface $(\mathbf{V_I}, P_I)$ sont celles proposées dans [23] par Gallouët *et al.* :

$$\mathbf{V_I} = (1-\mu)\mathbf{u}_1 + \mu\mathbf{u}_2, \quad \mu = \frac{\chi\alpha_1\rho_1}{\chi\alpha_1\rho_1 + (1-\chi)\alpha_2\rho_2}, \quad \chi\in\{0,1/2,1\}, \tag{0.2.3}$$

$$P_I = \beta p_1 + (1-\beta)p_2, \quad \beta = \frac{\mu T_1}{\mu T_1 + (1-\mu)T_2}, \tag{0.2.4}$$

où T_k est la température de la phase k. Le choix de la fermeture de $\mathbf{V_I}$ est motivé par l'exigence naturelle que le taux de présence soit porté par un champ linéairement dégénéré. Quant au choix de la fermeture de P_I, il est motivé par l'existence pour le système (0.2.2) d'une équation d'entropie conservative. En effet, en invoquant le second principe de la thermodynamique, on peut introduire l'entropie spécifique par phase $s_k(\rho_k, p_k)$ dont la différentielle exacte est donnée par

$$ds_k(\rho_k,p_k) = \frac{1}{T_k}de_k(\rho_k,p_k) + \frac{p_k}{T_k}d\tau_k, \tag{0.2.5}$$

où $\tau_k = \rho_k^{-1}$. On montre (voir [23]) que, si l'on omet les termes sources (*i.e.* si l'on prend $\Phi=0$, $\mathbf{D}_k=0,\ k\in\{1,2\}$ et $\Psi_k=0,\ k\in\{1,2\}$), alors les solutions régulières de (0.2.2) vérifient les deux équations supplémentaires suivantes:

$$\partial_t(\alpha_k\rho_k s_k) + \nabla\cdot(\alpha_k\rho_k s_k\mathbf{u}_k) + \frac{(p_k - P_I)}{T_k}(\mathbf{V_I}-\mathbf{u}_k)\cdot\nabla\alpha_k = 0, \quad k\in\{1,2\}. \tag{0.2.6}$$

Or, en sommant ces deux équations, le terme non conservatif $\sum_{k=1}^2 \frac{1}{T_k}(p_k - P_I)(\mathbf{V_I}-\mathbf{u}_k)\cdot\nabla\alpha_k$ s'annule par le choix (0.2.4), ce qui donne la loi de conservation supplémentaire

$$\partial_t\eta + \nabla\cdot\mathcal{F}_\eta = 0, \tag{0.2.7}$$

où $\eta = -\alpha_1\rho_1 s_1 - \alpha_2\rho_2 s_2$ et $\mathcal{F}_\eta = -\alpha_1\rho_1 s_1\mathbf{u}_1 - \alpha_2\rho_2 s_2\mathbf{u}_2$. La fonction η est convexe (voir l'annexe A pour une preuve de la convexité de η). Bien que non strictement convexe (la convexité est perdue dans la direction de α_1), η sera considérée comme une entropie mathématique pour le système homogène (0.2.2).

Considérons à présent les fermetures des termes sources d'ordre zéro. Le terme source Φ est un terme de relaxation sur la différence entre les pressions $p_1 - p_2$. Les termes $\mathbf{D}_k,\ k\in\{1,2\}$ sont

des termes de forces volumiques appliquées (gravité, etc.) et des termes d'échange de quantité de mouvement par friction entre les phases. Ces termes de friction étant généralement proportionnels à la différence $\mathbf{u}_1 - \mathbf{u}_2$, ils agissent également comme des termes de relaxation sur la différence des vitesses. Enfin, les termes $\Psi_k,\ k \in \{1,2\}$ modélisent l'apport éventuel d'énergie au système (par gravité par exemple) ainsi que les échanges d'énergie entre les phases. Notant $\overline{\mathbf{V}} = (\mathbf{u}_1 + \mathbf{u}_2)/2$, un choix usuel pour ces termes sources est donné par

$$\Phi = \Theta_p(p_1 - p_2), \tag{0.2.8}$$
$$\mathbf{D}_k = \alpha_k\rho_k\mathbf{g} - \Theta_u(\mathbf{u}_k - \mathbf{u}_{3-k}), \tag{0.2.9}$$
$$\Psi_k = \alpha_k\rho_k\mathbf{g}\cdot\mathbf{u}_k - \Theta_T(T_k - T_{3-k}) - P_I(-1)^{k+1}\Phi - \overline{\mathbf{V}}\cdot\mathbf{D}_k, \tag{0.2.10}$$

où Θ_p, Θ_u et Θ_T sont des termes positifs pouvant êtres pris comme suit:

$$\Theta_p = \frac{1}{\tau_p}\frac{\alpha_1\alpha_2}{p_1+p_2}, \quad \Theta_u = \frac{1}{\tau_u}\frac{(\alpha_1\rho_1)(\alpha_2\rho_2)}{\alpha_1\rho_1+\alpha_2\rho_2}, \quad \Theta_T = \frac{1}{\tau_T}\frac{(\alpha_1\rho_1C_1)(\alpha_2\rho_2C_2)}{\alpha_1\rho_1C_1+\alpha_2\rho_2C_2}. \tag{0.2.11}$$

Les grandeurs τ_p, τ_u et τ_T sont des temps caractéristiques liés aux phénomènes de relaxation en pression, vitesse et température. Le coefficient C_k est homogène à une capacité thermique massique. Notons qu'en l'absence de forces extérieures, tous ces termes d'ordre zéro doivent assurer la conservation de la quantité de mouvement totale ainsi que de l'énergie totale si bien que

$$\sum_{k=1}^{2}\mathbf{D}_k = 0, \quad \text{et} \quad \sum_{k=1}^{2}\Psi_k = 0. \tag{0.2.12}$$

Ces termes sources sont compatibles avec l'équation d'entropie (0.2.7). En effet, sans termes de gravité, les solutions régulières du système (0.2.2) muni des fermetures (0.2.3)-(0.2.4) et (0.2.8)-(0.2.9)-(0.2.10) vérifient l'équation de bilan suivante :

$$\partial_t\eta + \nabla\cdot\mathcal{F}_\eta = -\Theta_p(p_1-p_2)^2 - \Theta_u|\mathbf{u}_1-\mathbf{u}_2|^2 - \Theta_T(T_1-T_2)^2 \le 0. \tag{0.2.13}$$

Notons enfin que toutes ces fermetures préservent l'invariance par rotation du système.

0.2.2 Le modèle avec énergie en une dimension d'espace

Dans le cadre d'une approximation numérique par des techniques de volumes finis, il suffit, grâce à l'invariance par rotation, de savoir traiter ces équations dans une direction quelconque. En choisissant par exemple la direction x (mais toute autre direction aurait convenu), on se ramène à l'étude du cas 1D, qui s'écrit de manière condensée :

$$\partial_t\mathbb{U} + \partial_x\mathbf{F}(\mathbb{U}) + \mathbf{C}(\mathbb{U})\partial_x\mathbb{U} = \mathbf{S}(\mathbb{U}), \quad x\in\mathbb{R},\ t>0, \tag{0.2.14}$$

où $\mathbb{U} = (\alpha_1, \alpha_1\rho_1, \alpha_1\rho_1u_1, \alpha_1\rho_1E_1, \alpha_2\rho_2, \alpha_2\rho_2u_2, \alpha_2\rho_2E_2)^T$ est le vecteur d'état et

$$\mathbf{F}(\mathbb{U}) = \begin{bmatrix} 0 \\ \alpha_1\rho_1u_1 \\ \alpha_1\rho_1u_1^2 + \alpha_1p_1 \\ \alpha_1\rho_1E_1u_1 + \alpha_1p_1u_1 \\ \alpha_2\rho_2u_2 \\ \alpha_2\rho_2u_2^2 + \alpha_2p_2 \\ \alpha_2\rho_2E_2u_2 + \alpha_2p_2u_2 \end{bmatrix}, \quad \mathbf{C}(\mathbb{U})\partial_x\mathbb{U} = \begin{bmatrix} V_I \\ 0 \\ -P_I \\ -V_IP_I \\ 0 \\ P_I \\ V_IP_I \end{bmatrix}\partial_x\alpha_1, \quad \mathbf{S}(\mathbb{U}) = \begin{bmatrix} \Phi \\ 0 \\ \mathbf{D}_1 \\ \Psi_1 \\ 0 \\ \mathbf{D}_2 \\ \Psi_2 \end{bmatrix}. \tag{0.2.15}$$

Les lois de fermeture (0.2.3) et (0.2.4) sur le couple vitesse et pression d'interface, de même que les lois de fermeture pour les termes sources (0.2.8)-(0.2.9)-(0.2.10) se déduisent directement dans le cas unidimensionnel. De même que dans le cas multidimensionnel, en l'absence de termes sources, les solutions régulières du système (0.2.14) admettent comme entropie mathématique la projection de l'équation (0.2.7) dans la direction x et si les termes sources sont présents, c'est la projection de l'équation de bilan (0.2.13) dans la direction x qui est vérifiée.

A présent, précisons quelques définitions que nous serons amenés à utiliser par la suite. Nous dirons qu'un système de taille N est *faiblement hyperbolique* s'il n'admet que des valeurs propres réelles. Si de plus, la famille associée de vecteurs propres à droite engendre tout l'espace $\mathbb{R}^N$, alors le système est dit *hyperbolique*. La proposition suivante permet de caractériser la structure convective de ce système:

Proposition 0.1. *La partie homogène du système (0.2.14) est faiblement hyperbolique et admet les valeurs propres réelles suivantes:*

$$V_I, \quad et \quad u_k, \quad u_k - c_k, \quad u_k + c_k, \quad k \in \{1,2\} \tag{0.2.16}$$

où $c_k^2 = \frac{1}{\rho_k}\left(\frac{p_k}{\rho_k} - \rho_k \partial_{\rho_k} e_k\right)\left(\partial_{p_k} e_k\right)^{-1}$, $k \in \{1,2\}$, *est le carré de la vitesse du son dans la phase* k. *Le système est hyperbolique si et seulement si*

$$\alpha_k \neq 0 \quad et \quad |u_k - V_I| \neq c_k, \quad pour\ k \in \{1,2\}. \tag{0.2.17}$$

Les champs associés aux valeurs propres u_k, $k \in \{1,2\}$ *sont linéairement dégénérés, et les champs associés aux valeurs propres* $u_k \pm c_k$, $k \in \{1,2\}$ *sont vraiment non linéaires. De plus, si* V_I *est défini comme dans (0.2.3) alors le champ associé est linéairement dégénéré.*

Ainsi, la perte d'hyperbolicité du sytème peut être due à deux causes distinctes. La première est l'annulation d'un des taux de présence α_k, $k \in \{1,2\}$ et la seconde est la superposition de la valeur propre V_I, associé à l'onde de taux de présence, avec l'une des valeurs propres des champs acoustiques $u_k \pm c_k$, $k \in \{1,2\}$. Dans ces deux cas, on dit alors que le système est *résonnant*. Le traitement des difficultés liées à cette perte de base, notamment celle conséquente à l'annulation d'un taux de présence, concerne l'essentiel des travaux réalisés dans cette thèse.

0.2.3 Le modèle barotrope en une dimension d'espace

En ce qui concerne les solutions régulières, le système (0.2.14) muni de la fermeture $(V_I, P_I) = (u_2, p_1)$ peut être décrit de façon équivalente en remplaçant les équations d'énergie par les équations d'entropie par phase:

$$\partial_t(\alpha_k \rho_k s_k) + \nabla \cdot (\alpha_k \rho_k s_k u_k) = 0, \quad k \in \{1,2\}. \tag{0.2.18}$$

Dans ce contexte, les lois d'états thermodynamiques de chaque phase s'expriment alors en fonction des variables ρ_k et de l'entropie spécifique s_k. On a par exemple $p_k = p_k(\rho_k, s_k)$ et $e_k = e_k(\rho_k, s_k)$.

Le modèle barotrope correspond à l'évolution *isentropique par phase* du mélange, pour laquelle les deux équations (0.2.18) disparaissent, et la pression p_k de même que l'énergie interne spécifique

e_k, ne dépend plus que de la variable densité. Le modèle est alors composé de cinq équations sur le taux de présence α_1, les masses partielles $\alpha_k\rho_k$, et les quantités de mouvement partielles $\alpha_k\rho_k u_k$:

$$\begin{aligned}
&\partial_t\alpha_1 + V_I\partial_x\alpha_1 = \Theta_p(p_1 - p_2),\\
&\partial_t(\alpha_1\rho_1) + \partial_x(\alpha_1\rho_1 u_1) = 0,\\
&\partial_t(\alpha_1\rho_1 u_1) + \partial_x(\alpha_1\rho_1 u_1^2 + \alpha_1 p_1) - P_I\partial_x\alpha_1 = -\Theta_u(u_1 - u_2),\\
&\partial_t(\alpha_2\rho_2) + \partial_x(\alpha_2\rho_2 u_2) = 0,\\
&\partial_t(\alpha_2\rho_2 u_2) + \partial_x(\alpha_2\rho_2 u_2^2 + \alpha_2 p_2) + P_I\partial_x\alpha_1 = -\Theta_u(u_2 - u_1).
\end{aligned} \tag{0.2.19}$$

Ce système admet cinq valeurs propres réelles qui sont V_I et $u_k \pm c_k,\ k \in \{1,2\}$ où $c_k^2 = p_k'(\rho_k)$. Il est hyperbolique si et seulement $\alpha_1\alpha_2 \neq 0$ et $|u_k - V_I| \neq c_k,\ k \in \{1,2\}$. Les champs associés aux valeurs propres $u_k \pm c_k,\ k \in \{1,2\}$, sont vraiment non linéaires. De plus, muni des fermetures

$$V_I = (1-\mu)u_1 + \mu u_2, \quad \mu = \frac{\chi\alpha_1\rho_1}{\chi\alpha_1\rho_1 + (1-\chi)\alpha_2\rho_2}, \quad \chi \in \{0, 1/2, 1\}, \tag{0.2.20}$$

$$P_I = \mu p_1 + (1-\mu)p_2, \tag{0.2.21}$$

le champ associé à V_I est linéairement dégénéré et il existe une entropie mathématique pour le système, qui cette fois-ci est l'énergie totale de mélange. Sans les termes sources, les solutions régulières de (0.2.19) vérifient l'équation de conservation supplémentaire

$$\partial_t\left\{\sum_{k=1}^{2}\alpha_k\rho_k E_k\right\} + \partial_x\left\{\sum_{k=1}^{2}\alpha_k\rho_k E_k u_k + \alpha_k p_k(\rho_k)u_k\right\} = 0. \tag{0.2.22}$$

Avec les termes sources, l'équation de bilan vérifiée par les solutions régulières est

$$\partial_t\left\{\sum_{k=1}^{2}\alpha_k\rho_k E_k\right\} + \partial_x\left\{\sum_{k=1}^{2}\alpha_k\rho_k E_k u_k + \alpha_k p_k(\rho_k)u_k\right\} = -\Theta_p(p_1 - p_2)^2 - \Theta_u(u_1 - u_2)^2. \tag{0.2.23}$$

0.3 Produits non conservatifs, entropie et résonance

Les modèles de type Baer-Nunziato, présentent des produits non conservatifs. Pour le cas barotrope par exemple, les termes du premier ordre en espace ne peuvent pas être mis sous forme conservative à cause du terme $P_I\partial_x\alpha_k$. En général, la définition de ce type de produits n'est pas immédiate dans le contexte des solutions faibles puisqu'ils peuvent impliquer le produit de fonctions discontinues avec des mesures.

Dans le cas du système barotrope sans termes sources, une éventuelle discontinuité du taux de présence α_k est seulement portée par l'onde associée à la valeur propre V_I. Or, ayant considéré les fermetures (0.2.20) pour V_I, le champ associé est linéairement dégénéré. Ceci implique qu'**il n'y a pas d'ambiguité dans la définition du produit non conservatif tant que le système est hyperbolique**. En effet, pour définir le produit non conservatif à travers une discontinuité de α_k, on décompte les relations de Rankine-Hugoniot issues des lois de conservation vérifiées par les solutions faibles du système. Afin d'illustrer ceci, plaçons nous dans le cadre barotrope, et supposons que la fermeture choisie est $(V_I, P_I) = (u_2, p_1)$. On obtient trois relations de saut

correspondant à la conservation de la valeur propre $V_I = u_2$ à travers l'onde, à l'équation de conservation de la masse partielle de phase 1 $\alpha_1\rho_1$, et à l'équation de conservation de la quantité de mouvement totale $\alpha_1\rho_1u_1 + \alpha_2\rho_2u_2$. La valeur propre $V_I = u_2$ étant simple, il manque alors une relation supplémentaire (à noter que la conservation de la masse partielle de la phase 2 ne donne pas d'information). Or, un résultat classique (voir [34, 9, 23]) sur les systèmes hyperboliques énonce que toute loi de conservation supplémentaire pour les solutions régulières est encore une loi de conservation au sens faible le long des champs linéairement dégénérés. Ainsi, la relation de Rankine-Hugoniot pour la loi de conservation de l'énergie totale (0.2.22) fournit la dernière relation permettant de définir le saut à travers la discontinuité de α_k et donc le produit non conservatif $P_I\partial_x\alpha_k = p_1\partial_x\alpha_k$. Evidemment, tout ceci ne vaut que dans le cadre hyperbolique.

En ce qui concerne le système avec énergie, il y a *a priori* deux produits non conservatifs à définir : $P_I\partial_x\alpha_k = p_1\partial_x\alpha_k$ et $P_IV_I\partial_x\alpha_k = p_1u_2\partial_x\alpha_k$. En réalité, comme la valeur propre $V_I = u_2$ est continue le long de ce champ linéairement dégénéré, il n'y a qu'un seul produit non conservatif à définir qui est $P_I\partial_x\alpha_k = p_1\partial_x\alpha_k$. Les relations de Rankine-Hugoniot à travers une discontinuité de α_k sont données par la continuité de $V_I = u_2$, la conservation de la masse partielle de phase 1, de la quantité de mouvement totale et de l'énergie totale. Il ne manque alors de nouveau qu'une information. Celle-ci est obtenue, toujours dans le cadre hyperbolique, en appliquant la relation de Rankine-Hugoniot à l'équation de conservation de l'entropie du mélange (0.2.7). Un décompte analogue peut être mené dans le cas plus général des fermetures (0.2.20).

Pour résumer, dans le cadre hyperbolique, le caractère linéairement dégénéré du champ V_I implique que la connaissance de l'ensemble des invariants de Riemann suffit à fermer le produit non conservatif. Soulignons de nouveau que contrairement à une croyance ancrée, il n'y a pas ici d'ambiguïté, contrairement au cas de produits non conservatifs associés à des champs non linéaires (voir [37, 19]).

Lorsque la résonance apparaît, le système n'est plus que *faiblement hyperbolique*. Les valeurs propres sont toutes réelles mais il y a perte de la base de vecteurs propres. Pour $(V_I, P_I) = (u_2, p_1)$, les relations de saut sur u_2, $\alpha_1\rho_1$ et $\alpha_1\rho_1u_1 + \alpha_2\rho_2u_2$ dans le cas barotope (ainsi que sur l'énergie totale dans le cas avec énergie) restent vrai. On perd cependant un invariant de Riemann et c'est nécessairement celui exprimant la conservation de l'entropie mathématique. Autrement dit, la loi de conservation de l'entropie mathématique du système n'a donc plus aucune raison d'être vérifiée à travers l'onde V_I. Dans ce cas résonnant, il apparaît nécessaire de garantir que si l'entropie ne peut pas être conservée, elle doit diminuer strictement, pour des raisons évidentes de stabilité. Il faut donc modéliser des mécanismes de régularisation le long du champ V_I. A ces mécanismes, est associée *a priori* ou *a posteriori* une dissipation de l'entropie mathématique, conduisant à la définition d'une **relation cinétique**, qui est une relation de type Rankine-Hugoniot supplémentaire permettant en pratique de calculer les sauts à travers la discontinuité de taux de présence. Notons par exemple que ces relations cinétiques interviennent dans le contexte des transitions de phases afin de les caractériser (voir [1]). Si la solution est loin de la résonance, cette relation cinétique doit naturellement se réduire à la conservation de l'entropie mathématique à travers l'onde.

Evidemment, il n'y a pas unicité du choix des mécanismes de régularisation. Une modélisation usuelle qui concerne une classe de modèles incluant le modèle de Baer-Nunziato (voir [25, 28]), revient à supposer une évolution monotone de α_k à travers la discontinuité. Ceci conduit en particulier à l'existence de plusieurs solutions auto-semblables du problème de Riemann en présence de résonance. D'autres mécanismes de régularisation ont été introduits dans le contexte du couplage non

conservatif de systèmes hyperboliques conduisant à des situations résonnantes (voir [5, 4, 11, 12]). De nouveau, il n'y a génériquement pas unicité de la solution, chaque solution étant associée à un taux de dissipation particulier. Notons que toutes les situations de résonance évoquées dans ces travaux correspondent à un type de résonance lié à l'interaction entre un champ linéairement dégénéré et un champ vraiment non linéaire.

Le phénomène de résonance lié à la disparition de phase dans le cadre d'un modèle diphasique (avec au moins une phase compressible) a été étudié dans un travail de Bouchut *et al.* [10]. Le modèle considéré est un modèle à quatre équations pour un liquide incompressible (*i.e.* de densité constante) et un gaz barotrope. La motivation de ce travail est d'examiner les équations obtenues asymptotiquement dans la limite de disparition du gaz. A cet effet, les auteurs ont montré que le mécanisme de régularisation par friction joue un rôle crucial dans l'obtention du modèle limite. Le modèle asymptotique est de type incompressible au sens où il implique un multiplicateur de Lagrange assurant la contrainte d'un taux de présence (celui du liquide) inférieur ou égal à un.

Dans le cas des modèles moyennés incluant au moins une phase compressible, nous n'avons pas connaissance d'autres travaux. Ceci n'est pas surprenant car l'ensemble des résultats mathématiques d'existence concernant les systèmes différentiels s'arrêtent au premier instant où l'inconnue atteint la frontière de l'espace des états. Nous renvoyons en particulier à [37] où l'utilisation de mécanismes de régularisation visqueuse permet d'obtenir une existence locale en temps, le temps étant fini dès que l'un des taux de vide s'annule. Citons également les résultats de Bresch *et al.* [13] utilisant des mécanismes de régularisation d'ordre plus élevé.

D'autres mécanismes de régularisation peuvent être envisagés dans le cadre des modèles de type Baer-Nunziato, notamment les termes sources de relaxation sur l'écart des pressions et les termes de friction sur l'écart des vitesses, par ailleurs incontournables pour obtenir une description réaliste des écoulements diphasiques. Ces mécanismes dissipent tous deux l'entropie et ils ont pour conséquence de faire tendre les écarts vers zéro en temps. De nombreux travaux, dont ceux par exemple de Yong [44], de Kawashima-Yong [33] ou encore Chen *et al.* [15], sont consacrés au caractère stabilisant des termes d'ordre zéro dans un cadre des systèmes d'équations de bilan à structure convective strictement hyperbolique. Cependant, l'absence de stricte convexité de l'entropie du modèle de Baer-Nunziato et la résonance rendent difficile l'exploitation de ces travaux.

Dans cette thèse, nous proposons d'examiner mathématiquement des mécanismes originaux de stabilisation permettant de résoudre le problème de Riemann dans le régime des phases évanescentes. Ces mécanismes sont basés d'une part sur l'emploi d'une relaxation de type Suliciu et d'autre part sur des mécanismes de dissipation à travers l'onde de taux de présence. Nous montrons que dissiper peut être à nouveau nécessaire dans certains cas. Les approches proposées sont notamment motivées par la simulation numérique des écoulements diphasiques, et la prise en compte, lors de ces simulations, des cas difficiles de phases évanescentes.

0.4 Approximation par relaxation et passage du barotrope à l'énergie

L'approximation des modèles par relaxation de type Suliciu est un outil largement utilisé dans cette thèse. Cette approximation consiste en une linéarisation partielle du modèle, en ne relaxant que les lois de pression. Ceci aboutit à un système, certes plus large, mais uniquement composé de champs linéairement dégénérés, ce qui simplifie grandement la résolution du problème de Riemann. Dans le cas des équations d'Euler barotrope par exemple, cela conduit à des schémas positifs très simples et faisant diminuer l'entropie mathématique sous une condition sous-caractéristique dite de Whitham. Une modification introduite par Bouchut [9] permet d'étendre la méthode dans le cas d'apparition du vide.

L'un des grands intérêts de ce type de solveurs est qu'il admet une formulation indépendante de la loi de pression, ce qui permet de l'utiliser pour tout type de loi d'état, considérée thermodynamiquement admissible.

L'autre grand intérêt de ces solveurs de relaxation est qu'ils admettent une généralisation immédiate du cas barotrope au cas avec énergie, grâce à la dualité énergie/entropie [17, 9]. Pour les équations d'Euler, les formules définissant la solution auto-semblable dans le cas avec énergie sont **virtuellement les mêmes** que dans le cas barotrope, ces formules conduisant à mettre à jour de manière conservative l'énergie en faisant augmenter l'entropie physique. Enfin, la méthode préserve la positivité de chaque énergie interne phasique.

Nous montrons dans cette thèse que cette situation est inchangée pour le modèle de Baer-Nunziato dans le cadre des fermetures $(V_I, P_I) = (u_2, p_1)$ ou $(V_I, P_I) = (u_1, p_2)$. Ceci explique pourquoi une grande partie du travail de cette thèse a été consacré à l'étude du cas barotrope. Nous montrons également comment un schéma numérique peut être immédiatement obtenu dans le cadre avec énergie, même si dans le cadre de la thèse, nous n'avons pas eu le temps d'approfondir extensivement les simulations numériques dans ce cas.

Dans les quatre sections suivantes, nous donnons une présentation détaillée des travaux de la thèse, organisés sous la forme de quatre chapitres.

0.5 Chapitre 1: Approximation par relaxation pour les équations d'Euler en tuyère

L'analyse menée dans ce premier chapitre constitue la pierre angulaire de l'étude du chapitre 2 sur une approximation par relaxation du système diphasique de Baer-Nunziato. Cependant, il s'agit aussi d'une étude indépendante d'une approximation par relaxation des équations d'Euler en tuyère, aboutissant à un schéma de relaxation précis et robuste pour ce système.

Dans ce chapitre, nous construisons donc une approximation par relaxation pour le système des équations d'Euler en tuyère en configuration barotrope. Ce système étant composé de champs vraiment non linéaires liés aux ondes acoustiques qui rendent la résolution du problème de Riemann difficile (mais néanmoins possible), nous proposons une approximation par relaxation de type Suliciu

qui prend la forme suivante:

$$\begin{cases} \partial_t \alpha^\varepsilon = 0, \\ \partial_t (\alpha\rho)^\varepsilon + \partial_x (\alpha\rho w)^\varepsilon = 0, \\ \partial_t (\alpha\rho w)^\varepsilon + \partial_x (\alpha\rho w^2 + \alpha\pi(\tau, \mathcal{T}))^\varepsilon - \pi(\tau, \mathcal{T})^\varepsilon \partial_x \alpha^\varepsilon = 0, \\ \partial_t (\alpha\rho\mathcal{T})^\varepsilon + \partial_x (\alpha\rho\mathcal{T} w)^\varepsilon = \dfrac{1}{\varepsilon} (\alpha\rho)^\varepsilon (\tau - \mathcal{T})^\varepsilon, \end{cases} \tag{0.5.1}$$

avec $\pi(\tau, \mathcal{T}) = p(\mathcal{T}) + a^2(\mathcal{T} - \tau)$, $\tau = \rho^{-1}$, où a est un paramètre strictement positif représentant une vitesse lagrangienne gelée. Ce système a des propriétés de résonance similaires à celles du modèle de Baer-Nunziato. Il admet toujours quatre valeurs propres réelles associées à des champs linéairement dégénérés qui sont 0, w et $w \pm a\tau$. Cependant, la base de diagonalisation dégénère dans deux cas distincts. Premièrement lorsque la section α s'annule et deuxièmement lorsque l'onde stationnaire interagit avec les ondes acoustiques. Notons que l'interaction entre les ondes 0 et w n'est pas résonnante car la base de diagonalisation est préservée et que l'interaction entre l'onde w et les ondes acoustiques $w \pm a\tau$ est exclue pour des raisons de positivité de la densité.

Nous menons une étude approfondie du problème de Riemann associé à la partie homogène de ce sytème (*i.e.* sans le terme source). L'objectif est de fournir une résolution complète dans tous les régimes d'écoulement, qu'ils soient subsoniques ($|w| < a\tau$), supersoniques ($|w| > a\tau$) ou même résonnants ($|w| = a\tau$). Nous introduisons une classe de solutions généralisées assurant l'existence dans tous les régimes d'écoulement. Dans le but de prendre en compte la résonance due à l'annulation de α, les solutions considérées sont susceptibles d'introduire une dissipation de l'énergie de relaxation du système (0.5.1) à travers l'onde stationnaire, alors que ce système est à champs linéairement dégénérés. En effet, rapportons que l'existence de rapports des sections droite et gauche $\frac{\alpha_L}{\alpha_R}$ (ou le rapport inverse) très grands, conduit à des valeurs anormalement basses voire négatives, du volume spécifique à l'intérieur du cône d'ondes de la solution du problème de Riemann. Nous proposons de dissiper l'énergie à la traversée de l'onde stationnaire et montrons qu'il est ainsi possible de restaurer la positivité de ces volumes spécifiques. Nous proposons en annexe de ce chapitre une relation cinétique particulière permettant d'assurer cette propriété.

En ce qui concerne la résonance due à l'interaction de l'onde stationnaire avec les ondes acoustiques linéarisées, les solutions considérées peuvent prendre des valeurs mesures lorsqu'une onde $w \pm a\tau$ voit sa vitesse s'annuler. Cette apparition d'une mesure stationnaire (valeurs ponctuelles infinies en $x = 0$ mais masse L^1 bornée) est tout à fait naturelle dans un contexte où toutes les ondes sont linéairement dégénérées. Voir par exemple [8] dans le contexte des gaz sans pression où des solutions δ-choc sont construites.

Le résultat principal de ce chapitre est un théorème d'existence de solutions au problème de Riemann dans la classe de solutions introduites (solutions dissipatives et éventuellement mesures). En particulier, nous exposons une cartographie basée sur des **conditions algébriques explicites** portant sur les conditions initiales, dont on déduit l'ordre des ondes et la valeur des états intermédiaires. Nous montrons en fait que dans chaque configuration d'onde, il existe un continuum de solutions paramétrées par un nombre de Mach qui pilote directement le taux de dissipation d'énergie à travers l'onde stationnaire. La relation cinétique que nous proposons permet de choisir une solution en fixant la valeur de ce nombre de Mach.

Nous attirons également l'attention du lecteur sur le fait que malgré une analyse du problème de Riemann qui peut paraître compliquée, le solveur de Riemann qui en résulte est extrêmement

simple dans la mesure où la solution s'exprime de façon **explicite par des relations algébriques fonctions des données initiales**.

En nous basant sur ce solveur de Riemann, nous construisons un schéma numérique de type Harten-Lax-van Leer (HLL) [27] pour les équations d'Euler barotrope en tuyère. Outre la discrétisation conservative de l'équation de masse, l'autre propriété classique de positivité de la densité est facilement démontrée grâce au formalisme HLL. Nous prouvons aussi que le schéma vérifie la propriété de préserver de façon exacte les équilibres stationnaires (vitesse nulle et densité constante). Nous prouvons également la stabilité non linéaire du schéma sous une condition de type Whitham affaiblie. Classiquement, l'analyse par entropie amène à imposer une condition dite sous-caractéristique sur la taille du paramètre a. La condition revient à définir une valeur locale de a pour chaque problème de Riemann, qui majore les valeurs ponctuelles de la vitesse du son lagrangienne $\sqrt{-\partial_\tau p(\tau)}$. Or pour les configurations qui sont proches de la résonance (interaction entre ondes), les valeurs mesure de la densité imposeraient un a potentiellement infini sous une telle condition restrictive. Pour contourner cet obstacle, nous menons l'analyse sur des inégalités d'entropies discrètes en moyenne. Cela permet de définir une condition de Whitham «faible» portant sur des valeurs moyennées des densités. Les solutions mesures ayant des masses bornées, on garantit alors la stabilité non linéaire du schéma avec des valeurs de a raisonnables.

Enfin, des tests numériques illustrent l'intérêt de la méthode pour l'approximation des équations d'Euler barotrope en tuyère.

0.6 Chapitre 2: Approximation par relaxation pour le modèle de Baer-Nunziato

Dans ce chapitre, on étend les travaux du chapitre 1 au cadre du modèle de Baer-Nunziato avec la fermeture $(V_I, P_I) = (u_2, p_1)$. De même que pour le premier chapitre, l'étude se fait sur un système de relaxation pour le modèle, qui consiste en une linéarisation sélective des lois de pression:

$$\left\{\begin{array}{l} \partial_t \alpha_1^\varepsilon + u_2^\varepsilon \partial_x \alpha_1^\varepsilon = 0, \\ \partial_t (\alpha_k \rho_k)^\varepsilon + \partial_x (\alpha_k \rho_k u_k)^\varepsilon = 0, \\ \partial_t (\alpha_k \rho_k u_k)^\varepsilon + \partial_x (\alpha_k \rho_k u_k^2 + \alpha_k \pi_k(\tau_k, \mathcal{T}_k))^\varepsilon - \pi_1(\tau_1, \mathcal{T}_1)^\varepsilon \partial_x \alpha_k^\varepsilon = 0, \\ \partial_t (\alpha_k \rho_k \mathcal{T}_k)^\varepsilon + \partial_x (\alpha_k \rho_k \mathcal{T}_k u_k)^\varepsilon = \dfrac{1}{\varepsilon} (\alpha_k \rho_k)^\varepsilon (\tau_k - \mathcal{T}_k)^\varepsilon, \end{array}\right. \tag{0.6.1}$$

avec $\alpha_1 + \alpha_2 = 1$ et $\pi_k(\tau_k, \mathcal{T}_k) = p_k(\mathcal{T}_k) + a_k^2(\mathcal{T}_k - \tau_k)$, $k \in \{1, 2\}$, où les a_k, $k \in \{1, 2\}$ sont des paramètres strictement positifs. Ce système admet les valeurs propres réelles u_k et $u_k \pm a_k \tau_k$ pour $k \in \{1, 2\}$, la valeur propre u_2 étant double. Il est hyperbolique si et seulement si $\alpha_1 \alpha_2 \neq 0$ et $|u_1 - u_2| \neq a_1 \tau_1$. On s'intéresse à nouveau au problème de Riemann pour la partie homogène de (0.6.1).

Etant données les applications qui nous intéressent (mélanges liquide/vapeur dans les réacteurs nucléaires), ne seront considérées dans ce chapitre que les solutions ayant un *ordre subsonique des ondes* c'est-à-dire les solutions pour lesquelles $u_1 - a_1 \tau_1 < u_2 < u_1 + a_1 \tau_1$. En conséquence, l'interaction des ondes ainsi que l'apparition d'éventuelles solutions mesure sont exclues *de facto*. La résonance liée à l'évanescence de phase ($\alpha_1 \to 0$ ou $\alpha_1 \to 1$) est quant à elle toujours possible et cette difficulté retient ici toute notre attention.

Comme dans le chapitre précédent, nous introduisons pour le problème de Riemann une classe de solutions généralisées qui autorise une dissipation de l'énergie de relaxation du système (0.6.1) à la traversée de l'onde de taux de présence u_2. En effet et à l'instar du premier chapitre, de grandes valeurs du rapport des taux de présence droit et gauche peuvent conduire les volumes spécifiques à prendre des valeurs anormalement basses voires négatives. Nous montrons à nouveau que dissiper l'énergie de mélange permet de contourner cette difficulté dans les régimes de phases évanescentes. La relation cinétique que nous proposons est similaire à celle du chapitre 1, elle consiste à choisir le taux de dissipation de manière à imposer une borne inférieure sur les volumes spécifiques. La donnée du taux de dissipation d'énergie par cette relation cinétique caractérise alors une unique solution dans cette classe de solutions dissipatives.

Le résultat princial de ce deuxième chapitre est un théorème d'existence de solutions au problème de Riemann dans la classe de solutions considérée (solutions subsoniques en vitesse relative éventuellement dissipatives), sous certaines **conditions explicites sous forme de relations algébriques** portant sur les données initiales. Ces conditions d'existence prennent la forme d'une condition de *subsonicité*:

$$-a_1\tau_1^\sharp < U^\sharp < a_1\tau_1^\sharp, \tag{0.6.2}$$

où les quantités $^\sharp$ dépendent explicitement de la condition initiale et où la vitesse $U^\sharp$ mesure les différences de vitesse $u_1 - u_2$ et de pression $\pi_1 - \pi_2$ dans la donnée initiale (voir le chapitre 2 pour l'expression exacte de ces quantités). L'unicité de la solution est également assurée une fois spécifiée une relation cinétique indiquant le taux d'énergie dissipée à travers l'onde de taux de présence. Par ailleurs, nous obtenons des **conditions explicites** portant sur les conditions initiales, caractérisant l'ordre des ondes les unes par rapport aux autres. Ainsi, au vu uniquement des conditions initiales du problème de Riemann, il est possible de savoir s'il existe ou non une solution subsonique en vitesse relative, et de prédire quel ordre des ondes a l'éventuelle solution. La valeur des états intermédiaires est également obtenue très facilement. A notre connaissance, ce type de résulat n'existe pas dans la littérature concernant le système équilibre de Baer-Nunziato.

Donnons quelques indications sur la stratégie utilisée pour la preuve de ce théorème. L'idée de départ (qui était déjà présente dans un travail de Ambroso *et al.* [3]) est de remarquer que si l'on peut prédire la valeur du produit non conservatif $\pi_1\partial_x\alpha_1$ en fonction des données, alors il est possible de résoudre le système (0.6.1) puisque les deux phases sont alors découplées. En particulier, si l'on note $\pi_1^*\partial_x\alpha_1$ la prédiction du produit non conservatif, alors les équations de la phase 2 sont indépendantes de la phase 1 et s'écrivent

$$\begin{aligned}
&\partial_t\alpha_2 + u_2\partial_x\alpha_2 = 0,\\
&\partial_t(\alpha_2\rho_2) + \partial_x(\alpha_2\rho_2u_2) = 0,\\
&\partial_t(\alpha_2\rho_2u_2) + \partial_x(\alpha_2\rho_2u_2^2 + \alpha_2\pi_2) + \pi_1^*\partial_x\alpha_1 = 0,\\
&\partial_t(\alpha_2\rho_2\mathcal{T}_2) + \partial_x(\alpha_2\rho_2\mathcal{T}_2u_2) = 0.
\end{aligned} \tag{0.6.3}$$

En résolvant le problème de Riemann pour ce système, on peut alors calculer une prédiction u_2^* de la vitesse de propagation de l'onde de taux de présence. Les équations de la phase 1, réécrites dans

le référentiel galiléen se déplaçant à la vitesse constante u_2^* donnent alors le système

$$\begin{aligned}
&\partial_t \alpha_1 = 0,\\
&\partial_t(\alpha_1\rho_1) + \partial_x(\alpha_1\rho_1 w_1) = 0,\\
&\partial_t(\alpha_1\rho_1 w_1) + \partial_x(\alpha_1\rho_1 w_1^2 + \alpha_1\pi_1) - \pi_1\partial_x\alpha_1 = 0,\\
&\partial_t(\alpha_1\rho_1\mathcal{T}_1) + \partial_x(\alpha_1\rho_1\mathcal{T}_1 w_1) = 0,
\end{aligned} \tag{0.6.4}$$

où $w_1 = u_1 - u_2^*$. Ce système n'est autre que le système de relaxation pour les équations d'Euler en tuyère introduit dans le chapitre 1 et pour lequel le problème de Riemann est complètement résolu. En particulier, la résolution fournit une nouvelle valeur pour la prédiction du produit non conservatif $\pi_1^*\partial_x\alpha_1$. La technique consiste alors à faire un point fixe sur le couple (π_1^*, u_2^*), consistant à résoudre tour à tour les phases 1 et 2. En réalité, ce point fixe se ramène de manière remarquable à un point fixe de la forme :

$$\text{Trouver} \quad \mathcal{M}_L^* \in (-1,1) \quad \text{tel que} \quad \Psi(\mathcal{M}_L^*) = 0, \tag{0.6.5}$$

où Ψ est une **fonction scalaire strictement monotone** dépendant de la condition initiale et $\mathcal{M}_L^*$ est un nombre de Mach relatif construit sur la différence $u_1 - u_2$. Les conditions de subsonicité (0.6.2) qui sont données dans le théorème sont alors des conditions d'existence d'une solution au point fixe (0.6.5). Le fait que Ψ soit une fonction scalaire monotone est crucial car dans les applications pratiques utilisant ce solveur de Riemann, il sera possible d'utiliser les algorithmes classiques de recherche de racine pour déterminer la solution $\mathcal{M}_L^*$. Une fois déterminée la valeur de $\mathcal{M}_L^*$ solution de (0.6.5), il est alors possible de construire un autre Mach relatif $\mathcal{M}$ pilotant directement la dissipation d'énergie à travers l'onde de taux de présence. Ce deuxième nombre de Mach relatif $\mathcal{M}$, qui paramétrise tous les états intermédiaires, évolue dans un intervalle, ce qui explique la non-unicité de la solution. Une fois spécifié le taux de dissipation, le nombre $\mathcal{M}$ est alors fixé, ce qui aboutit à l'unicité.

0.7 Chapitre 3: Un schéma numérique de relaxation pour le modèle de Baer-Nunziato

Dans ce troisième chapitre, la solution du problème de Riemann construite au chapitre 2 est exploitée dans le but de construire un solveur de Riemann approché pour les solutions subsoniques en vitesse relative du modèle de Baer-Nunziato, c'est-à-dire les solutions telles que $|u_1 - u_2| < c_1$ (rappelons qu'ici $(V_I, P_I) = (u_2, p_1)$). Ce solveur est conçu dans le but de gérer les cas de phases evanescentes quitte à dissiper l'énergie de relaxation à travers l'onde de taux de présence.

Nous soulignons que si l'analyse mathématique développée au chapitre 2 peut paraître compliquée, le solveur de Riemann qui en résulte est là encore extrêmement simple. En effet, une fois déterminée la valeur de $\mathcal{M}_L^*$, solution du point fixe (0.6.5), grâce à un algorithme classique de recherche de racine, la solution du problème de Riemann s'exprime par des **relations algébriques simples** faisant intervenir $\mathcal{M}_L^*$ et les données initiales du problème de Riemann. Notons que dans le cadre de nos applications (mélanges liquide/vapeur fortement subsoniques en vitesse relative), les conditions de subsonicité (0.6.2) du théorème sont toujours vérifiées.

Dans un premier temps, le solveur de Riemann ainsi construit est exploité pour approcher des solutions du modèle barotrope homogène de Baer-Nunziato en une dimension d'espace. Nous montrons que ce solveur de type HLL (voir [27]) admet une formulation volumes finis classique à deux flux par interface (voir [9]) ce qui permet une extension simple et naturelle du schéma à des cas multi-dimensionnels. Nous prouvons le caractère conservatif de la discrétisation des équations de masses partielles et de la quantité de mouvement totale, de même que la positivité des taux de présence et des densités. Nous démontrons aussi que le schéma vérifie une inégalité d'entropie discrète sous des conditions de type Whitham sur les paramètres a_1 et a_2. Les solutions mesures étant exclues du cadre d'application, il n'est pas nécessaire ici de faire appel à une version affaiblie de la condition de Whitham, comme c'était le cas au chapitre 1.

La précision de ce schéma de relaxation est évaluée en comparant la solution approchée calculée par le schéma à la solution exacte d'un problème de Riemann. Il apparaît que sur un maillage grossier de cent mailles, la précision obtenue est très bonne dans la mesure où les états intermédiaires sont correctement capturés.

La nécessité d'utiliser une procédure de résolution itérative à chaque interface pour le calcul de $\mathcal{M}_L^*$ (en réalité, seules les interfaces où $\alpha_{1,L} \neq \alpha_{1,R}$ sont concernées) nous a amenés à évaluer les performances du schéma en terme de temps CPU. Dans ce but, nous avons comparé les performances du schéma de relaxation à celles d'un schéma dont les coûts sont réputés très faibles : le schéma de Rusanov (pour une référence sur le schéma de Rusanov, voir [23]). L'outil classique de calcul scientifique utilisé pour cette étude de performance est le suivant : considérant une solution exacte connue, il s'agit de se donner un niveau de précision (en terme d'erreur L^1 par exemple) et de comparer alors les temps CPU nécessaires à chaque schéma pour atteindre ce niveau de précision. Il apparaît que malgré le calcul du point fixe à chaque cellule où $\alpha_{1,L} \neq \alpha_{1,R}$, le schéma de relaxation est beaucoup plus rapide que le schéma de Rusanov à précision égale. A titre d'exemple, la figure 2 présente les courbes (erreur L^1) $= f$(temps CPU) obtenues pour deux variables d'intérêt. On y voit par exemple que concernant le taux de présence α_1, le schéma de relaxation est 12 fois plus rapide que le schéma de Rusanov, à précision égale.

Nous avons également évalué la robustesse du schéma dans les régimes de phases evanescentes. Pour cela, nous avons construit deux solutions exactes de problèmes de Riemann à phases evanescentes. Dans un premier cas, la phase 2 est absente de la donnée gauche du problème de Riemann tandis que dans la donnée droite, les deux phases sont en présence. Le deuxième cas est plus délicat encore. Il consiste en une donnée gauche où seule la phase 1 est présente et une donnée droite où seule la phase 2 est présente. La construction de telles solutions exactes est détaillée en annexe de ce chapitre, elle fut notamment abordée dans l'article de Schwedeman *et al.* [40]. En pratique, il est impossible de considérer des valeurs réellemement nulles des taux de présence mais l'objectif ici était de prescrire des valeurs extrêmement petites des taux de présence (de l'ordre de $\alpha_k \approx 10^{-9}$, à comparer à $\alpha_k \approx 10^{-6}$ dans Schwedeman etal [40]) et d'observer le comportement qualitatif de la solution approchée vis-à-vis de la solution exacte. L'étude numérique montre une grande robustesse du schéma de relaxation, en particulier pour les variables phasiques se trouvant dans une zone où la phase en question est quasiment absente, et ce malgré les divisions par α_k. Nous observons aussi une stabilité de la solution approchée quand des perturbations non négligeables sont apportées aux données de la phase quasiment absente.

Dans un deuxième temps, le schéma est naturellement étendu, grâce à sa formulation volumes finis à deux flux, à des applications 2D sur maillage non structuré général. Ce solveur 2D hérite alors

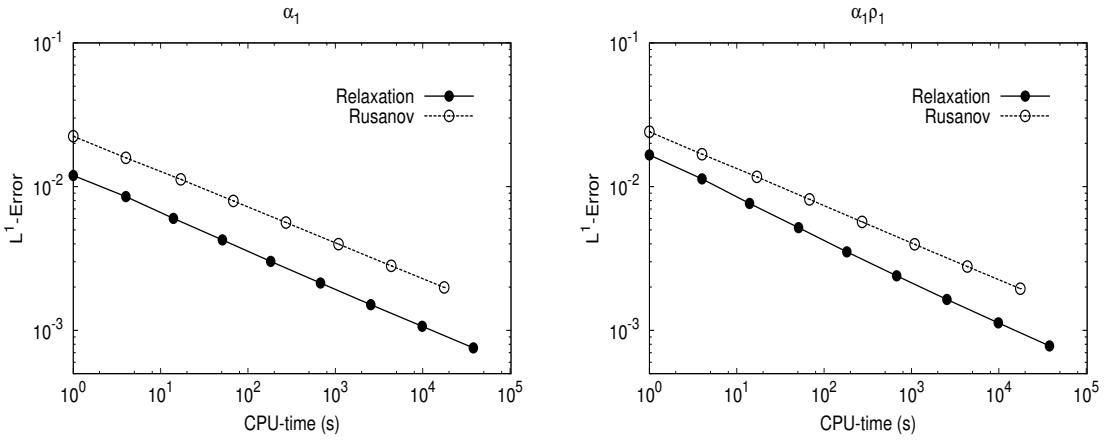

Figure 2: Erreur L^1 en fonction du coût CPU (en secondes) pour les variables α_1 (à gauche) et $\alpha_1\rho_1$ (à droite).

sous CFL des mêmes propriétés de positivité du schéma 1D ainsi que de la propriété de stabilité non linéaire sous une condition de Whitham adaptée. En vue de la réalisation d'applications 2D réalistes, nous avons également discrétisé les termes sources de relaxation en pression et en vitesse ainsi que la force de gravité. L'application numérique étudiée en 2D considère un cas de ballotement d'une poche de liquide dans une citerne. Là encore, la robustesse du schéma dans des configurations de phases évanescentes est vérifiée. A cet égard, les résultats sont très satisfaisants.

Enfin, la dernière partie de ce chapitre considère l'extension du schéma au modèle complet avec énergie, en une dimension d'espace. Après avoir expliqué comment le schéma barotrope s'étend naturellement au cas avec énergie grâce à la dualité énergie/entropie, nous illustront la méthode avec un cas test. Soulignons de nouveau qu'il importe de dissiper l'entropie mathématique *via* un argument de dualité énergie/entropie, pour définir une méthode de volumes finis stable, positive et entropique, y compris dans le régime des phases évanescentes.

0.8 Chapitre 4: Une méthode à pas fractionnaires pour le modèle de Baer-Nunziato

Le schéma de relaxation introduit aux chapitres 2 et 3 est conçu pour l'approximation du modèle de Baer-Nunziato muni de la fermeture $(V_I, P_I) = (u_2, p_1)$. Nous proposons dans ce chapitre un schéma numérique, reposant sur une décomposition en opérateurs, permettant de prendre en compte tout type de fermeture sur le couple (V_I, P_I). Le schéma est d'abord construit pour le cas barotrope pour toute fermeture (V_I, P_I), il est ensuite étendu au cas avec énergie dans le cadre de la fermeture $(V_I, P_I) = (u_2, p_1)$. L'extension au cas avec énergie est possible pour des fermetures plus générales, mais elle nécessite un travail supplémentaire qui n'a pas été mené ici.

Suivant les travaux de Chalons *et al.* [14], le splitting considéré propose un traitement séparé

des ondes acoustiques rapides et des ondes de transport matériel lentes. Cette séparation des phénomènes propagatifs selon leurs célérités respectives a pour objectif ultime (non réalisé dans cette thèse) d'impliciter le traitement des ondes rapides, ce qui permettrait d'adapter la condition CFL aux ondes lentes, traitées elles de façon explicite de manière à minimiser la diffusion numérique sur ces dernières. L'autre objectif recherché par ce splitting est de s'affranchir de l'interaction résonnante entre ondes lentes et ondes rapides. Ainsi, le schéma que nous proposons permet de traiter tous les régimes d'écoulement (subsoniques et supersoniques en vitesses relatives $u_k - V_I$), sans se soucier de l'interaction entre les ondes. Partant du système

$$\begin{aligned}
&\partial_t \alpha_1 + V_I \partial_x \alpha_1 = 0, \\
&\partial_t (\alpha_k \rho_k) + \partial_x (\alpha_k \rho_k u_k) = 0, \\
&\partial_t (\alpha_k \rho_k u_k) + \partial_x (\alpha_k \rho_k u_k^2 + \alpha_k p_k) - P_I \partial_x \alpha_k = 0,
\end{aligned}$$

la décomposition proposée pour le cas barotrope est motivée par un calcul simple:

$$\begin{aligned}
&\partial_t \alpha_1 + V_I \partial_x \alpha_1 = 0, \\
&\partial_t (\alpha_k \rho_k) + \rho_k \partial_x (\alpha_k u_k) - (\rho_k V_I) \partial_x \alpha_k + \alpha_k (u_k - V_I) \partial_x \rho_k - \alpha_k \rho_k \partial_x V_I + \partial_x (\alpha_k \rho_k V_I) = 0, \\
&(\alpha_k \rho_k) \partial_t u_k + \alpha_k \partial_x p_k + (p_k - P_I) \partial_x \alpha_k + (\alpha_k \rho_k)(u_k - V_I) \partial_x u_k - u_k \partial_x (\alpha_k \rho_k V_I) + \partial_x (\alpha_k \rho_k u_k V_I) \\
&\qquad + u_k \underbrace{\{\partial_t \alpha_k \rho_k + \partial_x \alpha_k \rho_k u_k\}}_{=0} = 0.
\end{aligned}$$

Ceci aboutit à la décomposition suivante:

Premier pas : Propagation des ondes acoustiques dues aux déséquilibres de pression:

$$\begin{aligned}
&\partial_t \alpha_1 = 0, \\
&\partial_t (\alpha_k \rho_k) + \rho_k \partial_x (\alpha_k u_k) - (\rho_k V_I) \partial_x \alpha_k = 0, \qquad k \in \{1, 2\} \\
&(\alpha_k \rho_k) \partial_t u_k + \alpha_k \partial_x p_k + (p_k - P_I) \partial_x \alpha_k = 0.
\end{aligned}$$

Deuxième pas : Transport à la vitesse $u_k - V_I$:

$$\begin{aligned}
&\partial_t \alpha_1 = 0, \\
&\partial_t \rho_k + (u_k - V_I) \partial_x \rho_k - \rho_k \partial_x V_I = 0, \qquad k \in \{1, 2\} \\
&\partial_t u_k + (u_k - V_I) \partial_x u_k = 0.
\end{aligned}$$

Troisième pas : Mise à jour de α_k et convection par V_I:

$$\begin{aligned}
&\partial_t \alpha_1 + V_I \partial_x \alpha_1 = 0, \\
&\partial_t (\alpha_k \rho_k) + \partial_x (\alpha_k \rho_k V_I) = 0, \qquad k \in \{1, 2\}. \\
&\partial_t (\alpha_k \rho_k u_k) + \partial_x (\alpha_k \rho_k u_k V_I) = 0.
\end{aligned}$$

En revanche, on n'évite toujours pas le problème de résonance lié à la disparition d'une ou des deux phases, difficulté sur laquelle ici encore nous concentrons nos efforts. Ainsi, il apparaît impératif de développer une discrétisation de chacun de ces trois pas de manière à supporter les

régimes de phases évanescentes. Dans le pas 2, qui traite des phénomènes de convection par les vitesses $u_k - V_I$, les taux de présence se simplifient des équations. Pourvu que l'on puisse définir correctement les quantités physiques (densités et vitesses) à la sortie du premier pas, on peut alors les mettre à jour dans le pas 2 sans faire intervenir α_k. On peut donc assurer lors de ce deuxième pas la stabilité de la méthode dans les régimes de phases évanescentes. Le dernier pas est consacré à la mise à jour de α_k. Une adaptation d'un schéma très simple et classique (le schéma décentré amont) permet de discrétiser ce dernier pas de manière à préserver la positivité des densités et un principe du maximum sur les taux de présence et ce même dans les cas de phases évanescentes.

Reste alors le traitement du premier pas. Motivés par les résultats du chapitre 2, nous introduisons un nouveau mécanisme de dissipation d'énergie reposant sur des corrections des lois de fermeture (V_I, P_I). Certaines fermetures dissipant l'entropie ont déjà été proposées par Saurel *et al.* [39], Abgrall-Saurel [2] et Papin-Abgrall [35]. La correction que nous proposons donne un cadre général à ces travaux en faisant intervenir une matrice symétrique positive de la forme

$$\mathcal{D} = \begin{pmatrix} b\, D_u & d \\ d & D_\pi / b \end{pmatrix}. \tag{0.8.1}$$

Etant donnée une loi de fermeture

$$V_I^c = (1-\mu)u_1 + \mu u_2, \quad P_I^c = \mu p_1 + (1-\mu)p_2, \quad \mu \in [0,1], \tag{0.8.2}$$

assurant une conservation de l'énergie (pour les solutions régulières), nous proposons de la corriger localement dans les régimes de phases évanescentes de la façon suivante:

$$\begin{pmatrix} V_I \\ P_I \end{pmatrix} = \begin{pmatrix} V_I^c \\ P_I^c \end{pmatrix} + \text{signe}(-\partial_x \alpha) \begin{pmatrix} d & D_\pi/b \\ b\, D_u & d \end{pmatrix} \begin{pmatrix} u_1 - u_2 \\ p_1 - p_2 \end{pmatrix}, \tag{0.8.3}$$

où

$$\text{signe}(-\partial_x \alpha) = \begin{cases} -1, & \text{si } \partial_x \alpha > 0, \\ +1, & \text{sinon.} \end{cases} \tag{0.8.4}$$

Ainsi, la matrice $\mathcal{D}$ permet de recoupler les vitesses et pressions relatives $u_1 - u_2$ et $p_1 - p_2$ dans la définition du couple (V_I, P_I). De plus, grâce au résultat suivant, on montre que cette matrice permet de piloter directement la dissipation d'énergie à la traversée de l'onde de taux de présence (l'onde stationnaire dans le pas 1):

Propriété 0.2. *Si la matrice symétrique $\mathcal{D}$ est positive, alors la correction (0.8.3) des vitesse et pression d'interface fait décroître l'énergie dans le premier pas au sens où les solutions régulières du pas 1 satisfont :*

$$\partial_t \left\{ \sum_{k=1}^{2} \alpha_k \rho_k E_k \right\} + \partial_x \left\{ \sum_{k=1}^{2} \alpha_k p_k(\rho_k) u_k \right\} = -\Big(u_1 - u_2, p_1 - p_2\Big) \mathcal{D} \begin{pmatrix} u_1 - u_2 \\ p_1 - p_2 \end{pmatrix} |\partial_x \alpha_1| \leq 0, \tag{0.8.5}$$

avec $E_k = \frac{u_k^2}{2} + e_k$.

Le premier pas est approché à l'aide d'un système de relaxation. L'analyse du problème de Riemann de relaxation montre que les corrections (0.8.3) peuvent être nécessaires quand les rapports $\frac{\alpha_{k,L}}{\alpha_{k,R}}$ (ou leurs inverses) tendent vers $+\infty$. En effet, pour certaines relations de fermeture, les vitesses

et pressions relatives de la solution du problème de Riemann peuvent devenir non bornées dans ces régimes de phases évanescentes. Afin d'assurer que ces quantités restent bornées dans ces régimes, nous obtenons des conditions de dissipation très simples portant sur la matrice $\mathcal{D}$ et le coefficient μ de (0.8.2). On vérifie alors que les fermetures usuelles (0.2.3) correspondant à un champ linéairement dégénéré pour l'onde de taux de présence vérifient automatiquement cette condition dans les régimes de phases évanescentes, et ce **sans avoir à dissiper de l'énergie**. Autrement dit, en prenant la matrice $\mathcal{D}$ **nulle**, il est possible d'assurer une discrétisation stable du premier pas dès lors qu'on a choisi une des fermetures classiques (0.2.3). Cet argument mathématique semble accréditer ce choix de fermeture, par ailleurs largement préconisé par des spécialistes des écoulements diphasiques, selon qui l'onde de taux de présence devrait être linéairement dégénérée. Soulignons qu'avec ou sans la correction, les formules donnant la solution du problème de Riemann sont explicites, ce qui rend facile la mise en oeuvre du schéma.

Le schéma global qui résulte de cette décomposition en opérateurs est très simple, et il admet une formulation volumes finis à sept points. On montre que sous une condition CFL naturelle, il vérifie les propriétés classiques de consistance et de positivité des grandeurs concernées. De plus, la définition des trois pas est menée de telle sorte que globalement, **les masses partielles ainsi que la quantité de mouvement totale sont discrétisées de manière conservative**, ceci grâce à une définition judicieuse des vitesses $u_k - V_I$ dans le second pas. De même, dans la version du schéma étendu au modèle avec énergie, l'énergie totale est aussi discrétisée de manière conservative.

Les performances du schéma en fonctionnement «normal» (*i.e.* sans phase évanescente) sont testées sur un problème de Riemann dans le cas barotrope. De même qu'au chapitre 3, on trace les courbes (erreur L^1) $= f$(temps CPU) de manière à comparer les coûts CPU à précision donnée avec le schéma de Rusanov. Non seulement le schéma à pas fractionnaires obtenu apparaît alors bien plus performant que le schéma de Rusanov, mais il est aussi plus performant que le schéma de relaxation introduit au chapitre 3. Cela est probablement dû à l'absence de procédure itérative de calcul de racine à chaque interface, dans le cas de la décomposition en opérateurs.

Enfin, la dernière partie de ce chapitre considère l'extension du schéma, grâce à la dualité énergie/entropie, au modèle complet avec énergie dans le cas $(V_I, P_I) = (u_2, p_1)$. Par manque de temps, cette partie n'est pas rédigée, mais nous proposons néanmoins des résultats numériques qui illustrent la méthode.

0.9 Publications

Les travaux présentés dans ce manuscrit ont fait l'objet de publications.

1. Les travaux du chapitre 1 ont fait l'objet d'un article soumis à la revue Mathematics of Computations, et actuellement en révision: F. Coquel, K. Saleh, N. Seguin. *Relaxation and numerical approximation for fluid flows in a nozzle.*

   Par ailleurs, ils ont été présentés au congrès FVCA 6 et sont référencés dans les actes du congrès: F. Coquel, K. Saleh, N. Seguin. *A relaxation approach for simulating fluid flows in a nozzle.* Finite volumes for complex applications VI, **Vol 1**, pp 273-281, 2011.

2. Un article reprenant les travaux du chapitre 2 est en cours de finalisation: F. Coquel, J-M. Hérard, K. Saleh, N. Seguin. *Relaxation and numerical approximation for the isentropic model of Baer-Nunziato with vanishing phases.*

3. Les travaux du chapitre 3 ont été soumis à la revue Mathematical Modelling and Numerical Analysis: K. Saleh. *An entropy-satisfying and efficient relaxation scheme for the isentropic Baer-Nunziato model.*

   Par ailleurs, une partie des travaux associés à ces deux chapitres doit faire l'objet de proceendings du congrès HYP 2012.

4. Les travaux du chapitre 4 font l'objet d'un article en cours de finalisation.

5. Un article présentant un schéma à pas fractionnaires similaire à celui du chapitre 4 (mais ne traitant pas les cas de phases évanescentes) a été accepté pour publication dans la revue ESAIM Proceedings. Il est présenté en annexe. F. Coquel, J-M. Hérard, K. Saleh. *A splitting method for the isentropic Baer-Nunziato two-phase flow model.* ESAIM Proceedings.

6. Enfin, nous joignons en annexe un travail complémentaire présenté dans les actes du congrès AIAA [18] sur un modèle bifluide à huit équations, visant à généraliser le modèle de Baer-Nunziato en considérant une fermeture dynamique pour le couple (V_I, P_I): Frédéric Coquel, J-M. Hérard, K. Saleh, N. Seguin. *A class of two-fluid two-phase flow models.* AIAA paper 2012-3356, https://www.aiaa.org/.

Bibliographie

[1] R. Abeyaratne and J.K. Knowles. Kinetic relations and the propagation of phase boundaries in solids. *Archive for Rational Mechanics and Analysis*, 114:119–154, 1991.

[2] R. Abgrall and R. Saurel. Discrete equations for physical and numerical compressible multiphase mixtures. *Journal of Computational Physics*, 186(2):361–396, 2003.

[3] A. Ambroso, C. Chalons, F. Coquel, and T. Galié. Relaxation and numerical approximation of a two-fluid two-pressure diphasic model. *M2AN Math. Model. Numer. Anal.*, 43(6):1063–1097, 2009.

[4] A. Ambroso, C. Chalons, F. Coquel, E. Godlewski, F. Lagoutière, P-A. Raviart, and N. Seguin. The coupling of homogeneous models for two-phase flows. *Int. J. Finite Vol.*, 4(1):39, 2007.

[5] A. Ambroso, C. Chalons, F. Coquel, E. Godlewski, F. Lagoutière, P.-A. Raviart, and N. Seguin. Coupling of general Lagrangian systems. *Math. Comp.*, 77(262):909–941, 2008.

[6] A. Ambroso, C. Chalons, and P.-A. Raviart. A Godunov-type method for the seven-equation model of compressible two-phase flow. *Computers and Fluids*, 54(0):67 – 91, 2012.

[7] M.R. Baer and J.W. Nunziato. A two-phase mixture theory for the deflagration-to-detonation transition (DDT) in reactive granular materials. *International Journal of Multiphase Flow*, 12(6):861 – 889, 1986.

[8] F. Bouchut. On zero pressure gas dynamics. In *Advances in kinetic theory and computing*, volume 22 of *Ser. Adv. Math. Appl. Sci.*, pages 171–190. World Sci. Publishing, River Edge, NJ, 1994.

[9] F. Bouchut. *Nonlinear stability of finite volume methods for hyperbolic conservation laws and well-balanced schemes for sources*. Frontiers in Mathematics. Birkhäuser Verlag, Basel, 2004.

[10] F. Bouchut, Y. Brenier, J. Cortes, and J.-F. Ripoll. A hierarchy of models for two-phase flows. *J. Nonlinear Sci.*, 10(6):639–660, 2000.

[11] B. Boutin, F. Coquel, and P.G. LeFloch. Coupling techniques for nonlinear hyperbolic equations. i self-similar diffusion for thin interfaces. *Proceedings of the Royal Society of Edinburgh, Section: A Mathematics*, 141(05):921–956, 2011.

[12] B. Boutin, F. Coquel, and P.G. LeFloch. Coupling nonlinear hyperbolic equations (iii). a regularization method based on thick interfaces. *Submitted*, 2012.

[13] D. Bresch, B. Desjardins, J.-M. Ghidaglia, and E. Grenier. Global weak solutions to a generic two-fluid model. *Arch. Ration. Mech. Anal.*, 196(2):599–629, 2010.

[14] C. Chalons, F. Coquel, S. Kokh, and N. Spillane. Large time-step numerical scheme for the seven-equation model of compressible two-phase flows. *Springer Proceedings in Mathematics, FVCA 6, 2011*, 4:225–233, 2011.

[15] G-Q. Chen, C. D. Levermore, and T-P. Liu. Hyperbolic conservation laws with stiff relaxation terms and entropy. *Communications on Pure and Applied Mathematics*, 47(6):787–830, 1994.

[16] F. Coquel, T. Gallouët, J-M. Hérard, and N. Seguin. Closure laws for a two-fluid two pressure model. *C. R. Acad. Sci.*, I-334(5):927–932, 2002.

[17] F. Coquel, E. Godlewski, B. Perthame, A. In, and P. Rascle. Some new Godunov and relaxation methods for two-phase flow problems. In *Godunov methods (Oxford, 1999)*, pages 179–188. Kluwer/Plenum, New York, 2001.

[18] F. Coquel, J-M. Hérard, K. Saleh, and N. Seguin. A class of two-fluid two-phase flow models. *AIAA paper 2012-3356. https://www.aiaa.org/.*

[19] G. Dal Maso, P.G. LeFloch, and F. Murat. Definition and weak stability of nonconservative products. *J. de Math. Pures et Appl.*, 74(6):483–548, 1995.

[20] V. Deledicque and M. V. Papalexandris. A conservative approximation to compressible two-phase flow models in the stiff mechanical relaxation limit. *J. Comput. Phys.*, 227(21):9241–9270, 2008.

[21] D.A. Drew and S. L. Passman. *Theory of multicomponent fluids*, volume 135 of *Applied Mathematical Sciences*. Springer-Verlag, New York, 1999.

[22] T. Gallouët, P. Helluy, J-M. Hérard, and J. Nussbaum. Hyperbolic relaxation models for granular flows. *M2AN Math. Model. Numer. Anal.*, 44(2):371–400, 2010.

[23] T. Gallouët, J-M. Hérard, and N. Seguin. Numerical modeling of two-phase flows using the two-fluid two-pressure approach. *Math. Models Methods Appl. Sci.*, 14(5):663–700, 2004.

[24] S. Gavrilyuk and R. Saurel. Mathematical and numerical modeling of two-phase compressible flows with micro-inertia. *Journal of Computational Physics*, 175(1):326 – 360, 2002.

[25] P. Goatin and P. G. LeFloch. The Riemann problem for a class of resonant hyperbolic systems of balance laws. *Ann. Inst. H. Poincaré Anal. Non Linéaire*, 21(6):881–902, 2004.

[26] A. Guelfi, D. Bestion, M. Boucker, P. Boudier, P. Fillion, M. Grandotto, J-M. Hérard, E. Hervieu, and P. Péturaud. Neptune: a new software platform for advanced nuclear thermal hydraulics. *Nuclear Science and Engineering*, 76(4):281–324.

[27] A. Harten, P. D. Lax, and B. van Leer. On upstream differencing and Godunov-type schemes for hyperbolic conservation laws. *SIAM Rev.*, 25(1):35–61, 1983.

[28] E. Isaacson and B. Temple. Convergence of the 2×2 Godunov method for a general resonant nonlinear balance law. *SIAM J. Appl. Math.*, 55(3):625–640, 1995.

[29] M. Ishii and T. Hibiki. *Thermo-fluid dynamics of two-phase flow*. Springer, New York, 2006. With a foreword by Lefteri H. Tsoukalas.

[30] A. K. Kapila, S. F. Son, J. B. Bdzil, R. Menikoff, and D. S. Stewart. Two-phase modeling of DDT: Structure of the velocity-relaxation zone. *Physics of Fluids*, 9(12):3885–3897, 1997.

[31] A.K. Kapila, R. Menikoff, and D.S. Stewart. Two-phase modeling of deflagration-to-detonation transition in granular materials: Reduced equations. *Physics of Fluids*, 13(6):3002–3024, 2001.

[32] S. Karni and G. Hernàndez-Dueñas. A hybrid algorithm for the Baer-Nunziato model using the Riemann invariants. *Journal of Scientific Computing*, 45:382–403, 2010.

[33] S. Kawashima and W.-A. Yong. Dissipative structure and entropy for hyperbolic systems of balance laws. *Archive for Rational Mechanics and Analysis*, 174:345–364, 2004.

[34] P.G. LeFloch. Shock waves for nonlinear hyperbolic systems in nonconservative form. *IMA, Minneapolis*, Preprint 593, 1991.

[35] M. Papin and R. Abgrall. Fermetures entropiques pour les systèmes bifluides à sept équations. *Compt. Rendu. Acad. Sci. Mécanique*, 333:838–842, 2005.

[36] V.H Ransom and D.L Hicks. Hyperbolic two-pressure models for two-phase flow. *Journal of Computational Physics*, 53(1):124 – 151, 1984.

[37] L. Sainsaulieu. Contribution à la modélisation mathématique et numérique des écoulements diphasiques constitués d'un nuage de particules dans un écoulement de gaz. *Thèse d'habilitation à diriger des recherches. Université Paris VI*, 1995.

[38] R. Saurel and R. Abgrall. A multiphase godunov method for compressible multifluid and multiphase flows. *Journal of Computational Physics*, 150(2):425 – 467, 1999.

[39] R. Saurel, S. Gavrilyuk, and F. Renaud. A multiphase model with internal degrees of freedom: application to shock–bubble interaction. *Journal of Fluid Mechanics*, 495:283–321, 2003.

[40] D.W. Schwendeman, C.W. Wahle, and A.K. Kapila. The Riemann problem and a high-resolution Godunov method for a model of compressible two-phase flow. *Journal of Computational Physics*, 212(2):490 – 526, 2006.

[41] H B. Stewart and B. Wendroff. Two-phase flow: Models and methods. *Journal of Computational Physics*, 56(3):363 – 409, 1984.

[42] M. D. Thanh, D. Kröner, and N. T. Nam. Numerical approximation for a Baer–Nunziato model of two-phase flows. *Applied Numerical Mathematics*, 61(5):702 – 721, 2011.

[43] S.A. Tokareva and E.F. Toro. HLLC-type Riemann solver for the Baer-Nunziato equations of compressible two-phase flow. *Journal of Computational Physics*, 229(10):3573 – 3604, 2010.

[44] W-A. Yong. Entropy and global existence for hyperbolic balance laws. *Archive for Rational Mechanics and Analysis*, 172:247–266, 2004.

Chapter 1

Approximation par relaxation pour les équations d'Euler en tuyère

RELAXATION AND NUMERICAL APPROXIMATION FOR FLUID FLOWS IN A NOZZLE[1]

Frédéric Coquel, Khaled Saleh, Nicolas Seguin

Abstract

We propose in this work an original numerical scheme for the system of gas dynamics in a nozzle. The method is based on a piecewise constant discretisation of the cross-section and on a linearized Riemann solver. Such a solver is obtained by the use of a relaxation approximation and therefore, this leads to a positive and entropy satisfying numerical scheme. The solution of the relaxation Riemann problem and the stability properties of the numerical scheme are deeply investigated, in particular in the case of resonance. Some numerical illustrations are provided at the end.

1.1 Introduction

The design of stable and accurate numerical schemes for hyperbolic systems is still a difficult problem and the challenge becomes much more difficult in presence of stiff source terms. Such an issue may occur in the frame of flows which are influenced by external effects, due for instance to the surrounding domain, another fluid, external forces... We are interested here in the numerical approximation of the solutions of a model describing one-dimensional barotropic flows in a nozzle. In this model, ρ and w are respectively the density and the velocity of the fluid while α stands for the cross-section of the nozzle, which is assumed to be constant in time. Under the classical assumption that α (and its variations) is small with respect to a characteristic length in the mainstream direction, the flow can be supposed to be one-dimensional and described by the following set of partial differential equations:

$$\left\{ \begin{array}{l} \partial_t(\alpha\rho) + \partial_x(\alpha\rho w) = 0, \\ \partial_t(\alpha\rho w) + \partial_x(\alpha\rho w^2 + \alpha p(\tau)) - p(\tau)\partial_x\alpha = 0, \end{array} \right. \tag{1.1.1}$$

where $\tau = \rho^{-1}$ is the specific volume and $\tau \mapsto p(\tau)$ is a barotropic pressure law. The first equation is the classical conservation of mass and the second equation governs the dynamics of the horizontal mean momentum.

[1] Les travaux de ce chapitre font l'objet d'un article soumis à la revue *Mathematics of Computations*, et actuellement en révision.

We propose a new numerical scheme for gas dynamics in a nozzle. Even if many numerical methods have already been proposed for System (1.1.1), very few of them possess all the features which could guarantee accurate results even for very complex flows. Among these features, we emphasize properties of numerical stability: preservation of the positivity of the density ρ and decrease of the total energy. The numerical scheme we develop here possesses all these properties (see later for precise statements). The two main ingredients which enable us to obtain them are: a piecewise constant discretisation of the cross-section α and the construction of a simple Riemann problem to compute the numerical fluxes. The idea of taking a constant-by-cell cross-section goes back to the works of LeRoux and co-workers [14, 13] and also to the paper of Isaacson and Temple [16]. The consequence of such a discretisation is to concentrate the source term at the interfaces of the mesh and to ease the construction of well-balanced schemes. In all these pioneer works, the numerical fluxes are obtained by solving each interfacial Riemann problem exactly, which is not an easy task because of the presence of a singular source term. Several attempts to simplify this Riemann solver have been proposed (see for instance [10]), but the overall resulting numerical scheme may lack for stability properties for severe test cases. Here, we construct a simple Riemann solver, in the spirit of [15]. It is only composed by constant states separated by discontinuities, which makes its practical implementation easy. In order to ensure the positivity of the density and the decrease of the total energy, we interprete this simple solver as the exact solver of a relaxation approximation of System (1.1.1), following [7, 6].

The cornerstone of this scheme is the resolution of the Riemann problem associated with the homogeneous relaxation model for arbitrary data. Even if the relaxation approximation provides a linearly degenerate system, the *resonance phenomenon* persists since the source term is singular (the cross-section is discontinuous at the interface). In few words, resonance in hyperbolic systems consists in the superimposition of an acoustic wave on the discontinuity of the cross-section, also called the *standing wave*, leading the associated eigenvectors to be colinear (as a consequence, the system is no longer hyperbolic). In the frame of the original model of gas dynamics in a nozzle, the resonance causes nonuniqueness of the solution of the Riemann problem, as proved in [16] and [11] (see also [18]). Here, the troubles are different. Global existence still remains true but, for particular initial data, measure solutions have to be considered. They naturally appear when resonance occurs, as parts of the solution in some limit regimes for given patterns of solutions. Measure solutions have been studied in the context of conservation laws by DiPerna [9] and Bouchut and James [4] (see also the references therein). Even if such solutions appear here, we are able to circumvent these solutions by slightly increasing the relaxation coefficient a which governs the acoustic part of the relaxation model. As a result, the solutions we consider for the final numerical scheme belong the the classical setting of piecewise constant solutions seperated by linearly degenerate waves. Therefore, despite this difficulty, we can obtain a positive and entropy satisfying relaxation numerical scheme.

The outline of this paper is the following. The next section is devoted to the presentation of the main features of the model for gas dynamics in a nozzle. Section 1.3 is the core of this work: the relaxation approximation is presented and the associated Riemann solver is solved. With the help of this analysis, the numerical approximation is studied in Section 1.4. Basic and more tricky properties are described with a special care to non linear stability and the computation of the CFL condition. Some numerical tests are also presented to attest the good behavior of our numerical scheme. Two appendices about some technical developments complete this work.

1.2 The Euler equations in a nozzle with variable cross-section

1.2.1 Presentation and main properties

The model describing one-dimensional barotropic flows in a nozzle can be described by the following set of partial differential equations:

$$\begin{cases} \partial_t \alpha = 0, \\ \partial_t(\alpha\rho) + \partial_x(\alpha\rho w) = 0, \\ \partial_t(\alpha\rho w) + \partial_x(\alpha\rho w^2 + \alpha p(\tau)) - p(\tau)\partial_x \alpha = 0, \end{cases} \tag{1.2.1}$$

where $\tau = \rho^{-1}$ is the specific volume and $\tau \mapsto p(\tau)$ is a barotropic pressure law. The first equation expresses the constancy of the section α, while the second and the third equations are respectively the mass and the momentum conservation equations. All along this paper, we assume that the pressure p is a smooth function of τ satisfying the following classical properties. For all $\tau > 0$, $p(\tau) > 0$, $p'(\tau) < 0$, and $\lim_{\tau \to 0} p(\tau) = +\infty$ and $\lim_{\tau \to +\infty} p(\tau) = 0$. An example of such a pressure law is an ideal gas barotropic pressure law $p(\tau) = S\tau^{-\gamma}$ with $S > 0$ and $\gamma > 0$. System (1.2.1) takes the following condensed form:

$$\partial_t \mathbb{U} + \partial_x \mathbf{f}(\mathbb{U}) + \mathbf{c}(\mathbb{U})\partial_x \mathbb{U} = 0, \tag{1.2.2}$$

where $\mathbb{U} = (\alpha, \alpha\rho, \alpha\rho w)^T$ is the vector of unknowns and the functions $\mathbf{f}$ and $\mathbf{c}$ are given by

$$\mathbf{f}(\mathbb{U}) = \begin{bmatrix} 0 \\ \alpha\rho w \\ \alpha\rho w^2 + \alpha p(\tau) \end{bmatrix}, \quad \mathbf{c}(\mathbb{U})\partial_x \mathbb{U} = \begin{bmatrix} 0 \\ 0 \\ -p(\tau)\partial_x \alpha \end{bmatrix}. \tag{1.2.3}$$

In practice, the constant section α is determined once and for all by the initial condition, and thus it is not properly speaking an unknown function. However, the section α appears in the mass and momentum equations, especially in the pressure terms. Therefore, in the numerical simulations, where the solutions of system (1.2.1) are approximated by a Finite Volume method, it is more appropriate to consider α as an unknown function, since it allows us to use the convenient machinery of hyperbolic systems theory. In particular, we will be able to construct self-similar solutions to system (1.2.1) (*i.e.* solution depending only on x/t). The following proposition holds, that characterizes the fields of this system.

Proposition 1.2.1. *For any $\mathbb{U}$ in the phase space Ω defined by*

$$\Omega = \left\{ \mathbb{U} = (\alpha, \alpha\rho, \alpha\rho w)^T \in \mathbb{R}^3, \alpha > 0, \alpha\rho > 0 \right\}, \tag{1.2.4}$$

system (1.2.1) admits the three following eigenvalues

$$\sigma_0(\mathbb{U}) = 0,$$
$$\sigma_1(\mathbb{U}) = w - c(\tau), \qquad \sigma_2(\mathbb{U}) = w + c(\tau), \tag{1.2.5}$$

where $c(\tau) = \tau\sqrt{-p'(\tau)}$ is the speed of sound. The system is hyperbolic on Ω (i.e. the corresponding right eigenvectors span $\mathbb{R}^3$) if, and only if $(w - c(\tau))(w + c(\tau)) \neq 0$. Moreover, the characteristic field associated with σ_0 is linearly degenerate, while the characteristic fields associated with σ_1 and σ_2 are genuinely nonlinear.

Proof. The proof is classical and it results from direct calculations that are left to the reader. □

The phase space Ω introduced in (1.2.4) is the physically relevant domain where the solutions of (1.2.1) have to lie. Indeed, the section α has to be positive (which is trivially imposed by the initial condition) as well as the fluid density ρ. In the sequel Ω will be referred to as the phase space of *positive solutions*. As regards the smooth solutions of system (1.2.1), we have the following property:

Proposition 1.2.2. *The smooth solutions of (1.2.1) obey the following additional conservation law*

$$\partial_t \left(\alpha\rho E\right) + \partial_x \left(\alpha\rho E w + \alpha p(\tau) w\right) = 0, \tag{1.2.6}$$

where $E = \dfrac{w^2}{2} + e(\tau)$ *is the total energy and where the function* $\tau \mapsto e(\tau)$ *is given by* $e'(\tau) = -p(\tau)$.

Proof. This follows from classical manipulations of system (1.2.1). □

When one considers non-smooth weak solutions of system (1.2.1), it is well known that there is no uniqueness of such solutions and one has to add a so-called entropy selection criterion in order to select the relevant physical solutions of (1.2.1).

Definition 1.2.1. *A solution of system (1.2.1) is said to be an* ***entropy*** *solution if it satisfies the following inequality in the weak sense*

$$\partial_t \left(\alpha\rho E\right) + \partial_x \left(\alpha\rho E w + \alpha p(\tau) w\right) \leq 0. \tag{1.2.7}$$

As the function $(\alpha, \alpha\rho, \alpha\rho w) \mapsto \alpha\rho E$ is convex, this selection criterion can be formally justified by the *vanishing viscosity method* (see for example [12]). When the solution contains strong shocks, inequality (1.2.7) is strict, and this accounts for the loss of energy due to viscosity.

1.2.2 Standing wave and resonance

For the sake of numerical applications, one has to consider the case of discontinuous cross-sections α, the simpler example of which is given by a Riemann-type initial condition $\alpha(x) = \alpha_L$ if $x < 0$ and $\alpha(x) = \alpha_R$ if $x > 0$. Since α is constant throughout time, this gives rise to a standing discontinuity across which one has to define jump relations. The main difficulty lies in the treatment of the non-conservative product $p(\tau)\partial_x\alpha$ since this product cannot be represented in the sense of distributions. Nevertheless, in the region of hyperbolicity of system (1.2.1), *i.e.* when $w \neq \pm c(\tau)$, this non-conservative product is supported by the standing wave associated with the linearly degenerate field $\sigma_0 = 0$, and the natural definition of $p(\tau)\partial_x\alpha$ is drawn from the conservation of the Riemann invariants associated with σ_0. These two Riemann invariants are obtained by applying the Rankine-Hugoniot jump conditions to the mass conservation equation and to the energy conservation equation (1.2.6):

$$\left[\alpha\rho w\right]^0 = \left[\alpha\rho E w + \alpha p(\tau) w\right]^0 = 0, \tag{1.2.8}$$

where $[X]^0$ denotes the jump of any quantity X across the standing wave.

When the *resonance* phenomenon appears, *i.e.* when there exists in the solution a state $(\alpha, \alpha\rho, \alpha\rho w)$ such that $w = \pm c(\tau)$, the hyperbolicity of the system is lost, and the standing wave superimposes with a non linear field associated with one of the extreme eigenvalues σ_1 or σ_2. In this very particular case, defining the non-conservative product is difficult and the uniqueness of solutions is lost in general (even with the entropy criterion given by Definition 1.2.1), see [11, 16]. Besides, if the standing wave superimposes with a stationary shock, the energy is no longer preserved across the wave and we rather have

$$[\alpha\rho E w + \alpha p(\tau) w]^0 < 0 \tag{1.2.9}$$

since the energy strictly decreases through the shock.

1.2.3 Numerical approximation and Riemann solvers

One of the most classical approaches for the numerical approximation of the solutions of (1.2.1) is the so-called *well-balanced approach* (see [14, 13, 5]) which relies on the construction of the exact solution of system (1.2.1) for the particular case where the initial condition is given by a constant state $\mathbb{U}_L$ for $x < 0$ and a constant state $\mathbb{U}_R$ for $x > 0$ (one speaks of a Riemann problem):

$$\mathbb{U}_0(x) = \begin{cases} \mathbb{U}_L & \text{if} \quad x < 0, \\ \mathbb{U}_R & \text{if} \quad x > 0. \end{cases} \tag{1.2.10}$$

Unfortunately, the exact solution of this Riemann problem is quite uneasy to obtain (see [18, 2]) due to the non linearities of the pressure law and to the difficulties linked with the resonance phenomenon (definition of the non-conservative product, non-uniqueness...). Therefore, an other approach is preferred, where solving the Riemann problem for system (1.2.1) is replaced by solving an easier Riemann problem for an enlarged system obtained by a relaxation approximation method.

1.3 Relaxation approximation

1.3.1 The relaxation system and its main properties

In this section, we propose a suitable relaxation approximation of the entropy weak solutions of system (1.2.1). For this purpose, we first recall that the genuine nonlinearity of the two extreme fields (also referred to as the $\{\sigma_1, \sigma_2\}$-fields in the sequel) is closely related to the nonlinearities of the pressure law $\tau \mapsto p(\tau)$. In the spirit of [17], we consider an enlarged system involving an additional unknown $\mathcal{T}$ associated with a linearization π of the pressure law. This linearization is designed to get a quasilinear enlarged system, shifting the initial nonlinearity from the convective part to a stiff relaxation source term. The relaxation approximation is based on the idea that the solutions of the original system are formally recovered as the limit of the solutions of the proposed enlarged system, in the regime of a vanishing relaxation coefficient $\varepsilon > 0$. As a relaxation approximation of (1.2.1), we propose the following system:

$$\begin{cases} \partial_t \alpha^\varepsilon = 0, \\ \partial_t (\alpha\rho)^\varepsilon + \partial_x (\alpha\rho w)^\varepsilon = 0, \\ \partial_t (\alpha\rho w)^\varepsilon + \partial_x (\alpha\rho w^2 + \alpha\pi(\tau, \mathcal{T}))^\varepsilon - \pi(\tau, \mathcal{T})^\varepsilon \partial_x \alpha^\varepsilon = 0, \\ \partial_t (\alpha\rho\mathcal{T})^\varepsilon + \partial_x (\alpha\rho\mathcal{T} w)^\varepsilon = \dfrac{1}{\varepsilon} (\alpha\rho)^\varepsilon (\tau - \mathcal{T})^\varepsilon, \end{cases} \tag{1.3.1}$$

where the linearization of the pressure law is given by

$$\pi(\tau, \mathcal{T}) = p(\mathcal{T}) + a^2 (\mathcal{T} - \tau). \tag{1.3.2}$$

System (1.3.1) takes the following condensed form:

$$\partial_t \mathbb{W}^\varepsilon + \partial_x \mathbf{g}(\mathbb{W}^\varepsilon) + \mathbf{d}(\mathbb{W}^\varepsilon) \partial_x \mathbb{W}^\varepsilon = \frac{1}{\varepsilon} \mathcal{R}(\mathbb{W}^\varepsilon), \tag{1.3.3}$$

where $\mathbb{W} = (\alpha, \alpha\rho, \alpha\rho w, \alpha\rho\mathcal{T})^T$ is the vector of unknowns and the functions $\mathbf{g}$, $\mathbf{d}$ and $\mathcal{R}$ are given by

$$\mathbf{g}(\mathbb{W}) = \begin{bmatrix} 0 \\ \alpha\rho w \\ \alpha\rho w^2 + \alpha\pi \\ \alpha\rho\mathcal{T} w \end{bmatrix}, \ \mathbf{d}(\mathbb{W}) \partial_x \mathbb{W} = \begin{bmatrix} 0 \\ 0 \\ -\pi \partial_x \alpha \\ 0 \end{bmatrix}, \ \mathcal{R}(\mathbb{W}) = \begin{bmatrix} 0 \\ 0 \\ 0 \\ \alpha\rho(\tau - \mathcal{T}) \end{bmatrix}. \tag{1.3.4}$$

To ease the notation hereafter, we will omit the superscript $^\varepsilon$. From this point, we will refer to the original system (1.2.1) as the *equilibrium system*, while system (1.3.1) will be referred to as the *relaxation system*. We can see that in the formal limit $\varepsilon \to 0$, the additionned variable $\mathcal{T}$ tends towards the specific volume τ, and the linearized pressure π tends towards the original nonlinear pressure p (seen as a function of τ), thus recovering the equilibrium system (1.2.1) in the first three equations of (1.3.1). The constant a in (1.3.2) is a constant positive parameter that must be taken large enough to prevent system (1.3.1) from instabilities in the regime of small values of ε. This will be clarified in section 1.4.4.

It is relevant to focus on the convective part of system (1.3.1) since a fractional step method is commonly used in the implementation of relaxation methods: the first step is a time-advancing step using the solution of the Riemann problem for the convective part of (1.3.1):

$$\begin{cases} \partial_t \alpha = 0, \\ \partial_t (\alpha\rho) + \partial_x (\alpha\rho w) = 0, \\ \partial_t (\alpha\rho w) + \partial_x (\alpha\rho w^2 + \alpha\pi(\tau, \mathcal{T})) - \pi(\tau, \mathcal{T}) \partial_x \alpha = 0, \\ \partial_t (\alpha\rho\mathcal{T}) + \partial_x (\alpha\rho\mathcal{T} w) = 0, \end{cases} \tag{1.3.5}$$

while the second step consists in an instantaneous relaxation towards the equilibrium system by imposing $\mathcal{T} = \tau$ in the solution obtained by the first step. This second step is equivalent to sending ε to 0 instantaneously (see section 1.4 for details).

We now state the main property that motivates the introduction of the proposed relaxation system:

Proposition 1.3.1. *For any $\mathbb{W}$ in the phase space Ω^r defined by*

$$\Omega^r = \left\{ \mathbb{W} = (\alpha, \alpha\rho, \alpha\rho w, \alpha\rho\mathcal{T})^T \in \mathbb{R}^4, \alpha > 0, \alpha\rho > 0, \alpha\rho\mathcal{T} > 0 \right\}, \tag{1.3.6}$$

system (1.3.5) admits the four following eigenvalues

$$\sigma_0^r(\mathbb{W}) = 0,$$

$$\sigma_1^r(\mathbb{W}) = w - a\tau, \qquad \sigma_2^r(\mathbb{W}) = w, \qquad \sigma_3^r(\mathbb{W}) = w + a\tau, \tag{1.3.7}$$

and is hyperbolic on Ω^r (i.e. the corresponding right eigenvectors span $\mathbb{R}^4$) if, and only if $(w - a\tau)(w + a\tau) \neq 0$. Moreover, all the characteristic fields associated with $\{\sigma_i^r\}_{i=0..3}$ are linearly degenerate.

Proof. The proof results from direct calculations that are left to the reader. □

Note that the crucial property here is the linear degeneracy of the two extreme fields. This enables us to easily define jump relations across these originally nonlinear fields. More precisely, the first equation of (1.3.5) shows that for any solution of the Riemann problem, the jump of α only occurs through the σ_0 standing wave, therefore α is a Riemann invariant for both acoustic fields. Similarly, equation four in (1.3.5) shows that $\mathcal{T}$ is also a Riemann invariant for the acoustic fields and the last Riemann invariant is determined by remarking that for any linearly degenerated wave, the eigenvalue is also constant through this field (any other invariant of the field can be expressed as a continuous function of these three Riemann invariants). Thus it is much easier to connect two intermediate states by an acoustic field since the whole discussion of the definition and calculation of rarefaction and shock waves is avoided.

Remark 1.3.1. *System (1.3.5) could be studied for itself without relaxation consideration, i.e. without considering that it is precisely designed to approximate the natural physical system (1.2.1). In that case, there is no reason to impose the positivity of the density in the solutions and the phase space for (1.3.5) turns to be larger than Ω^r defined in (1.3.6). For our relaxation approximation purposes though, we ask the solutions of 1.3.5 to stay within the phase space Ω^r. The positivity of the additioned variable $\mathcal{T}$ is necessary in order for the relaxed pressure $\pi(\tau, \mathcal{T})$ to be well-defined. Subsequently, any vector $\mathbb{W}$ is said to be positive if it satisfies $\mathbb{W} \in \Omega^r$, and any solution $(x,t) \mapsto \mathbb{W}(x,t)$ is said to be a positive solution if for all (x,t) in $\mathbb{R}_x \times \mathbb{R}_t^+$, $\mathbb{W}(x,t)$ belongs to Ω^r.*

1.3.2 Jump relations across the stationary contact discontinuity

We now focus on the definition of jump relations across the standing wave in the PDE model (1.3.5). Applying the Rankine-Hugoniot jump relation to the mass conservation equation as well as to the transport equation of $\mathcal{T}$ yields two Riemann invariants for the standing wave provided that system (1.3.5) is hyperbolic (see hereafter). But as the non conservative product $\pi(\tau, \mathcal{T})\partial_x \alpha$ is not well defined across the standing wave ($\pi(\tau, \mathcal{T})$ may not be continuous across this wave), we cannot apply the Rankine-Hugoniot relation to the momentum conservation equation. Instead, we seek an additional conservation law satisfied by the smooth solutions of (1.3.5) eventually leading to a full set of jump relations. We have the following statement:

Proposition 1.3.2. *The smooth solutions of (1.3.5) obey the following additional conservation law*

$$\partial_t \left(\alpha\rho\mathcal{E}\right) + \partial_x \left(\alpha\rho\mathcal{E}w + \alpha\pi(\tau, \mathcal{T})w\right) = 0, \tag{1.3.8}$$

where

$$\mathcal{E} = \frac{w^2}{2} + e(\mathcal{T}) + \frac{\pi^2(\tau,\mathcal{T}) - p^2(\mathcal{T})}{2a^2}, \tag{1.3.9}$$

is the total energy and where the function $\tau \mapsto e(\tau)$ *is given by* $e'(\tau) = -p(\tau)$.

Proof. This follows from classical manipulations. The details are left to the reader. □

For a hyperbolic conservative system, the conservation of energy (1.3.8) holds true in the weak sense for any solution presenting only contact discontinuities, and the Riemann invariant obtained by applying the Rankine-Hugoniot jump relation to equation (1.3.8) can be expressed as a continuous function of the other Riemann invariants. Nevertheless, system (1.3.5) *is not* conservative in the neighborhood of the standing wave and this is the reason why applying the Rankine-Hugoniot relation to (1.3.8) yields a *new* jump relation. Note that there are no theoretical results that impose relation (1.3.8) to be exactly maintained across the standing wave when the resonance occurs (*i.e.* when $w = \pm a\tau$), and we will see that, if equation (1.3.8) is exactly satisfied in the weak sense, we will not be able to impose the invariance of the domain Ω^r. Indeed, it will be proved that keeping domain Ω^r invariant requires the decrease of the energy in general. This is related to the fact that Ω^r is not the natural space for the solutions of system (1.3.5) (see Remark 1.3.1). These considerations motivate the construction of solutions to the Riemann problem where the energy decreases (in the weak sense) across the standing wave:

$$\partial_t\left(\alpha\rho\mathcal{E}\right) + \partial_x\left(\alpha\rho\mathcal{E}w + \alpha\pi(\tau,\mathcal{T})w\right) \leq 0, \quad \text{in} \quad \mathcal{D}', \tag{1.3.10}$$

as it may happen for the equilibrium system.

1.3.3 Solving the Riemann problem for the relaxation system

Definition of the solutions and existence theorem

Let be given $\mathbb{W}_L$ and $\mathbb{W}_R$, two positive states in Ω^r. We are now interested in solving the Riemann problem for system (1.3.5), *i.e.* we seek solutions satisfying the initial condition

$$\mathbb{W}_0(x) = \begin{cases} \mathbb{W}_L & \text{if} \quad x < 0, \\ \mathbb{W}_R & \text{if} \quad x > 0. \end{cases} \tag{1.3.11}$$

Before defining the solutions of the Riemann problem (1.3.5)-(1.3.11), let us first define the solutions of a slightly more general Cauchy problem where the initial data $\mathbb{W}_0$ is in $L^1_{\text{loc}}(\mathbb{R}_x)$, and where only the variable α is a Heavyside function:

$$\alpha_0(x) = \begin{cases} \alpha_L & \text{if} \quad x < 0, \\ \alpha_R & \text{if} \quad x > 0, \end{cases} \qquad \text{and} \qquad (\alpha_0, (\alpha\rho)_0, (\alpha\rho w)_0, (\alpha\rho\mathcal{T})_0) \quad \text{is in} \quad L^1_{\text{loc}}\left(\mathbb{R}_x, \Omega^r\right). \tag{1.3.12}$$

Thus, by the first equation of (1.3.5), the non conservative product $\pi(\tau,\mathcal{T})\partial_x\alpha$ is supported by the half line $\{x = 0, t \geq 0\}$. We also introduce the initial energy:

$$(\alpha\rho\mathcal{E})(\mathbb{W}_0) = (\alpha\rho)_0\left(\frac{w_0^2}{2} + e(\mathcal{T}_0) + \frac{\pi^2(\tau_0,\mathcal{T}_0) - p^2(\mathcal{T}_0)}{2a^2}\right), \tag{1.3.13}$$

which we assume to be in $L^1_{\rm loc}(\mathbb{R}_x)$ for the initial data $\mathbb{W}_0$ under consideration.

Definition 1.3.1. *A solution of the Cauchy problem (1.3.5)-(1.3.12) is a function* $\mathbb{W}:(x,t)\in\mathbb{R}_x\times\mathbb{R}_t^+\mapsto\mathbb{W}(x,t)\in\Omega^r$ *such that* $\mathbb{W}=(\alpha,\alpha\rho,\alpha\rho w,\alpha\rho\mathcal{T})$ *belongs to* $L^1_{\rm loc}\left(\mathbb{R}_x^{-,*}\times\mathbb{R}_t^+,\Omega^r\right)\cap L^1_{\rm loc}\left(\mathbb{R}_x^{+,*}\times\mathbb{R}_t^+,\Omega^r\right)$ *and* $(\alpha\rho w\mathcal{T},\alpha\rho\mathcal{E},\alpha\rho w\mathcal{E}+\alpha\pi w)$ *belongs to*

$$\left(L^1_{\rm loc}\left(\mathbb{R}_x^{-,*}\times\mathbb{R}_t^+,\mathbb{R}\right)\cap L^1_{\rm loc}\left(\mathbb{R}_x^{+,*}\times\mathbb{R}_t^+,\mathbb{R}\right)\right)^3.$$

Besides α *is such that*

$$\alpha(x,t)=\left\{\begin{array}{ll}\alpha_L & \text{if}\quad x<0,\\ \alpha_R & \text{if}\quad x>0,\end{array}\right.\qquad \text{for all}\quad t\geq 0, \tag{1.3.14}$$

and for all test functions (φ_1,φ_2) *in* $\left(\mathcal{D}(\mathbb{R}_x^*\times\mathbb{R}_t^+)\right)^2$

$$\int_{\mathbb{R}_x\times\mathbb{R}_t^+}(\alpha\rho w)\partial_t\varphi_1+\int_{\mathbb{R}_x\times\mathbb{R}_t^+}(\alpha\rho w^2+\alpha\pi)\partial_x\varphi_1+\int_{\mathbb{R}}(\alpha\rho w)_0(x)\varphi_1(x,0)dx=0, \tag{1.3.15}$$

$$\int_{\mathbb{R}_x\times\mathbb{R}_t^+}(\alpha\rho\mathcal{T})\partial_t\varphi_2+\int_{\mathbb{R}_x\times\mathbb{R}_t^+}(\alpha\rho w\mathcal{T})\partial_x\varphi_2+\int_{\mathbb{R}}(\alpha\rho\mathcal{T})_0(x)\varphi_2(x,0)dx=0, \tag{1.3.16}$$

while for all ψ *in* $\mathcal{D}(\mathbb{R}_x\times\mathbb{R}_t^+)$,

$$\int_{\mathbb{R}_x\times\mathbb{R}_t^+}(\alpha\rho)\partial_t\psi+\int_{\mathbb{R}_x\times\mathbb{R}_t^+}(\alpha\rho w)\partial_x\psi+\int_0^{+\infty}\left[\alpha\rho w\right]^0(t)\psi(0,t)dt+\int_{\mathbb{R}}(\alpha\rho)_0(x)\psi(x,0)dx=0, \tag{1.3.17}$$

where

$$\left[\alpha\rho w\right]^0(t)=\lim_{x\to 0^+}(\alpha\rho w)(x,t)-\lim_{x\to 0^-}(\alpha\rho w)(x,t),\qquad a.e.\quad t>0. \tag{1.3.18}$$

Remark 1.3.2. *The space* $\mathcal{D}(\mathbb{R}_x^*\times\mathbb{R}_t^+)$ *is the space of functions* φ *that can be written as a sum* $\varphi=\varphi^-+\varphi^+$ *where* φ^- *is a* $\mathcal{C}^\infty$ *function with compact support in* $\mathbb{R}_x^{-,*}\times\mathbb{R}_t^+$ *and* φ^+ *is a* $\mathcal{C}^\infty$ *function with compact support in* $\mathbb{R}_x^{+,*}\times\mathbb{R}_t^+$. *In particular all the derivatives of* φ *vanish at* $x=0$, $\partial_x^i\partial_t^j\varphi(0,t)=0$ *for all* i *and* j *in* $\mathbb{N}$ *and all* t *in* $\mathbb{R}$.

We draw the reader's attention on the fact that Definition 1.3.1 is not enough to wholly determine the solution with respect to the initial data. As a matter of fact, few specifications have been given so far for the treatment of the stationary discontinuity at $x=0$ (except equation (1.3.17)), and some choices have to be made in order to calculate a solution, especially for the Riemann problem for which the solution is self-similar. However, before giving a more complete definition of self-similar solutions for the Riemann problem, we first discuss Definition 1.3.1 which indeed deserves a few comments. Let us start with a property satisfied by the solutions of the Cauchy problem (1.3.5)-(1.3.12).

Proposition 1.3.3. *Assume that* $\mathbb{W}:(x,t)\in\mathbb{R}_x\times\mathbb{R}_t^+\mapsto\mathbb{W}(x,t)\in\Omega^r$ *is a solution of the Cauchy problem (1.3.5)-(1.3.12) in the sense of Definition 1.3.1. Then, for all test function* φ_3 *in* $\mathcal{D}(\mathbb{R}_x^*\times\mathbb{R}_t^+)$

$$\int_{\mathbb{R}_x\times\mathbb{R}_t^+}(\alpha\rho\mathcal{E})\partial_t\varphi_3+\int_{\mathbb{R}_x\times\mathbb{R}_t^+}\left(\alpha\rho w\mathcal{E}+\alpha\pi w\right)\partial_x\varphi_3+\int_{\mathbb{R}}(\alpha\rho\mathcal{E})_0(x)\varphi_3(x,0)dx=0. \tag{1.3.19}$$

Proof. Equations (1.3.15), (1.3.16) and (1.3.17) imply that outside a neighborhood of $x = 0$, any solution satisfies

$$\begin{cases} \partial_t(\alpha\rho) + \partial_x(\alpha\rho w) = 0, \\ \partial_t(\alpha\rho w) + \partial_x(\alpha\rho w^2 + \alpha\pi(\tau, \mathcal{T})) = 0, \\ \partial_t(\alpha\rho\mathcal{T}) + \partial_x(\alpha\rho\mathcal{T} w) = 0, \end{cases} \tag{1.3.20}$$

in the usual weak sense (take ψ in $\mathcal{D}(\mathbb{R}_x^* \times \mathbb{R}_t^+)$), *i.e.* $\mathbb{W}(x,t)$ is the solution of a conservative hyperbolic system whose fields are linearly degenerate. Hence, any additional conservation law satisfied by the smooth solutions is also satisfied in the weak sense. Thus, the result follows from Proposition 1.3.2. □

On the one hand, equations (1.3.15) to (1.3.17) imply that outside of a neighborhood of $x = 0$, any solution satisfies

$$\begin{cases} \partial_t(\alpha\rho) + \partial_x(\alpha\rho w) = 0, \\ \partial_t(\alpha\rho w) + \partial_x(\alpha\rho w^2 + \alpha\pi(\tau, \mathcal{T})) = 0, \\ \partial_t(\alpha\rho\mathcal{T}) + \partial_x(\alpha\rho\mathcal{T} w) = 0, \end{cases} \tag{1.3.21}$$

in the usual weak sense, and the energy is also exaclty preserved:

$$\partial_t\left(\alpha\rho\mathcal{E}\right) + \partial_x\left(\alpha\rho\mathcal{E}w + \alpha\pi(\tau, \mathcal{T})w\right) = 0. \tag{1.3.22}$$

On the other hand, equation (1.3.17) shows that the mass conservation equation is modified by a non classical term which can be seen as the consequence of a Dirac measure supported by the half-line $\{x = 0, t > 0\}$. Indeed, if $[\alpha\rho w]^0(t)$ is independent of t, we can write

$$\int_0^{+\infty} [\alpha\rho w]^0(t)\psi(0,t)dt = [\alpha\rho w]^0 \langle \delta_0, \psi \rangle_{\mathcal{D}',\mathcal{D}}. \tag{1.3.23}$$

Remark 1.3.3 (**Important remark**). *In the literature concerning hyperbolic systems of conservation laws, several approaches have been implemented to consider measure-valued solutions. One of the most common approaches is the measure-valued solutions introduced by Diperna [9] where the solution consists in a measurable family of probability measures. Another approach is introduced in [3] by Bouchut, where the solutions of a system describing pressureless gas flows are expressed in terms of so-called δ-shocks. Here again, the solution is defined in the sense of measures. In our particular case, we decided not to consider measure-valued solutions in the usual sense. Indeed the solutions given by Definition 1.3.1 are* ***functions*** *belonging to $L^1_{\text{loc}}\left(\mathbb{R}_x^{-,*} \times \mathbb{R}_t^+, \Omega^r\right) \cap L^1_{\text{loc}}\left(\mathbb{R}_x^{+,*} \times \mathbb{R}_t^+, \Omega^r\right)$, and the non-classical term supported by the half-line $\{x = 0, t > 0\}$ is accounted for by a direct modification of the mass conservation equation (1.3.17). This is motivated by the fact that the measure solutions that may arise when solving the Riemann problem have a very simple form. They are L^∞ functions with a non-zero mass flux across the standing wave, which can be interpreted as a mass concentration at $x = 0$. In fact, it will be shown that these measure solutions only arise when the resonance phenomenon occurs (i.e. when $w = \pm a\tau$), whereas in most cases, we will have $[\alpha\rho w]^0 = 0$.*

Note that $[\alpha\rho w]^0(t)$ is well defined. Indeed, if a balance law $\partial_t u + \partial_x \mathbf{F}(u) = 0$ is satisfied on a bounded open subset $\mathscr{D}$ of $\mathbb{R}_x \times \mathbb{R}_t^+$, then its flux $\mathbf{F}(u)$ is well defined as a measurable function on $\partial\mathscr{D}$ (see Theorem 1.2.1 in [8]).

We may now state the following definition for the solutions of the Riemann problem (1.3.5)-(1.3.11).

Definition 1.3.2. *A solution of the Riemann problem (1.3.5)-(1.3.11) is a function* $\mathbb{W} : (x,t) \in \mathbb{R}_x \times \mathbb{R}_t^+ \mapsto \mathbb{W}(x,t) \in \Omega^r$ *in* $L^1_{\text{loc}}\left(\mathbb{R}_x^{-,*} \times \mathbb{R}_t^+, \Omega^r\right) \cap L^1_{\text{loc}}\left(\mathbb{R}_x^{+,*} \times \mathbb{R}_t^+, \Omega^r\right)$ *satisfying the following properties:*

1. $\mathbb{W}$ *is a self similar mapping and we can write* $\mathbb{W}(x/t; \mathbb{W}_L, \mathbb{W}_R)$,

2. $\mathbb{W}$ *is a solution of the Cauchy problem determined by the initial condition* $(\mathbb{W}_L, \mathbb{W}_R)$ *in the sense of Definition 1.3.1,*

3. $\mathbb{W}$ *is composed with constant intermediate states separated by waves whose constant speeds are eigenvalues* $\{\sigma_i^r\}_{i=0..3}$ *of the system, and each eigenvalue* σ_i^r *appears at most once in* $\mathbb{W}$.

4. *The dissipation of energy across the standing wave is non-positive in the sense that*

$$\left[\alpha\rho w\mathcal{E} + \alpha\pi w\right]^0 \leq 0. \tag{1.3.24}$$

Moreover, we impose the following alternative

- *if* $\left[\alpha\rho w\right]^0 = 0$ *then* $\left[\alpha\rho w\mathcal{T}\right]^0 = 0$,
- *if* $\left[\alpha\rho w\right]^0 \neq 0$ *then* $\left[\mathcal{T}\right]^0 = 0$.

Here again, this definition deserves some comments. We will see that, on the one hand, the conditions on the solution that are imposed by definition 1.3.2 are restrictive enough to enable us to calculate all the intermediate sates of the solution. But on the other hand, these restrictions are broad enough to guarantee a global existence theorem on Ω^r for the Riemann problem, even when resonance occurs (see theorem 1.3.4 below). The solution is built so as to preserve the energy equality (1.3.8) at the interface $x = 0$ or at least to be *dissipative*, even if we have to accept a non zero mass flux $\left[\alpha\rho w\right]^0 \neq 0$ in order to ensure this dissipation. For any solution, we may formally write

$$\partial_t\left(\alpha\rho\mathcal{E}\right) + \partial_x\left(\alpha\rho\mathcal{E}w + \alpha\pi(\tau,\mathcal{T})w\right) = -f\delta_0, \tag{1.3.25}$$

where f is a positive function. Again, despite the linear degeneracy of the 0-field, we here allow a non zero energy dissipation through the standing wave recalling that for the equilibrium system, such a dissipation of energy may occur when the resonance appears. To be more precise, in the resonant cases (where $\left[\alpha\rho w\right]^0$ may be non zero), we will see that f is a given function wholly determined by the initial states $\mathbb{W}_L$ and $\mathbb{W}_R$, whereas in the non resonant cases (where $\left[\alpha\rho w\right]^0 = 0$), f depends on a parameter and will be chosen so as to guarantee the positivity of the intermediate states (*c.f.* remark 1.3.1).

Let us now define some notations depending only on the physical data $\mathbb{V}_L := (\rho_L, w_L, \mathcal{T}_L)$ and

$\mathbb{V}_R := (\rho_R, w_R, \mathcal{T}_R)$ and that will be useful afterwards:

$$w^\sharp := \frac{1}{2}(w_L + w_R) - \frac{1}{2a}(\pi_R - \pi_L), \tag{1.3.26}$$

$$\pi^\sharp := \frac{1}{2}(\pi_R + \pi_L) - \frac{a}{2}(w_R - w_L), \tag{1.3.27}$$

$$\tau_L^\sharp := \tau_L + \frac{1}{a}(w^\sharp - w_L) = \tau_L + \frac{1}{2a}(w_R - w_L) - \frac{1}{2a^2}(\pi_R - \pi_L), \tag{1.3.28}$$

$$\tau_R^\sharp := \tau_R - \frac{1}{a}(w^\sharp - w_R) = \tau_R + \frac{1}{2a}(w_R - w_L) + \frac{1}{2a^2}(\pi_R - \pi_L). \tag{1.3.29}$$

In fact, these quantities are respectively the speed, the linearized pressure, and the specific volumes of the solution obtained with a constant initial section $\alpha_L = \alpha_R$, provided that the specific volumes $\tau_L^\sharp$ and $\tau_R^\sharp$ are positive. Let stress from now on that a will be chosen large for stability matters (see section 1.4.4) and in particular large enough to enforce the positivity of $\tau_L^\sharp$ and $\tau_R^\sharp$. In the sequel, we always assume that the constant a is such that $\tau_L^\sharp$ and $\tau_R^\sharp$ are positive. It can be seen that this is equivalent to the natural ordering of the waves $w_L - a\tau_L < w^\sharp < w_R + a\tau_R$.

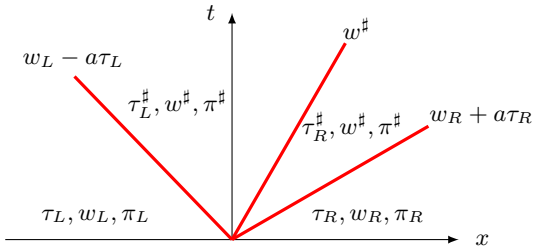

Self-similar solution in the case of an initial data with $\alpha_L = \alpha_R$.

Thereafter, the self-similar function depicted above will be referred to as the *constant section solution*. We also introduce the Mach numbers of the intermediate states for the constant section solution:

$$\mathcal{M}_L := \frac{w_L}{a\tau_L}, \qquad \mathcal{M}_L^\sharp := \frac{w^\sharp}{a\tau_L^\sharp}, \qquad \mathcal{M}_R^\sharp := \frac{w^\sharp}{a\tau_R^\sharp}, \qquad \mathcal{M}_R := \frac{w_R}{a\tau_R}. \tag{1.3.30}$$

The main result of this section is the following existence theorem for the Riemann problem.

Theorem 1.3.4. *Let $\mathbb{W}_L$ and $\mathbb{W}_R$ be two positive states in Ω^r. Assume that a is such that $\tau_L^\sharp > 0$ and $\tau_R^\sharp > 0$. Then the Riemann problem (1.3.5)-(1.3.11) admits a positive solution in the sense of Definition 1.3.2, whatever the ratio $\nu = \frac{\alpha_L}{\alpha_R}$ is.*

The proof of this existence theorem follows from an actual construction of the solution for every given initial data $\mathbb{W}_L$ and $\mathbb{W}_R$. For strictly hyperbolic systems of conservation laws, the characteristic eigenvalues are naturally ordered (see for example the Euler equations). Consequently, if all the characteristic fields are linearly degenerate, the solution is sought in the form of constant states separated by contact discontinuities whose speeds are equal to the corresponding eigenvalues. For system (1.3.5), the eigenvalues are not naturally ordered because of the existence of a standing

wave, and a resonance phenomenon does appear for sonic flows (*i.e.* flows with vanishing $(w - a\tau)(w + a\tau)$). Therefore, the classical proof must be slightly modified. We first focus our attention on a particular non resonant ordering of the eigenvalues (for instance $w - a\tau < 0 < w < w + a\tau$) and we determine sufficient conditions (that sometimes appear to be necessary) on the initial states $\mathbb{W}_L$ and $\mathbb{W}_R$ for the solution to have this particular ordering. We do the same for the other possible non resonant orderings (that may be supersonic). Resonant solutions are then studied as limits of non resonant solutions as the acoustic speeds tend to zero. Eventually, we check *a posteriori* that the determined conditions totally cover the entire domain of initial conditions $\Omega^r \times \Omega^r$. We show that the conditions that give the ordering of the wave speeds can be expressed in terms of the physical data $\mathbb{V}_L$,$\mathbb{V}_R$ and of the ratio of left and right sections : $\nu = \frac{\alpha_L}{\alpha_R}$. In addition, for certain values of ν (large or small values depending on the flow direction) the solution may have to dissipate energy in the standing wave in order to preserve the positivity of the densities (again, see Remark 1.3.1).

The following figure provides a schematic representation of the solution given by Theorem 1.3.4. It represents the map of the admissible solutions with respect to the initial states $\mathbb{W}_L$ and $\mathbb{W}_R$. The right part of the chart corresponds to the solutions with positive material speed, while the left part depicts the symmetric configurations with negative material speed. The blue lines represent the solutions whose structure needs to refer to a measure concentrated at $x = 0$.

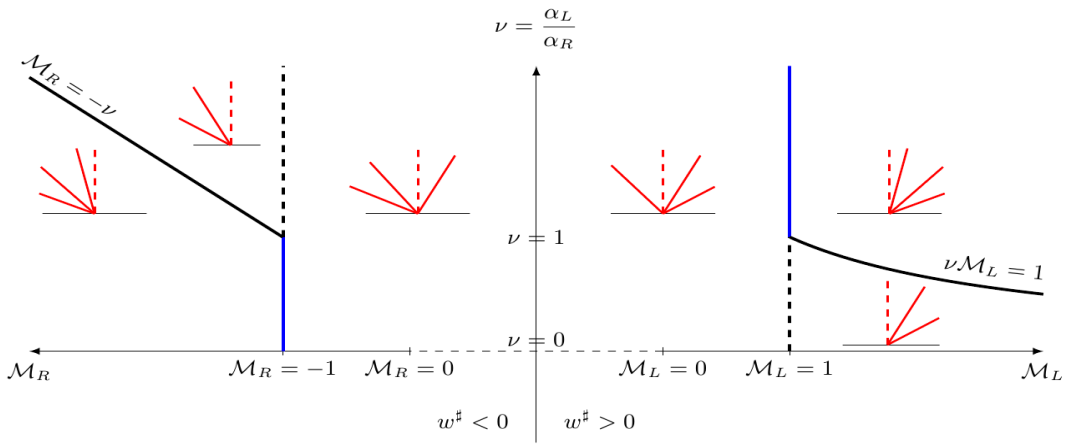

In the sequel, a solution of the Riemann problem is said to have *signature* $< i, j >$ with i and j in $\{0, 1, 2, 3\}$ if it is composed with i left-going waves and j right-going waves. For example, the solution with the ordering of the eigenvalues $w - a\tau < 0 < w < w + a\tau$ is said to have signature $< 1, 2 >$.

Non resonant solutions

Solutions with signature $< 1, 1 >$*:*

We first seek solutions with the subsonic non resonant ordering of the eigenvalues $w - a\tau < 0 = w < w + a\tau$ *i.e.* solutions with signature $< 1, 1 >$.

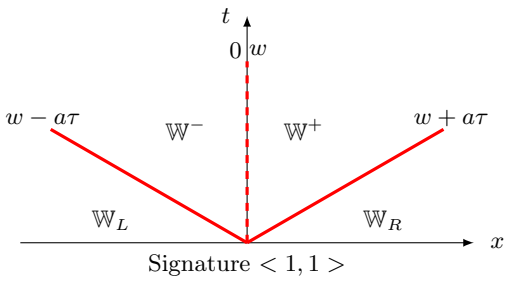

We have the following result:

Proposition 1.3.5. *Let $\mathbb{W}_L$ and $\mathbb{W}_R$ be two positive states in Ω^r. The Riemann problem (1.3.5)-(1.3.11) admits a positive solution in the sense of Definition 1.3.2 with signature $< 1, 1 >$, if*

$$w^\sharp = 0. \tag{1.3.31}$$

The intermediate states of this solution are given by:

$$\tau^- = \tau_L^\sharp, \qquad w^- = 0, \qquad \mathcal{T}^- = \mathcal{T}_L, \tag{1.3.32}$$

$$\tau^+ = \tau_R^\sharp, \qquad w^+ = 0, \qquad \mathcal{T}^+ = \mathcal{T}_R, \tag{1.3.33}$$

and the energy equality (1.3.8) is exactly preserved across the standing wave.

Proof. We assume that $w^\sharp = 0$. Let us prove that the intermediate states given by equations (1.3.32)-(1.3.33) determine a positive solution of signature $< 1, 1 >$. For the left-going acoustic wave, we have $\alpha = \text{cst} = \alpha_L$ and $\mathcal{T} = \text{cst} = \mathcal{T}_L$. Besides, we have $w_L - a\tau_L = w^\sharp - a\tau_L^\sharp = -a\tau_L^\sharp = -a\tau^- = w^- - a\tau^-$. Thus the Rankine-Hugoniot jump relations for (1.3.21) are clearly satisfied. Similarly, we prove that the jump relations corresponding to the right-going acoustic wave are also satisfied. As for the 0-w wave, the fact that $w^- = w^+ = 0$, clearly yields

$$[\alpha\rho w]^0 = 0, \qquad [\alpha\rho w\mathcal{T}]^0 = 0 \qquad \text{and} \qquad [\alpha\rho w\mathcal{E} + \alpha\pi w]^0 = 0. \tag{1.3.34}$$

Thus Definition 1.3.2 is satisfied. □

Solutions with signature $< 1, 2 >$:

Let us now turn on to solutions with the subsonic non resonant ordering of the eigenvalues $w - a\tau < 0 < w < w + a\tau$ *i.e.* solutions with the wave signature $< 1, 2 >$.

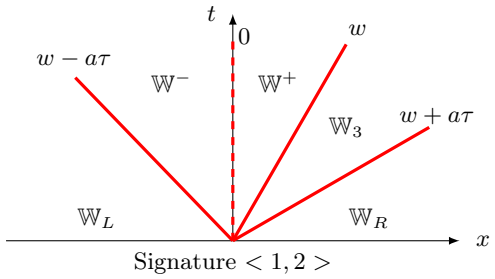

Signature $< 1, 2 >$

The following result shows that, provided a sufficient (and necessary) condition on the initial states, one can build a one-parameter family of solutions (in the sense of Definition 1.3.2) of signature $< 1, 2 >$, and the dissipation of energy across the standing wave is directly driven by the underlying parameter.

Proposition 1.3.6. *Let $\mathbb{W}_L$ and $\mathbb{W}_R$ be two positive states in Ω^r. The Riemann problem (1.3.5)-(1.3.11) admits positive solutions in the sense of Definition 1.3.2 with signature $< 1, 2 >$, if and only if*

$$w^\sharp > 0 \quad \text{and} \quad \mathcal{M}_L < 1, \tag{1.3.35}$$

where $w^\sharp$ and $\mathcal{M}_L$ are defined respectively in (1.3.26) and (1.3.30). These solutions are parametrized by $\mathcal{M} := \mathcal{M}^- = \frac{w^-}{a\tau^-}$, the Mach number of the state on the left of the standing wave, and the intermediate states are given by:

$$\tau^- = \tau_L^\sharp \frac{1 - \mathcal{M}_L^\sharp}{1 - \mathcal{M}}, \qquad w^- = a\mathcal{M}\tau^-, \qquad \mathcal{T}^- = \mathcal{T}_L, \tag{1.3.36}$$

$$\tau^+ = \tau_L^\sharp \frac{1 + \mathcal{M}_L^\sharp}{1 + \nu\mathcal{M}}, \qquad w^+ = \nu a\mathcal{M}\tau^+, \qquad \mathcal{T}^+ = \mathcal{T}_L, \tag{1.3.37}$$

$$\tau_3 = \tau_R^\sharp + \tau_L^\sharp \frac{\mathcal{M}_L^\sharp - \nu\mathcal{M}}{1 + \nu\mathcal{M}}, \qquad w_3 = \nu a\mathcal{M}\tau^+, \qquad \mathcal{T}_3 = \mathcal{T}_R. \tag{1.3.38}$$

Besides, there exists a critical value $\nu^\sharp$ in $(1, +\infty]$ depending only on the physical data $(\mathbb{V}_L, \mathbb{V}_R)$ and possibly infinite such that the following alternative holds

- *Either $\nu < \nu^\sharp$, and in this case, $\mathcal{M}$ belongs to the interval $(0, \mathcal{M}_0(\omega, \nu)] \subset (0, \min(1, 1/\nu))$ with*

$$\mathcal{M}_0(\omega, \nu) = \frac{1}{2}\left(\frac{1+\omega^2}{1-\omega^2}\left(1 + \frac{1}{\nu}\right) - \sqrt{\left(\frac{1+\omega^2}{1-\omega^2}\right)^2\left(1 + \frac{1}{\nu}\right)^2 - \frac{4}{\nu}}\right), \tag{1.3.39}$$

  where

$$\omega = \frac{1 - \mathcal{M}_L^\sharp}{1 + \mathcal{M}_L^\sharp} \in (0, 1). \tag{1.3.40}$$

  The value $\mathcal{M} = \mathcal{M}_0(\omega, \nu)$ gives the unique solution that exactly preserves the energy equality (1.3.8) across the standing wave, and for $\mathcal{M} < \mathcal{M}_0(\omega, \nu)$, the energy is dissipated.

- *Or $\nu \geq \nu^\sharp$, and in that case, no positive solution can preserve the energy equality (1.3.8). The initial data is such that $0 < \frac{\mathcal{M}_L^\sharp}{\nu} < \mathcal{M}_0(\omega,\nu)$ where $\mathcal{M}_0(\omega,\nu)$ is given by (1.3.39). $\mathcal{M}$ must be strictly less than $\mathcal{M}_0(\omega,\nu)$, and by taking $\mathcal{M}$ close enough to $\frac{\mathcal{M}_L^\sharp}{\nu}$ we ensure that all the densities remain positive.*

In both cases, the choice of the value of $\mathcal{M}$ determines the dissipation of energy across the standing wave through

$$[\alpha\rho w\mathcal{E} + \alpha\pi w]^0 = \frac{1}{2}(w_L^\sharp + a\tau_L^\sharp)^2 \mathcal{Q}_0(\mathcal{M})\Psi(\mathcal{M};\nu,\omega) \leq 0, \tag{1.3.41}$$

where $\mathcal{Q}_0(\mathcal{M}) = \alpha_L\rho^- w^- = \alpha_R\rho^+ w^+ > 0$ is the mass flux across the standing wave and Ψ is a nonpositive function defined by

$$\Psi(\mathcal{M};\nu,\omega) = \frac{\nu\mathcal{M}-1}{\nu\mathcal{M}+1} - \omega^2\frac{\mathcal{M}+1}{\mathcal{M}-1}, \quad \text{with} \quad \omega = \frac{1-\mathcal{M}_L^\sharp}{1+\mathcal{M}_L^\sharp}. \tag{1.3.42}$$

Proof. The proof relies on lengthly but easy calculations and therefore, we only sketch it. We look for a classical weak solution *i.e.* we impose the mass conservation across the standing wave $[\alpha\rho w]^0 = 0$. We first focus our attention on energy preserving solutions and we express the jump relation corresponding to the energy conservation equation (1.3.8) across the standing wave in terms of the left and right states $\mathbb{W}^-$ and $\mathbb{W}^+$, which reads

$$[\alpha\rho w\mathcal{E} + \alpha\pi w]^0 = -f \qquad \text{with} \qquad f = 0. \tag{1.3.43}$$

This, combined with the mass conservation implies that

$$\tau^{+^2}\left((\nu\mathcal{M})^2 - 1\right) - \tau^{-^2}\left(\mathcal{M}^2 - 1\right) = 0. \tag{1.3.44}$$

In addition, the solution must satisfy equations (1.3.21) outside a neighborhood of $x = 0$ which results in a full set of classical Rankine-Hugoniot jump relations. Using these jump relations through the other waves, we can wind up the information to the initial left and right states, showing that (1.3.44) is equivalent to

$$\Psi(\mathcal{M};\nu,\mathcal{M}_L^\sharp) = \frac{\nu\mathcal{M}-1}{\nu\mathcal{M}+1} - \omega^2\frac{\mathcal{M}+1}{\mathcal{M}-1} = 0 \tag{1.3.45}$$

$$\iff \quad (\nu\mathcal{M}-1)(\mathcal{M}-1) - \omega^2(\nu\mathcal{M}+1)(\mathcal{M}+1) = 0, \tag{1.3.46}$$

where the expression of ω is given in (1.3.40). Then we observe that for the solution to be of signature $< 1, 2 >$, w^+ has to be positive and so has to be w^- (by the mass conservation). Moreover, the $\{w - a\tau\}$-wave must be negative which means that $w_L - a\tau_L = w^- - a\tau^- < 0$, *i.e.* $\mathcal{M}_L < 1$ and $\mathcal{M} < 1$. By (1.3.44), this implies that $\mathcal{M} < 1/\nu$. Consequently, $\mathcal{M}$ must be sought in the interval $(0, \min(1, 1/\nu))$. Let us now check that (1.3.46) has a (unique) root in $(0, \min(1, 1/\nu))$ if and only if $w^\sharp > 0$, and that this root is given by (1.3.39). Defining $\varphi(\mathcal{M}) = (\nu\mathcal{M}-1)(\mathcal{M}-1) - \omega^2(\nu\mathcal{M}+1)(\mathcal{M}+1)$, its first derivative reads

$$\varphi'(\mathcal{M}) = \nu(\mathcal{M}-1) + (\nu\mathcal{M}-1) - \omega^2(\nu(\mathcal{M}+1) + \nu\mathcal{M}+1),$$

which is negative on the interval $(0, \min(1, 1/\nu))$. In addition, we have $\varphi(\min(1, 1/\nu)) = -2\omega^2(1 + \min(\nu, 1/\nu)) < 0$. Hence, by the intermediate value theorem, φ has a unique root in $(0, \min(1, 1/\nu))$ if and only if $\varphi(0) = 1 - \omega^2 > 0$. From the definition (1.3.40) of ω, we have $\omega^2 < 1 \Leftrightarrow \mathcal{M}_L^\sharp > 0 \Leftrightarrow w^\sharp > 0$. The expressions of the intermediate states follow from the Rankine-Hugoniot jump relations. Conversely, if $w^\sharp > 0$, then (1.3.46) has a unique root $\mathcal{M}_0$ in $(0, \min(1, 1/\nu))$, and formulas (1.3.36)-(1.3.38) give a positive solution of signature $< 1, 2 >$ provided that $w_L - a\tau_L < 0$ *i.e.* $\mathcal{M}_L < 1$.
The existence of $\nu^\sharp$ is related to the expression of τ_3 in (1.3.38) which is the only intermediate specific volume that may be nonpositive. It is possible to show that for fixed $\mathbb{V}_L$ and $\mathbb{V}_R$, the function

$$\nu \mapsto \tau_3(\nu, \mathcal{M}_0(\omega, \nu)) = \tau_R^\sharp + \tau_L^\sharp \frac{\mathcal{M}_L^\sharp - \nu \mathcal{M}_0(\omega, \nu)}{1 + \nu \mathcal{M}_0(\omega, \nu)} \tag{1.3.47}$$

is a non-increasing function that may become negative for large values of ν. Then, in order to impose the positivity of τ_3 we must no longer exactly conserve the energy at the standing wave (by taking $\mathcal{M} = \mathcal{M}_0(\omega, \nu)$) but dissipate it by taking $\mathcal{M}$ smaller than $\mathcal{M}_0(\omega, \nu)$. The expression of τ_3 clearly shows that if $\mathcal{M}$ is taken close enough to $\frac{\mathcal{M}_L^\sharp}{\nu}$, we have τ_3 close to $\tau_R^\sharp$ which is positive. □

Remark 1.3.4. *We can compute explicitly the expression of $\nu^\sharp$: it is the value of ν which cancels τ_3 in equation (1.3.47) If we introduce*

$$\tau_3^\infty = \lim_{\nu \to +\infty} \tau_3(\nu, \mathcal{M}_0(\omega, \nu)) = \tau_R^\sharp - \tau_L^\sharp \mathcal{M}_L^\sharp \frac{1 - \mathcal{M}_L^\sharp}{1 + \mathcal{M}_L^\sharp}, \tag{1.3.48}$$

we can prove that

$$\nu^\sharp = \begin{cases} +\infty & \text{if} \quad \tau_3^\infty \geq 0, \\ \dfrac{\mathcal{M}_L^\sharp + \frac{\tau_R^\sharp}{\tau_L^\sharp}}{1 - \frac{\tau_R^\sharp}{\tau_L^\sharp}} \dfrac{(1 - \frac{\tau_R^\sharp}{\tau_L^\sharp})(1 + \omega^2) - (1 - \omega^2)(\mathcal{M}_L^\sharp + \frac{\tau_R^\sharp}{\tau_L^\sharp})}{(1 - \frac{\tau_R^\sharp}{\tau_L^\sharp})(1 - \omega^2) - (1 + \omega^2)(\mathcal{M}_L^\sharp + \frac{\tau_R^\sharp}{\tau_L^\sharp})} > 1 & \text{if} \quad \tau_3^\infty < 0. \end{cases} \tag{1.3.49}$$

Moreover, for $\nu \geq \nu^\sharp$, appendix A gives a procedure to choose the value of $\mathcal{M}$ and determine the corresponding energy dissipation.

Solutions of signature $< 0, 3 >$:

We now seek solutions with the supersonic non resonant ordering of the eigenvalues $0 < w - a\tau < w < w + a\tau$ *i.e.* solutions of signature $< 0, 3 >$.

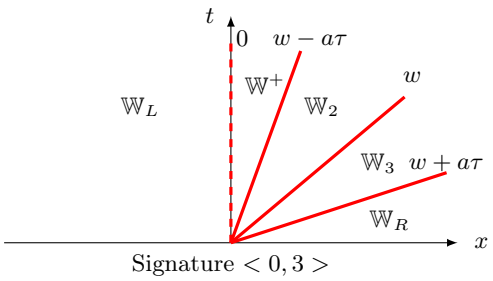

Again, a one-parameter family of solutions is built, the involved parameter being directly related to the energy dissipation across the standing wave.

Proposition 1.3.7. *Let $\mathbb{W}_L$ and $\mathbb{W}_R$ be two positive states in Ω^r. The Riemann problem (1.3.5)-(1.3.11) admits positive solutions in the sense of Definition 1.3.2 with signature $< 0, 3 >$ if and only if*

$$w^\sharp > 0, \quad \mathcal{M}_L > 1 \quad \text{and} \quad \nu\mathcal{M}_L > 1. \tag{1.3.50}$$

These solutions can be parametrized by a real parameter $\theta \in (0, 1]$ measuring the dissipation of energy across the standing wave, and the intermediate states are given by:

$$\tau^+ = \theta\tau_L\sqrt{\frac{\mathcal{M}_L^2 - 1}{\nu^2\mathcal{M}_L^2 - 1}}, \qquad w^+ = \nu a\mathcal{M}_L\tau^+, \qquad \mathcal{T}^+ = \mathcal{T}_L, \tag{1.3.51}$$

$$\tau_2 = \tau_L^\sharp + \frac{\tau_L}{2}(\mathcal{M}_L - 1)\left(1 - \theta\sqrt{\frac{(\mathcal{M}_L + 1)(\nu\mathcal{M}_L - 1)}{(\mathcal{M}_L - 1)(\nu\mathcal{M}_L + 1)}}\right), \quad w_2 = w^+ + a(\tau_2 - \tau^+), \quad \mathcal{T}_2 = \mathcal{T}_L, \tag{1.3.52}$$

$$\tau_3 = \tau_R^\sharp + \frac{\tau_L}{2}(\mathcal{M}_L - 1)\left(1 - \theta\sqrt{\frac{(\mathcal{M}_L + 1)(\nu\mathcal{M}_L - 1)}{(\mathcal{M}_L - 1)(\nu\mathcal{M}_L + 1)}}\right), \quad w_3 = w_2, \qquad \mathcal{T}_3 = \mathcal{T}_R. \tag{1.3.53}$$

Besides, there exists a critical value $\nu^\sharp \in (1, +\infty]$ depending only on the physical data $(\mathbb{V}_L, \mathbb{V}_R)$ and possibly infinite such that the following alternative holds

- *Either $\nu < \nu^\sharp$, and in this case the value $\theta = 1$ gives the unique solution that exactly preserves the energy equality (1.3.8) across the standing wave.*

- *Or $\nu \geq \nu^\sharp$, and in that case, no positive solution can preserve the energy equality (1.3.8). The parameter θ must be strictly less than 1, and by taking θ close enough to 0, we ensure that all the densities remain positive.*

In both cases, the choice of the value of θ determines the dissipation of energy across the standing wave through

$$[\alpha\rho w\mathcal{E} + \alpha\pi w]^0 = \frac{1}{2}a^2{\tau_L}^2({\mathcal{M}_L}^2 - 1)(\theta^2 - 1)\alpha_L\rho_L w_L \leq 0. \tag{1.3.54}$$

Proof. Here again, we only sketch the proof. We look for a classical weak solution by imposing the mass conservation across the stationary wave $[\alpha\rho w]^0 = 0$. The jump relation corresponding to the energy inequality (1.3.10) leads to nearly the same equation as (1.3.44):

$$\tau^{+2}\left((\nu\mathcal{M}_L)^2 - 1\right) - {\tau_L}^2\left({\mathcal{M}_L}^2 - 1\right) \leq 0. \tag{1.3.55}$$

Hence there exists θ in $(0,1)$ such that

$$\tau^+ = \theta\tau_L\sqrt{\frac{\mathcal{M}_L^2 - 1}{\nu^2\mathcal{M}_L^2 - 1}}, \tag{1.3.56}$$

and the value $\theta = 1$ corresponds to the exact preservation of energy. The intermediate states are then computed thanks to the Rankine-Hugoniot jump relations. Eventually, we observe that the functions

$$\nu \quad \mapsto \quad \tau_2(\nu,\theta) = \tau_L^\sharp + \frac{\tau_L}{2}(\mathcal{M}_L - 1)\left(1 - \theta\sqrt{\frac{(\mathcal{M}_L+1)(\nu\mathcal{M}_L - 1)}{(\mathcal{M}_L - 1)(\nu\mathcal{M}_L + 1)}}\right), \tag{1.3.57}$$

$$\nu \quad \mapsto \quad \tau_3(\nu,\theta) = \tau_R^\sharp + \frac{\tau_L}{2}(\mathcal{M}_L - 1)\left(1 - \theta\sqrt{\frac{(\mathcal{M}_L+1)(\nu\mathcal{M}_L - 1)}{(\mathcal{M}_L - 1)(\nu\mathcal{M}_L + 1)}}\right), \tag{1.3.58}$$

with θ identically equal to 1, are non-increasing functions that may become negative for large values of ν. Then, in order to impose the positivity of τ_2 and τ_3, we must no longer exactly preserve the energy at the standing wave but dissipate it by taking θ in the interval $(0,1)$ close enough to 0. □

Remark 1.3.5. *We can compute explicitly the expression of $\nu^\sharp$. If we introduce*

$$\tau^\infty = \min\left(\lim_{\nu\to+\infty}\tau_2(\nu,\theta=1), \lim_{\nu\to+\infty}\tau_3(\nu,\theta=1)\right) = \min(\tau_L^\sharp,\tau_R^\sharp) - \frac{\tau_L}{2}(\mathcal{M}_L - 1)\left(\sqrt{\frac{\mathcal{M}_L+1}{\mathcal{M}_L-1}} - 1\right), \tag{1.3.59}$$

we can prove that

$$\nu^\sharp = \begin{cases} +\infty & \text{if} \quad \tau^\infty \geq 0, \\ \dfrac{1}{\mathcal{M}_L}\dfrac{\mathcal{M}_L^2 - 1 + \left(\frac{2\min(\tau_L^\sharp,\tau_R^\sharp)}{\tau_L} + \mathcal{M}_L - 1\right)^2}{\mathcal{M}_L^2 - 1 - \left(\frac{2\min(\tau_L^\sharp,\tau_R^\sharp)}{\tau_L} + \mathcal{M}_L - 1\right)^2} > 1 & \text{if} \quad \tau^\infty < 0. \end{cases} \tag{1.3.60}$$

Moreover, for $\nu \geq \nu^\sharp$, appendix A describes a procedure to choose the value of θ and determine the corresponding energy dissipation.

Resonant solutions

We now study resonant solutions that are obtained by formally passing to the limit in non resonant configurations $< 1,2 >$ or $< 0,3 >$ when letting the acoustic wave speed $w - a\tau$ tend to zero. We distinguish the case of a divergent section $\alpha_R > \alpha_L$ *i.e.* $\nu < 1$ and the case of a convergent section $\alpha_R < \alpha_L$ *i.e.* $\nu > 1$.

Resonant solution for $\nu < 1$:

We consider initial left and right states $\mathbb{W}_L$ and $\mathbb{W}_R$ such that $w^\sharp > 0$ and $\mathcal{M}_L < 1$ which means that the corresponding solution is of signature $< 1, 2 >$ according to Proposition 1.3.6. Then, we study the formal limit of the solution as $\mathcal{M}_L$ goes to 1^- which is equivalent to sending $w_L - a\tau_L$ to 0^-. We expect the $\{w - a\tau\}$-wave to cross the standing wave and reappear on its right, thus letting the solution to shift from signature $< 1, 2 >$ to signature $< 0, 3 >$. However, Proposition 1.3.7 shows that signature $< 0, 3 >$ is possible only if $\nu\mathcal{M}_L > 1$. This implies that in the case of a divergent section $\nu < 1$, there exists a range of values of $\mathcal{M}_L$, namely $[1, \frac{1}{\nu}]$, on which the acoustic wave $w - a\tau$ does not appear in the solution. Therefore, we are brought to study the resonant signature $< 0, 2 >$ represented in the figure below.

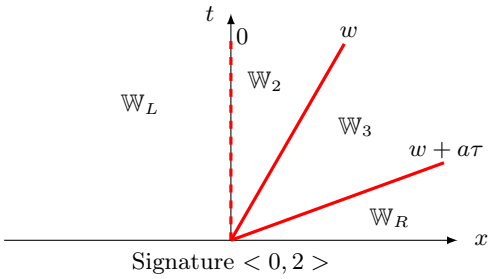

Proposition 1.3.8 shows that in this resonant case where $\nu < 1$, one can build a dissipative solution in the sense of Definition 1.3.2 where the $w - a\tau$-wave does not appear.

Proposition 1.3.8. *Let $\mathbb{W}_L$ and $\mathbb{W}_R$ be two positive states in Ω^r. The Riemann problem (1.3.5)-(1.3.11) admits a unique positive solution in the sense of Definition 1.3.2 with signature $< 0, 2 >$, if*

$$w^\sharp > 0, \quad \mathcal{M}_L \geq 1 \quad \text{and} \quad \nu\mathcal{M}_L \leq 1. \tag{1.3.61}$$

The intermediate states are given by

$$\tau_2 = \frac{2\tau_L^\sharp + \tau_L(\mathcal{M}_L - 1)}{1 + \nu\mathcal{M}_L}, \qquad w_2 = \nu a\mathcal{M}_L\tau_2, \qquad \mathcal{T}_2 = \mathcal{T}_L, \tag{1.3.62}$$

$$\tau_3 = \tau_R^\sharp + \tau_L^\sharp\frac{1 - \nu\mathcal{M}_L}{1 + \nu\mathcal{M}_L} + \tau_L\frac{\mathcal{M}_L - 1}{1 + \nu\mathcal{M}_L}, \qquad w_3 = w_2 = \nu a\mathcal{M}_L\tau_2, \qquad \mathcal{T}_3 = \mathcal{T}_R. \tag{1.3.63}$$

This solution dissipates energy across the standing wave and the dissipation is given by

$$[\alpha\rho w\mathcal{E} + \alpha\pi w]^0 = \frac{1}{2}\left(a^2(2\tau_L^\sharp + \tau_L(\mathcal{M}_L - 1))^2\frac{\nu\mathcal{M}_L - 1}{\nu\mathcal{M}_L + 1} - a^2\tau_L^2(\mathcal{M}_L^2 - 1)\right)\alpha_L\rho_L w_L \leq 0. \tag{1.3.64}$$

Proof. There are eight unknowns since we have to determine only two intermediate states. Thus we need eight independent jump relations in order to calculate these intermediate states. For the discontinuities located at $\frac{x}{t} = w_2$ and $\frac{x}{t} = w_3 + a\tau_3$, we use the classical Rankine-Hugoniot jump

relations associated with system (1.3.5) which provides us with six independent equations (three for each wave). And for the stationary discontinuity, we use the mass conservation equation (*i.e.* $[\alpha\rho w]^0 = 0$) as well as the conservation equation of $\mathcal{T}$ (*i.e.* $[\alpha\rho w\mathcal{T}]^0 = 0$) which provides us with two more equations. It is then possible to verify that for given $\mathbb{W}_L$ and $\mathbb{W}_R$, there exists a unique solution of signature $< 0, 2 >$ given by equations (1.3.62)-(1.3.63). Eventually, we calculate the flux related to the energy equation (1.3.10) on the standing wave:

$$[\alpha\rho w\mathcal{E} + \alpha\pi w]^0 = \frac{a^2}{2}\left({\tau_2}^2\left((\nu\mathcal{M}_L)^2 - 1\right) - {\tau_L}^2\left({\mathcal{M}_L}^2 - 1\right)\right)\alpha_L\rho_L w_L. \tag{1.3.65}$$

This dissipation is wholly determined by $\mathbb{W}_L$ and $\mathbb{W}_R$, and is nonpositive since $M_L \geq 1$ and $\nu\mathcal{M}_L \leq 1$. □

Resonant solution for $\nu > 1$:

Following similar steps as previously, we consider initial left and right states $\mathbb{W}_L$ and $\mathbb{W}_R$ such that $w^\sharp > 0$ and $\mathcal{M}_L < 1$ .The corresponding solution is of signature $< 1, 2 >$, and we study the formal limit of the solution as $\mathcal{M}_L$ goes to 1^- which is equivalent to sending $w_L - a\tau_L$ to 0^-. It is easy to verify that for M_L close to 1, $\nu^\sharp = +\infty$ which means that the Mach number of the state on the left of the standing wave is given by $\mathcal{M} = \mathcal{M}_0(\omega, \nu)$ (see equation (1.3.39)). Simple calculations show that

$$\lim_{\mathcal{M}_L\to 1^-}\mathcal{M}_0(\omega,\nu) = \lim_{\mathcal{M}_L^\sharp\to 1^-}\mathcal{M}_0(\omega,\nu) = \lim_{\omega\to 0^+}\mathcal{M}_0(\omega,\nu) = \frac{1}{\nu} \tag{1.3.66}$$

as soon as $\nu > 1$. This implies that the specific volume on the left of the standing wave tends to zero:

$$\lim_{\mathcal{M}_L\to 1^-}\tau^- = \lim_{\mathcal{M}_L^\sharp\to 1^-}\tau_L^\sharp\frac{1-\mathcal{M}_L^\sharp}{1-\mathcal{M}_0(\omega,\nu)} = 0, \tag{1.3.67}$$

which means that the partial mass tends to infinity:

$$\lim_{\mathcal{M}_L\to 1^-}\alpha^-\rho^- = +\infty. \tag{1.3.68}$$

However, the Lebesgue measure of the cone supporting this intermediate state tends to zero as $\mathcal{M}_L$ goes to 1^-

$$\mu\left\{(x,t),\ w_L - a\tau_L < \frac{x}{t} < 0\right\} \underset{\mathcal{M}_L\to 1^-}{\longrightarrow} 0, \tag{1.3.69}$$

and we expect a Dirac measure to appear whose weight is given by

$$\begin{aligned}
\lim_{\mathcal{M}_L\to 1^-}\int_{w_L - a\tau_L}^0 (\alpha^-\rho^-)(\xi)d\xi &= \lim_{\mathcal{M}_L\to 1^-}\int_{w^- - a\tau^-}^0 (\alpha^-\rho^-)(\xi)d\xi \\
&= \lim_{\mathcal{M}_L\to 1^-} -(w^- - a\tau^-)\alpha_L\rho^- \\
&= \lim_{\mathcal{M}_L\to 1^-} -a(\mathcal{M}_0 - 1)\alpha_L \\
&= -a\left(\frac{1}{\nu} - 1\right)\alpha_L \\
&= -a(\alpha_R - \alpha_L) > 0.
\end{aligned}$$

Therefore, we are brought to study the resonant signature $< 0, 2 > + \delta_0$, with little abuse in the notation, depicted in the figure below,

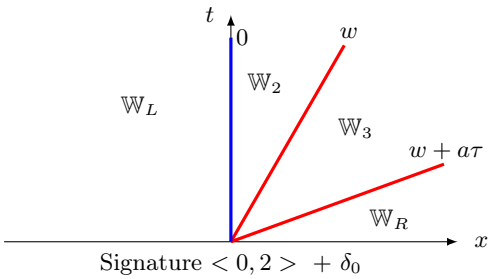

This non classical solution may be represented by a **function** that however does not satisfy the mass conservation across the standing wave. The missing mass between the states at the left and right of the standing wave is precisely supported by a Dirac measure on the half-line $(x = 0, t > 0)$ represented in blue in the above figure. Thus Proposition 1.3.9 shows that there exists a solution in the sense of Definition 1.3.2 which is a piecewise constant function with non zero mass flux across the standing wave $[\alpha\rho w]^0 = a(\alpha_R - \alpha_L) \neq 0$.

Proposition 1.3.9. *Let $\mathbb{W}_L$ and $\mathbb{W}_R$ be two positive states in Ω^r. The Riemann problem (1.3.5)-(1.3.11) admits a solution in the sense of Definition 1.3.2 with signature $< 0, 2 >$ $+ \delta_0$, if*

$$\nu > 1, \quad w^\sharp > 0 \quad \text{and} \quad \mathcal{M}_L = 1. \tag{1.3.70}$$

The intermediate states are given by

$$\tau_2 = \tau_L^\sharp, \qquad w_2 = w^\sharp = a\tau_L^\sharp, \qquad \mathcal{T}_2 = \mathcal{T}_L, \tag{1.3.71}$$

$$\tau_3 = \tau_R^\sharp, \qquad w_3 = w^\sharp = a\tau_L^\sharp, \qquad \mathcal{T}_3 = \mathcal{T}_R. \tag{1.3.72}$$

The mass flux across the standing wave is non zero:

$$[\alpha\rho w]^0 = a(\alpha_R - \alpha_L). \tag{1.3.73}$$

Moreover, this solution dissipates energy across the standing wave, and the dissipation is completely determined by the initial condition:

$$[\alpha\rho w\mathcal{E} + \alpha\pi w]^0 = a(\alpha_R - \alpha_L)\left(\frac{a^2\mathcal{T}_L^2}{2} + e(\mathcal{T}_L) + p_L\mathcal{T}_L\right), \tag{1.3.74}$$

which is negative since $\alpha_R < \alpha_L$.

Proof. The intermediate states are obtained by passing to the limit as $\mathcal{M}_L \to 1^-$ in the expressions (1.3.36)-(1.3.38) of the intermediate states of signature $< 1, 2 >$. Note that when $\mathcal{M}_L \to 1^-$, we have $\mathcal{M}_L^\sharp \to 1^-$ and $\mathcal{M} = \mathcal{M}_0 \to \frac{1}{\nu}$. Easy manipulations show that the jump relations corresponding to the w and $w + a\tau$ waves are satisfied. Indeed $\pi_2 = \pi(\tau_L^\sharp, \mathcal{T}_L) = \pi^\sharp = \pi(\tau_R^\sharp, \mathcal{T}_R) = \pi_3$, and therefore we have

$$[\alpha, w, \pi]^w = 0 \qquad \text{and} \qquad [\alpha, w + a\tau, \mathcal{T}]^{w+a\tau} = 0. \tag{1.3.75}$$

This implies that equations (1.3.15) and (1.3.16) are satisfied for all test functions (φ_1, φ_2) in $\mathcal{D}(\mathbb{R}_x^* \times \mathbb{R}_t^+)$, as well as equation (1.3.17) for any given ψ in $\mathcal{D}(\mathbb{R}^* \times \mathbb{R}_t^+)$. If ψ belongs to $\mathcal{D}(\mathbb{R} \times \mathbb{R}_t^+)$, it is sufficient to assume that $\mathrm{supp}(\psi)$ does not contain any other wave than the standing one. We denote by $\Omega^- = \mathrm{supp}(\psi) \cap \{(x < 0, t > 0)\}$ and $\Omega^+ = \mathrm{supp}(\psi) \cap \{(x > 0, t > 0)\}$. We also divide the boundary of $\mathrm{supp}(\psi)$ into three curves Γ_0, Γ^- and Γ^+, as shown in the figure below. Finally, we denote $\Sigma = \mathrm{supp}(\psi) \cap \{x = 0, t > 0\}$.

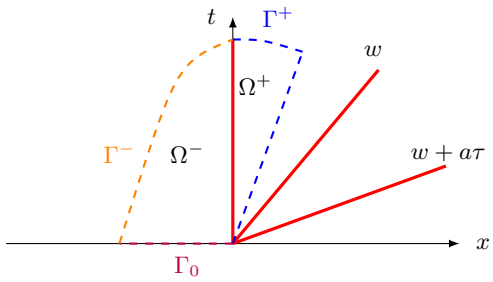

As we decided to represent the solution by functions, any integral of the solution on a bounded domain is well-defined and we can write

$$\begin{aligned}\int_{\mathbb{R}_x \times \mathbb{R}_t^+} \{(\alpha\rho)\partial_t\psi + (\alpha\rho w)\partial_x\psi\}\, dxdt &= \int_{\Omega^-} \{(\alpha\rho)\partial_t\psi + (\alpha\rho w)\partial_x\psi\}\, dxdt \\ &\quad + \int_{\Omega^+} \{(\alpha\rho)\partial_t\psi + (\alpha\rho w)\partial_x\psi\}\, dxdt \qquad (1.3.76)\end{aligned}$$

with

$$\begin{aligned}\int_{\Omega^-} \{(\alpha\rho)\partial_t\psi + (\alpha\rho w)\partial_x\psi\}\, dxdt &= \int_{\Omega^-} \mathrm{div}_{t,x}\left(\alpha_L\rho_L\psi, \alpha_L\rho_L w_L\psi\right) dxdt \\ &= \int_{\Gamma_0} \{(\alpha_L\rho_L\psi)n_t + (\alpha_L\rho_L w_L\psi)n_x\}\, d\Gamma_0 \\ &+ \int_{\Sigma} \{(\alpha_L\rho_L\psi)n_t + (\alpha_L\rho_L w_L\psi)n_x\}\, d\Sigma \\ &+ \underbrace{\int_{\Gamma^-} \{(\alpha_L\rho_L\psi)n_t + (\alpha_L\rho_L w_L\psi)n_x\}\, d\Gamma^-}_{=0}\end{aligned}$$

where (n_x, n_t) is the unit normal vector to the boundary pointing outside of $\mathrm{supp}(\psi)$. Hence

$$\int_{\Omega^-} \{(\alpha\rho)\partial_t\psi + (\alpha\rho w)\partial_x\psi\}\, dxdt = -\int_{-\infty}^{0} (\alpha\rho)_0(x)\psi(x,0)dx + \int_0^{+\infty} (\alpha_L\rho_L w_L)\psi(0,t)dt \qquad (1.3.77)$$

and in the same way, we show that

$$\int_{\Omega^+} \{(\alpha\rho)\partial_t\psi + (\alpha\rho w)\partial_x\psi\}\, dxdt = -\int_0^{+\infty} (\alpha_2\rho_2 w_2)\psi(0,t)dt. \qquad (1.3.78)$$

Casting this in (1.3.76), we get (1.3.17). □

Proof of the main result Theorem 1.3.4

In sections 1.3.3 and 1.3.3, we constructed solutions for $w^\sharp \geq 0$. These solutions correspond to a material wave with positive speed $w \geq 0$. We can also construct the symmetric solutions for $w^\sharp < 0$ which are denoted by $< 2,1 >$, $< 3,0 >$, $< 2,0 >$ and $< 2,0 > \ + \delta_0$ with clear notations. Thanks to the Gallilean invariance of system (1.3.5) (see [12]), the intermediate states of these symmetric solutions are obtained by exchanging the subscripts L and R and by applying the mapping $(\alpha, \alpha\rho, \alpha\rho w, \alpha\rho\mathcal{T}) \mapsto (\alpha, \alpha\rho, -\alpha\rho w, \alpha\rho\mathcal{T})$ to the solutions constructed above. The details are left to the reader. Finally the proof of theorem 1.3.4 is straightforward. If the constant a is such that $\tau_L^\sharp > 0$ and $\tau_R^\sharp > 0$, then Propositions 1.3.5, 1.3.6, 1.3.7, 1.3.8 and 1.3.9 as well as their symmetric counterparts show that, for all positive initial sates $\mathbb{W}_L$ and $\mathbb{W}_R$, there exists a solution in the sense of Definition 1.3.2. Indeed, the conditions stated in the propositions cover the whole domain of initial conditions $\Omega^r \times \Omega^r$. □

1.4 Numerical approximation

In this section, we use the relaxation approximation defined in section 1.3 in order to derive a numerical scheme for approximating the entropy weak solutions of the equilibrium system (1.2.1). We consider a Cauchy problem

$$\begin{cases} \partial_t \mathbb{U} + \partial_x \mathbf{f}(\mathbb{U}) + \mathbf{c}(\mathbb{U})\partial_x \mathbb{U} = 0, & x \in \mathbb{R}, t > 0, \\ \mathbb{U}(x,0) = \mathbb{U}_0(x). \end{cases} \tag{1.4.1}$$

For simplicity in the notations, we assume a constant positive time step Δt and a constant space step $\Delta x > 0$ and we define $\lambda = \frac{\Delta t}{\Delta x}$. We introduce a partition of the space $\mathbb{R} = \bigcup_{j\in\mathbb{Z}} [x_{j-\frac{1}{2}}, x_{j+\frac{1}{2}}[$ where $x_{j+\frac{1}{2}} - x_{j-\frac{1}{2}} = \Delta x$ for all j in $\mathbb{Z}$. We also introduce the discrete intermediate times $t^n = n\Delta t,\ n \in \mathbb{N}$. The approximate solution at time t^n, $x \in \mathbb{R} \mapsto \mathbb{U}_\lambda(x, t^n) \in \Omega$ is a piecewise constant function whose value on each cell $C_j = [x_{j-\frac{1}{2}}, x_{j+\frac{1}{2}}[$ is a constant value denoted by $\mathbb{U}_j^n$:

$$\mathbb{U}_\lambda(x, t^n) = \mathbb{U}_j^n, \quad \text{for all} \quad x \text{ in } C_j, \quad j \text{ in } \mathbb{Z}, \quad \text{in } n \in \mathbb{N}. \tag{1.4.2}$$

Endwise, we denote by $x_j = \frac{1}{2}(x_{j-\frac{1}{2}} + x_{j+\frac{1}{2}})$ the center of each cell C_j. At time $t = 0$, we use the initial condition $\mathbb{U}_0$ to define the sequence $(\mathbb{U}_j^0)_{j\in\mathbb{Z}}$ by

$$\mathbb{U}_j^0 = \frac{1}{\Delta x} \int_{x_{j-\frac{1}{2}}}^{x_{j+\frac{1}{2}}} \mathbb{U}_0(x)dx, \qquad j \text{ in } \mathbb{Z}. \tag{1.4.3}$$

1.4.1 The relaxation method

We now describe the two-step splitting method associated with the relaxation system (1.3.1) in order to calculate $\mathbb{U}_\lambda(\cdot, t^{n+1})$ from $\mathbb{U}_\lambda(\cdot, t^n)$. The first step consists in a time-advancing step for the convective part of the relaxation system (1.3.1), and the second step takes into account the

relaxation source term. We first introduce the piecewise constant approximate solution at time t^n of system (1.3.5) $x \mapsto \mathbb{W}_\lambda(x,t^n) = \mathbb{W}_j^n$ in C_j with

$$\mathbb{W}_j^n = \begin{bmatrix} \alpha_j^n \\ (\alpha\rho)_j^n \\ (\alpha\rho w)_j^n \\ (\alpha\rho\mathcal{T})_j^n \end{bmatrix}. \tag{1.4.4}$$

At time $t=0$, $\mathbb{W}_j^0$ is set at equilibrium which means that $(\alpha\rho\mathcal{T})_j^0 = \alpha_j^0$. The two steps are defined as follows.

Step 1: Evolution in time ($t^n \to t^{n+1-}$)

In the first step, the following Cauchy problem is exactly solved for $t \in [0,\Delta t]$ with Δt small enough (see condition (1.4.6) below)

$$\begin{cases} \partial_t \widetilde{\mathbb{W}} + \partial_x \mathbf{g}(\widetilde{\mathbb{W}}) + \mathbf{d}(\widetilde{\mathbb{W}})\partial_x \widetilde{\mathbb{W}} = 0, \\ \widetilde{\mathbb{W}}(x,0) = \mathbb{W}_\lambda(x,t^n). \end{cases} \tag{1.4.5}$$

Since $x \mapsto \mathbb{W}_\lambda(x,t^n)$ is piecewise constant, the exact solution of (1.4.5) is obtained by gluing together the solutions of the Riemann problems set at each cell interface $x_{j+\frac{1}{2}}$, provided that these solutions do not interact during the period Δt, *i.e.* provided the following classical CFL condition

$$\frac{\Delta t}{\Delta x} \max_{\mathbb{W}} |\sigma_i^r(\mathbb{W})| < \frac{1}{2}, \ i \in \{0,...,3\}, \tag{1.4.6}$$

for all the $\mathbb{W}$ under consideration. More precisely,

$$\text{If} \quad (x,t) \in [x_j, x_{j+1}] \times [0,\Delta t], \quad \text{then} \quad \widetilde{\mathbb{W}}_\lambda(x,t) = \mathbb{W}_r\left(\frac{x - x_{j+1/2}}{t}; \mathbb{W}_j^n, \mathbb{W}_{j+1}^n\right), \tag{1.4.7}$$

where $(x,t) \mapsto \mathbb{W}_r\left(\frac{x}{t}; \mathbb{W}_L, \mathbb{W}_R\right)$ is the solution of the Riemann problem

$$\begin{cases} \partial_t \mathbb{W} + \partial_x \mathbf{g}(\mathbb{W}) + \mathbf{d}(\mathbb{W})\partial_x \mathbb{W} = 0, \\ \\ \mathbb{W}(x,0) = \begin{cases} \mathbb{W}_L & \text{if} \quad x < 0, \\ \mathbb{W}_R & \text{if} \quad x > 0. \end{cases} \end{cases} \tag{1.4.8}$$

constructed in section 1.3. In order to define a piecewise constant approximate solution at time t^{n+1-}, the solution $\widetilde{\mathbb{W}}_\lambda(x,t)$ is averaged on each cell C_j at time Δt:

$$\mathbb{W}_\lambda(x,t^{n+1-}) = \mathbb{W}_j^{n+1-} = \begin{bmatrix} \alpha_j^{n+1-} \\ (\alpha\rho)_j^{n+1-} \\ (\alpha\rho w)_j^{n+1-} \\ (\alpha\rho\mathcal{T})_j^{n+1-} \end{bmatrix} = \frac{1}{\Delta x}\int_{x_{j-\frac{1}{2}}}^{x_{j-\frac{1}{2}}} \widetilde{\mathbb{W}}_\lambda(x,\Delta t)dx, \quad \forall x \in C_j, \quad \forall j \in \mathbb{Z}. \tag{1.4.9}$$

Step 2: Instantaneous relaxation ($t^{n+1-} \to t^{n+1}$)

In the second step, we solve at time $t^n + \Delta t$ the ordinary differential equation

$$\partial_t \mathbb{W}^\varepsilon = \frac{1}{\varepsilon}\mathcal{R}(\mathbb{W}^\varepsilon), \tag{1.4.10}$$

in the asymptotic regime $\varepsilon \to 0$. As an initial condition, we take the function $\mathbb{W}_\lambda(x, t^{n+1-})$ obtained at the end of the first step. Using the definition (1.3.4) of the relaxation term $\mathcal{R}$, we see that this amounts to imposing $\mathcal{T}_j^{n+1} := \tau_j^{n+1}$, thus we have

$$\mathbb{W}_j^{n+1} = \begin{bmatrix} \alpha_j^{n+1-} \\ (\alpha\rho)_j^{n+1-} \\ (\alpha\rho w)_j^{n+1-} \\ \alpha_j^{n+1-} \end{bmatrix}, \tag{1.4.11}$$

and the new cell value at time t^{n+1} of the approximate solution $\mathbb{U}_\lambda(\cdot, t^{n+1})$ is given by

$$\mathbb{U}_j^{n+1} = \begin{bmatrix} \alpha_j^{n+1-} \\ (\alpha\rho)_j^{n+1-} \\ (\alpha\rho w)_j^{n+1-} \end{bmatrix}. \tag{1.4.12}$$

This completes the description of the two-step relaxation method.

Remark 1.4.1 (**Choice of the parameter** a)**.** *In the first step, the solution of the Riemann problem at each interface $x_{j+\frac{1}{2}}$ always exists if the constant a is chosen large enough. As a matter of fact, at each interface, since $\mathbb{W}_L$ and $\mathbb{W}_R$ are set to equilibrium, we have $\mathcal{T}_L = \tau_L$ and $\mathcal{T}_R = \tau_R$. Thus*

$$\tau_L^\sharp = \tau_L + \frac{1}{2a}(w_R - w_L) - \frac{1}{2a^2}\left(p(\tau_R) - p(\tau_L)\right), \tag{1.4.13}$$

$$\tau_R^\sharp = \tau_R + \frac{1}{2a}(w_R - w_L) + \frac{1}{2a^2}\left(p(\tau_R) - p(\tau_L)\right), \tag{1.4.14}$$

and if a is taken large enough, we ensure that $\tau_L^\sharp > 0$ and $\tau_R^\sharp > 0$ since τ_L and τ_R are strictly positive. Besides, a can be chosen locally at each interface $x_{j+\frac{1}{2}}$ since the Riemann problems do not interact under the CFL condition (1.4.6), and it can be chosen so as to avoid any non classical solution with a mass concentration at one of the interfaces, this in order to guarantee the conservativity of the partial mass $\alpha\rho$ in the method (see Property 1.4.3 and section 1.4.5).

1.4.2 Finite volume formulation

It this section, we show that the two-step relaxation method described in the previous section can be written in the form of a non conservative finite volume scheme

$$\mathbb{U}_j^{n+1} = \mathbb{U}_j^n - \frac{\Delta t}{\Delta x}\left(\mathcal{F}^-_{j+\frac{1}{2}} - \mathcal{F}^+_{j-\frac{1}{2}}\right), \tag{1.4.15}$$

where $\mathcal{F}^-_{j+\frac{1}{2}} = \mathcal{F}^-(\mathbb{U}^n_j, \mathbb{U}^n_{j+1})$ and $\mathcal{F}^+_{j-\frac{1}{2}} = \mathcal{F}^+(\mathbb{U}^n_{j-1}, \mathbb{U}^n_j)$ are the left and right numerical fluxes at the cell interfaces $x_{j-\frac{1}{2}}$ and $x_{j+\frac{1}{2}}$. Here, the left and right fluxes $\mathcal{F}^-$ and $\mathcal{F}^+$ are two distinct functions in order to take into account the non conservative product.

The first step of the relaxation method shows that $\mathbb{W}_\lambda(x,t)$ is the **exact** solution of

$$\partial_t \mathbb{W} + \partial_x \mathbf{g}(\mathbb{W}) + \mathbf{d}(\mathbb{W})\partial_x \mathbb{W} = 0, \tag{1.4.16}$$

on $\mathbb{R} \times [t^n, t^{n+1}]$ with the initial data $\mathbb{W}_\lambda(x, t^n) = \mathbb{W}^n_j$ for all x in C_j, with j in $\mathbb{Z}$. Integrating on the rectangle $C_j \times [t^n, t^{n+1}]$, we get

$$\mathbb{W}^{n+1-}_j = \mathbb{W}^n_j - \frac{\Delta t}{\Delta x}\left(\mathbf{g}(\mathbb{W}_r(0^-; \mathbb{W}^n_j, \mathbb{W}^n_{j+1})) - \mathbf{g}(\mathbb{W}_r(0^+; \mathbb{W}^n_{j-1}, \mathbb{W}^n_j))\right), \tag{1.4.17}$$

since $\alpha = \alpha^n_j$ is constant on $C_j \times [t^n, t^{n+1}]$ so that the product $\mathbf{d}(\mathbb{W})\partial_x \mathbb{W}$ identically vanishes within C_j. We then recall that the initial values $\mathbb{W}^n_j$ are set to equilibrium which means that $\mathbb{W}^n_j = (\mathbb{U}^n_j, \alpha^n_j)$, *i.e.* $\mathbb{W}^n_j = \mathscr{M}(\mathbb{U}^n_j)$ where the mapping $\mathscr{M}$ is defined as

$$\begin{aligned} \mathscr{M} : \quad \mathbb{R}^3 &\longrightarrow \mathbb{R}^4 \\ (x,y,z) &\longmapsto (x,y,z,x). \end{aligned} \tag{1.4.18}$$

This mapping, which happens here to be linear, maps $\mathbb{U}$ to its so-called *maxwellian equilibrium* $\mathscr{M}(\mathbb{U})$ according to the terminology used in [4]. Moreover, the relaxation step shows that $\mathbb{U}^{n+1}_j = \mathscr{P}\mathbb{W}^{n+1-}_j$ where $\mathscr{P}$ is the linear operator

$$\begin{aligned} \mathscr{P} : \quad \mathbb{R}^4 &\longrightarrow \mathbb{R}^3 \\ (x,y,z,t) &\longmapsto (x,y,z). \end{aligned} \tag{1.4.19}$$

Eventually, when applying operator $\mathscr{P}$ to equation (1.4.17) (note that $\mathscr{P} \circ \mathscr{M} = Id_{\mathbb{R}^3}$) we obtain the finite volume formulation of our scheme

$$\mathbb{U}^{n+1}_j = \mathbb{U}^n_j - \frac{\Delta t}{\Delta x}\left(\mathcal{F}^-(\mathbb{U}^n_j, \mathbb{U}^n_{j+1}) - \mathcal{F}^+(\mathbb{U}^n_{j-1}, \mathbb{U}^n_j)\right), \tag{1.4.20}$$

with

$$\mathcal{F}^\pm(\mathbb{U}_L, \mathbb{U}_R) = \mathscr{P}\ \mathbf{g}\left(\mathbb{W}_r\left(0^\pm; \mathscr{M}(\mathbb{U}_L), \mathscr{M}(\mathbb{U}_R)\right)\right). \tag{1.4.21}$$

In the sequel, $\mathcal{F}^\pm_\alpha$, $\mathcal{F}^\pm_{\alpha\rho}$ and $\mathcal{F}^\pm_{\alpha\rho w}$ are respectively the first, the second and the third coordinates of the fluxes vectors $\mathcal{F}^-$ and $\mathcal{F}^+$. In practice, it is the finite volume formulation that is used to implement the numerical simulation. Subsequently, we denote by $(\mathcal{RS})$ the relaxation scheme described in sections 1.4.1-1.4.2, and whose finite volume form is given by equations (1.4.20)-(1.4.21). In the following two sections, we state the main properties of the relaxation scheme.

1.4.3 Basic properties of the scheme

The relaxation approximation method provides a very convenient framework for the L^1-stability of finite volume methods since the preservation of the phase space Ω by the scheme is almost straightforward. Indeed, the following property states the positivity of the approximated values of the section α^n_j as well as the the positivity of the partial masses $(\alpha\rho)^n_j$.

Property 1.4.1 (L^1**-stability**). *Under the CFL condition (1.4.6), the relaxation Finite Volume scheme* $(\mathcal{RS})$ *preserves positive values for the section and for the density. Indeed, if the initial condition* $x \mapsto \mathbb{U}_0(x)$ *is in* Ω*, then the values* $(\mathbb{U}_j^n)_{j\in\mathbb{Z},n\in\mathbb{N}}$ *computed by the scheme are such that,*

$$\alpha_j^n = \alpha_j^0 > 0, \quad (\alpha\rho)_j^n > 0, \qquad \text{for all } j \text{ in } \mathbb{Z} \text{ and all } n \text{ in } \mathbb{N}, \tag{1.4.22}$$

that is to say, the section α *is preserved throughout time at the discrete level, and the piecewise constant approximate solution* $\mathbb{U}_\lambda(x,t)$ *is also in* Ω*.*

Proof. The first line of equation (1.4.20) reads $\alpha_j^{n+1} = \alpha_j^n$ for all j in $\mathbb{Z}$ and all n in $\mathbb{N}$. Thus, if $\alpha_j^0 > 0$, this gives the result on α_j^n. For the positivity of the partial masses $(\alpha\rho)_j^n$, it is more convenient to consider the two-step splitting formulation of the scheme. The second line of equation (1.4.9) shows that $(\alpha\rho)_j^{n+1}$ is the $\mathbb{P}_0$ projection of the partial mass in the solution $\widetilde{\mathbb{W}}_\lambda(x,\Delta t)$ of the relaxation system. Under the CFL condition (1.4.6), this solution is obtained by gluing together the Riemann solutions arising from each interface $x_{j+1/2}$. Since these solutions are positive according to Theorem 1.3.4, this concludes the proof. □

We also have the following classical consistency property for the relaxation scheme $(\mathcal{RS})$ which guarantees that the constant solutions of system (1.2.1) are exactly computed.

Property 1.4.2 (**Consistency**). *The relaxation Finite Volume scheme* $(\mathcal{RS})$ *is consistent in the sense that, for all* $\mathbb{U}$ *in the phase space* Ω*, the numerical fluxes* $\mathcal{F}^-$ *and* $\mathcal{F}^+$ *satisfy*

$$\mathcal{F}^-(\mathbb{U},\mathbb{U}) = \mathcal{F}^+(\mathbb{U},\mathbb{U}) = \mathbf{f}(\mathbb{U}), \tag{1.4.23}$$

where $\mathbf{f}(\mathbb{U})$*, which is defined in (1.2.3), is the conservative part of the exact flux of the equilibrium system (1.2.1).*

Proof. The proof is almost straightforward, denoting $\mathbb{W} = \mathscr{M}(\mathbb{U})$, we immediately see that $\mathbb{W}_r(0^\pm;\mathbb{W},\mathbb{W}) = \mathbb{W}$ (see equations (1.3.32) and (1.3.33)). And $\mathscr{P}\,\mathbf{g}(\mathbb{W}) = \mathbf{f}(\mathbb{U})$ since $\mathbb{W} = \mathscr{M}(\mathbb{U})$ is at equilibrium. □

addition, under some condition on the choice of the numerical parameter a, the relaxation method is conservative for the mass equation:

Property 1.4.3 (**Conservativity**). *Denote* $\nu_{j+\frac12} = \frac{\alpha_j^n}{\alpha_{j+1}^n}$*. If for each interface* $x_{j+\frac12}$*, the local value of the parameter* $a = a_{j+\frac12}$ *is chosen so as*

$$\begin{cases} \nu_{j+\frac12} > 1 \Longrightarrow \mathcal{M}_{L,j+\frac12} = \dfrac{w_j^n}{a_{j+\frac12}\tau_j^n} \neq 1, \\[2ex] \nu_{j+\frac12} < 1 \Longrightarrow \mathcal{M}_{R,j+\frac12} = \dfrac{w_{j+1}^n}{a_{j+\frac12}\tau_{j+1}^n} \neq -1, \end{cases} \tag{1.4.24}$$

then the relaxation scheme $(\mathcal{RS})$ *is conservative for the partial mass* $\alpha\rho$*, in the sense that*

$$\mathcal{F}_{\alpha\rho}^-(\mathbb{U}_j^n,\mathbb{U}_{j+1}^n) = \mathcal{F}_{\alpha\rho}^+(\mathbb{U}_j^n,\mathbb{U}_{j+1}^n) \quad \text{for all } j \text{ in } \mathbb{Z}. \tag{1.4.25}$$

Proof. We have

$$\mathcal{F}^+_{\alpha\rho}(\mathbb{U}^n_j,\mathbb{U}^n_{j+1})-\mathcal{F}^-_{\alpha\rho}(\mathbb{U}^n_j,\mathbb{U}^n_{j+1})=[\alpha\rho w]^0\left(\mathbb{W}_r(\ .\ ;\mathscr{M}(\mathbb{U}^n_j),\mathscr{M}(\mathbb{U}^n_{j+1}))\right). \tag{1.4.26}$$

If $a_{j+\frac{1}{2}}$ is chosen as in (1.4.24), then the solution $\mathbb{W}_r(\ .\ ;\mathscr{M}(\mathbb{U}^n_j),\mathscr{M}(\mathbb{U}^n_{j+1}))$ of the relaxation Riemann problem is a classical solution without mass concentration at $x=x_{j+\frac{1}{2}}$. Hence $[\alpha\rho w]^0=0$. □

Property 1.4.4 (Well-balanced property). *The relaxation scheme ($\mathcal{RS}$) exactly preserves the steady states at rest: $w=0$ and $\rho=cst$. Indeed, if there exists $w^0\in\mathbb{R}$ and $\rho^0>0$ such that $(\alpha\rho w)^0_j=0$ and $\frac{(\alpha\rho)^0_j}{\alpha^0_j}=\rho^0$ for all j in $\mathbb{Z}$ then*

$$(\alpha\rho w)^n_j=0\quad\text{and}\quad\frac{(\alpha\rho)^n_j}{\alpha^n_j}=\rho^0,\quad\text{for all } j \text{ in } \mathbb{Z} \text{ and all } n \text{ in } \mathbb{N}. \tag{1.4.27}$$

Proof. Let us assume that at time t^n, $(\alpha\rho w)^n_j=0$ and $\frac{(\alpha\rho)^n_j}{\alpha^n_j}=\rho^0$ for all j in $\mathbb{Z}$, *i.e.* $w^n_j=0$ and $\rho^n_j=\rho^0$ for all j in $\mathbb{Z}$. At each interface, one has $w_L=w_R=0$ and $\tau_L=\tau_R=1/\rho^0$. Hence $w^\sharp=0$ and the solution has the signature $<1,1>$ with $w^-=w^+=0$ and $\tau^\sharp_L=\tau^\sharp_R=1/(\rho^0)$ *i.e.* all the intermediate states are at equilibrium ($w=0$ and $\rho=\rho^0$). After averaging the solution we obtain $(\alpha\rho w)^{n+1}_j=0$ and $\frac{(\alpha\rho)^{n+1}_j}{\alpha^{n+1}_j}=\rho^0$ for all j in $\mathbb{Z}$. The proof follows from an induction argument. □

1.4.4 Non linear stability

General points

Non linear stability matters are usually dealt with through a so-called *discrete entropy inequality*. Before describing what a discrete entropy inequality is, let us briefly recall what an *entropy* is:

Definition 1.4.1. *An entropy associated with the system*

$$\partial_t\mathbb{U}+\partial_x\boldsymbol{f}(\mathbb{U})+\boldsymbol{c}(\mathbb{U})\partial_x\mathbb{U}=0, \tag{1.4.28}$$

is a real valued function $\eta(\mathbb{U})$ such that there exists $\mathcal{G}(\mathbb{U})\in\mathbb{R}$ such that the smooth solutions of (1.4.28) satisfy the following additional conservation law

$$\partial_t\eta(\mathbb{U})+\partial_x\mathcal{G}(\mathbb{U})=0. \tag{1.4.29}$$

The real valued function $\mathcal{G}(\mathbb{U})$ is called the entropy flux associated with the entropy η.

Of course, if $\mathbb{U}(x,t)$ is a discontinuous solution, (1.4.29) cannot be exactly satisfied and a common criterion to select weak solutions is to impose an *entropy inequality*

$$\partial_t\eta(\mathbb{U})+\partial_x\mathcal{G}(\mathbb{U})\leq 0. \tag{1.4.30}$$

for non smooth weak solutions. If η is convex, this can be formally justified by the vanishing viscosity method (see [12]). Let us now assume that a non conservative finite volume scheme is used to approximate the solutions of (1.4.28):

$$\mathbb{U}_j^{n+1} = \mathbb{U}_j^n - \frac{\Delta t}{\Delta x}\left(\mathcal{F}^-(\mathbb{U}_j^n, \mathbb{U}_{j+1}^n) - \mathcal{F}^+(\mathbb{U}_{j-1}^n, \mathbb{U}_j^n)\right). \tag{1.4.31}$$

We have the following stability definition

Definition 1.4.2. *We say that the numerical scheme (1.4.31) satisfies a discrete entropy inequality associated with the entropy η if there exists a numerical entropy flux $G(\mathbb{U}_L, \mathbb{U}_R)$ which is consistent with the exact entropy flux $\mathcal{G}$ (in the sense that $G(\mathbb{U}, \mathbb{U}) = \mathcal{G}(\mathbb{U})$ for all $\mathbb{U}$ in Ω) such that, under some CFL condition, the discrete values computed by (1.4.31) automatically satisfy*

$$\eta(\mathbb{U}_j^{n+1}) - \eta(\mathbb{U}_j^n) + \frac{\Delta t}{\Delta x}(G(\mathbb{U}_j^n, \mathbb{U}_{j+1}^n) - G(\mathbb{U}_{j-1}^n, \mathbb{U}_j^n)) \leq 0. \tag{1.4.32}$$

This can be seen as a stability condition because if we denote by $\sum_{j\in\mathbb{Z}} \eta(\mathbb{U}_j^n)\Delta x$ the discrete L^1-norm of the total entropy at time t^n, then summing inequality (1.4.32) over the cells yields

$$\sum_{j\in\mathbb{Z}} \eta(\mathbb{U}_j^{n+1})\Delta x \leq \sum_{j\in\mathbb{Z}} \eta(\mathbb{U}_j^n)\Delta x, \quad \text{for all } n \text{ in } \mathbb{N}, \tag{1.4.33}$$

which means that the total entropy is decreasing in time.

According to Definition 1.2.1, $\alpha\rho E$ with $E(\mathbb{U}) = \frac{w^2}{2} + e(\tau)$ is an entropy for the equilibrium system and the associated entropy flux is given by $\mathcal{G}(\mathbb{U}) = \alpha\rho w E + \alpha w p$. Similarly, by Proposition 1.3.2, $\alpha\rho\mathcal{E}$ with $\mathcal{E}(\mathbb{W}) = \dfrac{w^2}{2} + e(\mathcal{T}) + \dfrac{1}{2a^2}(\pi^2(\tau, \mathcal{T}) - p^2(\mathcal{T}))$ is an entropy for the relaxation system and the associated entropy flux reads $\mathcal{G}_r(\mathbb{W}) = \alpha\rho w\mathcal{E} + \alpha w\pi$.

Sufficient conditions for the discrete entropy inequality

The aim of this section is to exhibit sufficient conditions on the constant a, which so far is still not determined, that ensure a discrete entropy inequality of the form

$$(\alpha\rho E)(\mathbb{U}_j^{n+1}) - (\alpha\rho E)(\mathbb{U}_j^n) + \frac{\Delta t}{\Delta x}(G(\mathbb{U}_j^n, \mathbb{U}_{j+1}^n) - G(\mathbb{U}_{j-1}^n, \mathbb{U}_j^n)) \leq 0, \tag{1.4.34}$$

with the numerical entropy flux $G(\mathbb{U}_L, \mathbb{U}_R)$ to be determined. Recall that the non conservative numerical fluxes of the scheme are given by

$$\mathcal{F}^-(\mathbb{U}_j^n, \mathbb{U}_{j+1}^n) = \mathscr{P}\,\mathbf{g}(\mathbb{W}_r(0^-; \mathscr{M}(\mathbb{U}_j^n), \mathscr{M}(\mathbb{U}_{j+1}^n))), \tag{1.4.35}$$

$$\mathcal{F}^+(\mathbb{U}_{j-1}^n, \mathbb{U}_j^n) = \mathscr{P}\,\mathbf{g}(\mathbb{W}_r(0^+; \mathscr{M}(\mathbb{U}_{j-1}^n), \mathscr{M}(\mathbb{U}_j^n))), \tag{1.4.36}$$

where each Riemann solution $\mathbb{W}_r(\xi; \mathscr{M}(\mathbb{U}_{j-1}^n), \mathscr{M}(\mathbb{U}_j^n))$ and $\mathbb{W}_r(\xi; \mathscr{M}(\mathbb{U}_j^n), \mathscr{M}(\mathbb{U}_{j+1}^n))$ clearly depends on the local choice of the constant a, denoted by $a_{j+\frac{1}{2}}$. A classical condition on $a_{j+\frac{1}{2}}$ is the so-called *Whitham condition* reading (see [4, 1])

Definition 1.4.3. *The parameter $a_{j+\frac{1}{2}}$ is said to satisfy the* ***classical Whitham condition*** *if $a_{j+\frac{1}{2}}$ is such that*

$$a_{j+\frac{1}{2}}^2 > \max\left(-\partial_\tau p(\tau), -\partial_\tau p(\mathcal{T})\right), \tag{1.4.37}$$

for all τ and all $\mathcal{T}$ encountered in the solution $\mathbb{W}_r(\xi; \mathscr{M}(\mathbb{U}_j^n), \mathscr{M}(\mathbb{U}_{j+1}^n))$ of the relaxation Riemann problem defined by $\mathbb{U}_j^n$ and $\mathbb{U}_{j+1}^n$.

A well-known result is that if $a_{j+\frac{1}{2}}$ satisfies this condition for all j in $\mathbb{Z}$ and at every time t^n then the relaxation approximation method satisfies a discrete entropy inequality (1.4.34) (see again [4]). However, for solutions near the resonance phenomenon, we have seen that the specific volume τ might be close to zero near the standing wave, thus making it meaningless to enforce the *classical Whitham condition*. Indeed, $-\partial_\tau p(\tau)$ tends to $+\infty$ as τ goes to 0. In the sequel, we exhibit a less restrictive condition on a that still ensures a discrete entropy inequality of the form (1.4.34) but that can also handle resonant solutions. This new condition will be referred to as the *weak Whitham condition*. We start by defining some useful notations.

Definition 1.4.4. *Let Δx and Δt be respectively a space and a time steps, and let σ be a real number in the interval $\left]-\frac{\Delta x}{2\Delta t}, \frac{\Delta x}{2\Delta t}\right[$. For any given self-similar function $X(x/t)$ in $L^1_{loc}(\mathbb{R}_\xi)$ with $\xi = x/t$, we introduce the following space averages of X at time $t = \Delta t$:*

$$\langle X\rangle^L = \frac{2}{\Delta x}\int_{-\frac{\Delta x}{2}}^0 X(x/\Delta t)dx = \frac{2\Delta t}{\Delta x}\int_{-\frac{\Delta x}{2\Delta t}}^0 X(\xi)d\xi, \tag{1.4.38}$$

$$\langle X\rangle^R = \frac{2}{\Delta x}\int_0^{\frac{\Delta x}{2}} X(x/\Delta t)dx = \frac{2\Delta t}{\Delta x}\int_0^{\frac{\Delta x}{2\Delta t}} X(\xi)d\xi, \tag{1.4.39}$$

<u>If $\sigma > 0$,</u> define

$$\langle X\rangle^1 = \frac{1}{\sigma\Delta t}\int_0^{\sigma\Delta t} X(x/\Delta t)dx = \frac{1}{\sigma}\int_0^{\sigma} X(\xi)d\xi, \tag{1.4.40}$$

$$\langle X\rangle^2 = \frac{1}{\frac{\Delta x}{2} - \sigma\Delta t}\int_{\sigma\Delta t}^{\frac{\Delta x}{2}} X(x/\Delta t)dx = \frac{1}{\frac{\Delta x}{2\Delta t} - \sigma}\int_{\sigma}^{\frac{\Delta x}{2\Delta t}} X(\xi)d\xi, \tag{1.4.41}$$

then $\langle X\rangle^R$ is a convex combination of $\langle X\rangle^1$ and $\langle X\rangle^2$:

$$\langle X\rangle^R = 2\sigma\frac{\Delta t}{\Delta x}\langle X\rangle^1 + \left(1 - 2\sigma\frac{\Delta t}{\Delta x}\right)\langle X\rangle^2. \tag{1.4.42}$$

<u>If $\sigma < 0$,</u> define

$$\langle X\rangle^1 = \frac{1}{\sigma\Delta t + \frac{\Delta x}{2}}\int_{-\frac{\Delta x}{2}}^{\sigma\Delta t} X(x/\Delta t)dx = \frac{1}{\sigma + \frac{\Delta x}{2\Delta t}}\int_{-\frac{\Delta x}{2\Delta t}}^{\sigma} X(\xi)d\xi, \tag{1.4.43}$$

$$\langle X\rangle^2 = \frac{1}{|\sigma|\Delta t}\int_{\sigma\Delta t}^0 X(x/\Delta t)dx = \frac{1}{|\sigma|}\int_{\sigma}^0 X(\xi)d\xi, \tag{1.4.44}$$

then $\langle X\rangle^L$ is a convex combination of $\langle X\rangle^1$ and $\langle X\rangle^2$:

$$\langle X\rangle^L = \left(1 + 2\sigma\frac{\Delta t}{\Delta x}\right)\langle X\rangle^1 + 2|\sigma|\frac{\Delta t}{\Delta x}\langle X\rangle^2. \tag{1.4.45}$$

Provided that $1/X$ belongs to $L^1_{loc}(\mathbb{R}_\xi)$, we also define the ***harmonic mean*** *of a strictly positive self-similar function $X(x/t)$ as*

$$\widehat{X}^i = \frac{1}{\langle \frac{1}{X} \rangle^i}, \quad i \in \{L, 1, 2, R\}. \tag{1.4.46}$$

Hereunder, we state the *weak Whitham condition* on a which ensures that the relaxation scheme satisfies the discrete entropy inequality (1.4.34).

Definition 1.4.5. *Let $(\mathbb{U}_L, \mathbb{U}_R)$ be two admissible initial states, and let*

$$\mathbb{U}_{app}(\xi; \mathbb{U}_L, \mathbb{U}_R) = \mathscr{P}\mathbb{W}_r(\xi; \mathscr{M}(\mathbb{U}_L), \mathscr{M}(\mathbb{U}_R))$$

be the approximate solution of the Riemann problem obtained by the relaxation approximation. We denote by σ the material speed of the Riemann solution for the ***relaxation system*** *i.e. the effective value of the w-wave speed in $\mathbb{W}_r(\xi; \mathscr{M}(\mathbb{U}_L), \mathscr{M}(\mathbb{U}_R))$. Let Δx and Δt be respectively a space and a time steps satisfying the CFL condition (1.4.6).*

We say that the parameter a satisfies the ***weak Whitham condition for*** *$(\mathbb{U}_L, \mathbb{U}_R)$ if*

in the case $\sigma = 0$, a is such that

$$a^2 > \max\left(-2\int_0^1 \partial_\tau p(s\ \widehat{\tau_{app}}^L + (1-s)\tau_L)(1-s)ds, -2\int_0^1 \partial_\tau p(s\ \widehat{\tau_{app}}^R + (1-s)\tau_R)(1-s)ds \right), \tag{1.4.47}$$

in the case $\sigma > 0$, a is such that

$$a^2 > \max\left(-2\int_0^1 \partial_\tau p(s\ \widehat{\tau_{app}}^L + (1-s)\tau_L)(1-s)ds, -2\int_0^1 \partial_\tau p(s\ \widehat{\tau_{app}}^1 + (1-s)\tau_L)(1-s)ds, \right.$$
$$\left. -2\int_0^1 \partial_\tau p(s\ \widehat{\tau_{app}}^2 + (1-s)\tau_R)(1-s)ds \right), \tag{1.4.48}$$

in the case $\sigma < 0$, a is such that

$$a^2 > \max\left(-2\int_0^1 \partial_\tau p(s\ \widehat{\tau_{app}}^1 + (1-s)\tau_L)(1-s)ds, -2\int_0^1 \partial_\tau p(s\ \widehat{\tau_{app}}^2 + (1-s)\tau_R)(1-s)ds, \right.$$
$$\left. -2\int_0^1 \partial_\tau p(s\ \widehat{\tau_{app}}^R + (1-s)\tau_R)(1-s)ds \right). \tag{1.4.49}$$

Remark 1.4.2. *For strictly convex pressure laws, the weak Whitham condition is indeed less restrictive than the classical Whitham condition since we have for all $i \in \{L, 1, 2, R\}$*

$$\forall s \in [0,1], \quad s\ \widehat{\tau_{app}}^i + (1-s)\tau_L \geq \min(\widehat{\tau_{app}}^i, \tau_L) \geq \min_\tau\ \tau \Longrightarrow \min_{s\in[0,1]} \left(s\ \widehat{\tau_{app}}^i + (1-s)\tau_L \right) \geq \min_\tau\ \tau. \tag{1.4.50}$$

where $\min_{\tau}\ \tau$ *denotes the smaller specific volume in* $\mathbb{W}_r(\xi;\mathscr{M}(\mathbb{U}_L),\mathscr{M}(\mathbb{U}_R))$. *Thus, we have*

$$\max_{s\in[0,1]}\ -\partial_\tau p\left(s\ \widehat{\tau_{app}}^{\,i}+(1-s)\tau_L\right)\leq \max_{\tau}\left(\ -\partial_\tau p(\tau)\right) \tag{1.4.51}$$

since $\tau\mapsto -\partial_\tau p(\tau)$ *decreases by the strict convexity of the pressure law. Hence*

$$\begin{aligned} -2\int_0^1 \partial_\tau p(s\ \widehat{\tau_{app}}^{\,i}+(1-s)\tau_L)(1-s)ds &\leq \max_{s\in[0,1]}\ -\partial_\tau p\left(s\ \widehat{\tau_{app}}^{\,i}+(1-s)\tau_L\right)2\int_0^1(1-s)ds \\ &\leq \max_{\tau}\left(\ -\partial_\tau p(\tau)\right). \end{aligned} \tag{1.4.52}$$

In the same way, we find that for $i\in\{L,1,2,R\}$, $-2\int_0^1 \partial_\tau p(s\ \widehat{\tau_{app}}^{\,i}+(1-s)\tau_R)(1-s)ds\leq \max_{\tau}\left(\ -\partial_\tau p(\tau)\right)$ *which proves that the weak Whitham condition is less restrictive than the classical one.*

Theorem 1.4.5 shows that the weak Whitham condition is still a sufficient condition to guarantee an entropy inequality.

Theorem 1.4.5. *Under the CFL condition (1.4.6), the weak Whitham condition guarantees a discrete entropy inequality for the relaxation Finite Volume scheme* $(\mathcal{RS})$. *Indeed, assume that for all* $n\in\mathbb{N}$ *and* $j\in\mathbb{Z}$, $a_{j+\frac{1}{2}}$ *satisfies the weak Whitham condition for* $(\mathbb{U}_j^n,\mathbb{U}_{j+1}^n)$ *in the sense of Definition 1.4.5, then the relaxation scheme* $(\mathcal{RS})$ *satisfies the discrete entropy inequality*

$$(\alpha\rho E)(\mathbb{U}_j^{n+1})-(\alpha\rho E)(\mathbb{U}_j^n)+\frac{\Delta t}{\Delta x}(G(\mathbb{U}_j^n,\mathbb{U}_{j+1}^n)-G(\mathbb{U}_{j-1}^n,\mathbb{U}_j^n))\leq 0, \tag{1.4.53}$$

where the numerical entropy flux $G(\mathbb{U}_L,\mathbb{U}_R)$ *is given by* $G(\mathbb{U}_L,\mathbb{U}_R)=\mathcal{G}_r\left(\mathbb{W}_r\left(0^+;\mathscr{M}(\mathbb{U}_L),\mathscr{M}(\mathbb{U}_R)\right)\right)$.

In order to prove theorem 1.4.5, we first establish the following Lemma

Lemma 1.4.6. *Let* $(\mathbb{U}_L,\mathbb{U}_R)$ *be two given admissible states in* Ω, *and let*

$$\mathbb{U}_{app}(\xi;\mathbb{U}_L,\mathbb{U}_R)=\mathscr{P}\mathbb{W}_r(\xi;\mathscr{M}(\mathbb{U}_L),\mathscr{M}(\mathbb{U}_R))$$

be the approximate solution of the Riemann problem obtained by the relaxation approximation. We denote by σ *the material speed of the Riemann solution for the* ***relaxation system*** *i.e. the effective value of the w-wave speed in* $\mathbb{W}_r(\xi;\mathscr{M}(\mathbb{U}_L),\mathscr{M}(\mathbb{U}_R))$. *Let* Δx *and* Δt *be respectively a space and a time steps satisfying the CFL condition (1.4.6). In order to ease notations, we write* $\mathbb{U}_{app}(\xi)$ *instead of* $\mathbb{U}_{app}(\xi;\mathbb{U}_L,\mathbb{U}_R)$ *and* $\mathbb{W}_r(\xi)$ *instead of* $\mathbb{W}_r(\xi;\mathscr{M}(\mathbb{U}_L),\mathscr{M}(\mathbb{U}_R))$.

If the parameter a *satisfies the weak Whitham condition for* $(\mathbb{U}_L,\mathbb{U}_R)$ *in the sense of Definition 1.4.5, then*

if $\sigma=0$, *the following inequalities hold*

$$(\alpha\rho E)(\langle \mathbb{U}_{app}\rangle^L) - (\alpha\rho E)(\mathbb{U}_L) + \frac{2\Delta t}{\Delta x}\left(\mathcal{G}_r(\mathbb{W}_r(0^+)) - \mathcal{G}(\mathbb{U}_L)\right) \leq 0, \tag{1.4.54}$$

$$(\alpha\rho E)(\langle \mathbb{U}_{app}\rangle^R) - (\alpha\rho E)(\mathbb{U}_R) + \frac{2\Delta t}{\Delta x}\left(\mathcal{G}(\mathbb{U}_R) - \mathcal{G}_r(\mathbb{W}_r(0^+))\right) \leq 0, \tag{1.4.55}$$

if $\sigma > 0$, the following inequalities hold

$$(\alpha\rho E)(\langle \mathbb{U}_{app}\rangle^L) - (\alpha\rho E)(\mathbb{U}_L) + \frac{2\Delta t}{\Delta x}\left(\mathcal{G}_r(\mathbb{W}_r(0^+)) - \mathcal{G}(\mathbb{U}_L)\right) \leq 0, \tag{1.4.56}$$

$$(\alpha\rho E)(\langle \mathbb{U}_{app}\rangle^1) - (\alpha\rho E)(\mathbb{U}_R) + \frac{1}{\sigma}\left(\frac{1}{\Delta t}\int_0^{\Delta t} \mathcal{G}_r(\mathbb{W}_r((\sigma\Delta t)/t))dt - \mathcal{G}_r(\mathbb{W}_r(0^+))\right) \leq 0, \tag{1.4.57}$$

$$(\alpha\rho E)(\langle \mathbb{U}_{app}\rangle^2) - (\alpha\rho E)(\mathbb{U}_R) + \frac{1}{\frac{\Delta x}{2\Delta t} - \sigma}\left(\mathcal{G}(\mathbb{U}_R) - \frac{1}{\Delta t}\int_0^{\Delta t} \mathcal{G}_r(\mathbb{W}_r((\sigma\Delta t)/t))dt\right) \leq 0, \tag{1.4.58}$$

if $\sigma < 0$, the following inequalities hold

$$(\alpha\rho E)(\langle \mathbb{U}_{app}\rangle^1) - (\alpha\rho E)(\mathbb{U}_L) + \frac{1}{\sigma + \frac{\Delta x}{2\Delta t}}\left(\frac{1}{\Delta t}\int_0^{\Delta t} \mathcal{G}_r(\mathbb{W}_r((\sigma\Delta t)/t))dt - \mathcal{G}(\mathbb{U}_L)\right) \leq 0, \tag{1.4.59}$$

$$(\alpha\rho E)(\langle \mathbb{U}_{app}\rangle^2) - (\alpha\rho E)(\mathbb{U}_L) + \frac{1}{-\sigma}\left(\mathcal{G}_r(\mathbb{W}_r(0^+)) - \frac{1}{\Delta t}\int_0^{\Delta t} \mathcal{G}_r(\mathbb{W}_r((\sigma\Delta t)/t))dt\right) \leq 0, \tag{1.4.60}$$

$$(\alpha\rho E)(\langle \mathbb{U}_{app}\rangle^R) - (\alpha\rho E)(\mathbb{U}_R) + \frac{2\Delta t}{\Delta x}\left(\mathcal{G}(\mathbb{U}_R) - \mathcal{G}_r(\mathbb{W}_r(0^+))\right) \leq 0. \tag{1.4.61}$$

Proof. We only give the proof for $\sigma > 0$. The proofs for $\sigma = 0$ and $\sigma < 0$ are similar and are left to the reader. We consider the Riemann problem for the relaxation system with initial conditions at equilibrium $(\mathbb{W}_L, \mathbb{W}_R) = (\mathscr{M}(\mathbb{U}_L), \mathscr{M}(\mathbb{U}_R))$. Since the CFL condition (1.4.6) holds, all the wave speeds of the Riemann solution $\mathbb{W}_r(\xi; \mathbb{W}_L, \mathbb{W}_R)$ lie in $[-\frac{\Delta x}{2\Delta t}, \frac{\Delta x}{2\Delta t}]$. In particular, we have $0 < \sigma < \frac{\Delta x}{2\Delta t}$.

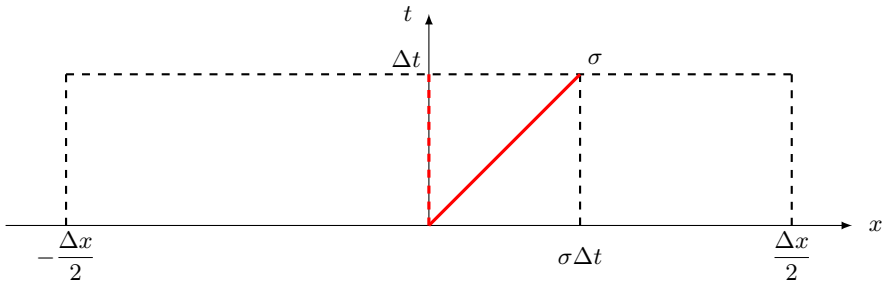

Within each rectangle $]-\frac{\Delta x}{2}, 0[\times]0, \Delta t[$, $]0, \sigma\Delta t[\times]0, \Delta t[$, and $]\sigma\Delta t, \frac{\Delta x}{2}[\times]0, \Delta t[$, the function $\mathbb{W}_r(x/t; \mathbb{W}_L, \mathbb{W}_R)$ satisfies exactly the scalar conservation law, valid for the relaxation equations

(1.3.5)

$$\partial_t \left((\alpha\rho\mathcal{E})(\mathbb{W}_r) \right) + \partial_x \left(\mathcal{G}_r(\mathbb{W}_r) \right) = 0. \tag{1.4.62}$$

Integrating this equation over $]-\frac{\Delta x}{2}, 0[\times]0, \Delta t[$, and dividing by $\frac{\Delta x}{2}$, we get

$$\frac{2\Delta t}{\Delta x} \int_{-\frac{\Delta x}{2\Delta t}}^{0} (\alpha\rho\mathcal{E})(\mathbb{W}_r(\xi))d\xi - (\alpha\rho\mathcal{E})(\mathbb{W}_L) + \frac{2\Delta t}{\Delta x} \left(\mathcal{G}_r(\mathbb{W}_r(0^-)) - \mathcal{G}_r(\mathbb{W}_L) \right) = 0. \tag{1.4.63}$$

Now, as $(\mathbb{W}_L, \mathbb{W}_R)$ are at equilibrium, we have $(\alpha\rho\mathcal{E})(\mathbb{W}_L) = (\alpha\rho E)(\mathbb{U}_L)$ and $\mathcal{G}_r(\mathbb{W}_L) = \mathcal{G}(\mathbb{U}_L)$. Moreover, the Riemann solution is constructed such that $\mathcal{G}_r(\mathbb{W}_r(0^+)) - \mathcal{G}_r(\mathbb{W}_r(0^-)) \leq 0$. Replacing in (1.4.63) this yields

$$-(\alpha\rho E)(\mathbb{U}_L) + \frac{2\Delta t}{\Delta x} \left(\mathcal{G}_r(\mathbb{W}_r(0^+)) - \mathcal{G}(\mathbb{U}_L) \right) \leq -\frac{2\Delta t}{\Delta x} \int_{-\frac{\Delta x}{2\Delta t}}^{0} (\alpha\rho\mathcal{E})(\mathbb{W}_r(\xi))d\xi. \tag{1.4.64}$$

Hence, in order to prove inequality (1.4.56) of the Lemma, it is sufficient to establish that

$$(\alpha\rho E)(\langle \mathbb{U}_{app} \rangle^L) - \frac{2\Delta t}{\Delta x} \int_{-\frac{\Delta x}{2\Delta t}}^{0} (\alpha\rho\mathcal{E})(\mathbb{W}_r(\xi))d\xi \leq 0, \tag{1.4.65}$$

which we can rewrite $(\alpha\rho E)(\langle \mathbb{U}_{app} \rangle^L) - \langle (\alpha\rho\mathcal{E})(\mathbb{W}_r) \rangle^L \leq 0$. In the same way, integrating equation (1.4.62) over $]0, \sigma\Delta t[\times]0, \Delta t[$ and dividing by $\sigma\Delta t$ gives

$$\frac{1}{\sigma} \int_0^{\sigma} (\alpha\rho\mathcal{E})(\mathbb{W}_r(\xi))d\xi - (\alpha\rho\mathcal{E})(\mathbb{W}_R) + \frac{1}{\sigma} \left(\frac{1}{\Delta t} \int_0^{\Delta t} \mathcal{G}_r(\mathbb{W}_r((\sigma\Delta t)/t))dt - \mathcal{G}_r(\mathbb{W}_r(0^+)) \right) = 0. \tag{1.4.66}$$

As the initial states are at equilibrium and using the notations of Definition 1.4.4, this reads

$$-(\alpha\rho E)(\mathbb{U}_R) + \frac{1}{\sigma} \left(\frac{1}{\Delta t} \int_0^{\Delta t} \mathcal{G}_r(\mathbb{W}_r((\sigma\Delta t)/t))dt - \mathcal{G}_r(\mathbb{W}_r(0^+)) \right) = -\langle (\alpha\rho\mathcal{E})(\mathbb{W}_r) \rangle^1. \tag{1.4.67}$$

Therefore, in order to prove inequality (1.4.57) of the Lemma, it is sufficient to show that

$$(\alpha\rho E)(\langle \mathbb{U}_{app} \rangle^1) - \langle (\alpha\rho\mathcal{E})(\mathbb{W}_r) \rangle^1 \leq 0. \tag{1.4.68}$$

Similarly, integrating equation (1.4.62) over $]\sigma\Delta t, \frac{\Delta x}{2}[\times]0, \Delta t[$ shows that it is sufficient to establish

$$(\alpha\rho E)(\langle \mathbb{U}_{app} \rangle^2) - \langle (\alpha\rho\mathcal{E})(\mathbb{W}_r) \rangle^2 \leq 0, \tag{1.4.69}$$

in order to prove inequality (1.4.58) of the Lemma. Thus it remains to show that for all $i \in \{L, 1, 2\}$,

$$(\alpha\rho E)(\langle \mathbb{U}_{app} \rangle^i) - \langle (\alpha\rho\mathcal{E})(\mathbb{W}_r) \rangle^i \leq 0, \tag{1.4.70}$$

which is equivalent to proving

$$(\rho E)(\langle \mathbb{U}_{app} \rangle^i) - \langle (\rho\mathcal{E})(\mathbb{W}_r) \rangle^i \leq 0 \tag{1.4.71}$$

since on each domain of integration α is a positive constant.

We have

$$
\begin{aligned}
&(\rho E)(\langle \mathbb{U}_{app} \rangle^i) - \langle (\rho \mathcal{E})(\mathbb{W}_r) \rangle^i \\
&= \langle \rho_{app} \rangle^i \left(\frac{\langle (\rho w)_{app} \rangle^{i\,2}}{2 \langle \rho_{app} \rangle^{i\,2}} + e(\widehat{\tau_{app}}^i) \right) - \left\langle \rho \left(\frac{(\rho w)_r^2}{2\rho_r^2} + e(\mathcal{T}_r) + \frac{1}{2a^2} (\pi^2 (\tau_r, \mathcal{T}_r) - p^2(\mathcal{T}_r)) \right) \right\rangle^i .
\end{aligned}
\tag{1.4.72}
$$

The relaxation method is such that $(\rho_{app}, (\rho w)_{app}) = (\rho_r, (\rho w)_r)$ and we omit the subscripts for more clarity. Besides, as the function $(\rho, \rho w) \mapsto \frac{(\rho w)^2}{2\rho}$ is convex, Jensen's inequality implies that it is sufficient to prove

$$
\langle \rho \rangle^i \, e(\widehat{\tau}^i) - \left\langle \rho \left(e(\mathcal{T}) + \frac{1}{2a^2} \left(\pi^2(\tau, \mathcal{T}) - p^2(\mathcal{T}) \right) \right) \right\rangle^i \leq 0. \tag{1.4.73}
$$

Let $\mathcal{I}$ be the expression on the left hand side of inequality (1.4.73). Then,

$$
\mathcal{I} = \left\langle \rho \left(e(\widehat{\tau}^i) - e(\mathcal{T}) - \frac{1}{2a^2} \left(\pi^2(\tau, \mathcal{T}) - p^2(\mathcal{T}) \right) \right) \right\rangle^i , \tag{1.4.74}
$$

with

$$
\begin{aligned}
\pi^2(\tau, \mathcal{T}) - p^2(\mathcal{T}) &= (\pi(\tau, \mathcal{T}) - p(\mathcal{T}))\,(\pi(\tau, \mathcal{T}) + p(\mathcal{T})) \\
&= a^2(\mathcal{T} - \tau)\left(2p(\mathcal{T}) + a^2(\mathcal{T} - \tau)\right) \\
&= -2a^2 e'(\mathcal{T})(\mathcal{T} - \tau) + a^4(\mathcal{T} - \tau)^2,
\end{aligned}
$$

by definition of e. Casting this in (1.4.73), we get

$$
\begin{aligned}
\mathcal{I} &= \left\langle \rho \left(e(\widehat{\tau}^i) - e(\mathcal{T}) - e'(\mathcal{T})(\tau - \mathcal{T}) - \frac{a^2}{2}(\mathcal{T} - \tau)^2 \right) \right\rangle^i \\
&= \left\langle \rho \left(e(\widehat{\tau}^i) - e(\mathcal{T}) - e'(\mathcal{T})(\widehat{\tau}^i - \mathcal{T}) - \frac{a^2}{2}(\mathcal{T} - \widehat{\tau}^i)^2 \right) \right\rangle^i \\
&+ \left\langle \rho \, e'(\mathcal{T})(\widehat{\tau}^i - \tau) \right\rangle^i \\
&+ \frac{a^2}{2} \left\langle \rho \left((\mathcal{T} - \widehat{\tau}^i)^2 - (\mathcal{T} - \tau)^2 \right) \right\rangle^i .
\end{aligned}
\tag{1.4.75}
$$

As the variable $\mathcal{T}$ only jumps through the w-wave whose speed is equal to σ, $\mathcal{T}$ is constant in each one of the integration areas at time $t = \Delta t$ (equal to τ_L if $i = L$ or $i = 1$ and to τ_R if $i = 2$), and any function of $\mathcal{T}$ can be factored out of the averages which gives, for the second term of equation (1.4.75),

$$
\left\langle \rho \, e'(\mathcal{T})(\widehat{\tau}^i - \tau) \right\rangle^i = e'(\mathcal{T}) \left\langle \rho(\widehat{\tau}^i - \tau) \right\rangle^i = e'(\mathcal{T})(\widehat{\tau}^i \langle \rho \rangle^i - \langle \rho\tau \rangle^i) = e'(\mathcal{T})(1 - \langle 1 \rangle^i) = 0, \tag{1.4.76}
$$

since by Definition 1.4.4, $\widehat{\tau}^i = 1/ < \rho >^i$. For the third term of equation (1.4.75), we can write

$$\begin{aligned}\frac{a^2}{2}\left\langle \rho\left((\mathcal{T}-\widehat{\tau}^i)^2-(\mathcal{T}-\tau)^2\right)\right\rangle^i &= \frac{a^2}{2}\left\langle \rho\left((\mathcal{T}-\widehat{\tau}^i-(\mathcal{T}-\tau)\right)\left(\mathcal{T}-\widehat{\tau}^i+(\mathcal{T}-\tau)\right)\right\rangle^i \\ &= \frac{a^2}{2}\left\langle \rho\left(\tau-\widehat{\tau}^i\right)\left(2\mathcal{T}-\widehat{\tau}^i-\tau\right)\right\rangle^i\end{aligned}$$

$\mathcal{T}$ and $\widehat{\tau}^i$ are two constants we can factor out

$$\begin{aligned}&= \frac{a^2}{2}(2\mathcal{T}-\widehat{\tau}^i)\underbrace{\left\langle \rho\left(\tau-\widehat{\tau}^i\right)\right\rangle^i}_{=0}-\frac{a^2}{2}\left\langle \rho\left(\tau-\widehat{\tau}^i\right)\tau\right\rangle^i \\ &= \frac{a^2}{2}\left\langle \widehat{\tau}^i-\tau\right\rangle^i \\ &= \frac{a^2}{2}\left(\widehat{\tau}^i-\langle\tau\rangle^i\right) \\ &\leq 0, \end{aligned} \tag{1.4.77}$$

since the harmonic mean of a strictly positive function is always less than its average. Finally, for the first term of equation (1.4.75), a Taylor expansion with integral remainder gives

$$e(\widehat{\tau}^i)-e(\mathcal{T})-e'(\mathcal{T})(\widehat{\tau}^i-\mathcal{T}) = (\mathcal{T}-\widehat{\tau}^i)^2\int_0^1 e''(s\,\widehat{\tau}^i+(1-s)\mathcal{T})(1-s)ds \tag{1.4.78}$$

Then, observing that $e'' = -\partial_\tau p$ and replacing in the first term of (1.4.75), we get

$$\begin{aligned}&\left\langle \rho\left(e(\widehat{\tau}^i)-e(\mathcal{T})-e'(\mathcal{T})(\widehat{\tau}^i-\mathcal{T})-\frac{a^2}{2}(\mathcal{T}-\widehat{\tau}^i)^2\right)\right\rangle^i \\ &= \langle\rho\rangle^i\left(\int_0^1 -\partial_\tau p(s\,\widehat{\tau}^i+(1-s)\mathcal{T})(1-s)ds-\frac{a^2}{2}\right)(\mathcal{T}-\widehat{\tau}^i)^2\end{aligned} \tag{1.4.79}$$

which is negative since the parameter a is supposed to verify the weak Whitham condition. Thus $\mathcal{I} \leq 0$ and we have proved that inequality (1.4.70) holds for all $i \in \{L, 1, 2\}$ which concludes the proof of the Lemma. □

We have the following consequence of Lemma 1.4.6

Lemma 1.4.7. *With the same notations as in Lemma 1.4.6, if a satisfies the weak Whitham condition for $(\mathbb{U}_L, \mathbb{U}_R)$ in the sense of Definition 1.4.5, then*

$$(\alpha\rho E)(\langle\mathbb{U}_{app}\rangle^L)-(\alpha\rho E)(\mathbb{U}_L)+\frac{2\Delta t}{\Delta x}\left(\mathcal{G}_r\left(\mathbb{W}_r(0^+;\mathscr{M}(\mathbb{U}_L),\mathscr{M}(\mathbb{U}_R)\right)-\mathcal{G}(\mathbb{U}_L)\right)\leq 0, \tag{1.4.80}$$

$$(\alpha\rho E)(\langle\mathbb{U}_{app}\rangle^R)-(\alpha\rho E)(\mathbb{U}_R)+\frac{2\Delta t}{\Delta x}\left(\mathcal{G}(\mathbb{U}_R)-\mathcal{G}_r\left(\mathbb{W}_r(0^+;\mathscr{M}(\mathbb{U}_L),\mathscr{M}(\mathbb{U}_R)\right)\right)\leq 0. \tag{1.4.81}$$

Proof. Let σ be the material speed of the Riemann solution for the **relaxation system**. If $\sigma = 0$, the result is straightforward from Lemma 1.4.6. If $\sigma > 0$, multiplying inequality (1.4.57) by $2\sigma\frac{\Delta t}{\Delta x}$

and inequality (1.4.58) by $1-2\sigma\frac{\Delta t}{\Delta x}$ then summing gives

$$2\sigma\frac{\Delta t}{\Delta x}(\alpha\rho E)(\langle\mathbb{U}_{app}\rangle^1)+\left(1-2\sigma\frac{\Delta t}{\Delta x}\right)(\alpha\rho E)(\langle\mathbb{U}_{app}\rangle^2)$$
$$-(\alpha\rho E)(\mathbb{U}_R)+\frac{2\Delta t}{\Delta x}\left(\mathcal{G}(\mathbb{U}_R)-\mathcal{G}_r\left(\mathbb{W}_r(0^+)\right)\right)\leq 0 \tag{1.4.82}$$

which yields inequality (1.4.81) since $\alpha\rho E$ is convex . The case $\sigma<0$ follows similar steps. □

Remark 1.4.3. *Following the terminology used in [4], Lemma 1.4.7 says that the numerical scheme satisfies an entropy inequality by interface.*

We can now prove Theorem 1.4.5. A proof is given in [4], but we reproduce it here for the sake of completeness.

Proof of theorem *1.4.5.* We first define the averages for each half-cell $[x_{j-\frac12},x_j]$ and $[x_j,x_{j+\frac12}]$:

$$\langle\mathbb{U}_{app}\rangle^R_{j-\frac12} = \frac{2}{\Delta x}\int_{x_{j-\frac12}}^{x_j}\mathbb{U}_{app}\left(x/\Delta t;\mathbb{U}^n_{j-1},\mathbb{U}^n_j\right)dx \quad \text{for the half-cell} \quad [x_{j-\frac12},x_j], \tag{1.4.83}$$
$$\langle\mathbb{U}_{app}\rangle^L_{j+\frac12} = \frac{2}{\Delta x}\int_{x_j}^{x_{j+\frac12}}\mathbb{U}_{app}\left(x/\Delta t;\mathbb{U}^n_{j},\mathbb{U}^n_{j+1}\right)dx \quad \text{for the half-cell} \quad [x_{j},x_{j+\frac12}]. \tag{1.4.84}$$

Thus we have $\mathbb{U}^{n+1}_j=\frac12\langle\mathbb{U}_{app}\rangle^R_{j-\frac12}+\frac12\langle\mathbb{U}_{app}\rangle^L_{j+\frac12}$, and as $\alpha\rho E$ is convex

$$(\alpha\rho E)\left(\mathbb{U}^{n+1}_j\right)\leq\frac12(\alpha\rho E)\left(\langle\mathbb{U}_{app}\rangle^R_{j-\frac12}\right)+\frac12(\alpha\rho E)\left(\langle\mathbb{U}_{app}\rangle^L_{j+\frac12}\right). \tag{1.4.85}$$

As $a_{j-\frac12}$ satisfies the weak Whitham condition, we can apply inequality (1.4.81) of Lemma 1.4.7 with $\mathbb{U}_L=\mathbb{U}^n_{j-1}$ and $\mathbb{U}_R=\mathbb{U}^n_j$, which yields

$$(\alpha\rho E)\left(\langle\mathbb{U}_{app}\rangle^R_{j-\frac12}\right)-(\alpha\rho E)(\mathbb{U}^n_j)+\frac{2\Delta t}{\Delta x}\left(\mathcal{G}(\mathbb{U}^n_j)-\mathcal{G}_r\left(\mathbb{W}_r(0^+;\mathscr{M}(\mathbb{U}^n_{j-1}),\mathscr{M}(\mathbb{U}^n_j))\right)\right)\leq 0. \tag{1.4.86}$$

In the same way, as $a_{j+\frac12}$ satisfies the weak Whitham condition, we can apply inequality (1.4.80) of Lemma 1.4.7 with $\mathbb{U}_L=\mathbb{U}^n_j$ and $\mathbb{U}_R=\mathbb{U}^n_{j+1}$, which gives

$$(\alpha\rho E)\left(\langle\mathbb{U}_{app}\rangle^L_{j+\frac12}\right)-(\alpha\rho E)(\mathbb{U}^n_j)+\frac{2\Delta t}{\Delta x}\left(\mathcal{G}_r\left(\mathbb{W}_r(0^+;\mathscr{M}(\mathbb{U}^n_j),\mathscr{M}(\mathbb{U}^n_{j+1}))\right)-\mathcal{G}(\mathbb{U}^n_j)\right)\leq 0. \tag{1.4.87}$$

Summing equations (1.4.86) and (1.4.87) and using (1.4.85) we obtain

$$(\alpha\rho E)(\mathbb{U}^{n+1}_j)-(\alpha\rho E)(\mathbb{U}^n_j)+\frac{\Delta t}{\Delta x}(G(\mathbb{U}^n_j,\mathbb{U}^n_{j+1})-G(\mathbb{U}^n_{j-1},\mathbb{U}^n_j))\leq 0, \tag{1.4.88}$$

where the numerical entropy flux $G(\mathbb{U}_L,\mathbb{U}_R)$ is given by $G(\mathbb{U}_L,\mathbb{U}_R)=\mathcal{G}_r\left(\mathbb{W}_r\left(0^+;\mathscr{M}(\mathbb{U}_L),\mathscr{M}(\mathbb{U}_R)\right)\right)$. Finally, it remains to prove that the numerical entropy flux $G(\mathbb{U}_L,\mathbb{U}_R)$ is consistent with the exact entropy flux $\mathcal{G}$. We notice that for any $\mathbb{W}$ in Ω^r, we have $\mathbb{W}_r\left(0^+;\mathbb{W},\mathbb{W}\right)=\mathbb{W}$. And if $\mathbb{W}=\mathscr{M}(\mathbb{U})$ is at equilibrium, we get $\mathcal{G}^r(\mathbb{W})=\mathcal{G}(\mathbb{U})$. This concludes the proof of Theorem 1.4.5. □

For general equations of state $\tau \mapsto p(\tau)$, evaluating explicitly the integrals involved in the weak Witham condition might be difficult or even impossible. A notable exception though is obtained in the case of an ideal gas $p(\tau) = A\tau^{-\gamma}$ for which the integrals can be calculated explicitly. In practice, for general strictly convex equations of state, the weak Whitham condition will be replaced by a stronger condition for the sake of numerical applications. This new condition will be referred to as the weak$^\sharp$ Whitham condition. It reads

Definition 1.4.6. *Let $(\mathbb{U}_L, \mathbb{U}_R)$ be two admissible initial states, and let*

$$\mathbb{U}_{app}(\xi; \mathbb{U}_L, \mathbb{U}_R) = \mathscr{P}\mathbb{W}_r(\xi; \mathscr{M}(\mathbb{U}_L), \mathscr{M}(\mathbb{U}_R))$$

*be the approximate solution of the Riemann problem obtained by the relaxation approximation. We denote by σ the material speed of the Riemann solution for the **relaxation system** i.e. the effective value of the w-wave speed in $\mathbb{W}_r(\xi; \mathscr{M}(\mathbb{U}_L), \mathscr{M}(\mathbb{U}_R))$. Let Δx and Δt be respectively a space and a time steps satisfying the CFL condition (1.4.6).*

*We say that a satisfies the **weak$^\sharp$ Whitham condition for** $(\mathbb{U}_L, \mathbb{U}_R)$ if*

- *in the case $\sigma = 0$, a is such that*

$$a^2 > \max\left(-\partial_\tau p(\tau_L), -\partial_\tau p(\widehat{\tau_{app}}^L), -\partial_\tau p(\widehat{\tau_{app}}^R), -\partial_\tau p(\tau_R)\right), \tag{1.4.89}$$

- *in the case $\sigma > 0$, a is such that*

$$a^2 > \max\left(-\partial_\tau p(\tau_L), -\partial_\tau p(\widehat{\tau_{app}}^L), -\partial_\tau p(\widehat{\tau_{app}}^1), -\partial_\tau p(\widehat{\tau_{app}}^2), -\partial_\tau p(\tau_R)\right). \tag{1.4.90}$$

- *in the case $\sigma < 0$, a is such that*

$$a^2 > \max\left(-\partial_\tau p(\tau_L), -\partial_\tau p(\widehat{\tau_{app}}^1), -\partial_\tau p(\widehat{\tau_{app}}^2), -\partial_\tau p(\widehat{\tau_{app}}^R), -\partial_\tau p(\tau_R)\right). \tag{1.4.91}$$

The fact that the weak$^\sharp$ Whitham condition implies the weak Whitham condition for strictly convex equations of states directly comes from the monotonicity of $\tau \mapsto -\partial_\tau p(\tau)$. Indeed, we have for instance

$$\begin{aligned} -2\int_0^1 \partial_\tau p(s\,\widehat{\tau_{app}}^L + (1-s)\tau_L)(1-s)ds &\leq \max\left(-\partial_\tau p(\widehat{\tau_{app}}^L), -\partial_\tau p(\tau_L)\right) 2\int_0^1 (1-s)ds \\ &= \max\left(-\partial_\tau p(\widehat{\tau_{app}}^L), -\partial_\tau p(\tau_L)\right). \end{aligned} \tag{1.4.92}$$

Comparison between the classical Whitham condition and the weak Whitham condition

In section 1.4.5, we prove that we can always determine a constant a so as to satisfy the weak Whitham condition, even if we have to take $a \to +\infty$, thus falling in subsonic wave configurations with large acoustic speeds. However, for subsonic wave configurations with large acoustic speeds,

the classical Whitham condition $a^2 > \max\left(-\partial_\tau p(\tau), -\partial_\tau p(\mathcal{T})\right)$ for all τ and $\mathcal{T}$, is possible to satisfy since in that case, the specific volumes are not close to zero. Besides, the classical Whitham condition is easier to implement since it does not require the calculation of the averages and the simultaneous coupling of the time step calculation (see section 1.4.5). Consequently, a legitimate question does arise: is it relevant to try to satisfy the weak Whitham condition instead of the classical one ? An answer to this question can be formulated by saying that, when the flow described by the equilibrium system, which we intend to approximate, is supersonic or near the resonance, it appears more interesting to approximate it with supersonic relaxation Riemann solutions. Therefore, it is relevant to choose a constant a large enough to ensure the non linear stability of the scheme but small enough to stay in the supersonic regime for the relaxation system. In addition, the larger is the parameter a, the more dissipative is the numerical scheme and it is always preferable, for precision purposes, to guarantee the non linear stability of the scheme all the while minimizing the numerical dissipation.

Hereunder we show that for some initial states $(\mathbb{U}_L, \mathbb{U}_R)$, the classical Whitham condition cannot be fulfilled in the supersonic regime while the weak Whitham condition still allows an entropy inequality. In order to build such an initial condition, we have to locate near the resonance where some specific volume is close to zero. For this purpose, we first consider an initial condition with constant section $\alpha_L = \alpha_R$, *i.e.* $\nu = 1$, and we build the initial specific volumes and speeds so as to be in a supersonic regime and to satisfy the classical Whitham condition. We take $\tau_L = \tau_R$, $\mathcal{T}_L = \mathcal{T}_R = \tau_L$ and we fix $a := a_0 > \sqrt{-\partial_\tau p(\tau_L)}$. Let ε be a small positive parameter (intended to be close to zero), we fix $w_L = a_0\tau_L(1+\varepsilon)$, and $w_R = 2w_L = 2a_0\tau_L(1+\varepsilon)$. Thus,

$$w^\sharp = \frac{1}{2}(w_L + w_R) - \frac{1}{2a_0}(p_R - p_L) = \frac{3}{2}w_L = \frac{3}{2}a_0\tau_L(1+\varepsilon) > 0 \quad \text{and} \quad \mathcal{M}_L = \frac{w_L}{a_0\tau_L} = 1+\varepsilon, \tag{1.4.93}$$

which means that the left Mach number is slightly supersonic. Besides, as the intermediate specific volumes are larger than τ_L: $\tau_L^\sharp = \tau_R^\sharp = \tau_L + \frac{1}{2}\tau_L(1+\varepsilon) > \tau_L$, the classical Whitham condition is satisfied by a_0:

$$a_0^2 > \max\left(-\partial_\tau p(\tau_L), -\partial_\tau p(\tau_L^\sharp), -\partial_\tau p(\tau_R^\sharp), -\partial_\tau p(\tau_R)\right) = -\partial_\tau p(\tau_L). \tag{1.4.94}$$

The idea then is to take $\alpha_L > \alpha_R$, *i.e.* $\nu > 1$, so as to give rise to a standing wave at $x = 0$ while all the other initial variables are fixed as described above. As $\nu > 1$ and $\mathcal{M}_L = 1 + \varepsilon$, the solution of the relaxation system is of signature $< 0, 3 >$ and is close to the resonance if ε is small. Consequently, if ε is small, the specific volume τ^+ on the right of the standing wave is close to zero since equation (1.3.51) gives

$$\tau^+ = \tau_L\sqrt{\frac{\mathcal{M}_L^2 - 1}{\nu^2\mathcal{M}_L^2 - 1}} \sim \tau_L\sqrt{\frac{2}{\nu^2 - 1}}\sqrt{\varepsilon}, \tag{1.4.95}$$

and the classical Whitham condition $a_0^2 > -\partial_\tau p(\tau^+)$ will be impossible to satisfy unless the parameter a is taken significantly larger than a_0, thus falling in the subsonic regime and increasing the numerical dissipation. Nevertheless, we can prove that with the same constant $a = a_0$, the weak Whitham condition (in fact the weak$^\sharp$ Whitham condition) still holds thus allowing an entropy

inequality. Indeed, let be given Δt a time step satisfying the CFL condition

$$\frac{\Delta x}{2\Delta t} > \max\left(|w_L - a_0\tau_L|, |w_R + a_0\tau_R|\right), \quad \text{for all} \quad \varepsilon \leq 1. \tag{1.4.96}$$

Let us prove that for some $\nu > 1$, a_0 satisfies the weak$^\sharp$ Whitham condition that is to say

$$a_0^2 > \max\left(-\partial_\tau p(\tau_L), -\partial_\tau p(\widehat{\tau_{app}}^L), -\partial_\tau p(\widehat{\tau_{app}}^1), -\partial_\tau p(\widehat{\tau_{app}}^2), -\partial_\tau p(\tau_R)\right). \tag{1.4.97}$$

We already have $\widehat{\tau_{app}}^L = \tau_L = \tau_R$ and $a_0^2 > -\partial_\tau p(\tau_L)$. As for $\widehat{\tau_{app}}^1$ and $\widehat{\tau_{app}}^2$, we can prove that

$$\widehat{\tau_{app}}^1 = \frac{3}{2\nu}\tau_L + \mathcal{O}(\sqrt{\varepsilon}) \qquad \text{and} \qquad \widehat{\tau_{app}}^2 = \tau_L \frac{\frac{\Delta x}{2\Delta t} - \frac{3}{2}a_0\tau_L}{\frac{\Delta x}{2\Delta t} - 2a_0\tau_L} + \mathcal{O}(\sqrt{\varepsilon}). \tag{1.4.98}$$

Hence, for $1 < \nu < \frac{3}{2}$, if we take ε small enough, we ensure that $\widehat{\tau_{app}}^1 > \tau_L$ and $\widehat{\tau_{app}}^2 > \tau_L$ which implies that the weak$^\sharp$ Whitham condition is satisfied for a_0. Therefore, this example points out the advantages in considering the weak Whitham condition instead of the classical one.

1.4.5 Practical choice of the parameter a

In the numerical applications, the parameter a must be chosen locally at each interface, *i.e.* for each given pair of two positive initial states $(\mathbb{U}_L, \mathbb{U}_R)$, so as to satisfy the three following conditions

- $C1$: The specific volumes $\tau_L^\sharp$ and $\tau_R^\sharp$ must be strictly positive so that Theorem 1.3.4 ensures the existence of a positive solution to the relaxation Riemann problem built on $(\mathbb{U}_L, \mathbb{U}_R)$.
- $C2$: If $\nu = \frac{\alpha_L}{\alpha_R} > 1$ then $\mathcal{M}_L = \frac{w_L}{a\tau_L}$ must be different from 1 and if $\nu < 1$ then $\mathcal{M}_R = \frac{w_R}{a\tau_R}$ must be different from -1 so as to impose the conservativity of the numerical method.
- $C3$: The parameter a must satisfy the weak$^\sharp$ Whitham condition in order to guarantee the non linear stability of the scheme.

In this section, we prove that being given two positive initial states $\mathbb{U}_L$ and $\mathbb{U}_R$, there exists a parameter a, large enough, satisfying conditions $C1$, $C2$ and $C3$, and we propose an iterative procedure to calculate such an a. In fact, the determination of a must be carried out with special carefulness since it must be coupled simultaneously with the calculation of the time step Δt. Indeed, on the one hand, a depends on Δt through the weak Whitham condition since the averaged specific volumes $\widehat{\tau}^{L,1,2,R}$ involved in definition 1.4.6 clearly depend on Δt. On the other hand, Δt depends on a because it must be small enough to ensure the CFL condition (1.4.6) which amounts to

$$\frac{\Delta x}{2\Delta t} > \max\left(|w_L - a\tau_L|, |w_R + a\tau_R|\right). \tag{1.4.99}$$

In order to reduce the problem to a single variable, we take a time step explicitly depending on the parameter a according to

$$\Delta t(a) := (1-\kappa)\frac{\Delta x}{2}\Big(\max\left(|w_L - a\tau_L|, |w_R + a\tau_R|\right)\Big)^{-1}, \tag{1.4.100}$$

where $0 < \kappa < 1$ denotes a fixed parameter. Thus, for the couple $(a, \Delta t(a))$, the CFL condition (1.4.99) is automatically satisfied. Besides, $\lim_{a\to+\infty} \Delta t(a) = 0$, and we have the following proposition

Proposition 1.4.8. *Let $(\mathbb{U}_L, \mathbb{U}_R)$ be two admissible states in Ω. Let be given $0 < \kappa < 1$ and assume (1.4.100). We have the following limit values as a goes to infinity.*

$$\begin{aligned}
&\lim_{a\to+\infty} \tau_L^\sharp(a) = \tau_L, && \lim_{a\to+\infty} \tau_R^\sharp(a) = \tau_R,\\
&\lim_{a\to+\infty} \widehat{\tau_{app}}^{\,L}(a, \Delta t(a)) = \tau_L, && \lim_{a\to+\infty} \widehat{\tau_{app}}^{\,R}(a, \Delta t(a)) = \tau_R,\\
&\lim_{a\to+\infty} \widehat{\tau_{app}}^{\,1}(a, \Delta t(a)) = \tau_L \text{ or } \tau_R, && \lim_{a\to+\infty} \widehat{\tau_{app}}^{\,2}(a, \Delta t(a)) = \tau_L \text{ or } \tau_R.
\end{aligned} \tag{1.4.101}$$

Proof. The proof is given in appendix B. □

Hence, for any couple of positive initial states $(\mathbb{U}_L, \mathbb{U}_R)$, it is always possible, by taking a large enough, to find a parameter a and the corresponding time step $\Delta t(a)$ in such a manner that $\tau_L^\sharp > 0$, $\tau_R^\sharp > 0$, and that the weak$^\sharp$ Whitham condition is satisfied for $(\mathbb{U}_L, \mathbb{U}_R)$. Indeed, in the expression

$$a^2 > \max\left(-\partial_\tau p(\tau_L), -\partial_\tau p(\widehat{\tau_{app}}^{\,L,1,2,R}), -\partial_\tau p(\tau_R)\right), \tag{1.4.102}$$

the left-hand side goes to infinity while the right-hand side remains bounded. Fulfilling the remaining condition $C2$ is easy since it is sufficient to perturb the parameter a so that $\mathcal{M}_L \neq 1$ or $\mathcal{M}_R \neq -1$.

It remains now to apply these observations to the relaxation method. Thereafter, we give a procedure that describes precisely the advancement of the scheme during a time step $t^n \to t^{n+1}$.

Beginning of the time step $t^n \to t^{n+1}$.

- Chose κ and κ' two (small) parameters in the interval $(0,1)$.
- For all interface $x_{j+\frac{1}{2}},\ j \in \mathbb{Z}$, calculate $a_{j+\frac{1}{2}}$ and $\Delta t_{j+\frac{1}{2}}$ as follows
  - Initialize $a_{j+\frac{1}{2}}$ and $\Delta t_{j+\frac{1}{2}}$:

$$\begin{aligned} a_{j+\frac{1}{2}}^2 &> \max\left(-\partial_\tau p(\tau_j^n), -\partial_\tau p(\tau_{j+1}^n)\right), \\ \Delta t_{j+\frac{1}{2}} &:= (1-\kappa)\frac{\Delta x}{2}\Big(\max\Big(|w_j^n - a_{j+\frac{1}{2}}\tau_j^n|, |w_{j+1}^n + a_{j+\frac{1}{2}}\tau_{j+1}^n|\Big)\Big)^{-1}, \end{aligned}$$

  - while $\Big($ the pair $(a_{j+\frac{1}{2}}, \Delta t_{j+\frac{1}{2}})$ is such that:

$$\begin{aligned} &\tau_L^\sharp(a_{j+\frac{1}{2}}) \le 0 \text{ or } \tau_R^\sharp(a_{j+\frac{1}{2}}) \le 0, \\ &\text{or the weak}^\sharp \text{ Whitham condition is not satisfied for } (\mathbb{U}_j^n, \mathbb{U}_{j+1}^n), \\ &\text{or } (\alpha_j^n/\alpha_{j+1}^n > 1 \text{ and } \mathcal{M}_L(\mathbb{U}_j^n, \mathbb{U}_{j+1}^n) = 1), \\ &\text{or } (\alpha_j^n/\alpha_{j+1}^n < 1 \text{ and } \mathcal{M}_R(\mathbb{U}_j^n, \mathbb{U}_{j+1}^n) = -1) \end{aligned}$$

    $\Big)$ do

$$\begin{aligned} a_{j+\frac{1}{2}} &:= (1+\kappa')a_{j+\frac{1}{2}}, \\ \Delta t_{j+\frac{1}{2}} &:= (1-\kappa)\frac{\Delta x}{2}\Big(\max\Big(|w_j^n - a_{j+\frac{1}{2}}\tau_j^n|, |w_{j+1}^n + a_{j+\frac{1}{2}}\tau_{j+1}^n|\Big)\Big)^{-1}, \end{aligned}$$

    End of the while loop.

  End of the loop on the interfaces $x_{j+\frac{1}{2}},\ j \in \mathbb{Z}$.
- Set $\Delta t = \min\limits_{j\in\mathbb{Z}} \Delta t_{j+\frac{1}{2}}$.
- Apply the relaxation scheme with the time step Δt.

End of the time step $t^n \to t^{n+1}$.

Remark 1.4.4. *The reader is invited to verify that for a fixed parameter a, if a satisfies the weak$^\sharp$ Whitham condition for a time step Δt, then it still satisfies this condition for any time step $\overline{\Delta t} \le \Delta t$. Therefore, when we set $\Delta t = \min\limits_{j\in\mathbb{Z}} \Delta t_{j+\frac{1}{2}}$ without changing the parameters $a_{j+\frac{1}{2}}$ at each interface, the weak$^\sharp$ Whitham condition is not deteriorated. This observation follows from the monotonicity of the harmonic means $\widehat{\tau}^i$ with respect to Δt, holding for every wave configuration.*

1.4.6 Numerical results

In this section we present two test cases in which we compare the results obtained with the relaxation approximation method with those obtained with the Rusanov scheme. The chosen pressure law is

an ideal gas pressure law

$$p(\tau) = \tau^{-\gamma}, \tag{1.4.103}$$

where the heat capacity ratio γ is taken equal to 3. The computations have been run on a refined mesh of 10^5 cells, and the CFL condition is fixed to 0.45.

A subsonic Riemann problem

We consider the Riemann problem where the initial left and right states are given by

$$\begin{array}{lll} \alpha_L = .3 & & \alpha_R = .4 \\ \rho_L = .2 & \text{and} & \rho_R = 0.1 \\ w_L = 0. & & w_R = 0. \end{array} \tag{1.4.104}$$

for which the solution is composed of the standing wave associated with the constant section α, a left-going σ_1-rarefaction wave and a right-going σ_2-shock. Figure 1.1 displays the cell values, at the final time $T = 1.0$, of some classical quantities. The *Cell entropy budget* (top left of Figure 1.1)denotes the cell value

$$(\alpha\rho E)(\mathbb{U}_j^{n+1}) - (\alpha\rho E)(\mathbb{U}_j^n) + \frac{\Delta t}{\Delta x}(G(\mathbb{U}_j^n, \mathbb{U}_{j+1}^n) - G(\mathbb{U}_{j-1}^n, \mathbb{U}_j^n)) \tag{1.4.105}$$

computed for the Relaxation scheme.

As expected, we can see that the cell entropy budget is nonpositive. Especially, it is strictly negative across the shock, which is natural, and also across the standing wave since the approximate relaxation Riemann solution has been allowed to dissipate energy across this wave. The Rusanov scheme and the Relaxation scheme provide similar results. However, it appears that the intermediate states captured by the two schemes are slightly different. Note that, at $x = 0$, *i.e.* where the cross-section jumps, the Rusanov scheme generates over and under-shoots. Such a behavior, which is "dangerous" since the computed values of the density might come close to zero, does not occur with the relaxation scheme.

A transonic Riemann problem

We consider the Riemann problem where the initial left and right states are given by

$$\begin{array}{lll} \alpha_L = 3. & & \alpha_R = 1. \\ \rho_L = 1. & \text{and} & \rho_R = 0.1 \\ w_L = 0. & & w_R = 0. \end{array} \tag{1.4.106}$$

for which the solution is composed of the standing wave associated with the constant section α, a left-going σ_1-rarefaction wave, a sonic right-going σ_1-rarefaction wave and a right-going σ_2-shock. Figure 1.2 displays the cell values, at the final time $T = 0.2$, of some classical quantities.

Again, we can see that the cell entropy budget (computed for the relaxation scheme) is nonpositive, and that it is strictly negative across the shock and across the standing wave. Note that this transonic case is much more energy dissipative than the sonic case (the order of magnitude of the

cell entropy budget is much higher). This is due to the resonance phenomenon which imposes more energy dissipation for the stability of the scheme. It appears on this case that the Rusanov scheme provides a notably unsatisfactory result compared with the Relaxation scheme. The intermediate states and the wave speeds are not correctly captured by the Rusanov scheme and there is no trace of the sonic rarefaction wave.

Appendix A

Choice of $\mathcal{M}$ for signature $< 1, 2 >$ and corresponding dissipation

When $\nu^\sharp < +\infty$ and $\nu \geq \nu^\sharp$, $\mathcal{M}$ must be chosen in the open interval $(0, \mathcal{M}_0(\omega, \nu))$, small enough so as to guarantee the positivity of τ_3. Being given a fixed real number μ in $(0, 1)$, we may choose $\mathcal{M}$ by prescribing τ_3 to a fixed strictly positive value

$$\tau_3 = \mu \tau_R^\sharp, \tag{1.4.107}$$

for every $\nu \geq \nu_c$ where ν_c is the only value of ν that satisfies

$$\tau_3(\nu) = \tau_R^\sharp + \tau_L^\sharp \frac{\mathcal{M}_L^\sharp - \nu \mathcal{M}_0(\omega, \nu)}{1 + \nu \mathcal{M}_0(\omega, \nu)} = \mu \tau_R^\sharp \tag{1.4.108}$$

and whose expression is

$$\nu_c = \frac{\mathcal{M}_L^\sharp + (1-\mu)\frac{\tau_R^\sharp}{\tau_L^\sharp}}{1 - (1-\mu)\frac{\tau_R^\sharp}{\tau_L^\sharp}} \frac{(1 - (1-\mu)\frac{\tau_R^\sharp}{\tau_L^\sharp})(1+\omega^2) - (1-\omega^2)(\mathcal{M}_L^\sharp + (1-\mu)\frac{\tau_R^\sharp}{\tau_L^\sharp})}{(1 - (1-\mu)\frac{\tau_R^\sharp}{\tau_L^\sharp})(1-\omega^2) - (1+\omega^2)(\mathcal{M}_L^\sharp + (1-\mu)\frac{\tau_R^\sharp}{\tau_L^\sharp})}. \tag{1.4.109}$$

Hence, for $\nu < \nu_c$, we take $\mathcal{M} = \mathcal{M}_0(\omega, \nu)$ and for $\nu \geq \nu_c$, the chosen value of $\mathcal{M}$ is obtained by evaluating the inverse function of $\mathcal{M} \mapsto \tau_3$ at $\tau_3 = \mu \tau_R^\sharp$, which gives

$$\mathcal{M}_\mu := \frac{1}{\nu} \frac{\mathcal{M}_L^\sharp + (1-\mu)\frac{\tau_R^\sharp}{\tau_L^\sharp}}{1 - (1-\mu)\frac{\tau_R^\sharp}{\tau_L^\sharp}}, \tag{1.4.110}$$

and the corresponding dissipation reads

$$\left[\alpha \rho w \left(\mathcal{E} + \frac{\pi}{\rho}\right)\right]^0 := \frac{1}{2}(w_L^\sharp + a\tau_L^\sharp)^2 \mathcal{Q}_0(\mathcal{M}_\mu)\Psi(\mathcal{M}_\mu; \nu, \omega). \tag{1.4.111}$$

Choice of θ for signature $< 0, 3 >$ and corresponding dissipation

When $\nu^\sharp < +\infty$ and $\nu \geq \nu^\sharp$, the parameter θ must be chosen in the open interval $(0, 1)$ small enough so as to guarantee the positivity of τ_2 and τ_3. For the sake of clarity, let us assume that

$\tau_L^\sharp \leq \tau_R^\sharp$. The case $\tau_L^\sharp \geq \tau_R^\sharp$ is straightforward. Being given a fixed real number μ in $(0,1)$, we may choose θ by prescribing τ_2 to a fixed strictly positive value

$$\tau_2 = \mu\tau_L^\sharp, \tag{1.4.112}$$

for every $\nu \geq \nu_c$ where ν_c is the only value of ν that satisfies

$$\tau_2 = \tau_L^\sharp - \frac{\tau_L}{2}(\mathcal{M}_L - 1)\left(\sqrt{\frac{(\mathcal{M}_L+1)(\nu\mathcal{M}_L-1)}{(\mathcal{M}_L-1)(\nu\mathcal{M}_L+1)}} - 1\right) = \mu\tau_L^\sharp \tag{1.4.113}$$

and whose expression is

$$\nu_c = \frac{1}{\mathcal{M}_L}\,\frac{\mathcal{M}_L^2 - 1 + \left(\frac{2(1-\mu)\tau_L^\sharp}{\tau_L} + \mathcal{M}_L - 1\right)^2}{\mathcal{M}_L^2 - 1 - \left(\frac{2(1-\mu)\tau_L^\sharp}{\tau_L} + \mathcal{M}_L - 1\right)^2}. \tag{1.4.114}$$

Hence, for $\nu < \nu_c$, we take $\theta = 1$ and for $\nu \geq \nu_c$, the chosen value of θ is obtained by evaluating the inverse function of $\theta \mapsto \tau_2$ at $\tau_2 = \mu\tau_L^\sharp$, which gives

$$\theta_\mu := \left(\frac{2(1-\mu)\tau_L^\sharp}{\tau_L(\mathcal{M}_L-1)} + 1\right)\left(\frac{(\mathcal{M}_L+1)(\nu\mathcal{M}_L-1)}{(\mathcal{M}_L-1)(\nu\mathcal{M}_L+1)}\right)^{-1/2}, \tag{1.4.115}$$

and the corresponding dissipation reads

$$\left[\alpha\rho w\left(\mathcal{E} + \frac{\pi}{\rho}\right)\right]^0 := \frac{1}{2}({w_L}^2 - a^2{\tau_L}^2)({\theta_\mu}^2 - 1)\alpha_L\rho_L w_L. \tag{1.4.116}$$

Appendix B : Proof of Proposition 1.4.8

We have

$$\tau_L^\sharp(a) = \tau_L + \frac{1}{2a}(w_R - w_L) - \frac{1}{2a^2}(\pi_R - \pi_L) \longrightarrow \tau_L, \tag{1.4.117}$$

$$\tau_R^\sharp(a) = \tau_R + \frac{1}{2a}(w_R - w_L) + \frac{1}{2a^2}(\pi_R - \pi_L) \longrightarrow \tau_R. \tag{1.4.118}$$

We then notice that as a goes to infinity, we have $\mathcal{M}_L \to 0$ and $\mathcal{M}_R \to 0$. Thus, the possible signatures in the regime of large parameters a are the subsonic signatures $< 1.2 >$, $< 1,1 >$ and $< 2,1 >$. In order to know which one of these configurations holds in the regime of large a, we have to investigate the sign of $w^\sharp$. Recall that

$$w^\sharp = \frac{1}{2}(w_L + w_R) - \frac{1}{2a}\left(p(\tau_R) - p(\tau_L)\right). \tag{1.4.119}$$

Thus, there are three different cases to take into account:

(i) $\frac{1}{2}(w_L + w_R) > 0$ or $\left(\frac{1}{2}(w_L + w_R) = 0 \quad \text{and} \quad \tau_R > \tau_L\right)$ in which case the solution is of signature $< 1,2 >$ for large parameters a,

(ii) $\frac{1}{2}(w_L+w_R) < 0$ or $\left(\frac{1}{2}(w_L+w_R) = 0 \text{ and } \tau_R < \tau_L\right)$ in which case the solution is of signature $< 2, 1 >$ for large parameters a,

(iii) $\frac{1}{2}(w_L + w_R) = 0$ and $\tau_R = \tau_L$ in which case the solution is always of signature $< 1, 1 >$ for all a.

Let us focus on the first case *(i)*. After some calculation using formulae (1.3.36) we get the expressions of $\widehat{\tau_{app}}^L$, $\widehat{\tau_{app}}^1$ and $\widehat{\tau_{app}}^2$:

$$\widehat{\tau_{app}}^L = \tau_L \frac{1}{1 + 2\frac{\Delta t(a)}{\Delta x}\left(w_L - \tau_L a \mathcal{M}_0(a)\right)}, \quad \widehat{\tau_{app}}^1 = \tau_L^\sharp(a)\frac{1+\mathcal{M}_L^\sharp(a)}{1+\nu\mathcal{M}_0(a)}, \quad \widehat{\tau_{app}}^2 = \tau_R \frac{\frac{\Delta x}{2\Delta t(a)} - w^+(a)}{\frac{\Delta x}{2\Delta t(a)} - w_R}. \tag{1.4.120}$$

We have $\tau_L^\sharp(a) \to \tau_L$ and we can prove that $\mathcal{M}_0(a) \to 0$, $\mathcal{M}_L^\sharp(a) \to 0$ and that the quantities $a\mathcal{M}_0(a)$ and $w^+(a)$ are bounded. As $\Delta t(a) \to 0$, this yields the result for the first case *(i)*. The second case *(ii)* can be obtained as a corollary of the first one by invoking the Galilean invariance of the system. As for the third and last case *(iii)*, we have

$$\widehat{\tau_{app}}^L = \tau_L \frac{1}{1 + \frac{2\Delta t(a)}{\Delta x} w_L}, \qquad \widehat{\tau_{app}}^R = \tau_R \frac{1}{1 - \frac{2\Delta t(a)}{\Delta x} w_R}, \tag{1.4.121}$$

which gives the result for case *(iii)* since $\Delta t(a) \to 0$.

Acknowledgements. The second author receives a financial support by ANRT through an EDF-CIFRE contract 529/2009. The third author is partially supported by the LRC Manon (Modélisation et Approximation Numérique Orientées pour l'énergie Nucléaire — CEA DM2S/LJLL).

References

[1] A. Ambroso, C. Chalons, F. Coquel, and T. Galié. Relaxation and numerical approximation of a two-fluid two-pressure diphasic model. *M2AN Math. Model. Numer. Anal.*, 43(6):1063–1097, 2009.

[2] N. Andrianov and G. Warnecke. On the solution to the Riemann problem for the compressible duct flow. *SIAM J. Appl. Math.*, 64(3):878–901 (electronic), 2004.

[3] F. Bouchut. On zero pressure gas dynamics. In *Advances in kinetic theory and computing*, volume 22 of *Ser. Adv. Math. Appl. Sci.*, pages 171–190. World Sci. Publishing, River Edge, NJ, 1994.

[4] F. Bouchut. *Nonlinear stability of finite volume methods for hyperbolic conservation laws and well-balanced schemes for sources*. Frontiers in Mathematics. Birkhäuser Verlag, Basel, 2004.

[5] A. Chinnayya, A.-Y. LeRoux, and N. Seguin. A well-balanced numerical scheme for the approximation of the shallow-water equations with topography: the resonance phenomenon. *Int. J. Finite Volumes*, pages 1–33, 2004.

[6] F. Coquel, E. Godlewski, B. Perthame, A. In, and P. Rascle. Some new Godunov and relaxation methods for two-phase flow problems. In *Godunov methods (Oxford, 1999)*, pages 179–188. Kluwer/Plenum, New York, 2001.

[7] F. Coquel and B. Perthame. Relaxation of energy and approximate Riemann solvers for general pressure laws in fluid dynamics. *SIAM J. Numer. Anal.*, 35(6):2223–2249 (electronic), 1998.

[8] C. M. Dafermos. *Hyperbolic conservation laws in continuum physics*, volume 325 of *Grundlehren der Mathematischen Wissenschaften [Fundamental Principles of Mathematical Sciences]*. Springer-Verlag, Berlin, second edition, 2005.

[9] R. J. DiPerna. Measure-valued solutions to conservation laws. *Arch. Rational Mech. Anal.*, 88(3):223–270, 1985.

[10] T. Gallouët, J.-M. Hérard, and N. Seguin. Some approximate Godunov schemes to compute shallow-water equations with topography. *Comput. & Fluids*, 32(4):479–513, 2003.

[11] P. Goatin and P. G. LeFloch. The Riemann problem for a class of resonant hyperbolic systems of balance laws. *Ann. Inst. H. Poincaré Anal. Non Linéaire*, 21(6):881–902, 2004.

[12] E. Godlewski and P.-A. Raviart. *Numerical approximation of hyperbolic systems of conservation laws*, volume 118 of *Applied Mathematical Sciences*. Springer-Verlag, New York, 1996.

[13] L. Gosse and A.-Y. LeRoux. Un schéma-équilibre adapté aux lois de conservation scalaires non-homogènes. *C. R. Acad. Sci. Paris Sér. I Math.*, 323(5):543–546, 1996.

[14] J. M. Greenberg and A.-Y. LeRoux. A well-balanced scheme for the numerical processing of source terms in hyperbolic equations. *SIAM J. Numer. Anal.*, 33(1):1–16, 1996.

[15] A. Harten, P. D. Lax, and B. van Leer. On upstream differencing and Godunov-type schemes for hyperbolic conservation laws. *SIAM Rev.*, 25(1):35–61, 1983.

[16] E. Isaacson and B. Temple. Convergence of the 2×2 Godunov method for a general resonant nonlinear balance law. *SIAM J. Appl. Math.*, 55(3):625–640, 1995.

[17] S. Jin and Z. P. Xin. The relaxation schemes for systems of conservation laws in arbitrary space dimensions. *Comm. Pure Appl. Math.*, 48(3):235–276, 1995.

[18] P. G. Lefloch and M. D. Thanh. The Riemann problem for fluid flows in a nozzle with discontinuous cross-section. *Commun. Math. Sci.*, 1(4):763–797, 2003.

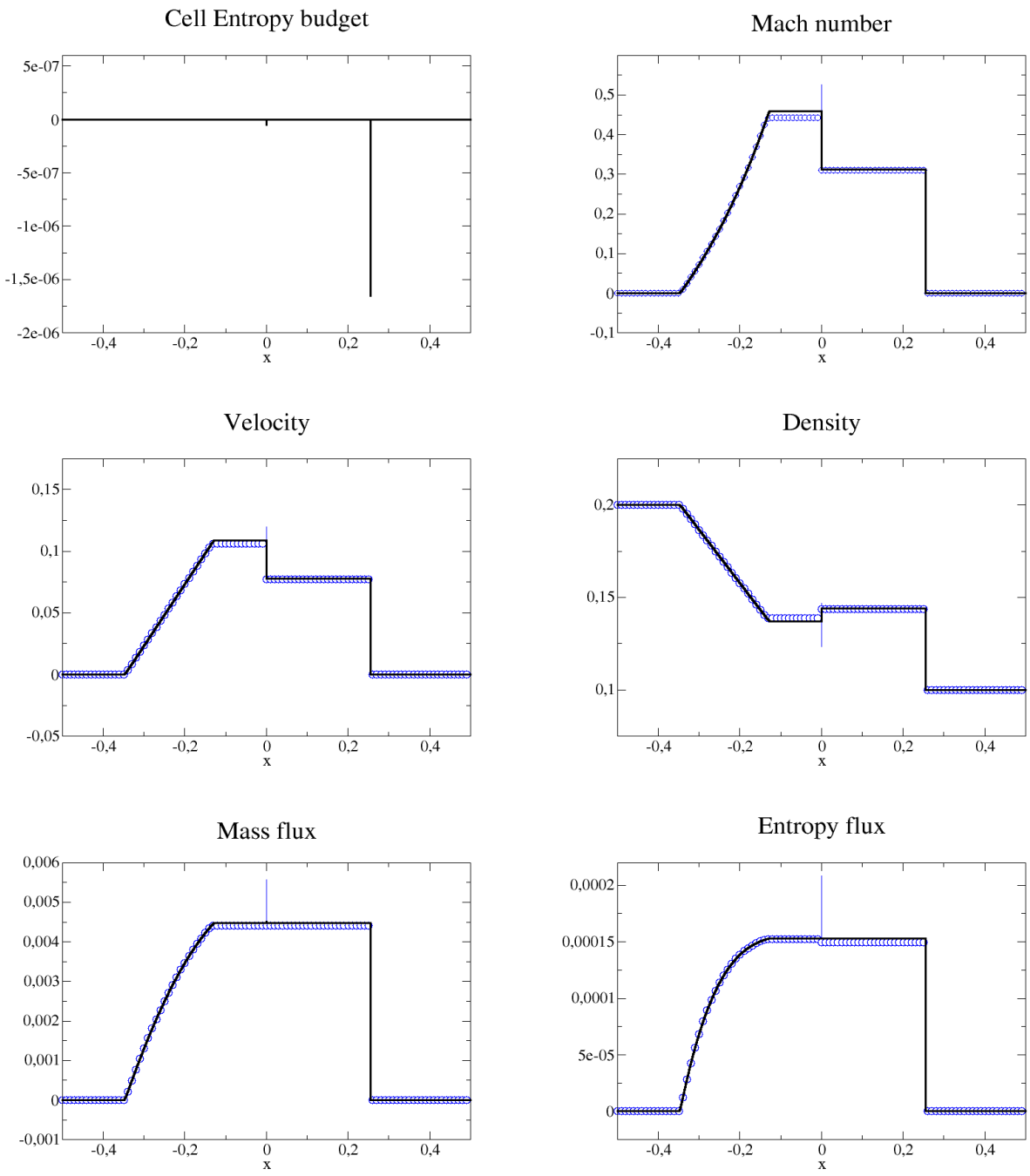

Figure 1.1: Solution of the subsonic Riemann problem (1.4.104) at time $T = 1.0$. Space step $\Delta x = 10^{-5}$. Straight line: relaxation scheme, circles: Rusanov scheme.

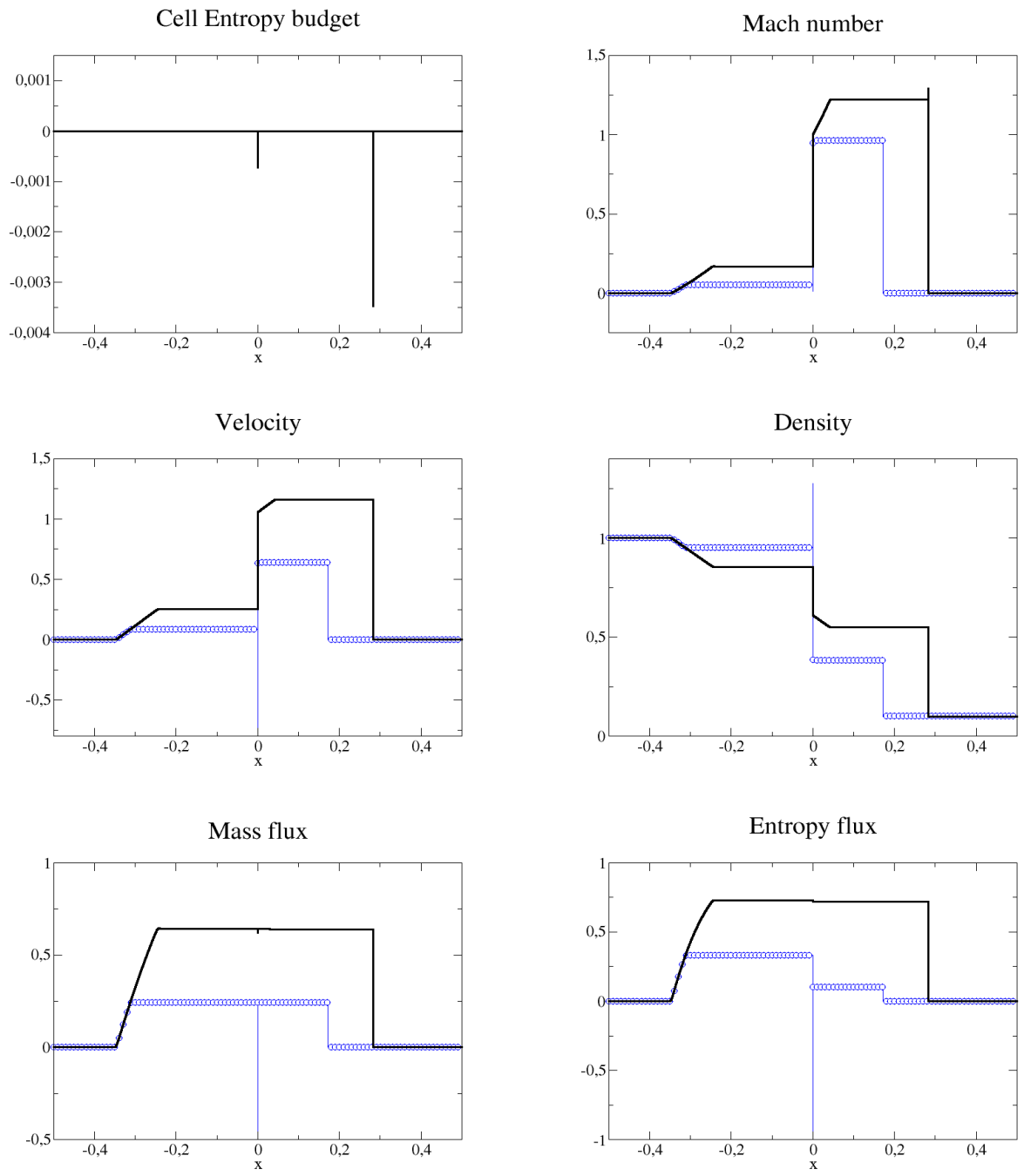

Figure 1.2: Solution of the transonic Riemann problem (1.4.106) at time $T = 0.2$. Space step $\Delta x = 10^{-5}$. Straight line: relaxation scheme, circles: Rusanov scheme.

Chapter 2

Approximation par relaxation pour le modèle de Baer-Nunziato

RELAXATION APPROXIMATION FOR THE ISENTROPIC BAER-NUNZIATO MODEL WITH VANISHING PHASES

Frédéric Coquel, Jean-Marc Hérard, Khaled Saleh, Nicolas Seguin

2.1 Introduction

The two-fluid approach is relevant for a detailed investigation of some patterns occurring in water-vapor flows such as those encountered in pressurized water reactors. In this framework, a major issue is the prediction of the boiling crisis, where the flow is initially dominated by the liquid phase while the vapor phase is dilute. Due to a failure in the heat evacuation, the liquid may reach the boiling point in some areas of the flow (mainly near the fuel rods) thus causing a phase transition towards vapor that could possibly isolate the fuel rods from the liquid. The modeling as well as the numerical simulation of such phenomena remains challenging since both models that can handle phase transitions and robust numerical schemes are needed.

This paper is concerned with the isentropic version of the two-fluid model introduced by Baer and Nunziato in [1], in the context of reactive granular materials, and studied in various papers [4, 10, 14] (see also [16] for a related framework). This model is a suitable candidate that enables the computation of two-phase flows in which few bubbles are statistically present in a liquid phase. It consists in two sets of partial differential equations accounting for the evolution of mass, momentum and total energy for each phase, in addition to an evolution equation for the phase fraction. A major feature of the Baer-Nunziato model is to assume two different velocities and two different pressures for the two phases. This approach is not genuinely usual in the nuclear industry where the commonly implemented methods assume the same pressure for the two phases at every time and everywhere in the flow. This latter assumption is justified by the very short time-scale associated with the relaxation of the phasic pressures towards an equilibrium. In the two-fluid two-pressure models (such as Baer & Nunziato's), source terms are explicitly written in order to account for this pressure relaxation phenomenon as well as friction terms for the relaxation of the phasic velocities towards an equilibrium. However, this work is mainly concerned with the convective effects and these relaxation source terms are not considered here (see [4] for some modeling choices of these terms and [12] for their numerical treatment). Contrary to the single pressure models, the Baer-Nunziato model provides a pleasant property which is the hyperbolicity of its convective part. Indeed, unlike single pressure models, where the characteristic eigenvalues may be complex, the

Baer-Nunziato model admits seven real eigenvalues and the associated right eigenvectors form a basis unless the relative velocity between the phases equals the sound speed in the liquid (see [8]). However, such a situation is unlikely to arise in the context of nuclear reactor simulations and therefore, the present paper is restricted to the cases where the relative velocity between the phases remains small compared to the liquid speed of sound.

In the present work, we introduce a larger system, in which the pressure laws have been linearized, and which relaxes towards the actual system of Baer-Nunziato in the regime of a small relaxation parameter (for a general framework on relaxation schemes we refer to [5, 7, 6, 2]). The Riemann problem associated with the relaxation system is exactly solved, in the framework of solutions with *subsonic wave ordering*, *i.e.* solutions for which the relative velocity between the phases is less than the acoustic wave speeds. Moreover, for this relaxation Riemann problem, it is proved that the relative ordering of the waves can be determined *a priori* with respect to the initial data.

2.1.1 The isentropic model of Baer-Nunziato

In the present work, we consider a model formulated in Eulerian coordinates where balance equations account for the evolution of mass and momentum of each phase. For compressible isentropic one-dimensional flows there are five unknowns that describe the evolution of the two-phase flow: the velocities of each phase u_i (where $i \in \{1,2\}$), the densities of each phase ρ_i and the phase fractions α_i (with the saturation constraint $\alpha_1 + \alpha_2 = 1$). The isentropic version of the model -firstly introduced by Baer & Nunziato in [1]- reads

$$\left\{\begin{array}{l} \partial_t \alpha_1 + u_2 \partial_x \alpha_1 = 0, \\ \partial_t(\alpha_1\rho_1) + \partial_x(\alpha_1\rho_1 u_1) = 0, \\ \partial_t(\alpha_1\rho_1 u_1) + \partial_x(\alpha_1\rho_1 u_1^2 + \alpha_1 p_1(\rho_1)) - p_1(\rho_1)\partial_x\alpha_1 = 0, \\ \partial_t(\alpha_2\rho_2) + \partial_x(\alpha_2\rho_2 u_2) = 0, \\ \partial_t(\alpha_2\rho_2 u_2) + \partial_x(\alpha_2\rho_2 u_2^2 + \alpha_2 p_2(\rho_2)) - p_1(\rho_1)\partial_x\alpha_2 = 0. \end{array}\right. \tag{2.1.1}$$

We assume barotropic pressure laws for each phase $\rho_i \mapsto p_i(\rho_i),\ i \in \{1,2\}$ with smooth dependence on the density, and which satisfy the following natural assumptions for all $\rho_i > 0$:

$$p_i(\rho_i) > 0, \quad \frac{dp_i}{d\rho_i}(\rho_i) > 0, \quad \lim_{\rho_i \to 0} p_i(\rho_i) = 0, \quad \lim_{\rho_i \to +\infty} p_i(\rho_i) = +\infty. \tag{2.1.2}$$

In practice, the usually considered pressure laws, also satisfy the following condition which implies the genuine non-linearity of the acoustic fields in each phase:

$$\frac{d^2 p_i}{d\rho_i^2}(\rho_i) + \frac{2}{\rho_i}\frac{dp_i}{d\rho_i}(\rho_i) > 0. \tag{2.1.3}$$

This system can be written in condensed form as

$$\partial_t \mathbb{U} + \partial_x \mathbf{f}(\mathbb{U}) + \mathbf{c}(\mathbb{U})\partial_x \mathbb{U} = 0, \tag{2.1.4}$$

where

$$\mathbb{U} = \begin{bmatrix} \alpha_1 \\ \alpha_1\rho_1 \\ \alpha_1\rho_1 u_1 \\ \alpha_2\rho_2 \\ \alpha_2\rho_2 u_2 \end{bmatrix}, \qquad \mathbf{f}(\mathbb{U}) = \begin{bmatrix} 0 \\ \alpha_1\rho_1 u_1 \\ \alpha_1\rho_1 u_1^2 + \alpha_1 p_1(\rho_1) \\ \alpha_2\rho_2 u_2 \\ \alpha_2\rho_2 u_2^2 + \alpha_2 p_2(\rho_2) \end{bmatrix}, \qquad \mathbf{c}(\mathbb{U})\partial_x\mathbb{U} = \begin{bmatrix} u_2\partial_x\alpha_1 \\ 0 \\ -p_1\partial_x\alpha_1 \\ 0 \\ -p_1\partial_x\alpha_2 \end{bmatrix}. \tag{2.1.5}$$

The following proposition characterizes the fields of this system:

Proposition 2.1.1. *System (2.1.1) is weakly hyperbolic since it admits the following real eigenvalues*

$$\sigma_1 = u_1 - c_1(\rho_1), \quad \sigma_2 = u_1 + c_1(\rho_1), \quad \sigma_3 = u_2 - c_2(\rho_2), \quad \sigma_4 = u_2, \quad \sigma_5 = u_2 + c_2(\rho_2), \tag{2.1.6}$$

where $c_i(\rho_i) = \sqrt{p_i'(\rho_i)}$ is the speed of sound for phase i. The corresponding right eigenvectors are linearly independent if, and only if

$$\alpha_1 \neq 0, \quad \alpha_2 \neq 0, \quad |u_1 - u_2| \neq c_1(\rho_1). \tag{2.1.7}$$

The characteristic fields associated with σ_1, σ_2, σ_3 and σ_5 are genuinely non-linear, while the characteristic filed associated with σ_4 is linearly degenerate.

We donote the phasic energies by $E_i := E_i(u_i, \tau_i) = \frac{u_i^2}{2} + e_i(\tau_i),\ i \in \{1, 2\}$. Here, the function $\tau \mapsto e_i(\tau)$ is such that $e_i'(\tau) = -\mathcal{P}_i(\tau)$, where $\mathcal{P}_i(\tau) = p_i(\tau^{-1})$ is the pressure seen as a function of the specific volume $\tau = \rho^{-1}$. And we have the following proposition:

Proposition 2.1.2. *The smooth solutions of system (2.1.1) satisfy the following phasic energy equations:*

$$\partial_t(\alpha_i\rho_i E_i) + \partial_x\left(\alpha_i\rho_i E_i + \alpha_i p_i(\rho_i)\right) u_i - u_2 p_1(\rho_1)\partial_x\alpha_i = 0, \quad i \in \{1, 2\}. \tag{2.1.8}$$

Summing over $i = 1, 2$ yields the following additional conservation law, also satisfied by the smooth solutions of system (2.1.1):

$$\partial_t\left(\alpha_1\rho_1 E_1 + \alpha_2\rho_2 E_2\right) + \partial_x\left(\left(\alpha_1\rho_1 E_1 + \alpha_1 p_1(\rho_1)\right) u_1 + \left(\alpha_2\rho_2 E_2 + \alpha_2 p_2(\rho_2)\right) u_2\right) = 0. \tag{2.1.9}$$

As regards the non-smooth weak solutions of (2.1.1), there is no uniqueness results and one has to add a so-called entropy criterion in order to select the relevant physical solutions. Thus, an entropy weak solution of (2.1.1) is a function $\mathbb{U}(x, t)$ that satisfies (2.1.1) in the sense of distributions as well as the following entropy inequality:

$$\partial_t\left(\alpha_1\rho_1 E_1 + \alpha_2\rho_2 E_2\right) + \partial_x\left(\left(\alpha_1\rho_1 E_1 + \alpha_1 p_1(\rho_1)\right) u_1 + \left(\alpha_2\rho_2 E_2 + \alpha_2 p_2(\rho_2)\right) u_2\right) \leq 0. \tag{2.1.10}$$

When the solution contains strong shocks, inequality (2.1.10) is strict in order to account for the physical loss of energy due to viscous phenomena that are not modeled in system (2.1.1).

2.1.2 A relaxation approximation

In this section, we consider a suitable relaxation approximation of the entropy weak solutions of system (2.1.1). For this purpose, we first recall that the genuine non-linearity of the acoustic fields is closely related to the non-linearities of the pressure laws $\rho_i \mapsto p_i(\rho_i)$, as seen in (2.1.3). In the spirit of [13], we consider an augmented system involving two additional phasic unknowns $\mathcal{T}_1$ and $\mathcal{T}_2$ associated with some linearization of the pressure laws. This linearization is designed to get a quasi-linear enlarged system, shifting the initial non-linearity from the convective part to a stiff relaxation source term. The relaxation approximation is based on the idea that the solutions of the original system are formally recovered as the limit of the solutions of the proposed enlarged system, in the regime of a vanishing relaxation coefficient $\varepsilon > 0$. Denoting $\mathbb{W} = (\alpha_1, \alpha_1\rho_1, \alpha_1\rho_1 u_1, \alpha_2\rho_2, \alpha_2\rho_2 u_2,\ alpha_1\rho_1\mathcal{T}_1, \alpha_2\rho_2\mathcal{T}_2)^T$ the relaxation state vector, we propose the following approximation for system (2.1.1):

$$\partial_t \mathbb{W}^\varepsilon + \partial_x \mathbf{g}(\mathbb{W}^\varepsilon) + \mathbf{d}(\mathbb{W}^\varepsilon)\partial_x \mathbb{W}^\varepsilon = \frac{1}{\varepsilon}\mathcal{R}(\mathbb{W}^\varepsilon), \tag{2.1.11}$$

where

$$\mathbf{g}(\mathbb{W}) = \begin{bmatrix} 0 \\ \alpha_1\rho_1 u_1 \\ \alpha_1\rho_1 u_1^2 + \alpha_1\pi_1(\tau_1, \mathcal{T}_1) \\ \alpha_2\rho_2 u_2 \\ \alpha_2\rho_2 u_2^2 + \alpha_2\pi_2(\tau_2, \mathcal{T}_2) \\ \alpha_1\rho_1\mathcal{T}_1 u_1 \\ \alpha_2\rho_2\mathcal{T}_2 u_2 \end{bmatrix}, \quad \mathbf{d}(\mathbb{W})\partial_x\mathbb{W} = \begin{bmatrix} u_2\partial_x\alpha_1 \\ 0 \\ -\pi_1(\tau_1, \mathcal{T}_1)\partial_x\alpha_1 \\ 0 \\ -\pi_1(\tau_1, \mathcal{T}_1)\partial_x\alpha_2 \\ 0 \\ 0 \end{bmatrix}, \quad \mathcal{R}(\mathbb{W}) = \begin{bmatrix} 0 \\ 0 \\ 0 \\ 0 \\ 0 \\ \alpha_1\rho_1(\tau_1 - \mathcal{T}_1) \\ \alpha_2\rho_2(\tau_2 - \mathcal{T}_2) \end{bmatrix}. \tag{2.1.12}$$

For each phase i in $\{1, 2\}$ the linearized pressure $\pi_i(\tau_i, \mathcal{T}_i)$ is a function defined as

$$\pi_i(\tau_i, \mathcal{T}_i) = \mathcal{P}_i(\mathcal{T}_i) + a_i^2(\mathcal{T}_i - \tau_i), \tag{2.1.13}$$

where $\tau_i = \rho_i^{-1}$ is the specific volume of phase i. We can see that in the formal limit $\varepsilon \to 0$, the additional variable $\mathcal{T}_i$ tends towards the specific volume τ_i, and the linearized pressure π_i tends towards the original nonlinear pressure p_i, thus recovering system (2.1.1) in the first five equations of (2.1.11). From this point and to ease the notation, we will omit the superscript $^\varepsilon$. In the sequel, the original system (2.1.1) will be referred to as the *equilibrium system* as opposed to the *relaxation system*. The constants a_i in (2.1.13) are two constant positive parameters that must be taken large enough to prevent system (2.1.11) from instabilities in the regime of small values of ε.

Let us now focus on the convective part of system (2.1.11):

$$\partial_t \mathbb{W} + \partial_x \mathbf{g}(\mathbb{W}) + \mathbf{d}(\mathbb{W})\partial_x \mathbb{W} = 0. \tag{2.1.14}$$

Proposition 2.1.3. *System (2.1.14) is weakly hyperbolic since it admits the following real eigenvalues*

$$\sigma_1 = u_1 - a_1\tau_1, \quad \sigma_2 = u_1, \quad \sigma_3 = u_1 + a_1\tau_1, \quad \sigma_4 = u_2 - a_2\tau_2, \quad \sigma_5 = \sigma_6 = u_2, \quad \sigma_7 = u_2 + a_2\tau_2. \tag{2.1.15}$$

The corresponding right eigenvectors are linearly independent if, and only if

$$\alpha_1 \neq 0, \quad \alpha_2 \neq 0, \quad |u_1 - u_2| \neq a_1\tau_1. \tag{2.1.16}$$

All the characteristic fields associated with these eigenvalues are linearly degenerate.

Unlike system (2.1.1), one remarkable property of the relaxation system (2.1.14) is the linear degeneracy of all the characteristic fields. This has the helpful consequence that jump relations can be easily derived through each wave. The relaxation approximation is therefore a pleasant way to get around the difficulties due to non-linearity (discrimination between shocks and rarefaction waves, jump relations for shocks...) which arise when solving the Riemann problem for (2.1.1).

In a similar way to that for the equilibrium system, we have balance equations on the phasic energies as well as a total mixture energy conservation equation satisfied by the smooth solutions of system (2.1.14):

Proposition 2.1.4. *The smooth solutions of system (2.1.14) satisfy the following phasic energy equations:*

$$\partial_t \left(\alpha_i\rho_i\mathcal{E}_i\right) + \partial_x \left(\alpha_i\rho_i\mathcal{E}_i + \alpha_i\pi_i\right) u_i - u_2\pi_1(\tau_1, \mathcal{T}_1)\partial_x\alpha_i = 0, \quad i \in \{1, 2\}. \tag{2.1.17}$$

where the phasic energies are defined as

$$\mathcal{E}_i := \mathcal{E}_i(u_i, \tau_i, \mathcal{T}_i) = \frac{u_i^2}{2} + e_i(\mathcal{T}_i) + \frac{\pi_i^2(\tau_i, \mathcal{T}_i) - \mathcal{P}_i^2(\mathcal{T}_i)}{2a_i^2}, \qquad i \in \{1, 2\}. \tag{2.1.18}$$

Summing over $i = 1, 2$ yields the following additional conservation law, also satisfied by the smooth solutions of system (2.1.14):

$$\partial_t \left(\alpha_1\rho_1\mathcal{E}_1 + \alpha_2\rho_2\mathcal{E}_2\right) + \partial_x \left(\left(\alpha_1\rho_1\mathcal{E}_1 + \alpha_1\pi_1\right) u_1 + \left(\alpha_2\rho_2\mathcal{E}_2 + \alpha_2\pi_2\right) u_2\right) = 0, \tag{2.1.19}$$

Regarding the discontinuous solutions, as system (2.1.14) has only linearly degenerate fields, one would expect to see no energy dissipation in the solutions, which makes it natural to construct discontinuous solutions that also satisfy equation (2.1.19) (see [15, 2, 9]). In particular, any solution composed of constant states separated by contact discontinuities should satisfy the corresponding Rankine-Hugoniot's jump relation associated with (2.1.19). Nevertheless, building solutions with strict energy dissipation appears to be compulsory when solving the Riemann problem for (2.1.14), especially in the vanishing phase regimes. Indeed, as discussed in section 2.2.5, computing solutions with positive densities while exaclty preserving the total energy in the weak sense, is in some cases impossible when one of the phase fractions is close to zero. Instead, one has to *weaken* this condition by authorizing strict energy dissipation. It is not surprising to lose energy-conservation in these particular regimes of vanishing phases, since the hyperbolicity property, which is necessary for using an additional conservation law as a Riemann invariant is lost in these regimes.

2.2 The Riemann problem for the relaxation system

The aim of this section is to solve the Riemann problem associated with the homogeneous part of the relaxation system. Being given a pair of initial states $(\mathbb{W}_L, \mathbb{W}_R)$, we seek solutions of the

following Cauchy problem:

$$\partial_t \mathbb{W} + \partial_x \mathbf{g}(\mathbb{W}) + \mathbf{d}(\mathbb{W})\partial_x \mathbb{W} = 0, \tag{2.2.1}$$

with the initial condition

$$\mathbb{W}(x, t=0) = \begin{cases} \mathbb{W}_L & \text{if} \quad x < 0, \\ \mathbb{W}_R & \text{if} \quad x > 0. \end{cases} \tag{2.2.2}$$

We recall that $\pi_i(\tau_i, \mathcal{T}_i) = \mathcal{P}_i(\mathcal{T}_i) + a_i^2(\mathcal{T}_i - \tau_i)$, with $\tau_i = {\rho_i}^{-1}$, $i \in \{1, 2\}$, and where $a_i,\ i \in \{1, 2\}$ are two positive constant parameters. The solutions are sought in the domain of positive densities ρ_i and positive $\mathcal{T}_i$:

$$\Omega^r = \Big\{ \mathbb{W} \in \mathbb{R}^7, 0 < \alpha_1 < 1,\ \alpha_i \rho_i > 0,\ \alpha_i \rho_i \mathcal{T}_i > 0,\ i \in \{1, 2\} \Big\}. \tag{2.2.3}$$

2.2.1 Definition of the solutions to the Riemann problem

The solution is sought in the form of a *self-similar* function only depending on the variable $\xi = \frac{x}{t}$, that's to say $\mathbb{W}(x, t) = \mathbb{W}_r(x/t)$, where $\xi \mapsto \mathbb{W}_r(\xi)$ is a weak solution of

$$-\xi \mathbb{W}'(\xi) + \mathbf{g}(\mathbb{W}(\xi))' + \mathbf{d}(\mathbb{W}(\xi))\mathbb{W}'(\xi) = 0. \tag{2.2.4}$$

As all the fields are linearly degenerate, the function $\mathbb{W}_r(\xi)$ is a piecewise constant function, where each discontinuity corresponds to a traveling wave in the (x, t)-plane. In addition, if the solution remains in the domain of hyperbolicity, $\mathbb{W}_r(\xi)$ is expected to be composed of at most six discontinuities, associated with the six eigenvalues $u_1 \pm a_1\tau_1$, $u_2 \pm a_2\tau_2$, u_1 and u_2, separating (at most) seven constant intermediate states (see Lax's theory for Riemann problems [11]). In the ξ-line, the position of each discontinuity is equal to the propagation speed of the corresponding traveling wave in the (x, t)-plane.

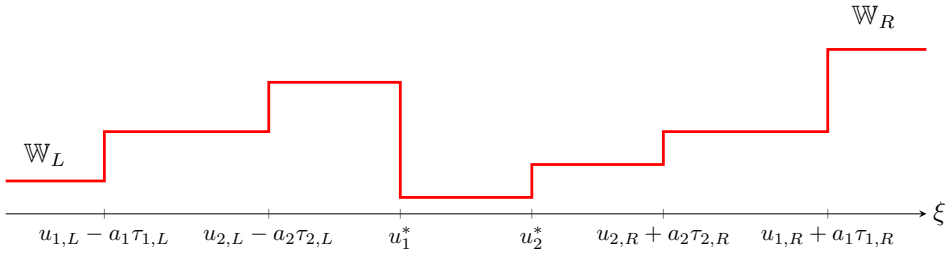

In our application context (nuclear flows), we are only interested in solutions which have a ***subsonic wave ordering***, *i.e.* solutions for which the propagation velocity u_2^* of the void fraction α_1 lies in-between the acoustic waves of phase 1 namely $u_{1,L} - a_1\tau_{1,L}$ and $u_{1,R} + a_1\tau_{1,R}$. In the sequel, these solutions are classified in three categories depending on the ordering between the u_1-contact discontinuity, and the u_2-contact discontinuity.

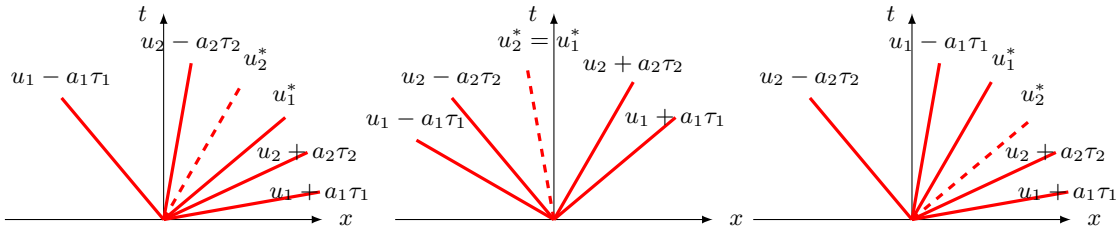

A solution with $u_2^* < u_1^*$. A solution with $u_2^* = u_1^*$. A solution with $u_2^* > u_1^*$.

Remark 2.2.1. *We draw the reader's attention on the fact that the considered solutions are allowed to have* ***phasic supersonic speeds*** $|u_i| > a_i\tau_i$ *as represented here. Indeed, the subsonic property considered here is related to the* ***relative velocity*** $u_1 - u_2$.

For each one of these discontinuous waves, one has to provide jump relations that ensure the constructed solution to be an entropy weak solution. For all the discontinuities except the one associated with the eigenvalue u_2, the system is locally conservative (the product $\pi_1\partial_x\alpha_i$ locally vanishes) and the jump conditions are simply obtained by the Rankine-Hugoniot relations applied to each equation of the system (except the transport equation on α_1).

On the contrary, for the u_2-wave, we have $\partial_x\alpha_i \neq 0$. In fact $\partial_x\alpha_i$ identifies with a Dirac measure given by

$$\partial_x\alpha_i = \Delta\alpha_i\delta_0(x - u_2^*t), \text{ with } \Delta\alpha_i := \alpha_{i,R} - \alpha_{i,L}, \tag{2.2.5}$$

where u_2^* is the constant propagation speed of this wave. Hence, as the pressure π_1 may be discontinuous across this wave, the product $\pi_1\partial_x\alpha_i$ is not clearly defined at this stage. Actually, as long as the system is hyperbolic, there is non ambiguity in its definition since the classical theory [15, 2, 9] shows that the jump relations across this discontinuity is totally determined by the Riemann invariants of this linearly degenerate field. A first relation is given by the continuity of the eigenvalue u_2 across this linearly degenerate wave, and we get three more independent jump relations by applying Rankine-Hugoniot's formula to the conservative equations of phase 1 and to the total momentum conservation:

$$\begin{aligned}
&[u_2]_{\xi=u_2^*} = 0,\\
-u_2^*&[\alpha_1\rho_1]_{\xi=u_2^*} + [\alpha_1\rho_1u_1]_{\xi=u_2^*} = 0,\\
-u_2^*&[\alpha_1\rho_1\mathcal{T}_1]_{\xi=u_2^*} + [\alpha_1\rho_1u_1\mathcal{T}_1]_{\xi=u_2^*} = 0,\\
-u_2^*&[\alpha_1\rho_1u_1 + \alpha_2\rho_2u_2]_{\xi=u_2^*} + \left[\alpha_1\rho_1u_1^2 + \alpha_1\pi_1 + \alpha_2\rho_2u_2^2 + \alpha_2\pi_2\right]_{\xi=u_2^*} = 0.
\end{aligned} \tag{2.2.6}$$

Here, $[X]_{\xi=u_2^*} = X^r - X^l$ denotes the difference between the values taken by the quantity X on the right and on the left of the u_2-wave. Finally, if the system is hyperbolic, a last jump relation (recall that the eigenvalue u_2 has multiplicity 2) is obtained by applying Rankine-Hugoniot's formula to the total energy preservation (2.1.19) which yields

$$-u_2^*\left[\alpha_1\rho_1\mathcal{E}_1 + \alpha_2\rho_2\mathcal{E}_2\right]_{\xi=u_2^*} + \left[\left(\alpha_1\rho_1\mathcal{E}_1 + \alpha_1\pi_1\right)u_1 + \left(\alpha_2\rho_2\mathcal{E}_2 + \alpha_2\pi_2\right)u_2\right]_{\xi=u_2^*} = 0. \tag{2.2.7}$$

Hence, each wave is equipped with a set of independent jump relations which enables the resolution of the Riemann problem in the hyperbolic case, provided that one is capable of finding a

solution to such a non-linear set of equations. On the basis of this discussion, we give the following definition for the solutions of the Riemann problem (2.2.1)-(2.2.2) for the relaxation system. Note that in this work, we only consider solutions **with subsonic wave ordering**, as specified in the following definition:

Definition 2.2.1. *Let $(\mathbb{W}_L, \mathbb{W}_R)$ be two states in Ω^r. A solution to the Riemann problem (2.2.1)-(2.2.2) **with subsonic wave ordering** is a self-similar mapping $\mathbb{W}(x,t) = \mathbb{W}_r(x/t; \mathbb{W}_L, \mathbb{W}_R)$ where the function $\xi \mapsto \mathbb{W}_r(\xi; \mathbb{W}_L, \mathbb{W}_R)$ belongs to $L^1_{loc}(\mathbb{R}, \Omega^r)$ and satisfies the following properties:*

(i) $\mathbb{W}_r(\xi; \mathbb{W}_L, \mathbb{W}_R)$ is a piecewise constant function, composed of (at most) seven intermediate states separated by (at most) six contact discontinuities associated with the eigenvalues $u_1 \pm a_1\tau_1$, $u_2 \pm a_2\tau_2$, u_1, u_2 and such that

$$\lim_{\xi \to -\infty} \mathbb{W}_r(\xi; \mathbb{W}_L, \mathbb{W}_R) = \mathbb{W}_L, \quad \lim_{\xi \to +\infty} \mathbb{W}_r(\xi; \mathbb{W}_L, \mathbb{W}_R) = \mathbb{W}_R. \tag{2.2.8}$$

(ii) There exists two real numbers u_2^* and π_1^* depending on $(\mathbb{W}_L, \mathbb{W}_R)$ such that, for all test function φ in $\mathcal{D}(\mathbb{R})$,

$$\int_{\mathbb{R}} \mathbb{W}_r(\xi; \mathbb{W}_L, \mathbb{W}_R)\varphi(\xi)d\xi + \int_{\mathbb{R}} \left\{\xi \mathbb{W}_r(\xi; \mathbb{W}_L, \mathbb{W}_R) - \boldsymbol{g}(\mathbb{W}_r(\xi; \mathbb{W}_L, \mathbb{W}_R))\right\} \varphi'(\xi)d\xi + \mathbf{D}^*\varphi(u_2^*) = 0, \tag{2.2.9}$$

where $\mathbf{D}^* = \Delta\alpha_1(u_2^*, 0, -\pi_1^*, 0, 0, \pi_1^*, 0)^T$.

(iii) The solution has a subsonic wave ordering in the following sense:

$$u_{1,L} - a_1\tau_{1,L} < u_2^* < u_{1,R} + a_1\tau_{1,R}. \tag{2.2.10}$$

(iv) The energy jump across the u_2-contact discontinuity is non-positive:

$$-u_2^* \left[\alpha_1\rho_1\mathcal{E}_1 + \alpha_2\rho_2\mathcal{E}_2\right]_{\xi=u_2^*} + \left[\left(\alpha_1\rho_1\mathcal{E}_1 + \alpha_1\pi_1\right)u_1 + \left(\alpha_2\rho_2\mathcal{E}_2 + \alpha_2\pi_2\right)u_2\right]_{\xi=u_2^*} \leq 0. \tag{2.2.11}$$

*If (2.2.11) is a strict inequality, the solution is said to be **energy-dissipating**. Otherwise the solution is **energy-preserving**.*

This definition deserves a few comments. Equation (2.2.9) in the second item, provides some important information. In particular, it implies for all the waves except u_2, that the discontinuities are defined by the Rankine-Hugoniot jump relations. It also defines rigourously the non-conservative product $\mathbf{d}(\mathbb{W}_r(\xi))\mathbb{W}_r'(\xi)$ by introducing u_2^*, the propagation velocity of the void fraction wave and π_1^*, the weight of the non-conservative product $\pi_1\partial_x\alpha_1$. Actually, this weight is obtained by the Rankine-Hugoniot jump relation applied to any of the momentum equations:

$$-u_2^*\left[\alpha_i\rho_i u_i\right] + \left[\alpha_i\rho_i u_i^2 + \alpha_i\pi_i\right]_{\xi=u_2^*} = \pi_1^*\Delta\alpha_i.$$

The third item states that the solution has the expected subsonic wave ordering. Observe that this requirement prevents the loss of hyperbolicity due to wave interactions. However, the system may still be resonant in the regimes of vanishing phases.

The fourth required property *(iv)* expresses that the total energy is either preserved or dissipated through the u_2-contact discontinuity. As this discontinuity is associated with a linearly degenerate field, the total energy is actually expected to be preserved when the system is hyperbolic. However, in the regimes of vanishing phases, where the system becomes resonant, there are no more reasons for this exact energy conservation to hold true. In the sequel, we will see that in most cases, preserving the total energy (2.2.7) through the u_2-contact is possible for constructing admissible solutions of the Riemann problem. In this case, one may speak of *energy-preserving solutions*. However, it appears that when the ratio $\frac{\alpha_{1,L}}{\alpha_{1,R}}$ (or its inverse) is large, constructing solutions with positive densities while maintaining the exact energy conservation across the u_2-contact discontinuity is impossible. It will be shown that positive solutions cannot be obtained unless one authorizes some dissipation of the total energy through the u_2-contact, and one speaks of *energy-dissipating solutions* in that particular case. Once again, it is not surprising to lose energy-conservation in these particular regimes of vanishing phases, since the hyperbolicity property, which is necessary for using an additional conservation law as a Riemann invariant is lost in these regimes. Through all the waves except u_2, the energy conservation (2.1.19) is exactly satisfied as a consequence of the other jump relations. Hence, the global energy equation may be formally written as

$$\partial_t \left(\alpha_1\rho_1\mathcal{E}_1 + \alpha_2\rho_2\mathcal{E}_2\right) + \partial_x \left(\left(\alpha_1\rho_1\mathcal{E}_1 + \alpha_1\pi_1\right)u_1 + \left(\alpha_2\rho_2\mathcal{E}_2 + \alpha_2\pi_2\right)u_2\right) = -\mathcal{Q}(\mathbb{W}_L,\mathbb{W}_R)\delta_0(x-u_2^*t). \tag{2.2.12}$$

where $\mathcal{Q}(\mathbb{W}_L,\mathbb{W}_R) \geq 0$ is a non-negative real number measuring the dissipation of the total energy through the u_2-wave.

Before describing the strategy for solving the Riemann problem (2.2.1)-(2.2.2), let us give a technical result which will be useful in the sequel. It aims at giving an equivalent alternative choice for the fifth jump relation.

Lemma 2.2.1. *Let $\mathcal{Q}$ be a given non-negative number, and consider the jump relations*

(i)
$$-u_2^*\left[\alpha_1\rho_1\mathcal{E}_1 + \alpha_2\rho_2\mathcal{E}_2\right]_{\xi=u_2^*} + \left[\left(\alpha_1\rho_1\mathcal{E}_1 + \alpha_1\pi_1\right)u_1 + \left(\alpha_2\rho_2\mathcal{E}_2 + \alpha_2\pi_2\right)u_2\right]_{\xi=u_2^*} = -\mathcal{Q}, \tag{2.2.13}$$

(ii)
$$\left[\alpha_1\rho_1\overline{\mathcal{E}}_1(u_1-u_2^*) + \alpha_1\pi_1(u_1-u_2^*)\right]_{\xi=u_2^*} = -\mathcal{Q}, \tag{2.2.14}$$

where $\overline{\mathcal{E}}_1 := \frac{(u_1-u_2^*)^2}{2} + e_1(\mathcal{T}_1) + \frac{\pi_1^2(\tau_1,\mathcal{T}_1)-p_1^2(\mathcal{T}_1)}{2a_1^2}$. Then, the set of jump relations (2.2.6)-(2.2.13) across the u_2-wave is equivalent to the set of jump relations (2.2.6)-(2.2.14).

Proof. The proof follows from easy manipulations and is therefore left to the reader. □

2.2.2 The resolution strategy: an iterative procedure

Following Definition 2.2.1, the non-conservative product of the momentum equations identifies with the following Dirac measure

$$\pi_1^*\Delta\alpha_1\delta_0(x-u_2^*t). \tag{2.2.15}$$

The key challenge to solving the Riemann problem for the relaxation system consists in determining this non-conservative product $\pi_1^*\Delta\alpha_1\delta_0(x-u_2^*t)$ in the case $\alpha_{1,L} \neq \alpha_{1,R}$. Indeed, if

$\alpha_{1,L} = \alpha_{1,R}$, the two phases are *decoupled* and the resolution is straightforward as stated in the following lemma.

Lemma 2.2.2. *Consider the Riemann problem (2.2.1)-(2.2.2) with $\alpha_{1,L} = \alpha_{1,R}$. Then, a self-similar solution $\xi \mapsto \mathbb{W}(\xi; \mathbb{W}_L, \mathbb{W}_R)$ is such that $\alpha_1(\xi) = cst = \alpha_{1,L} = \alpha_{1,R}$, so that the non-conservative product $\pi_1(\tau_1, \mathcal{T}_1)\partial_x \alpha_i$ vanishes. As a consequence, the evolutions of the two phases are completely decoupled and the intermediate states for each phase are given for $i \in \{1, 2\}$ by*

$$u_i^\sharp := \frac{1}{2}(u_{i,L} + u_{i,R}) - \frac{1}{2a_i}(\pi_{i,R} - \pi_{i,L}), \tag{2.2.16}$$

$$\pi_i^\sharp := \frac{1}{2}(\pi_{i,R} + \pi_{i,L}) - \frac{a_i}{2}(u_{i,R} - u_{i,L}), \tag{2.2.17}$$

$$\tau_{i,L}^\sharp := \tau_{i,L} + \frac{1}{a_i}(u_i^\sharp - u_{i,L}) = \tau_{i,L} + \frac{1}{2a_i}(u_{i,R} - u_{i,L}) - \frac{1}{2a_i^2}(\pi_{i,R} - \pi_{i,L}), \tag{2.2.18}$$

$$\tau_{i,R}^\sharp := \tau_{i,R} - \frac{1}{a_i}(u_i^\sharp - u_{i,R}) = \tau_{i,R} + \frac{1}{2a_i}(u_{i,R} - u_{i,L}) + \frac{1}{2a_i^2}(\pi_{i,R} - \pi_{i,L}). \tag{2.2.19}$$

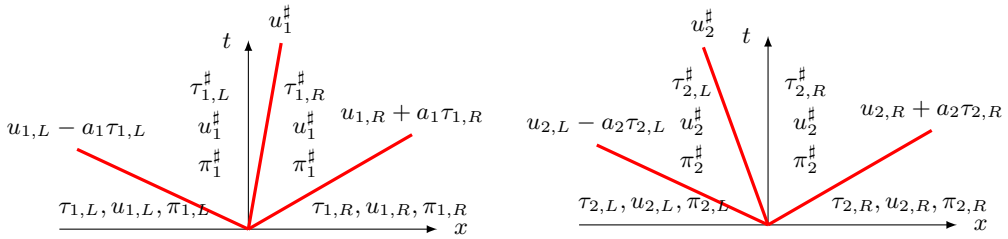

Phase solutions in the case of constant initial phase fractions $\alpha_{i,L} = \alpha_{i,R}$. In each case, $\mathcal{T}_{i,L}^\sharp = \mathcal{T}_{i,L}$ and $\mathcal{T}_{i,R}^\sharp = \mathcal{T}_{i,R}$.

The value of u_2^* is given by $u_2^\sharp$ and the solution has a subsonic wave ordering if and only if, these quantities satisfy the following constraint:

$$u_1^\sharp - a_1\tau_{1,L}^\sharp < u_2^\sharp < u_1^\sharp + a_1\tau_{1,R}^\sharp. \tag{2.2.20}$$

Observe that the quantities defined in (2.2.16) to (2.2.19) are independent of the phase fractions $\alpha_{1,L} = \alpha_{1,R}$. They only depend on the pair $(\mathbb{V}_L, \mathbb{V}_R)$ where $\mathbb{V}$ is the vector of physical variables $\mathbb{V} = (\rho_1, u_1, \rho_2, u_2, \mathcal{T}_1, \mathcal{T}_2)^T$. On the contrary, if $\alpha_{i,L} \neq \alpha_{i,R}$, the evolutions of both phases are affected by the u_2-wave (which has multiplicity 2) and the physical quantities of the two phases are **coupled** through this wave.

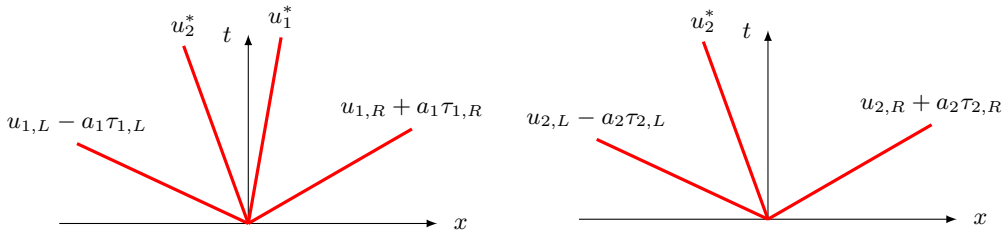

Phase solutions in the case of non-constant initial phase fractions $\alpha_{i,L} \neq \alpha_{i,R}$.

Starting from the known solution in the decoupled case $|\alpha_{1,L} - \alpha_{1,R}| = 0$, we seek to construct a *branch of solutions* with subsonic wave ordering, in the non-conservative cases $|\alpha_{1,L} - \alpha_{1,R}| \neq 0$. Actually the aim is to expose a subsonic type condition, similar to (2.2.20) which accounts for the subsonic ordering requirement

$$u_1^\sharp - a_1\tau_{1,L}^\sharp < u_2^* < u_1^\sharp + a_1\tau_{1,R}^\sharp, \tag{2.2.21}$$

and ensures the existence of such a solution. Of course, the main difficulty here is that the value of u_2^* is not *a priori* known with respect to the initial data unlike in the case $\alpha_{1,L} = \alpha_{1,R}$. However, the analysis carried out in this paper will expose a very simple generalization of condition (2.2.20) valid for the case $\alpha_{1,L} \neq \alpha_{1,R}$ and that can be explicitely tested with respect to the initial data just as (2.2.20).

For this purpose, we make the following key remark, which is the cornerstone of the whole resolution strategy.

Key remark: *Consider the case $\alpha_{1,L} \neq \alpha_{1,R}$. If one is able to **make a prediction** of the pressure π_1^* that defines the non-conservative product $\pi_1\partial_x\alpha_i$ and therefore shift it to a **known right hand side of the system**, then one can see that the governing equations for phase 2 are completely independent of the phase 1 quantities, namely ρ_1, u_1 and $\mathcal{T}_1$.*

Indeed, the governing equations for phase 2 form the following independent system:

$$\begin{cases} \partial_t\alpha_2 + u_2\partial_x\alpha_2 = 0, \\ \partial_t(\alpha_2\rho_2) + \partial_x(\alpha_2\rho_2u_2) = 0, \\ \partial_t(\alpha_2\rho_2u_2) + \partial_x(\alpha_2\rho_2u_2^2 + \alpha_2\pi_2(\tau_2, \mathcal{T}_2)) = \pi_1^*\partial_x\alpha_2, \\ \partial_t(\alpha_2\rho_2\mathcal{T}_2) + \partial_x(\alpha_2\rho_2\mathcal{T}_2u_2) = 0, \end{cases} \tag{2.2.22}$$

where π_1^* **is here assumed to be known**. Hence, the Riemann problem for (2.2.22) can be solved regardless of the quantities related to phase 1. A pleasant property is the hyperbolicity of this system. Thus, knowing a prediction of the pressure π_1^*, one can explicitly compute the value of the kinematic speed u_2^* by solving the Riemann problem associated with phase 2.

Based on this important remark, we decide to adopt an iterative procedure for the resolution of the Riemann problem (2.2.1)-(2.2.2) for a given pair of initial left and right data $(\mathbb{W}_L, \mathbb{W}_R) \in \Omega^r \times \Omega^r$. Formally, it amounts to iterating on the pair (u_2^*, π_1^*):

First step: The pressure π_1^* defining the non-conservative product $\pi_1\partial_x\alpha_1 = \pi_1^*\Delta\alpha_1\delta_0(x-u_2^*t)$ is first assumed to be known, and one determines u_2^* by solving the Riemann problem for the governing system (2.2.22) of phase 2. This first step enables to define a function

$$\mathscr{F}[\mathbb{W}_L,\mathbb{W}_R;a_2]:\left\{\begin{array}{ccc}\mathbb{R}&\longrightarrow&\mathbb{R}\\ \pi_1^*&\longmapsto&u_2^*.\end{array}\right. \tag{2.2.23}$$

Second step: The advection velocity u_2^* of the phase fraction α_1 is then assumed to be known. Thus, the governing equations for phase 1 read

$$\left\{\begin{array}{l}\partial_t\alpha_1+u_2^*\partial_x\alpha_1=0,\\ \partial_t(\alpha_1\rho_1)+\partial_x(\alpha_1\rho_1u_1)=0,\\ \partial_t(\alpha_1\rho_1u_1)+\partial_x(\alpha_1\rho_1u_1^2+\alpha_1\pi_1(\tau_1,\mathcal{T}_1))=\pi_1\partial_x\alpha_1,\\ \partial_t(\alpha_1\rho_1\mathcal{T}_1)+\partial_x(\alpha_1\rho_1\mathcal{T}_1u_1)=0.\end{array}\right. \tag{2.2.24}$$

In addition to the kinematic velocity u_1 and the acoustic speeds $u_1\pm a_1\tau_1$, the Riemann problem for (2.2.24) involves an *additional wave* whose *known* constant velocity is u_2^*. This wave is weighted with an *unknown* weight $\pi_1^*\Delta\alpha_1$ (only for the momentum equation) which is calculated by solving the Riemann problem for (2.2.24) and then applying Rankine-Hugoniot's jump relation to the momentum equation for the traveling wave u_2^*. This second step amounts to defining a function

$$\mathscr{G}[\mathbb{W}_L,\mathbb{W}_R;a_1]:\left\{\begin{array}{ccc}\mathbb{R}&\longrightarrow&\mathbb{R}\\ u_2^*&\longmapsto&\pi_1^*.\end{array}\right. \tag{2.2.25}$$

Performing an iterative procedure on these two steps actually boils down to the following fixed-point research.

Find u_2^* *in* $(u_1^\sharp-a_1\tau_{1,L}^\sharp,u_1^\sharp+a_1\tau_{1,R}^\sharp)\bigcap(u_2^\sharp-a_1\tau_{2,L}^\sharp,u_2^\sharp+a_2\tau_{2,R}^\sharp)$ *such that*

$$u_2^*=\Big(\mathscr{F}[\mathbb{W}_L,\mathbb{W}_R;a_2]\circ\mathscr{G}[\mathbb{W}_L,\mathbb{W}_R;a_1]\Big)(u_2^*). \tag{2.2.26}$$

The interval where u_2^* must be sought corresponds to the subsonic wave ordering condition (2.2.10) in the one hand, and to the positivity of the intermediate states of phase 2 in the other hand (see Proposition (2.2.6)). It is worth noting that, within each step 1 and 2, where a Riemann problem is solved for each phase, one will have to introduce some restrictions on the initial data $(\mathbb{W}_L,\mathbb{W}_R)$ so as to guarantee the existence of admissible solutions. Actually, these restrictions will provide sufficient conditions for an existence theorem (see section 2.2.3). As a matter of fact, the ultimate objective would be to establish a partition of the space of initial conditions $\Omega^r\times\Omega^r$, each element of this partition corresponding to a particular ordering of the waves. In this paper however, we only consider subsonic wave orderings according to Definition 2.2.1.

Section 2.2.3 is devoted to presenting and commenting the main results of the paper while in sections 2.2.4 to 2.2.6, the iterative procedure described above is handled. As a matter of fact, in section 2.2.4, the first step of the iterative process is performed and we give the explicit formula of function $\mathscr{F}[\mathbb{W}_L,\mathbb{W}_R;a_2]$ defined in (2.2.23). Then, in section 2.2.5, we perform a change of

variables which facilitates the resolution of the governing equations for phase 1. Once, the value of u_2^* is predicted by the first step, this change of variables consists in re-writing the governing equations of phase 1 in the moving frame associated with the traveling wave of velocity u_2^*. In section 2.2.4 however, we restrict the presentation to the wave configurations $u_2^* < u_1^*$. This second step allows us to define an explicit formula for function $\mathscr{G}[\mathbb{W}_L, \mathbb{W}_R; a_1]$ introduced in (2.2.25). Finally, in section 2.2.6, we prove that, under some assumptions on the initial data $(\mathbb{W}_L, \mathbb{W}_R)$ (see Theorem 2.2.3), there exists a unique energy-preserving solution to the fixed point problem (2.2.26). This unique solution corresponds to the exact conservation of the total energy across the u_2-contact discontinuity. It will be shown however that in some cases where the ratio $\frac{\alpha_{1,L}}{\alpha_{1,R}}$ is large, this solution may have non-positive densities. By relaxing the conservation of the total energy, we recover the existence of positive solutions.

The results for the other wave configurations $u_2^* = u_1^*$ and $u_2^* > u_1^*$ can be obtained through the same process, or can be inferred from the Galilean invariance of the equations.

2.2.3 An existence theorem for solutions with subsonic wave ordering

We may now state the main result of this paper, an existence theorem for the Riemann problem (2.2.1)-(2.2.2). We refer to equations (2.2.16) to (2.2.19) for the definition of the quantities $^\sharp$ used in the theorem, an we define the following number which solely depends on the initial phase fractions:

$$\Lambda^\alpha := \frac{\alpha_{2,R} - \alpha_{2,L}}{\alpha_{2,R} + \alpha_{2,L}}. \tag{2.2.27}$$

Theorem 2.2.3. *Let be given a pair of admissible initial states $(\mathbb{W}_L, \mathbb{W}_R) \in \Omega^r \times \Omega^r$ and assume that the parameter a_i is such that $\tau_{i,L}^\sharp > 0$ and $\tau_{i,R}^\sharp > 0$ for i in $\{1,2\}$. There exists solutions with subsonic wave ordering to the Riemann problem (2.2.1)-(2.2.2) in the sense of Definition 2.2.1 if the following condition holds:*

$$(\boldsymbol{A}) \qquad -a_1\tau_{1,R}^\sharp < \frac{u_1^\sharp - u_2^\sharp - \frac{1}{a_2}\Lambda^\alpha(\pi_1^\sharp - \pi_2^\sharp)}{1 + \frac{a_1}{a_2}|\Lambda^\alpha|} < a_1\tau_{1,L}^\sharp.$$

*In addition, if the ratio $\frac{\alpha_{1,L}}{\alpha_{1,R}}$ is in a neighbourhood of 1, condition $(\boldsymbol{A})$ is a **necessary and sufficient** condition for the existence of a **unique** energy-preserving solution. If $\frac{\alpha_{1,L}}{\alpha_{1,R}}$ is too large, or too small depending on the wave ordering, ensuring positive densities for phase 1 may require strict energy dissipation, and it is always possible under assumption $(\boldsymbol{A})$ to ensure the posivity of the phase 1 densities by dissipating the total energy. The densities of phase 2 are positive if and only if,*

$$(\boldsymbol{B}) \qquad u_2^\sharp - a_2\tau_{2,L}^\sharp < u_2^* < u_2^\sharp + a_2\tau_{2,R}^\sharp. \tag{2.2.28}$$

Moreover, we have the following proposition which specifies the wave ordering of the solution depending on the sign of the quantity

$$U^\sharp = \frac{u_1^\sharp - u_2^\sharp - \frac{1}{a_2}\Lambda^\alpha(\pi_1^\sharp - \pi_2^\sharp)}{1 + \frac{a_1}{a_2}|\Lambda^\alpha|}.$$

Proposition 2.2.4. *Let $(\mathbb{W}_L, \mathbb{W}_R) \in \Omega^r \times \Omega^r$ be two initial states satisfying the existence conditions of Theorem 2.2.3. Condition (**A**) can be decomposed into the three following conditions defining the wave configuration:*

1. *Either*

$$(\boldsymbol{A1}) \qquad 0 < \frac{u_1^\sharp - u_2^\sharp - \frac{1}{a_2}\Lambda^\alpha(\pi_1^\sharp - \pi_2^\sharp)}{1 + \frac{a_1}{a_2}|\Lambda^\alpha|} < a_1\tau_{1,L}^\sharp,$$

   and the solutions have the wave configuration $u_2^* < u_1^*$.

2. *Or*

$$(\boldsymbol{A2}) \qquad -a_1\tau_{1,R}^\sharp < \frac{u_1^\sharp - u_2^\sharp - \frac{1}{a_2}\Lambda^\alpha(\pi_1^\sharp - \pi_2^\sharp)}{1 + \frac{a_1}{a_2}|\Lambda^\alpha|} < 0,$$

   and the solutions have the wave configuration $u_2^* > u_1^*$.

3. *Or*

$$(\boldsymbol{A3}) \qquad u_1^\sharp - u_2^\sharp - \frac{1}{a_2}\Lambda^\alpha(\pi_1^\sharp - \pi_2^\sharp) = 0,$$

   and the solutions have the wave configuration $u_2^* = u_1^*$.

The proofs of these two results follow from the steps described in the three following sections 2.2.4 2.2.5 and 2.2.6. Before giving the details of these steps, let us first make some comments on these results:

(i) Assumption (**A**) (actually (**A1**), (**A2**) or (**A3**)) **can be very easily tested** in terms of the initial data and the parameters a_i, $i \in \{1, 2\}$. To our knowledge, there is no similar result concerning the Riemann problem for the isentropic non-relaxed Baer-Nunziato system (2.1.1).

(ii) Assumption (**A**) allows to compute the value of the wave propagation velocity u_2^*, while assumption (**B**) is not needed for this computation. Actually, with the obtained value of u_2^*, one has to *check* that assumption (**B**), which is equivalent to the positivity of the phase 2 densities, is satisfied. In the numerical applications using this Riemann solver (see chapter 3), it will always be possible to ensure condition (**B**) by taking a large enough value of the relaxation parameter a_2.

(iii) Assumption (**A**) reduces to (2.2.20) when $\alpha_{1,L} = \alpha_{1,R}$ since in this case $\Lambda^\alpha = 0$. In this sense, assumption (**A**) is a generalization of (2.2.20) for the non-conservative case $\alpha_{1,L} \neq \alpha_{1,R}$.

(iv) The quantities $a_1\tau_{1,L}^\sharp$ and $a_1\tau_{1,R}^\sharp$ can be seen as two sound propagation speeds, while the quantity $U^\sharp$, which has the dimension of a velocity, measures the difference between the pressures and kinematic velocities of the two phases, in the initial data. Observe that if the initial data is close to the pressure and velocity equilibrium between the two phases, this quantity is expected to be small compared to $a_1\tau_{1,L}^\sharp$ and $a_1\tau_{1,R}^\sharp$.

(v) One may formulate a geometrical interpretation of Theorem 2.2.3. Assuming that there exists a solution with subsonic relative speeds when $|\alpha_{1,R} - \alpha_{1,L}| = 0$ (*i.e.* assuming (2.2.20)), the theorem shows that if $|\alpha_{1,R} - \alpha_{1,L}| \neq 0$ is sufficiently small, then the Riemann problem still admits energy-preserving subsonic solutions. Provided that one allows some energy-dissipation across the u_2-wave, this branch of solutions can be followed for Riemann problems in which $|\alpha_{1,R} - \alpha_{1,L}|$ increases (holding the other quantities in the initial left and right data fixed) until assumption (**A**) is violated, or until $|\alpha_{1,R} - \alpha_{1,L}| = 1$.

(vi) Again, we emphasize that for most of the initial data $(\mathbb{W}_L, \mathbb{W}_R)$, it is possible to construct energy-preserving solutions that exactly preserve the total energy conservation in the weak sense:

$$\partial_t \left(\alpha_1\rho_1\mathcal{E}_1 + \alpha_2\rho_2\mathcal{E}_2\right) + \partial_x \left(\left(\alpha_1\rho_1\mathcal{E}_1 + \alpha_1\pi_1\right)u_1 + \left(\alpha_2\rho_2\mathcal{E}_2 + \alpha_2\pi_2\right)u_2\right) = 0. \tag{2.2.29}$$

However, in some cases where the ratio $\frac{\alpha_{1,L}}{\alpha_{1,R}}$ (or its inverse depending on the wave ordering between u_1^* and u_2^*) is large, it may be necessary to dissipate some energy across the kinematic wave u_2 in order to enforce positive densities for phase 1. In section 2.2.6, we propose a ***kinetic relation*** for the determination of one solution, among all the admissible dissipative solutions given by the theorem. Actually, the total mixture energy is dissipated only because of the dissipation of the phase 1 energy. Indeed, according the Proposition 2.2.7 thereafter, the energy of phase 2 is preserved in the sense that it still satisfies the equation

$$\partial_t \left(\alpha_2\rho_2\mathcal{E}_2\right) + \partial_x \left(\alpha_2\rho_2\mathcal{E}_2 + \alpha_2\pi_2\right)u_2 - u_2^*\pi_1^*\partial_x\alpha_2 = 0, \tag{2.2.30}$$

in the weak sense, while the energy of phase 1 satisfies

$$\partial_t \left(\alpha_1\rho_1\mathcal{E}_1\right) + \partial_x \left(\alpha_1\rho_1\mathcal{E}_1 + \alpha_1\pi_1\right)u_1 - u_2^*\pi_1^*\partial_x\alpha_1 < 0, \tag{2.2.31}$$

thus dissipating the total mixture energy.

2.2.4 The Riemann problem for phase 2 with a predicted value of π_1^*

In this step, we assume that the pressure π_1^* defining the non-conservative product $\pi_1\partial_x\alpha_1 = \pi_1^*\Delta\alpha_1\delta_0(x - u_2^*t)$ is known while the propagation speed u_2^* is an unknown that must be calculated. Thus, the governing equations for phase 2 form the following system

$$\begin{cases} \partial_t\alpha_2 + u_2\partial_x\alpha_2 = 0, \\ \partial_t(\alpha_2\rho_2) + \partial_x(\alpha_2\rho_2u_2) = 0, \\ \partial_t(\alpha_2\rho_2u_2) + \partial_x(\alpha_2\rho_2u_2^2 + \alpha_2\pi_2(\tau_2, \mathcal{T}_2)) = \pi_1^*\partial_x\alpha_2, \\ \partial_t(\alpha_2\rho_2\mathcal{T}_2) + \partial_x(\alpha_2\rho_2\mathcal{T}_2u_2) = 0, \end{cases} \tag{2.2.32}$$

with $\pi_2(\tau_2, \mathcal{T}_2) = \mathcal{P}_2(\mathcal{T}_2) + a_2^2(\mathcal{T}_2 - \tau_2)$, $\tau_2 = {\rho_2}^{-1}$. The following proposition characterizes the convective behavior of system (2.2.32).

Proposition 2.2.5. *System (2.2.32) is a hyperbolic system of conservation laws, with linearly degenerate fields associated with the eigenvalues $u_2 - a_2\tau_2$, u_2 and $u_2 + a_2\tau_2$.*

Proof. The proof is left to the reader. □

Denoting $\mathbb{W}_2 = (\alpha_2, \alpha_2\rho_2, \alpha_2\rho_2 u_2, \alpha_2\rho_2\mathcal{T}_2)^T$, the state vector for phase 2, we consider the following Riemann initial condition

$$\mathbb{W}_2(x, t=0; \mathbb{W}_{2,L}, \mathbb{W}_{2,R}) = \begin{cases} \mathbb{W}_{2,L} & \text{if} \quad x < 0, \\ \mathbb{W}_{2,R} & \text{if} \quad x > 0, \end{cases} \tag{2.2.33}$$

where $(\mathbb{W}_{2,L}, \mathbb{W}_{2,R})$ are the restriction of the complete initial data $(\mathbb{W}_L, \mathbb{W}_R)$ to the phase 2 variables. When solving this Riemann problem, the source term in (2.2.32) is to be understood as a **known weight** $\pi_1^*\Delta\alpha_1$ supported by the existing contact discontinuity associated with the u_2-wave. Hence, there is no additional wave due to this source term, and the solution of the Riemann problem (2.2.32)-(2.2.33) is sought in the form of four constant states separated by three discontinuities:

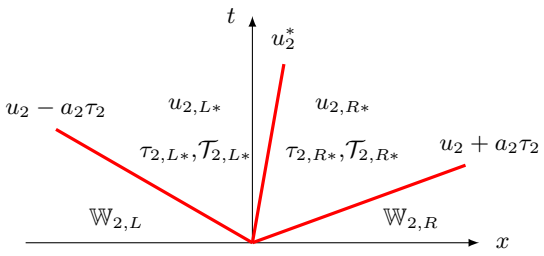

We have the following existence result for the governing equations of phase 2:

Proposition 2.2.6. *Assume that the parameter a_2 is such that $\tau_{2,L}^\sharp > 0$ and $\tau_{2,R}^\sharp > 0$. Then the Riemann problem (2.2.32)-(2.2.33) admits a unique solution whose intermediate states are defined by:*

$$\tau_{2,L*} = \tau_{2,L}^\sharp + \frac{\Delta\alpha_1}{a_2^2}\frac{\pi_2^\sharp - \pi_1^*}{\alpha_{2,L} + \alpha_{2,R}}, \quad u_{2,L*} = u_2^* = u_2^\sharp + \frac{\Delta\alpha_1}{a_2}\frac{\pi_2^\sharp - \pi_1^*}{\alpha_{2,L} + \alpha_{2,R}}, \quad \mathcal{T}_{2,L*} = \mathcal{T}_{2,L}, \tag{2.2.34}$$

$$\tau_{2,R*} = \tau_{2,R}^\sharp - \frac{\Delta\alpha_1}{a_2^2}\frac{\pi_2^\sharp - \pi_1^*}{\alpha_{2,L} + \alpha_{2,R}}, \quad u_{2,R*} = u_2^*, \quad \mathcal{T}_{2,R*} = \mathcal{T}_{2,R}. \tag{2.2.35}$$

Moreover, the intermediate densities $\rho_{2,L*}$ and $\rho_{2,R*}$ are positive if and only if

$$u_2^\sharp - a_2\tau_{2,L}^\sharp < u_2^* < u_2^\sharp + a_2\tau_{2,R}^\sharp. \tag{2.2.36}$$

Proof. We only sketch the proof. The expressions of the intermediate states directly follow from classical manipulations of Rankine-Hugoniot's jump relations. The only non classical relation is the jump relation across the u_2-wave for the momentum equation, where the source term is taken into account:

$$-u_2^*\left[\alpha_2\rho_2 u_2\right] + \left[\alpha_2\rho_2 u_2^2 + \alpha_2\pi_2\right] = \pi_1^*\Delta\alpha_2 = -\pi_1^*\Delta\alpha_1. \tag{2.2.37}$$

The densities $\rho_{2,L*}$ and $\rho_{2,R*}$ are positive if and only if $u_2^* - a_2\tau_{2,L*} < u_2^* < u_2^* + a_2\tau_{2,R*}$. As the fields are linearly degenerate, the corresponding eigenvalues are Riemann invariants and we have $u_2^* - a_2\tau_{2,L*} = u_{2,L} - a_2\tau_{2,L} = u_2^\sharp - a_2\tau_{2,L}^\sharp$. In the same way, $u_2^* + a_2\tau_{2,R*} = u_{2,R} + a_2\tau_{2,R} = u_2^\sharp + a_2\tau_{2,R}^\sharp$. □

Observe that the expression of u_2^* given in equation (2.2.34) defines the function $\mathscr{F}[\mathbb{W}_L, \mathbb{W}_R; a_2]$ introduced in (2.2.23), since u_2^* is expressed as a function of π_1^*. It clearly appears that if $\alpha_{1,L} = \alpha_{1,R}$, the non-conservative product vanishes and the resolution of the Riemann problem yields $u_2^* = u_2^\sharp$ as seen in Lemma 2.2.2.

Moreover, we have the following property satisfied by the unique solution given in Proposition 2.2.6.

Proposition 2.2.7. *The unique solution of the Riemann problem (2.2.32)-(2.2.33) given in Proposition 2.2.6 satisfies the following energy equation in the usual weak sense:*

$$\partial_t \left(\alpha_2\rho_2\mathcal{E}_2\right) + \partial_x \left(\alpha_2\rho_2\mathcal{E}_2 + \alpha_2\pi_2\right) u_2 - u_2\pi_1^*\partial_x\alpha_2 = 0. \tag{2.2.38}$$

Proof. The proof is left to the reader. □

2.2.5 The Riemann problem for phase 1 with a predicted value of u_2^*

In this step, we assume that the velocity u_2^* of the wave supporting the α_1 discontinuity is known, while the pressure π_1^* defining the non-conservative product $\pi_1\partial_x\alpha_1 = \pi_1^*\Delta\alpha_1\delta_0(x - u_2^*t)$ is an unknown that must be calculated. Thus, the governing equations for the evolution of phase 1 read

$$\begin{cases} \partial_t\alpha_1 + u_2^*\partial_x\alpha_1 = 0, \\ \partial_t(\alpha_1\rho_1) + \partial_x(\alpha_1\rho_1u_1) = 0, \\ \partial_t(\alpha_1\rho_1u_1) + \partial_x(\alpha_1\rho_1u_1^2 + \alpha_1\pi_1(\tau_1, \mathcal{T}_1)) = \pi_1\partial_x\alpha_1, \\ \partial_t(\alpha_1\rho_1\mathcal{T}_1) + \partial_x(\alpha_1\rho_1\mathcal{T}_1u_1) = 0, \end{cases} \tag{2.2.39}$$

with $\pi_1(\tau_1, \mathcal{T}_1) = \mathcal{P}_1(\mathcal{T}_1) + a_1^2(\mathcal{T}_1 - \tau_1)$, $\tau_1 = {\rho_1}^{-1}$. The following proposition characterizes the convective behavior of system (2.2.39).

Proposition 2.2.8. *System (2.2.39) admits four real eigenvalues $u_1 - a_1\tau_1$, u_1, $u_1 + a_1\tau_1$ and u_2^*, this last eigenvalue being a known constant. All the fields are linearly degenerate and the system is hyperbolic (i.e. the corresponding right eigenvectors are linearly independent) if and only,*

$$\alpha_1 \neq 0, \quad \textit{and} \quad |u_1 - u_2^*| \neq a_1\tau_1. \tag{2.2.40}$$

Proof. The proof is left to the reader. □

Denoting $\mathbb{W}_1 = (\alpha_1, \alpha_1\rho_1, \alpha_1\rho_1u_1, \alpha_1\rho_1\mathcal{T}_1)^T$, the state vector for phase 1, we consider the following Riemann initial condition

$$\mathbb{W}_1(x, t = 0; \mathbb{W}_{1,L}, \mathbb{W}_{1,R}) = \begin{cases} \mathbb{W}_{1,L} & \text{if} \quad x < 0, \\ \mathbb{W}_{1,R} & \text{if} \quad x > 0, \end{cases} \tag{2.2.41}$$

where $(\mathbb{W}_{1,L}, \mathbb{W}_{1,R})$ are the restriction of the complete initial data $(\mathbb{W}_L, \mathbb{W}_R)$ to the phase 1 variables. The solutions we are interested in are solutions with subsonic wave ordering *i.e.* solutions for which

$$u_1^\sharp - a_1\tau_{1,L}^\sharp < u_2^* < u_1^\sharp + a_1\tau_{1,R}^\sharp. \tag{2.2.42}$$

As for the global Riemann problem (2.2.1)-(2.2.2), these solutions are classified in three categories depending on the ordering between the u_1-contact and the u_2-contact in the solution.

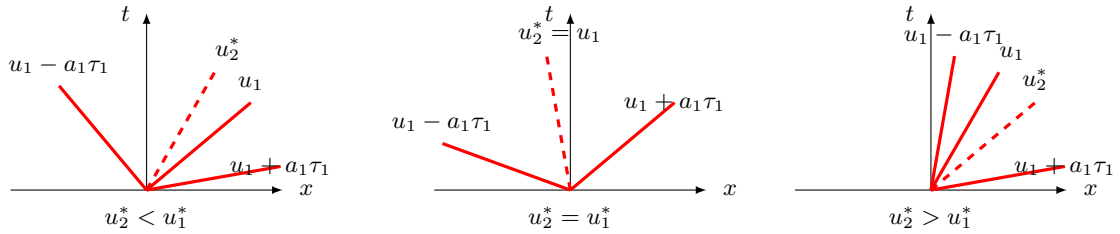

Actually, we only consider the solutions with the wave ordering $u_2^* < u_1^*$ since the other possible wave orderings can be obtained by the Galilean invariance of the equations. Solving the Riemann problem requires three jump relations for each one of the four contact discontinuities associated with the eigenvalues $u_1 - a_1\tau_1$, u_1, $u_1 + a_1\tau_1$ and u_2^*. These jump relations are inherited from the jump relations of the global system (2.2.1). In particular, for all the eigenvalues except u_2^*, the three jump relations directly follow from Rankine-Hugoniot's formula applied to the three last equations of (2.2.39) as the system is locally conservative away from the u_2^*-wave.

Concerning the u_2^*-wave, two jump relations are obtained by applying Rankine-Hugoniot's formula to the mass conservation and to the conservation equation on $\mathcal{T}_1$. The last jump relation is provided by the total energy conservation equality taken in its second form (see Lemma 2.2.1):

$$\left[\alpha_1\rho_1\overline{\mathcal{E}}_1(u_1 - u_2^*) + \alpha_1\pi_1(u_1 - u_2^*)\right]_{\frac{x}{t}=u_2^*} = 0, \tag{2.2.43}$$

with $\overline{\mathcal{E}}_1 := \frac{(u_1-u_2^*)^2}{2} + e_1(\mathcal{T}_1) + \frac{\pi_1^2(\tau_1,\mathcal{T}_1)-p_1^2(\mathcal{T}_1)}{2a_1^2}$. However, it will appear that if this energy conservation is exaclty satisfied, non-positive densities may appear in the solutions with the wave ordering $u_2^* < u_1^*$ for large values of the ratio $\frac{\alpha_{1,L}}{\alpha_{1,R}}$. (For the wave ordering $u_2^* > u_1^*$ large values of the inverse ratio should be considered). In these vanishing phase cases, one must relax the energy conservation by allowing

$$\left[\alpha_1\rho_1\overline{\mathcal{E}}_1(u_1 - u_2^*) + \alpha_1\pi_1(u_1 - u_2^*)\right]_{\frac{x}{t}=u_2^*} = -\mathcal{Q}. \tag{2.2.44}$$

with $\mathcal{Q} > 0$. In practice, the solutions are built so as to preserve the energy equality (2.2.43) through the u_2^*-wave *whenever it is possible*, or at least to be dissipative. In most of the cases, conservative solutions may be built. Nevertheless, for some cases, ensuring positive densities involves a strict energy dissipation through the u_2^*-wave.

A convenient change of variables: Before actually solving the Riemann problem, it is judicious to rewrite equations (2.2.39) in the moving frame of constant speed u_2^*. For this purpose, we perform the following change of variables: $(x,t) \mapsto (y,t) = (x - u_2^*t, t)$. Any function $\mathbb{W}$ of the variables (x,t), is associated with a function $\mathcal{W}$ of the variables (y,t) such that

$$\mathcal{W}(y,t) = \mathbb{W}(x,t) = \mathbb{W}(y + u_2^*t, t) \quad \Longleftrightarrow \quad \mathbb{W}(x,t) = \mathcal{W}(x - u_2^*t, t). \tag{2.2.45}$$

The following differentiation formulae hold

$$\begin{cases} \partial_x\mathbb{W}(x,t) = \partial_y\mathcal{W}(y,t), \\ \\ \partial_t\mathbb{W}(x,t) = -u_2^*\partial_y\mathcal{W}(y,t) + \partial_t\mathcal{W}(y,t). \end{cases} \tag{2.2.46}$$

Denoting $w_1 = u_1 - u_2^*$ the fluid velocity of phase 1 in the frame of the u_2^*-wave, system (2.2.39) rewrites

$$\begin{cases} \partial_t \alpha_1 = 0, \\ \partial_t(\alpha_1\rho_1) + \partial_y(\alpha_1\rho_1 w_1) = 0, \\ \partial_t(\alpha_1\rho_1 w_1) + \partial_y(\alpha_1\rho_1 w_1^2 + \alpha_1\pi_1(\tau_1, \mathcal{T}_1)) = \pi_1 \partial_y \alpha_1, \\ \partial_t(\alpha_1\rho_1\mathcal{T}_1) + \partial_y(\alpha_1\rho_1\mathcal{T}_1 w_1) = 0, \end{cases} \tag{2.2.47}$$

As a direct consequence of Proposition 2.2.8, we may assert that system (2.2.47) admits four real eigenvalues that are $w_1 - a_1\tau_1$, w_1, $w_1 + a_1\tau_1$ and 0. All the fields are linearly degenerate and the system is hyperbolic if and only $\alpha_1 \neq 0$ and $|w_1| \neq a_1\tau_1$. The u_2^*-wave in (2.2.39) corresponds to the standing wave in (2.2.47) across which the the energy jump relation (2.2.44) becomes

$$\left[\alpha_1\rho_1\overline{\mathcal{E}}_1 w_1 + \alpha_1\pi_1 w_1\right]_{\frac{y}{t}=0} = -\mathcal{Q}. \tag{2.2.48}$$

Hence, we actually calculate a solution $\mathcal{W}(y,t)$ of the Riemann problem associated with system (2.2.47), and the solution for the original Riemann problem (2.2.39)-(2.2.41) is obtained by $\mathbb{W}(x,t) = \mathcal{W}(x - u_2^* t, t)$, and by adding u_2^* to the velocities w_1.

Remark 2.2.2. *System (2.2.47) is exactly the relaxation system introduced for the approximation of nozzle flows in [3][1]. Moreover, the jump relation (2.2.48) can be formally written as*

$$\partial_t\left(\alpha_1\rho_1\overline{\mathcal{E}}_1\right) + \partial_y\left(\alpha_1\rho_1\overline{\mathcal{E}}_1 w_1 + \alpha_1\pi_1 w_1\right) = -\mathcal{Q}\delta_0(y), \tag{2.2.49}$$

thus taking the same form of the energy equation satisfied by the solutions of the relaxation nozzle flow system introduced in [3]. Hence, one may reproduce the very same analysis developed in [3] for the resolution of the Riemann problem.

As already mentioned, we only consider solutions with the subsonic wave ordering $u_2^* < u_1^*$ since the other possible wave orderings can be obtained by the Galilean invariance of the equations:

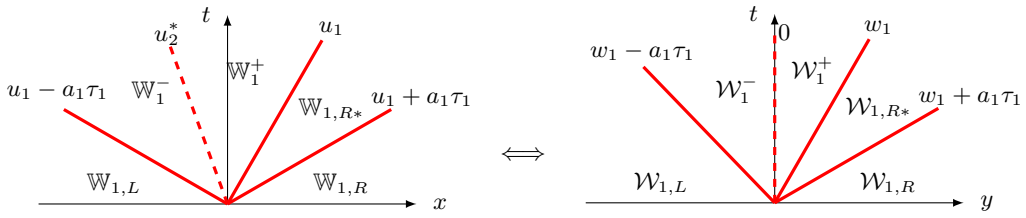

Let us introduce the following notations,

$$\nu = \frac{\alpha_{1,L}}{\alpha_{1,R}}, \qquad \mathcal{M}_L^* = \frac{u_1^\sharp - u_2^*}{a_1\tau_{1,L}^\sharp}. \tag{2.2.50}$$

Lemma 2.2.9 and Proposition 2.2.10 prove that, one can build a one-parameter family of solutions with the subsonic wave ordering $u_2 < u_1$ for the Riemann problem (2.2.39)-(2.2.41), and the dissipation of energy across the standing wave is directly driven by the underlying parameter.

[1] *i.e.* in the first chapter of this thesis.

Lemma 2.2.9. *Assume that there exists a solution to the Riemann problem (2.2.39)-(2.2.41) with the subsonic wave ordering $u_2 < u_1$. Then, denoting $\mathcal{M}$ the relative Mach number of the state on the left of the standing wave:*

$$\mathcal{M} := \frac{w_1^-}{a_1\tau_1^-} = \frac{u_1^- - u_2^*}{a_1\tau_1^-}, \tag{2.2.51}$$

all the intermediate states can be expressed in terms of $\mathcal{M}$ as follows:

$$\tau_1^- = \tau_{1,L}^\sharp \frac{1-\mathcal{M}_L^*}{1-\mathcal{M}}, \qquad w_1^- = a_1\mathcal{M}\tau_1^-, \qquad \mathcal{T}_1^- = \mathcal{T}_{1,L}, \tag{2.2.52}$$

$$\tau_1^+ = \tau_{1,L}^\sharp \frac{1+\mathcal{M}_L^*}{1+\nu\mathcal{M}}, \qquad w_1^+ = \nu a_1\mathcal{M}\tau_1^+, \qquad \mathcal{T}_1^+ = \mathcal{T}_{1,L}, \tag{2.2.53}$$

$$\tau_{1,R*} = \tau_{1,R}^\sharp + \tau_{1,L}^\sharp \frac{\mathcal{M}_L^* - \nu\mathcal{M}}{1+\nu\mathcal{M}}, \qquad w_{1,R*} = \nu a_1\mathcal{M}\tau_1^+, \qquad \mathcal{T}_{1,R*} = \mathcal{T}_{1,R}. \tag{2.2.54}$$

Besides, denoting

$$\varphi(\mathcal{M};\nu,\omega) = \omega^2(\nu\mathcal{M}+1)(\mathcal{M}+1) - (\nu\mathcal{M}-1)(\mathcal{M}-1), \tag{2.2.55}$$

the energy jump across the standing wave is given by

$$\left[\alpha_1\rho_1\overline{\mathcal{E}}_1 w_1 + \alpha_1\pi_1 w_1\right]_{\frac{y}{t}=0} = \frac{1}{2}(u_{1,L} - u_2^* + a_1\tau_{1,L}^\sharp)^2 \frac{\mathcal{Q}_0(\mathcal{M})}{(1+\nu\mathcal{M})(1-\mathcal{M})}\varphi\left(\mathcal{M};\nu,\frac{1-\mathcal{M}_L^*}{1+\mathcal{M}_L^*}\right), \tag{2.2.56}$$

where $\mathcal{Q}_0(\mathcal{M}) = \alpha_{1,L}\rho_1^- w_1^- = \alpha_{1,R}\rho_1^+ w_1^+ > 0$ is the mass flux across the standing wave. Hence, $\varphi\left(\mathcal{M};\nu,\frac{1-\mathcal{M}_L^*}{1+\mathcal{M}_L^*}\right)$ and the energy jump across the standing wave have the same sign.

Proof. This Lemma directly follows from applying Rankine-Hugoniot's jump relations to the four waves of the solution. These easy but tedious calculations are left to the reader. □

Proposition 2.2.10. *Assume that a_1 is such that $\tau_{1,L}^\sharp > 0$ and $\tau_{1,R}^\sharp > 0$. Then the Riemann problem (2.2.39)-(2.2.41) admits solutions with the subsonic wave ordering $w_1 > 0$ (i.e. $u_2^* < u_1^*$), if and only if*

$$0 < \mathcal{M}_L^* < 1. \tag{2.2.57}$$

These solutions can be parametrized by $\mathcal{M}$, the Mach number of the state on the left of the standing wave as seen in Lemma 2.2.9. Besides, there exists a critical value $\nu^\sharp$ in $(1,+\infty]$ independent of $(\alpha_{1,L},\alpha_{1,R})$ and possibly infinite such that the following alternative holds.

- *Either $\nu < \nu^\sharp$, and in this case, $\mathcal{M}$ belongs to the interval $(0,\mathcal{M}_0(\nu,\omega)] \subsetneq (0,\min(1,1/\nu))$ with*

$$\mathcal{M}_0(\nu,\omega) = \frac{1}{2}\left(\frac{1+\omega^2}{1-\omega^2}\left(1+\frac{1}{\nu}\right) - \sqrt{\left(\frac{1+\omega^2}{1-\omega^2}\right)^2\left(1+\frac{1}{\nu}\right)^2 - \frac{4}{\nu}}\right), \quad \text{where} \quad \omega = \frac{1-\mathcal{M}_L^*}{1+\mathcal{M}_L^*} \tag{2.2.58}$$

  lies in the open interval $(0,1)$. The value $\mathcal{M} = \mathcal{M}_0(\nu,\omega)$ gives the unique solution that exactly preserves the energy equality (2.2.43) across the standing wave, and for $0 < \mathcal{M} < \mathcal{M}_0(\nu,\omega)$, the energy is dissipated.

- *Or $\nu \geq \nu^\sharp$, and in that case, no solution with positive densities can preserve the energy equality (2.2.43). The initial data is such that $0 < \frac{\mathcal{M}_L^*}{\nu} < \mathcal{M}_0(\nu,\omega)$ where $\mathcal{M}_0(\nu,\omega)$ is given by (2.2.58). $\mathcal{M}$ must be strictly less than $\mathcal{M}_0(\nu,\omega)$, and by taking $\mathcal{M}$ close enough to $\frac{\mathcal{M}_L^*}{\nu}$ it is always possible to ensure that all the densities remain positive.*

In both cases ($\nu < \nu^\sharp$ or $\nu \geq \nu^\sharp$), the choice of $\mathcal{M}$ determines the value of $\varphi(\mathcal{M};\nu,\omega) \leq 0$ i.e. the energy dissipation across the standing wave through equation (2.2.56) in Lemma 2.2.9.

Proof. The proof is exactly the same as in [3] for the wave configuration $< 1, 2 >$ (see chapter 1 Proposition 1.3.6 for the details). It is not reproduced here. □

As explained in [3] (chapter 1), the existence of $\nu^\sharp$ is related to the expression of $\tau_{1,R*}$ in (2.2.54) which is the only intermediate specific volume that may be non-positive. It is possible to show that for fixed physical quantities $\mathbb{V}_L$ and $\mathbb{V}_R$, the function

$$\nu \mapsto \tau_{1,R}^\sharp - \tau_{1,L}^\sharp \frac{\nu\mathcal{M}_0(\nu,\omega) - \mathcal{M}_L^*}{1+\nu\mathcal{M}_0(\nu,\omega)}, \quad \omega = \frac{1-\mathcal{M}_L^*}{1+\mathcal{M}_L^*}, \tag{2.2.59}$$

is a non-increasing function that may become negative for large values of ν. Observe that for $\nu = 1$, we have $\nu\mathcal{M}_0(\nu,\omega) = \mathcal{M}_L^*$ which implies that the pathological values of ν are larger than one (*i.e.* $\nu^\sharp > 1$). In such pathological cases, in order to impose the positivity of $\tau_{1,R*}$ we must no longer exactly conserve the energy at the standing wave (by taking $\mathcal{M} = \mathcal{M}_0(\nu,\omega)$) but dissipate it by taking $\mathcal{M}$ smaller than $\mathcal{M}_0(\nu,\omega)$. Indeed, $\varphi(\mathcal{M};\nu,\omega) \leq 0$ for all $\mathcal{M} \in (0, \mathcal{M}_0(\nu,\omega)]$. The expression of $\tau_{1,R*}$ clearly shows that if $\mathcal{M}$ is taken close enough to $\frac{\mathcal{M}_L^*}{\nu}$ (remember that $\nu > 1$), we have $\tau_{1,R*}$ close to $\tau_{1,R}^\sharp$ which is positive. Actually, the function

$$\mathcal{M} \mapsto \tau_{1,R}^\sharp - \tau_{1,L}^\sharp \frac{\nu\mathcal{M} - \mathcal{M}_L^*}{1+\nu\mathcal{M}}, \tag{2.2.60}$$

is a non-increasing function. Hence, as in [3] (chapter 1), being given a fixed real number μ in $(0,1)$, we may choose $\mathcal{M}$ by prescribing the following lower-bound for $\tau_{1,R*}$:

$$\tau_{1,R*} \geq \mu\tau_{1,R}^\sharp. \tag{2.2.61}$$

For $\mathcal{M} = \mathcal{M}_\mu(\nu, \mathcal{M}_L^*)$ where

$$\mathcal{M}_\mu(\nu,\mathcal{M}_L^*) := \frac{1}{\nu}\frac{\mathcal{M}_L^* + (1-\mu)\frac{\tau_{1,R}^\sharp}{\tau_{1,L}^\sharp}}{1-(1-\mu)\frac{\tau_{1,R}^\sharp}{\tau_{1,L}^\sharp}}, \tag{2.2.62}$$

expression (2.2.60) gives $\tau_{1,R*} = \mu\tau_{1,R}^\sharp$. As a result, the lower-bound (2.2.61) on $\tau_{1,R*}$ may be obtained by replacing the function $\mathcal{M}_0\left(\nu, \frac{1-\mathcal{M}_L^*}{1+\mathcal{M}_L^*}\right)$ with the new function $\mathcal{M}(\nu,\mathcal{M}_L^*)$ given by

$$\mathcal{M}(\nu,\mathcal{M}_L^*) := \min\left(\mathcal{M}_0\left(\nu, \frac{1-\mathcal{M}_L^*}{1+\mathcal{M}_L^*}\right), \mathcal{M}_\mu(\nu,\mathcal{M}_L^*)\right). \tag{2.2.63}$$

Note that if $\nu \leq 1$, then $\mathcal{M}_0\left(\nu, \frac{1-\mathcal{M}_L^*}{1+\mathcal{M}_L^*}\right) < \mathcal{M}_\mu(\nu, \mathcal{M}_L^*)$, which means that no dissipative correction is added since the lower-bound on $\tau_{1,R*}$ is already satisfied by the energy-preserving choice $\mathcal{M}_0(\nu, \omega)$. If $\nu > 1$, for μ close enough to one, one has $\mathcal{M}_\mu(\nu, \mathcal{M}_L^*)$ close to $\frac{\mathcal{M}_L^*}{\nu}$ and then $\mathcal{M}(\nu, \mathcal{M}_L^*) \in (0, \mathcal{M}_0(\nu, \omega)]$ which implies that the energy is now dissipted since $\varphi(\mathcal{M}; \nu, \omega) \leq 0$ for all $\mathcal{M} \in (0, \mathcal{M}_0(\nu, \omega)]$.

Expression of $\pi_1^* \Delta\alpha_1$: We may now give the expression of $\pi_1^* \Delta\alpha_1$. For this purpose, we write the jump relation across the standing wave for the momentum equation in (2.2.47):

$$\begin{aligned}
\pi_1^* \Delta\alpha_1 &= \left[\alpha_1 \rho_1 w_1^2 + \alpha_1 \pi_1\right]_{\frac{y}{t}=0} && (2.2.64)\\
&= (\alpha_1^+ \rho_1^+ {w_1^+}^2 - \alpha_1^- \rho_1^- {w_1^-}^2) - a_1^2(\alpha_1^+ \tau_1^+ - \alpha_1^- \tau_1^-) && (2.2.65)\\
&+ (p_1(\mathcal{T}_{1,L}) + a_1^2 \mathcal{T}_{1,L}) \Delta\alpha_1, && (2.2.66)
\end{aligned}$$

because $\mathcal{T}_1$ is constant across the standing wave and is equal to $\mathcal{T}_{1,L}$. Moreover, $\alpha_1^- = \alpha_{1,L}$ and $\alpha_1^+ = \alpha_{1,R}$. Thus

$$\begin{aligned}
\pi_1^* \Delta\alpha_1 &= a_1^2 \left(\alpha_{1,R} \frac{{w_1^+}^2}{a_1^2 {\tau_1^+}^2} \tau_1^+ - \alpha_{1,L} \frac{{w_1^-}^2}{a_1^2 {\tau_1^-}^2} \tau_1^- \right) - a_1^2(\alpha_{1,R}\tau_1^+ - \alpha_{1,L}\tau_1^-)\\
&\quad + (p_1(\mathcal{T}_{1,L}) + a_1^2 \mathcal{T}_{1,L}) \Delta\alpha_1\\
&= a_1^2 \left(\alpha_{1,R}({\mathcal{M}^+}^2 - 1)\tau_1^+ - \alpha_{1,L}(\mathcal{M}^2 - 1)\tau_1^- \right) + (p_1(\mathcal{T}_{1,L}) + a_1^2 \mathcal{T}_{1,L}) \Delta\alpha_1,
\end{aligned}$$

where $\mathcal{M}^+ = \nu\mathcal{M}$ thanks to the mass conservation equation, and $\nu = \frac{\alpha_{1,L}}{\alpha_{1,R}}$, $\tau_1^- = \tau_{1,L}^\sharp \frac{1-\mathcal{M}_L^*}{1-\mathcal{M}}$, $\tau_1^+ = \tau_{1,L}^\sharp \frac{1+\mathcal{M}_L^*}{1+\nu\mathcal{M}}$. Hence

$$\begin{aligned}
\pi_1^* \Delta\alpha_1 &= -a_1^2 \left((1 - \nu^2\mathcal{M}^2) \frac{\tau_1^+}{\tau_{1,L}^\sharp} - \nu(1 - \mathcal{M}^2) \frac{\tau_1^-}{\tau_{1,L}^\sharp} \right) \alpha_{1,R} \tau_{1,L}^\sharp + (p_1(\mathcal{T}_{1,L}) + a_1^2 \mathcal{T}_{1,L}) \Delta\alpha_1\\
&= -a_1^2 \left((1 - \nu\mathcal{M})(1 + \mathcal{M}_L^*) - \nu(1 + \mathcal{M})(1 - \mathcal{M}_L^*) \right) \alpha_{1,R} \tau_{1,L}^\sharp + (p_1(\mathcal{T}_{1,L}) + a_1^2 \mathcal{T}_{1,L}) \Delta\alpha_1\\
&= -a_1^2 \left(1 + \mathcal{M}_L^* - \nu\mathcal{M} - \nu\mathcal{M}\mathcal{M}_L^* - \nu + \nu\mathcal{M}_L^* - \nu\mathcal{M} + \nu\mathcal{M}\mathcal{M}_L^* \right) \alpha_{1,R} \tau_{1,L}^\sharp\\
&\quad + (p_1(\mathcal{T}_{1,L}) + a_1^2 \mathcal{T}_{1,L}) \Delta\alpha_1\\
&= (p_1(\mathcal{T}_{1,L}) + a_1^2 \mathcal{T}_{1,L}) \Delta\alpha_1 - a_1^2 \left(1 - \nu + (1 + \nu)\mathcal{M}_L^* - 2\nu\mathcal{M} \right) \alpha_{1,R} \tau_{1,L}^\sharp\\
&= (p_1(\mathcal{T}_{1,L}) + a_1^2 (\mathcal{T}_{1,L} - \tau_{1,L}^\sharp)) \Delta\alpha_1 - a_1^2 \left((1 + \nu)\mathcal{M}_L^* - 2\nu\mathcal{M} \right) \alpha_{1,R} \tau_{1,L}^\sharp,
\end{aligned}$$

with $\pi_1^\sharp = p_1(\mathcal{T}_{1,L}) + a_1^2(\mathcal{T}_{1,L} - \tau_{1,L}^\sharp)$. Finally:

$$\pi_1^* \Delta\alpha_1 = \pi_1^\sharp \Delta\alpha_1 - a_1^2 \left((\alpha_{1,R} + \alpha_{1,L})\mathcal{M}_L^* - 2\alpha_{1,L}\mathcal{M} \right) \tau_{1,L}^\sharp. \tag{2.2.67}$$

In this expression, the value of $\mathcal{M}$ may be taken equal to $\mathcal{M}_0(\nu, \omega)$, $\omega = \frac{1-\mathcal{M}_L^*}{1+\mathcal{M}_L^*}$ in order to exactly preserve the energy across the standing wave as long as $\tau_{1,R*} > 0$. However in some cases, ensuring

positive densities for phase 1 requires that $\mathcal{M}$ be taken sufficiently smaller than $\mathcal{M}_0(\nu,\omega)$ so as to ensure positive densities. As explained above, this can be achieved by prescribing a lower-bound on $\tau_{1,R*}$ which amounts to taking $\mathcal{M} := \mathcal{M}(\nu,\mathcal{M}_L^*)$ (see equation (2.2.63)) instead of $\mathcal{M}_0(\nu,\omega)$. Finally, observe that expression (2.2.67) defines the function $\mathscr{G}[\mathbb{W}_L,\mathbb{W}_R;a_1]$ introduced in (2.2.25).

2.2.6 Solution of the fixed point problem and proof of Theorem 2.2.3

In this section, we prove that condition (**A1**) is a necessary and sufficient condition for the existence of solutions to the fixed point problem :

$$\textit{Find } u_2^* \textit{ in } (u_1^\sharp - a_1\tau_{1,L}^\sharp, u_1^\sharp + a_1\tau_{1,R}^\sharp)\bigcap(u_2^\sharp - a_1\tau_{2,L}^\sharp, u_2^\sharp + a_2\tau_{2,R}^\sharp) \textit{ such that}$$
$$u_2^* = \Big(\mathscr{F}[\mathbb{W}_L,\mathbb{W}_R;a_2]\circ\mathscr{G}[\mathbb{W}_L,\mathbb{W}_R;a_1]\Big)(u_2^*), \quad \text{with } u_2^* < u_1^*, \tag{2.2.68}$$

and therefore, for the existence of solutions to the Riemann problem (2.2.1)-(2.2.2) with the subsonic wave ordering $u_{1,L} - a_1\tau_{1,L} < u_2^* < u_1^*$. Let us first introduce some non-dimensional numbers built on the quantities defined in (2.2.16)-(2.2.19) :

$$\mathcal{M}_L^\sharp := \frac{u_1^\sharp - u_2^\sharp}{a_1\tau_{1,L}^\sharp}, \qquad \mathcal{M}_R^\sharp := \frac{u_1^\sharp - u_2^\sharp}{a_1\tau_{1,R}^\sharp}, \qquad \mathcal{P}_L^\sharp := \frac{\pi_1^\sharp - \pi_2^\sharp}{a_1^2\tau_{1,L}^\sharp}, \qquad \mathcal{P}_R^\sharp := \frac{\pi_1^\sharp - \pi_2^\sharp}{a_1^2\tau_{1,R}^\sharp}. \tag{2.2.69}$$

Solving the fixed-point (2.2.68) amounts to *recoupling* the two phases that have been decoupled for a separate resolution. We start by rewriting the expression of $\pi_1^*\Delta\alpha_1$ obtained for phase 2 in (2.2.34):

$$\begin{aligned}\pi_1^*\Delta\alpha_1 &= \Delta\alpha_1\pi_2^\sharp + a_2(\alpha_{2,L}+\alpha_{2,R})\left(u_2^\sharp - u_2^*\right)\\ &= \Delta\alpha_1\pi_2^\sharp + a_2(\alpha_{2,L}+\alpha_{2,R})\left(u_1^\sharp - u_2^* + u_2^\sharp - u_1^\sharp\right),\end{aligned} \tag{2.2.70}$$

Hence, solving the fixed point problem (2.2.68) amounts to seeking u_2^* such that the two expressions of $\pi_1^*\Delta\alpha_1$ given in (2.2.67) and (2.2.70) are equal, *i.e.* such that

$$\begin{aligned}\pi_1^\sharp\Delta\alpha_1 - a_1^2\left((\alpha_{1,R}+\alpha_{1,L})\mathcal{M}_L^* - 2\alpha_{1,L}\mathcal{M}\right)\tau_{1,L}^\sharp &= \pi_2^\sharp\Delta\alpha_1 + a_2(\alpha_{2,L}+\alpha_{2,R})a_1\tau_{1,L}^\sharp\mathcal{M}_L^*\\ &\quad - a_2(\alpha_{2,L}+\alpha_{2,R})(u_1^\sharp - u_2^\sharp).\end{aligned} \tag{2.2.71}$$

The energy-preserving case :

We first look for solutions that exactly preserve the energy equality across the u_2^*-wave. Therefore, we take $\mathcal{M} := \mathcal{M}_0\left(\frac{\alpha_{1,L}}{\alpha_{1,R}}, \frac{1-\mathcal{M}_L^*}{1+\mathcal{M}_L^*}\right)$, where $\mathcal{M}_0(\nu,\omega)$ is defined in (2.2.58). Introducing the non-dimensional quantities $\mathcal{M}_L^\sharp$, $\mathcal{P}_L^\sharp$ and Λ^α, equation (2.2.71) re-writes as

$$\mathcal{M}_L^\sharp - \frac{a_1}{a_2}\Lambda^\alpha\mathcal{P}_L^\sharp = \mathcal{M}_L^* + \frac{a_1}{a_2}\frac{1}{\alpha_{2,L}+\alpha_{2,R}}\left((\alpha_{1,R}+\alpha_{1,L})\mathcal{M}_L^* - 2\alpha_{1,L}\mathcal{M}_0\left(\frac{\alpha_{1,L}}{\alpha_{1,R}}, \frac{1-\mathcal{M}_L^*}{1+\mathcal{M}_L^*}\right)\right). \tag{2.2.72}$$

Now, considering the change of variables $u_2^* \longmapsto \mathcal{M}_L^* = \frac{u_1^\sharp - u_2^*}{a_1 \tau_{1,L}^\sharp}$, solving the fixed point problem (2.2.68) is equivalent to finding $\mathcal{M}_L^*$ such that equation (2.2.72) holds. Observe that by Proposition 2.2.10, the solution has the subsonic wave ordering $u_1 - a_1\tau_1 < u_2 < u_1$ if and only if $\mathcal{M}_L^*$ belongs to $(0,1)$. Defining the function

$$\Psi_0 \ : \begin{cases} (0,1) \longrightarrow \mathbb{R} \\ m \quad \longmapsto m + \dfrac{a_1}{a_2} \dfrac{1}{\alpha_{2,L} + \alpha_{2,R}} \left((\alpha_{1,R} + \alpha_{1,L})m - 2\alpha_{1,L} \mathcal{M}_0 \left(\frac{\alpha_{1,L}}{\alpha_{1,R}}, \frac{1-m}{1+m} \right) \right), \end{cases} \tag{2.2.73}$$

the following proposition proves that condition (**A1**) is equivalent to the existence of a unique solution $\mathcal{M}_L^*$ in $(0,1)$ to our fixed point problem:

Proposition 2.2.11. *Function $m \mapsto \Psi_0(m)$ is a differentiable and strictly increasing function from 0 to 1, whose limit values are*

$$\lim_{m \to 0} \Psi_0(m) = 0, \qquad \lim_{m \to 1} \Psi_0(m) = 1 + \frac{a_1}{a_2} |\Lambda^\alpha|. \tag{2.2.74}$$

*Hence, if the following condition, which is equivalent to (**A1**) holds,*

$$0 < \mathcal{M}_L^\sharp - \frac{a_1}{a_2} \Lambda^\alpha \mathcal{P}_L^\sharp < 1 + \frac{a_1}{a_2} |\Lambda^\alpha|, \tag{2.2.75}$$

then there exists a unique $\mathcal{M}_L^*$ in $(0,1)$ such that

$$\Psi_0(\mathcal{M}_L^*) = \mathcal{M}_L^\sharp - \frac{a_1}{a_2} \Lambda^\alpha \mathcal{P}_L^\sharp. \tag{2.2.76}$$

Proof. The function Ψ_0 is clearly differentiable on the interval $(0,1)$. Differentiating *w.r.t* m, one gets

$$\Psi_0'(m) = 1 + \frac{a_1}{a_2} \frac{\alpha_{1,R} + \alpha_{1,L}}{\alpha_{2,L} + \alpha_{2,R}} - \frac{a_1}{a_2} \frac{2\alpha_{1,L}}{\alpha_{2,L} + \alpha_{2,R}} \frac{d}{dm} \left\{ \mathcal{M}_0 \left(\frac{\alpha_{1,L}}{\alpha_{1,R}}, \frac{1-m}{1+m} \right) \right\} \tag{2.2.77}$$

$$= 1 + \frac{a_1}{a_2} \frac{\alpha_{1,R} + \alpha_{1,L}}{\alpha_{2,L} + \alpha_{2,R}} - \frac{a_1}{a_2} \frac{2\alpha_{1,L}}{\alpha_{2,L} + \alpha_{2,R}} \frac{\partial \mathcal{M}_0}{\partial \omega} \left(\frac{\alpha_{1,L}}{\alpha_{1,R}}, \frac{1-m}{1+m} \right) \cdot \frac{d\omega}{dm}, \tag{2.2.78}$$

where $\omega = \frac{1-m}{1+m}$. We have $\frac{d\omega}{dm} = -\frac{2}{(1+m)^2}$, hence

$$\Psi_0'(m) = 1 + \frac{a_1}{a_2} \frac{\alpha_{1,R} + \alpha_{1,L}}{\alpha_{2,L} + \alpha_{2,R}} + \frac{a_1}{a_2} \frac{2\alpha_{1,L}}{\alpha_{2,L} + \alpha_{2,R}} \frac{\partial \mathcal{M}_0}{\partial \omega} \left(\frac{\alpha_{1,L}}{\alpha_{1,R}}, \frac{1-m}{1+m} \right) \cdot \frac{2}{(1+m)^2}. \tag{2.2.79}$$

The ratio $\frac{a_1}{a_2}$ is a positive number that somehow measures the distance between the acoustic waves of the two phases 1 and 2. In numerical applications, this ratio may take small or large values depending on the physical test-case. Nevertheless, it is sufficient for the derivative $\Psi_0'(m)$ to be positive, that the term before $\frac{a_1}{a_2} \frac{1}{\alpha_{2,L} + \alpha_{2,R}}$ is positive, *i.e.* that

$$\alpha_{1,R} + \alpha_{1,L} + 2\alpha_{1,L} \frac{\partial \mathcal{M}_0}{\partial \omega} \left(\frac{\alpha_{1,L}}{\alpha_{1,R}}, \frac{1-m}{1+m} \right) \cdot \frac{2}{(1+m)^2} \geq 0, \quad \text{for all } m \text{ in } (0,1), \tag{2.2.80}$$

or in an equivalent manner (again denoting $\nu = \frac{\alpha_{1,L}}{\alpha_{1,R}}$ and $\omega = \frac{1-m}{1+m}$) that

$$1 + \nu + \nu(1+\omega)^2 \frac{\partial \mathcal{M}_0}{\partial \omega}(\nu, \omega) \geq 0, \qquad \text{for all } \omega \text{ in } (0,1), \tag{2.2.81}$$

$$\iff \quad 1 + (1+\omega)^2 \frac{\partial}{\partial \omega} \left\{ \frac{\nu}{1+\nu} \mathcal{M}_0(\nu, \omega) \right\} \geq 0, \qquad \text{for all } \omega \text{ in } (0,1). \tag{2.2.82}$$

With the expression of $\mathcal{M}_0(\nu, \omega)$ in (2.2.58), one gets

$$\frac{\nu}{1+\nu} \mathcal{M}_0(\nu, \omega) = \frac{1}{2} \left(\frac{1+\omega^2}{1-\omega^2} - \sqrt{\left(\frac{1+\omega^2}{1-\omega^2} \right)^2 - \frac{4\nu}{(1+\nu)^2}} \right).$$

Differentiating this with respect to ω yields

$$\begin{aligned} \frac{\partial}{\partial \omega} \left\{ \frac{\nu}{1+\nu} \mathcal{M}_0(\nu, \omega) \right\} = & \frac{1}{2} \left(\frac{4\omega}{(1-\omega^2)^2} - \frac{4\omega}{(1-\omega^2)^2} \frac{1+\omega^2}{1-\omega^2} \left(\left(\frac{1+\omega^2}{1-\omega^2} \right)^2 - \frac{4\nu}{(1+\nu)^2} \right)^{-1/2} \right) \\ = & \frac{2\omega}{(1-\omega^2)^2} \left(1 - \left(1 - \frac{4\nu}{(1+\nu)^2} \left(\frac{1-\omega^2}{1+\omega^2} \right)^2 \right)^{-1/2} \right). \end{aligned} \tag{2.2.83}$$

Casting this in (2.2.82), the sufficient condition for the function Ψ_0 to be strictly increasing becomes

$$1 + 2\omega \frac{(1+\omega)^2}{(1-\omega^2)^2} \left(1 - \left(1 - \frac{4\nu}{(1+\nu)^2} \left(\frac{1-\omega^2}{1+\omega^2} \right)^2 \right)^{-1/2} \right) \geq 0, \quad \text{for all } \omega \text{ in } (0,1). \tag{2.2.84}$$

Now, isolating the terms in ν and those in ω, (2.2.84) is equivalent to

$$\frac{4\nu}{(1+\nu)^2} \leq \left(\frac{1+\omega^2}{1-\omega^2} \right)^2 \left(1 - \frac{1}{\left(1 + \frac{(1-\omega^2)^2}{2\omega(1+\omega)^2} \right)^2} \right), \quad \text{for all } \omega \text{ in } (0,1). \tag{2.2.85}$$

An easy calculation shows that the right-hand side term of (2.2.85) is independent of ω and equals 1. Hence, a sufficient condition for the function Ψ_0 to be strictly increasing is

$$\frac{4\nu}{(1+\nu)^2} \leq 1, \tag{2.2.86}$$

which is true for any ν in $\mathbb{R}^+$. As for the limit values of Ψ_0, observe that the function $\mathcal{M}_0(\nu, \omega)$ is such that $\lim_{\omega \to 0} \mathcal{M}_0(\nu, \omega) = \min\left(1, \frac{1}{\nu}\right)$ and $\lim_{\omega \to 1} \mathcal{M}_0(\nu, \omega) = 0$. Hence the limits (2.2.74) as m tends to 0 and 1. Finally, Proposition 2.2.11 follows from the intermediate value theorem. □

Thus, provided positive values of the densities, Proposition 2.2.11 proves that (**A1**) is a necessary and sufficient condition for the existence and uniqueness of an energy-preserving solution. If the phase 1 densities are not positive, one must authorize some energy dissipation as detailed hereunder.

The energy-dissipating case :

It may happen that the solution $\mathcal{M}_L^*$ of the fixed point problem (2.2.68) is such that

$$\tau_{1,R*} = \tau_{1,R}^\sharp - \tau_{1,L}^\sharp \frac{\nu \mathcal{M}_0\left(\nu, \frac{1-\mathcal{M}_L^*}{1+\mathcal{M}_L^*}\right) - \mathcal{M}_L^*}{1+\nu\mathcal{M}_0\left(\nu, \frac{1-\mathcal{M}_L^*}{1+\mathcal{M}_L^*}\right)} \leq 0. \tag{2.2.87}$$

In such pathological case, which may occur when the ratio $\nu = \frac{\alpha_{1,L}}{\alpha_{1,R}}$ is large, any energy-preserving solution is not admissible since the phase 1 densities cannot be positive. Consequently, one has to authorize energy dissipation introducing some *kinetic relation* which defines the dissipation rate. This kinetic relation is obtained by prescribing a lower-bound on $\tau_{1,R*}$ through the definition of a new value of the Mach number $\mathcal{M}$. Following section 2.2.5, we propose to take $\mathcal{M} := \mathcal{M}(\nu, m)$ where

$$\mathcal{M}(\nu, m) = \min\left(\mathcal{M}_0\left(\nu, \frac{1-m}{1+m}\right), \mathcal{M}_\mu(\nu, m)\right), \tag{2.2.88}$$

with

$$\mathcal{M}_\mu(\nu, m) := \frac{1}{\nu}\frac{m + (1-\mu)\frac{\tau_{1,R}^\sharp}{\tau_{1,L}^\sharp}}{1-(1-\mu)\frac{\tau_{1,R}^\sharp}{\tau_{1,L}^\sharp}}. \tag{2.2.89}$$

If μ is close enough to one, then $\mathcal{M}_\mu(\nu, m)$ is close to m/ν which implies that the solution has positive densities for phase 1 according to Proposition 2.2.10. With these definitions, the fixed point research must now be performed for the new function

$$\Psi \ : \begin{cases} (0,1) & \longrightarrow \mathbb{R} \\ m & \longmapsto m + \dfrac{a_1}{a_2}\dfrac{1}{\alpha_{2,L}+\alpha_{2,R}}\left((\alpha_{1,R}+\alpha_{1,L})m - 2\alpha_{1,L}\mathcal{M}\left(\frac{\alpha_{1,L}}{\alpha_{1,R}}, m\right)\right). \end{cases} \tag{2.2.90}$$

Observe that if m is such that $\mathcal{M}_0\left(\nu, \frac{1-m}{1+m}\right) \leq \mathcal{M}_\mu(\nu, m)$ then $\Psi(m) = \Psi_0(m)$. In particular, if $\alpha_{1,L} \leq \alpha_{1,R}$, then Ψ identifies with Ψ_0 on the whole interval $(0,1)$. We have the following proposition which shows that, provided an appropriate choice of the parameter $\mu \in (0,1)$, there still exists a unique solution $\mathcal{M}_L^* \in (0,1)$ under condition (**A1**).

Proposition 2.2.12. *If the parameter $\mu \in (0,1)$ is close enough to one, the function $m \mapsto \Psi(m)$ is a Lipschitz-continuous strictly increasing function on the interval $(0,1)$, whose limit values are*

$$\lim_{m\to 0}\Psi(m) = 0, \qquad \lim_{m\to 1}\Psi(m) = 1 + \frac{a_1}{a_2}|\Lambda^\alpha|. \tag{2.2.91}$$

*Hence, if condition (**A1**) holds, then there exists a unique $\mathcal{M}_L^*$ in $(0,1)$ such that*

$$\Psi(\mathcal{M}_L^*) = \mathcal{M}_L^\sharp - \frac{a_1}{a_2}\Lambda^\alpha \mathcal{P}_L^\sharp. \tag{2.2.92}$$

Proof. If $\alpha_{1,L} \leq \alpha_{1,R}$ then $\Psi \equiv \Psi_0$ and the result follows from the energy-preserving case. Let us turn to the case $\alpha_{1,L} > \alpha_{1,R}$. As the minimum of two differentiable functions, $\mathcal{M}(\nu, m)$ is Lipschitz-continuous and so is Ψ. Actually, Ψ is almost everywhere differentiable on $(0,1)$. For the limit values

of Ψ, we know from the energy-preserving case that $\lim_{m\to 0}\mathcal{M}_0\left(\nu,\frac{1-m}{1+m}\right)=0$, $\lim_{m\to 1}\mathcal{M}_0\left(\nu,\frac{1-m}{1+m}\right)=\min(1,1/\nu)$, and if μ is close enough to one, we have

$$\mathcal{M}_\mu(\nu,0)=\frac{1}{\nu}\frac{(1-\mu)\frac{\tau^\sharp_{1,R}}{\tau^\sharp_{1,L}}}{1-(1-\mu)\frac{\tau^\sharp_{1,R}}{\tau^\sharp_{1,L}}}>0,\qquad \mathcal{M}_\mu(\nu,1)=\frac{1}{\nu}\frac{1+(1-\mu)\frac{\tau^\sharp_{1,R}}{\tau^\sharp_{1,L}}}{1-(1-\mu)\frac{\tau^\sharp_{1,R}}{\tau^\sharp_{1,L}}}>\min\left(1,\frac{1}{\nu}\right). \tag{2.2.93}$$

Hence, Ψ and Ψ_0 share the same limit values at 0 and 1. As for the monotony of function Ψ, we may write that for almost every m in $(0,1)$:

$$\Psi'(m)\geq\min\left(\Psi_0'(m),1+\frac{a_1}{a_2}\frac{1}{\alpha_{2,L}+\alpha_{2,R}}\left(\alpha_{1,R}+\alpha_{1,L}-2\frac{\alpha_{1,R}}{1-(1-\mu)\frac{\tau^\sharp_{1,R}}{\tau^\sharp_{1,L}}}\right)\right). \tag{2.2.94}$$

For $\mu=1$, this expression gives $\Psi'(m)\geq\min\left(\Psi_0'(m),1+\frac{a_1}{a_2}\frac{|\alpha_{1,R}-\alpha_{1,L}|}{\alpha_{2,L}+\alpha_{2,R}}\right)$ since $\alpha_{1,L}>\alpha_{1,R}$. As $\Psi_0'(m)>0$ by the study of the energy-preserving case, this proves that Ψ is strictly increasing if μ is close enough to one, which conludes the proof. □

In practice, the parameter $\mu\in(0,1)$ which determines the lower-bound on $\tau_{1,R*}$ is chosen small enough so as to minimize the energy-dissipation, but close enough to one so as to ensure the uniqueness of the solution in the fixed point research procedure.

Proof of Theorem 2.2.3 :

We may now complete the proof of Theorem 2.2.3. If the ratio $\frac{\alpha_{1,L}}{\alpha_{1,R}}$ is close to one, Proposition 2.2.10 concerning phase 1, asserts that no energy-dissipation is needed for ensuring the positivity of the densities. Hence, for $\frac{\alpha_{1,L}}{\alpha_{1,R}}$ in a neighbourhood of 1, by Proposition 2.2.11, condition (**A1**) is a necessary and sufficient condition for the existence of a unique solution to the fixed point problem (2.2.72), *i.e.* for the existence and uniqueness of an energy-preserving solution to the Riemann problem (2.2.1)-(2.2.2) with the subsonic wave ordering $u_2^*<u_1^*$. For large values of the ratio $\frac{\alpha_{1,L}}{\alpha_{1,R}}$, Proposition 2.2.10 shows that ensuring positive densities for phase 1 may require strict energy dissipation across the u_2-wave. In this case, still assuming condition (**A1**), Proposition 2.2.12 proves that using the kinetic relation (2.2.88) defining $\mathcal{M}$ with respect to the pair $\left(\frac{\alpha_{1,L}}{\alpha_{1,R}},\mathcal{M}_L^*\right)$, it is always possible to ensure the existence of a solution with positive densities for phase 1 by dissipating the total energy. Condition (**B**) on the positivity of the phase 2 densities is proved in Proposition 2.2.6.

Finally, thanks to the Galilean invariance of system (2.2.1), one can prove that the symmetric wave-configuration $u_2^*>u_1^*$ is implied by (**A3**) by exchanging the subscripts L and R and changing the velocities to their opposite values. As for condition (**A3**), it can be obtained by passing to the limit in (**A1**). The corresponding $\mathcal{M}_L^*$ is equal to zero, and we obtain the $u_2^*=u_1^*$ configuration. This observation consludes the proof of Theorem 2.2.3.

2.2.7 Expression of the Riemann solution

In this section, we construct the solution $\mathbb{W}(x,t;\mathbb{W}_L,\mathbb{W}_R) = \mathbb{W}_r(x/t;\mathbb{W}_L,\mathbb{W}_R)$ for a given pair of initial conditions $(\mathbb{W}_L,\mathbb{W}_R)$ in Ω^r and two parameters a_1 and a_2 such that the conditions of Theorem 2.2.3 are met. We distinguish the three different cases corresponding respectively to (**A1**), (**A2**) and (**A3**).

- If (**A1**) holds, the phasic solutions have the following form:

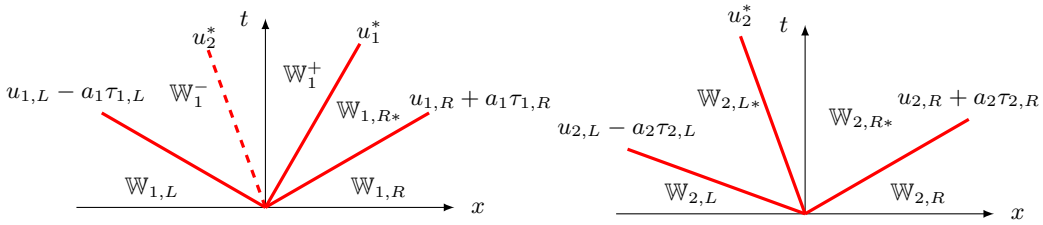

  The values u_2^* and π_1^* are calculated as follows. First use an iterative method (Newton's method or a dichotomy algorithm for instance) to compute $\mathcal{M}_L^*$ such that

$$\Psi(\mathcal{M}_L^*) = \mathcal{M}_L^\sharp - \frac{a_1}{a_2}\Lambda^\alpha \mathcal{P}_L^\sharp.$$

  According to section 2.2.6, $\mathcal{M}_L^*$ always exists under (**A1**) and is unique if μ is close enough to one. We then obtain u_2^* by $u_2^* = u_1^\sharp - a_1\tau_{1,L}^\sharp \mathcal{M}_L^*$, while π_1^* is obtained through (2.2.70). Then the intermediate states for phase 2 are given by equations (2.2.34) and (2.2.35) in Proposition 2.2.6. Once prescribed the value $\mathcal{M} := \mathcal{M}(\nu,\mathcal{M}_L^*)$ according to (2.2.88), the intermediate states for phase 1 are given in equations (2.2.52) to (2.2.54) of Lemma 2.2.9, except for the velocities to which one must add u_2^*: $u_1^- = w_1^- + u_2^*$, $u_1^+ = w_1^+ + u_2^*$, $u_{1,R*} = w_{1,R*} + u_2^*$.

- If (**A2**) holds, we exploit the Galilean invariance of the equations. The solution is obtained by the transformation

$$\mathbb{W}_r(\xi;\mathbb{W}_L,\mathbb{W}_R) := \mathcal{V}\mathbb{W}_r(-\xi;\mathcal{V}\mathbb{W}_R,\mathcal{V}\mathbb{W}_L), \tag{2.2.95}$$

  where the operator $\mathcal{V}$ changes the velocities into their opposite values:

$$\mathcal{V} : (x_1,x_2,x_3,x_4,x_5,x_6,x_7) \mapsto (x_1,x_2,-x_3,x_4,-x_5,x_6,x_7). \tag{2.2.96}$$

  Of course, the function $\mathbb{W}_r(-\xi;\mathcal{V}\mathbb{W}_R,\mathcal{V}\mathbb{W}_L)$ is computed through the first case, since for these new initial data $(\mathcal{V}\mathbb{W}_R,\mathcal{V}\mathbb{W}_L)$, it is condition (**A1**) that holds.

- If (**A3**) holds, u_2^* is equal to $u_1^\sharp$ (*i.e.* $\mathcal{M}_L^* = 0$). The intermediate states for phase 2 are obtained through equations (2.2.34) and (2.2.35) in Proposition 2.2.6, and the intermediate states for phase 1 are computed by passing to the limit as $\mathcal{M}_L^*$ goes to zero (*i.e.* $\omega \to 1$)in equations (2.2.52) to (2.2.54), for $\mathcal{M} = \mathcal{M}_0(\nu,\omega)$.

Acknowledgements. The authors would like to thank Jean-Paul Daniel for his helpful remarks. The third author receives a financial support by ANRT through an EDF-CIFRE contract 529/2009. The forth author is partially supported by the LRC Manon (Modélisation et Approximation Numérique Orientées pour l'énergie Nucléaire — CEA DM2S/LJLL).

References

[1] M.R. Baer and J.W. Nunziato. A two-phase mixture theory for the deflagration-to-detonation transition (DDT) in reactive granular materials. *International Journal of Multiphase Flow*, 12(6):861 – 889, 1986.

[2] F. Bouchut. *Nonlinear stability of finite volume methods for hyperbolic conservation laws and well-balanced schemes for sources*. Frontiers in Mathematics. Birkhäuser Verlag, Basel, 2004.

[3] C. Coquel, K. Saleh, and N. Seguin. Relaxation and numerical approximation for fluid flows in a nozzle. *Under revision*.

[4] F. Coquel, T. Gallouët, J-M. Hérard, and N. Seguin. Closure laws for a two-fluid two pressure model. *C. R. Acad. Sci.*, I-334(5):927–932, 2002.

[5] F. Coquel, E. Godlewski, B. Perthame, A. In, and P. Rascle. Some new Godunov and relaxation methods for two-phase flow problems. In *Godunov methods (Oxford, 1999)*, pages 179–188. Kluwer/Plenum, New York, 2001.

[6] F. Coquel, E. Godlewski, and N. Seguin. Relaxation of fluid systems. *Math. Models Methods Appl. Sci.*, 22(8), 2012.

[7] F. Coquel and B. Perthame. Relaxation of energy and approximate Riemann solvers for general pressure laws in fluid dynamics. *SIAM J. Numer. Anal.*, 35(6):2223–2249 (electronic), 1998.

[8] P. Embid and M. Baer. Mathematical analysis of a two-phase continuum mixture theory. *Contin. Mech. Thermodyn.*, 4(4):279–312, 1992.

[9] T. Gallouët, J-M. Hérard, and N. Seguin. Numerical modeling of two-phase flows using the two-fluid two-pressure approach. *Math. Models Methods Appl. Sci.*, 14(5):663–700, 2004.

[10] S. Gavrilyuk and R. Saurel. Mathematical and numerical modeling of two-phase compressible flows with micro-inertia. *Journal of Computational Physics*, 175(1):326 – 360, 2002.

[11] E. Godlewski and P.-A. Raviart. *Numerical approximation of hyperbolic systems of conservation laws*, volume 118 of *Applied Mathematical Sciences*. Springer-Verlag, New York, 1996.

[12] J-M. Hérard and O. Hurisse. A fractional step method to compute a class of compressible gas-luiquid flows. *Computers & Fluids. An International Journal*, 55:57–69, 2012.

[13] S. Jin and Z. P. Xin. The relaxation schemes for systems of conservation laws in arbitrary space dimensions. *Comm. Pure Appl. Math.*, 48(3):235–276, 1995.

[14] A. K. Kapila, S. F. Son, J. B. Bdzil, R. Menikoff, and D. S. Stewart. Two-phase modeling of DDT: Structure of the velocity-relaxation zone. *Physics of Fluids*, 9(12):3885–3897, 1997.

[15] P.G. LeFloch. Shock waves for nonlinear hyperbolic systems in nonconservative form. *IMA, Minneapolis*, Preprint 593, 1991.

[16] R. Saurel and R. Abgrall. A multiphase godunov method for compressible multifluid and multiphase flows. *Journal of Computational Physics*, 150(2):425 – 467, 1999.

Chapter 3

Un schéma numérique de relaxation pour le modèle de Baer-Nunziato

AN ENTROPY-SATISFYING AND EFFICIENT RELAXATION SCHEME FOR THE BAER-NUNZIATO MODEL[1]

Khaled Saleh

Abstract

In this work, we present a relaxation scheme for computing approximate solutions of the isentropic Baer-Nunziato two-phase flow model. The scheme is derived from the relaxation approximation of the model introduced in [10][2], which has been shown to be particularly suitable for subsonic flows, meaning that the relative velocity between the phases remains moderate compared to the speed of sound. The method is proved to satisfy a discrete entropy inequality and to preserve positive values of the statistical fractions and densities. The numerical simulations show that this first oder scheme provides a much higher precision than Rusanov's scheme, and a much more moderate computational cost, assuming the same level of precision. Finally, two test-cases assess the good behavior of the scheme when approximating vanishing phase solutions.

3.1 Introduction

The two-fluid approach is relevant for a detailed investigation of some patterns occurring in water-vapor flows such as those encountered in pressurized water reactors. In this framework, a major issue is the prediction of the boiling crisis, where the flow is initially dominated by the liquid phase while the vapor phase is dilute. Due to a failure in the heat evacuation, the liquid may reach the boiling point in some areas of the flow (mainly near the fuel rods) thus causing a phase transition towards vapor that could possibly isolate the fuel rods from the liquid. The modeling as well as the numerical simulation of such phenomena remains challenging since both models that can handle phase transitions and robust numerical schemes are needed.

This paper is concerned with the isentropic version of the two-fluid model introduced by Baer and Nunziato in [4], in the context of reactive granular materials, and studied in various papers

[1] Les travaux de ce chapitre font l'objet d'un article soumis à la revue *M2AN: Mathematical Modelling and Numerical Analysis.*

[2] Dans tout ce chapitre, la référence [10] renvoie en fait aux travaux du chapitre 2.

[6, 16, 20] (see also [22] for a related framework). This model is a suitable candidate that enables the computation of two-phase flows in which few bubbles are statistically present in a liquid phase. It consists in two sets of partial differential equations accounting for the evolution of mass, momentum and total energy for each phase, in addition to an evolution equation for the phase fraction. A major feature of the Baer-Nunziato model is to assume two different velocities and two different pressures for the two phases. This approach is not genuinely usual in the nuclear industry where the commonly implemented methods assume the same pressure for the two phases at every time and everywhere in the flow. This latter assumption is justified by the very short time-scale associated with the relaxation of the phasic pressures towards an equilibrium. In the two-fluid two-pressure models (such as Baer & Nunziato's), source terms are explicitly written in order to account for this pressure relaxation phenomenon as well as friction terms for the relaxation of the phasic velocities towards an equilibrium. However, this work is mainly concerned with the convective effects and these relaxation source terms are not considered here (see [6] for some modeling choices of these terms and [19] for their numerical treatment). Contrary to the single pressure models, the Baer-Nunziato model provides a pleasant property which is the hyperbolicity of its convective part. Indeed, unlike single pressure models, where the characteristic eigenvalues may be complex, the Baer-Nunziato model admits seven real eigenvalues and the associated right eigenvectors form a basis unless the relative velocity between the phases equals the sound speed in the liquid (see [13]). However, such a situation is unlikely to arise in the context of nuclear reactor simulations and therefore, the present paper is restricted to the cases where the relative velocity between the phases remains small compared to the liquid speed of sound.

Several schemes have already been proposed in the literature in order to build consistent and stable approximations of the Baer-Nunziato model. Many of them rely on the construction of interface Riemann solvers. Schwendeman, Wahle and Kapila [23] propose a Godunov scheme relying on an exact Riemann solver for the Baer-Nunziato model; see also Deledicque and Papalexandris [12] for an exact Riemann solver constructed through a different approach, and Andrianov and Warnecke [3], for a related work. The major drawback of such approaches is the difficulty of calculating the exact solution of the Riemann problem. One main hindrance is that the characteristic eigenvalues of the system are not naturally ordered, and no method has been found yet that could determine *a priori* their ordering, with respect to the initial data. In addition, the strong non-linearities of the pressure laws make even more difficult the derivation of exact Riemann solvers. Following the pioneering work of Harten, Lax and van Leer [18], other approaches consider approximate Riemann solvers. Tokareva and Toro [26] design an HLLC-type approximate Riemann solver that considers all of the seven characteristic waves. Ambroso, Chalons and Raviart [2] propose an approximate Riemann solver where the acoustic waves are linearized and which takes into account the relaxation source terms. Finally, we also mention some other finite volume techniques that have been used. In [15], the authors extend Rusanov's scheme and the VFRoe method to the context of non-conservative systems. Lastly, some schemes grounded on operator splitting techniques have been recently used [9, 25, 21].

The method considered in the present paper relies on a *relaxation approximation* of the isentropic version of the model, similar to that in Ambroso, Chalons, Coquel and Galié [1]. Actually, the numerical scheme, which reveals to be robust and highly precise, is grounded on a relaxation approach introduced and studied in a previous work [10]. The main idea consists in introducing a

larger system, in which the pressure laws have been linearized, and which relaxes towards the actual system of Baer-Nunziato in the regime of a small relaxation parameter (for a general framework on relaxation schemes we refer to [7, 11, 8, 5]). In [10], the Riemann problem associated with the relaxation system has been exactly solved, in the framework of solutions with *subsonic wave ordering*. Moreover, for this relaxation Riemann problem, it is proved that the relative ordering of the waves can be determined *a priori* with respect to the initial data. In the present paper, we implement a numerical scheme which is naturally derived from this relaxation approximation. The scheme is proved to satisfy a discrete entropy-inequality under a sub-characteristic condition (Whitham's condition). In addition, for the same level of refinement, the scheme is shown to be much more accurate than Lax-Friedrichs type schemes (such as Rusanov's scheme), and for a given level of approximation error, the relaxation scheme is shown to perform much better in terms of computational cost than Lax-Friedrichs type schemes. Finally, two test-cases assess that the scheme provides a robust numerical treatment of vanishing phase solutions, which is an important step towards the simulation of challenging phenomena such as the boiling crisis.

The paper is organized as follows. In section 3.2, we first recall the isentropic Baer-Nunziato two-phase flow model and we introduce the relaxation approximation studied in [10]. Section 3.3 then considers the Riemann problem for the relaxation system. The main results of [10] (necessary and sufficient conditions for the existence and uniqueness of solutions with subsonic wave ordering) are reminded and the construction of the exact solution is provided in details. In section 3.4, the relaxation Riemann solver is used to derive a numerical scheme whose main properties are described and proved, and notably a discrete entropy inequality. Finally, section 3.5 is devoted to the numerical applications. In the first test-case, a classical Riemann solution is approximated. A mesh refinement is implemented in order to prove the convergence of the method and its good performances in terms of precision and computational cost. The last two test- cases consider quite difficult configurations of vanishing phases.

3.2 The model and its relaxation approximation

The isentropic Baer-Nunziato model is a model formulated in Eulerian coordinates where balance equations account for the evolution of mass and momentum of each phase. The velocities of each phase are denoted $u_i,\ i \in \{1,2\}$, while the densities are denoted $\rho_i,\ i \in \{1,2\}$. Each phase has a statistical presence fraction $\alpha_i,\ i \in \{1,2\}$, with the saturation constraint $\alpha_1 + \alpha_2 = 1$. The model reads:

$$\partial_t \mathbb{U} + \partial_x \mathbf{f}(\mathbb{U}) + \mathbf{c}(\mathbb{U})\partial_x \mathbb{U} = 0, \quad x \in \mathbb{R}, t > 0, \tag{3.2.1}$$

with

$$\mathbb{U} = \begin{bmatrix} \alpha_1 \\ \alpha_1\rho_1 \\ \alpha_1\rho_1 u_1 \\ \alpha_2\rho_2 \\ \alpha_2\rho_2 u_2 \end{bmatrix}, \qquad \mathbf{f}(\mathbb{U}) = \begin{bmatrix} 0 \\ \alpha_1\rho_1 u_1 \\ \alpha_1\rho_1 u_1^2 + \alpha_1 p_1(\rho_1) \\ \alpha_2\rho_2 u_2 \\ \alpha_2\rho_2 u_2^2 + \alpha_2 p_2(\rho_2) \end{bmatrix}, \qquad \mathbf{c}(\mathbb{U})\partial_x \mathbb{U} = \begin{bmatrix} u_2 \\ 0 \\ -p_1(\rho_1) \\ 0 \\ +p_1(\rho_1) \end{bmatrix} \partial_x \alpha_1. \tag{3.2.2}$$

The state vector $\mathbb{U}$ is expected to belong to the natural physical space

$$\Omega = \left\{ \mathbb{U} \in \mathbb{R}^5, 0 < \alpha_1 < 1 \text{ and } \alpha_i\rho_i > 0 \text{ for } i \in \{1,2\} \right\}. \tag{3.2.3}$$

We assume barotropic pressure laws for each phase $\rho_i \mapsto p_i(\rho_i),\ i \in \{1,2\}$ with smooth dependence on the density, and which satisfy the following natural assumptions for all $\rho_i > 0$:

$$p_i(\rho_i) > 0, \quad p_i'(\rho_i) > 0, \quad \lim_{\rho_i \to 0} p_i(\rho_i) = 0, \quad \lim_{\rho_i \to +\infty} p_i(\rho_i) = +\infty. \tag{3.2.4}$$

We define the mapping $\tau \mapsto \mathcal{P}_i(\tau) := p_i(\tau^{-1})$ which is the phasic pressure seen as a function of the specific volume $\tau = \rho^{-1}$. In the whole paper, this smooth function is assumed to be strictly convex:

$$\mathcal{P}_i''(\tau_i) > 0, \quad \text{for all } \tau_i > 0,\ i \in \{1,2\}. \tag{3.2.5}$$

For the main mathematical properties of system (3.2.1), we refer to appendix A. Let us just recall that the entropy weak solutions of (3.2.1) satisfy the following energy inequality in the weak sense:

$$\partial_t \eta(\mathbb{U}) + \partial_x \mathcal{F}_\eta(\mathbb{U}) \leq 0, \tag{3.2.6}$$

where $\eta(\mathbb{U}) := \sum_{i=1}^2 \alpha_i \rho_i E_i$ and $\mathcal{F}_\eta(\mathbb{U}) := \sum_{i=1}^2 \alpha_i(\rho_i E_i + p_i(\rho_i))u_i$. The phasic energies are defined for $i \in \{1,2\}$ by $E_i := \frac{u_i^2}{2} + e_i(\tau_i)$ where the function $\tau \mapsto e_i(\tau)$ is such that $e_i' = -\mathcal{P}_i$. In addition, the following crucial property holds:

Proposition 3.2.1. *The mapping* $\eta : \left\{ \begin{array}{ccc} \Omega & \longrightarrow & \mathbb{R} \\ \mathbb{U} & \longmapsto & \eta(\mathbb{U}) \end{array} \right.$ *is convex.*

Proof. The proof is tedious but involves no particular difficulties. It is left to the reader. □

The numerical scheme presented in this paper is directly derived from the relaxation approximation of system (3.2.1) introduced in [10]. It is shown in [10] that this approach is particularly suitable for the cases of interest since it provides a very accurate relaxation Riemann solver for solutions with subsonic wave ordering. The considered relaxation system reads

$$\partial_t \mathbb{W} + \partial_x \mathbf{g}(\mathbb{W}) + \mathbf{d}(\mathbb{W})\partial_x \mathbb{W} = \frac{1}{\varepsilon}\mathcal{R}(\mathbb{W}), \quad x \in \mathbb{R}, t > 0, \tag{3.2.7}$$

where $\mathbb{W} = (\alpha_1, \alpha_1\rho_1, \alpha_1\rho_1 u_1, \alpha_2\rho_2, \alpha_2\rho_2 u_2, \alpha_1\rho_1\mathcal{T}_1, \alpha_2\rho_2\mathcal{T}_2)^T$ is the relaxation state vector and

$$\mathbf{g}(\mathbb{W}) = \begin{bmatrix} 0 \\ \alpha_1\rho_1 u_1 \\ \alpha_1\rho_1 u_1^2 + \alpha_1\pi_1(\tau_1, \mathcal{T}_1) \\ \alpha_2\rho_2 u_2 \\ \alpha_2\rho_2 u_2^2 + \alpha_2\pi_2(\tau_2, \mathcal{T}_2) \\ \alpha_1\rho_1\mathcal{T}_1 u_1 \\ \alpha_2\rho_2\mathcal{T}_2 u_2 \end{bmatrix}, \quad \mathbf{d}(\mathbb{W})\partial_x \mathbb{W} = \begin{bmatrix} u_2 \\ 0 \\ -\pi_1(\tau_1, \mathcal{T}_1) \\ 0 \\ +\pi_1(\tau_1, \mathcal{T}_1) \\ 0 \\ 0 \end{bmatrix} \partial_x \alpha_1, \quad \mathcal{R}(\mathbb{W}) = \begin{bmatrix} 0 \\ 0 \\ 0 \\ 0 \\ 0 \\ \alpha_1\rho_1(\tau_1 - \mathcal{T}_1) \\ \alpha_2\rho_2(\tau_2 - \mathcal{T}_2) \end{bmatrix}. \tag{3.2.8}$$

For each phase i in $\{1,2\}$ the linearized pressure $\pi_i(\tau_i, \mathcal{T}_i)$ is a function defined as

$$\pi_i(\tau_i, \mathcal{T}_i) = \mathcal{P}_i(\mathcal{T}_i) + a_i^2(\mathcal{T}_i - \tau_i). \tag{3.2.9}$$

In the formal limit $\varepsilon \to 0$, the additional variable $\mathcal{T}_i$ tends towards the specific volume τ_i, and the linearized pressure π_i tends towards the original non-linear pressure p_i, thus recovering system

(3.2.1) in the first five equations of (3.2.7). Actually, the solution of (3.2.7) should be parametrized by ε as in $\mathbb{W}^\varepsilon(x,t)$. However, in order to ease the notation, we omit the superscript $^\varepsilon$. The constants a_i in (3.2.9) are two positive parameters that must be taken large enough so as to satisfy the following sub-characteristic condition (also called Whitham's condition):

$$a_i^2 > \max(-\mathcal{P}_i'(\tau_i), -\mathcal{P}_i'(\mathcal{T}_i)), \quad i \text{ in } \{1,2\}, \tag{3.2.10}$$

for all τ_i and $\mathcal{T}_i$ encountered in the solution of (3.2.7). Performing a Chapman-Enskog expansion, we can see that Whitham's condition expresses that system (3.2.7) is a viscous perturbation of system (3.2.1) in the regime of small ε. Hence, it aims at enforcing the stability of the relaxation approximation (see section 3.4.4 for details).

At the numerical level, a fractional step method is commonly used in the implementation of relaxation methods: the first step is a time-advancing step using the solution of the Riemann problem for the convective part of (3.2.7):

$$\partial_t \mathbb{W} + \partial_x \mathbf{g}(\mathbb{W}) + \mathbf{d}(\mathbb{W})\partial_x \mathbb{W} = 0, \tag{3.2.11}$$

while the second step consists in an instantaneous relaxation towards the equilibrium system by imposing $\mathcal{T}_i = \tau_i$ in the solution obtained by the first step. This second step is equivalent to sending ε to 0 instantaneously (see section 3.4 for the details).

3.3 The relaxation Riemann solver

This section summarizes the main results of [10] concerning the relaxation Riemann problem:

$$\left\{ \begin{array}{l} \partial_t \mathbb{W} + \partial_x \mathbf{g}(\mathbb{W}) + \mathbf{d}(\mathbb{W})\partial_x \mathbb{W} = 0, \\ \\ \mathbb{W}(x,0) = \left\{ \begin{array}{ll} \mathbb{W}_L & \text{if} \quad x < 0, \\ \mathbb{W}_R & \text{if} \quad x > 0. \end{array} \right. \end{array} \right. \tag{3.3.1}$$

As required by the numerical method (see section 3.4), the initial states $(\mathbb{W}_L, \mathbb{W}_R)$ considered here are assumed to be *at equilibrium* which means that $\mathcal{T}_{i,L} = \tau_{i,L}$ and $\mathcal{T}_{i,R} = \tau_{i,R}$ for $i = 1,2$. The solutions are sought in the domain of positive densities ρ_i and positive $\mathcal{T}_i$:

$$\Omega^r = \Big\{ \mathbb{W} \in \mathbb{R}^7, 0 < \alpha_1 < 1, \ \alpha_i \rho_i > 0, \ \alpha_i \rho_i \mathcal{T}_i > 0, \ \text{for } i \in \{1,2\} \Big\}. \tag{3.3.2}$$

After introducing some notations and recalling the existence and uniqueness theorem for subsonic solutions proved in [10], the construction of the self-similar solution of (3.3.1) is fully displayed.

3.3.1 An existence theorem for subsonic solutions

It is shown in [10] that (3.2.11) has only linearly degenerate characteristic fields with uniquely defined jump relations across each field. Hence, the solution constructed in [10] is a *self-similar*

piecewise constant function $\mathbb{W}(x,t;\mathbb{W}_L,\mathbb{W}_R) = \mathbb{W}_r(x/t;\mathbb{W}_L,\mathbb{W}_R)$. Each discontinuity of $\xi \mapsto \mathbb{W}_r(\xi;\mathbb{W}_L,\mathbb{W}_R)$ corresponds to a contact discontinuity in the solution. More precisely, the position of each discontinuity in the ξ-line, is equal to the propagation speed of the corresponding contact discontinuity in the (x,t)-plane.

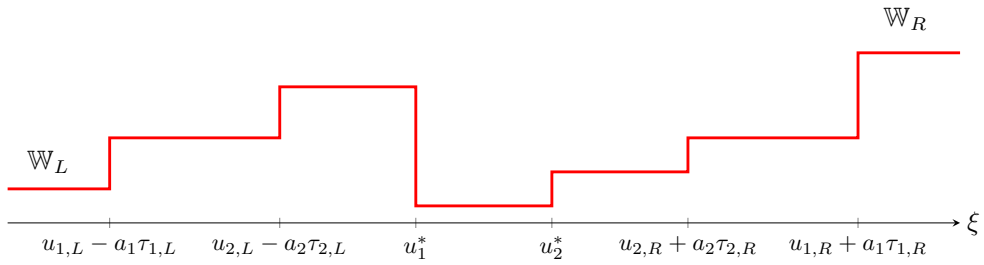

Figure 3.1: Representation of a solution with subsonic wave ordering. The velocities are such that $u_{1,L} - a_1\tau_{1,L} < u_2^* < u_{1,R} + a_1\tau_{1,R}$.

Following the framework of [10], we restrict to a class of solutions referred to as solutions with *subsonic wave ordering* (see [10] for details). Essentially, it means that the kinematic velocity u_2^* lies in between the acoustic speeds of phase 1, $u_{1,L} - a_1\tau_{1,L}$ and $u_{1,R} + a_1\tau_{1,R}$. In most cases, the constructed solutions preserve the following equation on the total energy which is exactly conserved for the smooth solutions of (3.2.11):

$$\partial_t \eta^r(\mathbb{W}) + \partial_x \mathcal{F}_\eta^r(\mathbb{W}) = 0, \tag{3.3.3}$$

where $\eta^r(\mathbb{W}) := \sum_{i=1}^2 \alpha_i\rho_i\mathcal{E}_i$ and $\mathcal{F}_\eta^r(\mathbb{W}) := \sum_{i=1}^2 \alpha_i(\rho_i\mathcal{E}_i + \pi_i(\tau_i,\mathcal{T}_i))u_i$. The relaxation phasic energies are defined for $i \in \{1,2\}$ by $\mathcal{E}_i := \frac{u_i^2}{2} + e_i(\mathcal{T}_i) + \frac{1}{2a_i^2}(\pi_i^2(\tau_i,\mathcal{T}_i) - p_i^2(\mathcal{T}_i))$. Nevertheless, it is shown in [10] that, in some rare cases, the construction of solutions with subsonic wave ordering requires that the total energy be dissipated through the u_2^*-wave in order to ensure the positivity of phase 1 densities. Hence, in such cases, the constructed solution satisfies the equality

$$\partial_t \eta^r(\mathbb{W}) + \partial_x \mathcal{F}_\eta^r(\mathbb{W}) = -\mathcal{Q}(\mathbb{W}_L,\mathbb{W}_R)\delta_{x-u_2^*t}, \tag{3.3.4}$$

where $\mathcal{Q}(\mathbb{W}_L,\mathbb{W}_R)\delta_{x-u_2^*t}$ is a positive measure supported by the discontinuity associated with u_2^*, and the weight $\mathcal{Q}(\mathbb{W}_L,\mathbb{W}_R)$ is strictly positive.

Before stating the existence theorem for solutions with subsonic wave ordering, let us introduce some notations built on the initial states $(\mathbb{W}_L,\mathbb{W}_R)$.

For i in $\{1,2\}$,

$$u_i^\sharp := \frac{1}{2}(u_{i,L}+u_{i,R}) - \frac{1}{2a_i}(p_i(\tau_{i,R})-p_i(\tau_{i,L})), \tag{3.3.5}$$

$$\pi_i^\sharp := \frac{1}{2}(p_i(\tau_{i,R})+p_i(\tau_{i,L})) - \frac{a_i}{2}(u_{i,R}-u_{i,L}), \tag{3.3.6}$$

$$\tau_{i,L}^\sharp := \tau_{i,L} + \frac{1}{a_i}(u_i^\sharp - u_{i,L}) = \tau_{i,L} + \frac{1}{2a_i}(u_{i,R}-u_{i,L}) - \frac{1}{2a_i^2}(p_i(\tau_{i,R})-p_i(\tau_{i,L})), \tag{3.3.7}$$

$$\tau_{i,R}^\sharp := \tau_{i,R} - \frac{1}{a_i}(u_i^\sharp - u_{i,R}) = \tau_{i,R} + \frac{1}{2a_i}(u_{i,R}-u_{i,L}) + \frac{1}{2a_i^2}(p_i(\tau_{i,R})-p_i(\tau_{i,L})). \tag{3.3.8}$$

We also introduce the following dimensionless number that only depends on the initial phase fractions:

$$\Lambda^\alpha := \frac{\alpha_{2,R}-\alpha_{2,L}}{\alpha_{2,R}+\alpha_{2,L}}. \tag{3.3.9}$$

We have the following result:

Theorem 3.3.1. *Let be given a pair of admissible initial states $(\mathbb{W}_L,\mathbb{W}_R)\in\Omega^r\times\Omega^r$ and assume that the parameter a_i is such that $\tau_{i,L}^\sharp>0$ and $\tau_{i,R}^\sharp>0$ for i in $\{1,2\}$. There exists solutions with subsonic wave ordering to the Riemann problem (2.2.1)-(2.2.2) (see Definition 2.2.1 in chapter 2) if the following condition holds:*

$$(\boldsymbol{A}) \qquad -a_1\tau_{1,R}^\sharp < \frac{u_1^\sharp - u_2^\sharp - \frac{1}{a_2}\Lambda^\alpha(\pi_1^\sharp-\pi_2^\sharp)}{1+\frac{a_1}{a_2}|\Lambda^\alpha|} < a_1\tau_{1,L}^\sharp.$$

*In addition, if the ratio $\frac{\alpha_{1,L}}{\alpha_{1,R}}$ is in a neighbourhood of 1, condition $(\boldsymbol{A})$ is a **necessary and sufficient** condition for the existence of a **unique** energy-preserving solution. If $\frac{\alpha_{1,L}}{\alpha_{1,R}}$ is too large, or too small depending on the wave ordering, ensuring positive densities for phase 1 may require strict energy dissipation, and it is always possible under assumption $(\boldsymbol{A})$ to ensure the posivity of the phase 1 densities by dissipating the total energy. The densities of phase 2 are positive if and only if,*

$$(\boldsymbol{B}) \qquad u_2^\sharp - a_2\tau_{2,L}^\sharp < u_2^* < u_2^\sharp + a_2\tau_{2,R}^\sharp. \tag{3.3.10}$$

Now, given $(\mathbb{W}_L,\mathbb{W}_R,a_1,a_2)$ (verifying $\mathcal{T}_{i,L}=\tau_{i,L}$ and $\mathcal{T}_{i,R}=\tau_{i,R}$ for $i=1,2$) such that the conditions of Theorem 3.3.1 are met, we may display the expression of the piecewise constant solution $\xi\mapsto\mathbb{W}_r(\xi;\mathbb{W}_L,\mathbb{W}_R)$.

3.3.2 Construction of the solution

Following [10], we distinguish three different cases corresponding to different orderings of the kinematic waves, $u_1^*<u_2^*$, $u_1^*=u_2^*$ or $u_1^*>u_2^*$. With each one of these wave configurations, is associated a different expression of assumption $(\mathbf{A})$ depending on the sign of

$$U^\sharp := \frac{u_1^\sharp - u_2^\sharp - \frac{1}{a_2}\Lambda^\alpha(\pi_1^\sharp-\pi_2^\sharp)}{1+\frac{a_1}{a_2}|\Lambda^\alpha|}. \tag{3.3.11}$$

Solution with the wave ordering $\mathbf{u_2^* < u_1^*}$

If together with (**B**), assumption

$$(\mathbf{A1}) \qquad 0 < U^\sharp < a_1 \tau_{1,L}^\sharp$$

holds, the solution has the wave ordering $u_2^* < u_1^*$.

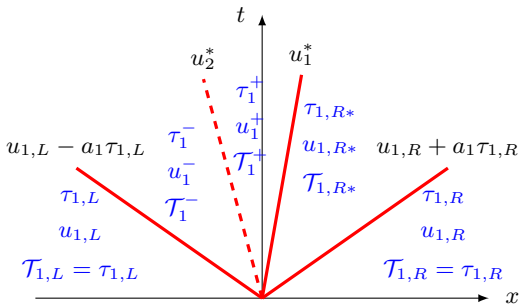

Phase 1 solution.

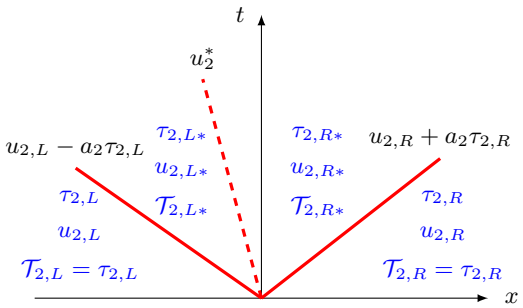

Phase 2 solution.

The intermediate states and the velocities u_1^* and u_2^* are computed through the following steps performed in the very same order.

1. Define $\nu := \dfrac{\alpha_{1,L}}{\alpha_{1,R}}$, $\mathcal{M}_L^\sharp := \dfrac{u_1^\sharp - u_2^\sharp}{a_1 \tau_{1,L}^\sharp}$ and $\mathcal{P}_L^\sharp := \dfrac{\pi_1^\sharp - \pi_2^\sharp}{a_1^2 \tau_{1,L}^\sharp}$.

2. Define successively the functions

$$\mathcal{M}_0(\omega) := \frac{1}{2}\left(\frac{1+\omega^2}{1-\omega^2}\left(1+\frac{1}{\nu}\right) - \sqrt{\left(\frac{1+\omega^2}{1-\omega^2}\right)^2\left(1+\frac{1}{\nu}\right)^2 - \frac{4}{\nu}}\right), \tag{3.3.12}$$

$$\mathcal{M}_\mu(m) := \frac{1}{\nu}\frac{m + (1-\mu)\frac{\tau_{1,R}^\sharp}{\tau_{1,L}^\sharp}}{1 - (1-\mu)\frac{\tau_{1,R}^\sharp}{\tau_{1,L}^\sharp}}, \quad \text{with } \mu \in (0,1). \text{ For instance } \mu = 0.1, \tag{3.3.13}$$

$$\mathcal{M}(m) := \min\left(\mathcal{M}_0\left(\frac{1-m}{1+m}\right), \mathcal{M}_\mu(m)\right), \tag{3.3.14}$$

$$\Psi(m) := m + \frac{a_1}{a_2}\frac{\alpha_{1,R}}{\alpha_{2,L} + \alpha_{2,R}}\left((1+\nu)m - 2\nu\mathcal{M}(m)\right). \tag{3.3.15}$$

3. Use an iterative method (*e.g.* Newton's method or a dichotomy algorithm) to compute $\mathcal{M}_L^* \in (0,1)$ such that

$$\Psi(\mathcal{M}_L^*) = \mathcal{M}_L^\sharp - \frac{a_1}{a_2}\Lambda^\alpha \mathcal{P}_L^\sharp. \tag{3.3.16}$$

According to [10], $\mathcal{M}_L^*$ always exists under (**A1**) and is unique if μ is close enough to one. In practice, the iterative method is initialized at $m^0 = \max(0, \min(\mathcal{M}_L^\sharp, 1))$.

4. The velocity u_2^* is obtained by
$$u_2^* = u_1^\sharp - a_1 \tau_{1,L}^\sharp \mathcal{M}_L^*. \tag{3.3.17}$$

5. The velocity u_1^* is obtained by
$$u_1^* = u_2^* + a_1 \tau_{1,L}^\sharp \mathcal{M}(\mathcal{M}_L^*) \frac{1-\mathcal{M}_L^*}{1-\mathcal{M}(\mathcal{M}_L^*)}. \tag{3.3.18}$$

6. The intermediate states for phase 1 are given by
$$\tau_1^- = \tau_{1,L}^\sharp \frac{1-\mathcal{M}_L^*}{1-\mathcal{M}(\mathcal{M}_L^*)}, \qquad u_1^- = u_2^* + a_1 \tau_{1,L}^\sharp \mathcal{M}(\mathcal{M}_L^*) \frac{1-\mathcal{M}_L^*}{1-\mathcal{M}(\mathcal{M}_L^*)}, \quad \mathcal{T}_1^- = \tau_{1,L}, \tag{3.3.19}$$
$$\tau_1^+ = \tau_{1,L}^\sharp \frac{1+\mathcal{M}_L^*}{1+\nu\mathcal{M}(\mathcal{M}_L^*)}, \qquad u_1^+ = u_1^*, \qquad \mathcal{T}_1^+ = \tau_{1,L}, \tag{3.3.20}$$
$$\tau_{1,R*} = \tau_{1,R}^\sharp + \tau_{1,L}^\sharp \frac{\mathcal{M}_L^* - \nu\mathcal{M}(\mathcal{M}_L^*)}{1+\nu\mathcal{M}(\mathcal{M}_L^*)}, \quad u_{1,R*} = u_1^*, \qquad \mathcal{T}_{1,R*} = \tau_{1,R}. \tag{3.3.21}$$

7. The intermediate states for phase 2 are then given by
$$\tau_{2,L*} = \tau_{2,L} + \frac{1}{a_2}(u_2^* - u_{2,L}), \qquad u_{2,L*} = u_2^*, \qquad \mathcal{T}_{2,L*} = \tau_{2,L}, \tag{3.3.22}$$
$$\tau_{2,R*} = \tau_{2,R} - \frac{1}{a_2}(u_2^* - u_{2,R}), \qquad u_{2,R*} = u_2^*, \qquad \mathcal{T}_{2,R*} = \tau_{2,R}. \tag{3.3.23}$$

Remark 3.3.1. *In [10], a kinetic relation is designed in order to define the Mach number $\mathcal{M}$ that parametrizes the phase 1 solution. It consists in imposing the lower-bound $\mu\tau_{1,R}^\sharp$ on the specific volume $\tau_{1,R*}$. If $\mathcal{M}(\mathcal{M}_L^*) = \mathcal{M}_0\left(\frac{1-\mathcal{M}_L^*}{1+\mathcal{M}_L^*}\right)$ is such that this lower-bound is satisfied, then the chosen solution is the unique energy-preserving solution. Otherwise, maintaining the lower-bound $\mu\tau_{1,R}^\sharp$ for $\tau_{1,R*}$ requires an energy dissipation which is ensured by taking $\mathcal{M}(\mathcal{M}_L^*) = \mathcal{M}_\mu(\mathcal{M}_L^*)$ (see [10] for more details).*

Solution with the wave ordering $\mathbf{u_2^* > u_1^*}$

If together with (**B**), assumption
$$(\mathbf{A2}) \qquad -a_1\tau_{1,R}^\sharp < U^\sharp < 0$$
holds, then the solution has the wave ordering $u_2^* > u_1^*$. For the determination of the wave velocities and the intermediate states, the simplest thing to do is to exploit the Galilean invariance of the equations. In this case indeed, the solution is obtained by the transformation
$$\mathbb{W}_r(\xi; \mathbb{W}_L, \mathbb{W}_R) := \mathcal{V}\mathbb{W}_r(-\xi; \mathcal{V}\mathbb{W}_R, \mathcal{V}\mathbb{W}_L), \tag{3.3.24}$$

where the operator $\mathcal{V}$ changes the velocities into their opposite values:

$$\mathcal{V} : (x_1, x_2, x_3, x_4, x_5, x_6, x_7) \mapsto (x_1, x_2, -x_3, x_4, -x_5, x_6, x_7). \tag{3.3.25}$$

Of course, the function $\mathbb{W}_r(-\xi; \mathcal{V}\mathbb{W}_R, \mathcal{V}\mathbb{W}_L)$ is computed through the first case, since for these new initial data $(\mathcal{V}\mathbb{W}_R, \mathcal{V}\mathbb{W}_L)$, it is condition (**A1**) that holds.

Solution with the wave ordering $\mathbf{u_2^* = u_1^*}$

If together with (**B**), assumption

$$(\mathbf{A3}) \qquad U^\sharp = 0$$

holds, then the solution has the wave ordering $u_2^* = u_1^*$.

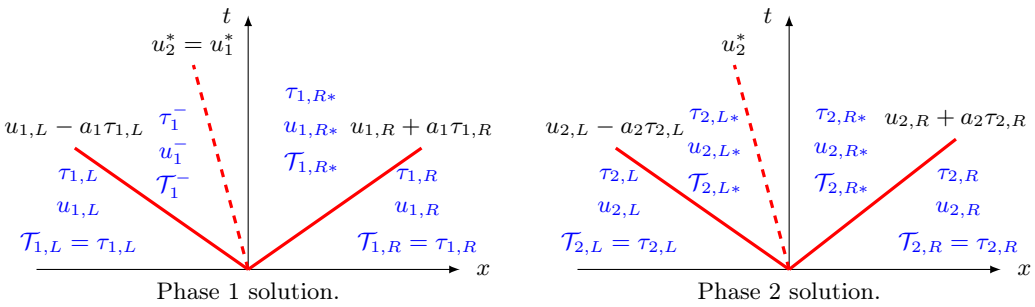

The kinematic velocities are given by

$$u_2^* = u_1^* = u_1^\sharp. \tag{3.3.26}$$

The intermediate states for phase 2 are obtained by the same formulas as in (3.3.22) and (3.3.23) while the intermediate states for phase 1 read

$$\tau_1^- = \tau_{1,L}^\sharp, \qquad u_1^- = u_1^\sharp, \qquad \mathcal{T}_1^- = \tau_{1,L}, \tag{3.3.27}$$

$$\tau_{1,R*} = \tau_{1,R}^\sharp, \qquad u_{1,R*} = u_1^\sharp, \qquad \mathcal{T}_{1,R*} = \tau_{1,R}. \tag{3.3.28}$$

The non-conservative product $\mathbf{d}(\mathbb{W})\partial_{\mathbf{x}}\mathbb{W}$

When $\alpha_{1,L} \neq \alpha_{1,R}$, the non-conservative product $\mathbf{d}(\mathbb{W})\partial_x\mathbb{W}$ identifies with a Dirac measure propagating at the constant velocity u_2^*. This Dirac measure is given by

$$\mathbf{D}^*(\mathbb{W}_L, \mathbb{W}_R)\delta_{x-u_2^*t}, \tag{3.3.29}$$

where $\mathbf{D}^*(\mathbb{W}_L, \mathbb{W}_R) := (\alpha_{1,R} - \alpha_{1,L})\,(u_2^*, 0, -\pi_1^*, 0, 0, +\pi_1^*, 0)^T$. The pressure π_1^* is defined for $\alpha_{1,R} \neq \alpha_{1,L}$ by

$$\pi_1^* := \pi_2^\sharp - a_2 \frac{\alpha_{2,R} + \alpha_{2,L}}{\alpha_{1,R} - \alpha_{1,L}}(u_2^* - u_2^\sharp). \tag{3.3.30}$$

3.4 The relaxation scheme

In this section, the relaxation Riemann solver is used in order to derive a numerical scheme, the aim being to approximate the entropy weak solutions of a Cauchy problem associated with system (3.2.1):

$$\begin{cases} \partial_t \mathbb{U} + \partial_x \mathbf{f}(\mathbb{U}) + \mathbf{c}(\mathbb{U})\partial_x \mathbb{U} = 0, & x \in \mathbb{R}, t > 0, \\ \mathbb{U}(x,0) = \mathbb{U}_0(x), & x \in \mathbb{R}. \end{cases} \tag{3.4.1}$$

For simplicity in the notations, we assume constant positive time and space steps Δt and Δx, and we define $\lambda = \frac{\Delta t}{\Delta x}$. The space is partitioned into cells $\mathbb{R} = \bigcup_{j\in\mathbb{Z}} C_j$ where $C_j = [x_{j-\frac{1}{2}}, x_{j+\frac{1}{2}}[$ with $x_{j+\frac{1}{2}} = (j+\frac{1}{2})\Delta x$ for all j in $\mathbb{Z}$. The centers of the cells are denoted $x_j = j\Delta x$ for all j in $\mathbb{Z}$. We also introduce the discrete intermediate times $t^n = n\Delta t$, $n \in \mathbb{N}$. The approximate solution at time t^n, $x \in \mathbb{R} \mapsto \mathbb{U}_\lambda(x,t^n) \in \Omega$ is a piecewise constant function whose value on each cell C_j is a constant value denoted by $\mathbb{U}_j^n$:

$$\mathbb{U}_\lambda(x,t^n) = \mathbb{U}_j^n, \quad \text{for all} \quad x \text{ in } C_j, \quad j \text{ in } \mathbb{Z}, \quad n \text{ in } \mathbb{N}. \tag{3.4.2}$$

3.4.1 Description of the relaxation algorithm

We now describe the two-step splitting method associated with the relaxation system (3.2.7) in order to calculate $\mathbb{U}_\lambda(\cdot,t^{n+1})$ from $\mathbb{U}_\lambda(\cdot,t^n)$. The first step consists in a time-advancing step for the convective part of the relaxation system (3.2.11), and the second step takes into account the relaxation source term. We first introduce the piecewise constant approximate solution at time t^n of system (3.2.11) $x \mapsto \mathbb{W}_\lambda(x,t^n) = \mathbb{W}_j^n$ in C_j with

$$\mathbb{W}_j^n = \left(\alpha_{1,j}^n, (\alpha_1\rho_1)_j^n, (\alpha_1\rho_1 u_1)_j^n, (\alpha_2\rho_2)_j^n, (\alpha_2\rho_2 u_2)_j^n, (\alpha_1\rho_1\mathcal{T}_1)_j^n, (\alpha_2\rho_2\mathcal{T}_2)_j^n, \right)^T. \tag{3.4.3}$$

At time $t = 0$, $\mathbb{W}_j^0$ is set at equilibrium which means that $(\alpha_i\rho_i\mathcal{T}_i)_j^0 = \alpha_{i,j}^0$ for i in $\{1,2\}$. The two steps are defined as follows.

Step 1: Evolution in time ($t^n \to t^{n+1,-}$)

In the first step, the following Cauchy problem is exactly solved for $t \in [0,\Delta t]$ with Δt small enough (see condition (3.4.5) below)

$$\begin{cases} \partial_t \widetilde{\mathbb{W}} + \partial_x \mathbf{g}(\widetilde{\mathbb{W}}) + \mathbf{d}(\widetilde{\mathbb{W}})\partial_x \widetilde{\mathbb{W}} = 0, \\ \widetilde{\mathbb{W}}(x,0) = \mathbb{W}_\lambda(x,t^n). \end{cases} \tag{3.4.4}$$

Since $x \mapsto \mathbb{W}_\lambda(x,t^n)$ is piecewise constant, the exact solution of (3.4.4) is obtained by gluing together the solutions of the Riemann problems set at each cell interface $x_{j+\frac{1}{2}}$, provided that these solutions do not interact during the period Δt, *i.e.* provided the following classical CFL condition

$$\frac{\Delta t}{\Delta x} \max_{i\in\{1,2\}, j\in\mathbb{Z}} \max(|(u_i - a_i\tau_i)_j|, |(u_i + a_i\tau_i)_{j+1}|) < \frac{1}{2}. \tag{3.4.5}$$

More precisely,

$$\text{If} \quad (x,t) \in [x_j, x_{j+1}] \times [0, \Delta t], \quad \text{then} \quad \widetilde{\mathbb{W}}_\lambda(x,t) = \mathbb{W}_r\left(\frac{x - x_{j+1/2}}{t}; \mathbb{W}_j^n, \mathbb{W}_{j+1}^n\right), \tag{3.4.6}$$

where $(x,t) \mapsto \mathbb{W}_r\left(\frac{x}{t}; \mathbb{W}_L, \mathbb{W}_R\right)$ is the solution of the Riemann problem (3.3.1) whose construction is detailed in section 3.3. Then, we get a piecewise constant function by averaging $\widetilde{\mathbb{W}}_\lambda(x,t)$ on each cell C_j at time Δt:

$$\mathbb{W}_\lambda(x, t^{n+1,-}) = \mathbb{W}_j^{n+1,-} := \frac{1}{\Delta x} \int_{x_{j-\frac{1}{2}}}^{x_{j+\frac{1}{2}}} \widetilde{\mathbb{W}}_\lambda(x, \Delta t) dx, \quad \forall x \in C_j, \quad \forall j \in \mathbb{Z}. \tag{3.4.7}$$

Step 2: Instantaneous relaxation ($t^{n+1,-} \to t^{n+1}$)

In the second step, we solve at time $t^n + \Delta t$ the ordinary differential equation

$$\begin{cases} \partial_t \mathbb{W} = \frac{1}{\varepsilon} \mathcal{R}(\mathbb{W}), & \text{in the asymptotic regime } \varepsilon \to 0, \\ \mathbb{W}(x,0) = \mathbb{W}_\lambda(x, t^{n+1,-}). \end{cases} \tag{3.4.8}$$

Using the definition (3.2.7) of the relaxation term $\mathcal{R}$, we see that this amounts to imposing $\mathcal{T}_{i,j}^{n+1} := \tau_{i,j}^{n+1}$ for i in $\{1,2\}$ and j in $\mathbb{Z}$. Hence we have

$$\mathbb{W}_j^{n+1} = \left(\alpha_{1,j}^{n+1,-}, (\alpha_1\rho_1)_j^{n+1,-}, (\alpha_1\rho_1 u_1)_j^{n+1,-}, (\alpha_2\rho_2)_j^{n+1,-}, (\alpha_2\rho_2 u_2)_j^{n+1,-}, (\alpha_1)_j^{n+1,-}, (\alpha_2)_j^{n+1,-}\right)^T \tag{3.4.9}$$

and the new cell value at time t^{n+1} of the approximate solution $\mathbb{U}_\lambda(\cdot, t^{n+1})$ is obtained by dropping the variables $\mathcal{T}_i$, $i \in \{1,2\}$:

$$\mathbb{U}_j^{n+1} = \left(\alpha_{1,j}^{n+1,-}, (\alpha_1\rho_1)_j^{n+1,-}, (\alpha_1\rho_1 u_1)_j^{n+1,-}, (\alpha_2\rho_2)_j^{n+1,-}, (\alpha_2\rho_2 u_2)_j^{n+1,-}\right)^T \tag{3.4.10}$$

This completes the description of the two-step relaxation method.

3.4.2 Finite volume formulation

It this section, we show that the two-step relaxation method described in the previous section can be written in the form of a non-conservative finite volume scheme

$$\mathbb{U}_j^{n+1} = \mathbb{U}_j^n - \frac{\Delta t}{\Delta x}\left(\mathbf{F}_{j+\frac{1}{2}}^- - \mathbf{F}_{j-\frac{1}{2}}^+\right), \tag{3.4.11}$$

where $\mathbf{F}_{j+\frac{1}{2}}^- = \mathbf{F}^-(\mathbb{U}_j^n, \mathbb{U}_{j+1}^n)$ and $\mathbf{F}_{j-\frac{1}{2}}^+ = \mathbf{F}^+(\mathbb{U}_{j-1}^n, \mathbb{U}_j^n)$ are the left and right numerical fluxes at the cell interfaces $x_{j-\frac{1}{2}}$ and $x_{j+\frac{1}{2}}$. Here, the left and right fluxes $\mathbf{F}^-$ and $\mathbf{F}^+$ are two distinct functions in order to take into account the non-conservative product. In practice, it is the finite volume formulation that is used when implementing the scheme. Note that such a formulation allows a straightforward extension of the method to the multi-D framework (see [17] for instance).

The first step of the relaxation method states that $\widetilde{\mathbb{W}}_\lambda(x,t)$ is the **exact** solution of

$$\partial_t \widetilde{\mathbb{W}} + \partial_x \mathbf{g}(\widetilde{\mathbb{W}}) + \mathbf{d}(\widetilde{\mathbb{W}})\partial_x \widetilde{\mathbb{W}} = 0, \tag{3.4.12}$$

on $\mathbb{R}\times[t^n,t^{n+1}]$ with the initial data $\mathbb{W}_\lambda(x,t^n)=\mathbb{W}_j^n$ for all x in C_j, with j in $\mathbb{Z}$. Integrating on the rectangle $C_j\times[t^n,t^{n+1}]$, we get

$$\mathbb{W}_j^{n+1-} = \mathbb{W}_j^n - \frac{\Delta t}{\Delta x}\left(\mathbf{G}_{j+\frac12}^n - \mathbf{G}_{j-\frac12}^n\right) - \frac{\Delta t}{\Delta x}\left(\mathbf{D}_{j-\frac12}^n \mathbf{1}_{\left\{u^*_{2,j-\frac12}>0\right\}} + \mathbf{D}_{j+\frac12}^n \mathbf{1}_{\left\{u^*_{2,j+\frac12}<0\right\}}\right), \tag{3.4.13}$$

where

$$\mathbf{G}_{j+\frac12}^n = \mathbf{G}(\mathbb{W}_j^n,\mathbb{W}_{j+1}^n) = \mathbf{g}(\mathbb{W}_r(0;\mathbb{W}_j^n,\mathbb{W}_{j+1}^n)), \tag{3.4.14}$$

$$\mathbf{D}_{j+\frac12}^n = \mathbf{D}^*(\mathbb{W}_j^n,\mathbb{W}_{j+1}^n) = (\Delta\alpha_1)_{j+\frac12}^n\,(u_2^*,0,-\pi_1^*,0,0,+\pi_1^*,0)_{j+\frac12}^T, \tag{3.4.15}$$

with $(\Delta\alpha_1)_{j+\frac12}^n = \alpha_{1,j+1}^n - \alpha_{1,j}^n$. See section 3.3.2 for the expressions of u_2^* and π_1^*. The non-conservative term has zero, one or two contributions, depending on whether the u_2-contact waves from the Riemann problems centered respectively at $x_{j-\frac12}$ and $x_{j+\frac12}$ enter cell C_j respectively from the left and from the right or not. We then recall that the initial values $\mathbb{W}_j^n$ are set to equilibrium which means that $\mathbb{W}_j^n = \mathscr{M}(\mathbb{U}_j^n)$ where the mapping $\mathscr{M}$ is defined as

$$\begin{array}{rccc} \mathscr{M}: & \mathbb{R}^5 & \longrightarrow & \mathbb{R}^7 \\ & (x_1,x_2,x_3,x_4,x_5) & \longmapsto & (x_1,x_2,x_3,x_4,x_5,x_1,1-x_1). \end{array} \tag{3.4.16}$$

Moreover, the relaxation step shows that $\mathbb{U}_j^{n+1} = \mathscr{P}\mathbb{W}_j^{n+1-}$ where $\mathscr{P}$ is the linear operator

$$\begin{array}{rccc} \mathscr{P}: & \mathbb{R}^7 & \longrightarrow & \mathbb{R}^5 \\ & (x_1,x_2,x_3,x_4,x_5,x_6,x_7) & \longmapsto & (x_1,x_2,x_3,x_4,x_5). \end{array} \tag{3.4.17}$$

Eventually, when applying operator $\mathscr{P}$ to equation (3.4.13) (note that $\mathscr{P}\circ\mathscr{M} = Id_{\mathbb{R}^5}$) we obtain the finite volume formulation of our scheme

$$\mathbb{U}_j^{n+1} = \mathbb{U}_j^n - \frac{\Delta t}{\Delta x}\left(\mathbf{F}^-(\mathbb{U}_j^n,\mathbb{U}_{j+1}^n) - \mathbf{F}^+(\mathbb{U}_{j-1}^n,\mathbb{U}_j^n)\right), \tag{3.4.18}$$

with

$$\mathbf{F}^-(\mathbb{U}_L,\mathbb{U}_R) = \mathscr{P}\ \mathbf{G}\left(\mathscr{M}(\mathbb{U}_L),\mathscr{M}(\mathbb{U}_R)\right) + \mathscr{P}\ \mathbf{D}^*\left(\mathscr{M}(\mathbb{U}_L),\mathscr{M}(\mathbb{U}_R)\right)\mathbf{1}_{\left\{u_2^*<0\right\}}, \tag{3.4.19}$$

$$\mathbf{F}^+(\mathbb{U}_L,\mathbb{U}_R) = \mathscr{P}\ \mathbf{G}\left(\mathscr{M}(\mathbb{U}_L),\mathscr{M}(\mathbb{U}_R)\right) - \mathscr{P}\ \mathbf{D}^*\left(\mathscr{M}(\mathbb{U}_L),\mathscr{M}(\mathbb{U}_R)\right)\mathbf{1}_{\left\{u_2^*>0\right\}}. \tag{3.4.20}$$

3.4.3 Basic properties of the scheme

The relaxation approximation method provides a very convenient framework for the preservation of the invariant domain Ω. Indeed, the following property states a maximum principle on the approximated phase fraction $\alpha_{1,j}^n$ as well as the positivity of the approximated partial masses $(\alpha_i\rho_i)_j^n$.

Property 3.4.1. *Under the CFL condition (3.4.5), if the initial condition $x \mapsto \mathbb{U}_0(x)$ is in Ω, then the values $(\mathbb{U}_j^n)_{j\in\mathbb{Z},n\in\mathbb{N}}$ computed by the scheme are such that,*

$$0 < \alpha_{i,j}^n < 1, \quad \text{and} \quad (\alpha_i\rho_i)_j^n > 0, \qquad \text{for all } i \text{ in } \{1,2\},\ j \text{ in } \mathbb{Z} \text{ and } n \text{ in } \mathbb{N}. \tag{3.4.21}$$

that is to say, the piecewise constant approximate solution $\mathbb{U}_\lambda(x,t^n)$ is also in Ω.

Proof. Let us consider the two-step splitting formulation of the scheme. The second line of equation (3.4.7) shows that $\alpha_{1,j}^{n+1}$ is the L^2-projection of the phase fraction α_1 in the solution $\widetilde{\mathbb{W}}_\lambda(x,\Delta t)$ of the homogeneous relaxation system. Under the CFL condition (3.4.5), this solution is obtained by gluing together the Riemann solutions arising from each interface $x_{j+1/2}$. Thus, by Theorem 3.3.1, we have $0 < \alpha_1(x,t^{n+1,-}) < 1$ for all x in $\mathbb{R}$ before the projection. The conclusion follows from the convexity of the L^2-projection. The same argument can be reproduced for the positivity of the partial masses. □

We also have the following classical consistency property for the relaxation scheme which guarantees that the constant solutions of system (3.2.1) are exactly computed.

Property 3.4.2 (Consistency). *The relaxation scheme is consistent in the sense that, for all $\mathbb{U}$ in the phase space Ω, the numerical fluxes $\mathbf{F}^-$ and $\mathbf{F}^+$ satisfy*

$$\mathbf{F}^-(\mathbb{U},\mathbb{U}) = \mathbf{F}^+(\mathbb{U},\mathbb{U}) = \mathbf{f}(\mathbb{U}), \tag{3.4.22}$$

where $\mathbf{f}(\mathbb{U})$, which is defined in (3.2.2), is the conservative part of the exact flux of the equilibrium system (3.2.1).

Proof. The proof is almost straightforward, denoting $\mathbb{W} = \mathscr{M}(\mathbb{U})$, we can check that $\mathbb{W}_r(0;\mathbb{W},\mathbb{W}) = \mathbb{W}$ and $\mathscr{P}\,\mathbf{g}(\mathbb{W}) = \mathbf{f}(\mathbb{U})$ since $\mathbb{W} = \mathscr{M}(\mathbb{U})$ is at equilibrium. In addition, we have $\mathbf{D}^*(\mathbb{W},\mathbb{W}) = 0$ since $\alpha_{1,L} = \alpha_{1,R}$. □

Finally, the relaxation method is conservative for the partial masses and for the total momentum:

Property 3.4.3 (Conservativity). *For all pair $(\mathbb{U}_L,\mathbb{U}_R)$ in Ω,*

$$\mathbf{F}_k^-(\mathbb{U}_L,\mathbb{U}_R) = \mathbf{F}_k^+ \quad \text{for } k \text{ in } \{2,4\}, \tag{3.4.23}$$

$$\mathbf{F}_3^-(\mathbb{U}_L,\mathbb{U}_R) + \mathbf{F}_5^-(\mathbb{U}_L,\mathbb{U}_R) = \mathbf{F}_3^+(\mathbb{U}_L,\mathbb{U}_R) + \mathbf{F}_5^+(\mathbb{U}_L,\mathbb{U}_R), \tag{3.4.24}$$

where $\mathbf{F}_k^\pm$ is the k^{th} component of vector $\mathbf{F}^\pm$.

Proof. The proof is left to the reader. □

3.4.4 Non-linear stability

In the first step of the relaxation method, the solution of the Riemann problem (3.3.1) is computed at each interface $x_{j+\frac{1}{2}}$, and therefore, one must determine the values of the numerical parameters

a_1 and a_2. Observe that, under the CFL condition (3.4.5), the Riemann problems do not interact and the parameters (a_1, a_2) can be chosen locally at each cell interface $x_{j+\frac{1}{2}}$. In this section, we prove that if a so-called sub-characteristic condition (also known as Whitham's condition, see [5]) is verified by the parameters a_1 and a_2 at each cell interface, then the discrete values computed by the relaxation scheme satisfy a discrete entropy inequality, which is a discrete counterpart of the energy inequality (3.2.6) verified by the exact solutions, thus assessing the stability of the method.

Definition 3.4.1. *Consider $(\mathbb{U}_L, \mathbb{U}_R) \in \Omega \times \Omega$ and let $(\mathbb{W}_L, \mathbb{W}_R) = (\mathscr{M}(\mathbb{U}_L), \mathscr{M}(\mathbb{U}_R)) \in \Omega^r \times \Omega^r$ be the corresponding relaxation initial data. Let Δx and Δt be two space and time steps satisfying the CFL condition (3.4.5). Denoting $\tau_i(\xi)$ the specific volumes $\rho_i^{-1}(\xi)$ in the solution $\mathbb{W}_r(\xi; \mathbb{W}_L, \mathbb{W}_R)$ of the Riemann problem (3.3.1), the parameters (a_1, a_2) are said to satisfy* ***Whitham's condition for*** *$(\mathbb{U}_L, \mathbb{U}_R)$ if*

$$\text{for } i \text{ in } \{1,2\}, \quad a_i^2 > -\mathcal{P}_i'(\tau_i(\xi)), \text{ for almost every } \xi \text{ in } \left[-\frac{\Delta x}{2\Delta t}, \frac{\Delta x}{2\Delta t}\right]. \tag{3.4.25}$$

Recall that $\tau \mapsto \mathcal{P}_i(\tau) = p_i(\tau^{-1})$ is the pressure of phase i seen as a function of the specific volume.

Lemma 3.4.4. *With the same notations as in Definition 3.4.1 and denoting $\mathbb{W}_r(\xi)$ so as to ease the notation, if (a_1, a_2) satisfy Whitham's condition for $(\mathbb{U}_L, \mathbb{U}_R)$, then the relaxation approximate Riemann solver satisfies a discrete entropy inequality by interface (see [18]) in the sense that*

$$\eta(\langle \mathbb{U} \rangle^L) - \eta(\mathbb{U}_L) + \frac{2\Delta t}{\Delta x}\left(\mathcal{F}_\eta^r\left(\mathbb{W}_r(0^+)\right) - \mathcal{F}_\eta(\mathbb{U}_L)\right) \leq 0, \tag{3.4.26}$$

$$\eta(\langle \mathbb{U} \rangle^R) - \eta(\mathbb{U}_R) + \frac{2\Delta t}{\Delta x}\left(\mathcal{F}_\eta(\mathbb{U}_R) - \mathcal{F}_\eta^r\left(\mathbb{W}_r(0^+)\right)\right) \leq 0, \tag{3.4.27}$$

where

$$\langle \mathbb{U} \rangle^L = \frac{2}{\Delta x}\int_{-\frac{\Delta x}{2}}^0 \mathscr{P}\mathbb{W}_r(x/\Delta t)dx = \frac{2\Delta t}{\Delta x}\int_{-\frac{\Delta x}{2\Delta t}}^0 \mathscr{P}\mathbb{W}_r(\xi)d\xi, \tag{3.4.28}$$

$$\langle \mathbb{U} \rangle^R = \frac{2}{\Delta x}\int_0^{\frac{\Delta x}{2}} \mathscr{P}\mathbb{W}_r(x/\Delta t)dx = \frac{2\Delta t}{\Delta x}\int_0^{\frac{\Delta x}{2\Delta t}} \mathscr{P}\mathbb{W}_r(\xi)d\xi. \tag{3.4.29}$$

Proof. We only prove inequality (3.4.26) (the proof of (3.4.27) is similar). By Jensen's inequality, the convexity of the map $\mathbb{U} \mapsto \eta(\mathbb{U})$ (see Proposition 3.2.1) implies that it is sufficient to prove

$$\frac{2\Delta t}{\Delta x}\int_{-\frac{\Delta x}{2\Delta t}}^0 \eta\left(\mathscr{P}\mathbb{W}_r(\xi)\right)d\xi - \eta(\mathbb{U}_L) + \frac{2\Delta t}{\Delta x}\left(\mathcal{F}_\eta^r\left(\mathbb{W}_r(0^+)\right) - \mathcal{F}_\eta(\mathbb{U}_L)\right) \leq 0, \tag{3.4.30}$$

under Whitham's condition (3.4.25). The solution $\mathbb{W}_r(\xi)$ of the Riemann problem (3.3.1) satisfies

$$\partial_t \eta^r(\mathbb{W}_r) + \partial_x \mathcal{F}_\eta^r(\mathbb{W}_r) = -\mathcal{Q}(\mathbb{W}_L, \mathbb{W}_R)\delta_{x-u_2^* t}, \tag{3.4.31}$$

in the weak sense, where $\mathcal{Q}(\mathbb{W}_L, \mathbb{W}_R)\delta_{x-u_2^* t}$ is a positive measure. Integrating this equation over $]-\frac{\Delta x}{2}, 0[\times]0, \Delta t[$, and dividing by $\frac{\Delta x}{2}$, we get

$$\frac{2\Delta t}{\Delta x}\int_{-\frac{\Delta x}{2\Delta t}}^0 \eta^r(\mathbb{W}_r(\xi))d\xi - \eta^r(\mathbb{W}_L) + \frac{2\Delta t}{\Delta x}\left(\mathcal{F}_\eta^r(\mathbb{W}_r(0^-)) - \mathcal{F}_\eta^r(\mathbb{W}_L)\right) \leq 0. \tag{3.4.32}$$

Now, as $(\mathbb{W}_L, \mathbb{W}_R) = (\mathscr{M}(\mathbb{U}_L), \mathscr{M}(\mathbb{U}_R))$ are at equilibrium, we have $\eta^r(\mathbb{W}_L) = \eta(\mathbb{U}_L)$ and $\mathcal{F}^r_\eta(\mathbb{W}_L) = \mathcal{F}_\eta(\mathbb{U}_L)$. Moreover, the Riemann solution is constructed such that $\mathcal{F}^r_\eta(\mathbb{W}_r(0^+)) - \mathcal{F}^r_\eta(\mathbb{W}_r(0^-)) \leq 0$ (indeed, we have $\mathcal{F}^r_\eta(\mathbb{W}_r(0^+)) - \mathcal{F}^r_\eta(\mathbb{W}_r(0^-)) = 0$ unless $u_2^* = 0$ in which case $\mathcal{F}^r_\eta(\mathbb{W}_r(0^+)) - \mathcal{F}^r_\eta(\mathbb{W}_r(0^-)) = -\mathcal{Q}(\mathbb{W}_L, \mathbb{W}_R) \leq 0$). Replacing in (3.4.32) this yields

$$-\eta(\mathbb{U}_L) + \frac{2\Delta t}{\Delta x}\left(\mathcal{F}^r_\eta\left(\mathbb{W}_r(0^+)\right) - \mathcal{F}_\eta(\mathbb{U}_L)\right) \leq -\frac{2\Delta t}{\Delta x}\int_{-\frac{\Delta x}{2\Delta t}}^0 \eta^r\left(\mathbb{W}_r(\xi)\right)d\xi. \tag{3.4.33}$$

Hence, a sufficient condition for (3.4.30) (and thus for (3.4.26)) to hold true is

$$\frac{2\Delta t}{\Delta x}\int_{-\frac{\Delta x}{2\Delta t}}^0 \left\{\eta\left(\mathscr{P}\mathbb{W}_r(\xi)\right) - \eta^r\left(\mathbb{W}_r(\xi)\right)\right\}d\xi \leq 0. \tag{3.4.34}$$

Now, for almost every ξ in $\left[-\frac{\Delta x}{2\Delta t}, 0\right]$, we have

$$\begin{aligned}&\eta\left(\mathscr{P}\mathbb{W}_r(\xi)\right) - \eta^r\left(\mathbb{W}_r(\xi)\right) = \\ &\qquad \sum_{i=1}^{2}(\alpha_i\rho_i)(\xi)\left(e(\tau_i(\xi)) - e_i(\mathcal{T}_i(\xi)) - \frac{1}{2a_i^2}\left(\pi_i^2(\tau_i(\xi),\mathcal{T}_i(\xi)) - \mathcal{P}_i^2(\mathcal{T}_i(\xi))\right)\right).\end{aligned} \tag{3.4.35}$$

Omitting the dependence on ξ, we have for $i = 1, 2$:

$$\begin{aligned}\pi_i^2(\tau_i,\mathcal{T}_i) - \mathcal{P}_i^2(\mathcal{T}_i) &= \left(\pi_i(\tau_i,\mathcal{T}_i) - \mathcal{P}_i(\mathcal{T}_i)\right)\left(\pi_i(\tau_i,\mathcal{T}_i) + \mathcal{P}_i(\mathcal{T}_i)\right)\\ &= a_i^2(\mathcal{T}_i - \tau_i)\left(2\mathcal{P}_i(\mathcal{T}_i) + a_i^2(\mathcal{T}_i - \tau_i)\right)\\ &= -2a_i^2 e_i'(\mathcal{T}_i)(\mathcal{T}_i - \tau_i) + a_i^4(\mathcal{T}_i - \tau_i)^2,\end{aligned}$$

since $e_i' = -\mathcal{P}_i$. Hence,

$$e_i(\tau_i) - e_i(\mathcal{T}_i) - \frac{1}{2a_i^2}\left(\pi_i^2(\tau_i,\mathcal{T}_i) - \mathcal{P}_i^2(\mathcal{T}_i)\right) = e_i(\tau_i) - e_i(\mathcal{T}_i) - e_i'(\mathcal{T}_i)(\tau_i - \mathcal{T}_i) - \frac{a_i^2}{2}(\mathcal{T}_i - \tau_i)^2. \tag{3.4.36}$$

A Taylor expansion with integral remainder gives

$$e_i(\tau_i) - e_i(\mathcal{T}_i) - e_i'(\mathcal{T}_i)(\tau_i - \mathcal{T}_i) = (\mathcal{T}_i - \tau_i)^2\int_0^1 e_i''(s\tau_i + (1-s)\mathcal{T}_i)(1-s)ds. \tag{3.4.37}$$

Then, replacing in (3.4.36) and observing that $e_i'' = -\mathcal{P}_i'$ we get a sufficient condition for (3.4.30) (and thus for (3.4.26)):

$$2\int_0^1 -\mathcal{P}_i'(s\tau_i(\xi) + (1-s)\mathcal{T}_i(\xi))(1-s)ds - a_i^2 \leq 0 \quad \text{for } a.e.\ \xi \text{ in } \left[-\frac{\Delta x}{2\Delta t}, 0\right]. \tag{3.4.38}$$

Noticing that in the solution $\mathcal{T}_i(\xi) = \tau_{i,L}$ or $\tau_{i,R}$ and using the strict convexity of $\tau \mapsto \mathcal{P}_i(\tau)$, we get for $a.e.\ \xi$ in $\left[-\frac{\Delta x}{2\Delta t}, 0\right]$:

$$\begin{aligned}2\int_0^1 -\mathcal{P}_i'(s\tau_i(\xi) + (1-s)\mathcal{T}_i(\xi))(1-s)ds &\leq \max_{s\in[0,1]}\left\{-\mathcal{P}_i'(s\tau_i(\xi) + (1-s)\mathcal{T}_i(\xi))\right\}2\int_0^1(1-s)ds\\ &\leq \operatorname*{ess\,sup}_{\xi\in[-\frac{\Delta x}{2\Delta t},\frac{\Delta x}{2\Delta t}]}\left\{-\mathcal{P}_i'(\tau_i(\xi))\right\}\\ &< a_i^2\end{aligned} \tag{3.4.39}$$

by Whitham's condition. This concludes the proof of inequality (3.4.26) under Whitham's condition. □

We may now prove the following theorem which states that under the CFL condition (3.4.5), Whitham's condition (3.4.25) guarantees a discrete entropy inequality for the relaxation finite volume scheme.

Theorem 3.4.5. *Assume the CFL condition (3.4.5) and suppose that for all $n \in \mathbb{N}$ and $j \in \mathbb{Z}$, the pair $(a_1, a_2)_{j+\frac{1}{2}}$ satisfies Whitham's condition for $(\mathbb{U}_j^n, \mathbb{U}_{j+1}^n)$. Then the relaxation scheme satisfies the following discrete entropy inequality:*

$$\eta(\mathbb{U}_j^{n+1}) - \eta(\mathbb{U}_j^n) + \frac{\Delta t}{\Delta x}(H(\mathbb{U}_j^n, \mathbb{U}_{j+1}^n) - H(\mathbb{U}_{j-1}^n, \mathbb{U}_j^n)) \leq 0, \tag{3.4.40}$$

where the numerical entropy flux is given by $H(\mathbb{U}_L, \mathbb{U}_R) = \mathcal{F}_\eta^r\left(\mathbb{W}_r\left(0^+; \mathscr{M}(\mathbb{U}_L), \mathscr{M}(\mathbb{U}_R)\right)\right)$.

This can be seen as a stability condition because if one considers the discrete L^1-norm of the total mixture energy at time t^n: $\sum_{j\in\mathbb{Z}} \eta(\mathbb{U}_j^n)\Delta x$, then summing inequality (3.4.40) over the cells yields

$$\sum_{j\in\mathbb{Z}} \eta(\mathbb{U}_j^{n+1})\Delta x \leq \sum_{j\in\mathbb{Z}} \eta(\mathbb{U}_j^n)\Delta x, \quad \text{for all } n \text{ in } \mathbb{N}, \tag{3.4.41}$$

which means that the total mixture energy is decreasing in time.

Proof. The proof is given in [5], but for the sake of completeness, we reproduce it here. Defining the averages for each half-cell $[x_{j-\frac{1}{2}}, x_j]$ and $[x_j, x_{j+\frac{1}{2}}]$:

$$\langle \mathbb{U} \rangle_{j-\frac{1}{2}}^R = \frac{2}{\Delta x}\int_{x_{j-\frac{1}{2}}}^{x_j} \mathscr{P}\mathbb{W}_r\left(x/\Delta t; \mathscr{M}(\mathbb{U}_{j-1}^n), \mathscr{M}(\mathbb{U}_j^n)\right) dx, \tag{3.4.42}$$

$$\langle \mathbb{U} \rangle_{j+\frac{1}{2}}^L = \frac{2}{\Delta x}\int_{x_j}^{x_{j+\frac{1}{2}}} \mathscr{P}\mathbb{W}_r\left(x/\Delta t; \mathscr{M}(\mathbb{U}_j^n), \mathscr{M}(\mathbb{U}_{j+1}^n)\right) dx, \tag{3.4.43}$$

we have, under the CFL condition (3.4.5): $\mathbb{U}_j^{n+1} = \frac{1}{2}\langle \mathbb{U} \rangle_{j-\frac{1}{2}}^R + \frac{1}{2}\langle \mathbb{U} \rangle_{j+\frac{1}{2}}^L$, and as η is convex

$$\eta\left(\mathbb{U}_j^{n+1}\right) \leq \frac{1}{2}\eta\left(\langle \mathbb{U} \rangle_{j-\frac{1}{2}}^R\right) + \frac{1}{2}\eta\left(\langle \mathbb{U} \rangle_{j+\frac{1}{2}}^L\right). \tag{3.4.44}$$

As the pair $(a_1, a_2)_{j-\frac{1}{2}}$ satisfies Whitham's condition for $(\mathbb{U}_{j-1}^n, \mathbb{U}_j^n)$, we can apply inequality (3.4.27) of Lemma 3.4.4 with $\mathbb{U}_L = \mathbb{U}_{j-1}^n$ and $\mathbb{U}_R = \mathbb{U}_j^n$, which yields

$$\eta\left(\langle \mathbb{U} \rangle_{j-\frac{1}{2}}^R\right) - \eta(\mathbb{U}_j^n) + \frac{2\Delta t}{\Delta x}\left(\mathcal{F}_\eta(\mathbb{U}_j^n) - \mathcal{F}_\eta^r\left(\mathbb{W}_r(0^+; \mathscr{M}(\mathbb{U}_{j-1}^n), \mathscr{M}(\mathbb{U}_j^n))\right)\right) \leq 0. \tag{3.4.45}$$

In the same way, as $(a_1, a_2)_{j+\frac{1}{2}}$ satisfies Whitham's condition for $(\mathbb{U}_j^n, \mathbb{U}_{j+1}^n)$, we can apply inequality (3.4.26) of Lemma 3.4.4 with $\mathbb{U}_L = \mathbb{U}_j^n$ and $\mathbb{U}_R = \mathbb{U}_{j+1}^n$, which gives

$$\eta\left(\langle \mathbb{U} \rangle_{j+\frac{1}{2}}^L\right) - \eta(\mathbb{U}_j^n) + \frac{2\Delta t}{\Delta x}\left(\mathcal{F}_\eta^r\left(\mathbb{W}_r(0^+; \mathscr{M}(\mathbb{U}_j^n), \mathscr{M}(\mathbb{U}_{j+1}^n)\right) - \mathcal{F}_\eta(\mathbb{U}_j^n)\right) \leq 0. \tag{3.4.46}$$

Summing equations (3.4.45) and (3.4.46) and using (3.4.44) we obtain

$$\eta(\mathbb{U}_j^{n+1}) - \eta(\mathbb{U}_j^n) + \frac{\Delta t}{\Delta x}(H(\mathbb{U}_j^n, \mathbb{U}_{j+1}^n) - H(\mathbb{U}_{j-1}^n, \mathbb{U}_j^n)) \leq 0, \tag{3.4.47}$$

where the numerical entropy flux is given by $H(\mathbb{U}_L, \mathbb{U}_R) = \mathcal{F}_\eta^r\left(\mathbb{W}_r\left(0^+; \mathscr{M}(\mathbb{U}_L), \mathscr{M}(\mathbb{U}_R)\right)\right)$. Finally, observe that H is consistent with the exact entropy flux $\mathcal{F}_\eta$ since $H(\mathbb{U}, \mathbb{U}) = \mathcal{F}_\eta(\mathbb{U})$ for all $\mathbb{U}$ in Ω. Indeed, for any $\mathbb{W}$ in Ω^r, we have $\mathbb{W}_r\left(0^+; \mathbb{W}, \mathbb{W}\right) = \mathbb{W}$. And if $\mathbb{W} = \mathscr{M}(\mathbb{U})$ is at equilibrium, we get $\mathcal{F}_\eta^r(\mathbb{W}) = \mathcal{F}_\eta(\mathbb{U})$. This concludes the proof of Theorem 3.4.5. □

3.4.5 Practical choice of the pair (a_1, a_2)

The pair of parameters (a_1, a_2), which is computed at each interface $x_{j+\frac{1}{2}}$ must chosen be large enough so as to satisfy several conditions:

- In order to ensure the stability of the relaxation approximation, a_i must satisfy Whitham's condition (3.4.25). For simplicity however, we do not impose Whitham's condition everywhere in the solution of the Riemann problem (3.3.1), but only for the left and right initial data at each interface:

$$\text{for } i \text{ in } \{1, 2\}, \quad a_i^2 > \max(-\mathcal{P}_i'(\tau_{i,L}), -\mathcal{P}_i'(\tau_{i,R})). \tag{3.4.48}$$

  In practice, no instabilities were observed during the numerical simulations due to this simpler Whitham-like condition.

- The specific volumes $\tau_{i,L}^\sharp$ and $\tau_{i,R}^\sharp$ must be positive. As the initial conditions of the local Riemann problems in (3.3.1) are set to equilibrium, we have $\mathcal{T}_{i,L} = \tau_{i,L}$ and $\mathcal{T}_{i,R} = \tau_{i,R}$. Thus

$$\tau_{i,L}^\sharp = \tau_{i,L} + \frac{1}{2a_i}(u_{i,R} - u_{i,L}) - \frac{1}{2a_i^2}\left(p_i(\tau_{i,R}) - p_i(\tau_{i,L})\right), \tag{3.4.49}$$

$$\tau_{i,R}^\sharp = \tau_{i,R} + \frac{1}{2a_i}(u_{i,R} - u_{i,L}) + \frac{1}{2a_i^2}\left(p_i(\tau_{i,R}) - p_i(\tau_{i,L})\right). \tag{3.4.50}$$

  Equations (3.4.49) and (3.4.50) are two second order polynomials in a_i^{-1}, and by taking a_i large enough, one can guarantee that $\tau_{i,L}^\sharp > 0$ and $\tau_{i,R}^\sharp > 0$, since the initial specific volumes $\tau_{i,L}$ and $\tau_{i,R}$ are positive.

- Finally, (a_1, a_2) must be chosen so as to meet the two conditions (**A**) and (**B**) of Theorem 3.3.1.

Thereafter, we propose an iterative algorithm for the computation of the parameters (a_1, a_2) at each interface. `Fixedpoint`(a_1, a_2) is a subroutine that computes a numerical approximation of the solution u_2^* of the fixed-point problem (3.3.16), using some numerical method such as Newton's method or a dichotomy algorithm. The notation `not`(**P**) is the negation of the logical statement **P**.

Choose κ a (small) parameter in the interval $(0,1)$.

For all interface $x_{j+\frac{1}{2}}$, $j \in \mathbb{Z}$, calculate $a_{1,j+\frac{1}{2}}$ and $a_{2,j+\frac{1}{2}}$ as follows

- For i in $\{1,2\}$ initialize $a_{i,j+\frac{1}{2}}$:
  $$a^2_{i,j+\frac{1}{2}} := (1+\kappa)\max\left(-\mathcal{P}_i'(\tau^n_{i,j}), -\mathcal{P}_i'(\tau^n_{i,j+1})\right).$$
- For i in $\{1,2\}$, do {
  $a_{i,j+\frac{1}{2}} := (1+\kappa)a_{i,j+\frac{1}{2}}$
  compute $u^\sharp_i$, $\pi^\sharp_i$, $\tau^\sharp_{i,L}$ and $\tau^\sharp_{i,R}$
  } while $\left(\tau^\sharp_{i,L} \leq 0 \text{ or } \tau^\sharp_{i,R} \leq 0\right)$
- do {
  $a_{2,j+\frac{1}{2}} := (1+\kappa)a_{2,j+\frac{1}{2}}$
  compute $u^\sharp_2$, $\pi^\sharp_2$, $\tau^\sharp_{2,L}$ and $\tau^\sharp_{2,R}$
  do {
  $a_{1,j+\frac{1}{2}} := (1+\kappa)a_{1,j+\frac{1}{2}}$
  compute $u^\sharp_1$, $\pi^\sharp_1$, $\tau^\sharp_{1,L}$ and $\tau^\sharp_{1,R}$
  } while $\left(\text{not(A)}\right)$
  compute ν, $\mathcal{M}^\sharp_L$ and $\mathcal{P}^\sharp_L$,
  compute $u^*_2 = \text{Fixedpoint}(a_{1,j+\frac{1}{2}}, a_{2,j+\frac{1}{2}})$
  } while $\left(\text{not(B)}\right)$

It is possible to prove that this algorithm always converges in the sense that there is non infinite looping due to the while-conditions. Moreover, this algorithm provides reasonable values of a_1 and a_2, since in all the numerical simulations, the time step obtained through the CFL condition (3.4.5) remains reasonably large and does not go to zero. In fact, the obtained values of a_1 and a_2 are quite satisfying since the relaxation scheme compares very favorably with Rusanov's scheme, in terms of CPU-time performances (see section 3.5).

3.5 Numerical tests for the barotropic 1D model

In this section, we present Riemann-type test-cases on which the performances of the relaxation scheme are tested. The phasic equations of state are given by the following ideal gas pressure laws:

$$\begin{aligned} p_1(\rho_1) &= \kappa_1 \rho_1^{\gamma_1}, \quad \text{with } \kappa_1 = 1 \text{ and } \gamma_1 = 3, \\ p_2(\rho_2) &= \kappa_2 \rho_2^{\gamma_2}, \quad \text{with } \kappa_2 = 1 \text{ and } \gamma_2 = 1.5. \end{aligned} \tag{3.5.1}$$

All the exact Riemann solutions considered in the sequel are constructed through classical steps that are reminded in Appendix B. In the sequel, $\mathcal{U} = (\alpha_1, \rho_1, u_1, \rho_2, u_2)^T$ denotes the state vector in **non-conservative variables**.

3.5.1 Test-case 1: a complete Riemann problem

We consider the following initial data,

$$\begin{aligned}
\mathcal{U}_L &= (0.1, 0.85, 0.4609513139, 0.96, 0.0839315299) && \text{if } x < 0,\\
\mathcal{U}_R &= (0.6, 1.2520240113, 0.7170741165, 0.2505659851, -0.3764790609) && \text{if } x > 0,
\end{aligned}$$

for which the exact solution is composed of a $\{u_1 - c_1\}$-shock wave, followed by a $\{u_2 - c_2\}$-rarefaction wave, followed by a u_2-contact discontinuity, followed by a $\{u_2 + c_2\}$-shock and finally followed by a $\{u_1 + c_1\}$-rarefaction wave (see Figure 3.2). The intermediate states are given by:

$$\begin{aligned}
\mathcal{U}_1 &= (0.1, 1., 0.2, 0.96, 0.0839315299),\\
\mathcal{U}_2 &= (0.1, 1., 0.2, 0.8, 0.3),\\
\mathcal{U}_3 &= (0.6, 1.0016192090, 0.2833602765, 0.5011319701, 0.3),\\
\mathcal{U}_4 &= (0.6, 1.0016192090, 0.2833602765, 0.2505659851, -0.3764790609).
\end{aligned}$$

At each interface $x_{j+\frac{1}{2}}$, Newton's method is used in order to compute the solution $\mathcal{M}_L^*$ of (3.3.16). The iterative procedure is stopped when the error is less than 10^{-12}.

In Figure 3.2, the approximate solution computed with the relaxation scheme is compared with both the exact solution and the approximate solution obtained with Rusanov's scheme (a Lax-Friedrichs type scheme see [15]). The results show that unlike Rusanov's scheme, the relaxation method correctly captures the intermediate states even for this rather coarse mesh of 100 cells. This coarse mesh is a typical example of an industrial mesh, reduced to one direction, since 100 cells in 1D correspond to a 10^6-cell mesh in 3D. It appears that the contact discontinuity is captured more sharply by the relaxation method than by Rusanov's scheme for which the numerical diffusion is larger. We can also see that for the phase 1 variables, there are no oscillations as one can see for Rusanov's scheme: the curves are monotone between the intermediate states. As for phase 2, the intermediate states are captured by the relaxation method while with Rusanov's scheme, this weak level of refinement is clearly not enough to capture any intermediate state. These observations assess that, for the same level of refinement, the relaxation method is more accurate than Rusanov's scheme.

A mesh refinement process has also been implemented in order to check numerically the convergence of the method, as well as it's performances in terms of CPU-time cost. For this purpose, we compute the discrete L^1-error between the approximate solution and the exact one at the final time T, normalized by the discrete L^1-norm of the exact solution:

$$E(\Delta x) = \frac{\sum_{\text{cells}j} |\varphi_j^n - \varphi_{ex}(x_j, T)|\Delta x}{\sum_{\text{cells}j} |\varphi_{ex}(x_j, T)|\Delta x}, \tag{3.5.2}$$

where φ is any of the **conservative** variables $(\alpha_1, \alpha_1\rho_1, \alpha_1\rho_1 u_1, \alpha_2\rho_2, \alpha_2\rho_2 u_2)$. The calculations have been implemented on several meshes composed of 100×2^n cells with $n = 0, 1, .., 10$ (knowing that the domain size is $L = 1$). In Figure 3.3, the error $E(\Delta x)$ at the final time $T = 0.14$, is plotted against Δx in a $log - log$ scale. Only the error on the phase fraction α_1 converges towards zero with

the expected order of $\Delta x^{1/2}$, while the other variables seem to converge with a higher rate. However, $\Delta x^{1/2}$ is only an asymptotic order of convergence, and in this particular case, one would have to implement the calculation on much more refined meshes in order to reach the expected order of $\Delta x^{1/2}$.

Figure 3.3 also displays the error on the conservative variables with respect to the CPU-time of the calculation expressed in seconds. Each point of the plot corresponds to one single calculation for a given mesh size (going from 400 to 102400 cells for the relaxation scheme and from 800 to 102400 cells for Rusanov's scheme). One can see that, for all the variables except $\alpha_1\rho_1u_1$, if one prescribes a given level of the error, the computational cost of Rusanov's scheme is significantly higher than that of the relaxation method. For instance, for the same error on the phase fraction α_1, the gain in computational cost is more than 13 when using the relaxation method rather than Rusanov's scheme. For the variable $\alpha_1\rho_1u_1$, even if the two methods seem to provide similar results, the relaxation method seems to give slightly better results for mesh sizes beyond 10000 cells.

3.5.2 Test-case 2: a vanishing phase case

We now consider a Riemann problem in which one of the two phases vanishes in one of the initial states, which means that the corresponding phase fraction α_1 or α_2 is equal to zero. For this kind of Riemann problem, the u_2-contact separates a mixture region where the two phases coexist from a single phase region with the remaining phase. Assuming for instance that $\alpha_{1,L} = 1$ and $0 < \alpha_{1,R} < 1$, the right state is a mixture of both phases while the left initial state is composed solely of phase 1. This type of vanishing-phase Riemann solution is introduced in [23] in the more general context of the complete Baer-Nunziato system with energy equations. The construction of an exact solution with vanishing phase fraction is not classical and we choose to follow the natural approach given in [23]. For more details, see appendix B. Consider the intermediate states

$$\mathcal{U}_L = (1.0, 1.8, 0.747051068928543, 3.979765198025580, 0.6),$$
$$\mathcal{U}_1 = (1.0, 2.0, 0.4, 3.979765198025580, 0.6),$$
$$\mathcal{U}_2 = (0.4, 1.982040094756841, 0.095469338564172, 3.979765198025580, 0.6),$$
$$\mathcal{U}_3 = (0.4, 1.9820400948, 0.0954693386, 5.1736947574, 1.0690676047),$$
$$\mathcal{U}_R = (0.4, 2.081142099494683, 0.267119045902047, 5.173694757433254, 1.069067604724276).$$

The solution is composed of a $\{u_1 - c_1\}$-shock wave from $\mathcal{U}_L$ to $\mathcal{U}_1$ in the left-hand side (LHS) region where only phase 1 is present. This region is separated by a u_2-contact discontinuity from the right-hand side (RHS) region where the two phases are mixed. In this RHS region, the solution is composed of a $\{u_2 + c_2\}$-rarefaction wave connecting $\mathcal{U}_2$ to $\mathcal{U}_3$ followed by a $\{u_1 + c_1\}$-rarefaction wave from $\mathcal{U}_3$ to $\mathcal{U}_R$ (see Figure 3.2).

In practice, the numerical method requires values of $\alpha_{1,L}$ and $\alpha_{1,R}$ that lie strictly in the interval $(0, 1)$. Therefore, in the numerical implementation, we take $\alpha_{1,L} = 1 - 10^{-9}$. The aim here is to give a qualitative comparison between the numerical approximation and the exact solution. Moreover, there is theoretically no need to specify left initial values for the phase 2 quantities since this phase is not present in the LHS region. For the sake of the numerical simulations however, one must provide such values. We choose to set $\rho_{2,L}$ and $u_{2,L}$ to the values on the right of the u_2-contact

discontinuity. For the relaxation scheme, this choice enables to avoid oscillations of phase 2 quantities in the region where phase 2 in not present. However, some tests have been conducted that assess that taking other values of $(\rho_{2,L}, u_{2,L})$ has little impact on the phase 1 quantities as well as on the phase 2 quantities where this phase is present.

At each interface $x_{j+\frac{1}{2}}$, a dichotomy algorithm is used in order to compute the solution $\mathcal{M}_L^*$ of (3.3.16). Indeed for such a vanishing phase test-case, Newton's method fails to converge. The dichotomy algorithm is stopped when the error is less than 10^{-12}. As for the first test-case, we can see that for the same level of refinement, the relaxation method is more accurate than Rusanov's scheme, which can be seen especially for phase 1. As regards the region where phase 2 does not exist, we can see that the relaxation method is much more stable than Rusanov's scheme. Indeed, the relaxation scheme behaves better than Rusanov's scheme when it comes to divisions by small values of α_2, since the solution approximated by Rusanov's scheme develops important oscillations.

3.5.3 Test-case 3: Coupling between two pure phases

The last test-case considers the coupling between two pure phases. A left region, where only phase 1 exists ($\alpha_{1,L} = 1$), is separated by a u_2-contact discontinuity from a right region, where only phase 2 is present ($\alpha_{1,R} = 0$). The intermediate states are given by

$$\begin{aligned}
\mathcal{U}_L &= (1.0, 0.861773876012754, 3.552800564555003, 4.641588833612778, 1.0),\\
\mathcal{U}_1 &= (1.0, 2.154434690031884, 1., 4.641588833612778, 1.),\\
\mathcal{U}_2 &= (0., 2.154434690031884, 1., 4.641588833612778, 1.),\\
\mathcal{U}_R &= (0., 2.154434690031884, 1.0, 6.962383250419167, 1.767119653712349).
\end{aligned} \tag{3.5.3}$$

The exact solution is composed of a $\{u_1 - c_1\}$-shock wave from $\mathcal{U}_L$ to $\mathcal{U}_1$ in the LHS region where only phase 1 is present. $\mathcal{U}_1$ is connected to $\mathcal{U}_2$ by a u_2-contact discontinuity separating the two pure phase regions. In the RHS region, where only phase 2 exists, $\mathcal{U}_2$ is connected to $\mathcal{U}_R$ by a $\{u_2 + c_2\}$-rarefaction wave. For more details on how the exact solution is constructed see appendix B.

In the numerical implementation, we set $\alpha_{1,L} = 1 - 10^{-9}$ and $\alpha_{1,R} = 10^{-9}$. A dichotomy procedure is used in order to compute the solution $\mathcal{M}_L^*$ of (3.3.16) at each interface $x_{j+\frac{1}{2}}$. The dichotomy algorithm is stopped when the error is less than 10^{-12}.

One can see that, in the LHS region, the quantities of the only present phase 1 are correctly approximated while the quantities of the vanishing phase 2 remain stable despite the division by small values of α_2. The same observation can be made for the RHS region. On the contrary, with Rusanov's scheme, strong oscillations pop up in the regions where a phase vanishes. Observe also that unlike Rusanov's scheme, the relaxation scheme does not fail to correctly approximate the evolution of the phase fraction α_1.

3.6 The multidimensional case

We are now interested in the numerical approximation of the multidimensional Baer-Nunziato model, on the basis of the numerical scheme developed before. Without loss of generality, we consider the two-dimensional case and denote $\mathbf{u}_i = (u_i, v_i) \in \mathbb{R}^2,\ i \in \{1,2\}$, the two-dimensional velocity of phase i: u_i and v_i respectively stand for the components of $\mathbf{u}_i$ in the x direction and in the y direction. All the variables depend on (x, y, t) and the 2D Baer-Nunziato model writes, using the same notations as in (3.2.1)-(3.2.2),

$$\partial_t \widetilde{\mathbb{U}} + \partial_x \mathbf{f}_x(\widetilde{\mathbb{U}}) + \partial_y \mathbf{f}_y(\widetilde{\mathbb{U}}) + \mathbf{c}_x(\widetilde{\mathbb{U}})\partial_x \widetilde{\mathbb{U}} + \mathbf{c}_y(\widetilde{\mathbb{U}})\partial_y \widetilde{\mathbb{U}} = 0, \quad (x,y) \in \mathbb{R}^2, t > 0, \tag{3.6.1}$$

with

$$\widetilde{\mathbb{U}} = \begin{bmatrix} \alpha_1 \\ \alpha_1\rho_1 \\ \alpha_1\rho_1 u_1 \\ \alpha_1\rho_1 v_1 \\ \alpha_2\rho_2 \\ \alpha_2\rho_2 u_2 \\ \alpha_2\rho_2 v_2 \end{bmatrix}, \quad \mathbf{f}_x(\widetilde{\mathbb{U}}) = \begin{bmatrix} 0 \\ \alpha_1\rho_1 u_1 \\ \alpha_1\rho_1 u_1^2 + \alpha_1 p_1(\rho_1) \\ \alpha_1\rho_1 u_1 v_1 \\ \alpha_2\rho_2 u_2 \\ \alpha_2\rho_2 u_2^2 + \alpha_2 p_2(\rho_2) \\ \alpha_2\rho_2 u_2 v_2 \end{bmatrix}, \quad \mathbf{f}_y(\widetilde{\mathbb{U}}) = \begin{bmatrix} 0 \\ \alpha_1\rho_1 v_1 \\ \alpha_1\rho_1 u_1 v_1 \\ \alpha_1\rho_1 v_1^2 + \alpha_1 p_1(\rho_1) \\ \alpha_2\rho_2 v_2 \\ \alpha_2\rho_2 u_2 v_2 \\ \alpha_2\rho_2 v_2^2 + \alpha_2 p_2(\rho_2) \end{bmatrix}, \tag{3.6.2}$$

and

$$\mathbf{c}_x(\widetilde{\mathbb{U}})\partial_x \widetilde{\mathbb{U}} = \begin{bmatrix} u_2 \\ 0 \\ -p_1(\rho_1) \\ 0 \\ 0 \\ +p_1(\rho_1) \\ 0 \end{bmatrix} \partial_x \alpha_1, \qquad \mathbf{c}_y(\widetilde{\mathbb{U}})\partial_y \widetilde{\mathbb{U}} = \begin{bmatrix} v_2 \\ 0 \\ 0 \\ -p_1(\rho_1) \\ 0 \\ 0 \\ +p_1(\rho_1) \end{bmatrix} \partial_y \alpha_1. \tag{3.6.3}$$

The physical space is now

$$\widetilde{\Omega} = \{\widetilde{\mathbb{U}} \in \mathbb{R}^7, 0 < \alpha_1 < 1 \text{ and } \alpha_i\rho_i > 0 \text{ for } i \in \{1,2\}\} \tag{3.6.4}$$

and the phasic energies become $E_i := \frac{|\mathbf{u}_i|^2}{2} + e_i(\tau_i)$ so that

$$(\eta, (\mathcal{F}_{\eta,x}, \mathcal{F}_{\eta,y}))(\widetilde{\mathbb{U}}) := \left(\sum_{i=1}^{2} \alpha_i\rho_i E_i, \left(\sum_{i=1}^{2} \alpha_i(\rho_i E_i + p_i(\rho_i))u_i, \sum_{i=1}^{2} \alpha_i(\rho_i E_i + p_i(\rho_i))v_i \right) \right)$$

defines a Lax entropy-entropy flux pair: η is a convex function of $\widetilde{\mathbb{U}}$ and entropy weak solutions of (3.6.1) satisfy

$$\partial_t \eta(\widetilde{\mathbb{U}}) + \partial_x \mathcal{F}_{\eta,x}(\widetilde{\mathbb{U}}) + \partial_y \mathcal{F}_{\eta,y}(\widetilde{\mathbb{U}}) \leq 0. \tag{3.6.5}$$

In section 3.4.2, the two-step relaxation method has been recast in a classical finite volume formulation by the use of two numerical fluxes by interface, $\mathbf{F}^-_{j+\frac{1}{2}}$ and $\mathbf{F}^+_{j+\frac{1}{2}}$. Moreover, one may easily check that the 2D Baer-Nunziato model is invariant by Galilean transformation. The classical but important consequence is that the (one-dimensional) relaxation Riemann solver can still be used to obtain a finite volume scheme on two-dimensional unstructured meshes.

3.6.1 The two-dimensionnal finite volume scheme

Let us first introduce several notations, beginning with the mesh. We follow [14] where an admissible *mesh* $\mathcal{M}$ is a family of disjoint polygonal subsets of $\mathbb{R}^2$, such that the union of the closure of its elements (the *cells*) is $\mathbb{R}^2$ and the common *interface* between two neighboring cells K and L of $\mathcal{M}$ is a line segment, denoted e_{KL}. With each interface e_{KL} is associated two unit vectors $\mathbf{n}_{KL}$ and $\mathbf{n}_{LK}$ which are orthogonal to e_{KL} and such that $\mathbf{n}_{KL}$ is oriented from K to L and $\mathbf{n}_{KL} = -\mathbf{n}_{LK}$. We also define the *neighborhood* $\mathcal{N}(K)$ of a cell K as the set of the neighboring cells to K, i.e. $\mathcal{N}(K) := \{L \in \mathcal{M} \setminus \{K\}, e_{KL} \neq \emptyset\}$.

Since we are dealing with cell-centered finite volume schemes, the initial datum u_0 is discretized in this way:

$$\forall K \in \mathcal{M}, \qquad \widetilde{\mathbb{U}}_K^0 = \frac{1}{|K|} \int_K \widetilde{\mathbb{U}}_0 \, dx \, dy \tag{3.6.6}$$

and the finite volume scheme may be written in the following form:

$$\forall K \in \mathcal{M}, \ \forall n \geq 0, \qquad \widetilde{\mathbb{U}}_K^{n+1} = \widetilde{\mathbb{U}}_K^n - \frac{\Delta t}{|K|} \sum_{L \in \mathcal{N}(K)} |e_{KL}| \, \mathbf{F}_{KL}^n \tag{3.6.7}$$

where the numerical fluxes $\mathbf{F}_{KL}^n$ depend on $\widetilde{\mathbb{U}}_K^n$, $\widetilde{\mathbb{U}}_L^n$ and $\mathbf{n}_{KL}$ and in the sequel, we also use the notation

$$\mathbf{F}_{KL}^n = \mathbf{F}(\widetilde{\mathbb{U}}_K^n, \widetilde{\mathbb{U}}_L^n; \mathbf{n}_{KL}).$$

Basically, $\mathbf{F}_{KL}^n$ for the cell K corresponds to $\mathbf{F}_{j+\frac{1}{2}}^-$ for the cell C_j while $\mathbf{F}_{LK}^n$ for the cell L corresponds to $-\mathbf{F}_{j+\frac{1}{2}}^+$ for the cell C_{j+1}. In the neighborhood of an interface e_{KL}, it may be considered that one has a local 1D Riemann problem for (3.6.1) in the direction of $\mathbf{n}_{KL}$. As a consequence, the solution is expected to be constant in the direction which is orthogonal to $\mathbf{n}_{KL}$ and the Riemann problem then takes the form after rotation in the (x, y) frame

$$\begin{cases} \partial_t \widetilde{\mathbb{U}} + \partial_x \mathbf{f}_x(\widetilde{\mathbb{U}}) + \mathbf{c}_x(\widetilde{\mathbb{U}}) \partial_x \widetilde{\mathbb{U}} = 0, \\ \widetilde{\mathbb{U}}(0, x, y) = \begin{cases} \mathcal{O}(\mathbf{n}_{KL}) \, \widetilde{\mathbb{U}}_K^n & \text{if } x < 0, \\ \mathcal{O}(\mathbf{n}_{KL}) \, \widetilde{\mathbb{U}}_L^n & \text{if } x > 0, \end{cases} \end{cases} \tag{3.6.8}$$

where $\mathcal{O} \colon \mathbb{R}^2 \to \mathbb{R}^{7\times 7}$ is defined by

$$\mathcal{O}(\mathbf{n}) = \begin{bmatrix} \mathbf{I}_2 & \mathbf{0}_2 & \begin{matrix} 0 \\ 0 \end{matrix} & \mathbf{0}_2 \\ \mathbf{0}_2 & \begin{matrix} n_x & n_y \\ -n_y & n_x \end{matrix} & \begin{matrix} 0 \\ 0 \end{matrix} & \mathbf{0}_2 \\ \begin{matrix} 0 & 0 \end{matrix} & \begin{matrix} 0 & 0 \end{matrix} & 1 & \begin{matrix} 0 & 0 \end{matrix} \\ \mathbf{0}_2 & \mathbf{0}_2 & \begin{matrix} 0 \\ 0 \end{matrix} & \begin{matrix} n_x & n_y \\ -n_y & n_x \end{matrix} \end{bmatrix}, \quad \forall \, \mathbf{n} = (n_x, n_y) \in \mathbb{S}^1, \tag{3.6.9}$$

where $\mathbf{I}_2$ and $\mathbf{0}_2$ respectively are the 2×2 identity matrix and the 2×2 null matrix. This Riemann problem is composed of two parts. The first part is exactly the one-dimensional Baer-Nunziato model, omitting the fourth and the seventh components of the system and of the data. The second

part, which is composed of the fourth and the seventh components, can be easily solved since they both are transport equations for the transverse velocities v_1 and v_2 with velocities u_1 and u_2, computed from the first part. As a consequence, the numerical flux associated with this Riemann problem can be obtained using the relaxation Riemann solver defined in section 3.3 for the first part, completed with a classical upwind scheme for the transverse velocities. To do so, let us introduce

$$\begin{array}{rccc} \Theta: & \mathbb{R}^7 & \longrightarrow & \mathbb{R}^5 \\ & (x_1,x_2,x_3,x_4,x_5,x_6,x_7) & \longmapsto & (x_1,x_2,x_3,x_5,x_6) \end{array} \tag{3.6.10}$$

and $\widetilde{\mathbb{V}}_j^n = \Theta\,\mathcal{O}(\mathbf{n}_{KL})\,\widetilde{\mathbb{U}}_j^n$, $j=K,L$. The local numerical flux (local in the sense that we still are in the frame of the interface) with respect to cell K can be written using the 1D numerical flux $\mathbf{F}^-$ defined in (3.4.19):

$$\begin{aligned}\widetilde{\mathbf{F}}\big(\mathcal{O}(\mathbf{n}_{KL})\,\widetilde{\mathbb{U}}_K^n, \mathcal{O}(\mathbf{n}_{KL})\,\widetilde{\mathbb{U}}_L^n\big) = \Big(&\mathbf{F}_1^-(\widetilde{\mathbb{V}}_K^n,\widetilde{\mathbb{V}}_L^n), \mathbf{F}_2^-(\widetilde{\mathbb{V}}_K^n,\widetilde{\mathbb{V}}_L^n), \mathbf{F}_3^-(\widetilde{\mathbb{V}}_K^n,\widetilde{\mathbb{V}}_L^n), \mathbf{F}_2^-(\widetilde{\mathbb{V}}_K^n,\widetilde{\mathbb{V}}_L^n)\ v_1^*, \\ &\mathbf{F}_4^-(\widetilde{\mathbb{V}}_K^n,\widetilde{\mathbb{V}}_L^n), \mathbf{F}_5^-(\widetilde{\mathbb{V}}_K^n,\widetilde{\mathbb{V}}_L^n), \mathbf{F}_4^-(\widetilde{\mathbb{V}}_K^n,\widetilde{\mathbb{V}}_L^n)\ v_2^*\Big)^T\end{aligned}$$

where the velocities v_i^*, $i=1,2$, are given by a classical upwinding according to the sign of u_i:

$$\begin{aligned} v_1^* &= \frac{\big[\mathcal{O}(\mathbf{n}_{KL})\,\widetilde{\mathbb{U}}_L^n\big]_4}{\big[\mathcal{O}(\mathbf{n}_{KL})\,\widetilde{\mathbb{U}}_L^n\big]_2} + \left(\frac{\big[\mathcal{O}(\mathbf{n}_{KL})\,\widetilde{\mathbb{U}}_K^n\big]_4}{\big[\mathcal{O}(\mathbf{n}_{KL})\,\widetilde{\mathbb{U}}_K^n\big]_2} - \frac{\big[\mathcal{O}(\mathbf{n}_{KL})\,\widetilde{\mathbb{U}}_L^n\big]_4}{\big[\mathcal{O}(\mathbf{n}_{KL})\,\widetilde{\mathbb{U}}_L^n\big]_2}\right)\mathbf{1}_{\{\mathbf{F}_2^-(\widetilde{\mathbb{V}}_K^n,\widetilde{\mathbb{V}}_L^n)>0\}}, \\ v_2^* &= \frac{\big[\mathcal{O}(\mathbf{n}_{KL})\,\widetilde{\mathbb{U}}_L^n\big]_7}{\big[\mathcal{O}(\mathbf{n}_{KL})\,\widetilde{\mathbb{U}}_L^n\big]_5} + \left(\frac{\big[\mathcal{O}(\mathbf{n}_{KL})\,\widetilde{\mathbb{U}}_K^n\big]_7}{\big[\mathcal{O}(\mathbf{n}_{KL})\,\widetilde{\mathbb{U}}_K^n\big]_5} - \frac{\big[\mathcal{O}(\mathbf{n}_{KL})\,\widetilde{\mathbb{U}}_L^n\big]_7}{\big[\mathcal{O}(\mathbf{n}_{KL})\,\widetilde{\mathbb{U}}_L^n\big]_5}\right)\mathbf{1}_{\{\mathbf{F}_4^-(\widetilde{\mathbb{V}}_K^n,\widetilde{\mathbb{V}}_L^n)>0\}}, \end{aligned}$$

and where the indices from 1 to 7 denote the component of the considered vector. It now remains to go back to the initial (x,y) frame. This simply amounts to take

$$\mathbf{F}\big(\widetilde{\mathbb{U}}_K^n,\widetilde{\mathbb{U}}_L^n;\mathbf{n}_{KL}\big) = \big[\mathcal{O}(\mathbf{n}_{KL})\big]^T\,\widetilde{\mathbf{F}}\big(\mathcal{O}(\mathbf{n}_{KL})\,\widetilde{\mathbb{U}}_K^n, \mathcal{O}(\mathbf{n}_{KL})\,\widetilde{\mathbb{U}}_L^n\big). \tag{3.6.11}$$

Since $\mathbf{F}^-$ is consistent with the 1D physical flux (Property 3.4.2), we have the consistency relation $\widetilde{\mathbf{F}}\big(\mathcal{O}(\mathbf{n})\,\widetilde{\mathbb{U}}, \mathcal{O}(\mathbf{n})\,\widetilde{\mathbb{U}}\big) = \mathbf{f}_x\big(\mathcal{O}(\mathbf{n})\widetilde{\mathbb{U}}\big)$. Hence, invoking the rotational invariance of system (3.6.1) which implies

$$\mathbf{f}_x\big(\mathcal{O}(\mathbf{n})\widetilde{\mathbb{U}}\big) = \mathcal{O}(\mathbf{n})\left[\mathbf{f}_x\big(\widetilde{\mathbb{U}}\big), \mathbf{f}_y\big(\widetilde{\mathbb{U}}\big)\right]\cdot\mathbf{n} := \mathcal{O}(\mathbf{n})\left(\mathbf{f}_x\big(\widetilde{\mathbb{U}}\big)n_x + \mathbf{f}_y\big(\widetilde{\mathbb{U}}\big)n_y\right),$$

for all $\widetilde{\mathbb{U}}\in\widetilde{\Omega}$, and all $\mathbf{n}=(n_x,n_y)$ in $\mathbb{S}^1$, we can see that the numerical flux $\mathbf{F}$ is consistent with the 2D physical flux, in the sense that

$$\forall\widetilde{\mathbb{U}}\in\widetilde{\Omega},\ \forall\mathbf{n}\in\mathbb{S}^1,\quad \mathbf{F}\big(\widetilde{\mathbb{U}},\widetilde{\mathbb{U}};\mathbf{n}\big) = \big[\mathcal{O}(\mathbf{n})\big]^T\,\mathbf{f}_x\big(\mathcal{O}(\mathbf{n})\widetilde{\mathbb{U}}\big) = \left[\mathbf{f}_x\big(\widetilde{\mathbb{U}}\big), \mathbf{f}_y\big(\widetilde{\mathbb{U}}\big)\right]\cdot\mathbf{n}. \tag{3.6.12}$$

On the other hand, using the classical geometric identity

$$\sum_{L\in\mathcal{N}(K)} |e_{KL}|\ \mathbf{n}_{KL} = 0$$

and the consistency property (3.6.12), one can rewrite the finite volume scheme (3.6.7) as

$$\widetilde{\mathbb{U}}_K^{n+1} = \sum_{L\in\mathcal{N}(K)} \frac{|e_{KL}|}{|\partial K|}\left[\widetilde{\mathbb{U}}_K^n - \frac{\Delta t|\partial K|}{|K|}\left(\mathbf{F}(\widetilde{\mathbb{U}}_K^n,\widetilde{\mathbb{U}}_L^n;\mathbf{n}_{KL}) - \mathbf{F}(\widetilde{\mathbb{U}}_K^n,\widetilde{\mathbb{U}}_K^n;\mathbf{n}_{KL})\right)\right] \tag{3.6.13}$$

$$= \sum_{L\in\mathcal{N}(K)} \frac{|e_{KL}|}{|\partial K|}\left[\mathcal{O}(\mathbf{n}_{KL})\right]^T \widetilde{\mathbb{U}}_{KL}^n \tag{3.6.14}$$

where

$$\widetilde{\mathbb{U}}_{KL}^n = \mathcal{O}(\mathbf{n}_{KL})\,\widetilde{\mathbb{U}}_K^n - \frac{\Delta t|\partial K|}{|K|}\left(\widetilde{\mathbf{F}}\big(\mathcal{O}(\mathbf{n}_{KL})\,\widetilde{\mathbb{U}}_K^n, \mathcal{O}(\mathbf{n}_{KL})\,\widetilde{\mathbb{U}}_L^n\big) - \mathbf{f}_x\big(\mathcal{O}(\mathbf{n}_{KL})\,\widetilde{\mathbb{U}}_K^n\big)\right). \tag{3.6.15}$$

The form (3.6.14)-(3.6.15) is the straightforward multidimensional extension of the one-dimensional half-cell decomposition of Harten, Lax and van Leer [18]. Moreover, formula (3.6.15) corresponds to the 1D Baer-Nunziato model completed by two transport equations for the transverse velocities, so that the positivity result (Property 3.4.1) and the theorem of non-linear stability (Theorem 3.4.5) can be extended to the 2D inequality (3.6.5) under a natural CFL condition, which is very similar to the 1D CFL condition (3.4.5):

$$\frac{\Delta t}{\min_{K\in\mathcal{M}}(|K|/|\partial K|)} \max_{K\in\mathcal{M},i\in\{1,2\}} \max_{L\in\mathcal{N}(K)} \max\big(\mathbf{u}_{i,K}^n\cdot\mathbf{n}_{KL} - a_i\tau_{i,K}^n, \mathbf{u}_{i,L}^n\cdot\mathbf{n}_{KL} + a_i\tau_{i,L}^n\big) < \frac{1}{2}. \tag{3.6.16}$$

3.6.2 Numerical approximation of the source terms

In order to obtain a realistic modelling of compressible two-phase flows, the model (3.6.1) has to be completed by source terms. The Baer-Nunziato model takes the form

$$\partial_t\widetilde{\mathbb{U}} + \partial_x\mathbf{f}_x(\widetilde{\mathbb{U}}) + \partial_y\mathbf{f}_y(\widetilde{\mathbb{U}}) + \mathbf{c}_x(\widetilde{\mathbb{U}})\partial_x\widetilde{\mathbb{U}} + \mathbf{c}_y(\widetilde{\mathbb{U}})\partial_y\widetilde{\mathbb{U}} = \mathbf{s}(\widetilde{\mathbb{U}}), \quad (x,y)\in\mathbb{R}^2, t>0, \tag{3.6.17}$$

and the vector-valued function $\mathbf{s}$ which represents the source terms writes

$$\mathbf{s}(\widetilde{\mathbb{U}}) = \begin{bmatrix} \dfrac{\alpha_1\alpha_2}{\tau_p}(p_1(\rho_1) - p_2(\rho_2)) \\ 0 \\ \dfrac{\alpha_1\rho_1\alpha_2\rho_2}{\tau_u}|\mathbf{u_2}-\mathbf{u_1}|(\mathbf{u_2}-\mathbf{u_1}) + (0,-\alpha_1\rho_1 g)^T \\ 0 \\ \dfrac{\alpha_1\rho_1\alpha_2\rho_2}{\tau_u}|\mathbf{u_2}-\mathbf{u_1}|(\mathbf{u_1}-\mathbf{u_2}) + (0,-\alpha_2\rho_2 g)^T \end{bmatrix} \tag{3.6.18}$$

where g is the gravity constant. The first component of $\mathbf{s}$ corresponds to the so-called pressure relaxation source term, which models the mechanical effects through the interfaces between the phases. The other source terms correspond to the drag force between the phases and to the gravity effects. The time scales τ_p and τ_u can be very small parameters, which leads to use implicit or semi-implicit schemes to approximate them. On the contrary, the gravity source term can be discretized by and explicit method.

Let us describe the different steps of the splitting method for the discretization of the source terms. For simplicity, we drop the space index and respectively note $\widetilde{\mathbb{U}}$ and $\widetilde{\mathbb{U}}^\star$ the approximated solutions at time t^n and at time $t^n+\Delta t$.

Discretization of the pressure relaxation source term

This source term only intervenes in the first equation. In order to be able to handle small τ_p, an implicit Euler method is used:

$$\alpha_1^\star = \alpha_1 + \frac{\Delta t}{\tau_p}\alpha_1^\star(1-\alpha_1^\star)\left(p_1\left(\frac{(\alpha_1\rho_1)^\star}{\alpha_1^\star}\right) - p_2\left(\frac{(\alpha_2\rho_2)^\star}{1-\alpha_1^\star}\right)\right), \tag{3.6.19}$$

$$(\alpha_i\rho_i)^\star = (\alpha_i\rho_i), \qquad i \in \{1,2\}, \tag{3.6.20}$$

$$(\alpha_i\rho_i\mathbf{u}_i)^\star = (\alpha_i\rho_i\mathbf{u}_i), \qquad i \in \{1,2\}. \tag{3.6.21}$$

Equation (3.6.19) is a nonlinear scalar equation to solve since, using (3.6.20), the partial masses $(\alpha_i\rho_i)^\star$ are known. Assuming (3.2.4), $\tau_p > 0$, $\Delta t > 0$, $(\alpha_i\rho_i)^\star > 0$ and $\alpha_1 \in (0,1)$, one may easily check that the derivative of the function

$$\mathcal{A}\colon \alpha \longmapsto 1-\alpha - \frac{\Delta t}{\tau_p}\alpha(1-\alpha)\left(p_1\left(\frac{(\alpha_1\rho_1)^\star}{\alpha}\right) - p_2\left(\frac{(\alpha_2\rho_2)^\star}{1-\alpha}\right)\right)$$

is positive and that $\lim_{\alpha\searrow 0}\mathcal{A} < 0$ and $\lim_{\alpha\nearrow 1}\mathcal{A} > 0$.

As a consequence, the numerical scheme (3.6.19)-(3.6.21) ensures $\widetilde{\mathbb{U}}^\star \in \widetilde{\Omega}$ for any $\Delta t > 0$ and $\tau_p > 0$, provided that $\widetilde{\mathbb{U}} \in \widetilde{\Omega}$. In practice, equation $\mathcal{A}(\alpha_1^\star) = 0$ is solved with the help of the bisection method.

Discretization of the drag force

In order to discretize the source term due to the drag force, we use the semi-implicit scheme

$$\alpha_1^\star = \alpha_1, \tag{3.6.22}$$

$$(\alpha_i\rho_i)^\star = (\alpha_i\rho_i), \qquad i \in \{1,2\}, \tag{3.6.23}$$

$$(\alpha_i\rho_i\mathbf{u}_i)^\star = \frac{(\alpha_i\rho_i)^\star}{(\alpha_1\rho_1)^\star + (\alpha_2\rho_2)^\star}\left(\mathbf{u}_m + (-1)^i(\alpha_{i'}\rho_{i'})^\star\mathbf{u}_r\right), \qquad i \in \{1,2\}, \tag{3.6.24}$$

where $i' = 3-i$ and

$$\mathbf{u}_m = \sum_{i\in\{1,2\}}\alpha_i\rho_i\mathbf{u}_i \quad \text{and} \quad \mathbf{u}_r = (\mathbf{u}_2-\mathbf{u}_1)\exp\left[\frac{\Delta t}{\tau_u}(\alpha_1\rho_1+\alpha_2\rho_2)|\mathbf{u}_2-\mathbf{u}_1|\right].$$

This numerical scheme obviously ensures $\widetilde{\mathbb{U}}^\star \in \widetilde{\Omega}$ as soon as $\widetilde{\mathbb{U}} \in \widetilde{\Omega}$.

Discretization of gravity source term

The last source can be discretized by an explicit Euler method, which actually turns out to be equivalent to the implicit Euler method:

$$\alpha_1^\star = \alpha_1, \tag{3.6.25}$$
$$(\alpha_i\rho_i)^\star = (\alpha_i\rho_i), \qquad i \in \{1,2\}, \tag{3.6.26}$$
$$(\alpha_i\rho_i u_i)^\star = (\alpha_i\rho_i u_i), \qquad i \in \{1,2\}, \tag{3.6.27}$$
$$(\alpha_i\rho_i v_i)^\star = (\alpha_i\rho_i v_i) - \Delta t(\alpha_i\rho_i)^\star g, \qquad i \in \{1,2\}. \tag{3.6.28}$$

Once again, we have $\widetilde{\mathbb{U}}^\star \in \widetilde{\Omega}$ after this step if $\widetilde{\mathbb{U}} \in \widetilde{\Omega}$.

3.6.3 Numerical illustration

Let us now present a numerical test which has been performed with the splitting algorithm described in the previous sections. In order to simply reproduce a liquid/vapor density ratio, the equations of state are

$$p_1(\rho_1) = \rho_1 \ \text{(liquid)}, \qquad p_2(\rho_2) = (\rho_2)^4 \ \text{(vapor)}.$$

The parameters in the source terms are $\tau_p = 10^{-9}$, $\tau_u = 10^{-4}$ and $g = 9.81$. The computational domain is the unit disk and the initial condition is

$$\widetilde{\mathbb{U}}(x,y,0) = \begin{cases} (0.99, 0.99\times 81, 0, 0, 0.01\times 3, 0, 0) & \text{if } x<0 \text{ and } y<0, \\ (0.01, 0.01\times 81, 0, 0, 0.99\times 3, 0, 0) & \text{otherwise,} \end{cases}$$

and wall boundary conditions are set on the whole frontier of the domain. These boundary conditions are approximated by the classical mirror technique. The mesh is composed by 6888 triangular cells and 3545 vertices (recall that a cell-centered discretization is used), see Figure 3.6.

We present in Figure 3.7 the void fraction α_1 and the partial mass $\alpha_1\rho_1$ at different times. The shapes of the approximate solution comply with the intuition: after the collapse of the initial step, the heaviest phase (phase 1) remains in the bottom of the cylinder and tends to an oscillating solution due to the inertia of the collapse. This solution is very similar to the Thacker's planar solution for shallow water equations [24], which is characterized by a plane surface with an exact periodic behavior. Here, one can observe that the surface becomes more and more planar and that the number of cells in the thickness of the interface decreases. Of course, for much larger time, one can check that the numerical solution is not fully periodic due to the numerical diffusion which introduces a small damping, letting the solution tend to a stationary solution with a horizontal surface. It is also clear that the numerical scheme is very robust, since the void fraction α_1 varies from about 10^{-2} to 1. Morevoer, due to the different relaxation source terms, the relative speed of the flow remains subsonic, so that our algorithm is applicable all along the simulation.

3.7 Extension to the full Baer-Nunziato model in 1D

In this section, we show how to extend the finite volume method devised in the barotropic setting to the framework with phasic energies. The proposed extension relies on two key ingredients. The

first one is the extension of the fixed point procedure based on two decoupled Euler like systems, respectively for phase 1 and phase 2, which was at the corner stone of the resolution of the Riemann problem for the Suliciu relaxation system in the barotropic setting. Such a strategy has been actually promoted to permit an easy extension to the full setting. The second ingredient is a duality principle in between entropy and energy that allows a trivial extension of Suliciu like approximations from barotropic pressure laws to the framework with energy. The combination of these two ingredients permits in turn a rather immediate extension, since most of the formulae derived in the barotropic setting are virtually kept unchanged.

The full Baer-Nunziato model writes :

$$\left\{\begin{array}{l} \partial_t\alpha_1 + V_I\partial_x\alpha_1 = 0, \\ \partial_t(\alpha_1\rho_1) + \partial_x(\alpha_1\rho_1 u_1) = 0, \\ \partial_t(\alpha_1\rho_1 u_1) + \partial_x(\alpha_1\rho_1 u_1^2 + \alpha_1 p_1(\tau_1, s_1)) - P_I\partial_x\alpha_1 = 0, \\ \partial_t(\alpha_1\rho_1 E_1) + \partial_x(\alpha_1\rho_1 E_1 u_1 + \alpha_1 p_1(\tau_1, s_1)u_1) - V_I P_I\partial_x\alpha_1 = 0, \\ \partial_t(\alpha_2\rho_2) + \partial_x(\alpha_2\rho_2 u_2) = 0, \\ \partial_t(\alpha_2\rho_2 u_2) + \partial_x(\alpha_2\rho_2 u_2^2 + \alpha_2 p_2(\tau_2, s_2)) - P_I\partial_x\alpha_2 = 0, \\ \partial_t(\alpha_2\rho_2 E_2) + \partial_x(\alpha_2\rho_2 E_2 u_2 + \alpha_2 p_2(\tau_2, s_2)u_2) - V_I P_I\partial_x\alpha_2 = 0. \end{array}\right. \tag{3.7.1}$$

Observe that the pressure closure laws $p_i(\tau_i, s_i)$ correspond to complete equations of state, namely functions of the specific volume $\tau_i = \rho_i^{-1}$ and the specific entropy s_i. Their evaluations follow from the definition of the phasic energies :

$$E_i := E_i(u_i, \tau_i, s_i) = \frac{u_i^2}{2} + e_i(\tau_i, s_i),\ i \in \{1, 2\}, \tag{3.7.2}$$

where the internal energy function $(\tau_i, s_i) \mapsto e_i(\tau_i, s_i)$ allows to define the corresponding pressure thanks to $\partial_{\tau_i} e_i(\tau_i, s_i) = -p_i(\tau_i, s_i)$. We assume the following classical thermodynamic assumptions :

$$\left\{\begin{array}{l} (\tau_i, s_i) \to e_i(\tau_i, s_i) \text{ is convex}, \\ T_i = -\partial_{s_i} e_i(\tau_i, s_i) > 0. \end{array}\right. \tag{3.7.3}$$

Thanks to these thermodynamic assumptions, the first order system (3.7.1) can be shown to be (weakly) hyperbolic. In addition, the specific entropy s_i can be understood as a function of (τ_i, e_i) with the property that the mapping $(\tau_i, e_i) \to s_i(\tau_i, e_i)$ is convex.

At last, the closure laws on the interfacial velocity and pressure laws are prescribed according to the original Baer-Nunziato proposal :

$$(V_I, P_I) = (u_2, p_1), \tag{3.7.4}$$

so that smooth solutions of (3.7.1) can be seen to obey the additional conservation laws

$$\left\{\begin{array}{l} \partial_t(\alpha_1\rho_1 s_1(\tau_1, e_1) + \partial_x(\alpha_1\rho_1 s_1(\tau_1, e_1)u_1) = 0, \\ \partial_t(\alpha_2\rho_2 s_2(\tau_2, e_2) + \partial_x(\alpha_2\rho_2 s_2(\tau_2, e_2)u_2) = 0. \end{array}\right. \tag{3.7.5}$$

The existence of these two additional conservation laws will play a central role in the numerical approximation of the solutions of the full Baer-Nunziato model. They permit an energy-entropy duality principle which we briefly revisit in the setting of the Euler equations. Recall that the fixed point procedure is precisely based on Euler like equations. Readers, familiar with this principle, can skip this section.

3.7.1 Entropy-Energy duality for the Euler equations

Let us consider the classical Euler equations

$$\left\{\begin{array}{l}\partial_t\rho+\partial_x(\rho u)=0,\\ \partial_t(\rho u)+\partial_x(\rho u^2+p(\tau,s))=0,\\ \partial_t(\rho E)+\partial_x(\rho E u+p(\tau,s)u)=0,\end{array}\right. \tag{3.7.6}$$

closed with a complete equation of state, namely a pressure law $p(\tau,s)$ function of the specific volume $\tau=\rho^{-1}$ and the specific entropy s. We again assume the following stability thermodynamic conditions :

$$\left\{\begin{array}{l}(\tau,s)\to e(\tau,s) \text{ is convex},\\ T=-\partial_s e(\tau,s)>0.\end{array}\right. \tag{3.7.7}$$

in symmetry with the assumptions stated in (3.7.3). Again, classical arguments allow to define the mapping $(\tau,e)\to s(\tau,e)$ with a convexity property inherited from the positiveness of the temperature T in (3.7.7). Smooth solutions of the hyperbolic system (3.7.6) are known to obey the additional conservation law

$$\partial_t(\rho s(\tau,e))+\partial_x(\rho s(\tau,e)u)=0, \tag{3.7.8}$$

while in view of the convexity property of the mapping $(\rho,\rho u,\rho E)\to\{\rho s\}(\rho,\rho u,\rho E)$, the relevant weak solutions are asked to obey the following differential entropy inequality

$$\partial_t\{\rho s\}(\rho,\rho u,\rho E)+\partial_x(\{\rho s\}(\rho,\rho u,\rho E)u)\leq 0, \tag{3.7.9}$$

for the sake of uniqueness.

In order to approximate at the discrete level the weak entropy solutions of (3.7.6)–(3.7.9), it is interesting to consider the following auxiliary system

$$\left\{\begin{array}{l}\partial_t\rho+\partial_x(\rho u)=0,\\ \partial_t(\rho u)+\partial_x(\rho u^2+p(\tau,s))=0,\\ \partial_t(\rho s)+\partial_x(\rho s u)=0,\end{array}\right. \tag{3.7.10}$$

where the entropy ρs now plays the role of an independent conservative variable. Since the mapping $(\rho,\rho u,\rho s)\to\{\rho E\}(\rho,\rho u,\rho s)$ is convex, it turns natural to select weak solutions of the hyperbolic model (3.7.10) according to the differential inequality

$$\partial_t\{\rho E\}(\rho,\rho u,\rho s)+\partial_x(\{\rho E\}(\rho,\rho u,\rho s)u+p(\tau,s)u)\leq 0. \tag{3.7.11}$$

The Riemann solutions of this auxiliary model are simpler to approximate than those of (3.7.6), because the specific entropy is now just advected by the flow

$$\partial_t s+u\partial_x s=0, \tag{3.7.12}$$

so that the derivation of the self-similar solutions is very close to the barotropic setting. But clearly, if smooth solutions of (3.7.6) and (3.7.10) are the same, their shock solutions are of course distinct. Hence, a numerical scheme for advancing in time discrete solutions of the original PDEs (3.7.6)–(3.7.9) based on solving a sequence of Riemann solutions for the auxiliary model (3.7.10)–(3.7.11) must be given a correction.

The required correction step turns in fact immediate because of the general thermodynamic assumptions made on the complete equation of state. Assuming an entropy satisfying Riemann solver for the auxiliary equations (3.7.10), we can in a first step update in conservation form the density ρ and momentum ρu, while preserving the entropy at the discrete level

$$(\rho s)_j^{n+1-} = (\rho s)_j^n - \frac{\Delta t}{\Delta x}\Big((\rho s u)_{j+\frac{1}{2}}^n - (\rho s u)_{j-\frac{1}{2}}^n\Big), \tag{3.7.13}$$

with standard notations. Since the scheme is entropy satisfying with respect to the energy inequality (3.7.11), one gets at the discrete level

$$(\rho E)_j^{n+1-} \leq (\rho E)_j^n - \frac{\Delta t}{\Delta x}\Big((\rho E u + p u)_{j+\frac{1}{2}}^n - (\rho E u + p u)_{j-\frac{1}{2}}^n\Big). \tag{3.7.14}$$

The correction step to perform readily follows : it simply consists in keeping unchanged the updates of the density and momentum,

$$\rho_j^{n+1} = \rho_j^{n+1-}, \quad (\rho u)_j^{n+1} = (\rho u)_j^{n+1-}, \tag{3.7.15}$$

while enforcing energy conservation in defining the energy update by

$$(\rho E)_j^{n+1} = (\rho E)_j^n - \frac{\Delta t}{\Delta x}\Big((\rho E u + p u)_{j+\frac{1}{2}}^n - (\rho E u + p u)_{j-\frac{1}{2}}^n\Big). \tag{3.7.16}$$

Obviously

$$(\rho E)_j^{n+1} \geq (\rho E)_j^{n+1-}. \tag{3.7.17}$$

Of course, the entropy $(\rho s)_j^{n+1} \equiv \{\rho s\}(\rho, \rho u, \rho E)_j^{n+1}$ has changed. But observe from the thermodynamic assumption (3.7.7) that $\partial_{\rho E}\{\rho s\}(\rho, \rho u, \rho E) = -1/T < 0$, we infer from (3.7.17) that

$$(\rho s)_j^{n+1} \leq (\rho s)_j^{n+1-}, \tag{3.7.18}$$

that is

$$(\rho s)_j^{n+1} \leq (\rho s)_j^n - \frac{\Delta t}{\Delta x}\Big((\rho s u)_{j+\frac{1}{2}}^n - (\rho s u)_{j-\frac{1}{2}}^n\Big). \tag{3.7.19}$$

We thus has defined a fully conservative and entropy satisfying scheme for the Euler equations while using the auxiliary model (3.7.10). This exchange step in between entropy and energy is referred as to a duality principle.

Application of this principle to the Suliciu relaxation procedure is straightforward. Indeed, the relaxation PDEs for approximating the solutions of the auxiliary model (3.7.10) read

$$\begin{cases} \partial_t \rho + \partial_x(\rho u) = 0, \\ \partial_t(\rho u) + \partial_x(\rho u^2 + \pi(\tau, \mathcal{T}, s)) = 0, \\ \partial_t(\rho \mathcal{T}) + \partial_x(\rho \mathcal{T} u) = \dfrac{1}{\epsilon}(\tau - \mathcal{T}), \\ \partial_t(\rho s) + \partial_x(\rho s u) = 0, \end{cases} \tag{3.7.20}$$

where the relaxation pressure law is the direct extension of the barotropic linearization

$$\pi(\tau, \mathcal{T}, s) = \mathcal{P}(\mathcal{T}, s) + a^2(\mathcal{T} - \tau). \tag{3.7.21}$$

For non-linear stability reasons, the frozen lagrangian sound speed a is asked to obey the following Whitham like condition

$$a^2 > -\partial_\tau \mathcal{P}(\mathcal{T}, s), \tag{3.7.22}$$

for all the (τ, s) under consideration. An central property of the homogeneous equations stems from the following additional balance law for ruling the time evolution of the relaxation pressure

$$\partial_t(\rho\pi(\tau, \mathcal{T}, s)) + \partial_x(\rho\pi(\tau, \mathcal{T}, s)u + a^2 u) = 0. \tag{3.7.23}$$

Under the sub-characteristic condition (3.7.22), the relaxation pressure can thus clearly serve as an admissible independent variable in place of $\mathcal{T}$ solving

$$\mathcal{P}(\mathcal{T}, s) + a^2\mathcal{T} = \pi + a^2\tau, \tag{3.7.24}$$

with root $\mathcal{T}$ such that $\partial_\tau \mathcal{P}(\mathcal{T}, s) + a^2 > 0$. This leads to the following equivalent form of the homogeneous part of (3.7.20) :

$$\left\{ \begin{array}{l} \partial_t \rho + \partial_x(\rho u) = 0, \\ \partial_t(\rho u) + \partial_x(\rho u^2 + \pi) = 0, \\ \partial_t(\rho\pi) + \partial_x(\rho\pi u + a^2 u) = 0, \\ \partial_t(\rho s) + \partial_x(\rho s u) = 0. \end{array} \right. \tag{3.7.25}$$

Obviously, the first three equations are decoupled from the entropy PDE. In other words, they can be solved independently

$$\left\{ \begin{array}{l} \partial_t \rho + \partial_x(\rho u) = 0, \\ \partial_t(\rho u) + \partial_x(\rho u^2 + \pi) = 0, \\ \partial_t(\rho\pi) + \partial_x(\rho\pi u + a^2 u) = 0. \end{array} \right. \tag{3.7.26}$$

These set of PDEs is nothing but the Suliciu relaxation model in the barotropic framework. Let be given two states $\mathbb{U}_L$ and $\mathbb{U}_R$ with π_L and π_R defined at equilibrium : $\pi_L = \mathcal{P}(\tau_L, s_L)$ and $\pi_R = \mathcal{P}(\tau_R, s_R)$. Then the self-similar solution of the corresponding Riemann problem for (3.7.26) is made of four states $\mathbb{U}_L$, $\mathbb{U}_{L*}$, $\mathbb{U}_{R*}$, $\mathbb{U}_R$ separated by three contats discontinuities, respectively propagating with speed $u_L - a\tau_L$, $u^* \equiv u_L^* = u_R^*$ and $u_R + a\tau_R$, with

$$\begin{array}{l} u^* = \frac{1}{2}(u_L + u_R) - \frac{1}{2a}(\pi_R - \pi_L), \quad \pi^* = \frac{1}{2}(\pi_L + \pi_R) - \frac{a}{2}(u_R - u_L), \\ \tau_{L*} = \tau_L + \frac{1}{a^2}(\pi_L - \pi^*), \quad \tau_{R*} = \tau_R + \frac{1}{a^2}(\pi_R - \pi^*). \end{array} \tag{3.7.27}$$

As expected, these formulae are identical to those derived in the barotropic setting, except of course that $\pi_L = \mathcal{P}(\tau_L, s_L) = \mathcal{P}_L$ and $\pi_R = \mathcal{P}(\tau_R, s_R) = \mathcal{P}_R$. In other words and within the Suliciu framework, the entropy (or say the energy) is entirely wrapped **in the initial data for** π !

To end up the derivation of the approximate solver, one needs to define the update of the total energy. In that aim, we observe that the solutions of the relaxation model (3.7.20) obey the additional energy like equation in the usual weak sense (all the fields are indeed LD)

$$\partial_t\{\rho\mathcal{E}\} + \partial_x\{\rho\mathcal{E}u + \pi u\} = 0, \tag{3.7.28}$$

with

$$\rho\mathcal{E} = \rho\Big(\frac{u^2}{2} + e(\mathcal{T}, s) + \frac{1}{2a^2}(\pi^2(\tau, \mathcal{T}, s) - p^2(\mathcal{T}, s)\Big). \tag{3.7.29}$$

Under the Whitham condition (3.7.22), one can infer from (3.7.28) the following discrete energy inequality

$$(\rho E)_j^{n+1-} \leq (\rho E)_j^n - \frac{\Delta t}{\Delta x}\Big((\rho\mathcal{E}u+\pi u)_{j+\frac{1}{2}}^n - (\rho\mathcal{E}u+\pi u)_{j-\frac{1}{2}}^n\Big). \tag{3.7.30}$$

For the details, we refer for instance the reader to the monograph by Bouchut. Restoring energy conservation at the discrete level yields the final update of the total energy

$$(\rho E)_j^{n+1} = (\rho E)_j^n - \frac{\Delta t}{\Delta x}\Big((\rho\mathcal{E}u+\pi u)_{j+\frac{1}{2}}^n - (\rho\mathcal{E}u+\pi u)_{j-\frac{1}{2}}^n\Big). \tag{3.7.31}$$

To conclude the method, we have to define the relaxation energy associated with the two intermediate states $\mathbb{U}_L^*$ and $\mathbb{U}_R^*$. The required values readily follow from the jump relations associated to the energy conservation law (3.7.28) :

$$\mathcal{E}_{L*} = E_L - \frac{1}{a}(\pi^* u^* - \pi_L u_L), \quad \mathcal{E}_{R*} = E_R + \frac{1}{a}(\pi^* u^* - \pi_R u_R). \tag{3.7.32}$$

This concludes the presentation of the method.

3.7.2 Extension to the Baer-Nunziato equations

Equipped with the additional laws (3.7.5) for the entropies $\alpha_i\rho_i s_i$, and motivated by the previous section, we introduce the following auxiliary system

$$\left\{\begin{array}{l}
\partial_t\alpha_1 + u_2\partial_x\alpha_1 = 0,\\
\partial_t(\alpha_1\rho_1) + \partial_x(\alpha_1\rho_1 u_1) = 0,\\
\partial_t(\alpha_1\rho_1 u_1) + \partial_x(\alpha_1\rho_1 u_1^2 + \alpha_1 p_1(\tau_1,s_1)) - p_1(\tau_1,s_1)\partial_x\alpha_1 = 0,\\
\partial_t(\alpha_1\rho_1 s_1) + \partial_x(\alpha_1\rho_1 s_1 u_1) = 0,\\
\partial_t(\alpha_2\rho_2) + \partial_x(\alpha_2\rho_2 u_2) = 0,\\
\partial_t(\alpha_2\rho_2 u_2) + \partial_x(\alpha_2\rho_2 u_2^2 + \alpha_2 p_2(\tau_2,s_2)) - p_1(\tau_2,s_2)\partial_x\alpha_2 = 0,\\
\partial_t(\alpha_2\rho_2 s_2) + \partial_x(\alpha_2\rho_2 s_2 u_2) = 0,
\end{array}\right. \tag{3.7.33}$$

where $\alpha_i\rho_i s_i$ play the role of independent conservative variables. Again smooth solutions of (3.7.1) also solve (3.7.33) in a classical sense but weak solutions of (3.7.1) and (3.7.33) do differ. Advancing in time discrete approximate solutions for (3.7.1) can be nevertheless performed when solving in each time slab (t^n, t^{n+1}) a sequence of Riemann problems for the auxiliary model (3.7.33). Consistency with the exact PDEs (3.7.1) is then recovered thanks to a duality principle in between energy and entropy, entirely similar to the one described in the previous section. We propose to approximate the Riemann problem for (3.7.33) by the self similar solution of a Suliciu relaxation model :

$$\partial_t\mathbb{W}^\varepsilon + \partial_x\mathbf{g}(\mathbb{W}^\varepsilon) + \mathbf{d}(\mathbb{W}^\varepsilon)\partial_x\mathbb{W}^\varepsilon = \frac{1}{\varepsilon}\mathcal{R}(\mathbb{W}^\varepsilon), \tag{3.7.34}$$

with state vector $\mathbb{W} = (\alpha_1, \alpha_1\rho_1, \alpha_1\rho_1 u_1, \alpha_2\rho_2, \alpha_2\rho_2 u_2, \alpha_1\rho_1\mathcal{T}_1, \alpha_2\rho_2\mathcal{T}_2, \alpha_1\rho_1 s_1, \alpha_2\rho_2 s_2)^T$ and

$$\mathbf{g}(\mathbb{W}) = \begin{bmatrix} 0 \\ \alpha_1\rho_1 u_1 \\ \alpha_1\rho_1 u_1^2 + \alpha_1\pi_1(\tau_1, \mathcal{T}_1, s_1) \\ \alpha_2\rho_2 u_2 \\ \alpha_2\rho_2 u_2^2 + \alpha_2\pi_2(\tau_2, \mathcal{T}_2, s_2) \\ \alpha_1\rho_1\mathcal{T}_1 u_1 \\ \alpha_2\rho_2\mathcal{T}_2 u_2 \\ \alpha_1\rho_1 s_1 u_1 \\ \alpha_2\rho_2 s_2 u_2 \end{bmatrix}, \quad \mathbf{d}(\mathbb{W})\partial_x\mathbb{W} = \begin{bmatrix} u_2\partial_x\alpha_1 \\ 0 \\ -\pi_1(\tau_1, \mathcal{T}_1, s_1)\partial_x\alpha_1 \\ 0 \\ -\pi_1(\tau_1, \mathcal{T}_1, s_1)\partial_x\alpha_2 \\ 0 \\ 0 \\ 0 \\ 0 \end{bmatrix}, \quad \mathcal{R}(\mathbb{W}) = \begin{bmatrix} 0 \\ 0 \\ 0 \\ 0 \\ 0 \\ \alpha_1\rho_1(\tau_1 - \mathcal{T}_1) \\ \alpha_2\rho_2(\tau_2 - \mathcal{T}_2) \\ 0 \\ 0 \end{bmatrix}. \tag{3.7.35}$$

For each phase i in $\{1, 2\}$ the (partially) linearized pressure $\pi_i(\tau_i, \mathcal{T}_i, s_i)$ are defined by

$$\pi_i(\tau_i, \mathcal{T}_i, s_i) = \mathcal{P}_i(\mathcal{T}_i, s_i) + a_i^2(\mathcal{T}_i - \tau_i). \tag{3.7.36}$$

Formally, the exact pressure laws $\mathcal{P}_i(\mathcal{T}_i, s_i)$ are recovered in the limit $\varepsilon \to 0^+$. Again, the frozen lagrangian sound speeds a_i in (3.7.36) have to be taken large enough to prevent the relaxation approximation from instabilities in the regime of a vanishing relaxation parameter (see the Whitham conditions in the next Lemma).

Let us now state simple but central properties of the homogeneous (weakly) hyperbolic relaxation system

$$\partial_t\mathbb{W} + \partial_x\mathbf{g}(\mathbb{W}) + \mathbf{d}(\mathbb{W})\partial_x\mathbb{W} = 0. \tag{3.7.37}$$

Such properties are directly inherited from the fact that both the relaxation volume fraction $\mathcal{T}_i$ and the specific entropy s_i are just advected by the flow velocity u_i

$$\begin{cases} \partial_t\mathcal{T}_i + u_i\partial_x\mathcal{T}_i = 0, \\ \partial_t s_i + u_i\partial_x s_i = 0, \end{cases} \tag{3.7.38}$$

so that any given nonlinear combination of these, say $\varphi(\mathcal{T}_i, s_i)$, is also advected by u_i. It is important to observe that for self-similar initial data, the Riemann solution, as soon as it exists, necessarily obeys

$$\mathcal{T}_i(\xi) = \begin{cases} (\mathcal{T}_i)_L, & \xi < u_i^* \\ (\mathcal{T}_i)_R, & u_i^* < \xi, \end{cases} \qquad s_i(\xi) = \begin{cases} (s_i)_L, & \xi < u_i^* \\ (s_i)_R, & u_i^* < \xi, \end{cases} \qquad \varphi(\mathcal{T}_i, s_i)(\xi) = \begin{cases} \varphi_L, & \xi < u_i^* \\ \varphi_R, & u_i^* < \xi. \end{cases} \tag{3.7.39}$$

Lemma 3.7.1. *Solutions of (3.7.37) obey the following additional laws in a usual weak sense*

$$\begin{cases} \partial_t(\alpha_1\rho_1\mathcal{E}_1) + \partial_x(\alpha_1\rho_1\mathcal{E}_1 u_1 + \alpha_1\pi_1(\tau_1, \mathcal{T}_1, s_1)u_1) - u_2\pi_1(\tau_1, \mathcal{T}_1, s_1)\partial_x\alpha_1 = 0, \\ \partial_t(\alpha_2\rho_2\mathcal{E}_2) + \partial_x(\alpha_2\rho_2\mathcal{E}_2 u_2 + \alpha_2\pi_2(\tau_2, \mathcal{T}_2, s_2)u_2) - u_2\pi_1(\tau_1, \mathcal{T}_2, s_1)\partial_x\alpha_2 = 0, \end{cases} \tag{3.7.40}$$

where the relaxation phasic energies read

$$\mathcal{E}_i := \mathcal{E}_i(u_i, \tau_i, \mathcal{T}_i, s_i) = \frac{u_i^2}{2} + e_i(\mathcal{T}_i, s_i) + \frac{\pi_i^2(\tau_i, \mathcal{T}_i, s_i) - p_i^2(\mathcal{T}_i, s_i)}{2a_i^2}, \qquad i \in \{1, 2\}. \tag{3.7.41}$$

Under the Whitham like conditions

$$a_i^2 > -\partial_{\tau_i} p_i(\mathcal{T}_i, s_i), \quad i \in \{1, 2\}, \tag{3.7.42}$$

to be met for all the $(\mathcal{T}_i, s_i)$ under consideration, the following Gibbs principles are satisfied

$$\tau_i = Argmin\ \{\mathcal{E}_i(\tau_i, u_i, \mathcal{T}_i, s_i),\ \ with\ (\tau_i, u_i, s_i)\ kept\ fixed\}, \quad E_i(\tau_i, u_i, s_i) = \mathcal{E}_i(\tau_i, u_i, \tau_i, s_i). \tag{3.7.43}$$

In addition, the following balance equations for governing the relaxation pressure laws $\pi_i(\tau_i, \mathcal{T}_i, s_i)$ hold

$$\partial_t \alpha_i \rho_i \pi_i(\tau_i, \mathcal{T}_i, s_i) + \partial_x(\alpha_i \rho_i \pi_i(\tau_i, \mathcal{T}_i, s_i) u_i + a_i^2 \alpha_i u_i) - a_i^2 u_2 \partial_x \alpha_i = 0. \tag{3.7.44}$$

Besides standard algebraic manipulations, this statement basically holds because of the advection equations (3.7.38). Details are left to the reader. From (3.7.39), let us stress that the laws under consideration evolve in the Riemann solution, virtually the same way as within the barotropic setting : entropies s_i are systematically involved in non-linear functions already depending on the variable $\mathcal{T}_i$: namely $\mathcal{P}_i(\mathcal{T}_i, s_i), e_i(\mathcal{T}_i, s_i)$. Such functions are solely evaluated on the left and right states in the self-similar initial data and hence always contribute to any given jump conditions in terms of $(\mathcal{P}_i, e_i)_L$ or $(\mathcal{P}_i, e_i)_R$.

In the regime of vanishing phases and following the strategy devised in the previous chapter, we intend to dissipate the mixture energy when needed :

$$\begin{array}{ll} \partial_t(\alpha_1\rho_1\mathcal{E}_1 + \alpha_2\rho_2\mathcal{E}_2) & +\partial_x(\alpha_1\rho_1\mathcal{E}_1 u_1 + \alpha_1\pi_1(\tau_1, \mathcal{T}_1, s_1)u_1) \\ & +\partial_x(\alpha_2\rho_2\mathcal{E}_2 u_2 + \alpha_2\pi_2(\tau_2, \mathcal{T}_2, s_2)u_2) \leq 0. \end{array} \tag{3.7.45}$$

Let us express the associated jump relation at the void fraction wave

$$[\alpha_1\rho_1\bar{\mathcal{E}}_1(u_1 - u_2^*) + \alpha_1\pi_1(u_1 - u_2^*)]_{\xi = u_2^*} \leq 0, \tag{3.7.46}$$

where

$$\bar{\mathcal{E}}_1 := \frac{(u_1 - u_2^*)^2}{2} + e_1(\mathcal{T}_1, s_1) + \frac{\pi_1^2(\tau_1, \mathcal{T}_1, s_1) - p_1^2(\mathcal{T}_1, s_1)}{2a_1^2}. \tag{3.7.47}$$

Let us again observe, from (3.7.39), that the jump relation (3.7.46) exactly coincides with the one derived within the barotropic setting.

We will prove that the duality principle in between energy and entropy will allow to restore at the discrete level the expected balance laws that govern both energies $\alpha_i\rho_i E_i$ (namely finite volume updates consitent with (3.7.40)) while dissipating the mixture entropy

$$\partial_t(\alpha_1\rho_1 s_1 + \alpha_2\rho_2 s_2) + \partial_x(\alpha_1\rho_1 s_1 u_1 + \alpha_2\rho_2 s_2 u_2) \leq 0, \tag{3.7.48}$$

in a convenient discrete sense.

The strategy for solving the Riemann problem for the homogeneous relaxation system (3.7.37) relies on a straightforward extension of the fixed point procedure we have devised within the barotropic framework. This procedure basically aims at defining an interfacial velocity u_2^* and an interfacial pressure π_1^* at the void fraction wave, involving mixture energy dissipation when needed. The extension to the energy setting is analyzed in the next section with the following first important result.

Proposition 3.7.2. *The mathematical formulae for defining the phasic quantities τ_i, u_i, π_i and the void fraction α_i within the Riemann fan read exactly the same as in the barotropic framework, provided that the relaxation pressures in the initial data are evaluated at equilibrium, namely*

$$\pi_i^0(x) = \left\{ \begin{array}{ll} (\mathcal{P}_i)_L, & x < 0, \\ (\mathcal{P}_i)_R, & x > 0. \end{array} \right. \tag{3.7.49}$$

The next statement allows to easily derive the values of the phasic energies within the Riemann fan, provided that some entropy-energy duality principle is used in case the mixture energy is dissipated at the void fraction wave. This is the matter of the last section.

Proposition 3.7.3. *Values of the phasic energies $\mathcal{E}_i$ within the Riemann fan are recovered when solving at each contact discontinuity, the jump relations associated with*

$$\partial_t(\alpha_i\rho_i\mathcal{E}_i) + \partial_x(\alpha_i\rho_i\mathcal{E}_i u_i + \alpha_i\pi_i u_i) = u_2^*\pi_1^*\Delta\alpha_i\delta_{x-u_2^*t}. \tag{3.7.50}$$

Here, the interfacial velocity u_2^* and the interfacial pressure π_1^* are defined from the fixed point procedure at convergence, and possibly corrected thanks to mixture energy dissipation.

Choosing the CFL number less than $1/2$, the updates of the phasic energies then read

$$\begin{array}{rl} (\alpha_i\rho_i E_i)_j^{n+1} & = (\alpha_i\rho_i E_i)_j^n - \frac{\Delta t}{\Delta x}\Delta(\alpha_i\rho_i\mathcal{E}_i u_i + \pi_i u_i)_{j+\frac{1}{2}}^n \\ & + \frac{\Delta t}{\Delta x}(\pi_1^*\max(u_2^*,0))_{j-\frac{1}{2}}^n\Delta(\alpha_i)_{j-\frac{1}{2}}^n + \frac{\Delta t}{\Delta x}(\pi_1^*\min(u_2^*,0))_{j+\frac{1}{2}}^n\Delta(\alpha_i)_{j+\frac{1}{2}}^n. \end{array} \tag{3.7.51}$$

Provided that the frozen lagrangian sound speeds a_i are chosen large enough, the positiveness of the phasic internal energies e_i is preserved and we have in addition the following discrete entropy inequalities per phase :

$$(\alpha_i\rho_i s_i)_j^{n+1} - (\alpha_i\rho_i s_i)_j^n + \frac{\Delta t}{\Delta x}\Delta(\alpha_i\rho_i s_i u_i)_{j+\frac{1}{2}}^n \leq 0, \quad i \in \{1,2\}, \tag{3.7.52}$$

3.7.3 The fixed point procedure

Let us describe in details the resolution of the Riemann problem for the homogeneous (weakly) hyperbolic relaxation system

$$\begin{array}{l} \partial_t\mathbb{W} + \partial_x\mathbf{g}(\mathbb{W}) + \mathbf{d}(\mathbb{W})\partial_x\mathbb{W} = 0, \\ \mathbb{W}(x, t=0) = \left\{ \begin{array}{lll} \mathbb{W}_L & \text{if} & x < 0, \\ \mathbb{W}_R & \text{if} & x > 0, \end{array} \right. \end{array} \tag{3.7.53}$$

for given states $(\mathbb{W}_L, \mathbb{W}_R)$ prescribed so that the self-similar solution exhibits subsonic wave ordering $u_1 - a_1\tau_1 < u_2 < u_1 + a_1\tau_1$. We adopt a direct extension of the strategy described in the barotropic cases, namely a fixed point procedure in between two Euler like models for defining the velocity u_2^* and the pressure π_1^* at the void fraction wave. The proposed extension thus reads as follows.

- Solve the system for phase 2 with corresponding self-similar data

$$\begin{cases} \partial_t \alpha_2 + u_2 \partial_x \alpha_2 = 0, \\ \partial_t(\alpha_2\rho_2) + \partial_x(\alpha_2\rho_2 u_2) = 0, \\ \partial_t(\alpha_2\rho_2 u_2) + \partial_x(\alpha_2\rho_2 u_2^2 + \alpha_2\pi_2(\tau_2, \mathcal{T}_2, s_2)) - \pi_1^* \partial_x \alpha_2 = 0, , \\ \partial_t(\alpha_2\rho_2 \mathcal{T}_2) + \partial_x(\alpha_2\rho_2 \mathcal{T}_2 u_2) = 0, \\ \partial_t(\alpha_2\rho_2 s_2) + \partial_x(\alpha_2\rho_2 s_2 u_2) = 0, \end{cases} \tag{3.7.54}$$

  for a prescribed value of the interfacial pressure π_1^* and define the interfacial velocity u_2^*. Recall that u_2^* is nothing but the velocity of the void fraction wave in the Riemann solution.

- Solve for this velocity u_2^*, the system for phase 1

$$\begin{cases} \partial_t \alpha_1 + u_2^* \partial_x \alpha_1 = 0, \\ \partial_t(\alpha_1\rho_1) + \partial_x(\alpha_1\rho_1 u_1) = 0, \\ \partial_t(\alpha_1\rho_1 u_1) + \partial_x(\alpha_1\rho_1 u_1^2 + \alpha_1\pi_1(\tau_1, \mathcal{T}_1, s_1)) - \pi_1(\tau_1, \mathcal{T}_1, s_1)\partial_x \alpha_1 = 0, \\ \partial_t(\alpha_1\rho_1 \mathcal{T}_1) + \partial_x(\alpha_1\rho_1 \mathcal{T}_1 u_1) = 0, \\ \partial_t(\alpha_1\rho_1 s_1) + \partial_x(\alpha_1\rho_1 s_1 u_1) = 0, \end{cases} \tag{3.7.55}$$

  so as to define a new value of the interfacial pressure π_1^*. The linear degeneracy of all the fields make the non-conservative product $\pi_1 \partial_x \alpha_1$ well defined despite that π is discontinuous across the void fraction wave. By definition, this product reads $\pi_1^* \Delta\alpha_1 \delta_{x-u_2^* t}$, with

$$\pi_1^* \Delta\alpha_1 = -u_2^*[\alpha_1\rho_1 u_1] + [\alpha_1\rho_1 u_1^2 + \alpha_1\pi_1], \tag{3.7.56}$$

  where the right-side is known since the Riemann solution is explicitely known. This in turn defines π_1^*.

- Iterate till convergence.

To further proceed, we observe that under the Whitham conditions (3.7.42), each relaxation pressure π can serve as new variables in place of the relaxation specific volume $\mathcal{T}_i$:

$$\mathcal{P}_i(\mathcal{T}_i, s_i) + a_i^2 \mathcal{T}_i = \pi_i + a_i^2 \tau_i. \tag{3.7.57}$$

Using the proposed change of variable, we can recast the fixed point procedure as follows :

- For a prescribed π_1^*, solve for u_2^*

$$\begin{cases} \partial_t \alpha_2 + u_2 \partial_x \alpha_2 = 0, \\ \partial_t(\alpha_2\rho_2) + \partial_x(\alpha_2\rho_2 u_2) = 0, \\ \partial_t(\alpha_2\rho_2 u_2) + \partial_x(\alpha_2\rho_2 u_2^2 + \alpha_2\pi_2) - \pi_1^* \partial_x \alpha_2 = 0, \\ \partial_t(\alpha_2\rho_2 \pi_2) + \partial_x(\alpha_2\rho_2 \pi_2 u_2 + \alpha_2 a_2^2 u_2) - a_2^2 u_2 \partial_x \alpha_2 = 0, \\ \partial_t(\alpha_2\rho_2 s_2) + \partial_x(\alpha_2\rho_2 s_2 u_2) = 0. \end{cases} \tag{3.7.58}$$

- For a prescribed u_2^*, solve for π_1^*

$$\begin{cases} \partial_t \alpha_1 + u_2^* \partial_x \alpha_1 = 0, \\ \partial_t(\alpha_1\rho_1) + \partial_x(\alpha_1\rho_1 u_1) = 0, \\ \partial_t(\alpha_1\rho_1 u_1) + \partial_x(\alpha_1\rho_1 u_1^2 + \alpha_1\pi_1) - \pi_1 \partial_x \alpha_1 = 0, \\ \partial_t(\alpha_1\rho_1 \pi_1) + \partial_x(\alpha_1\rho_1 \pi_1 u_1 + a_1^2 \alpha_1 u_1) - a_1^2 u_2^* \partial_x \alpha_1 = 0, , \\ \partial_t(\alpha_1\rho_1 s_1) + \partial_x(\alpha_1\rho_1 s_1 u_1) = 0. \end{cases} \tag{3.7.59}$$

- Iterate till convergence.

Clearly in (3.7.58) and (3.7.59), the corresponding specific entropy s_i is absent from the first four PDEs. Some coupling nevertheless exists *via* the Whitham condition $a_i^2 > -\partial_{\mathcal{T}_i}\mathcal{P}_i(\mathcal{T}_i, s_i)$ but as soon as a_i is prescribed, the advection equation for s_i is entirely decoupled from the PDEs governing the phasic quantities τ_i, u_i, π_i and the void fraction α_i. Put in other words and focusing for instance on the system (3.7.59), one can first solve

$$\left\{\begin{array}{l} \partial_t\alpha_1 + u_2^*\partial_x\alpha_1 = 0, \\ \partial_t(\alpha_1\rho_1) + \partial_x(\alpha_1\rho_1 u_1) = 0, \\ \partial_t(\alpha_1\rho_1 u_1) + \partial_x(\alpha_1\rho_1 u_1^2 + \alpha_1\pi_1) - \pi_1\partial_x\alpha_1 = 0, \\ \partial_t(\alpha_1\rho_1\pi_1) + \partial_x(\alpha_1\rho_1\pi_1 u_1 + a_1^2\alpha_1 u_1) - a_1^2 u_2^*\partial_x\alpha_1 = 0, \end{array}\right. \tag{3.7.60}$$

and then the advection equation for s_1

$$\partial_t s_1 + u_1\partial_x s_1 = 0. \tag{3.7.61}$$

Observe that the PDEs (3.7.60) have **exactly the same** PDE structure as those studied within the barotropic framework : indeed each relaxation pressure $\pi_i(\tau_i, \mathcal{T}_i) = \mathcal{P}_i(\mathcal{T}_i) + a_i^2(\mathcal{T}_i - \tau_i)$ can also serve there as an independent variable in place of $\mathcal{T}_i$ to give rise to the equivalent formulation (3.7.60). The only difference stays in the initial data for the respective Cauchy problems : $\pi_0(x) = \mathcal{P}_i((\tau_i)_0(x))$ versus $\pi_0(x) = \mathcal{P}_i((\tau_i)_0(x), (s_i)_0(x))$ and the correct prescription of the frozen Lagrangian sound speeds a_i ! This exactly means that the formulae for defining the phasic quantities ρ_i, u_i, π_i and the void fraction α_1 in the Riemann fan are **exactly the same** in the barotropic setting and in the framework with energies. Thus solving the respective Cauchy problems yields identical mathematical expressions for the phasic quantities τ_i, u_i, π_i and the void fraction α_i (of course, up to the precise definition of the quantities evaluated on the initial data), that can be again conveniently parametrized by the same relative Mach number $\mathcal{M} \equiv (u_1^- - u_2^*)/(a_1\tau_1^-) \to \tau_i(\mathcal{M}), u_i(\mathcal{M}), \pi_i(\mathcal{M})$ (recall that its precise value dictates the jump of the mixture energy across the void fraction wave).

Recall that solving the fixed point problem (3.7.54)–(3.7.55) relies on an iterative real parameter ω given by

$$\omega = \frac{1 - \mathcal{M}_L^*}{1 + \mathcal{M}_L^*}, \quad \mathcal{M}_L^* = \frac{u_1 - u_2^*}{a_1\tau_{1,L}}. \tag{3.7.62}$$

It again amounts to solve a scalar non-linear equation in ω which has the same form as in the barotropic setting. As a consequence, there exists a unique solution to the fixed point problem (3.7.54)–(3.7.55) under the assumptions stated in Chapter 2. Keeping unchanged the notations introduced in this chapter, the main output of the fixed point procedure is a relative Mach number $\mathcal{M}_0(\nu, \omega)$. Due to galilean invariance, it again suffices to restrict attention to $\mathcal{M}_0(\nu, \omega) > 0$. Recall that promoting this value in the formulae defining the Riemann solution, the mixture energy is by construction preserved at the void fraction wave :

$$\begin{array}{ll} \partial_t(\alpha_1\rho_1\mathcal{E}_1 + \alpha_2\rho_2\mathcal{E}_2) & +\partial_x(\alpha_1\rho_1\mathcal{E}_1 u_1 + \alpha_1\pi_1(\tau_1, \mathcal{T}_1, s_1)u_1) \\ & +\partial_x(\alpha_2\rho_2\mathcal{E}_2 u_2 + \alpha_2\pi_2(\tau_2, \mathcal{T}_2, s_2)u_2) = 0. \end{array} \tag{3.7.63}$$

In full symmetry with Chapter 2, positiveness of some specific volumes τ_i (namely $\tau_{1,R*}$) may be violated if we persist to preserve the mixture energy conservation law across the void fraction wave, in the case of a very large ratio of void fraction ν in the Riemann data.

As already claimed, we propose the same cure : namely dissipate the mixture energy to restore positivity

$$\begin{array}{ll} \partial_t(\alpha_1\rho_1\mathcal{E}_1+\alpha_2\rho_2\mathcal{E}_2) & +\partial_x(\alpha_1\rho_1\mathcal{E}_1u_1+\alpha_1\pi_1(\tau_1,\mathcal{T}_1,s_1)u_1) \\ & +\partial_x(\alpha_2\rho_2\mathcal{E}_2u_2+\alpha_2\pi_2(\tau_2,\mathcal{T}_2,s_2)u_2)\leq 0. \end{array} \tag{3.7.64}$$

The corresponding kinetic relation again amounts to enforce a lower bound $\mu\tau_{1,R}^\sharp$ on some specific volume in the Riemann fan. In order to implement this energy dissipation rule, we adopt exactly the same strategy : namely preserve the phasic energy for phase 2 and dissipate energy across the void fraction wave for phase 1 once the fixed point procedure has achieved convergence. This again amounts to prescribe in place of $\mathcal{M}_0(\nu,\omega)$, a relative Mach number $\mathcal{M}_\mu(\nu,\omega)$ conveniently chosen in the interval $(0,\mathcal{M}_0(\nu,\omega)[$. Small enough values of $\mathcal{M}$ again systematically guarantee that the Riemann solution achieves subsonic relative Mach number within the Riemann fan.

Let us now address how to handle the duality principle in between energy and entropy so as to restore consistency with the exact Baer-Nunziato equations. We propose to proceed into two steps, first assuming that $\mathcal{M}_0(\nu,\omega)$ gives rise to a solution with subsonic relative velocities and then addressing the case of energy dissipation at the void fraction wave in order to achieve the lower bound $\mu\tau_{1,R}^\sharp$.

First case : $\mathcal{M}_0(\nu,\omega)$ is relevant

Let us first observe that self-similar solutions of (3.7.54) obey the following energy like equation

$$\partial_t(\alpha_2\rho_2\mathcal{E}_2)+\partial_x(\alpha_2\rho_2\mathcal{E}_2u_2+\alpha_2\pi_2(\tau_2,\mathcal{T}_2,s_2)u_2)=u_2^*\pi_1^*\Delta\alpha_1\delta_0(x-u_2^*t), \tag{3.7.65}$$

where the relaxation energy is defined in (3.7.40). Again, note that the non-conservative product $u_2\times\delta_0(x-u_2^*t)$ is not ambiguous since u_2 stays constant across the void fraction wave, and takes the value u_2^*. Similarly, self-similar solutions of (3.7.55) verify the following energy like equation :

$$\partial_t(\alpha_1\rho_1\mathcal{E}_1)+\partial_x(\alpha_1\rho_1\mathcal{E}_1u_1+\alpha_1\pi_1(\tau_1,\mathcal{T}_1,s_1)u_1)=u_2^*\Delta\alpha_1\Big(\pi_1\times\delta_0(x-u_2^*t)\Big), \tag{3.7.66}$$

where by definition the mass of the product $\pi_1\times\delta_0(x-u_2^*t)$ equals π_1^* with π_1^* given by (3.7.56).

The energy-entropy duality principle is now at hand. We use classical notations from the framework of finite volume methods. The CFL condition is set to $1/2$. Assume a the discrete solution at time t^n for the Baer-Nunziato PDEs (3.7.1). Defining from this discrete solution an initial data $\mathbb{W}_\Delta(x,t^n)$ at equilibrium, that is with $\pi_i(x,t^n)=\mathcal{P}_i(\tau_i,s_i)(x,t^n)$, we solve a sequence of non-interacting Riemann problems for the relaxation system (3.7.37) to define an approximate solution $\mathbb{W}_\Delta(x,t^{n+1=})$ at time $t^{n+1=}=t^n+\Delta t$. This solution is then classically averaged in each computational cell and in particular, gives conservative updates for both entropies

$$(\alpha_i\rho_is_i)_j^{n+1-}=(\alpha_i\rho_is_i)_j^n-\frac{\Delta t}{\Delta x}\Delta(\alpha_i\rho_is_iu_i)_{j+\frac12}^n. \tag{3.7.67}$$

Averaging (3.7.65) and (3.7.66), one easily gets :

$$\frac{1}{\Delta x}\int_{x_{j-\frac{1}{2}}}^{x_{j+\frac{1}{2}}} \alpha_i\rho_i\mathcal{E}_i(\mathbb{W}_\Delta(x,t^{n+1=})dx = (\alpha_i\rho_iE_i)_j^n - \frac{\Delta t}{\Delta x}\Delta(\alpha_i\rho_i\mathcal{E}_iu_i+\alpha_i\pi_iu_i)_{j+\frac{1}{2}}^n \\ +\frac{\Delta t}{\Delta x}(\pi_1^*\max(u_2^*,0))_{j-\frac{1}{2}}^n\Delta(\alpha_i)_{j-\frac{1}{2}}^n + \frac{\Delta t}{\Delta x}(\pi_1^*\min(u_2^*,0))_{j+\frac{1}{2}}^n\Delta(\alpha_i)_{j+\frac{1}{2}}^n, \tag{3.7.68}$$

since $(\mathcal{E}_i)_j^n = (E_i)_j^n$ because the initial data $\mathbb{W}_\Delta(x,t^n)$ is at equilibrium. Then we set $\mathcal{T}_i(x,t^{n+1,=})$ at equilibrium, pointwisely in x at time $t^{n+1,=}$: namely we define $\mathcal{T}_i(x,t^{n+1,-}) = \tau_i(x,t^{n+1,=})$. Assuming the frozen lagrangian sound speed a_i large enough so that the Gibbs principles stated in (3.7.43) hold true, one gets as a by-product

$$\frac{1}{\Delta x}\int_{x_{j-\frac{1}{2}}}^{x_{j+\frac{1}{2}}} \alpha_i\rho_iE_i(\mathbb{U}_\Delta(x,t^{n+1-})dx \le \frac{1}{\Delta x}\int_{x_{j-\frac{1}{2}}}^{x_{j+\frac{1}{2}}} \alpha_i\rho_i\mathcal{E}_i(\mathbb{W}_\Delta(x,t^{n+1=})dx, \tag{3.7.69}$$

where $\mathbb{U}_\Delta(x,t^{n+1-})$ denotes a piecewise constant approximate solution of the auxiliary system (3.7.33). Invoking the convexity of the mapping $\mathbb{U}_i \to (\alpha_i\rho_iE_i)(\mathbb{U}_i)$, one deduces

$$(\alpha_i\rho_iE_i)^{n+1-} \le \frac{1}{\Delta x}\int_{x_{j-\frac{1}{2}}}^{x_{j+\frac{1}{2}}} \alpha_i\rho_iE_i(\mathbb{U}_\Delta(x,t^{n+1=})dx. \tag{3.7.70}$$

It now suffices to exchange energy and entropy along the lines developed in the first section to conclude.

To check that the proposed algorithm preserves the positiveness of the internal energies, namely $(e_i)_j^{n+1} > 0$, it suffices to notice that before the exchange in between entropy and energy, the update $(s_i)_j^{n+1-}$ obeys a discrete local maximum principle so that $(e_i)_j^{n+1-} \equiv e_i((\tau_i)_j^{n+1-},(s_i)_j^{n+1-})$ is well defined and thus positive provided that $(\alpha_i\rho_i)_j^{n+1-} > 0$. But this last property holds true since we are dealing with positive intermediate specific volume τ_i, and thus ρ_i, everywhere within the wave fan since no energy dissipation is needed here. Then the exchange step correction results in $(E_i)_j^{n+1} \ge (E_i)_j^{n+1-}$ while the kinetic energy has been kept unchanged. As a consequence, we infer $(e_i)_j^{n+1} \ge (e_i)_j^{n+1-} > 0$ and hence the required positiveness property for the proposed algorithm.

Second case : $\mathcal{M}_0(\nu,\omega)$ is irrelevant

Let us at last address the situation where one needs to dissipate energy for phase 1 across the void fraction wave

$$\partial_t(\alpha_1\rho_1\mathcal{E}_1) + \partial_x(\alpha_1\rho_1\mathcal{E}_1u_1+\alpha_1\pi_1u_1) - u_2^*\Delta\alpha_1\Big(\pi_1 \times \delta_0(x-u_2^*t)\Big) \le 0, \tag{3.7.71}$$

thanks to some conveniently chosen value of $\mathcal{M}_\mu(\nu,\omega) \in (0,\mathcal{M}_0(\nu,\omega)[$. Here again and by definition

$$\pi_1 \times \delta_0(x-u_2^*t) = \pi_1^*\delta_0(x-u_2^*t) \tag{3.7.72}$$

with π_1^* given by (3.7.56) and evaluated for the choice of the relative Mach number $\mathcal{M}_\mu(\nu,\omega)$ under consideration. Recall that this procedure is energy preserving for phase 2, in the sense that :

$$\partial_t(\alpha_2\rho_2\mathcal{E}_2) + \partial_x(\alpha_2\rho_2\mathcal{E}_2u_2 + \alpha_2\pi_2u_1) - \pi_1^*u_2^*\Delta\alpha_1\delta_0(x-u_2^*t) = 0, \tag{3.7.73}$$

for the pair (u_2^*,π_1^*) under consideration.

Here thanks to an energy-entropy duality principle, we propose to slightly modify the local Riemann solution of (3.7.55)–(3.7.71) so that it no longer solves these equations but instead

$$\left\{\begin{array}{l} \partial_t\alpha_1 + u_2^*\partial_x\alpha_1 = 0, \\ \partial_t(\alpha_1\rho_1) + \partial_x(\alpha_1\rho_1u_1) = 0, \\ \partial_t(\alpha_1\rho_1u_1) + \partial_x(\alpha_1\rho_1u_1^2 + \alpha_1\pi_1) - \pi_1^*\Delta\alpha_1\delta_{x-u_2^*t} = 0, \\ \partial_t(\alpha_1\rho_1\mathcal{T}_1) + \partial_x(\alpha_1\rho_1\mathcal{T}_1u_1) = 0, \\ \partial_t(\alpha_1\rho_1\mathcal{E}_1) + \partial_x(\alpha_1\rho_1\mathcal{E}_1u_1 + a_1^2\alpha_1\pi_1) - u_2^*\pi_1^*\Delta\alpha_1\delta_{x-u_2^*t} = 0, \end{array}\right. \tag{3.7.74}$$

with

$$\partial_t(\alpha_1\rho_1s_1) + \partial_x(\alpha_1\rho_1s_1u_1) \leq 0, \tag{3.7.75}$$

where entropy dissipation for phase 1 only takes place at the void fraction wave. In other words, energy conservation is restored at the expense of entropy dissipation. The main reason for restoring energy conservation at the PDE level stems from the need to assess clear conservative jump relations for defining the traces of $\mathcal{E}_1$ at the void fraction wave. Note that the Riemann solution for phase 2 is kept unchanged thanks to (3.7.73).

The duality principle under consideration relies on the following technical result

Lemma 3.7.4. *Under the Whitham condition, define the following admissible change of variables* $\mathbb{W}_i = (\alpha_i, \alpha_i\rho_i, \alpha_i\rho_iu_i, \alpha_i\rho_i\mathcal{T}_i, \alpha_i\rho_is_i) \to \bar{\mathbb{W}}_i = (\alpha_i, \alpha_i\rho_i, \alpha_i\rho_iu_i, \alpha_i\rho_iI_i, \alpha_i\rho_is_i)$ *with* $I_i = p_i(\mathcal{T}_i) + a_i^2\mathcal{T}_i$. *Then understanding the phasic energy* $\alpha_i\rho_i\mathcal{E}_i$ *as a function of* $\bar{\mathbb{W}}_i$, *one has*

$$\partial_{\alpha_i\rho_is_i}(\alpha_i\rho_i\mathcal{E}_i)(\bar{\mathbb{W}}_i) = -T_i(\mathcal{T}_i,s_i) < 0. \tag{3.7.76}$$

The proof of this statement is a straightforward adaptation of a result established by Christophe Chalons in his PhD dissertation (see Lemma 4, page 173). We skip the details.

In order to use this technical result, we propose to re-express the energy inequality (3.7.66) in the frame of the void fraction wave, as already performed in the barotropic setting. Introducing $w_1 = u_1 - u_2^*$, this inequality reads

$$\partial_t(\alpha_1\rho_1\bar{\mathcal{E}}_1) + \partial_x(\alpha_1\rho_1\bar{\mathcal{E}}_1w_1 + \alpha_1\pi_1w_1) - \pi_1^*u_2^*\Delta\alpha_1\delta_0(x) \leq 0, \tag{3.7.77}$$

with $\bar{\mathcal{E}}_1$ given in (3.7.46). Using the notation of Chapter 2, we denote by $\mathbb{W}^-$ and $\mathbb{W}^+$ the left and right traces at the standing wave (namely the void fraction wave in the proposed new frame). The jump relation at this standing wave coming with (3.7.77) reads

$$(\alpha_1\rho_1\bar{\mathcal{E}}w_1)(\mathbb{W}_1^+) \leq (\alpha_1\rho_1\bar{\mathcal{E}}w_1)(\mathbb{W}_1^-) - [\alpha_1\pi_1w_1] + \pi_1^*u_2^*\Delta\alpha_1. \tag{3.7.78}$$

By contrast, the entropy $\alpha_1\rho_1 s_1$ satisfies

$$(\alpha_1\rho_1 s_1 w_1)^+ = (\alpha_1\rho_1 s_1 w_1)^-. \tag{3.7.79}$$

We propose to modify the self similar Riemann solution $\mathbb{W}_1(\xi, \mathbb{W}_L, \mathbb{W}_R)$ of (3.7.55)–(3.7.66) into another self-similar function denoted by $\hat{\mathbb{W}}_1(\xi, \mathbb{W}_L, \mathbb{W}_R)$. This function is defined when keeping unchanged all the intermediate states except $\mathbb{W}_1^+$. This new state is built keeping unchanged the phasic quantities $\alpha_1, \tau_1, u_1, \pi_1$ of $\mathbb{W}_1^+$. By contrast, the phasic entropy s_1 is changed so that the energy for phase 1 is now preserved across the standing wave

$$(\alpha_1\rho_1\bar{\mathcal{E}}_1 w_1)(\hat{\mathbb{W}}_1^+) = (\alpha_1\rho_1\bar{\mathcal{E}}_1 w_1)(\mathbb{W}_1^-) - [\alpha_1\pi_1 w_1] + \pi_1^* u_2^* \Delta\alpha_1. \tag{3.7.80}$$

Since we focus ourselves on positive relative Mach number $\mathcal{M} = (u_1^- - u_2^*)(a_1\tau_1^-)$ without loss of generality, we have $\alpha_1^+\rho_1^+ w_1^+ = \alpha_1^-\rho_1^- w_1^- > 0$ so that we infer from (3.7.78) and (3.7.80)

$$\bar{\mathcal{E}}_1(\hat{\mathbb{W}}_1^+) \geq \bar{\mathcal{E}}_1(\mathbb{W}_1^+). \tag{3.7.81}$$

Recall that the modified inner state $\hat{\mathbb{W}}^+$ is built so as to keep unchanged $\alpha_1^+, (\alpha_1\rho_1)^+, (\alpha_1\rho_1 w_1)^+$ and π_1^+ that is to say $(\alpha_1\rho_1\mathcal{I})_1^+ = (\alpha_1\rho_1)^+(\pi_1^+ + a_1^2\tau_1^+)$. So that Lemma 3.7.4 applies to prove that the entropy s_1 in the modified right trace $\hat{\mathbb{W}}^+$ actually obeys

$$s_1(\hat{\mathbb{W}}_1^+) \leq s_1^- \quad \text{that is} \quad (\alpha_1\rho_1 s_1 w_1)(\hat{\mathbb{W}}_1^+) \leq (\alpha_1\rho_1 s_1 w_1)^-. \tag{3.7.82}$$

Turning back to the original frame, we have therefore defined a self similar function $\hat{\mathbb{W}}_1(\xi, \mathbb{W}_L, \mathbb{W}_R)$ which is solution of the Riemann problem (3.7.74)–(3.7.75) as expected.

The numerical procedure then follows when averaging the modified Riemann solution $\hat{\mathbb{W}}_1(\xi)$ in place of $\mathbb{W}_1(\xi)$ in order to get in the one hand

$$(\alpha_1\rho_1 s_1)_j^{n+1-} \leq (\alpha_1\rho_1 s_1)_j^n - \frac{\Delta t}{\Delta x}\Delta(\alpha_1\rho_1 s_1 u_1)_{j+\frac{1}{2}}^n, \tag{3.7.83}$$

and in the other hand

$$\begin{aligned}\frac{1}{\Delta x}\int_{x_{j-\frac{1}{2}}}^{x_{j+\frac{1}{2}}} \alpha_1\rho_1\mathcal{E}_1(\hat{\mathbb{W}}_\Delta(x, t^{n+1=})dx = (\alpha_1\rho_1\mathcal{E}_1)_j^n - \frac{\Delta t}{\Delta x}\Delta(\alpha_1\rho_1\mathcal{E}_1 u_1 + \alpha_1\pi_1 u_1)_{j+\frac{1}{2}}^n \\ + \frac{\Delta t}{\Delta x}(\pi_1^*\max(u_2^*, 0))_{j-\frac{1}{2}}^n \Delta(\alpha_1)_{j-\frac{1}{2}}^n + \frac{\Delta t}{\Delta x}(\pi_1^*\min(u_2^*, 0))_{j+\frac{1}{2}}^n \Delta(\alpha_1)_{j+\frac{1}{2}}^n.\end{aligned} \tag{3.7.84}$$

Using similar arguments to those developed in the previous section devoted to a relevant relative Mach number $\mathcal{M}_0(\nu, \omega)$, we pointwisely in x set $\mathcal{T}_1$ at equilibrium assuming a large enough value of a_1 so that energy for phase 1 is dissipated on average. Then the usual energy-entropy duality principle again applies to prove that energy for phase 1 can be preserved while further dissipating the entropy s_1 in (3.7.83)

$$(\alpha_1\rho_1 s_1)_j^{n+1} \leq (\alpha_1\rho_1 s_1)_j^n - \frac{\Delta t}{\Delta x}\Delta(\alpha_1\rho_1 s_1 u_1)_{j+\frac{1}{2}}^n. \tag{3.7.85}$$

As far as phase 2 is concerned, the situation is exactly the same as in the previous section. Exactly the same steps apply.

Checking the positiveness preserving property of the resulting algorithm comes along similar lines as those proposed in the previous section. It suffices to notice in the one hand that $(\alpha_i\rho_i)_j^{n+1-} > 0$ since energy dissipation ensures this property. In a second hand, one has to notice that we could directly average the Riemann solution without correction, then apply the standard entropy-energy duality principle to actually get an equivalent formula for the final update $(\alpha_i\rho_i E_i)_j^{n+1}$. The intermediate entropy-energy duality principle just aimed at proving that we can solve standard jump relations at the void fraction wave to get the requested traces. In other words and for the final update under consideration, the situation is just equivalent to the one treated in the previous section !

This concludes the proof.

3.7.4 Numerical illustration

In this section, we present the Riemann test-case for the complete model with energies, which is considered in [23]. The two phases follow two ideal gas equations of state with $\gamma_1 = \gamma_2 = 1.4$. Denoting $\mathcal{U} = (\alpha_1, \rho_1, u_1, p_1, \rho_2, u_2, p_2)$ the initial data is given by

$$\begin{aligned} \mathcal{U}_L &= (0.2, 0.2, 0, 0.3, 1.0, 0, 1.0) \qquad \text{if } x < 0, \\ \mathcal{U}_R &= (0.7, 1.0, 0, 1.0, 1.0, 0, 1.0) \qquad \text{if } x > 0. \end{aligned}$$

The computation has been implemented on three different meshes of respectively 100, 1000 and 10000 cells. The results are presented in Figure 3.8. As for the isentropic test-cases, we observe a very good behavior on the very coarse 100-cell mesh. Moreover, although the exact solution is not represented here, the scheme seems to be convergent as the space step tends to zero (with a constant CFL).

Appendix A: Mathematical properties of system (3.2.1)

Characteristic fields

Denoting $\mathcal{U} = (\alpha_1, \rho_1, u_1, \rho_2, u_2)^T$ the state vector of non-conservative variables, the smooth solutions of system (3.2.1) are equivalent to the following system

$$\partial_t \mathcal{U} + A(\mathcal{U})\partial_x \mathcal{U} = 0, \tag{3.7.86}$$

where

$$\mathbf{A}(\mathcal{U}) = \begin{bmatrix} u_2 & 0 & 0 & 0 & 0 \\ \frac{\rho_1}{\alpha_1}(u_1 - u_2) & u_1 & \rho_1 & 0 & 0 \\ 0 & \frac{p_1'(\rho_1)}{\rho_1} & u_1 & 0 & 0 \\ 0 & 0 & 0 & u_2 & \rho_2 \\ \frac{p_1(\rho_1)-p_2(\rho_2)}{(1-\alpha_1)\rho_2} & 0 & 0 & \frac{p_2'(\rho_2)}{\rho_2} & u_2 \end{bmatrix}. \tag{3.7.87}$$

This matrix admits five real characteristic eigenvalues which are:

$$\begin{aligned} &\sigma_1(\mathcal{U}) = u_2, \\ &\sigma_2(\mathcal{U}) = u_1 - c_1(\rho_1), \quad \sigma_3(\mathcal{U}) = u_1 + c_1(\rho_1), \\ &\sigma_4(\mathcal{U}) = u_2 - c_2(\rho_2), \quad \sigma_5(\mathcal{U}) = u_2 + c_2(\rho_2), \end{aligned} \tag{3.7.88}$$

where $c_i(\rho_i) = \sqrt{p_i'(\rho_i)}$, i in $\{1, 2\}$ are the phasic speeds of sound. The corresponding right eigenvectors are denoted $r_k(\mathcal{U})$, $k = 2, 3, 4, 5$. With a suitable normalisation, one can easily verify that

$$\begin{aligned} &\nabla_{\mathcal{U}}\sigma_1(\mathcal{U}).r_1(\mathcal{U}) = 0, \\ &\nabla_{\mathcal{U}}\sigma_k(\mathcal{U}).r_k(\mathcal{U}) = 1, \ k = 2, 3, 4, 5. \end{aligned} \tag{3.7.89}$$

Hence, the first characteristic field is linearly degenerate while the four others are genuinely nonlinear. Observe that the system is hyperbolic, *i.e.* the five eigenvectors $r_k(\mathcal{U})$, k in $\{1, .., 5\}$ span $\mathbb{R}^5$ if and only if $(u_1 - u_2)^2 \neq c_1^2(\rho_1)$.

Appendix B: Exact solutions to the Riemann problem

We are now interested in Cauchy problems for system (3.2.1) where the initial data (in non-conservative variables) is of the form

$$\mathcal{U}(x, t = 0) = \begin{cases} \mathcal{U}_L & \text{if } x < 0, \\ \mathcal{U}_R & \text{if } x > 0. \end{cases} \tag{3.7.90}$$

In the domain of hyperbolicity, the solution is self-similar (*i.e.* $\mathcal{U}(x, t) = V(x/t)$) and composed of five isolated waves separating six constant intermediate states, each wave corresponding to one characteristic field. In the sequel, we describe the different types of waves connecting two constant intermediate states. We restrict to solutions composed of **isolated** waves.

Rarefaction waves

A rarefaction wave is a **continuous and piecewise smooth** solution of system (3.2.1) of the form

$$U(x, t) = V(\xi), \quad \xi = \frac{x}{t}, \ x \in \mathbb{R}, \ t > 0. \tag{3.7.91}$$

Substituting this in (3.7.86), one can see that a rarefaction wave is a solution of the following Cauchy problem for ordinary differential equations:

$$\begin{cases} \dfrac{dV(\xi)}{d\xi} = r_k(V(\xi)), \quad \xi \geq \sigma_k(\mathcal{U}_0),\ k = 2,3,4,5, \\ V(\sigma_k(\mathcal{U}_0)) = \mathcal{U}_0. \end{cases} \tag{3.7.92}$$

A solution $V(\xi)$, $\xi \geq \sigma_k(\mathcal{U}_0)$ of (3.7.92) consists of all the right-hand states $V(\xi)$ that can be connected to a given left-hand state $\mathcal{U}_0$ by a σ_k-rarefaction wave. Considering the second characteristic field for example, system (3.7.92) is equivalent to the preservation of the following quantities, called the *Riemann invariants* of the field:

$$\frac{d\alpha_1(\xi)}{d\xi} = \frac{d\rho_2(\xi)}{d\xi} = \frac{du_2(\xi)}{d\xi} = \frac{d\Phi(\mathcal{U})(\xi)}{d\xi} = 0, \tag{3.7.93}$$

where $\Phi(\mathcal{U}) = u_1 + \int^{\rho_1} c_1(y)/y dy$. Consequently, α_1, ρ_2 and u_2 are constant through a σ_2-rarefaction wave, while ρ_1 and u_1 are respectively decreasing and increasing. The same study can be done for the other rarefaction waves associated with the genuinely non-linear fields σ_k, $k = 3,4,5$.

Shock waves

Shock waves are discontinuous solutions associated with one of the genuinely non-linear fields σ_k, $k = 2,3,4,5$. As we restrict to hyperbolic solutions, α_1 is constant across this type of discontinuity and the system reduces to two independent subsystems of isentropic gas dynamics equations for each phase. Two states $\mathcal{U}^-$ and $\mathcal{U}^+$ (or their conservative counterparts $\mathbb{U}^-$ and $\mathbb{U}^+$) are connected by an *admissible shock* whose velocity is equal to σ, if and only if the discontinuity satisfies the two following jump relation:

$$\sigma\,[\mathbb{U}] + [\mathbf{f}(\mathbb{U})] = 0, \tag{3.7.94}$$

together with the Lax admissibility condition. Such a discontinuous wave is purely phasic since if it is associated with one of the characteristic fields of phase i (σ_2 or σ_3 for $i = 1$ and σ_4 or σ_5 for $i = 2$), all the quantities related to the other phase are constant through the discontinuity. For instance, if the thermodynamics of phase 1 follow an ideal gas pressure law: $p_1(\rho_1) = \kappa_1 \rho_1^{\gamma_1}$, then given a left-hand state $\mathcal{U}^-$, the shock curves consisting of all the right-hand states $\mathcal{U}^+$ that can be connected to $\mathcal{U}^-$ by an admissible shock associated to σ_2 or σ_3 are given by

$$\sigma_2: \quad u_2^+ = u_2^-,\ \rho_2^+ = \rho_2^-,\ u_1^+ = u_1^- - \left(\kappa_1 \left(\frac{1}{\rho_1^-} - \frac{1}{\rho_1^+}\right)\left((\rho_1^+)^{\gamma_1} - (\rho_1^-)^{\gamma_1}\right)\right)^{1/2},\ \rho_1^+ > \rho_1^-, \tag{3.7.95}$$

$$\sigma_3: \quad u_2^+ = u_2^-,\ \rho_2^+ = \rho_2^-,\ u_1^+ = u_1^- - \left(\kappa_1 \left(\frac{1}{\rho_1^-} - \frac{1}{\rho_1^+}\right)\left((\rho_1^+)^{\gamma_1} - (\rho_1^-)^{\gamma_1}\right)\right)^{1/2},\ \rho_1^+ < \rho_1^-. \tag{3.7.96}$$

Contact discontinuity

A σ_1-contact discontinuity is associated to a jump in the phase fraction α_1 between $\alpha_{1,L}$ and $\alpha_{1,R}$, α_1 being constant in both the regions left and right of this discontinuity. Through such a contact

discontinuity, the eigenvalue u_2 is constant and we have the following jump relations (see for instance [13, 23] or [25])

$$[u_2] = 0, \tag{3.7.97}$$
$$[\alpha_1\rho_1(u_1 - u_2)] = 0, \tag{3.7.98}$$
$$[\alpha_1\rho_1(u_1 - u_2)u_1 + \alpha_1 p_1(\rho_1) + \alpha_2 p_2(\rho_2)] = 0, \tag{3.7.99}$$
$$[\alpha_1\rho_1(u_1 - u_2)E_1 + \alpha_1 p_1(\rho_1)u_1 + \alpha_2 p_2(\rho_2)u_2] = 0. \tag{3.7.100}$$

Hence, two states $\mathcal{U}^-$ and $\mathcal{U}^+$ are connected by a σ_1-contact discontinuity if they satisfy the four jump relations (3.7.97) to (3.7.100).

Vanishing-phase solution of test-case 2

The vanishing phase solution of test-case 2 is constructed as follows. First of all, two states $\mathcal{U}^-$ and $\mathcal{U}^+$ are constructed so as to be connected by a σ_1-contact discontinuity with $\alpha_1^- = \alpha_{1,L} = 1$ and $\alpha_1^+ = \alpha_{1,R} = 0.4$ ($\mathcal{U}^-$ *resp.* $\mathcal{U}^+$ is denoted $\mathcal{U}_1$ *resp.* $\mathcal{U}_2$ in (3.5.2)). For this purpose, observe that the jump relations associated with the contact discontinuity reduce to

$$\begin{aligned}
&u_2^- = u_2^+,\\
&\rho_1^-(u_1^- - u_2^-) = \alpha_1^+\rho_1^+(u_1^+ - u_2^+),\\
&\rho_1^-(u_1^- - u_2^-)u_1^- + p_1(\rho_1^-) = \alpha_1^+\rho_1^+(u_1^+ - u_2^+)u_1^+ + \alpha_1^+ p_1(\rho_1^+) + \alpha_2^+ p_2(\rho_2^+),\\
&\rho_1^-(u_1^- - u_2^-)E_1^- + p_1(\rho_1^-)u_1^- = \alpha_1^+\rho_1^+(u_1^+ - u_2^+)E_1^+ + \alpha_1^+ p_1(\rho_1^+)u_1^+ + \alpha_2^+ p_2(\rho_2^+)u_2^+,
\end{aligned}$$

since $\alpha_1^- = 1$ and $\alpha_2^- = 0$. Thanks to these jump relations, given the values $\rho_1^- = 2.0$, $u_1^- = 0.4$ and $u_2^- = 0.6$ (no value of ρ_2^- is needed), we compute the values of ρ_1^+, u_1^+, ρ_2^+ and u_2^+ which are given in the intermediate state $\mathcal{U}_2$ in (3.5.2). The value of ρ_2^- is then imposed to be equal to ρ_2^+. Then the state $\mathcal{U}^- = \mathcal{U}_1$ is connected on its left with the state $\mathcal{U}_L$ through a σ_2-shock. The state $\mathcal{U}_2$ is connected to $\mathcal{U}_3$ through a σ_5-rarefaction wave, and finally $\mathcal{U}_3$ is connected to $\mathcal{U}_R$ through a σ_3-rarefaction wave.

Coupling solution of test-case 3

The same procedure is implemented for the construction of the exact solution of test-case 3, which corresponds to a coupling between a pure phase 1 ($\alpha_1^- = \alpha_{1,L} = 1$) on the right and a pure phase 2 ($\alpha_1^+ = \alpha_{1,R} = 0$) on the left. This time, the jump relations of the σ_1-contact discontinuity reduce to

$$\begin{aligned}
&u_2^- = u_2^+,\\
&\rho_1^-(u_1^- - u_2^-) = 0,\\
&p_1(\rho_1^-) = p_2(\rho_2^+),\\
&p_1(\rho_1^-)u_1^- = p_2(\rho_2^+)u_2^+.
\end{aligned}$$

A solution is given by $u_2^- = u_2^+ = u_1^- = 1.0$ and $\rho_1^- = p_1^{-1}(p)$, $\rho_2^+ = p_2^{-1}(p)$ where $p = p_1^- = p_2^+ = 10$ is the common pressure. The values of ρ_1^+ and u_1^+, which are of no importance since phase 1 in

not present on the right of the contact discontinuity, are taken equal to ρ_1^- and u_1^-. Similarly, we set $\rho_2^- := \rho_2^+$. This concludes the construction of the intermediate states $\mathcal{U}^- = \mathcal{U}^1$ and $\mathcal{U}^+ = \mathcal{U}^2$. Then the state $\mathcal{U}_1$ is connected on its left with the state $\mathcal{U}_L$ through a σ_2-shock and the state $\mathcal{U}_2$ is connected to $\mathcal{U}_R$ through a σ_5-rarefaction wave.

Acknowledgements. The author receives a financial support by ANRT through an EDF-CIFRE contract 529/2009.

References

[1] A. Ambroso, C. Chalons, F. Coquel, and T. Galié. Relaxation and numerical approximation of a two-fluid two-pressure diphasic model. *M2AN Math. Model. Numer. Anal.*, 43(6):1063–1097, 2009.

[2] A. Ambroso, C. Chalons, and P.-A. Raviart. A Godunov-type method for the seven-equation model of compressible two-phase flow. *Computers and Fluids*, 54(0):67 – 91, 2012.

[3] N. Andrianov and G. Warnecke. The Riemann problem for the Baer-Nunziato two-phase flow model. *J. Comput. Phys.*, 195(2):434–464, 2004.

[4] M.R. Baer and J.W. Nunziato. A two-phase mixture theory for the deflagration-to-detonation transition (DDT) in reactive granular materials. *International Journal of Multiphase Flow*, 12(6):861 – 889, 1986.

[5] F. Bouchut. *Nonlinear stability of finite volume methods for hyperbolic conservation laws and well-balanced schemes for sources*. Frontiers in Mathematics. Birkhäuser Verlag, Basel, 2004.

[6] F. Coquel, T. Gallouët, J-M. Hérard, and N. Seguin. Closure laws for a two-fluid two-pressure model. *C. R. Math. Acad. Sci. Paris*, 334(10):927–932, 2002.

[7] F. Coquel, E. Godlewski, B. Perthame, A. In, and P. Rascle. Some new Godunov and relaxation methods for two-phase flow problems. In *Godunov methods (Oxford, 1999)*, pages 179–188. Kluwer/Plenum, New York, 2001.

[8] F. Coquel, E. Godlewski, and N. Seguin. Relaxation of fluid systems. *Math. Models Methods Appl. Sci.*, 22(8), 2012.

[9] F. Coquel, J-M. Hérard, and K. Saleh. A splitting method for the isentropic Baer-Nunziato two-phase flow model. *To appear in ESAIM Proceedings*.

[10] F. Coquel, J-M. Hérard, K. Saleh, and N. Seguin. Relaxation approximation for the isentropic Baer-Nunziato model with vanishing phases.

[11] F. Coquel and B. Perthame. Relaxation of energy and approximate Riemann solvers for general pressure laws in fluid dynamics. *SIAM J. Numer. Anal.*, 35(6):2223–2249 (electronic), 1998.

[12] V. Deledicque and M. V. Papalexandris. A conservative approximation to compressible two-phase flow models in the stiff mechanical relaxation limit. *J. Comput. Phys.*, 227(21):9241–9270, 2008.

[13] P. Embid and M. Baer. Mathematical analysis of a two-phase continuum mixture theory. *Contin. Mech. Thermodyn.*, 4(4):279–312, 1992.

[14] R. Eymard, T. Gallouët, and R. Herbin. Finite volume methods. In *Handbook of numerical analysis, Vol. VII*, Handb. Numer. Anal., VII, pages 713–1020. North-Holland, Amsterdam, 2000.

[15] T. Gallouët, J-M. Hérard, and N. Seguin. Numerical modeling of two-phase flows using the two-fluid two-pressure approach. *Math. Models Methods Appl. Sci.*, 14(5):663–700, 2004.

[16] S. Gavrilyuk and R. Saurel. Mathematical and numerical modeling of two-phase compressible flows with micro-inertia. *Journal of Computational Physics*, 175(1):326 – 360, 2002.

[17] E. Godlewski and P.-A. Raviart. *Numerical approximation of hyperbolic systems of conservation laws*, volume 118 of *Applied Mathematical Sciences*. Springer-Verlag, New York, 1996.

[18] A. Harten, P. D. Lax, and B. van Leer. On upstream differencing and Godunov-type schemes for hyperbolic conservation laws. *SIAM Rev.*, 25(1):35–61, 1983.

[19] J-M. Hérard and O. Hurisse. A fractional step method to compute a class of compressible gas-luiquid flows. *Computers & Fluids. An International Journal*, 55:57–69, 2012.

[20] A. K. Kapila, S. F. Son, J. B. Bdzil, R. Menikoff, and D. S. Stewart. Two-phase modeling of DDT: Structure of the velocity-relaxation zone. *Physics of Fluids*, 9(12):3885–3897, 1997.

[21] Y. Liu. PhD thesis, Université Aix-Marseille, to appear in 2013.

[22] R. Saurel and R. Abgrall. A multiphase godunov method for compressible multifluid and multiphase flows. *Journal of Computational Physics*, 150(2):425 – 467, 1999.

[23] D.W. Schwendeman, C.W. Wahle, and A.K. Kapila. The Riemann problem and a high-resolution Godunov method for a model of compressible two-phase flow. *Journal of Computational Physics*, 212(2):490 – 526, 2006.

[24] W. C. Thacker. Some exact solutions to the nonlinear shallow-water wave equations. *J. Fluid Mechanics*, 107:499–508, 1981.

[25] M. D. Thanh, D. Kröner, and N. T. Nam. Numerical approximation for a Baer–Nunziato model of two-phase flows. *Applied Numerical Mathematics*, 61(5):702 – 721, 2011.

[26] S.A. Tokareva and E.F. Toro. HLLC-type Riemann solver for the Baer-Nunziato equations of compressible two-phase flow. *Journal of Computational Physics*, 229(10):3573 – 3604, 2010.

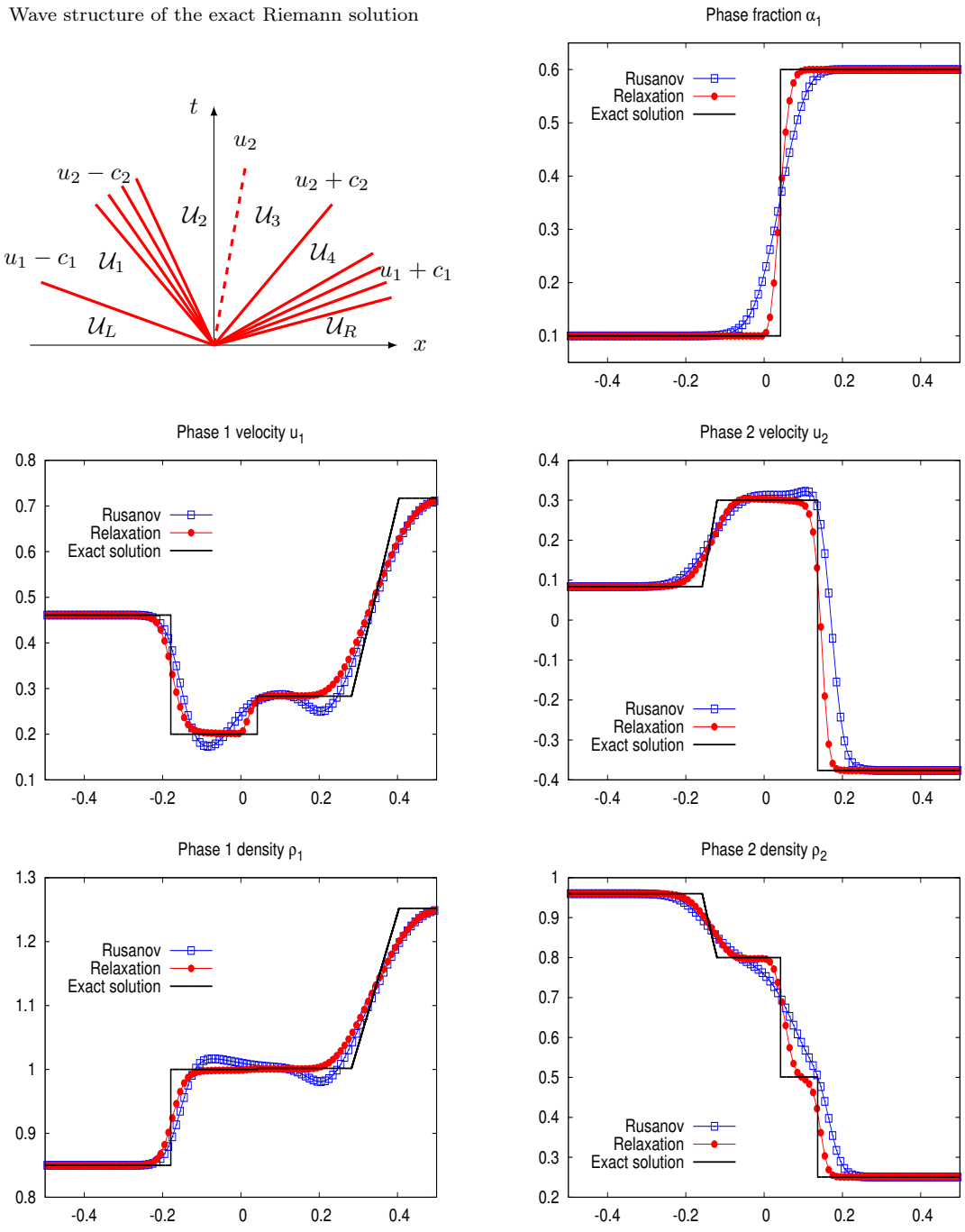

Figure 3.2: Test-case 1: Structure of the solution and space variations of the physical variables at the final time $T = 0.14$. Mesh size: 100 cells.

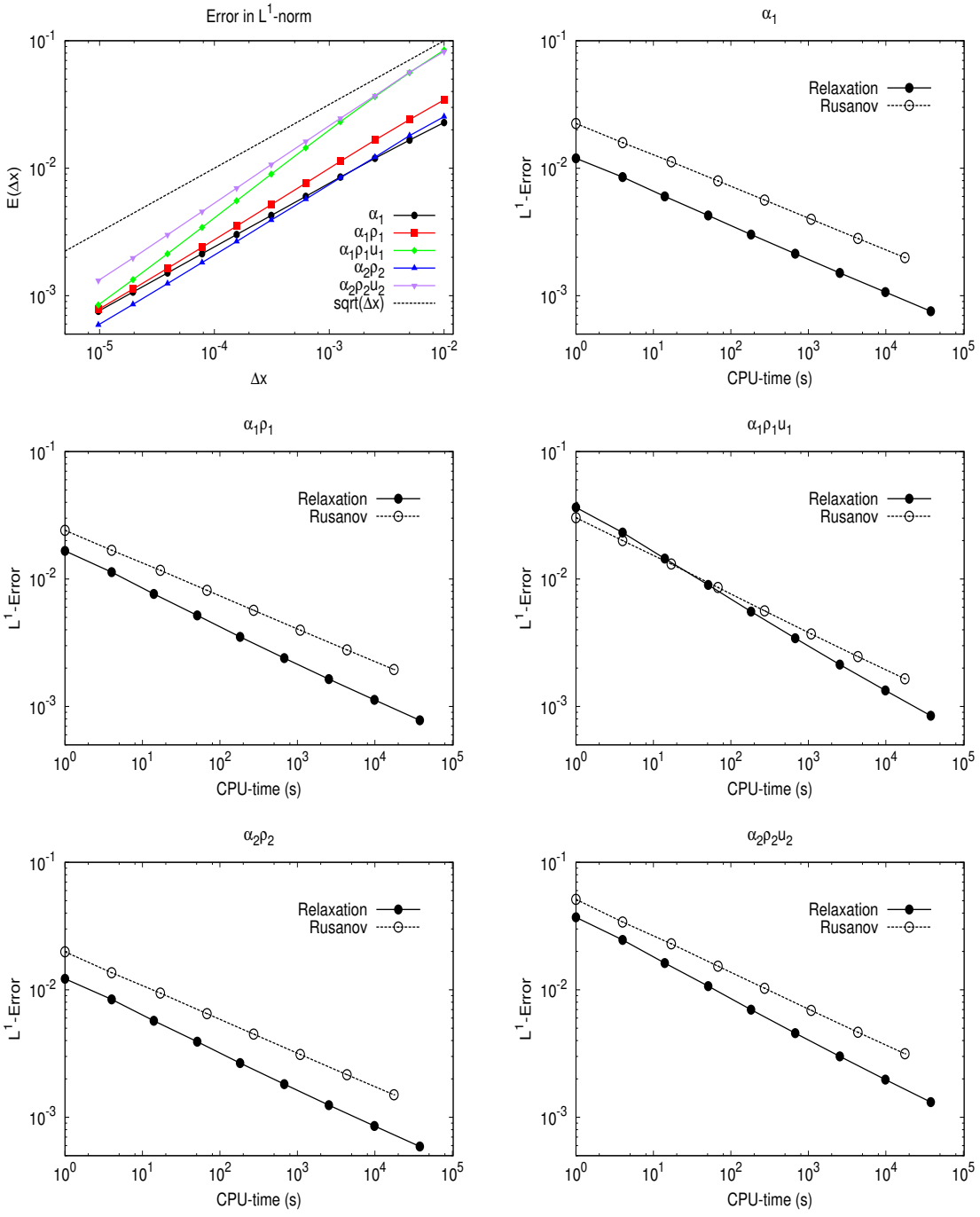

Figure 3.3: Test-case 1: L^1-Error with respect to Δx and L^1-Error with respect to computational cost (in seconds), for the conservative variables.

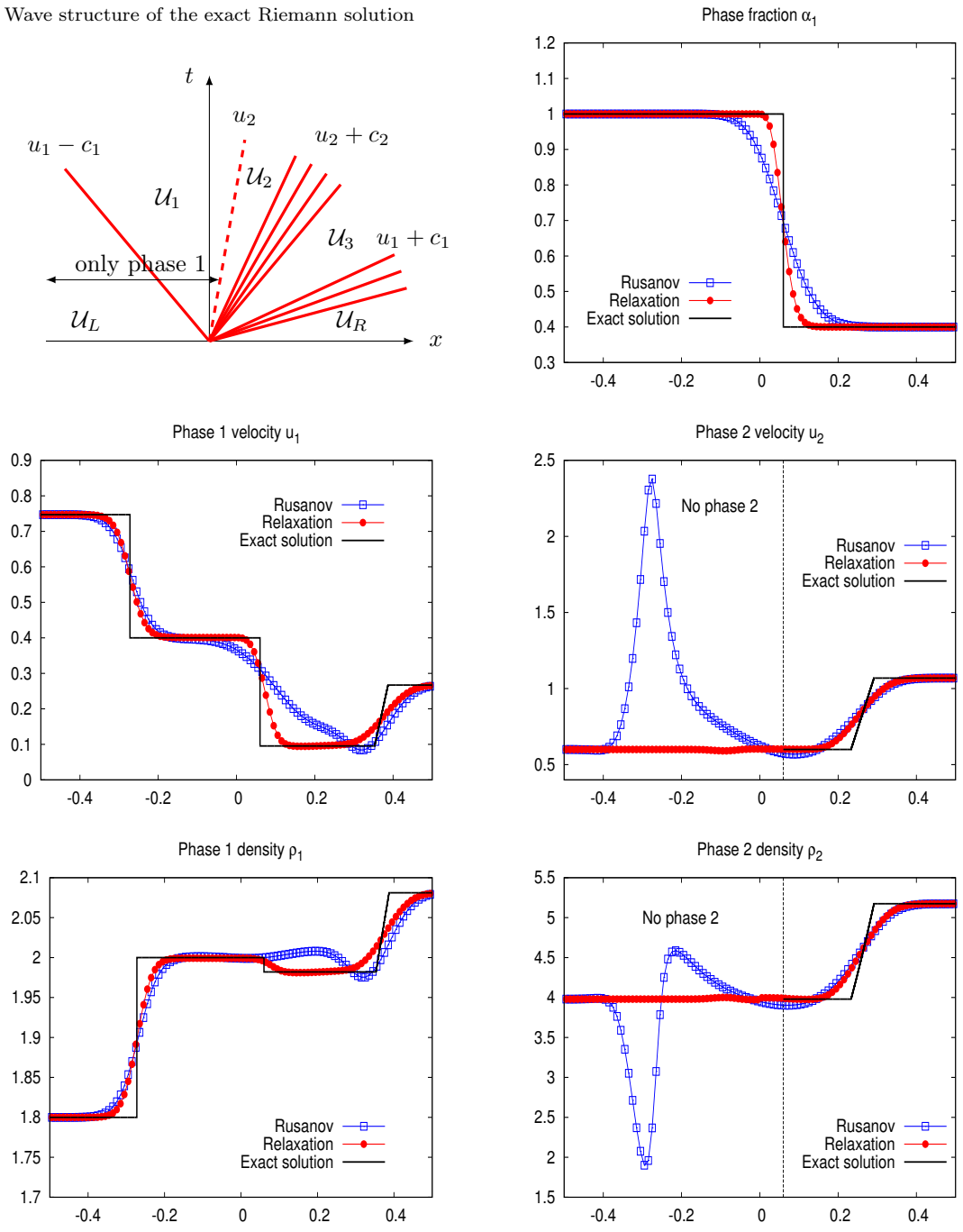

Figure 3.4: Test-case 2: Structure of the solution and space variations of the physical variables at the final time $T = 0.1$. Mesh size: 100 cells.

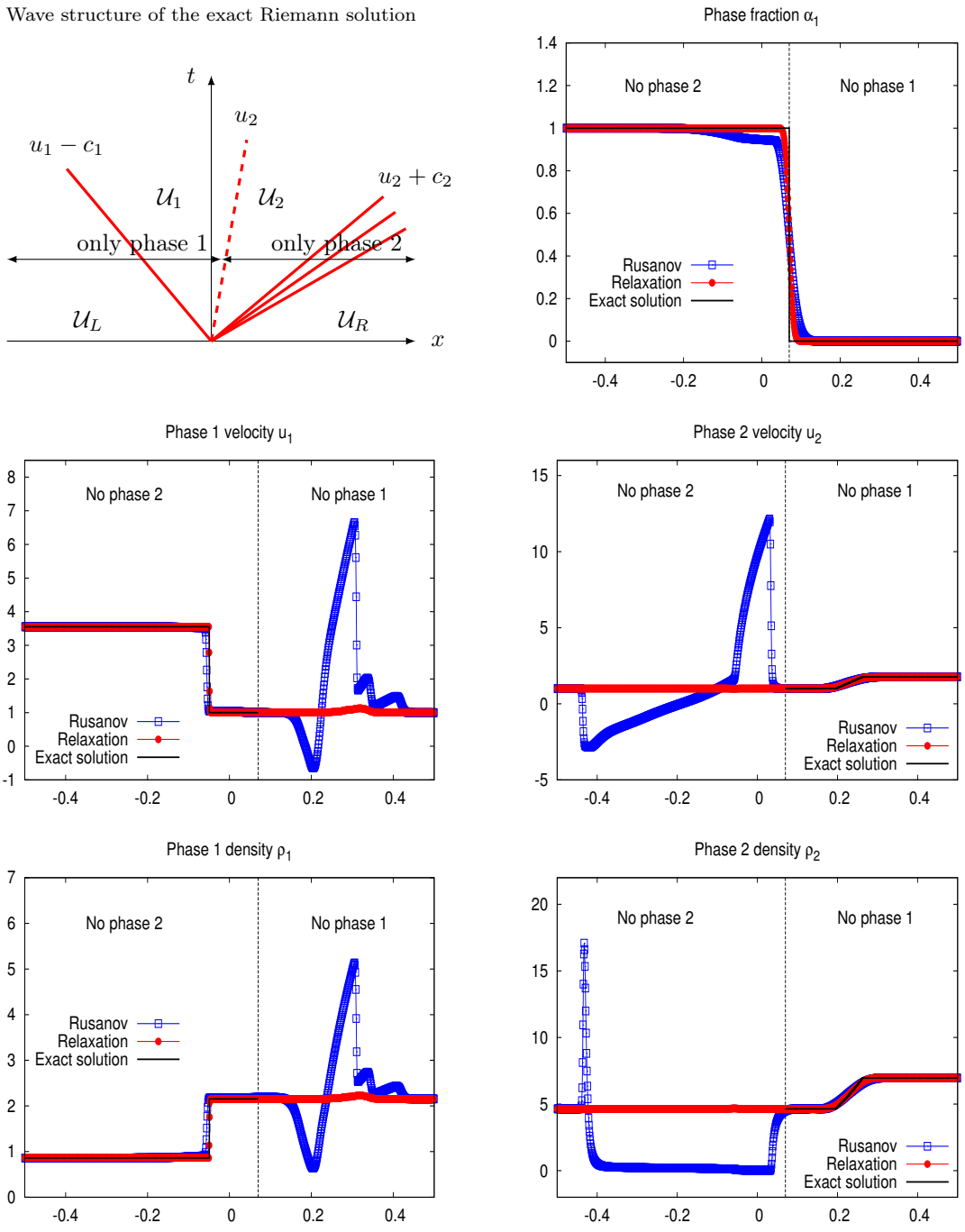

Figure 3.5: Test-case 3: Structure of the solution and space variations of the physical variables at the final time $T = 0.07$. Mesh size: 1000 cells.

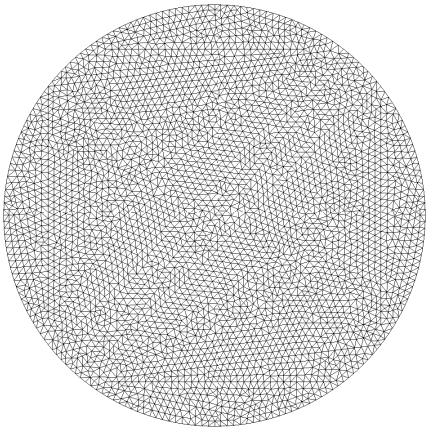

Figure 3.6: The mesh of the 2D numerical test.

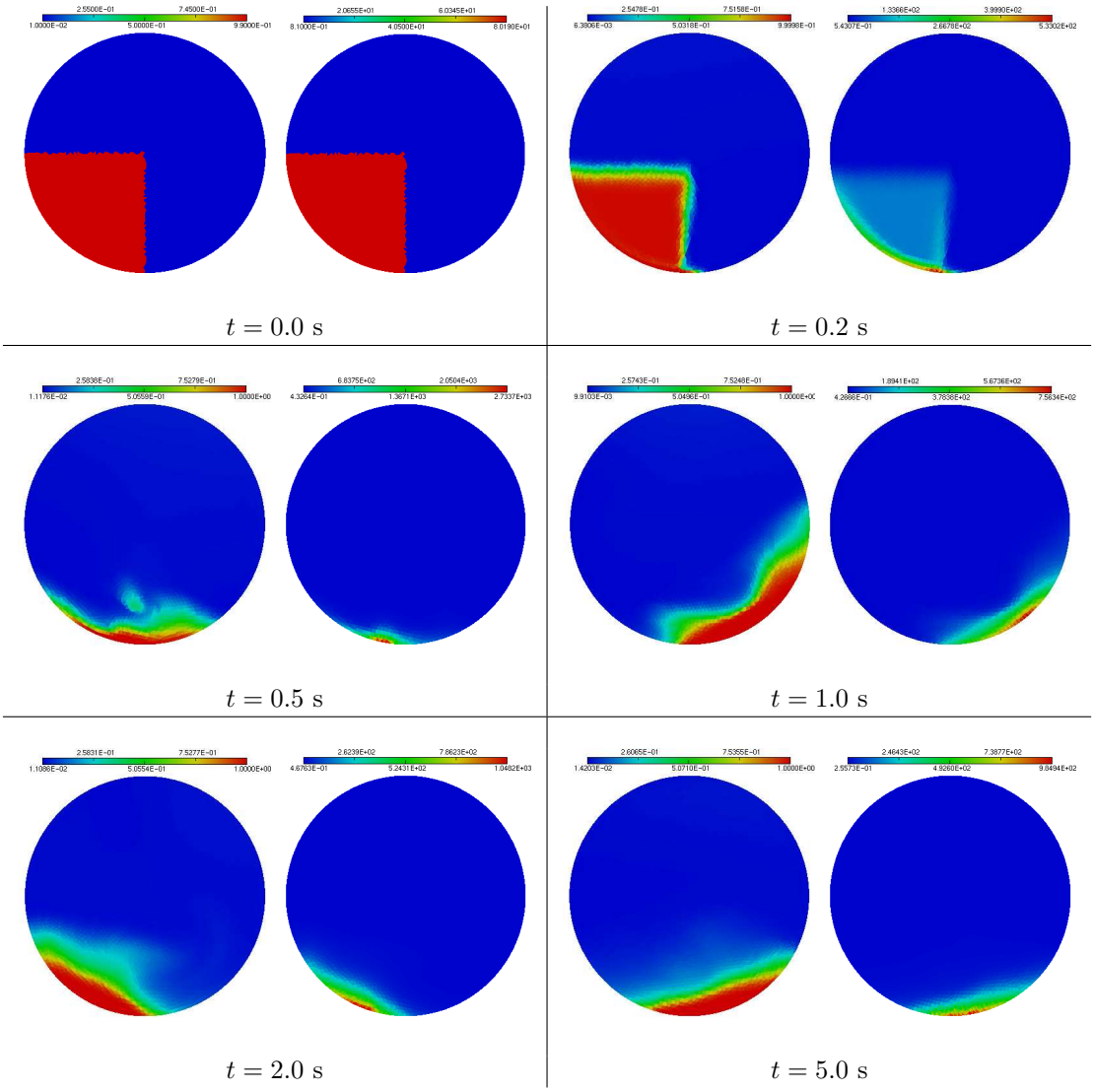

Figure 3.7: The void fraction α_1 (left figure in the cases) and the partial mass $\alpha_1\rho_1$ (right figure in the cases).

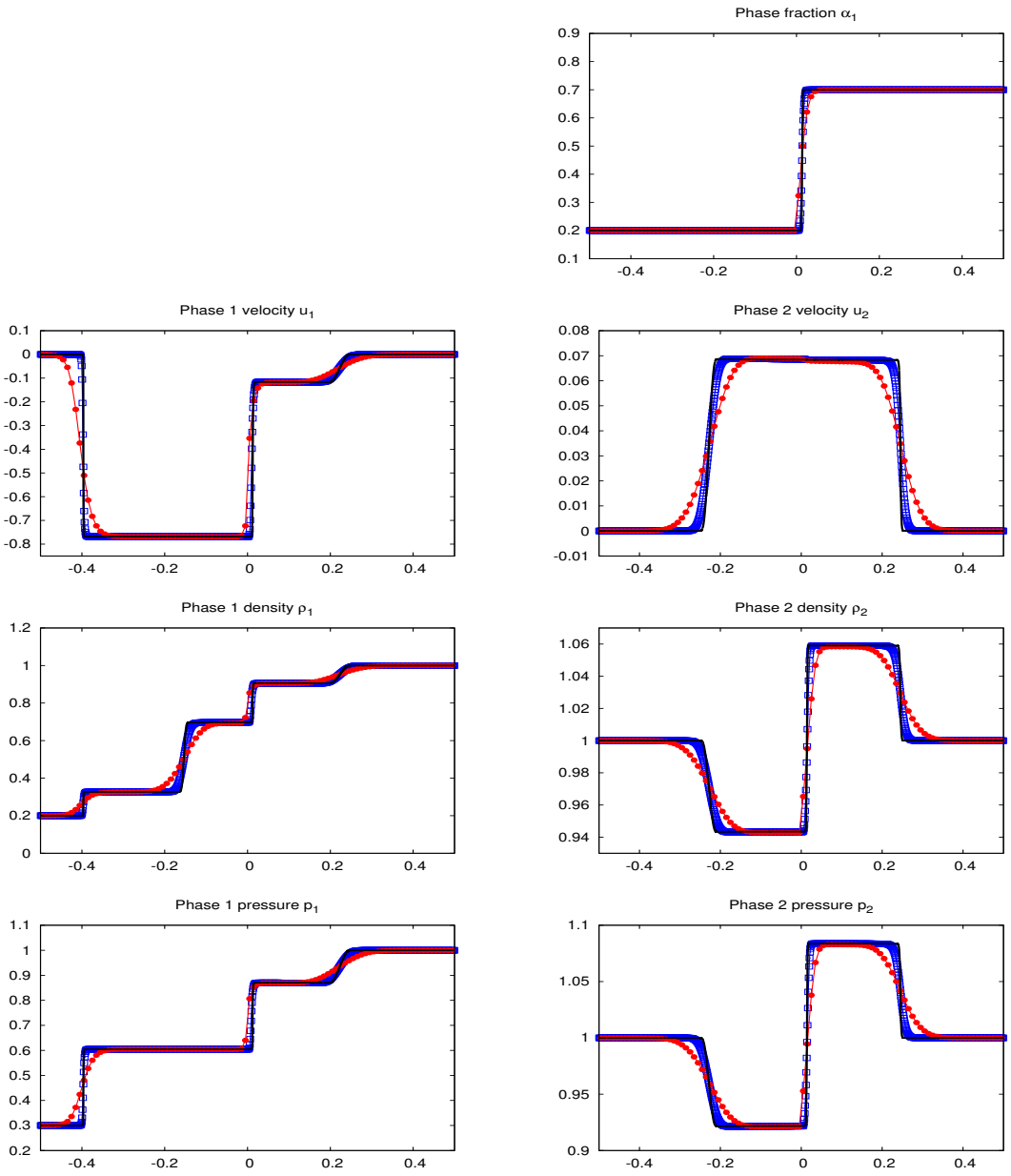

Figure 3.8: Model with energies: space variations of the physical variables at the final time $T = 0.2$. Red dots: 100-cell mesh. Blue squares: 1000-cell mesh. Straight line: 10000-cell mesh.

Chapter 4

Une méthode à pas fractionnaires pour le modèle de Baer-Nunziato

A SPLITTING METHOD FOR STABLE NUMERICAL APPROXIMATIONS OF THE BAER-NUNZIATO MODEL WITH VANISHING PHASES

Frédéric Coquel, Jean-Marc Hérard, Khaled Saleh

4.1 The isentropic Baer-Nunziato model

In the present work, we consider a model formulated in Eulerian coordinates where balance equations account for the evolution of mass and momentum of each phase. For compressible isentropic one-dimensional flows there are five unknowns that describe the evolution of the two-phase flow: the velocities of each phase u_k, the densities of each phase ρ_k and the phase fractions α_k, where $k \in \{1,2\}$ (knowing that $\alpha_1 + \alpha_2 = 1$). Denoting

$$\mathbb{U} = (\alpha_1, \alpha_1\rho_1, \alpha_1\rho_1 u_1, \alpha_2\rho_2, \alpha_2\rho_2 u_2)^T \tag{4.1.1}$$

the vector of unknowns, the isentropic version of the model –firstly introduced by Baer & Nunziato [3]– reads

$$\partial_t \mathbb{U} + \partial_x \mathbf{F}(\mathbb{U}) + \mathbf{C}(\mathbb{U})\partial_x \alpha_1 = \mathbf{S}(\mathbb{U}), \quad x \in \mathbb{R},\ t > 0, \tag{4.1.2}$$

where

$$\mathbf{F}(\mathbb{U}) = \begin{bmatrix} 0 \\ \alpha_1\rho_1 u_1 \\ \alpha_1\rho_1 u_1^2 + \alpha_1 p_1(\rho_1) \\ \alpha_2\rho_2 u_2 \\ \alpha_2\rho_2 u_2^2 + \alpha_2 p_2(\rho_2) \end{bmatrix}, \quad \mathbf{C}(\mathbb{U}) = \begin{bmatrix} V_I \\ 0 \\ -P_I \\ 0 \\ P_I \end{bmatrix}, \quad \mathbf{S}(\mathbb{U}) = \begin{bmatrix} \Theta_p\left(p_1(\rho_1) - p_2(\rho_2)\right) \\ 0 \\ \Theta_u(u_2 - u_1) \\ 0 \\ \Theta_u(u_1 - u_2) \end{bmatrix}. \tag{4.1.3}$$

In the absence of vacuum ($\rho_k > 0$ for $k \in \{1,2\}$) and if there exists no region of pure phases, *i.e.* if both the phase fractions $\alpha_k,\ k \in \{1,2\}$ lie in the *open interval* $(0,1)$, the vector of unkowns is expected to belong the physical space:

$$\Omega = \{\mathbb{U} \in \mathbb{R}^5, \alpha_k \in (0,1), \rho_k > 0, k \in \{1,2\}\}. \tag{4.1.4}$$

We assume barotropic pressure laws for each phase $\rho_k \mapsto p_k(\rho_k),\ k \in \{1,2\}$ with smooth dependence on the density, and which satisfy the following natural assumptions for all $\rho_k > 0$:

$$p_k(\rho_k) > 0, \quad p_k'(\rho_k) > 0, \quad \lim_{\rho_k \to 0} p_k(\rho_k) = 0, \quad \lim_{\rho_k \to +\infty} p_k(\rho_k) = +\infty. \tag{4.1.5}$$

We define the mapping $\tau \mapsto \mathcal{P}_k(\tau) := p_k(\tau^{-1})$ which is the phasic pressure seen as a function of the specific volume $\tau = \rho^{-1}$. In the whole paper, this smooth function is assumed to be strictly convex:

$$\mathcal{P}_k''(\tau_k) > 0, \quad \text{for all } \tau_k > 0,\ k \in \{1,2\}. \tag{4.1.6}$$

V_I and P_I are the so-called interfacial velocity and pressure for which one must provide closure laws as well as for the relaxation coefficients Θ_u and Θ_p in the source term $\mathbf{S}(\mathbb{U})$. Before turning to these closure laws, we may state the following important hyperbolicity property satisfied by system (4.1.2).

Proposition 4.1.1. *For every state vector $\mathbb{U}$ in Ω and whatever is the closure for V_I, the convective part of system (4.1.2) (i.e. system (4.1.2) with $\boldsymbol{S}(\mathbb{U}) = 0$) admits the following real eigenvalues:*

$$\sigma_1(\mathbb{U}) = V_I, \quad \sigma_2(\mathbb{U}) = u_1 - c_1, \quad \sigma_3(\mathbb{U}) = u_1 + c_1, \quad \sigma_4(\mathbb{U}) = u_2 - c_2, \quad \sigma_5(\mathbb{U}) = u_2 + c_2, \tag{4.1.7}$$

where

$$c_1 = \sqrt{p_1'(\rho_1)}, \qquad c_2 = \sqrt{p_2'(\rho_2)}, \tag{4.1.8}$$

are the speeds of sound in each phase. The system is hyperbolic (i.e. the corresponding family of right eigenvectors spans $\mathbb{R}^5$) if and only if $\alpha_1(1-\alpha_1) \neq 0$ and $|V_I - u_k| \neq c_k$ for both $k = 1$ and $k = 2$. In addition, the fields associated with the eigenvalues $\{\sigma_i\}_{i=2..5}$ are genuinely non linear.

Proof. The proof follows from classical calculations that are left to the reader. □

4.1.1 Classical Closure laws for the pair (V_I, P_I)

Choice of V_I: In the existing literature, a classical choice for the interfacial velocity is

$$V_I^c = (1-\mu)u_1 + \mu u_2, \quad \mu = \frac{\beta\alpha_1\rho_1}{\beta\alpha_1\rho_1 + (1-\beta)\alpha_2\rho_2}, \quad \beta \in [0,1]. \tag{4.1.9}$$

This choice is driven by several considerations among which a consistency requirement that states that ($u_1 = u_2 \Rightarrow V_I^c = u_1 = u_2$). An other important property which is often required is the linear degeneracy of the associated field. In the original model introduced by Baer and Nunziato [3], where a mixture of a dilute and a dominant phase is considered, the interfacial velocity is equal to the velocity of the dilute phase. This corresponds to taking a constant coefficient $\beta \equiv 1$ if phase 1 is the dilute phase (or symmetrically $\beta \equiv 0$ if phase 2 is dilute). This choice ensures the linear degenaracy of the field associated with $\sigma_1(\mathbb{U}) = V_I^c$. In [7], the authors prove that the choice $\beta \equiv \frac{1}{2}$ also provides a linearly degenerate field for $\sigma_1(\mathbb{U})$. In a recent work [6], the coefficient β is driven by an additional PDE of the form

$$\partial_t\beta + W_I(\mathbb{U},\beta)\partial_x\beta = s(\beta,\mathbb{U}), \tag{4.1.10}$$

while still ensuring the linear degeneracy of the $\sigma_1(\mathbb{U})$-field.

Choice of P_I: Once the choice for the closure of V_I is made in the form (4.1.9), the closure for the interfacial pressure P_I may be derived by energy considerations. Indeed for every pair (V_I, P_I) the following energy equation is satisfied by the smooth solutions of system (4.1.2) with $\mathbf{S}(\mathbb{U}) = 0$:

Proposition 4.1.2. *Denoting $E_k := \frac{u_k^2}{2} + e_k(\tau_k)$, the phasic energies, where the function $\tau \mapsto e_k(\tau)$ is such that $e_k' = -\mathcal{P}_k$, the smooth solutions of the homogeneous part of system (4.1.2) (i.e. assuming $\boldsymbol{S}(\mathbb{U}) = 0$) satisfy the equality:*

$$\begin{array}{ll} \partial_t \left\{ \sum_{k=1}^2 \alpha_k \rho_k E_k \right\} & + \partial_x \left\{ \sum_{k=1}^2 \alpha_k (\rho_k E_k + p_k(\rho_k)) u_k \right\} \\ & + \Big(p_1 u_1 - p_2 u_2 - P_I(u_1 - u_2) - V_I(p_1 - p_2) \Big) \partial_x \alpha_1 = 0. \end{array} \tag{4.1.11}$$

Hence, if P_I is chosen according to

$$P_I^c = \mu p_1 + (1 - \mu) p_2, \tag{4.1.12}$$

where μ is the same as in the definition (4.1.9) of V_I, then the total energy is conserved.

4.1.2 Closure laws for $\mathbf{S}(\mathbb{U})$ and stabilization effects

A first physical effect of the source term $\mathbf{S}(\mathbb{U})$ is to bring the phasic pressures and velocities towards an equilibrium by deacreasing the relative pressure between the phases $p_1 - p_2$ and the relative velocity $u_1 - u_2$. One classical choice in the existing literature (see [8]) for the coefficients Θ_p and Θ_u is

$$\Theta_p = \frac{\alpha_1 \alpha_2}{\tau_p (p_1 + p_2)}, \tag{4.1.13}$$

$$\Theta_u = \frac{1}{\tau_u} \frac{(\alpha_1 \rho_1)(\alpha_2 \rho_2)}{\alpha_1 \rho_1 + \alpha_2 \rho_2}, \tag{4.1.14}$$

where τ_p and τ_u are two characteristic times of the pressure and velocity relaxation processes. As $\Theta_p > 0$ and $\Theta_u > 0$, the source term acts as a relaxation term which deacreases the relative pressure $p_1 - p_2$ and the relative velocity $u_1 - u_2$.

Another important feature of these relaxation source terms is to come up with a dissipative effect on the model. Indeed, the following property is satisfied by system (4.1.2):

Proposition 4.1.3. *Considering the closure laws (4.1.9)-(4.1.12) for the pair (V_I, P_I), the smooth solutions of system (4.1.2) satisfy the equality:*

$$\partial_t \left\{ \sum_{k=1}^2 \alpha_k \rho_k E_k \right\} + \partial_x \left\{ \sum_{k=1}^2 \alpha_k (\rho_k E_k + p_k(\rho_k)) u_k \right\} = -\Theta_p (p_1 - p_2)^2 - \Theta_u (u_1 - u_2)^2, \tag{4.1.15}$$

while the entropy-weak solutions satisfy the inequality

$$\partial_t \left\{ \sum_{k=1}^2 \alpha_k \rho_k E_k \right\} + \partial_x \left\{ \sum_{k=1}^2 \alpha_k (\rho_k E_k + p_k(\rho_k)) u_k \right\} \leq -\Theta_p (p_1 - p_2)^2 - \Theta_u (u_1 - u_2)^2. \tag{4.1.16}$$

Hence, the coefficients Θ_p and Θ_u being positive, $\mathbf{S}(\mathbb{U})$ dissipates the total energy of the mixture.

4.1.3 Dissipative correction of the closure laws (V_I, P_I)

In the sequel, we assume a zero source term $\mathbf{S}(\mathbb{U}) = 0$, so that the system of interest is homogeneous and reads

$$\partial_t \mathbb{U} + \partial_x \mathbf{F}(\mathbb{U}) + \mathbf{C}(\mathbb{U})\partial_x \alpha_1 = 0, \quad x \in \mathbb{R},\ t > 0. \tag{4.1.17}$$

Among all the dissipative processes that can be added to the model, we explore some dissipative correction of the classical closure laws for (V_I, P_I) that may ensure bounded solutions in the regime of vanishing phases. We recall the classical pairs

$$V_I^c = (1-\mu)u_1 + \mu u_2, \quad P_I^c = \mu p_1 + (1-\mu)p_2, \quad \text{with } \mu \in [0,1]. \tag{4.1.18}$$

Such classical pairs (4.1.18) satisfy the Leibniz rule :

$$p_1 u_1 - p_2 u_2 = P_I^c(u_1 - u_2) + V_I^c(p_1 - p_2), \tag{4.1.19}$$

which actually implies energy conservation across the void fraction's wave as already seen. We propose a simple dissipative correction of the pairs (4.1.18) which is achieved introducing the following symmetric matrix

$$\mathcal{D} = \begin{pmatrix} b\, D_u & d \\ d & D_\pi / b \end{pmatrix}. \tag{4.1.20}$$

Here $b > 0$ stands for some frozen Lagrangian sound speed. Then parameters D_u, D_π and d are dimensionless numbers to be prescribed so that the symmetric matrix $\mathcal{D}$ is non-negative :

$$D_u \geq 0, \quad D_\pi \geq 0, \quad D_u D_\pi - d^2 \geq 0. \tag{4.1.21}$$

The interplay between the matrix $\mathcal{D}$ and the weight μ in (4.1.18) will actually ask for a slightly strengthened condition introduced on due time. The interfacial pairs we promote then read :

$$\begin{pmatrix} V_I \\ P_I \end{pmatrix} = \begin{pmatrix} V_I^c \\ P_I^c \end{pmatrix} + \text{sign}(-\partial_x \alpha) \begin{pmatrix} d & D_\pi / b \\ b\, D_u & d \end{pmatrix} \begin{pmatrix} u_1 - u_2 \\ p_1 - p_2 \end{pmatrix}, \tag{4.1.22}$$

where

$$\text{sign}(-\partial_x \alpha) = \begin{cases} -1, & \text{if } \partial_x \alpha > 0, \\ +1, & \text{otherwise.} \end{cases} \tag{4.1.23}$$

The dissipative nature of the proposed interfacial pairs (4.1.22) is revealed by the following preliminary result.

Lemma 4.1.4. *Assuming the non-negative condition (4.1.21) on the symmetric matrix $\mathcal{D}$, the closure (4.1.22) for the interfacial velocity and pressure decreases the energy in the sense that the smooth solutions od system (4.1.17) satisfy :*

$$\partial_t \left\{ \sum_{k=1}^{2} \alpha_k \rho_k E_k \right\} + \partial_x \left\{ \sum_{k=1}^{2} \alpha_k (\rho_k E_k + p_k(\rho_k)) u_k \right\} = -\Big(u_1 - u_2, p_1 - p_2\Big) \mathcal{D} \begin{pmatrix} u_1 - u_2 \\ p_1 - p_2 \end{pmatrix} |\partial_x \alpha_1| \leq 0. \tag{4.1.24}$$

Proof. Smooth solutions of system (4.1.17) are easily seen to obey the following balance energy law for each phase

$$\partial_t \alpha_k \rho_k E_k + \partial_x \alpha_k (\rho_k E_k + p_k(\rho_k)) u_k + \Big(p_k u_k - P_I u_k - V_I p_k \Big) \partial_x \alpha_k = 0. \tag{4.1.25}$$

Summing these two equations gives the expected result

$$\begin{array}{rcl} \partial_t \left\{ \sum_{k=1}^2 \alpha_k \rho_k E_k \right\} & + & \partial_x \left\{ \sum_{k=1}^2 \alpha_k (\rho_k E_k + p_k(\rho_k)) u_k \right\} \\ & = & -\Big(p_1 u_1 - p_2 u_2 - P_I (u_1 - u_2) - V_I (p_1 - p_2) \Big) \partial_x \alpha_1 \\ & = & -\Big((P_I^c - P_I)(u_1 - u_2) + (V_I^c - V_I)(p_1 - p_2) \Big) \partial_x \alpha_1 \\ & = & +\Big(b\ D_u (u_1 - u_2)^2 + \dfrac{D_\pi}{b} (p_1 - p_2)^2 + 2d (u_1 - u_2)(p_1 - p_2) \Big) \ \Big(s \partial_x \alpha_1 \Big) \\ & = & -\Big(u_1 - u_2, p_1 - p_2 \Big) \mathcal{D} \begin{pmatrix} u_1 - u_2 \\ p_1 - p_2 \end{pmatrix} |\partial_x \alpha_1| \end{array} \tag{4.1.26}$$

where we have successively used the Leibniz's rule (4.1.19) verified by the classical pair (V_I^c, P_I^c), the definition (4.1.22) of the modified interfacial closure (V_I, P_I) together with the sign of s prescribed in (4.1.23) so that $\Big(s \partial_x \alpha_1 \Big) = -|\partial_x \alpha_1|$, and at last the non-negative assumption (4.1.21) on the matrix $\mathcal{D}$. □

Similar dissipative closure laws for the pair (V_I, P_I) were proposed in previous works [10, 1, 9]. The correction we introduce here provides a general framework by considering the positive matrix $\mathcal{D}$.

4.2 An operator splitting method for the Baer-Nunziato model

In this section, we propose a numerical method for approximating the solutions of the homogeneous system (4.1.17). The main objective is to implement a method which allows a stable extension of the solution to the regimes of vanishing phases, by taking advantage of the new closure laws introduced in (4.1.22).

We start by writing the fluid transport in the frame of the V_I-wave which amounts to shifting the transport velocities by the quantity V_I:

$$\begin{array}{l} \partial_t \alpha_1 = 0, \\ \partial_t (\alpha_k \rho_k) + \partial_x (\alpha_k \rho_k (u_k - V_I)) = 0, \qquad\qquad k \in \{1, 2\}. \\ \partial_t (\alpha_k \rho_k u_k) + \partial_x (\alpha_k \rho_k u_k (u_k - V_I) + \alpha_k p_k) - P_I \partial_x \alpha_k = 0, \end{array} \tag{4.2.1}$$

After solving system (4.2.1), going back to the original frame is done through solving

$$\begin{array}{l} \partial_t \alpha_k + V_I \partial_x \alpha_k = 0, \\ \partial_t (\alpha_k \rho_k) + \partial_x (\alpha_k \rho_k V_I) = 0, \qquad\qquad k \in \{1, 2\}. \\ \partial_t (\alpha_k \rho_k u_k) + \partial_x (\alpha_k \rho_k u_k V_I) = 0. \end{array} \tag{4.2.2}$$

One first advantage of this decomposition, is that the void fractions α_k are stationary in the first step which eases the resolution of (4.2.1) while the last step (4.2.2) can be suitably approximated even in the regimes of vanishing phases $\alpha_k \to 0$ as it is shown in section 4.5. Observe that system (4.2.1) has similar characteristic features as system (4.1.17). Indeed, the system is still hyperbolic and the acoustic waves for instance are still genuinely non-linear. The only difference is that the V_I-wave whose nature depends on the chosen closure law for V_I is replaced here by a standing wave which is always linearly degenerate.

Actually we do not consider the approximation of system (4.2.1) directly. Inspired by the Lagrange-projection method for Euler's equations, we rather operate a further splitting of system (4.2.1) based on a separate treatment of fast propagation speeds related to the acoustic waves, and slow propagation speeds linked with the transport by $u_k - V_I$. Eventually, this further decomposition is aimed at designing a large time-step method by treating the acoustic effects with an implicit scheme while keeping a sensible precision for the appoximation of the material waves by treating the slow propagation speeds with an explicit scheme. This approach is similar to that studied in [4]. The decomposition of system (4.2.1) is motivated by the simple calculation

$$
\begin{aligned}
&\partial_t \alpha_1 = 0,\\
&\partial_t(\alpha_k\rho_k) + \rho_k\partial_x(\alpha_k u_k) - (\rho_k V_I)\partial_x\alpha_k + \alpha_k(u_k - V_I)\partial_x\rho_k - \alpha_k\rho_k\partial_x V_I = 0,\\
&(\alpha_k\rho_k)\partial_t u_k + \alpha_k\partial_x p_k + (p_k - P_I)\partial_x\alpha_k + (\alpha_k\rho_k)(u_k - V_I)\partial_x u_k + u_k \underbrace{\{\partial_t\alpha_k\rho_k + \partial_x\alpha_k\rho_k u_k\}}_{=0} = 0,
\end{aligned}
$$

which yields the following decomposition:

Lagrange step: propagation of acoustic waves due to pressure and phase fraction disequilibrium:

$$
(\mathscr{BN}_1) \qquad \begin{aligned}
&\partial_t \alpha_1 = 0,\\
&\partial_t \alpha_k\rho_k + \rho_k\partial_x(\alpha_k u_k) - (\rho_k V_I)\partial_x\alpha_k = 0, \qquad k \in \{1,2\}\\
&(\alpha_k\rho_k)\partial_t u_k + \alpha_k\partial_x p_k + (p_k - P_I)\partial_x\alpha_k = 0.
\end{aligned}
$$

Projection step: propagation of material waves due to the fluid motion:

$$
(\mathscr{BN}_2) \qquad \begin{aligned}
&\partial_t \alpha_1 = 0,\\
&\partial_t \rho_k + (u_k - V_I)\partial_x\rho_k - \rho_k\partial_x V_I = 0, \qquad k \in \{1,2\}\\
&\partial_t u_k + (u_k - V_I)\partial_x u_k = 0.
\end{aligned}
$$

Remap step: going back to the original frame:

$$
(\mathscr{BN}_3) \qquad \begin{aligned}
&\partial_t \alpha_k + V_I\partial_x\alpha_k = 0,\\
&\partial_t(\alpha_k\rho_k) + \partial_x(\alpha_k\rho_k V_I) = 0, \qquad k \in \{1,2\}.\\
&\partial_t(\alpha_k\rho_k u_k) + \partial_x(\alpha_k\rho_k u_k V_I) = 0.
\end{aligned}
$$

Before precisely describing the treatment of each step, let us emphasize a crucial point which actually led to considering the fluid motion in the frame of V_I. In the second step ($\mathscr{BN}_2$), the

quantities ρ_k and u_k evolve independently of α_k. This crucial feature clearly allows to consider vanishing phase fractions α_k since the latter do not influence the updating of ρ_k and u_k in this step. It is also shown in section 4.5 that the treatement of vanishing phase cases in the third step ($\mathscr{BN}_3$) is rather easy using an adaptation of the classical upwind scheme. Actually, the main difficulty is to approximate the solutions of system ($\mathscr{BN}_1$) while ensuring bounded solutions in the regimes of small void fractions. To this extent the key tool is the dissipative corrections of the (V_I, P_I) closure laws introduced in section 4.1.3.

Numerical approximation

Let us first introduce some classical notations for the numerical approximation. Let Δt be the time step and Δx the space step, which we assume here to be constant for simplicity in the notations. In the sequel we denote $\lambda = \frac{\Delta t}{\Delta x}$. The space is partitioned into cells

$$\mathbb{R} = \bigcup_{j\in\mathbb{Z}} C_j \quad \text{with} \quad C_j = [x_{j-\frac{1}{2}}, x_{j+\frac{1}{2}}[, \quad \forall j \ \in \mathbb{Z},$$

where $x_{j+\frac{1}{2}} = (j+\frac{1}{2})\Delta x$ are the cell interfaces. We also denote $x_j = j\Delta x$ the center of cell C_j. At the discrete times $t^n = n\Delta t$, the solution is approximated on each cell C_j by a constant value denoted by

$$\mathbb{U}_j^n = \left((\alpha_1)_j^n, (\alpha_1\rho_1)_j^n, (\alpha_1\rho_1 u_1)_j^n, (\alpha_2\rho_2)_j^n, (\alpha_2\rho_2 u_2)_j^n\right)^T.$$

Before giving the precise description of the fractional step method, we state the following result which summarizes the main properties of the scheme:

Theorem 4.2.1. *Under some natural CFL restriction (see (4.3.60), (4.3.61), (4.4.5), (4.4.6) and (4.5.4)), and a Whitham-like condition (see (4.3.56)), the fractional step numerical scheme presented in this paper has the following properties:*

(i) It preserves the maximum principle on the phase fractions α_k.

(ii) It preserves positive values of the densities ρ_k.

(iii) The discretization of the partial masses $\alpha_k\rho_k$ is conservative.

(iv) The discretization of the total momentum $\alpha_1\rho_1 u_1 + \alpha_2\rho_2 u_2$ is conservative.

(v) The physical quantities $(\rho_k)_j^n$ and $(u_k)_j^n$ have finite values even in the regime of vanishing phases.

Proof. The result follows from Propositions 4.3.9, 4.4.1, and 4.5.2 stated in sections 4.3 and 4.4 and 4.5 below as well as Proposition 4.6.3. □

In the following three sections, we describe the fractional-step procedure associated with the time operator-splitting method in order to calculate the values of the approximate solution at time t^{n+1}, $(\mathbb{U}_j^{n+1})_{j\in\mathbb{Z}}$ from those at time t^n. In section 4.3 we provide an extensive analysis which proves the existence of bounded approximate solutions for the first step ($\mathscr{BN}_1$). Section 4.4 deals with the material transport step ($\mathscr{BN}_2$) and finally, in section 4.5 we consider the last step ($\mathscr{BN}_3$).

4.3 Analysis and numerical treatment of the first step

For regular solutions, the first step $(\mathscr{BN}_1)$ is equivalent to

$$(\mathscr{BN}_1)\qquad \begin{aligned} &\partial_t \alpha_1 = 0,\\ &(\alpha_k\rho_k)\partial_t\tau_k - \alpha_k\partial_x u_k - (u_k - V_I)\partial_x\alpha_k = 0,\\ &(\alpha_k\rho_k)\partial_t u_k + \alpha_k\partial_x p_k + (p_k - P_I)\partial_x\alpha_k = 0, \end{aligned} \qquad k\in\{1,2\}$$

where $\tau_k = \rho_k^{-1}$. Dividing the last two equations by $\alpha_k = \alpha_k(x)$ and "freezing" the densities ρ_k before the time-derivatives to their initial values yields the following system which is still called $(\mathscr{BN}_1)$ with little abuse in the notation.

$$(\mathscr{BN}_1)\qquad \begin{aligned} &\partial_t \alpha_1 = 0,\\ &(\rho_k)^0\partial_t\tau_k - \partial_x u_k - (u_k - V_I)\frac{\partial_x\alpha_k}{\alpha_k} = 0,\\ &(\rho_k)^0\partial_t u_k + \partial_x \pi_k + (p_k - P_I)\frac{\partial_x\alpha_k}{\alpha_k} = 0, \end{aligned} \qquad k\in\{1,2\}.$$

With a heuristic argument we can see that in the regimes of small phase fractions α_k, the solution has to ensure small values of $u_k - V_I$ and $p_k - P_I$ in order to remain bounded.

4.3.1 A relaxation approximation

We choose to treat this first step with a relaxation scheme. For this purpose, we introduce the following relaxation system which relaxes towards $(\mathscr{BN}_1)$ in the limit $\varepsilon \to 0$:

$$\partial_t \alpha_1 = 0, \tag{4.3.1}$$

$$(\rho_k)^0\partial_t\tau_k - \partial_x u_k - (u_k - V_I)\frac{\partial_x\alpha_k}{\alpha_k} = 0, \tag{4.3.2}$$

$$(\rho_k)^0\partial_t u_k + \partial_x \pi_k + (\pi_k - \Pi_I)\frac{\partial_x\alpha_k}{\alpha_k} = 0, \tag{4.3.3}$$

$$(\rho_k)^0\partial_t \frac{\pi_k}{a_k^2} + \partial_x(u_k) + (u_k - V_I)\frac{\partial_x\alpha_k}{\alpha_k} = \frac{1}{\varepsilon}\left(p_k(\rho_k) - \pi_k\right). \tag{4.3.4}$$

π_k is an additional unknown which relaxes towards the actual pressure p_k as $\varepsilon \to 0$ and whose evolution is governed by the additional partial differential equation (4.3.4). The numbers $a_k > 0$ are two numerical parameters that need to be taken large enough so as to ensure the stability of the relaxation approximation in the regime of small ε. Typically, a_k must follow the so-called Whitham condition:

$$a_k^2 > \max_{\tau_k}\left(-\frac{\partial p_k}{\partial \tau_k}(\tau_k)\right), \qquad k\in\{1,2\}, \tag{4.3.5}$$

where the max is taken over all the specific volumes $\tau_k = \rho_k^{-1}$ in the solution of (4.3.1)-(4.3.4). We refer to [2] and [5] for a related framework.

Let us now focus on the convective part of this relaxation system which reads:

$$(\widetilde{\mathscr{BN}_1)} \qquad \begin{aligned} &\partial_t \alpha_1 = 0, \\ &(\rho_k)^0 \partial_t \tau_k - \partial_x u_k - (u_k - V_I)\frac{\partial_x \alpha_k}{\alpha_k} = 0, \\ &(\rho_k)^0 \partial_t u_k + \partial_x \pi_k + (\pi_k - \Pi_I)\frac{\partial_x \alpha_k}{\alpha_k} = 0, \\ &(\rho_k)^0 \partial_t \frac{\pi_k}{a_k^2} + \partial_x (u_k) + (u_k - V_I)\frac{\partial_x \alpha_k}{\alpha_k} = 0. \end{aligned} \qquad k \in \{1,2\}.$$

Denoting $\mathbb{W} = (\alpha_1, \tau_1, u_1, \pi_1, \tau_2, u_2, \pi_2)$ the enlarged vector of unknowns, it is expected to belong to the phase state

$$\Omega = \left\{ \mathbb{W} \in \mathbb{R}^7, \alpha_1 \in (0,1), \tau_k > 0, k \in \{1,2\} \right\}. \tag{4.3.6}$$

We are mostly interested in the Riemann problem associated with an initial condition:

$$\mathbb{W}(x, t=0) = \begin{cases} \mathbb{W}_L, & \text{if } x < 0, \\ \mathbb{W}_R, & \text{if } x > 0. \end{cases} \tag{4.3.7}$$

To this end, a first important result concerns the hyperbolicity of $(\widetilde{\mathscr{BN}_1})$:

Proposition 4.3.1. *For all state vector $\mathbb{W}$ in Ω_r, system $(\widetilde{\mathscr{BN}_1})$ has five real eigenvalues which are $-a_k/(\rho_k)^0$, 0, $a_k/(\rho_k)^0$, $k \in \{1,2\}$. The system is hyperbolic (i.e. the corresponding family of eigenvectors spans the whole space $\mathbb{R}^7$) if and only if $\alpha_1 \alpha_2 \neq 0$. Moreover, all the characteristic fields are linearly degenerate.*

Proof. The proof is left to the reader. □

We can see that the resonance due to the interaction between the acoustic waves and the V_I-wave has disappeared, and only the resonance implied by vanishing phases remains. This is due to the splitting procedure that has separated the fast phenomena from the slow ones. As a consequence, as long as $(\alpha_k)_L \neq 0$ and $(\alpha_k)_R \neq 0$ for $k \in \{1,2\}$, the solution of the Riemann problem consists in six constant states separated by five contact discontinuities. The jump relations across each contact discontinuity are given by the Riemann invariants of the corresponding wave. In the sequel, we construct this solution and we study its asymptotic behavior as the ratios $(\alpha_1)_L/(\alpha_1)_R$, $(\alpha_2)_L/(\alpha_2)_R$ (or the inverse ratios) go to infinity. Actually, in order for the solution to remain bounded in these regimes we chose to introduce the announced dissipative corrections to the classical closure laws (V_I^c, Π_I^c).

4.3.2 Dissipative closure laws for (V_I, Π_I)

In order to ensure stable approximations in the regimes of small α_k, we seek to construct solutions to the Riemann problem which are uniformly bounded even for vanishing values of the initial void fractions $(\alpha_k)_L$ and $(\alpha_k)_R$.

$$\overline{\Omega}_r^{\alpha} = \left\{ \mathbb{W} \in \mathbb{R}^7, \alpha_1 \in [0,1], \tau_k > 0, k \in \{1,2\} \right\}. \tag{4.3.8}$$

In this purpose, we introduce a dissipative correction of the classical interfacial pairs

$$V_I^c = (1-\mu)u_1 + \mu u_2, \quad \Pi_I^c = \mu\pi_1 + (1-\mu)\pi_2, \quad \text{with } \mu \in [0,1]. \tag{4.3.9}$$

Dissipation is achieved introducing the following symmetric matrix

$$\mathcal{D} = \begin{pmatrix} b\, D_u & d \\ d & D_\pi/b \end{pmatrix}. \tag{4.3.10}$$

Here $b > 0$ stands for some frozen Lagrangian sound speed, *i.e.* b has the dimension of a_1 and a_2, and will be chosen later on. Then parameters D_u, D_π and d are dimensionless numbers to be prescribed for each Riemann data for $(\widetilde{\mathscr{BN}}_1)$ so that the symmetric matrix $\mathcal{D}$ is non-negative :

$$D_u \geq 0, \quad D_\pi \geq 0, \quad D_u D_\pi - d^2 \geq 0. \tag{4.3.11}$$

The interplay between the matrix $\mathcal{D}$ and the weight μ in (4.3.9) will actually ask for a slightly strengthened condition introduced on due time. The interfacial pairs we promote then read :

$$\begin{pmatrix} V_I \\ \Pi_I \end{pmatrix} = \begin{pmatrix} V_I^c \\ \Pi_I^c \end{pmatrix} + s \begin{pmatrix} d & D_\pi/b \\ b\, D_u & d \end{pmatrix} \begin{pmatrix} u_1 - u_2 \\ \pi_1 - \pi_2 \end{pmatrix}, \tag{4.3.12}$$

where s is the sign of $-\partial_x \alpha_1$ in the Riemann solution, namely

$$s = \begin{cases} -1, & \text{if } (\alpha_1)_L \leq (\alpha_1)_R, \\ +1, & \text{otherwise.} \end{cases} \tag{4.3.13}$$

Note that the number μ in the definition of (V_I^c, Π_I^c) is assumed to be constant in both the space and time variables for each Riemann problem. This is an important property for the determination of the solution.

Remark 4.3.1. *Let us again underline that the proper definition of μ and $\mathcal{D}$ is to be performed for each Riemann data. For a given Riemann problem, those coefficients are given real parameters but whose values depend at least on the given void fractions $(\alpha_1)_L$ and $(\alpha_1)_R$. For simplicity in the notations, such a dependence has been skipped but has to be kept in mind.*

The dissipative nature of the proposed interfacial pairs (4.3.12) is revealed by the following preliminary result.

Property 4.3.2. *Assuming the non-negative condition (4.3.11) on the symmetric matrix $\mathcal{D}$, the closure (4.3.12) for the interfacial velocity and pressure decreases the energy*

$$\partial_t \Big\{ \sum_{k=1,2} \alpha_k \rho_k \big(\frac{u_k^2}{2} + \frac{\pi_k^2}{2a_k^2}\big) \Big\} + \partial_x \sum_{k=1,2} (\alpha_k u_k \pi_k) = -\Big(u_1 - u_2, \pi_1 - \pi_2\Big)\mathcal{D} \begin{pmatrix} u_1 - u_2 \\ \pi_1 - \pi_2 \end{pmatrix} |\partial_x \alpha_1| \leq 0. \tag{4.3.14}$$

Proof. Smooth solutions of system $(\widetilde{\mathscr{BN}}_1)$ are easily seen to obey the following balance energy law for each phase

$$\partial_t \zeta_k + \partial_x(\alpha_k u_k \pi_k) + \Big(\pi_k u_k - \Pi_I u_k - V_I \pi_k\Big)\partial_x \alpha_k = 0, \quad \zeta_k = \alpha_k \rho_k \big(\frac{u_k^2}{2} + \frac{\pi_k^2}{2a_k^2}\big), \quad k = 1, 2. \tag{4.3.15}$$

Summing these two equations gives the expected result

$$\begin{aligned}\partial_t \sum_{k=1,2} \zeta_k \quad &+\partial_x \textstyle\sum_{k=1,2}(\alpha_k u_k \pi_k) = -\Big(\pi_1 u_1 - \pi_2 u_2 - \Pi_I(u_1-u_2) - V_I(\pi_1-\pi_2)\Big)\partial_x\alpha_1,\\ &= -\Big((\Pi_I^c - \Pi_I)(u_1-u_2) + (V_I^c - V_I)(\pi_1-\pi_2)\Big)\partial_x\alpha_1,\\ &= +\Big(b\, D_u(u_1-u_2)^2 + \frac{D_\pi}{b}(\pi_1-\pi_2)^2 + 2d(u_1-u_2)(\pi_1-\pi_2)\Big)\ \Big(s\partial_x\alpha_1\Big),\\ &\leq 0\end{aligned} \tag{4.3.16}$$

where we have successively used the Leibniz's rule

$$\pi_1 u_1 - \pi_2 u_2 = \Pi_I^c(u_1-u_2) + V_I^c(\pi_1-\pi_2), \tag{4.3.17}$$

verified by the classical pair (V_I^c, Π_I^c), the definition (4.3.12) of the modified interfacial closure (V_I, Π_I) together with the sign of s prescribed in (4.3.13) so that $\Big(s\partial_x\alpha_1\Big) = -|\partial_x\alpha_1|$, and at last the non-negative assumption (4.3.11) on the matrix $\mathcal{D}$. Observe that this inequality also holds for weak solutions in a convenient sense thanks to the linear degeneracy of all the fields of the hyperbolic model $(\widetilde{\mathscr{BN}_1})$. □

4.3.3 Jump relations for the Riemann problem

Equipped with these corrected closure laws, we may now provide a careful study of the jump relations defining the various waves of the Riemann solution. In order to shorten the notations, let us first set

$$\alpha(\xi) := \alpha_1(\xi), \quad \text{so that} \quad \alpha_2(\xi) = (1-\alpha)(\xi), \tag{4.3.18}$$

where ξ denotes the usual self-similar variable. Correspondingly, we denote their left and right traces at the void fraction's standing wave (*i.e.* respectively at 0^- and 0^+) by

$$\alpha^- = \alpha(0^-) \equiv \alpha_L, \quad \alpha^+ = \alpha(0^+) \equiv \alpha_R. \tag{4.3.19}$$

It is also convenient to promote $\Delta u(\xi) = (u_1-u_2)(\xi)$ and $\Delta\pi(\xi) = (\pi_1-\pi_2)(\xi)$ while denoting

$$\Delta u^\pm = (u_1-u_2)(0^\pm), \quad \Delta\pi^\pm = (\pi_1-\pi_2)(0^\pm). \tag{4.3.20}$$

The following proposition displays the Riemann invariants of each wave. For the standing wave, it is convenient to parametrize the associated wave curve by α, with α varying from α^- to α^+. Velocities and pressures along this wave curve are thus functions of the void fraction, $\alpha \mapsto u_k(\alpha)$ and $\alpha \mapsto \pi_k(\alpha)$ with $\alpha \in [\alpha^-, \alpha^+]$ so that by construction, the initial and final values (*i.e.* respectively at $\alpha = \alpha^-$ and $\alpha = \alpha^+$) coincide with the left and right traces of the Riemann solution at the standing wave :

$$u_k(0^-) = u_k(\alpha^-), \quad \pi_k(0^-) = \pi_k(\alpha^-), \quad \text{while} \quad u_k(0^+) = u_k(\alpha^+), \quad \pi_k(0^+) = \pi_k(\alpha^+). \tag{4.3.21}$$

Proposition 4.3.3. *Denoting*

$$L_k = a_k u_k + \pi_k, \quad R_k = a_k u_k - \pi_k, \quad k = 1, 2, \tag{4.3.22}$$

the Riemann invariants of the acoustic waves are given by

$$-a_1/(\rho_1)^0 \ : \qquad \alpha_1,\ \pi_1 + a_1^2\tau_1,\ \pi_2 + a_2^2\tau_2,\ u_2,\ \pi_2,\ L_1. \tag{4.3.23}$$

$$-a_2/(\rho_2)^0 \ : \qquad \alpha_1,\ \pi_1 + a_1^2\tau_1,\ \pi_2 + a_2^2\tau_2,\ u_1,\ \pi_1,\ L_2. \tag{4.3.24}$$

$$+a_2/(\rho_2)^0 \ : \qquad \alpha_1,\ \pi_1 + a_1^2\tau_1,\ \pi_2 + a_2^2\tau_2,\ u_1,\ \pi_1,\ R_2. \tag{4.3.25}$$

$$+a_1/(\rho_1)^0 \ : \qquad \alpha_1,\ \pi_1 + a_1^2\tau_1,\ \pi_2 + a_2^2\tau_2,\ u_2,\ \pi_2,\ R_1. \tag{4.3.26}$$

As for the standing wave, we first define the following quantities parametrized by α *:*

$$I_1(\alpha) = \alpha u_1(\alpha) + (1-\alpha)u_2(\alpha), \quad I_2(\alpha) = \alpha\pi_1(\alpha) + (1-\alpha)\pi_2(\alpha), \tag{4.3.27}$$

$$I_3(\alpha) = \alpha^\mu(1-\alpha)^{1-\mu}\ \Delta u(\alpha), \qquad I_4(\alpha) = \alpha^{1-\mu}(1-\alpha)^\mu\ \Delta\pi(\alpha). \tag{4.3.28}$$

Then, the jump relations across the standing wave are defined by a set of ODEs: I_1 *and* I_2 *are two preserved Riemann invariants through the standing wave:*

$$\frac{dI_1(\alpha)}{d\alpha} = \frac{dI_2(\alpha)}{d\alpha} = 0, \quad \alpha \in [\alpha^-, \alpha^+], \tag{4.3.29}$$

while I_3 *and* I_4 *solve the* 2×2 *ODE system*

$$\frac{d}{d\alpha}\begin{pmatrix} I_3(\alpha) \\ I_4(\alpha)\end{pmatrix} = \frac{s}{\alpha(1-\alpha)}\begin{pmatrix} d & D_\pi/(bg(\alpha)) \\ bg(\alpha)D_u & d\end{pmatrix}\begin{pmatrix} I_3(\alpha) \\ I_4(\alpha)\end{pmatrix}, \quad \alpha\in[\alpha^-,\alpha^+] \tag{4.3.30}$$

with

$$g(\alpha) = \Big(\frac{\alpha}{1-\alpha}\Big)^{2\theta}, \quad \theta = \frac{1-2\mu}{2}, \tag{4.3.31}$$

and where the initial states $I_3(\alpha^-)$, $I_4(\alpha^-)$ *are defined from (4.3.21).*

4.3.4 Boundedness of the solution in the regime of vanishing phases

We may now display sufficient and necessary conditions on the corrected pressure laws for the boudedness of the solution in the asymptotic regimes of vanishing void fractions. Actually, in the first place we restrict the study to the case where $a_1 = a_2 \equiv a$, since this assumption largely simplifies the algebraic manipulations.

Proposition 4.3.4. *Assume that* $a_1 = a_2 \equiv a$ *and define the lagrangian speed* b *in the dissipation matrix* $\mathcal{D}$ *(4.3.10) to be equal to* $b = a\sqrt{D_\pi}/\sqrt{D_u}$*. Define from the weight* $\mu\in[0,1]$ *in the definition (4.3.9) of* (V_I^c, P_I^c) *:*

$$\theta = \frac{1-2\mu}{2} \tag{4.3.32}$$

as well as the dimensionless exponents

$$\Lambda_- = d - s\theta - \sqrt{D_uD_\pi + \theta^2}, \quad \Lambda_+ = d - s\theta + \sqrt{D_uD_\pi + \theta^2}. \tag{4.3.33}$$

The solution of the Riemann problem $(\widetilde{\mathscr{B}\mathscr{N}}_1)$*-(4.3.7) remains bounded in the regime of vanishing phases if and only if the following two functions* h_+, $1/h_-$ *of* $(\alpha^-,\alpha^+)\in(0,1)\times(0,1)$ *remain*

bounded as α^-/α^+, $(1-\alpha^-)/(1-\alpha^+)$ *(or the inverse ratios) go to infinity*

$$h_+(\alpha^-,\alpha^+) = \Big(\frac{\alpha^+}{\alpha^-}\Big)^{s\Lambda_+-\mu}\Big(\frac{1-\alpha^+}{1-\alpha^-}\Big)^{-s\Lambda_++\mu-1},$$
$$\frac{1}{h_-}(\alpha^+,\alpha^-) = \Big(\frac{\alpha^+}{\alpha^-}\Big)^{-s\Lambda_-+\mu}\Big(\frac{1-\alpha^+}{1-\alpha^-}\Big)^{+s\Lambda_--\mu+1}. \tag{4.3.34}$$

Assume the following compatibility condition in between μ*, the coefficients of the dissipation matrix* $\mathcal{D}$ *and the sign* s *in (4.3.13)*

$$D_uD_\pi - d^2 + 2s\theta d \geq 0, \tag{4.3.35}$$

then

$$\Lambda^- \leq 0 \leq \Lambda^+, \tag{4.3.36}$$

and $h_+(\alpha^-,\alpha^+)$ *and* $1/h_-(\alpha^-,\alpha^+)$ *are uniformly bounded as* α^- *and* α^+ *run in* $(0,1)$ *provided that the two exponents* Λ^+ *and* Λ^- *verify*

	$\alpha^- \to 0$	$\alpha^+ \to 0$	$\alpha^- \to 1$	$\alpha^+ \to 1$
$\alpha^- \to 0$	$\Lambda^- < -\mu$			$\Lambda^+ > 1-\mu$
$\alpha^+ \to 0$		$\Lambda^+ > \mu$	$\Lambda^- < -(1-\mu)$	
$\alpha^- \to 1$		$\Lambda^+ > \mu$	$\Lambda^- < -(1-\mu)$	
$\alpha^+ \to 1$	$\Lambda^- < -\mu$			$\Lambda^+ > 1-\mu$

Let us then briefly comment on the proposed table. Its main diagonal, starting from the upper left corner to the bottom right one, gives the leading condition on one of the exponents $\Lambda^\pm$: Λ^- has to be sufficiently negative or Λ^+ has to be sufficiently positive, depending on the weight μ. Observe that compatibility requirement (4.3.35) makes relevant the corresponding sign on the exponents $\Lambda^\pm$ since by assumption μ belongs to $[0,1]$. A given diagonal condition on such an exponent is to be read from the phase vanishing assumption stated in the corresponding row. The associated column just states the same limiting behavior. If the other traces of the void fractions stay away from 0 and 1, only the condition stated on the main diagonal has to be met. The situation where the traces $\alpha^\pm$ and $\alpha^\mp$ jump from 0 to 1 is examined in the counter-diagonal of the proposed table. The corresponding element then asks for a new condition on the second exponent. In such an extreme case, Λ^- and Λ^+ must be chosen respectively sufficiently negative and positive, depending on the choice of μ in (4.3.9). For example, let us focus on the first row, stating that α vanishes on the left of the standing wave : $\alpha^- \to 0$ with $\alpha^+/\alpha^- \to \infty$. Since $\alpha^- < \alpha^+$, we have $s = -1$ according to the definition (4.3.13). Boundedness of the mapping $1/h_-(\alpha^-,\alpha^+)$ clearly asks for

$$\mu + \Lambda^- \leq 0, \quad 1 - \mu - \Lambda^- \geq 0. \tag{4.3.37}$$

The second inequality holds true under the compatibility condition (4.3.35) since $\Lambda_- \leq 0$ while $\mu \in [0,1]$. The remaining condition resumes to $\Lambda^- \leq -\mu$. Boundedness of $h_+(\alpha^-,\alpha^+)$ requires the following additional conditions in the limit $\alpha^+ \to 1$:

$$-\mu - \Lambda^+ \leq 0, \quad \mu - 1 + \Lambda^+ \geq 0, \tag{4.3.38}$$

which boils down to $\Lambda^+ \geq 1-\mu$ as expected. Recall that we ask for strict version of the proposed inequalities. The three last rows of Table 1, devoted to other phase vanishing regimes, are derived following similar steps. Details are left to the reader.

Remark 4.3.2. *We underline that an "if and only if statement" is obtained when changing all the strict inequalities expressed in Table 1 into large ones. We indeed promote strict inequalities in these boundedness conditions. As a consequence, both $h_+(\alpha^-, \alpha^+)$ and $1/h_-(\alpha^-, \alpha^+)$ will be seen to go to zero in the corresponding phase vanishing regimes. Such an asymptotic behavior is of interest in the sequel.*

From the definition of the exponents $\Lambda^\pm$ in (4.3.33), it is easily seen that one's favorite closure law for the energy preserving pair (V_I^c, P_I^c) can be corrected, if needed in terms of the underlying weight μ, when choosing $d = 0$ and a large enough product $D_u D_\pi > 0$. Observe that the choice $d = 0$ makes valid the compatibility condition (4.3.35). More precisely, we have the following remarkable result:

Theorem 4.3.5. *Assume $d = 0$, then the two functions h_+ and $1/h_-$ defined in Proposition 4.3.4 are bounded if and only if the following simple condition holds*

$$D_u D_\pi \geq \mu(1-\mu). \tag{4.3.39}$$

Proof. The proof consists in considering each one of the configurations considered in Table 1 (replacing the strict inequalities by large ones). If $\alpha^- \to 0$ for instance, while α^+ remains away from 1, then we study the condition $\Lambda^- \leq -\mu$ with $\Lambda^- = \theta - \sqrt{D_u D_\pi + \theta^2}$ since $d = 0$ and $s = -1$. This gives $\theta + \mu \leq \sqrt{D_u D_\pi + \theta^2}$. Observing that $\theta + \mu = 1/2$ and raising to the power of two, we obtain $\frac{1}{4} \leq D_u D_\pi + \theta^2$. Using again the definition of θ, this is equivalent to $\mu(1-\mu) \leq D_u D_\pi$. If in addition $\alpha^+ \to 1$, one has also to ensure $\Lambda^+ \geq 1 - \mu$ with $\Lambda^+ = \theta + \sqrt{D_u D_\pi + \theta^2}$ since s is still equal to -1. As $1 - \mu - \theta = 1/2$, we clearly obtain the same condition $\mu(1-\mu) \leq D_u D_\pi$. Similar calculations (while being careful for the sign of s) prove the very same result for all the other cells of Table 1. □

Thanks to this very simple expression (4.3.39) we may propose a guideline for the determination of the dissipative correction of the closure laws (V_I, Π_I). Considering the usual closure laws

$$V_I^c = (1-\mu)u_1 + \mu u_2, \quad \mu = \frac{\beta\alpha_1\rho_1}{\beta\alpha_1\rho_1 + (1-\beta)\alpha_2\rho_2}, \quad \beta \in [0,1], \tag{4.3.40}$$

that ensure the linear degeneracy of the V_I-wave, it appears unnecessary to add a further dissipation by taking $D_u D_\pi > 0$. Indeed, in the regimes where α_1 goes to zero or one, this choice of μ goes also to zero or one, which makes condition (4.3.39) to be easily satisfied by simply taking $D_u = D_\pi = 0$, *i.e.* by taking a zero dissipation matrix $\mathcal{D}$. This observation seems to consolidate the requirement of a linearly degenerate field for the phase fraction wave.

For the other closure laws, dissipating appears compulsory in order to guarantee the boundedness of the solution. Of course, as μ belongs to $[0,1]$, any constant values of D_u and D_π larger than $1/2$ suffice. However, it may be judicious to minimize the dissipation since taking non-zero constant values of (D_u, D_π) brings an additional dissipation to the Riemann solution even in the non-problematic regimes where both void fractions α_1 and α_2 are away from zero. Instead, we rather recommend the following procedure:

1. Define a tolerance level L_{Tol} for the number $\delta(\alpha^-, \alpha^+) = \max\big(h_+(\alpha^-, \alpha^+), 1/h_-(\alpha^-, \alpha^+)\big)$.

2. Define the function $D(\delta)$ as follows:

$$D(\delta) := \begin{cases} 0 & \text{if } \delta \leq L_{\text{Tol}}, \\ (1+\kappa)\sqrt{\mu(1-\mu)}(\delta - L_{\text{Tol}}) & \text{if } \delta \in [L_{\text{Tol}}, L_{\text{Tol}}+1], \\ (1+\kappa)\sqrt{\mu(1-\mu)} & \text{if } \delta \geq L_{\text{Tol}}+1, \end{cases} \tag{4.3.41}$$

where κ is a small positive number.

3. Take $d := 0$, $b := a = a_1 = a_2$ and $D_u = D_\pi := D(\delta(\alpha^-, \alpha^+))$.

We may now turn to the proof of Proposition 4.3.4. The following preparatory statement asserts that the Riemann solution for $(\widetilde{\mathscr{B}\mathscr{N}_1})$ is actually bounded as soon as that the relative velocities and pressures (4.3.20) keep finite values at the standing wave. This Lemma actually holds even for non-equal values of a_1 and a_2.

Lemma 4.3.6. *Defining the following Riemann invariants for the extreme waves*

$$L_k = a_k u_{k,L} + \pi_{k,L}, \quad R_k = a_k u_{k,R} - \pi_{k,R}, \quad k = 1, 2. \tag{4.3.42}$$

The left and right traces at the standing wave of the velocities and the pressures read

$$\begin{aligned}
u_2^- &= \frac{1}{2}\Big\{\alpha^+\Big(\Delta u^+ - \frac{1}{a_2}\Delta\pi^+\Big) - \alpha^-\Big(\Delta u^- - \frac{1}{a_2}\Delta\pi^-\Big) + \frac{1}{a_2}(R_2 + L_2)\Big\}, \\
u_2^+ &= \frac{1}{2}\Big\{ -\alpha^+\Big(\Delta u^+ + \frac{1}{a_2}\Delta\pi^+\Big) + \alpha^-\Big(\Delta u^- + \frac{1}{a_2}\Delta\pi^-\Big) + \frac{1}{a_2}(R_2 + L_2)\Big\}, \\
\pi_2^- &= -a_2 u_2^- + L_2, \\
\pi_2^+ &= a_2 u_2^+ - R_2, \\
u_1^- &= \frac{1}{2}\Big\{ -(1-\alpha^+)\Big(\Delta u^+ - \frac{1}{a_1}\Delta\pi^+\Big) + (1-\alpha^-)\Big(\Delta u^- - \frac{1}{a_1}\Delta\pi^-\Big) + \frac{1}{a_1}(R_1 + L_1)\Big\}, \\
u_1^+ &= \frac{1}{2}\Big\{(1-\alpha^+)\Big(\Delta u^+ + \frac{1}{a_1}\Delta\pi^+\Big) - (1-\alpha^-)\Big(\Delta u^- + \frac{1}{a_1}\Delta\pi^-\Big) + \frac{1}{a_1}(R_1 + L_1)\Big\}, \\
\pi_1^- &= -a_1 u_1^- + L_1, \\
\pi_1^+ &= a_1 u_1^+ - R_1.
\end{aligned} \tag{4.3.43}$$

Proof. See Appendix A. □

The next statement displays the formulae of the relative velocities and pressures $\Delta u^\pm$ and $\Delta\pi^\pm$ at the standing wave in the simple case where $a_1 = a_2 \equiv a$.

Proposition 4.3.7. *Assume $a_1 = a_2 \equiv a$ and choose $b := a\sqrt{\frac{D_\pi}{D_u}}$ in the definition (4.3.10) of the dissipation matrix $\mathcal{D}$. Define from the Riemann invariants (4.3.42) of the extreme waves*

$$\Delta L = L_1 - L_2, \quad \Delta R = R_1 - R_2. \tag{4.3.44}$$

Then the relative pressures and velocities at the void fraction's wave are explicitly given by

$$\begin{aligned}
\Delta u^- &= \frac{1}{2a}\Big(\frac{1}{1+\frac{h_+(\alpha_-,\alpha_+)}{h_-(\alpha_-,\alpha_+)}\omega^2}\Big)\Big\{\ \frac{1+\omega^2}{h_-(\alpha_-,\alpha_+)}\Delta R + \Big(1+\omega - \frac{h_+(\alpha_-,\alpha_+)}{h_-(\alpha_-,\alpha_+)}\omega(1-\omega)\Big)\Delta L\Big\},\\
\Delta \pi^- &= \frac{1}{2}\ \Big(\frac{1}{1+\frac{h_+(\alpha_-,\alpha_+)}{h_-(\alpha_-,\alpha_+)}\omega^2}\Big)\Big\{-\frac{1+\omega^2}{h_-(\alpha_-,\alpha_+)}\Delta R + \Big(1-\omega + \frac{h_+(\alpha_-,\alpha_+)}{h_-(\alpha_-,\alpha_+)}\omega(1+\omega)\Big)\Delta L\Big\},
\end{aligned} \tag{4.3.45}$$

with

$$\begin{aligned}
\Delta u^+ &= \frac{1}{2a}\Big(\frac{1}{1+\frac{h_+(\alpha_-,\alpha_+)}{h_-(\alpha_-,\alpha_+)}\omega^2}\Big)\Big\{\ (1+\omega^2)h_+(\alpha_-,\alpha_+)\Delta L + \Big(1-\omega + \frac{h_+(\alpha_-,\alpha_+)}{h_-(\alpha_-,\alpha_+)}\omega(1-\omega)\Big)\Delta R\Big\},\\
\Delta \pi^+ &= \frac{1}{2}\ \Big(\frac{1}{1+\frac{h_+(\alpha_-,\alpha_+)}{h_-(\alpha_-,\alpha_+)}\omega^2}\Big)\Big\{-(1+\omega^2)h_+(\alpha_-,\alpha_+)\Delta L - \Big(1+\omega - \frac{h_+(\alpha_-,\alpha_+)}{h_-(\alpha_-,\alpha_+)}\omega(1-\omega)\Big)\Delta R\Big\}.
\end{aligned} \tag{4.3.46}$$

The proof of this claim comes as a corollary of the general case where $a_1 \neq a_2$ and which is studied thereafter for the sake of completeness. Observe that the proposed formulae clearly highlight that the boundedness conditions expressed on $h_+(\alpha^-,\alpha^+)$ and $1/h_-(\alpha^-,\alpha^+)$ in Proposition 4.3.4 are actually necessary and sufficient conditions.

Proposition 4.3.8. *Let us introduce the following bounded averages of the lagrangian sound speeds a_1 and a_2 as well as the new lagrangian speed r :*

$$\widehat{a}(\alpha^\pm) = (1-\alpha^\pm)a_1 + \alpha^\pm a_2, \quad \frac{\widehat{1}}{a}(\alpha^\pm) = \frac{(1-\alpha^\pm)}{a_1} + \frac{\alpha^\pm}{a_2}, \quad r = b\sqrt{\frac{D_u}{D_\pi}}. \tag{4.3.47}$$

We also define the dimensionless number

$$\omega = \frac{s\theta}{\sqrt{D_u D_\pi + \theta^2} + \sqrt{D_u D_\pi}}, \quad \omega \in [-1,1]. \tag{4.3.48}$$

Then, the relative pressures and velocities at the void fraction's wave are the solution of the 4×4 linear system :

$$\begin{aligned}
&r(1+\omega)\Delta u^+ + (1-\omega)\Delta\pi^+ - h_+(\alpha^-,\alpha^+)\Big\{r(1+\omega)\Delta u^- + (1-\omega)\Delta\pi^-\Big\} = 0\\
&\frac{1}{h_-(\alpha^-,\alpha^+)}\Big\{r(1-\omega)\Delta u^+ - (1+\omega)\Delta\pi^+\Big\} - \Big(r(1-\omega)\Delta u^- - (1+\omega)\Delta\pi^-\Big) = 0\\
&\widehat{a}(\alpha^+)\Delta u^+ - \Delta\pi^+ - \Big(\widehat{a}(\alpha^-)\Delta u^- + \Delta\pi^-\Big) = (R_1 - L_1) - (R_2 - L_2),\\
&-\Delta u^+ + \frac{\widehat{1}}{a}(\alpha^+)\Delta\pi^+ - \Big(\Delta u^- + \frac{\widehat{1}}{a}(\alpha^-)\Delta\pi^-\Big) = -\frac{1}{a_1}(R_1 + L_1) + \frac{1}{a_2}(R_2 + L_2).
\end{aligned} \tag{4.3.49}$$

The associated determinant may be expressed as a second order polynomial in terms of the free parameter $r > 0$:

$$\begin{aligned} det = \quad & (1-\omega^2)\Big(\widehat{\tfrac{1}{a}}(\alpha^+) + \widehat{\tfrac{1}{a}}(\alpha^-)\Big)\Big(1 - \tfrac{h_+(\alpha^-,\alpha^+)}{h_-(\alpha^-,\alpha^+)}\Big)r^2 \\ & + \Big\{2\Big(1 - \widehat{a}(\alpha^+)\widehat{\tfrac{1}{a}}(\alpha^+)\Big)h_+(\alpha^-,\alpha^+) \\ & + \Big(\widehat{a}(\alpha^-)\widehat{\frac{1}{a}}(\alpha^+)(1-\omega)^2 + \widehat{a}(\alpha^+)\widehat{\frac{1}{a}}(\alpha^-)(1+\omega)^2 + 2(1+\omega^2)\Big)\frac{h_+(\alpha^-,\alpha^+)}{h_-(\alpha^-,\alpha^+)} \\ & + \Big(\widehat{a}(\alpha^+)\widehat{\tfrac{1}{a}}(\alpha^-)(1-\omega)^2 + \widehat{a}(\alpha^-)\widehat{\tfrac{1}{a}}(\alpha^+)(1+\omega)^2 + 2(1+\omega^2)\Big)\Big\}r \\ & + (1-\omega^2)\Big(\widehat{a}(\alpha^+) + \widehat{a}(\alpha^-)\Big)\Big(1 - \frac{h_+(\alpha^-,\alpha^+)}{h_-(\alpha^-,\alpha^+)}\Big). \end{aligned} \tag{4.3.50}$$

Proof. See Appendix A. □

It seems out of reach to prove that this determinant never vanishes whatever are the void fractions and whatever is the value of the lagrangian sound speed $r > 0$. Let us first briefly discuss this issue for close values of the void fraction : $|\alpha^+ - \alpha^-| << 1$. Despite dissipation is not required in such cases since both are close to unity, the determinant is seen to be strictly positive since when $\alpha^+ = \alpha^- \equiv \alpha$ with $h + (\alpha, \alpha) = 1/h_-(\alpha, \alpha) = 1$, it resumes to :

$$2\Big\{1 + \widehat{a}(\alpha)\widehat{\frac{1}{a}}(\alpha)\Big((1-\omega)^2 + (1+\omega)^2 + 1 + 2\omega^2\Big)\Big\}r > 0, \tag{4.3.51}$$

as soon as r is strictly positive. Then considering the case of grossly different values of the left and right void fractions. One first notice that

$$\frac{h_+(\alpha_-,\alpha_+)}{h_-(\alpha_-,\alpha^+)} = \Big(\frac{\alpha^+}{\alpha^-}\Big)^{s\left(\Lambda^+ - \Lambda^-\right)}\Big(\frac{1-\alpha^+}{1-\alpha^-}\Big)^{-s\left(\Lambda^+ - \Lambda^-\right)} < 1, \tag{4.3.52}$$

while this ratio gets closer to zero as α^+ and α^- depart from each others. Indeed and according to the compatibility condition (4.3.35), we have $\Lambda^+ - \Lambda^- \geq 0$. Hence in the limit $\alpha^+/\alpha^- \to \infty$ (*i.e.* $\alpha^+ > \alpha^- \to 0$) with $s = -1$ according to the definition (4.3.13) and possibly $1 - \alpha^+/1 - \alpha^- \to 0$ (*i.e.* $\alpha^- < \alpha^+ \to 1$), the estimate (4.3.52) follows. As a consequence, large enough values of r systematically guarantee the unique solvability of the linear problem (4.3.49) provided that $|\omega| < 1$. Observe that this requirement can be readily achieved from the definition (4.3.48) of ω, choosing positive values of D_u, D_π. This explains why we promote strict inequalities in the boundedness conditions stated in Table 1. Observe that as a side effect, we get a much strengthened version of (4.3.52) :

$$\frac{h_+(\alpha_-,\alpha_+)}{h_-(\alpha_-,\alpha^+)} \to 0 \tag{4.3.53}$$

when ratios of void fractions go to infinity, namely when energy dissipation is required. This comes with the property that when $h_+(\alpha_-,\alpha_+)/h_-(\alpha_-,\alpha^+) = \mathcal{O}(\epsilon)$ the determinant (4.3.50) reads :

$$\begin{aligned} & (1-\omega^2)\Big(\widehat{\frac{1}{a}}(\alpha^+) + \widehat{\frac{1}{a}}(\alpha^-)\Big)\, r^2 \\ & + \Big\{\Big(\widehat{a}(\alpha^+)\widehat{\tfrac{1}{a}}(\alpha^-)(1-\omega)^2 + \widehat{a}(\alpha^-)\widehat{\tfrac{1}{a}}(\alpha^+)(1+\omega)^2 + 2(1+\omega^2)\Big)\Big\}\, r \\ & + (1-\omega^2)\Big(\widehat{a}(\alpha^+) + \widehat{a}(\alpha^-)\Big) \\ & + \mathcal{O}(\epsilon). \end{aligned} \tag{4.3.54}$$

Hence in case of real roots for this second order equation in r, the sum and product of roots are respectively negative and positive, so that both real roots must be negative. Since $r > 0$, the linear system (4.3.49) turns solvable for a user-free choice of r.

Of course, the solutions of the linear system (4.3.49) can be given exact formulae. But existence of products in the form $\widehat{a}(\alpha^{\pm}) \times \widehat{\frac{1}{a}}(\alpha^{\pm})$ together with $\widehat{a}(\alpha^{\pm}) \times \widehat{\frac{1}{a}}(\alpha^{\mp})$ make the resulting expressions somewhat cumbersome. In practice, we advocate the use of a linear solver to get numerical values for the relative velocities and pressures under consideration. For completeness, we display in Appendix A the exact expressions so that the reader can get convinced that these solely involve products by $h_+(\alpha_-, \alpha_+)$, $1/h_(\alpha_-, \alpha_+)$ and $h_+(\alpha_-, \alpha_+)/h_-(\alpha_-, \alpha_+)$. These formulae are indeed mandatory for the proof of Proposition 4.3.4. The algebraic situation turns to considerably simplify in the case $a_1 = a_2 \equiv a$. As expected, simplicity arises from the identities $\widehat{a}(\alpha^{\pm}) = a$ together with $\widehat{\frac{1}{a}}(\alpha^{\pm}) = \frac{1}{a}$ so that all the incriminated cumbersome products $\widehat{a}(\alpha)\widehat{\frac{1}{a}}(\alpha)$ boil down to 1.

4.3.5 Numerical approximation of the first step

Let us now describe the numerical treatment of the first step resulting from the relaxation Riemann solver for $(\widetilde{\mathscr{B}\mathscr{N}_1})$. Starting from the given data at time t^n: $\mathbb{U}_j^n$, the updated data at the fictive intermediate time $t^{n+\frac{1}{3}}$: $\mathbb{U}_j^{n+\frac{1}{3}}$ are computed as follows:

1. Take the additional variables $(\pi_k)_j^n$ equal to $p_k\left((\rho_k)_j^n\right)$.

2. Apply the exact Godunov scheme to the relaxation system $(\widetilde{\mathscr{B}\mathscr{N}_1})$ with the initial data

$$(\alpha_1, \tau_k, u_k, \pi_k)(x, t = 0) = (\alpha_1, \tau_k, u_k, \pi_k)_j^n \quad \text{if } x \in [x_{j-\frac{1}{2}}, x_{j+\frac{1}{2}}). \tag{4.3.55}$$

   At this level, as the Riemann problem has to be solved at each interface $x_{j+\frac{1}{2}}$, the numerical parameters a_k should be chosen, interface by interface, so as to satisfy Whitham's condition. In practice, Whitham's condition is replaced for simplicity by the following Whitham-like condition:

$$a_k^2 > \max\left(-\frac{\partial p_k}{\partial \tau_k}\left((\tau_k)_j^n\right), -\frac{\partial p_k}{\partial \tau_k}\left((\tau_k)_{j+1}^n\right)\right), \quad k \in \{1, 2\}. \tag{4.3.56}$$

   This condition is less restrictive than the classical Whitham condition stated in (4.3.5) but it appears that in practice, no instabilities pop up in the scheme.

3. Drop the additional variable π_k by taking

$$\mathbb{U}_j^{n+\frac{1}{3}} = \left((\alpha_1)_j^{n+\frac{1}{3}}, (\alpha_1\rho_1)_j^{n+\frac{1}{3}}, (\alpha_1\rho_1u_1)_j^{n+\frac{1}{3}}, (\alpha_2\rho_2)_j^{n+\frac{1}{3}}, (\alpha_2\rho_2u_2)_j^{n+\frac{1}{3}}\right)^T.$$

Points (1) to (3) provide the following scheme with non-conservative numerical fluxes at the interfaces:

$$(\alpha_1)_j^{n+\frac{1}{3}} = (\alpha_1)_j^n, \tag{4.3.57}$$

$$(\rho_k)_j^n \left((\tau_k)_j^{n+\frac{1}{3}} - (\tau_k)_j^n\right) - \lambda\left((u_k)^-_{j+\frac{1}{2}} - (u_k)^+_{j-\frac{1}{2}}\right) = 0, \tag{4.3.58}$$

$$(\rho_k)_j^n \left((u_k)_j^{n+\frac{1}{3}} - (u_k)_j^n\right) + \lambda\left((\pi_k)^-_{j+\frac{1}{2}} - (\pi_k)^+_{j-\frac{1}{2}}\right) = 0, \tag{4.3.59}$$

where $(u_k)^-_{j+\frac{1}{2}}$ and $(\pi_k)^-_{j+\frac{1}{2}}$ (*resp.* $(u_k)^+_{j+\frac{1}{2}}$ and $(\pi_k)^+_{j+\frac{1}{2}}$) are the values of u_k and π_k on the left (*resp.* on the right) of the standing wave in the Riemann problem (see Appendix A for their formulae).

Positivity of the densities and CFL restrictions

Or course, when applying Godunov's scheme to the relaxation system, one has to restrict the time step to a classical CFL condition in order for the waves coming from different Riemann problems not to interact:

$$\lambda \max_{j\in\mathbb{Z}} \max_{k\in\{1,2\}} |(a_k\tau_k)_j^n| < \frac{1}{2}. \tag{4.3.60}$$

Another CFL restriction must also be imposed for the densities to remain positive. A suitable reformulation of (4.3.58) shows that under the following CFL restriction, the densities remain positive in this first step:

$$\max_{j\in\mathbb{Z}} \max_{k\in\{1,2\}} \left\{1 + \lambda\left((u_k)^-_{j+\frac{1}{2}} - (u_k)^+_{j-\frac{1}{2}}\right)\right\} > 0. \tag{4.3.61}$$

The following proposition summarizes the main properties of the above discretization of the first step:

Proposition 4.3.9. *Under Whitham's condition (4.3.56) and the CFL restrictions (4.3.60) and (4.3.61), equations (4.3.57)-(4.3.58)-(4.3.59) provide a numerical scheme for the first step ($\mathscr{BN}_1$) of the splitting method which has the following properties:*

(i) It preserves positive values of the densities $\rho_k > 0$.

(ii) The updated physical quantities $(\rho_k)_j^{n+\frac{1}{3}}$ and $(u_k)_j^{n+\frac{1}{3}}$ have finite values even in the regime of vanishing phases.

Some important notations

Based on this Riemann solver, let us define some interface values that are needed for the discretization of the upcoming steps of the splitting method. In particular interface values of the velocities $(u_k - V_I)$ and V_I are needed for steps 2 and 3.

Definition 4.3.1. *If* $(\alpha_k)^n_{j+1} \neq (\alpha_k)^n_j$, *define*

$$(u_k - V_I)^*_{j+\frac{1}{2}} := \begin{cases} -(\alpha_k)^n_j \dfrac{(u_k)^+_{j+\frac{1}{2}} - (u_k)^-_{j+\frac{1}{2}}}{(\alpha_k)^n_{j+1} - (\alpha_k)^n_j}, & \text{if} \quad \dfrac{(u_k)^+_{j+\frac{1}{2}} - (u_k)^-_{j+\frac{1}{2}}}{(\alpha_k)^n_{j+1} - (\alpha_k)^n_j} < 0, \\ -(\alpha_k)^n_{j+1} \dfrac{(u_k)^+_{j+\frac{1}{2}} - (u_k)^-_{j+\frac{1}{2}}}{(\alpha_k)^n_{j+1} - (\alpha_k)^n_j}, & \text{otherwise.} \end{cases} \tag{4.3.62}$$

$$(V_I)^*_{j+\frac{1}{2}} := \frac{(\alpha_k)^n_{j+1}(u_k)^+_{j+\frac{1}{2}} - (\alpha_k)^n_j (u_k)^-_{j+\frac{1}{2}}}{(\alpha_k)^n_{j+1} - (\alpha_k)^n_j}, \tag{4.3.63}$$

and if $(\alpha_k)^n_{j+1} = (\alpha_k)^n_j$ *these quantities are replaced by their limits as* $(\alpha_k)^n_{j+1} - (\alpha_k)^n_j \to 0$.

Observe that there is no ambiguity in the definition of $(V_I)^*_{j+\frac{1}{2}}$ and $(\Pi_I)^*_{j+\frac{1}{2}}$ depending on whether $k = 1$ or $k = 2$. Indeed, as $\alpha_1 u_1 + \alpha_2 u_2$ is conserved across the interface (it is an invariant of the standing wave), one has

$$\begin{array}{ll} & (\alpha_1 u_1)^- + (\alpha_2 u_2)^- = (\alpha_1 u_1)^- + (\alpha_2 u_2)^- \\ \iff & (\alpha_1 u_1)^+ - (\alpha_1 u_1)^- = -\left((\alpha_2 u_2)^+ - (\alpha_2 u_2)^-\right) \\ \iff & \frac{(\alpha_1 u_1)^+ - (\alpha_1 u_1)^-}{(\alpha_1)^+ - (\alpha_1)^+} = \frac{(\alpha_2 u_2)^+ - (\alpha_2 u_2)^-}{(\alpha_1)^+ - (\alpha_1)^+}, \end{array}$$

with $(\alpha_1)^- = (\alpha_1)^n_j$ and $(\alpha_1)^+ = (\alpha_1)^n_{j+1}$. Hence the two definitions of $(V_I)^*_{j+\frac{1}{2}}$ coincide.

We also define the following **downwind-biased** values of $(\alpha_k)^\pm$, $(u_k)^\pm$ depending on the sign of the velocity $(u_k - V_I)^*_{j+\frac{1}{2}}$:

Definition 4.3.2.

$$(\alpha_k)^*_{j+\frac{1}{2}} := \begin{cases} (\alpha_k)^n_{j+1}, & \text{if } (u_k - V_I)^*_{j+\frac{1}{2}} > 0, \\ (\alpha_k)^n_j, & \text{otherwise.} \end{cases} \tag{4.3.64}$$

$$(u_k)^*_{j+\frac{1}{2}} := \begin{cases} (u_k)_{j+\frac{1}{2},+}, & \text{if } (u_k - V_I)^*_{j+\frac{1}{2}} > 0, \\ (u_k)_{j+\frac{1}{2},-}, & \text{otherwise,} \end{cases} \tag{4.3.65}$$

and we have the following useful property, whose proof is left to the reader:

Property 4.3.10. *With the above definitions of* $(u_k - V_I)^*_{j+\frac{1}{2}}$, $(V_I)^*_{j+\frac{1}{2}}$ *and* $(u_k)^*_{j+\frac{1}{2}}$, *one has*

$$(u_k - V_I)^*_{j+\frac{1}{2}} = (u_k)^*_{j+\frac{1}{2}} - (V_I)^*_{j+\frac{1}{2}}, \quad \forall\, j \in \mathbb{Z}. \tag{4.3.66}$$

Notice that these downwind-biased interface values $(\alpha_k)^*_{j+\frac{1}{2}}$ and $(u_k)^*_{j+\frac{1}{2}}$ can be interpreted as if in the exact Godunov scheme, the interface $x_{j+\frac{1}{2}}$ is included or not in the integration domain depending on whether the fictitious wave of velocity $(u_k - V_I)^*_{j+\frac{1}{2}}$ enters or not into the cell C_j.

If $(u_k - V_I)^*_{j+\frac{1}{2}} > 0$ then the interface is included in the integration domain, otherwise it is not. And the same criterion is applied to the interface $x_{j-\frac{1}{2}}$. This unusual manipulation appears to be crucial for ensuring the conservativity of the method. Observe also that one **does not** have $(\alpha_1)^*_{j+\frac{1}{2}} + (\alpha_2)^*_{j+\frac{1}{2}} = 1$ since $(u_1 - V_I)^*_{j+\frac{1}{2}}$ and $(u_2 - V_I)^*_{j+\frac{1}{2}}$ may have opposite signs. However, this does not have any impact in the sequel.

4.4 Numerical approximation of the second step

We now consider the numerical treatment of the time evolution corresponding to the second step. Starting from the output data of the first step, $\mathbb{U}_j^{n+\frac{1}{3}}$, we want to compute the updated data at time $t^{n+\frac{2}{3}}$: $\mathbb{U}_j^{n+\frac{2}{3}}$. To this intent, we must discretize the following system:

$$(\mathscr{BN}_2) \qquad \begin{aligned} &\partial_t \alpha_1 = 0, \\ &\partial_t \rho_k + (u_k - V_I)\partial_x \rho_k - \rho_k \partial_x V_I = 0, \qquad k \in \{1,2\}. \\ &\partial_t u_k + (u_k - V_I)\partial_x u_k = 0, \end{aligned}$$

Actually, in order to later impose the conservativity of the global method, we decide to discretize the equation on $\rho_k u_k$ rather than the transport equation on u_k. Hence, we rather consider the following equivalent system which is still denoted $(\mathscr{BN}_2)$ with little abuse in the notation.

$$(\mathscr{BN}_2) \qquad \begin{aligned} &\partial_t \alpha_1 = 0, \\ &\partial_t \rho_k + (u_k - V_I)\partial_x \rho_k - \rho_k \partial_x V_I = 0, \qquad k \in \{1,2\}. \\ &\partial_t (\rho_k u_k) + (u_k - V_I)\partial_x (\rho_k u_k) - (\rho_k u_k)\partial_x V_I = 0, \end{aligned}$$

Here $(u_k - V_I) = (u_k - V_I)(x)$ and $V_I = V_I(x)$ are seen as two *given* velocity fields defined by the first step and piecewise constant on shifted cells:

$$\begin{aligned} (u_k - V_I)(x) &= (u_k - V_I)^*_{j+\frac{1}{2}}, \quad x \in [x_j, x_{j+1}), \\ V_I(x) &= (V_I)^*_{j+\frac{1}{2}}, \qquad\quad x \in [x_j, x_{j+1}). \end{aligned}$$

This allows to discretize the equation on $\rho_k X_k = \rho_k(1, u_k)$ with the first order upwind scheme for the transport term $(u_k - V_I)\partial_x(\rho_k X_k)$ and with a centered discretization for the term $(\rho_k X_k)\partial_x V_I$:

$$(\alpha_k)_j^{n+\frac{2}{3}} = (\alpha_k)_j^{n+\frac{1}{3}}, \tag{4.4.1}$$

$$\begin{aligned} (\rho_k X_k)_j^{n+\frac{2}{3}} = (\rho_k X_k)_j^{n+\frac{1}{3}} \quad & -\lambda\, (u_k - V_I)^*_{j+\frac{1}{2}} \left((\rho_k X_k)_{j+\frac{1}{2}}^{n+\frac{1}{3}} - (\rho_k X_k)_j^{n+\frac{1}{3}} \right) \\ & -\lambda\, (u_k - V_I)^*_{j-\frac{1}{2}} \left((\rho_k X_k)_j^{n+\frac{1}{3}} - (\rho_k X_k)_{j-\frac{1}{2}}^{n+\frac{1}{3}} \right) \\ & +\lambda\, (\rho_k X_k)_j^{n+\frac{1}{3}} \left((V_I)^*_{j+\frac{1}{2}} - (V_I)^*_{j-\frac{1}{2}} \right), \end{aligned} \tag{4.4.2}$$

where for all j in $\mathbb{Z}$,

$$(\rho_k X_k)_{j+\frac{1}{2}}^{n+\frac{1}{3}} := \begin{cases} (\rho_k X_k)_j^{n+\frac{1}{3}} & \text{if } (u_k - V_I)^*_{j+\frac{1}{2}} > 0, \\ (\rho_k X_k)_{j+1}^{n+\frac{1}{3}} & \text{if } (u_k - V_I)^*_{j+\frac{1}{2}} \leq 0. \end{cases} \tag{4.4.3}$$

Observe that in this step, the evolution of ρ_k and u_k is absolutely not affected by α_k. Hence, the statistical fractions α_k, which are constant through this step, may take very small values without impinging on the densities or on the time step. This latter must however be restricted to a CFL condition in order to ensure the positivity of the densities out of this second step as studied hereunder.

Positivity of the densities and CFL restrictions

Using the fact that $(u_k - V_I)^*_{j+\frac{1}{2}} = (u_k)^*_{j+\frac{1}{2}} - (V_I)^*_{j+\frac{1}{2}}$ for all j in $\mathbb{Z}$, the updating formula for $(\rho_k)_j^{n+\frac{2}{3}}$ re-writes as follows:

$$\begin{aligned}(\rho_k)_j^{n+\frac{2}{3}} = & \left\{\lambda\left((u_k - V_I)^*_{j-\frac{1}{2}}\right)_+\right\}(\rho_k)_{j-1}^{n+\frac{1}{3}} \\ & + \left\{1+\lambda\left((V_I)^*_{j+\frac{1}{2}} - (V_I)^*_{j-\frac{1}{2}}\right) + \lambda\left((u_k - V_I)^*_{j-\frac{1}{2}}\right)_+ + \lambda\left((u_k - V_I)^*_{j+\frac{1}{2}}\right)_-\right\}(\rho_k)_j^{n+\frac{1}{3}} \\ & + \left\{-\lambda\left((u_k - V_I)^*_{j+\frac{1}{2}}\right)_-\right\}(\rho_k)_{j+1}^{n+\frac{1}{3}},\end{aligned} \tag{4.4.4}$$

where for any real number r, $(r)_+ = \max(0,r)$ and $(r)_- = \min(0,r)$. Introducing the density

$$\widetilde{(\rho_k)}_j^{n+\frac{1}{3}} = \frac{1+\lambda\left((u_k - V_I)^*_{j-\frac{1}{2}}\right)_+ + \lambda\left((u_k - V_I)^*_{j+\frac{1}{2}}\right)_-}{1+\lambda\left((V_I)^*_{j+\frac{1}{2}} - (V_I)^*_{j-\frac{1}{2}}\right) + \lambda\left((u_k - V_I)^*_{j-\frac{1}{2}}\right)_+ + \lambda\left((u_k - V_I)^*_{j+\frac{1}{2}}\right)_-}(\rho_k)_j^{n+\frac{1}{3}}$$

equation (4.4.4) becomes

$$\begin{aligned}(\rho_k)_j^{n+\frac{2}{3}} = & \left\{\lambda\left((u_k - V_I)^*_{j-\frac{1}{2}}\right)_+\right\}(\rho_k)_{j-1}^{n+\frac{1}{3}} \\ & + \left\{1+\lambda\left((u_k - V_I)^*_{j-\frac{1}{2}}\right)_+ + \lambda\left((u_k - V_I)^*_{j+\frac{1}{2}}\right)_-\right\}\widetilde{(\rho_k)}_j^{n+\frac{1}{3}} \\ & + \left\{-\lambda\left((u_k - V_I)^*_{j+\frac{1}{2}}\right)_-\right\}(\rho_k)_{j+1}^{n+\frac{1}{3}}.\end{aligned}$$

Hence, under the following double CFL condition, $(\rho_k)_j^{n+\frac{2}{3}}$ is positive as a convex combination of positive densities:

$$1+\lambda\left((V_I)^*_{j+\frac{1}{2}} - (V_I)^*_{j-\frac{1}{2}}\right) + \lambda\left((u_k - V_I)^*_{j-\frac{1}{2}}\right)_+ + \lambda\left((u_k - V_I)^*_{j+\frac{1}{2}}\right)_- > 0, \tag{4.4.5}$$

$$1+\lambda\left((u_k - V_I)^*_{j-\frac{1}{2}}\right)_+ + \lambda\left((u_k - V_I)^*_{j+\frac{1}{2}}\right)_- > 0. \tag{4.4.6}$$

The following proposition summarizes the the main properties of the discretization of the second step:

Proposition 4.4.1. *Under the CFL restrictions (4.4.5) and (4.4.6), equations (4.4.1)-(4.4.2) provide a numerical scheme for the second step ($\mathscr{BN}_2$) of the splitting method which has the following properties:*

(i) It preserves positive values of the densities $\rho_k > 0$.

(ii) The updated physical quantities $(\rho_k)_j^{n+\frac{2}{3}}$ and $(u_k)_j^{n+\frac{2}{3}}$ have finite values even in the regime of vanishing phases.

4.5 Numerical approximation of the third step

In the third and last step, we compute the evolution from the output data of the second step, $\mathbb{U}_j^{n+\frac{2}{3}}$, to the updated data at time t^{n+1}: $\mathbb{U}_j^{n+1}$. We recall the equations that need to be discretized:

$$(\mathscr{BN}_3) \qquad \begin{aligned} &\partial_t \alpha_k + V_I \partial_x \alpha_k = 0, \\ &\partial_t(\alpha_k \rho_k) + \partial_x(\alpha_k \rho_k V_I) = 0, \qquad k \in \{1,2\}. \\ &\partial_t(\alpha_k \rho_k u_k) + \partial_x(\alpha_k \rho_k u_k V_I) = 0, \end{aligned}$$

Here again, $V_I = V_I(x)$ is seen as a *given velocity field* defined as $V_I(x) = (V_I)^*_{j+\frac{1}{2}},\ x \in [x_j, x_{j+1})$. For regular solutions, system $(\mathscr{BN}_3)$ is equivalent to

$$\partial_t \alpha_k + V_I \partial_x \alpha_k = 0, \tag{4.5.1}$$
$$\partial_t \rho_k + \partial_x(\rho_k V_I) = 0, \tag{4.5.2}$$
$$\partial_t u_k + V_I \partial_x u_k = 0. \tag{4.5.3}$$

The numerical scheme we propose for this third step preserves the maximum principle on α_k and $u_k,\ k \in \{1,2\}$ and a conservative discretization of $\alpha_k\rho_k$ and $\alpha_k\rho_k u_k$. In addition we are able to compute the densities $\rho_k,\ k \in \{1,2\}$ even in the regimes of vanishing phases. The main idea is to replace the discretization of α_k in (4.5.1) by a discretization of ρ_k (4.5.2) when the phase fraction α_k is close to zero. The procedure mainly relies on the following Lemma whose proof is given in Appendix B.

Lemma 4.5.1. *Consider two physical quantities $\theta \geq 0$ and $\Theta \in \mathbb{R}$ such that the vector-valued quantity $[\theta, \theta\Theta]$ follows the convection equation $\partial_t[\theta,\theta\Theta] + \partial_x\left([\theta,\theta\Theta]V_I\right) = 0$. Then under the **strict** CFL condition*

$$\max_{j\in\mathbb{Z}} \lambda |(V_I)^*_{j+\frac{1}{2}}| < \frac{1}{2}, \tag{4.5.4}$$

the classical upwind scheme

$$[\theta,\theta\Theta]_j^{n+1} = [\theta,\theta\Theta]_j^{n+\frac{2}{3}} - \lambda\left([\theta,\theta\Theta]_{j+\frac{1}{2}}^{n+\frac{2}{3}}(V_I)^*_{j+\frac{1}{2}} - [\theta,\theta\Theta]_{j-\frac{1}{2}}^{n+\frac{2}{3}}(V_I)^*_{j-\frac{1}{2}}\right) \tag{4.5.5}$$

where for all j in $\mathbb{Z}$,

$$[\theta,\theta\Theta]_j^{n+\frac{2}{3}} := \begin{cases} [\theta,\theta\Theta]_j^{n+\frac{2}{3}} & \text{if } (V_I)^*_{j+\frac{1}{2}} > 0, \\ [\theta,\theta\Theta]_{j+1}^{n+\frac{2}{3}} & \text{if } (V_I)^*_{j+\frac{1}{2}} \leq 0, \end{cases} \tag{4.5.6}$$

preserves the positivity of θ in the following sense

$$\left(\forall j \in \mathbb{Z},\ \theta_j^{n+\frac{2}{3}} \geq 0\right) \Longrightarrow \left(\forall j \in \mathbb{Z},\ \theta_j^{n+1} \geq 0\right) \quad \text{and} \quad \forall j \in \mathbb{Z},\ \left(\theta_j^{n+\frac{2}{3}} > 0 \Longrightarrow\ \theta_j^{n+1} > 0\right), \tag{4.5.7}$$

and a maximum principle on Θ*:*

$$\left(\forall j \in \mathbb{Z},\ m \leq \Theta_j^{n+\frac{2}{3}} \leq M\right) \Longrightarrow \left(\forall j \in \mathbb{Z},\ m \leq \Theta_j^{n+1} \leq M\right). \tag{4.5.8}$$

Let us now use this lemma for the discretization of the third step under the strict CFL condition (4.5.4). The numerical scheme we propose, which guarantees finite values of the physical quantities ρ_k and u_k, is obtained by the following procedure:

1. For the updating of $\alpha_k\rho_k$ and $\alpha_k\rho_k u_k$, apply Lemma 4.5.1 with $\theta = \alpha_k\rho_k$ and $\theta\Theta = \alpha_k\rho_k u_k$ for $k \in \{1,2\}$. This preserves the positivity of $\alpha_k\rho_k, k \in \{1,2\}$ and a maximum principle on $u_k, k \in \{1,2\}$.

2. For the updating of α_k, define $\overline{k}$ such that $(\alpha_{\overline{k}})_j^{n+\frac{2}{3}} < (\alpha_{3-\overline{k}})_j^{n+\frac{2}{3}}$ (*i.e.* $\overline{k}$ is the possibly vanishing phase) and apply the lemma with $\theta = \rho_{\overline{k}}$ and $\theta\Theta = \alpha_{\overline{k}}\rho_{\overline{k}}$. This gives $(\rho_{\overline{k}})_j^{n+1} > 0$ and $(\alpha_{\overline{k}})_j^{n+1} = \frac{(\alpha\rho_{\overline{k}})_j^{n+1}}{(\rho_{\overline{k}})_j^{n+1}}$.

3. The other phase fraction is obtained by $(\alpha_{3-\overline{k}})_j^{n+1} = 1 - (\alpha_{\overline{k}})_j^{n+1}$ and the other density by $(\rho_{3-\overline{k}})_j^{n+1} = \frac{(\alpha_{3-\overline{k}}\rho_{3-\overline{k}})_j^{n+1}}{(\alpha_{3-\overline{k}})_j^{n+1}}$.

The following proposition summarizes the the main properties of the discretization of the third and last step:

Proposition 4.5.2. *Under the CFL restriction (4.5.4), the discretization of the third step* $(\mathscr{BN}_3)$ *of the splitting method has the following properties:*

(i) It preserves the maximum principle for the phase fractions : $0 < \alpha_k < 1$.

(ii) It preserves positive values of the densities $\rho_k > 0$.

(iii) The discretization of the partial masses $\alpha_k\rho_k$ *is conservative.*

(iv) The discretization of the total momentum $\alpha_1\rho_1u_1 + \alpha_2\rho_2u_2$ *is conservative.*

(v) The updated physical quantities $(\rho_k)_j^{n+1}$ *and* $(u_k)_j^{n+1}$ *have finite values even in the regime of vanishing phases.*

4.6 Global conservativity of the scheme

In this section, we prove that the splitting scheme defined above for the three steps $(\mathscr{BN}_1)$, $(\mathscr{BN}_2)$ and $(\mathscr{BN}_3)$ provides a conservative discretization of the partial masses $\alpha_k\rho_k$ and of the total momentum $\alpha_1\rho_1u_1 + \alpha_2\rho_2u_2$. Actually, as the third step has already a conservative formulation for these quantities, proving the global conservativity of the method amounts to proving that the combination of the first and second steps is conservative.

To this aim, we may first give an equivalent formulation of the discretization of the first step (4.3.58)-(4.3.59) which is consistent with the following formulation at the continuous level:

$$\begin{aligned}
&\partial_t \alpha_1 = 0,\\
&\partial_t(\alpha_k\rho_k) + \rho_k\partial_x(\alpha_k u_k) - (\rho_k V_I)\partial_x\alpha_k = 0, \qquad\qquad k\in\{1,2\}.\\
&(\alpha_k\rho_k)^0\partial_t u_k + \partial_x(\alpha_k\pi_k) - \Pi_I\partial_x\alpha_k = 0,
\end{aligned}$$

Indeed, the following result holds:

Lemma 4.6.1. *Equations (4.3.58)-(4.3.59) for the updating of* $(\rho_k)_j^{n+\frac{1}{3}} = 1/(\tau_k)_j^{n+\frac{1}{3}}$ *and* $(u_k)_j^{n+\frac{1}{3}}$ *in the first step are equivalent to*

$$\begin{aligned}
(\alpha_k\rho_k)_j^{n+\frac{1}{3}} = (\alpha_k\rho_k)_j^n \quad &- \lambda\ (\rho_k)_j^{n+\frac{1}{3}}\left((\alpha_k)^*_{j+\frac{1}{2}}(u_k)^*_{j+\frac{1}{2}} - (\alpha_k)^*_{j-\frac{1}{2}}(u_k)^*_{j-\frac{1}{2}}\right)\\
&+ \lambda\ (\rho_k)_{j+\frac{1}{2}}^{n+\frac{1}{3}}(V_I)^*_{j+\frac{1}{2}}\left((\alpha_k)^n_{j+1} - (\alpha_k)^n_j\right)\mathbb{1}_{(u_k-V_I)^*_{j+\frac{1}{2}}>0} \qquad (4.6.1)\\
&+ \lambda\ (\rho_k)_{j-\frac{1}{2}}^{n+\frac{1}{3}}(V_I)^*_{j-\frac{1}{2}}\left((\alpha_k)^n_j - (\alpha_k)^n_{j-1}\right)\mathbb{1}_{(u_k-V_I)^*_{j-\frac{1}{2}}\leq 0}.\\
(\alpha_k\rho_k)_j^n\left((u_k)_j^{n+\frac{1}{3}} - (u_k)_j^n\right) = \quad &- \lambda\ \left((\alpha_k\pi_k)^+_{j+\frac{1}{2}} - (\alpha_k\pi_k)^-_{j-\frac{1}{2}}\right) \qquad (4.6.2)
\end{aligned}$$

where $(u_k - V_I)^*_{j+\frac{1}{2}}$, $(V_I)^*_{j+\frac{1}{2}}$, $(\alpha_k)^*_{j+\frac{1}{2}}$, $(u_k)^*_{j+\frac{1}{2}}$ *are given in definitions 4.3.1 and 4.3.2.*

Proof. See appendix C. □

In the same way, we may give an equivalent discrete formulation of the second step which is consistent with the following formulation at the continuous level:

$$\begin{aligned}
&\partial_t \alpha_1 = 0,\\
&\partial_t(\alpha_k\rho_k) + (\alpha_k u_k)\partial_x\rho_k - \alpha_k\partial_x(\rho_k V_I) = 0, \qquad\qquad k\in\{1,2\}.\\
&\partial_t(\alpha_k\rho_k u_k) + (\alpha_k u_k)\partial_x(\rho_k u_k) - \alpha_k\partial_x(\rho_k u_k V_I) = 0.
\end{aligned}$$

We have the following lemma:

Lemma 4.6.2. *Equation (4.4.2) for the updating of* $(\rho_k X_k)_j^{n+\frac{2}{3}} = (\rho_k, \rho_k u_k)_j^{n+\frac{2}{3}}$ *in the second step is equivalent to*

$$\begin{aligned}
(\alpha_k\rho_k X_k)_j^{n+\frac{2}{3}} = (\alpha_k\rho_k X_k)_j^{n+\frac{1}{3}} \quad &-\lambda\ (\alpha_k)^*_{j+\frac{1}{2}}(u_k)^*_{j+\frac{1}{2}}\left((\rho_k X_k)_{j+\frac{1}{2}}^{n+\frac{1}{3}} - (\rho_k X_k)_j^{n+\frac{1}{3}}\right)\\
&-\lambda\ (\alpha_k)^*_{j-\frac{1}{2}}(u_k)^*_{j-\frac{1}{2}}\left((\rho_k X_k)_j^{n+\frac{1}{3}} - (\rho_k X_k)_{j-\frac{1}{2}}^{n+\frac{1}{3}}\right) \qquad (4.6.3)\\
&+\lambda\ (\alpha_k)^n_j\left((\rho_k X_k)_{j+\frac{1}{2}}^{n+\frac{1}{3}}(V_I)^*_{j+\frac{1}{2}} - (\rho_k X_k)_{j-\frac{1}{2}}^{n+\frac{1}{3}}(V_I)^*_{j-\frac{1}{2}}\right),
\end{aligned}$$

where for $j\in\mathbb{Z}$, $(V_I)^*_{j+\frac{1}{2}}$, $(\alpha_k)^*_{j+\frac{1}{2}}$ *and* $(u_k)^*_{j+\frac{1}{2}}$ *are given in definitions 4.3.1 and 4.3.2.*

Proof. See appendix C. □

We are now able to prove the following crucial result:

Proposition 4.6.3. *The combination of the first and second steps (4.3.58)-(4.3.59) and (4.4.2) provides a conservative discretization of the partial masses $\alpha_k\rho_k$ and of the total momentum $\alpha_1\rho_1u_1+\alpha_2\rho_2u_2$ from t^n to $t^{n+\frac{2}{3}}$.*

Proof. Considering firstly the discretization of the partial masses $\alpha_k\rho_k$, the combination of the second (see (4.6.3)) and first (see 4.6.1)) steps gives

$$\begin{aligned}(\alpha_k\rho_k)_j^{n+\frac{2}{3}} = (\alpha_k\rho_k)_j^n \quad & -\lambda\,(\rho_k)_j^{n+\frac{1}{3}}\left((\alpha_k)^*_{j+\frac{1}{2}}(u_k)^*_{j+\frac{1}{2}}-(\alpha_k)^*_{j-\frac{1}{2}}(u_k)^*_{j-\frac{1}{2}}\right)\\ & +\lambda\,(\rho_k)^{n+\frac{1}{3}}_{j+\frac{1}{2}}(V_I)^*_{j+\frac{1}{2}}\left((\alpha_k)^n_{j+1}-(\alpha_k)^n_j\right)\mathbb{1}_{(u_k-V_I)^*_{j+\frac{1}{2}}>0}\\ & +\lambda\,(\rho_k)^{n+\frac{1}{3}}_{j-\frac{1}{2}}(V_I)^*_{j-\frac{1}{2}}\left((\alpha_k)^n_{j}-(\alpha_k)^n_{j-1}\right)\mathbb{1}_{(u_k-V_I)^*_{j-\frac{1}{2}}\leq 0}\\ & -\lambda\,(\alpha_k)^*_{j+\frac{1}{2}}(u_k)^*_{j+\frac{1}{2}}\left((\rho_k)^{n+\frac{1}{3}}_{j+\frac{1}{2}}-(\rho_k)^{n+\frac{1}{3}}_{j}\right)\\ & -\lambda\,(\alpha_k)^*_{j-\frac{1}{2}}(u_k)^*_{j-\frac{1}{2}}\left((\rho_k)^{n+\frac{1}{3}}_{j}-(\rho_k)^{n+\frac{1}{3}}_{j-\frac{1}{2}}\right)\\ & +\lambda\,(\alpha_k)^n_j\left((\rho_k)^{n+\frac{1}{3}}_{j+\frac{1}{2}}(V_I)^*_{j+\frac{1}{2}}-(\rho_k)^{n+\frac{1}{3}}_{j-\frac{1}{2}}(V_I)^*_{j-\frac{1}{2}}\right).\end{aligned}$$

Eliminating the terms $(\rho_k)_j^{n+\frac{1}{3}}(\alpha_k)^*_{j+\frac{1}{2}}(u_k)^*_{j+\frac{1}{2}}$ and $(\rho_k)_j^{n+\frac{1}{3}}(\alpha_k)^*_{j-\frac{1}{2}}(u_k)^*_{j-\frac{1}{2}}$ and factoring the terms in $(\rho_k)^{n+\frac{1}{3}}_{j+\frac{1}{2}}(V_I)^*_{j+\frac{1}{2}}$ and $(\rho_k)^{n+\frac{1}{3}}_{j-\frac{1}{2}}(V_I)^*_{j-\frac{1}{2}}$ one gets

$$\begin{aligned}(\alpha_k\rho_k)_j^{n+\frac{2}{3}} = (\alpha_k\rho_k)_j^n \quad & -\lambda\,\left((\alpha_k)^*_{j+\frac{1}{2}}(\rho_k)^{n+\frac{1}{3}}_{j+\frac{1}{2}}(u_k)^*_{j+\frac{1}{2}}-(\alpha_k)^*_{j-\frac{1}{2}}(\rho_k)^{n+\frac{1}{3}}_{j-\frac{1}{2}}(u_k)^*_{j-\frac{1}{2}}\right)\\ & +\lambda\,(\rho_k)^{n+\frac{1}{3}}_{j+\frac{1}{2}}(V_I)^*_{j+\frac{1}{2}}\left\{(\alpha_k)^n_j+\left((\alpha_k)^n_{j+1}-(\alpha_k)^n_j\right)\mathbb{1}_{(u_k-V_I)^*_{j+\frac{1}{2}}>0}\right\}\\ & -\lambda\,(\rho_k)^{n+\frac{1}{3}}_{j-\frac{1}{2}}(V_I)^*_{j-\frac{1}{2}}\left\{(\alpha_k)^n_j-\left((\alpha_k)^n_{j}-(\alpha_k)^n_{j-1}\right)\mathbb{1}_{(u_k-V_I)^*_{j-\frac{1}{2}}\leq 0}\right\}.\end{aligned}$$

Now as by Definition 4.3.2, we have $(\alpha_k)^*_{j+\frac{1}{2}} = (\alpha_k)^n_j+\left((\alpha_k)^n_{j+1}-(\alpha_k)^n_j\right)\mathbb{1}_{(u_k-V_I)^*_{j+\frac{1}{2}}>0}$ and $(\alpha_k)^*_{j-\frac{1}{2}} = (\alpha_k)^n_j-\left((\alpha_k)^n_{j}-(\alpha_k)^n_{j-1}\right)\mathbb{1}_{(u_k-V_I)^*_{j-\frac{1}{2}}\leq 0}$, this re-writes in the conservative form

$$(\alpha_k\rho_k)_j^{n+\frac{2}{3}} = (\alpha_k\rho_k)_j^n \quad -\lambda\,\left((\alpha_k)^*_{j+\frac{1}{2}}(\rho_k)^{n+\frac{1}{3}}_{j+\frac{1}{2}}(u_k-V_I)^*_{j+\frac{1}{2}}-(\alpha_k)^*_{j-\frac{1}{2}}(\rho_k)^{n+\frac{1}{3}}_{j-\frac{1}{2}}(u_k-V_I)^*_{j-\frac{1}{2}}\right). \tag{4.6.4}$$

Let us now turn to the discretization of the partial momentums $\alpha_k\rho_ku_k$. According to the reformulation of the second step (4.6.3) we have:

$$\begin{aligned}(\alpha_k\rho_ku_k)_j^{n+\frac{2}{3}} = (\alpha_k\rho_ku_k)_j^{n+\frac{1}{3}} \quad & -\lambda\,(\alpha_k)^*_{j+\frac{1}{2}}(u_k)^*_{j+\frac{1}{2}}\left((\rho_ku_k)^{n+\frac{1}{3}}_{j+\frac{1}{2}}-(\rho_ku_k)^{n+\frac{1}{3}}_{j}\right)\\ & -\lambda\,(\alpha_k)^*_{j-\frac{1}{2}}(u_k)^*_{j-\frac{1}{2}}\left((\rho_ku_k)^{n+\frac{1}{3}}_{j}-(\rho_ku_k)^{n+\frac{1}{3}}_{j-\frac{1}{2}}\right)\\ & +\lambda\,(\alpha_k)^n_j\left((\rho_ku_k)^{n+\frac{1}{3}}_{j+\frac{1}{2}}(V_I)^*_{j+\frac{1}{2}}-(\rho_ku_k)^{n+\frac{1}{3}}_{j-\frac{1}{2}}(V_I)^*_{j-\frac{1}{2}}\right),\end{aligned} \tag{4.6.5}$$

Using the expression of $(\alpha_k\rho_k)_j^{n+\frac{1}{3}}$ given in (4.6.1), we have

$$\begin{aligned}(\alpha_k\rho_k u_k)_j^{n+\frac{1}{3}} &= (\alpha_k\rho_k)_j^{n+\frac{1}{3}}(u_k)_j^{n+\frac{1}{3}} \\ &= (\alpha_k\rho_k)_j^n(u_k)_j^{n+\frac{1}{3}} - \lambda(\rho_k)_j^{n+\frac{1}{3}}(u_k)_j^{n+\frac{1}{3}}\left((\alpha_k)^*_{j+\frac{1}{2}}(u_k)^*_{j+\frac{1}{2}} - (\alpha_k)^*_{j-\frac{1}{2}}(u_k)^*_{j-\frac{1}{2}}\right) \\ &\quad + \lambda(\rho_k)_{j+\frac{1}{2}}^{n+\frac{1}{3}}(u_k)_j^{n+\frac{1}{3}}(V_I)^*_{j+\frac{1}{2}}\left((\alpha_k)^n_{j+1} - (\alpha_k)^n_j\right)\mathbb{1}_{(u_k-V_I)^*_{j+\frac{1}{2}}>0} \\ &\quad + \lambda(\rho_k)_{j-\frac{1}{2}}^{n+\frac{1}{3}}(u_k)_j^{n+\frac{1}{3}}(V_I)^*_{j-\frac{1}{2}}\left((\alpha_k)^n_j - (\alpha_k)^n_{j-1}\right)\mathbb{1}_{(u_k-V_I)^*_{j-\frac{1}{2}}\leq 0}.\end{aligned} \tag{4.6.6}$$

As in the second step, $(u_k)_{j+\frac{1}{2}}^{n+\frac{1}{3}}$ is upwind-biased with respect to $(u_k - V_I)^*_{j+\frac{1}{2}}$, we may replace $(u_k)_j^{n+\frac{1}{3}}$ by $(u_k)_{j+\frac{1}{2}}^{n+\frac{1}{3}}$ in the second line of (4.6.6) and $(u_k)_j^{n+\frac{1}{3}}$ by $(u_k)_{j-\frac{1}{2}}^{n+\frac{1}{3}}$ in the third line of (4.6.6). Moreover, according to equation (4.6.2) of Lemma 4.6.1, we get

$$\begin{aligned}(\alpha_k\rho_k u_k)_j^{n+\frac{1}{3}} = (\alpha_k\rho_k u_k)_j^n &\ -\lambda\left((\alpha_k\pi_k)^-_{j+\frac{1}{2}} - (\alpha_k\pi_k)^+_{j-\frac{1}{2}}\right) \\ &\ -\lambda(\rho_k u_k)_j^{n+\frac{1}{3}}\left((\alpha_k)^*_{j+\frac{1}{2}}(u_k)^*_{j+\frac{1}{2}} - (\alpha_k)^*_{j-\frac{1}{2}}(u_k)^*_{j-\frac{1}{2}}\right) \\ &\ +\lambda(\rho_k u_k)_{j+\frac{1}{2}}^{n+\frac{1}{3}}(V_I)^*_{j+\frac{1}{2}}\left((\alpha_k)^n_{j+1} - (\alpha_k)^n_j\right)\mathbb{1}_{(u_k-V_I)^*_{j+\frac{1}{2}}>0} \\ &\ +\lambda(\rho_k u_k)_{j-\frac{1}{2}}^{n+\frac{1}{3}}(V_I)^*_{j-\frac{1}{2}}\left((\alpha_k)^n_j - (\alpha_k)^n_{j-1}\right)\mathbb{1}_{(u_k-V_I)^*_{j-\frac{1}{2}}\leq 0}.\end{aligned}$$

Casting this expression of $(\alpha_k\rho_k u_k)_j^{n+\frac{1}{3}}$ in (4.6.5) and eliminating the terms $(\rho_k u_k)_j^{n+\frac{1}{3}}(\alpha_k)^*_{j+\frac{1}{2}}(u_k)^*_{j+\frac{1}{2}}$ and $(\rho_k u_k)_j^{n+\frac{1}{3}}(\alpha_k)^*_{j-\frac{1}{2}}(u_k)^*_{j-\frac{1}{2}}$, we obtain:

$$\begin{aligned}(\alpha_k\rho_k u_k)_j^{n+\frac{2}{3}} = (\alpha_k\rho_k u_k)_j^n &\ -\lambda\left((\alpha_k)^*_{j+\frac{1}{2}}(u_k)^*_{j+\frac{1}{2}}(\rho_k u_k)_{j+\frac{1}{2}}^{n+\frac{1}{3}} - (\alpha_k)^*_{j-\frac{1}{2}}(u_k)^*_{j-\frac{1}{2}}(\rho_k u_k)_{j-\frac{1}{2}}^{n+\frac{1}{3}}\right) \\ &\ -\lambda\left((\alpha_k\pi_k)^-_{j+\frac{1}{2}} - (\alpha_k\pi_k)^+_{j-\frac{1}{2}}\right) \\ &\ +\lambda\ (\alpha_k)_j^n\left((\rho_k u_k)_{j+\frac{1}{2}}^{n+\frac{1}{3}}(V_I)^*_{j+\frac{1}{2}} - (\rho_k u_k)_{j-\frac{1}{2}}^{n+\frac{1}{3}}(V_I)^*_{j-\frac{1}{2}}\right) \\ &\ +\lambda(\rho_k u_k)_{j+\frac{1}{2}}^{n+\frac{1}{3}}(V_I)^*_{j+\frac{1}{2}}\left((\alpha_k)^n_{j+1} - (\alpha_k)^n_j\right)\mathbb{1}_{(u_k-V_I)^*_{j+\frac{1}{2}}>0} \\ &\ +\lambda(\rho_k u_k)_{j-\frac{1}{2}}^{n+\frac{1}{3}}(V_I)^*_{j-\frac{1}{2}}\left((\alpha_k)^n_j - (\alpha_k)^n_{j-1}\right)\mathbb{1}_{(u_k-V_I)^*_{j-\frac{1}{2}}\leq 0}.\end{aligned} \tag{4.6.7}$$

Again, using the downwind definitions of $(\alpha_k)^*_{j+\frac{1}{2}}$ and $(\alpha_k)^*_{j+\frac{1}{2}}$, we get:

$$\begin{aligned}(\alpha_k\rho_k u_k)_j^{n+\frac{2}{3}} = (\alpha_k\rho_k u_k)_j^n &\ -\lambda\left((\alpha_k)^*_{j+\frac{1}{2}}(u_k - V_I)^*_{j+\frac{1}{2}}(\rho_k u_k)_{j+\frac{1}{2}}^{n+\frac{1}{3}} - (\alpha_k)^*_{j-\frac{1}{2}}(u_k - V_I)^*_{j-\frac{1}{2}}(\rho_k u_k)_{j-\frac{1}{2}}^{n+\frac{1}{3}}\right) \\ &\ -\lambda\left((\alpha_k\pi_k)^-_{j+\frac{1}{2}} - (\alpha_k\pi_k)^+_{j-\frac{1}{2}}\right).\end{aligned} \tag{4.6.8}$$

Summing this last equation over $k = 1, 2$ yields a conservative discretization of the total momentum since $\sum_{k=1,2}(\alpha_k\pi_k)^- = \sum_{k=1,2}(\alpha_k\pi_k)^+$ by the conservation of the Riemann invariant $\sum_{k=1,2}(\alpha_k\pi_k)$ across the standing wave in the first step. □

4.7 Extension of the scheme to the model with energies

Although we provide some numerical illustration in the following section, the extension of the scheme to the full model with energies has not been written yet. We refer to section 3.7 of chapter 3 for a similar extension.

4.8 Numerical applications

4.8.1 The isentropic case

In this section, we present a Riemann-type test-case on which the performances of the splitting scheme are tested. The phasic equations of state are given by the following ideal gas pressure laws:

$$\begin{aligned} p_1(\rho_1) &= \kappa_1 \rho_1^{\gamma_1}, \quad \text{with } \kappa_1 = 1 \text{ and } \gamma_1 = 3, \\ p_2(\rho_2) &= \kappa_2 \rho_2^{\gamma_2}, \quad \text{with } \kappa_2 = 1 \text{ and } \gamma_2 = 1.5. \end{aligned} \tag{4.8.1}$$

We consider the following initial data, where $\mathcal{U} = (\alpha_1, \rho_1, u_1, \rho_2, u_2)^T$ denotes the state vector in **non-conservative variables**.

$$\begin{aligned} \mathcal{U}_L &= (0.1, 0.85, 0.4609513139, 0.96, 0.0839315299) && \text{if } x < 0, \\ \mathcal{U}_R &= (0.6, 1.2520240113, 0.7170741165, 0.2505659851, -0.3764790609) && \text{if } x > 0, \end{aligned}$$

for which the exact solution is composed of a $\{u_1 - c_1\}$-shock wave, followed by a $\{u_2 - c_2\}$-rarefaction wave, followed by a u_2-contact discontinuity, followed by a $\{u_2 + c_2\}$-shock and finally followed by a $\{u_1 + c_1\}$-rarefaction wave (see Figure 4.1). The intermediate states are given by:

$$\begin{aligned} \mathcal{U}_1 &= (0.1, 1., 0.2, 0.96, 0.0839315299), \\ \mathcal{U}_2 &= (0.1, 1., 0.2, 0.8, 0.3), \\ \mathcal{U}_3 &= (0.6, 1.0016192090, 0.2833602765, 0.5011319701, 0.3), \\ \mathcal{U}_4 &= (0.6, 1.0016192090, 0.2833602765, 0.2505659851, -0.3764790609). \end{aligned}$$

In Figure 4.1, the approximate solution computed with the splitting scheme is compared with both the exact solution and the approximate solution obtained with Rusanov's scheme (see [7]). The results show that unlike Rusanov's scheme, the splitting method correctly captures the intermediate states even for this rather coarse mesh of 100 cells. This coarse mesh is a typical example of an industrial mesh, reduced to one direction, since 100 cells in 1D correspond to a 10^6-cell mesh in 3D. It appears that the contact discontinuity is captured more sharply by the splitting method than by Rusanov's scheme for which the numerical diffusion is larger. We can also see that for the phase 1 variables, there are no oscillations as one can see for Rusanov's scheme: the curves are monotone between the intermediate states. As for phase 2, the intermediate states are captured by the splitting method while with Rusanov's scheme, this weak level of refinement is clearly not enough to capture any intermediate state. These observations assess that, for the same level of refinement, the splitting method is more accurate than Rusanov's scheme.

A mesh refinement process has also been implemented in order to check numerically the convergence of the method, as well as it's performances in terms of CPU-time cost. For this purpose, we compute the discrete L^1-error between the approximate solution and the exact one at the final time T, normalized by the discrete L^1-norm of the exact solution:

$$E(\Delta x) = \frac{\sum_{\text{cells}j} |\varphi_j^n - \varphi_{ex}(x_j, T)| \Delta x}{\sum_{\text{cells}j} |\varphi_{ex}(x_j, T)| \Delta x}, \tag{4.8.2}$$

where φ is any of the **conservative** variables $(\alpha_1, \alpha_1\rho_1, \alpha_1\rho_1 u_1, \alpha_2\rho_2, \alpha_2\rho_2 u_2)$. The calculations have been implemented on several meshes composed of 100×2^n cells with $n = 0, 1, .., 10$ (knowing that the domain size is $L = 1$). In Figure 4.2, the error $E(\Delta x)$ at the final time $T = 0.14$, is plotted against Δx in a $log - log$ scale. Only the error on the phase fraction α_1 converges towards zero with the expected order of $\Delta x^{1/2}$, while the other variables seem to converge with a higher rate. However, $\Delta x^{1/2}$ is only an asymptotic order of convergence, and in this particular case, one would have to implement the calculation on much more refined meshes in order to reach the expected order of $\Delta x^{1/2}$.

Figure 4.2 also displays the error on the conservative variables with respect to the CPU-time of the calculation expressed in seconds. Each point of the plot corresponds to one single calculation for a given mesh size (going from 400 to 102400 cells for the relaxation scheme and from 800 to 102400 cells for Rusanov's scheme). One can see that, for all the variables, if one prescribes a given level of the error, the computational cost of Rusanov's scheme is significantly higher than that of the splitting method.

4.8.2 Complete model with energies

In this section, we present the Riemann test-case for the complete model with energies, which is considered in [11]. The two phases follow two ideal gas equations of state with $\gamma_1 = \gamma_2 = 1.4$. Denoting $\mathcal{U} = (\alpha_1, \rho_1, u_1, p_1, \rho_2, u_2, p_2)$ the initial data is given by

$$\begin{aligned} \mathcal{U}_L &= (0.2, 0.2, 0, 0.3, 1.0, 0, 1.0) \qquad \text{if } x < 0, \\ \mathcal{U}_R &= (0.7, 1.0, 0, 1.0, 1.0, 0, 1.0) \qquad \text{if } x > 0. \end{aligned}$$

The computation has been implemented on a coarse mesh of 200 cells and a more refined one of 10^5 cells. The results are presented in Figure 4.3. We observe a rather good behavior on the coarse mesh. Moreover, although the exact solution is not represented here, the scheme seems to be convergent as the space step tends to zero (with a constant CFL).

Appendix A: Proofs related to the first step (section 4.3)

Proof of Proposition 4.3.3

Solving the jump relations at the void fraction's wave is conveniently performed recasting the PDEs in $(\mathscr{BN}_1)$ under the following equivalent form :

$$\left\{\begin{array}{ll} \partial_t\alpha_k & = 0, \qquad k\in\{1,2\}, \\ (\alpha_k\rho_k)^0\partial_t\Big(\pi_k+a_k^2\tau_k\Big) & = 0, \\ (\alpha_k\rho_k)^0\partial_t u_k+\partial_x\Big(\alpha_k\pi_k\Big)-P_I\partial_x\alpha_k & = 0, \\ (\alpha_k\rho_k)^0\partial_t\frac{\pi_k}{a_k^2}+\partial_x\Big(\alpha_k u_k\Big)-V_I\partial_x\alpha_k & = 0. \end{array}\right. \tag{4.8.3}$$

Expressing these PDEs in the self-similar variable $\xi=x/t$, the non trivial jump conditions at the standing wave, formally expressed in differential form, clearly resume to the following four equations

$$\left\{\begin{array}{l} (\alpha_k u_k)_{,\xi}-V_I(\xi)\ (\alpha_k)_{,\xi}=0, \quad k\in\{1,2\}, \\ (\alpha_k\pi_k)_{,\xi}-P_I(\xi)\ (\alpha_k)_{,\xi}=0, \end{array}\right. \tag{4.8.4}$$

where the notation $(\ )_{,\xi}$ classically stands for the differentiation with respect to the self-similar variable ξ. Summing the velocity equations and the pressure ones respectively gives

$$\begin{array}{l} \Big(\alpha u_1+(1-\alpha)u_2\Big)_{,\xi}=0, \\ \Big(\alpha\pi_1+(1-\alpha)\pi_2\Big)_{,\xi}=0, \end{array} \tag{4.8.5}$$

and yields the two Riemann invariants stated in (4.3.29). To exhibit the last two non trivial jump conditions, let us re-express (4.8.4) as follows

$$\left\{\begin{array}{l} \alpha_k(\xi)\ (u_k)_{,\xi}+(u_k-V_I)(\xi)\ (\alpha_k)_{,\xi}=0, \quad k\in\{1,2\}, \\ \alpha_k(\xi)\ (\pi_k)_{,\xi}+(\pi_k-P_I)(\xi)\ (\alpha_k)_{,\xi}=0. \end{array}\right. \tag{4.8.6}$$

At this stage, it is convenient to re-parametrize the wave curves under consideration by α with $\alpha\in(\alpha^-,\alpha^+)$ so as to arrive at the following EDOs :

$$\begin{array}{l} u_{1,\alpha}(\alpha)+\dfrac{1}{\alpha}\ (u_1-V_I)(\alpha)=0, \quad u_{2,\alpha}(\alpha)-\dfrac{1}{1-\alpha}\ (u_2-V_I)(\alpha)=0, \\ \pi_{1,\alpha}(\alpha)+\dfrac{1}{\alpha}(\pi_1-P_I)(\alpha)=0, \quad \pi_{2,\alpha}(\alpha)-\dfrac{1}{1-\alpha}\ (\pi_2-P_I)(\alpha)=0. \end{array} \tag{4.8.7}$$

Here and by construction, the initial and final values (*i.e.* respectively at $\alpha=\alpha^-$ and $\alpha=\alpha^+$) coincide with the left and right traces of the Riemann solution at the standing wave as already stated in (4.3.21). To shorten the notations, we will skip from now on the dependence on the parameter α unless otherwise needed. Subtracting respectively the velocity equations and the pressure ones while plugging the definition (4.3.12) of the interfacial pair (V_I,P_I) yield :

$$\begin{array}{l} \Delta u_{,\alpha}+(\dfrac{\mu}{\alpha}-\dfrac{1-\mu}{1-\alpha})\Delta u-s(\dfrac{1}{\alpha}+\dfrac{1}{1-\alpha})\Big(d\Delta u+D_\pi\Delta\pi/b\Big)=0, \\ \Delta\pi_{,\alpha}+(\dfrac{1-\mu}{\alpha}-\dfrac{\mu}{1-\alpha})\Delta\pi-s(\dfrac{1}{\alpha}+\dfrac{1}{1-\alpha})\Big(b\ D_u\Delta u+d\Delta\pi\Big)=0, \end{array} \tag{4.8.8}$$

where for convenience, we recall that $\Delta u = u_1 - u_2$ and $\Delta\pi = \pi_1 - \pi_2$. Invoking the definition of I_3 and I_4 defined in (4.3.28), the ODEs (4.8.8) can be seen to recast equivalently in the form (4.3.30). This concludes the proof.

Proof of Lemma 4.3.6

Let us start from the two Riemann invariants stated in (4.3.29)

$$\begin{array}{l} \alpha^+ u_1^+ + (1-\alpha^+)u_2^+ = \alpha^- u_1^- + (1-\alpha^-)u_2^-, \\ \alpha^+ \pi_1^+ + (1-\alpha^+)\pi_2^+ = \alpha^- \pi_1^- + (1-\alpha^-)\pi_2^-, \end{array} \tag{4.8.9}$$

which we rewrite as

$$\begin{array}{l} \alpha^+ \Delta u^+ + u_2^+ = \alpha^- \Delta u^- + u_2^-, \\ \alpha^+ \Delta \pi^+ + \pi_2^+ = \alpha^- \Delta \pi^- + \pi_2^-. \end{array} \tag{4.8.10}$$

Then invoking the Riemann invariants for phase two in the corresponding two extreme waves :

$$\pi_2^- = -a_2 u_2^- + L_2, \quad \pi_2^+ = a_2 u_2^+ - R_2, \tag{4.8.11}$$

allows to infer the following identities

$$\begin{array}{l} u_2^+ - u_2^- = -\alpha^+ \Delta u^+ + \alpha^- \Delta u^-. \\ u_2^+ + u_2^- = \dfrac{1}{a_2}\Big(-\alpha^+ \Delta \pi^+ + \alpha^- \Delta \pi^- + R_2 + L_2 \Big). \end{array} \tag{4.8.12}$$

These are easily seen to give the expected traces $u_2^\pm$ in terms of the jumps $\Delta u^\pm$ and $\Delta \pi^\pm$. Similar calculations but promoting $u_1^\pm$ in place of $u_2^\pm$ from (4.3.29) to (4.8.10) yield

$$\begin{array}{l} u_1^+ - u_1^- = (1-\alpha^+)\Delta u^+ - (1-\alpha^-)\Delta u^-, \\ u_1^+ + u_1^- = \dfrac{1}{a_1}\Big((1-\alpha^+)\Delta \pi^+ - (1-\alpha^-)\Delta \pi^- + R_1 + L_1 \Big). \end{array} \tag{4.8.13}$$

Details are left to the reader.

Proof of Proposition 4.3.8

The shape of the differential system (4.3.30), stated in Proposition 4.3.3, suggests to advocate the new parameter $\beta = \log\Big(\alpha/(1-\alpha)\Big)$ so as to re-express (4.3.30) according to

$$\begin{pmatrix} I_3(\beta) \\ I_4(\beta) \end{pmatrix}_{,\beta} = s\ \mathcal{A}(\beta) \begin{pmatrix} I_3(\beta) \\ I_4(\beta) \end{pmatrix}, \qquad \mathcal{A}(\beta) = \begin{pmatrix} d & e^{-2\theta\beta}\ D_\pi/b \\ e^{+2\theta\beta}\ bD_u & d \end{pmatrix} \tag{4.8.14}$$

where the notation $(\ )_{,\beta}$ stands for the differentiation with respect to β. A straightforward analysis of the eigenstructure of the matrix $\mathcal{A}(\beta)$ reveals under the non-negative assumption (4.3.11) on the dissipative matrix $\mathcal{D}$ the existence of two constant real eigenvalues with opposite signs :

$$\lambda_- = d - \sqrt{D_u D_\pi} \quad \leq 0 \leq \quad \lambda_+ = d + \sqrt{D_u D_\pi}, \tag{4.8.15}$$

respectively associated to the (β-weighted) characteristic variables :

$$\kappa_-(\beta) = r\ I_3(\beta) - e^{2\theta\beta}\ I_4(\beta), \quad \kappa_+(\beta) = r\ I_3(\beta) + e^{-2\theta\beta}\ I_4(\beta). \tag{4.8.16}$$

with $r = b\sqrt{\frac{D_u}{D_\pi}}$. In these variables, direct calculations show that the non-homogenous ODE model (4.3.30) actually takes the form of a constant coefficient ODE system (recall that $s^2 = 1$)

$$\begin{pmatrix} \kappa_+ \\ \kappa_- \end{pmatrix}_{,\beta} = s\mathcal{B}\begin{pmatrix} \kappa_+ \\ \kappa_- \end{pmatrix}, \qquad \mathcal{B} = \begin{pmatrix} \lambda_+ - s\theta & s\theta \\ s\theta & \lambda_- - s\theta \end{pmatrix}. \tag{4.8.17}$$

The characteristic polynomial of the underlying linear system $\mathcal{B}$ reads

$$\mathcal{P}(\Lambda) = \Lambda^2 - 2(d - s\theta)\Lambda - \Big\{D_u D_\pi - d^2 + 2s\theta d\Big\}, \tag{4.8.18}$$

and always ensures the existence of the following two real eigenvalues

$$\Lambda_- = d - s\theta - \sqrt{D_u D_\pi + \theta^2}, \quad \Lambda_+ = d - s\theta + \sqrt{D_u D_\pi + \theta^2}, \tag{4.8.19}$$

which we have already introduced in the main statement of this section, namely Theorem 4.3.4. Under the compatibility condition (4.3.35) which we recall for convenience

$$D_u D_\pi - d^2 + 2s\theta d \geq 0, \tag{4.8.20}$$

the shape (4.8.18) of the polynomial $\mathcal{P}(\Lambda)$ asserts that the eigenvalues under consideration have opposite sign, with

$$\Lambda^- \quad \leq 0 \leq \quad \Lambda^+. \tag{4.8.21}$$

Their associated left eigenvectors respectively reads $L^- = (-\omega, 1)$ and $L^+ = (1, \omega)$ with $\omega \in (-1, 1)$ defined in (4.3.48), so that the diagonal form of the ODE system (4.8.17) is

$$\begin{pmatrix} \eta_+ \\ \eta_- \end{pmatrix}_{,\beta} = s\begin{pmatrix} \Lambda_+ & 0 \\ 0 & \Lambda_- \end{pmatrix}\begin{pmatrix} \eta_+ \\ \eta_- \end{pmatrix}, \tag{4.8.22}$$

with $\eta_+ = \kappa_+ + \omega\kappa_-$, and $\eta_- = -\omega\kappa_+ + \kappa_-$. We thus get once integrated in the β-parameter but expressed in the α-variable :

$$\eta_+(\alpha^+) \quad = \Big(\tfrac{\alpha^+}{\alpha^-}\Big)^{s\Lambda_+}\Big(\tfrac{1-\alpha^-}{1-\alpha^+}\Big)^{s\Lambda_+}\ \eta_+(\alpha^-), \qquad \eta_-(\alpha^+) \quad = \Big(\tfrac{\alpha^+}{\alpha^-}\Big)^{s\Lambda_-}\Big(\tfrac{1-\alpha^-}{1-\alpha^+}\Big)^{s\Lambda_-}\ \eta_-(\alpha^-). \tag{4.8.23}$$

To further proceed, let us observe from the characteristic variables $\kappa_\pm$ in (4.8.16) but re-expressed in the α-parameter and developed according to the definition (4.3.28) of I_3 and I_4 :

$$\begin{aligned} \kappa_\pm(\alpha) \quad &\equiv r\ \alpha^\mu(1-\alpha)^{1-\mu}\Delta u(\alpha) \pm \Big\{\big(\tfrac{\alpha}{1-\alpha}\big)^{-2\theta}\alpha^{1-\mu}(1-\alpha)^\mu\Big\}\Delta\pi(\alpha) \\ &= \alpha^\mu(1-\alpha)^{1-\mu}\Big\{r\ \Delta u \pm \Delta\pi\Big\}(\alpha), \end{aligned} \tag{4.8.24}$$

since $2\theta = (1 - 2\mu)$. Hence, the variables $\eta^\pm$ in the linear system (4.8.22) just recast in terms of the α-variable as

$$\begin{aligned} \eta_+(\alpha) \quad &= \alpha^\mu(1-\alpha)^{1-\mu}\Big\{(1+\omega)r\ \Delta u + (1-\omega)\Delta\pi\Big\}(\alpha), \\ \eta_-(\alpha) \quad &= \alpha^\mu(1-\alpha)^{1-\mu}\Big\{(1-\omega)r\ \Delta u - (1+\omega)\Delta\pi\Big\}(\alpha). \end{aligned} \tag{4.8.25}$$

The jump formulae (4.8.23) together with the identities (4.3.21) linking the initial and final values, respectively at α^- and α^+, with the left and right traces of the Riemann solution at the standing wave yield the expected definition of $h_-(\alpha^-,\alpha^+)$ and $h_+(\alpha^-,\alpha^+)$:

$$\begin{aligned} h_+(\alpha^-,\alpha^+) &= \Big(\tfrac{\alpha^+}{\alpha^-}\Big)^{s\Lambda_+-\mu}\Big(\tfrac{1-\alpha^+}{1-\alpha^-}\Big)^{\mu-1-s\Lambda_+}, \\ h_-(\alpha^-,\alpha^+) &= \Big(\tfrac{\alpha^+}{\alpha^-}\Big)^{s\Lambda_--\mu}\Big(\tfrac{1-\alpha^+}{1-\alpha^-}\Big)^{\mu-1-s\Lambda_-}. \end{aligned} \tag{4.8.26}$$

The developed form of the solutions (4.8.23) just give the first two equations of the linear system (4.3.49). The last two equations can be derived as follows. Let us first rewrite the Riemann invariants (4.3.42) for the extreme waves of phase 1 according to

$$a_1\Delta u^- + \Delta\pi^- + (a_1\ u_2^- + \pi_2^-) = L_1, \quad a_1\Delta u^+ - \Delta\pi^+ + (a_1\ u_2^+ - \pi_2^+) = R_1. \tag{4.8.27}$$

Using the corresponding Riemann invariants for phase 2

$$\pi_2^- = -a_2u_2^- + L_2, \quad \pi_2^+ = a_2u_2^+ - R_2, \tag{4.8.28}$$

we get

$$(a_1-a_2)u_2^- = L_1 - L_2 - a_1\Delta u^- - \Delta\pi^-, \quad (a_1-a_2)u_2^+ = R_1 - R_2 - a_1\Delta u^+ + \Delta\pi^+. \tag{4.8.29}$$

Then we recast the two invariants (4.3.29) at the standing wave as follows

$$\alpha^+\Delta u^+ + u_2^+ = \alpha^-\Delta u^- + u_2^-, \quad \alpha^+\Delta\pi^+ + \pi_2^+ = \alpha^-\Delta\pi^- + \pi_2^-. \tag{4.8.30}$$

Multiplying the above first equation by (a_1-a_2) and plugging the identities (4.8.29) give the third equation in the linear system (4.3.49) :

$$\Big\{(1-\alpha^+)a_1 + \alpha^+a_2\Big\}\Delta u^+ - \Delta\pi^+ = \Big\{(1-\alpha^-)a_1 + \alpha^-a_2\Big\}\Delta u^- + \Delta\pi^- + \Delta R - \Delta L, \tag{4.8.31}$$

where we have set $\Delta R = R_1 - R_2$ and $\Delta L = L_1 - L_2$. The last equation of (4.3.49) is obtained multiplying the Riemann invariants (4.8.28) by (a_1-a_2) while again using (4.8.29) :

$$\Big\{\alpha^+a_1(1-\alpha^+)a_2\Big\}\Delta\pi^+ - a_1a_2\Delta u^+ = \Big\{\alpha^-a_1 + (1-\alpha^-)a_2\Big\}\Delta\pi^- + a_1a_2\Delta u^- - a_2(R_1+L_1) + a_1(R_2+L_2).$$

For the calculation of the determinant, let us define

$$\mathcal{G}_1 = (R_1 - L_1) - (R_2 - L_2), \quad \mathcal{G}_2 = -\frac{1}{a_1}(R_1 + L_1) + \frac{1}{a_2}(R_2 + L_2), \tag{4.8.32}$$

and

$$\zeta = \frac{1}{\widehat{a}(\alpha^-) + \widehat{a}(\alpha^+)}. \tag{4.8.33}$$

Then expressing the relative velocities in terms of the relative pressures from the last two equations in (4.3.49) writes

$$\begin{aligned} \Delta u^- &= -\zeta\Big\{\mathcal{G}_1 + \widehat{a}(\alpha^+)\mathcal{G}_2 + (1+\widehat{a}(\alpha^+)\widehat{\frac{1}{a}}(\alpha^-))\Delta\pi^- + (1-\widehat{a}(\alpha^+)\widehat{\frac{1}{a}}(\alpha^+))\Delta\pi^+\Big\}, \\ \Delta u^+ &= +\zeta\Big\{\mathcal{G}_1 - \widehat{a}(\alpha^-)\mathcal{G}_2 + (1-\widehat{a}(\alpha^-)\widehat{\frac{1}{a}}(\alpha^-))\Delta\pi^- + (1+\widehat{a}(\alpha^-)\widehat{\frac{1}{a}}(\alpha^+))\Delta\pi^+\Big\} \end{aligned} \tag{4.8.34}$$

Plugging these identities in the first two equations yields the following 2×2 linear system for the relative pressures :

$$\left\{ \begin{array}{l} A_{11}\Delta\pi^- + A_{12}\Delta\pi^+ = B_1, \\ A_{21}\Delta\pi^- + A_{22}\Delta\pi^+ = B_2. \end{array} \right. \tag{4.8.35}$$

where

$$\begin{aligned} A_{11} &:= -(1-\omega)h_+(\alpha^-,\alpha^+) + r\ \zeta(1+\omega)\Big(\big(1-\widehat{a}(\alpha^-)\widehat{\tfrac{1}{a}}(\alpha^-)\big) + \big(1+\widehat{a}(\alpha^+)\widehat{\tfrac{1}{a}}(\alpha^-)\big)h_+(\alpha^-,\alpha^+)\Big), \\ A_{12} &:= (1-\omega) + r\ \zeta(1+\omega)\Big(\big(1+\widehat{a}(\alpha^-)\widehat{\tfrac{1}{a}}(\alpha^+)\big) + \big(1-\widehat{a}(\alpha^+)\widehat{\tfrac{1}{a}}(\alpha^+)\big)h_+(\alpha^-,\alpha^+)\Big), \\ A_{21} &:= (1+\omega) + r\ \zeta(1-\omega)\Big(\big(1+\widehat{a}(\alpha^+)\widehat{\tfrac{1}{a}}(\alpha^-)\big) + \big(1-\widehat{a}(\alpha^-)\widehat{\tfrac{1}{a}}(\alpha^-)\big)\tfrac{1}{h_-(\alpha^-,\alpha^+)}\Big), \\ A_{22} &:= -(1+\omega)\tfrac{1}{h_-(\alpha^-,\alpha^+)} + b\ \zeta(1-\omega)\Big(\big(1-\widehat{a}(\alpha^+)\widehat{\tfrac{1}{a}}(\alpha^+)\big) + \big(1+\widehat{a}(\alpha^-)\widehat{\tfrac{1}{a}}(\alpha^+)\big)\tfrac{1}{h_-(\alpha^-,\alpha^+)}\Big), \end{aligned} \tag{4.8.36}$$

and

$$\begin{aligned} B_1 &:= r\ \zeta(1+\omega)\Big\{\big(1+h_+(\alpha^-,\alpha^+)\big)\mathcal{G}_1 + \big(\widehat{a}(\alpha^+)h_+(\alpha^-,\alpha^+) - \widehat{a}(\alpha^-)\big)\mathcal{G}_2\Big\}, \\ B_2 &:= r\ \zeta(1-\omega)\Big\{\big(1+\tfrac{1}{h_-(\alpha^-,\alpha^+)}\big)\mathcal{G}_1 + \big(\widehat{a}(\alpha^+) - \widehat{a}(\alpha^-)\tfrac{1}{h_-(\alpha^-,\alpha^+)}\big)\mathcal{G}_2\Big\}. \end{aligned} \tag{4.8.37}$$

Computing this 2×2 determinant $\det = A_{11}A_{22} - A_{21}A_{12}$ gives the expected expression after collecting the terms in powers of r. Using Cramer formulae, we obtain the expression of $\Delta\pi^-$ and $\Delta\pi^+$:

$$\Delta\pi^- = \frac{1}{\det}(B_1A_{22} - B_2A_{12}), \quad \Delta\pi^- = \frac{1}{\det}(B_2A_{11} - B_1A_{21}). \tag{4.8.38}$$

The expressions of Δu^- and Δu^+ are obtained by plugging theses expressions in (4.8.34). And using Lemma 4.3.6, we get the expression of all the intermediate states. Observe that all these expressions are bounded as soon as the two functions h_+ and $1/h_-$ are bounded and the determinant is not close to zero.

Appendix B: Proof of Lemma 4.5.1

Let us re-write the discretization of θ as follows

$$\theta_j^{n+1} = \theta_j^{n+\frac{2}{3}} - \lambda\left(\theta_{j+1}^{n+\frac{2}{3}}(V_I)^{*-}_{j+\frac{1}{2}} + \theta_j^{n+\frac{2}{3}}(V_I)^{*+}_{j+\frac{1}{2}} - \theta_j^{n+\frac{2}{3}}(V_I)^{*-}_{j-\frac{1}{2}} - \theta_{j-1}^{n+\frac{2}{3}}(V_I)^{*+}_{j-\frac{1}{2}}\right) \Longleftrightarrow \tag{4.8.39}$$

$$\theta_j^{n+1} = \left\{1 - \lambda\left((V_I)^{*+}_{j+\frac{1}{2}} - (V_I)^{*-}_{j-\frac{1}{2}}\right)\right\}\theta_j^{n+\frac{2}{3}} + \underbrace{\left\{-\lambda(V_I)^{*-}_{j+\frac{1}{2}}\right\}}_{\geq 0}\theta_{j+1}^{n+\frac{2}{3}} + \underbrace{\left\{\lambda(V_I)^{*+}_{j-\frac{1}{2}}\right\}}_{\geq 0}\theta_{j-1}^{n+\frac{2}{3}} \tag{4.8.40}$$

where for all j in $\mathbb{Z}$, $(V_I)^{*+}_{j+\frac{1}{2}} = \max(0,(V_I)^*_{j+\frac{1}{2}})$ and $(V_I)^{*-}_{j+\frac{1}{2}} = \min(0,(V_I)^*_{j+\frac{1}{2}})$. As

$$1 - \lambda\left((V_I)^{*+}_{j+\frac{1}{2}} - (V_I)^{*-}_{j-\frac{1}{2}}\right) \geq 1 - \lambda|(V_I)^*_{j+\frac{1}{2}}| - \lambda|(V_I)^*_{j-\frac{1}{2}}| > 0$$

by the CFL condition (4.5.4), we have proven (4.5.7). The discretization of $\theta\Theta$ re-writes

$$\begin{aligned} \theta_j^{n+1}\Theta_j^{n+1} = {} & \theta_j^{n+\frac{2}{3}}\Theta_j^{n+\frac{2}{3}} \\ & -\lambda\left(\theta_{j+1}^{n+\frac{2}{3}}\Theta_{j+1}^{n+\frac{2}{3}}(V_I)^{*-}_{j+\frac{1}{2}} + \theta_j^{n+\frac{2}{3}}\Theta_j^{n+\frac{2}{3}}(V_I)^{*+}_{j+\frac{1}{2}} - \theta_j^{n+\frac{2}{3}}\Theta_j^{n+\frac{2}{3}}(V_I)^{*-}_{j-\frac{1}{2}} - \theta_{j-1}^{n+\frac{2}{3}}\Theta_{j-1}^{n+\frac{2}{3}}(V_I)^{*+}_{j-\frac{1}{2}}\right). \end{aligned} \tag{4.8.41}$$

In order to prove the maximum principle on Θ, we distinguish two cases. First, if $\theta_j^{n+1} = 0$, equation (4.8.40) implies that $\theta_j^{n+\frac{2}{3}} = 0$ and $(V_I^*)^-_{j+\frac{1}{2}}\theta_{j+1}^{n+\frac{2}{3}} = (V_I^*)^+_{j-\frac{1}{2}}\theta_{j-1}^{n+\frac{2}{3}} = 0$ under the strict CFL condition (4.5.4). Hence, equation (4.8.41) is trivially true which means that Θ_j^{n+1} is not updated and one has $\Theta_j^{n+1} = \Theta_j^{n+\frac{2}{3}}$ and the maximum principle is staisfied for Θ. Now, if $\theta_j^{n+1} \neq 0$, dividing equation (4.8.40) by θ_j^{n+1} yields

$$1 = \left\{1 - \lambda\left((V_I)^{*+}_{j+\frac{1}{2}} - (V_I)^{*-}_{j-\frac{1}{2}}\right)\right\}\frac{\theta_j^{n+\frac{2}{3}}}{\theta_j^{n+1}} + C_{j+\frac{1}{2}} + D_{j-\frac{1}{2}} \tag{4.8.42}$$

where $C_{j+\frac{1}{2}} = \left\{-\lambda(V_I)^{*-}_{j+\frac{1}{2}}\right\}\frac{\theta_{j+1}^{n+\frac{2}{3}}}{\theta_j^{n+1}} \geq 0$ and $D_{j-\frac{1}{2}} = \left\{\lambda(V_I)^{*+}_{j-\frac{1}{2}}\right\}\frac{\theta_{j-1}^{n+\frac{2}{3}}}{\theta_j^{n+1}} \geq 0$. Thanks to (4.8.42), one has $C_{j+\frac{1}{2}} + D_{j-\frac{1}{2}} < 1$.

Multiplying equation (4.8.40) by $\Theta_j^{n+\frac{2}{3}}$ and substracting it from (4.8.41) yields

$$\theta_j^{n+1}\left(\Theta_j^{n+1} - \Theta_j^{n+\frac{2}{3}}\right) = -\lambda(V_I)^{*-}_{j+\frac{1}{2}}\theta_{j+1}^{n+\frac{2}{3}}\left(\Theta_{j+1}^{n+\frac{2}{3}} - \Theta_j^{n+\frac{2}{3}}\right) - \lambda(V_I)^{*+}_{j-\frac{1}{2}}\theta_{j-1}^{n+\frac{2}{3}}\left(\Theta_j^{n+\frac{2}{3}} - \Theta_{j-1}^{n+\frac{2}{3}}\right). \tag{4.8.43}$$

Dividing by θ_j^{n+1} we get a convexe combination for Θ_j^{n+1} which proves the maximum principle:

$$\Theta_j^{n+1} = \left\{1 - C_{j+\frac{1}{2}} - D_{j-\frac{1}{2}}\right\}\Theta_j^{n+\frac{2}{3}} + C_{j+\frac{1}{2}}\Theta_{j+1}^{n+\frac{2}{3}} + D_{j-\frac{1}{2}}\Theta_{j-1}^{n+\frac{2}{3}}. \tag{4.8.44}$$

Appendix C: Proofs related to Section 4.6

Proof of Lemma 4.6.1

We first prove (4.6.1). Multiplying equation (4.3.58) by $(\tau_k)_j^n = 1/(\rho_k)_j^n$, one gets

$$\begin{aligned}
& (\tau_k)_j^{n+\frac{1}{3}} = (\tau_k)_j^n\left\{1 + \lambda\ \left((u_k)^-_{j+\frac{1}{2}} - (u_k)^+_{j-\frac{1}{2}}\right)\right\} \\
\iff\quad & (\rho_k)_j^n = (\rho_k)_j^{n+\frac{1}{3}}\left\{1 + \lambda\ \left((u_k)^-_{j+\frac{1}{2}} - (u_k)^+_{j-\frac{1}{2}}\right)\right\} \\
\iff\quad & (\rho_k)_j^{n+\frac{1}{3}} = (\rho_k)_j^n - \ \lambda\ (\rho_k)_j^{n+\frac{1}{3}}\left((u_k)^-_{j+\frac{1}{2}} - (u_k)^+_{j-\frac{1}{2}}\right).
\end{aligned}$$

Multiplying by $(\alpha_k)_j^{n+\frac{1}{3}} = (\alpha_k)_j^n$, this gives

$$(\alpha_k\rho_k)_j^{n+\frac{1}{3}} = (\alpha_k\rho_k)_j^n - \ \lambda\ (\rho_k)_j^{n+\frac{1}{3}}(\alpha_k)_j^n\left((u_k)^-_{j+\frac{1}{2}} - (u_k)^+_{j-\frac{1}{2}}\right). \tag{4.8.45}$$

Now, with the definitions of $(u_k - V_I)^*_{j+\frac{1}{2}}$ (in 4.3.62), $(u_k)^*_{j+\frac{1}{2}}$ (in 4.3.65), we have

$$\begin{aligned}
(\alpha_k)_j^n\left((u_k)^-_{j+\frac{1}{2}} - (u_k)^+_{j-\frac{1}{2}}\right) \quad & = (\alpha_k)_j^n\left((u_k)^*_{j+\frac{1}{2}} - (u_k)^*_{j-\frac{1}{2}}\right) \\
& + (u_k - V_I)^*_{j+\frac{1}{2}}\left((\alpha_k)_{j+1}^n - (\alpha_k)_j^n\right)\mathbb{1}_{(u_k - V_I)^*_{j+\frac{1}{2}} > 0} \\
& + (u_k - V_I)^*_{j-\frac{1}{2}}\left((\alpha_k)_j^n - (\alpha_k)_{j-1}^n\right)\mathbb{1}_{(u_k - V_I)^*_{j-\frac{1}{2}} \leq 0}.
\end{aligned} \tag{4.8.46}$$

Using $(u_k - V_I)^*_{j+\frac{1}{2}} = (u_k)^*_{j+\frac{1}{2}} - (V_I)^*_{j+\frac{1}{2}}$ for $j \in \mathbb{Z}$ and collecting the terms in $(u_k)^*_{j+\frac{1}{2}}$ and $(u_k)^*_{j-\frac{1}{2}}$, this re-writes

$$\begin{aligned}(\alpha_k)^n_j \left((u_k)^-_{j+\frac{1}{2}} - (u_k)^+_{j-\frac{1}{2}}\right) &= \left((\alpha_k)^*_{j+\frac{1}{2}}(u_k)^*_{j+\frac{1}{2}} - (\alpha_k)^*_{j-\frac{1}{2}}(u_k)^*_{j-\frac{1}{2}}\right)\\ &+(V_I)^*_{j+\frac{1}{2}}\left((\alpha_k)^n_{j+1} - (\alpha_k)^n_j\right)\mathbb{1}_{(u_k-V_I)^*_{j+\frac{1}{2}}>0}\\ &+(V_I)^*_{j-\frac{1}{2}}\left((\alpha_k)^n_j - (\alpha_k)^n_{j-1}\right)\mathbb{1}_{(u_k-V_I)^*_{j-\frac{1}{2}}\leq 0},\end{aligned} \tag{4.8.47}$$

since by Definition 4.3.2, we have $(\alpha_k)^*_{j+\frac{1}{2}} = (\alpha_k)^n_j + \left((\alpha_k)^n_{j+1} - (\alpha_k)^n_j\right)\mathbb{1}_{(u_k-V_I)^*_{j+\frac{1}{2}}>0}$ and $(\alpha_k)^*_{j-\frac{1}{2}} = (\alpha_k)^n_j - \left((\alpha_k)^n_j - (\alpha_k)^n_{j-1}\right)\mathbb{1}_{(u_k-V_I)^*_{j-\frac{1}{2}}\leq 0}$. Replacing in (4.8.45) yields

$$\begin{aligned}(\alpha_k\rho_k)^{n+\frac{1}{3}}_j = (\alpha_k\rho_k)^n_j \quad &-\lambda(\rho_k)^{n+\frac{1}{3}}_j \left((\alpha_k)^*_{j+\frac{1}{2}}(u_k)^*_{j+\frac{1}{2}} - (\alpha_k)^*_{j-\frac{1}{2}}(u_k)^*_{j-\frac{1}{2}}\right)\\ &+\lambda(\rho_k)^{n+\frac{1}{3}}_j (V_I)^*_{j+\frac{1}{2}}\left((\alpha_k)^n_{j+1} - (\alpha_k)^n_j\right)\mathbb{1}_{(u_k-V_I)^*_{j+\frac{1}{2}}>0}\\ &+\lambda(\rho_k)^{n+\frac{1}{3}}_j (V_I)^*_{j-\frac{1}{2}}\left((\alpha_k)^n_j - (\alpha_k)^n_{j-1}\right)\mathbb{1}_{(u_k-V_I)^*_{j-\frac{1}{2}}\leq 0}.\end{aligned} \tag{4.8.48}$$

Since $(\rho_k)^{n+\frac{1}{3}}_{j+\frac{1}{2}}$ is upwind-biased with respect to $(u_k - V_I)^*_{j+\frac{1}{2}}$ according to (4.4.3), we have

$$\begin{aligned}(\rho_k)^{n+\frac{1}{3}}_j \mathbb{1}_{(u_k-V_I)^*_{j+\frac{1}{2}}>0} &= (\rho_k)^{n+\frac{1}{3}}_{j+\frac{1}{2}}\mathbb{1}_{(u_k-V_I)^*_{j+\frac{1}{2}}>0},\\ (\rho_k)^{n+\frac{1}{3}}_j \mathbb{1}_{(u_k-V_I)^*_{j-\frac{1}{2}}\leq 0} &= (\rho_k)^{n+\frac{1}{3}}_{j-\frac{1}{2}}\mathbb{1}_{(u_k-V_I)^*_{j-\frac{1}{2}}\leq 0}.\end{aligned}$$

Hence, in second line of (4.8.48), $(\rho_k)^{n+\frac{1}{3}}_j$ can be repaced by $(\rho_k)^{n+\frac{1}{3}}_{j+\frac{1}{2}}$ and in the third line of (4.8.48), $(\rho_k)^{n+\frac{1}{3}}_j$ can be repaced by $(\rho_k)^{n+\frac{1}{3}}_{j-\frac{1}{2}}$. This concludes the proof of (4.6.1).

Now for (4.6.2), the result is straightforward when multiply (4.3.59) by $(\alpha_k)^{n+\frac{1}{3}}_j = (\alpha_k)^n_j$. □

Proof of Lemma 4.6.2

Multiplying equation (4.4.2) by $(\alpha_k)^{n+\frac{2}{3}}_j = (\alpha_k)^{n+\frac{1}{3}}_j = (\alpha_k)^n_j$, we obtain

$$\begin{aligned}(\alpha_k\rho_k X_k)^{n+\frac{2}{3}}_j = (\alpha_k\rho_k X_k)^{n+\frac{1}{3}}_j \quad &-\lambda\ (\alpha_k)^n_j(u_k - V_I)^*_{j+\frac{1}{2}}\left((\rho_k X_k)^{n+\frac{1}{3}}_{j+\frac{1}{2}} - (\rho_k X_k)^{n+\frac{1}{3}}_j\right)\\ &-\lambda\ (\alpha_k)^n_j(u_k - V_I)^*_{j-\frac{1}{2}}\left((\rho_k X_k)^{n+\frac{1}{3}}_j - (\rho_k X_k)^{n+\frac{1}{3}}_{j-\frac{1}{2}}\right)\\ &+\lambda\ (\alpha_k)^n_j(\rho_k X_k)^{n+\frac{1}{3}}_j\left((V_I)^*_{j+\frac{1}{2}} - (V_I)^*_{j-\frac{1}{2}}\right).\end{aligned} \tag{4.8.49}$$

Using $(u_k - V_I)^*_{j+\frac{1}{2}} = (u_k)^*_{j+\frac{1}{2}} - (V_I)^*_{j+\frac{1}{2}}$ for $j \in \mathbb{Z}$ and collecting the terms in $(u_k)^*_{j+\frac{1}{2}}$ and $(u_k)^*_{j-\frac{1}{2}}$, this re-writes

$$\begin{aligned}(\alpha_k\rho_k X_k)^{n+\frac{2}{3}}_j = (\alpha_k\rho_k X_k)^{n+\frac{1}{3}}_j \quad &-\lambda\ (\alpha_k)^n_j(u_k)^*_{j+\frac{1}{2}}\left((\rho_k X_k)^{n+\frac{1}{3}}_{j+\frac{1}{2}} - (\rho_k X_k)^{n+\frac{1}{3}}_j\right)\\ &-\lambda\ (\alpha_k)^n_j(u_k)^*_{j-\frac{1}{2}}\left((\rho_k X_k)^{n+\frac{1}{3}}_j - (\rho_k X_k)^{n+\frac{1}{3}}_{j-\frac{1}{2}}\right)\\ &+\lambda\ (\alpha_k)^n_j\left((\rho_k X_k)^{n+\frac{1}{3}}_{j+\frac{1}{2}}(V_I)^*_{j+\frac{1}{2}} - (\rho_k X_k)^{n+\frac{1}{3}}_{j-\frac{1}{2}}(V_I)^*_{j-\frac{1}{2}}\right).\end{aligned} \tag{4.8.50}$$

Now, by definition of $(\alpha_k)^*_{j+\frac{1}{2}}$ and since $(\rho_k X_k)^{n+\frac{1}{3}}_{j+\frac{1}{2}}$ is upwind-biased with respect to $(u_k - V_I)^*_{j+\frac{1}{2}}$ according to (4.4.3), we get

$$\begin{aligned}(\alpha_k)^n_j \left((\rho_k X_k)^{n+\frac{1}{3}}_{j+\frac{1}{2}} - (\rho_k X_k)^{n+\frac{1}{3}}_j\right) &= (\alpha_k)^*_{j+\frac{1}{2}} \mathbb{1}_{(u_k - V_I)^*_{j+\frac{1}{2}} \leq 0} \left((\rho_k X_k)^{n+\frac{1}{3}}_{j+\frac{1}{2}} - (\rho_k X_k)^{n+\frac{1}{3}}_j\right) \\ &= (\alpha_k)^*_{j+\frac{1}{2}} \left((\rho_k X_k)^{n+\frac{1}{3}}_{j+\frac{1}{2}} - (\rho_k X_k)^{n+\frac{1}{3}}_j\right),\end{aligned}$$

and a similar argument gives

$$(\alpha_k)^n_j \left((\rho_k X_k)^{n+\frac{1}{3}}_j - (\rho_k X_k)^{n+\frac{1}{3}}_{j-\frac{1}{2}}\right) = (\alpha_k)^*_{j-\frac{1}{2}} \left((\rho_k X_k)^{n+\frac{1}{3}}_j - (\rho_k X_k)^{n+\frac{1}{3}}_{j-\frac{1}{2}}\right).$$

Replacing in (4.8.50) yields the result.

□

Acknowledgements. The third author receives a financial support by ANRT through an EDF-CIFRE contract 529/2009. The forth author is partially supported by the LRC Manon (Modélisation et Approximation Numérique Orientées pour l'énergie Nucléaire — CEA DM2S/LJLL).

References

[1] R. Abgrall and R. Saurel. Discrete equations for physical and numerical compressible multiphase mixtures. *Journal of Computational Physics*, 186(2):361–396, 2003.

[2] A. Ambroso, C. Chalons, F. Coquel, and T. Galié. Relaxation and numerical approximation of a two-fluid two-pressure diphasic model. *M2AN Math. Model. Numer. Anal.*, 43(6):1063–1097, 2009.

[3] M.R. Baer and J.W. Nunziato. A two-phase mixture theory for the deflagration-to-detonation transition (DDT) in reactive granular materials. *International Journal of Multiphase Flow*, 12(6):861 – 889, 1986.

[4] C. Chalons, F. Coquel, S. Kokh, and N. Spillane. Large time-step numerical scheme for the seven-equation model of compressible two-phase flows. *Springer Proceedings in Mathematics, FVCA 6, 2011*, 4:225–233, 2011.

[5] F. Coquel, E. Godlewski, and N. Seguin. Relaxation of fluid systems. *Math. Models Methods Appl. Sci.*, 22(8), 2012.

[6] F. Coquel, J-M. Hérard, K. Saleh, and N. Seguin. A class of two-fluid two-phase flow models. *AIAA paper 2012-3356. https://www.aiaa.org/.*

[7] T. Gallouët, J-M. Hérard, and N. Seguin. Numerical modeling of two-phase flows using the two-fluid two-pressure approach. *Math. Models Methods Appl. Sci.*, 14(5):663–700, 2004.

[8] J-M. Hérard and O. Hurisse. A fractional step method to compute a class of compressible gas-luiquid flows. *Computers & Fluids. An International Journal*, 55:57–69, 2012.

[9] M. Papin and R. Abgrall. Fermetures entropiques pour les systèmes bifluides à sept équations. *Compt. Rendu. Acad. Sci. Mécanique*, 333:838–842, 2005.

[10] R. Saurel, S. Gavrilyuk, and F. Renaud. A multiphase model with internal degrees of freedom: application to shock–bubble interaction. *Journal of Fluid Mechanics*, 495:283–321, 2003.

[11] D.W. Schwendeman, C.W. Wahle, and A.K. Kapila. The Riemann problem and a high-resolution Godunov method for a model of compressible two-phase flow. *Journal of Computational Physics*, 212(2):490 – 526, 2006.

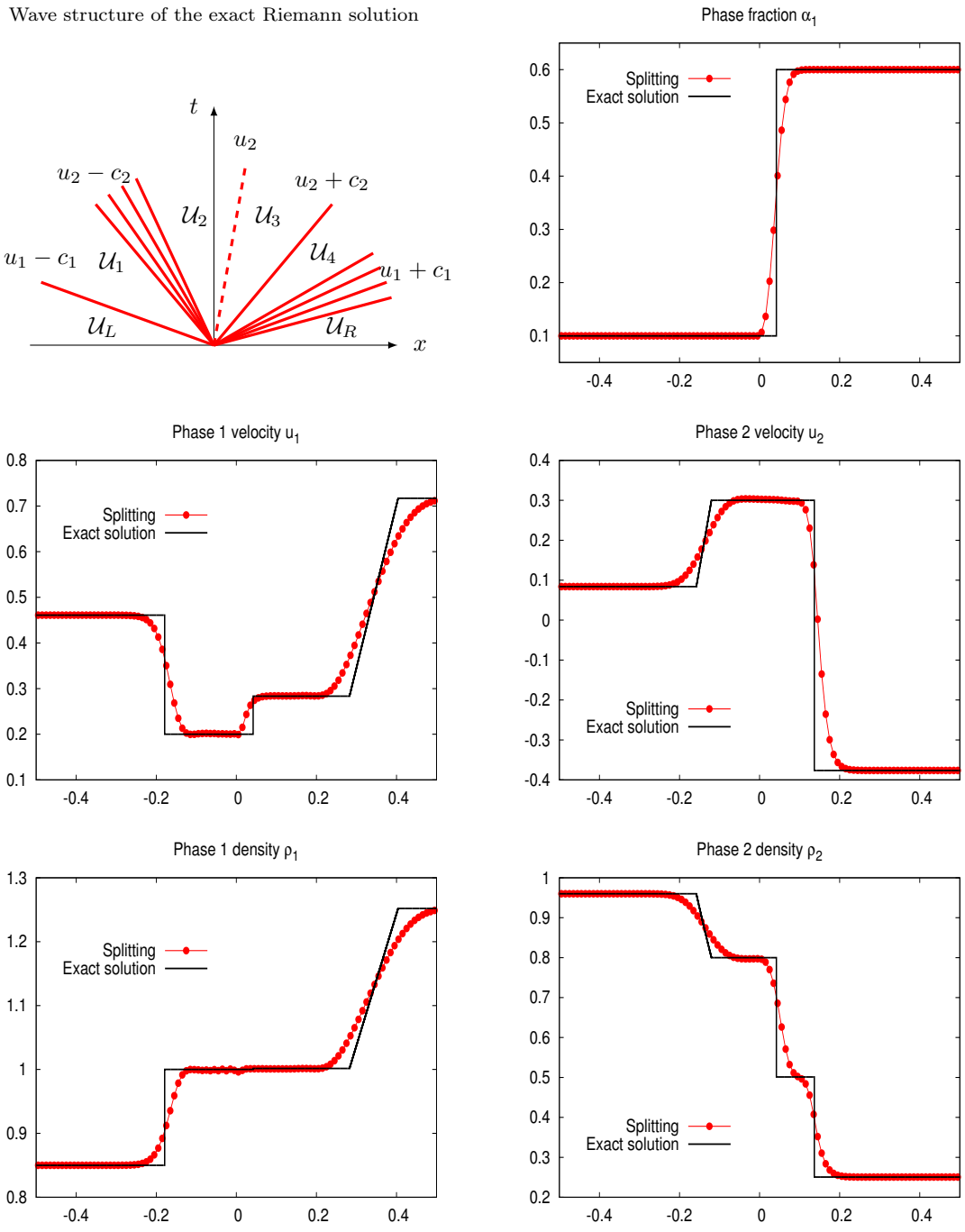

Figure 4.1: Isentropic case: Structure of the solution and space variations of the physical variables at the final time $T = 0.14$. Mesh size: 100 cells.

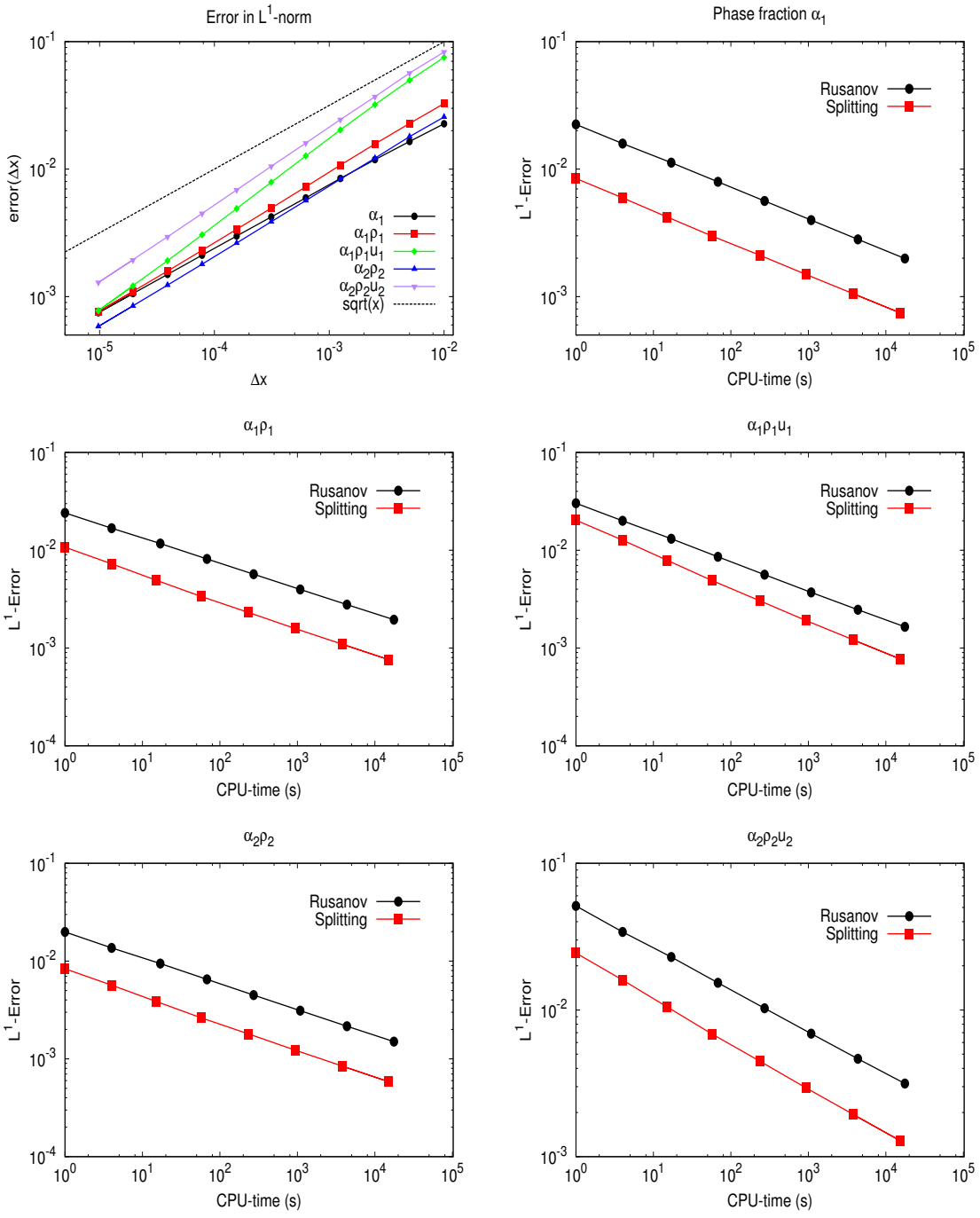

Figure 4.2: Isentropic case: L^1-Error with respect to Δx and L^1-Error with respect to computational cost (in seconds), for the conservative variables.

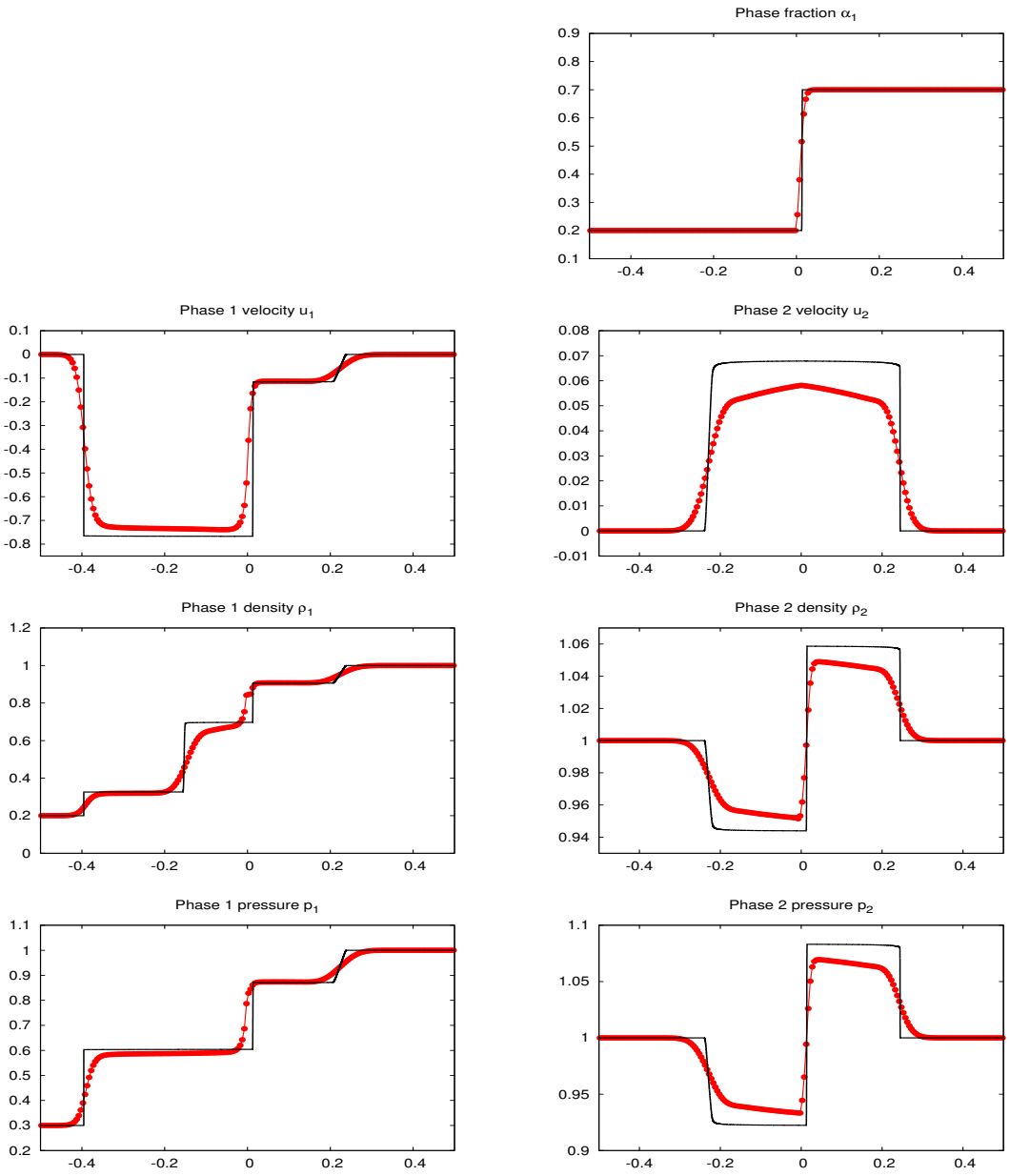

Figure 4.3: Model with energies: space variations of the physical variables at the final time $T = 0.2$. Red dots: 200-cell mesh. Straight line: 10^5-cell mesh.

Annexes

Appendix A

Convexité de l'entropie mathématique pour le modèle de Baer-Nunziato

This appendix is devoted to proving the convexity of the mathematical entropy of the Baer-Nunziato model.

Let us first introduce some notations:

$$\begin{aligned} \alpha = \alpha_1 = 1 - \alpha_2, \qquad & \mathbf{c}(\mathbf{u})^T = (V_I, 0, -P_I, -V_I P_I, 0, P_I, V_I P_I), \\ \mathbf{u}_k^T = (\rho_k, \rho_k u_k, \rho_k E_k), \qquad & \mathbf{f}_k(\mathbf{u}_k)^T = (\rho_k u_k, \rho_k u_k^2/2 + P_k, u_k(\rho_k E_k + P_k)), \\ \mathbf{u}^T = (\alpha, \alpha \mathbf{u}_1^T, (1-\alpha)\mathbf{u}_2^T), \qquad & \mathbf{f}(\mathbf{u})^T = (\alpha, \alpha \mathbf{f}_1(\mathbf{u}_1)^T, (1-\alpha)\mathbf{f}(\mathbf{u}_2)^T). \end{aligned}$$

We now define $\omega = \left\{(a_1, a_2, a_3) \in \mathbb{R}^3 \text{ such that } a_1 > 0, a_3/a_1 - a_2^2/(2a_1^2) > 0\right\}$ and from now on we assume that $\mathbf{u}$ lies in $\Omega = (0,1) \times \omega \times \omega$, which means that the phase fractions α_k, the densities ρ_k and the internal energies e_k are positive, for $k = 1, 2$.

The two-velocity two-pressure system can be written as:

$$\partial_t \mathbf{u} + \partial_x \mathbf{f}(\mathbf{u}) + \mathbf{c}(\mathbf{u}) \partial_x \alpha = 0. \tag{A.0.1}$$

Let us introduce the entropy pair (S_k, F_k) associated with the system $\partial_t \mathbf{u}_k + \partial_x \mathbf{f}_k(\mathbf{u}_k) = 0$ and defined by

$$S_k(\mathbf{u}_k) = -\rho_k s_k \quad \text{and} \quad F_k'(\mathbf{u}_k) = (S_k'(\mathbf{u}_k))^T \mathbf{f}_k'(\mathbf{u}_k), \tag{A.0.2}$$

where s_k is the physical entropy of phase k given by the second law of thermodynamics

$$de_k = T_k ds_k - p_k d\tau_k.$$

It is well-known that the mathematical entropy S_k is *strictly convex* with respect to $\mathbf{u}_k$ and that the pair (S_k, F_k) verifies for smooth solutions

$$\partial_t S_k + \partial_x F_k = 0.$$

We define now the entropy of the two-phase flow:

Definition A.0.1. *The mixture entropy for the system* (A.0.1) *is*

$$S(\mathbf{u}) = \alpha S_1(\mathbf{u}_1) + (1-\alpha) S_2(\mathbf{u}_2), \tag{A.0.3}$$

and the associated mixture entropy flux

$$F(\mathbf{u}) = \alpha F_1(\mathbf{u}_1) + (1-\alpha) F_2(\mathbf{u}_2). \tag{A.0.4}$$

Observe that this definition does not account for any phenomenon at the interface between the two phases.

We may now state the following important property of the mixture entropy:

Proposition A.0.1. *The mixture entropy S is (non strictly) convex in Ω.*

Proof. First, we write S as a function of $(\alpha, \alpha\mathbf{u}_1, (1-\alpha)\mathbf{u}_2)$:

$$S(\alpha, \alpha\mathbf{u}_1, (1-\alpha)\mathbf{u}_2) = \alpha S_1\Big(\frac{\alpha\mathbf{u}_1}{\alpha}\Big) + (1-\alpha)S_2\Big(\frac{(1-\alpha)\mathbf{u}_2}{1-\alpha}\Big).$$

Then, the hessian matrix of S has the form

$$S''(\mathbf{u}) = \begin{pmatrix} A & B^T & C^T \\ B & \frac{1}{\alpha}S_1''(\mathbf{u}_1) & 0 \\ C & 0 & \frac{1}{1-\alpha}S_2''(\mathbf{u}_2) \end{pmatrix}$$

with

$$A = \frac{1}{\alpha}\mathbf{u}_1^T S_1''(\mathbf{u}_1)\mathbf{u}_1 + \frac{1}{1-\alpha}\mathbf{u}_2^T S_2''(\mathbf{u}_2)\mathbf{u}_2,$$
$$B = -\frac{1}{\alpha}S_1''(\mathbf{u}_1)\mathbf{u}_1 \quad \text{and} \quad C = \frac{1}{1-\alpha}S_2''(\mathbf{u}_2)\mathbf{u}_2.$$

Let (a, b^T, c^T) be vector of $\mathbb{R}^7$. Let us check that the hessian S'' is positive as soon as S_1'' and S_2'' are positive. We have

$$(a, b^T, c^T)\ S''(\mathbf{u}) \begin{pmatrix} a \\ b \\ c \end{pmatrix} = a^2 A + aB^T b + aC^T c + ab^T B + \frac{1}{\alpha}b^T S_1''(\mathbf{u}_1)b + ac^T C + \frac{1}{1-\alpha}c^T S_2''(\mathbf{u}_2)c.$$

Using the definitions of A, B and C we obtain

$$(a, b^T, c^T)\ S''(\mathbf{u}) \begin{pmatrix} a \\ b \\ c \end{pmatrix} = \frac{1}{\alpha}(b - a\mathbf{u}_1)^T S_1''(\mathbf{u}_1)(b - a\mathbf{u}_1) + \frac{1}{1-\alpha}(c + a\mathbf{u}_2)^T S_2''(\mathbf{u}_2)(c + a\mathbf{u}_2).$$

This right-hand side is clear nonnegative since S_1 and S_2 are strictly convex. □

Let us rapidly study the case of the degeneracy of $S''(\mathbf{u})$. One can easily check that

$$(a, b^T, c^T)\ S''(\mathbf{u}) \begin{pmatrix} a \\ b \\ c \end{pmatrix} = 0 \Longleftrightarrow (a, b, c) \in \operatorname{span}\{(1, \mathbf{u}_1, -\mathbf{u}_2)\}.$$

Finally, we observe that the main key of the proof is the convexity of the phasic mathematical entropies. Hence, this proof can be immediately extended to the isentropic version of the Baer-Nunziato model, replacing $-s_k$ by the phasic energies $E_k = \frac{u_k^2}{2} + e_k(\rho_k)$.

Appendix B

Un schéma à pas fractionnaires simple pour le modèle de Baer-Nunziato

A SPLITTING METHOD FOR THE ISENTROPIC BAER-NUNZIATO TWO-PHASE FLOW MODEL[1]

Frédéric Coquel, Jean-Marc Hérard, Khaled Saleh

Abstract

In the present work, we propose a fractional step method for computing approximate solutions of the isentropic Baer-Nunziato two-phase flow model. The scheme relies on an operator splitting method corresponding to a separate treatment of fast propagation phenomena due to the acoustic waves on the one hand and slow propagation phonomena due to the fluid motion on the other. The scheme is proved to preserve positive values of the statistical fractions and densities. We also provide two test-cases that assess the convergence of the method.

Résumé

Nous proposons ici une méthode à pas fractionnaires pour le calcul de solutions approchées pour la version isentropique du modèle diphasique de Baer-Nunziato. Le schéma s'appuie sur un splitting de l'opérateur temporel correspondant à la prise en compte différenciée des phéno-mènes de propagation rapide dus aux ondes acoustiques et des phénomènes de propagation lente dus aux ondes matérielles. On prouve que le schéma permet de préserver des valeurs positives pour les taux statistiques de présence des phases ainsi que pour les densités. Deux cas tests numériques permettent d'illustrer la convergence de la méthode.

Introduction

The two-fluid approach is useful for a detailed investigation of some patterns occuring in gas-solid two-phase flows, or alternatively in water-vapour flows such as those encountered in pressurised water reactors. In the latter framework, a classical situation corresponds to the prediction of the boiling crisis, where the flow is initially dominated by the liquid phase while the vapour phase is dilute. Actually, the two-fluid model proposed in [2, 8, 6, 9, 11] is one suitable candidate that enables the computation of two-phase flows in which few bubbles are statistically present in a liquid phase. For other approaches relying on different assumptions, see [14, 4]. Several schemes have already been proposed in the literature in order to build consistent and stable approximations of the Baer-Nunziato model, among which we may cite those relying on interface Riemann solvers (see for instance [15, 17, 12, 16]) and other schemes relying on relaxation techniques (see for instance [1]).

[1] Cette annexe reprend un article accepté pour publication dans la revue *ESAIM Proceedings*.

However, one difficulty -among others- that immediately arises when computing approximations of the Baer-Nunziato model is due to the fact that the convective effects in this non-conservative model require accurate enough schemes ; otherwise, the numerical approximations provided by standard solvers seem to be useless, and one reason for that failure is that the mix of "fast" waves corresponding with acoustic waves and "slow" waves associated with material velocities requires the development of schemes which should be accurate for quantities governed by either fast or slow waves. We suggest here a possible way to tackle this difficult problem, which is grounded on the use of a fractional step method. Before going further on, we recall that this idea has already been used earlier within the framework of Euler equations (see for instance [3]), but also for the Baer-Nunziato model (see [5]). Roughly speaking, a two-step algorithem is introduced in order to account for acoustic waves in the two-phase medium within the first step, while the second step handles material waves. In order to simplify the presentation, we will restrict in this paper to the barotropic version of the BN model, but the extension to the standard BN model is straightforward. Moreover, the numerical treatment of source terms will be disregarded, and we refer to relevant references for that topic [10].

Actually, the paper is organized as follows. In Section B.1, we present the set of partial differential equations of the Baer-Nunziato two-phase flow model in the isentropic framework, and we recall its main mathematical properties. In Section B.2, we propose an operator splitting method for this model, and we describe the numerical treatment of each step. Finally, Section B.3 is devoted to the numerical experiments, where two test cases have been implemented with a mesh refinement procedure that proves the convergence of the method.

B.1 The Baer-Nunziato two-phase flow model and its mathematical properties

In the present work, we consider a model formulated in Eulerian coordinates where balance equations account for the evolution of mass and momentum of each phase. For compressible isentropic one-dimensional flows there are five unknowns that describe the evolution of the two-phase flow: the velocities of each phase u_k (where $k \in \{1,2\}$), the densities of each phase ρ_k and the phase fractions α_k (knowing that $\alpha_1 + \alpha_2 = 1$). The isentropic version of the model –firstly introduced by Baer & Nunziato– reads

$$
\begin{aligned}
&\partial_t \alpha_1 + v_I \partial_x \alpha_1 = \Theta_p (p_1 - p_2), \\
&\partial_t (\alpha_1 \rho_1) + \partial_x (\alpha_1 \rho_1 u_1) = 0, \\
&\partial_t (\alpha_1 \rho_1 u_1) + \partial_x (\alpha_1 \rho_1 u_1^2 + \alpha_1 p_1) - p_I \partial_x \alpha_1 = \Theta_u (u_2 - u_1), \\
&\partial_t (\alpha_2 \rho_2) + \partial_x (\alpha_2 \rho_2 u_2) = 0, \\
&\partial_t (\alpha_2 \rho_2 u_2) + \partial_x (\alpha_2 \rho_2 u_2^2 + \alpha_2 p_2) - p_I \partial_x \alpha_2 = \Theta_u (u_1 - u_2),
\end{aligned}
\tag{B.1.1}
$$

where v_I and p_I are the interfacial velocity and pressure for which one must provide closure laws as well as for the relaxation coefficients Θ_u and Θ_p. One classical choice in the existing literature

(see [10]) is

$$\Theta_p = \frac{\alpha_1\alpha_2}{\tau_p \Pi_0}, \tag{B.1.2}$$

$$\Theta_p = \frac{1}{\tau_u}\frac{(\alpha_1\rho_1)(\alpha_2\rho_2)}{\alpha_1\rho_1 + \alpha_2\rho_2}, \tag{B.1.3}$$

where Π_0 has the dimension of a pressure, and τ_p and τ_u are two characteristic times of the pressure and velocity relaxation processes. For liquid-vapor applications, where the vapor phase is assumed to be dilute (we also refer to [2] where one of the phases is dilute), a meaningful choice for the pair of interfacial velocity and pressure is

$$(v_I, p_I) = (u_2, p_1). \tag{B.1.4}$$

In this case, the index 1 refers to the liquid phase while the index 2 refers to the vapor phase. We also assume a barotropic pressure law for each phase $\rho_k \mapsto p_k(\rho_k), k \in \{1,2\}$ that can be deduced from the complete set of equations of the Baer-Nunziato model when assuming formally a constant entropy s_k for each phase. We only consider a smooth dependence of $p_k(\rho_k)$ such that $p_k(\rho_k) > 0$, $p_k'(\rho_k) > 0$, $p_k''(\rho_k) + \frac{2}{\rho_k}p_k'(\rho_k) > 0$, $\lim\limits_{\rho_k \to 0} p_k(\rho_k) = 0$, and $\lim\limits_{\rho_k \to +\infty} p_k(\rho_k) = +\infty$. We denote

$$\mathbb{U} = (\alpha_1, \alpha_1\rho_1, \alpha_1\rho_1 u_1, \alpha_2\rho_2, \alpha_2\rho_2 u_2) \tag{B.1.5}$$

the unknown vector which is expected to belong to the natural physical space

$$\Omega = \left\{ \mathbb{U} = (\alpha_1, \alpha_1\rho_1, \alpha_1\rho_1 u_1, \alpha_2\rho_2, \alpha_2\rho_2 u_2) \in \mathbb{R}^5, 0 < \alpha_k < 1, \rho_k > 0, k \in \{1,2\}, \alpha_1 + \alpha_2 = 1 \right\}. \tag{B.1.6}$$

System (B.1.1) takes the following condensed form

$$\partial_t \mathbb{U} + \partial_x \mathbf{F}(\mathbb{U}) + \mathbf{C}(\mathbb{U})\partial_x \mathbb{U} = \mathbf{S}(\mathbb{U}), \quad x \in \mathbb{R},\ t > 0, \tag{B.1.7}$$

where

$$\mathbf{F}(\mathbb{U}) = \begin{bmatrix} 0 \\ \alpha_1\rho_1 u_1 \\ \alpha_1\rho_1 u_1^2 + \alpha_1 p_1(\rho_1) \\ \alpha_2\rho_2 u_2 \\ \alpha_2\rho_2 u_2^2 + \alpha_2 p_2(\rho_2) \end{bmatrix}, \quad \mathbf{C}(\mathbb{U})\partial_x\mathbb{U} = \begin{bmatrix} u_2\partial_x\alpha_1 \\ 0 \\ -p_1\partial_x\alpha_1 \\ 0 \\ -p_1\partial_x\alpha_2 \end{bmatrix}, \quad \mathbf{S}(\mathbb{U}) = \begin{bmatrix} \Theta_p\left(p_1(\rho_1) - p_2(\rho_2)\right) \\ 0 \\ \Theta_u(u_2 - u_1) \\ 0 \\ \Theta_u(u_1 - u_2) \end{bmatrix}. \tag{B.1.8}$$

The following proposition holds:

Proposition B.1.1. *For every state vector $\mathbb{U}$ in Ω, the convective part of system (B.1.7) admits the following real eigenvalues:*

$$\sigma_1(\mathbb{U}) = u_2, \quad \sigma_2(\mathbb{U}) = u_1 - c_1, \quad \sigma_3(\mathbb{U}) = u_1 + c_1, \quad \sigma_4(\mathbb{U}) = u_2 - c_2, \quad \sigma_5(\mathbb{U}) = u_2 + c_2, \tag{B.1.9}$$

where

$$c_1 = \sqrt{p_1'(\rho_1)}, \qquad c_2 = \sqrt{p_2'(\rho_2)}, \tag{B.1.10}$$

are the speeds of sound is each phase. The system is hyperbolic (i.e. the corresponding family of right eigenvectors spans $\mathbb{R}^5$) if and only if $u_2 \neq u_1 + c_1$ and $u_2 \neq u_1 - c_1$. In addition, the fields associated with the eigenvalues $\{\sigma_i\}_{i=2..5}$ are genuinely non linear while the field associated with σ_1 is linearly degenerate.

Proof. The proof follows from classical calculations that are left to the reader. □

B.2 A Splitting method for the Baer-Nunziato model

Let us introduce the following operator splitting method for the Baer-Nunziato equations. It consists in separating the wave propagation phenomena according to their respective propagation speed.

The first step corresponds to the propagation of acoustic waves due to pressure and phase fraction disequilibrium:

$$(\mathscr{S}_1) \qquad \begin{aligned} &\partial_t \alpha_1 = 0, \\ &\partial_t \alpha_k \rho_k = 0, \qquad\qquad k \in \{1,2\} \\ &\partial_t \alpha_k \rho_k u_k + \partial_x \alpha_k p_k - p_1 \partial_x \alpha_k = 0. \end{aligned}$$

The second step considers the propagation of material waves due to the fluid motion:

$$(\mathscr{S}_2) \qquad \begin{aligned} &\partial_t \alpha_1 + u_2 \partial_x \alpha_1 = 0, \\ &\partial_t \alpha_k \rho_k + \partial_x \alpha_k \rho_k u_k = 0, \qquad\qquad k \in \{1,2\} \\ &\partial_t \alpha_k \rho_k u_k + \partial_x \alpha_k \rho_k u_k^2 = 0. \end{aligned}$$

Finally, the third step takes into account the relaxation terms

$$(\mathscr{S}_3) \qquad \begin{aligned} &\partial_t \alpha_1 = \Theta_p (p_1 - p_2), \\ &\partial_t \alpha_k \rho_k = 0, \qquad\qquad k \in \{1,2\} \\ &\partial_t \alpha_k \rho_k u_k = \Theta_u (u_{3-k} - u_k). \end{aligned}$$

Observe that the splitting steps $(\mathscr{S}_1)$ and $(\mathscr{S}_2)$ are an extension to the two-phase flow model of the work performed in [3] in the framework of Euler's equations. In the present work, we focus on physical configurations for which the characteristic times τ_p and τ_u of the relaxation terms are much larger than the simulation time T. As a consequence, we do not treat this last step $(\mathscr{S}_3)$ in the present paper, and we refer to [10] for the numerical treatment of these terms. From this point, we assume that $\mathbf{S}(\mathbb{U}) = 0$.

B.2.1 Numerical approximation

In this section, we use the operator splitting method in order to derive a fractional-step numerical scheme, the aim being to approximate the weak solutions of a Cauchy problem associated with the homogeneous part of system (B.1.7):

$$\left\{ \begin{array}{l} \partial_t \mathbb{U} + \partial_x \mathbf{F}(\mathbb{U}) + \mathbf{C}(\mathbb{U}) \partial_x \mathbb{U} = 0, \quad x \in \mathbb{R},\ t > 0, \\ \mathbb{U}(x,0) = \mathbb{U}_0(x). \end{array} \right. \tag{B.2.1}$$

Let Δt be the time step and Δx the space step, which we assume here to be constant for simplicity in the notations. The space is partitioned into cells

$$\mathbb{R} = \bigcup_{j \in \mathbb{Z}} C_j \quad \text{with} \quad C_j = [x_{j-\frac{1}{2}}, x_{j+\frac{1}{2}}[, \quad \forall j \ \in \mathbb{Z},$$

where $x_{j+\frac{1}{2}} = (j+\frac{1}{2})\Delta x$ are the cell interfaces. At the discrete times $t^n = n\Delta t$, the solution of (B.2.1) is approximated on each cell C_j by a constant value denoted by

$$\mathbb{U}_j^n = \left((\alpha_1)_j^n, (\alpha_1\rho_1)_j^n, (\alpha_1\rho_1 u_1)_j^n, (\alpha_2\rho_2)_j^n, (\alpha_2\rho_2 u_2)_j^n\right)^T.$$

Before giving the precise description of the fractional step method, we state the following result which summarizes the main properties of the scheme:

Theorem B.2.1. *Under some natural CFL restriction (see (B.2.25) and (B.2.39)), the fractional step numerical scheme presented in this paper has the following properties:*

(i) It preserves the maximum principle on the phase fractions α_k, in the sense that

$$\forall n \in \mathbb{N}, \qquad \left(0 < \alpha_{k,j}^n < 1, \ \forall j \in \mathbb{Z}\right) \quad \Longrightarrow \quad \left(0 < \alpha_{k,j}^{n+1} < 1, \ \forall j \in \mathbb{Z}\right),$$

(ii) It preserves positive values of the densities in the sense that

$$\forall n \in \mathbb{N}, \qquad \left(\rho_{k,j}^n > 0, \ \forall j \in \mathbb{Z}\right) \quad \Longrightarrow \quad \left(\rho_{k,j}^{n+1} > 0, \ \forall j \in \mathbb{Z}\right),$$

(iii) The discretization of the partial masses $\alpha_k\rho_k$ is conservative,

(iv) The discretization of the total momentum $\alpha_1\rho_1 u_1 + \alpha_2\rho_2 u_2$ is conservative.

Proof. The result follows from Propositions B.2.4 and B.2.5 stated in sections B.2.2 and B.2.3 below. □

In the following two sections, we describe the fractional-step procedure associated with the time operator -splitting method in order to calculate the values of the approximate solution at time t^{n+1}, $(\mathbb{U}_j^{n+1})_{j\in\mathbb{Z}}$ from those at time t^n. Section B.2.2 displays the numerical treatment of the Lagrangian step $(\mathscr{S}_1)$ while section B.2.3 deals with the material transport step $(\mathscr{S}_2)$.

B.2.2 Treatment of the first step

In this section, we consider the numerical treatment of the following set of PDE's.

$$(\mathscr{S}_1) \qquad \begin{aligned} &\partial_t \alpha_1 = 0, \\ &\partial_t \alpha_k \rho_k = 0, \\ &\partial_t \alpha_k \rho_k u_k + \partial_x \alpha_k p_k - p_1 \partial_x \alpha_k = 0. \end{aligned}$$

One can check that all the eigenvalues of this non conservative system are zero, which implies that no numerical method relying on the spectral radius of the Jacobian matrix (such as Rusanov's scheme) can be applied in the present case. Therefore we choose to treat this first step with a

relaxation scheme. For this purpose, we introduce the following relaxation system which relaxes towards $(\mathscr{S}_1)$ in the limit $\varepsilon \to 0$:

$$\partial_t \alpha_1 = 0, \tag{B.2.2}$$
$$\partial_t \alpha_k \rho_k = 0, \tag{B.2.3}$$
$$\partial_t \alpha_k \rho_k u_k + \partial_x \alpha_k \pi_k - \pi_1 \partial_x \alpha_k = 0, \tag{B.2.4}$$
$$\partial_t \alpha_k \rho_k \pi_k + a_k^2 \partial_x \alpha_k u_k - a_k^2 u_2 \partial_x \alpha_k = \frac{1}{\varepsilon} \alpha_k \rho_k (p_k - \pi_k). \tag{B.2.5}$$

π_k is an additional unknown which relaxes towards the actual pressure p_k as $\varepsilon \to 0$ and whose evolution is governed by the additional PDE (B.2.5). The numbers $a_k > 0$ are two numerical parameters that need to be taken large enough so as to ensure the stability of the relaxation approximation in the regime of small ε. Typically, a_k must follow the so-called Whitham condition:

$$a_k^2 > \max_{\tau_k} \left(-\frac{\partial p_k}{\partial \tau_k}(\tau_k) \right), \qquad k = 1, 2, \tag{B.2.6}$$

where the max is taken over all the specific volumes τ_k in the solution of (B.2.2)-(B.2.5). We refer to [1] and [7] for a related framework.

Let us now focus on the convective part of this relaxation system which reads:

$$(\mathscr{S}_1\mathscr{R}) \qquad \begin{aligned} &\partial_t \alpha_1 = 0, && \text{(B.2.7)}\\ &\partial_t \alpha_k \rho_k = 0, && \text{(B.2.8)}\\ &\partial_t \alpha_k \rho_k u_k + \partial_x \alpha_k \pi_k - \pi_1 \partial_x \alpha_k = 0, && \text{(B.2.9)}\\ &\partial_t \alpha_k \rho_k \pi_k + a_k^2 \partial_x \alpha_k u_k - a_k^2 u_2 \partial_x \alpha_k = 0. && \text{(B.2.10)} \end{aligned}$$

We have the following property on the characteristic fields of the relaxation system.

Proposition B.2.2. *For all state vector* $\mathbb{W} = (\alpha_1, \alpha_1\rho_1, \alpha_1\rho_1 u_1, \alpha_1\rho_1\pi_1, \alpha_2\rho_2, \alpha_2\rho_2 u_2, \alpha_2\rho_2\pi_2)$ *such that* $\rho_1 > 0$ *and* $\rho_2 > 0$, *system* $(\mathscr{S}_1\mathscr{R})$ *has the following eigenvalues:*

$$-a_k\tau_k, \quad 0, \quad a_k\tau_k, \quad k \in \{1, 2\},$$

where $\tau_k = \rho_k^{-1}$ *is the specific volume of phase k. Moreover, all the characteristic fields are linearly degenerate and system* $(\mathscr{S}_1\mathscr{R})$ *is hyperbolic in the sense that the corresponding family of eigenvectors spans the whole space* $\mathbb{R}^7$.

Proof. The proof is left to the reader. □

Thus, the solution of a Riemann problem for $(\mathscr{S}_1\mathscr{R})$ consists in six constant states separated by five contact discontinuities. The calculation of such a solution is easy since the jump relations across each contact discontinuity are given by the Riemann invariants of the corresponding wave. In the following array, we display the Riemann invariants for each wave:

Wave's velocity	Riemann invariants
$-a_1\tau_1$	$\alpha_1,\ \rho_1,\ \rho_2,\ u_2,\ \pi_2,\ \pi_1 + a_1u_1$
$-a_2\tau_2$	$\alpha_1,\ \rho_1,\ \rho_2,\ u_1,\ \pi_1,\ \pi_2 + a_2u_2$
0	$\alpha_1u_1 + \alpha_2u_2,\ \alpha_1\pi_1 + \alpha_2\pi_2,\ u_2,\ \pi_1$
$a_2\tau_2$	$\alpha_1,\ \rho_1,\ \rho_2,\ u_1,\ \pi_1,\ \pi_2 - a_2u_2$
$a_1\tau_1$	$\alpha_1,\ \rho_1,\ \rho_2,\ u_2,\ \pi_2,\ \pi_1 - a_1u_1$

And we have the following proposition:

Proposition B.2.3. *Let be given two initial states $\mathbb{W}_L$ and $\mathbb{W}_R$ such that $\rho_1 > 0$ and $\rho_2 > 0$. Then the Riemann problem for $(\mathscr{S}_1\mathscr{R})$ where the initial condition is given by*

$$\mathbb{W}_0(x) = \begin{cases} \mathbb{W}_L & \text{if} \quad x < 0, \\ \mathbb{W}_R & \text{if} \quad x > 0 \end{cases} \tag{B.2.11}$$

has a unique solution with positive densities ρ_k for every intermediate state. The states $\mathbb{W}^-$ and $\mathbb{W}^+$ respectively on the left and on the right of the standing wave are given in the Appendix.

Proof. We only sketch the proof. First of all, let us notice that from equations (B.2.7) and (B.2.8), we deduce that the densities are constant in time $\partial_t\rho_k = 0$. As $\rho_k > 0$ at time $t = 0$, we get $\rho_k > 0$ for every time $t > 0$. The solution is composed of constant states separated by contact discontinuities:

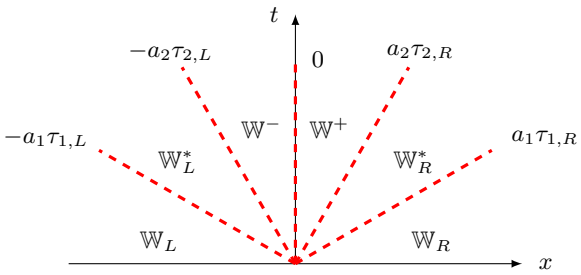

Note that the relative order of the acoustic waves ($a_1\tau_1 < a_2\tau_2$ or $a_1\tau_1 > a_2\tau_2$) is of no importance here since it does not change the values of the intermediate states. The solution is calculated by solving a linear system of eight equations where the eight unknowns are the values of $(\alpha_k u_k)^-$, and $(\alpha_k\pi_k)^-$ evaluated on the left of the standing wave as well as $(\alpha_k u_k)^+$, and $(\alpha_k\pi_k)^+$ evaluated on the right of the standing wave. In order to ease the notation, we define $x_k := (\alpha_k u_k)$ and $y_k := (\alpha_k\pi_k)$. These quantities are linked together through the Riemann invariants of the standing wave:

$$y_1^- = \varphi y_1^+, \quad \text{with} \quad \varphi = \alpha_1^-/\alpha_1^+, \tag{B.2.12}$$

$$x_2^- = \psi x_2^+, \quad \text{with} \quad \psi = \alpha_2^-/\alpha_2^+, \tag{B.2.13}$$

$$y_1^- + y_2^- = y_1^+ + y_2^+, \tag{B.2.14}$$

$$x_1^- + x_2^- = x_1^+ + x_2^+. \tag{B.2.15}$$

Note that $(\alpha_i^-, \alpha_i^+) = (\alpha_{i,L}, \alpha_{i,R})$ since α_i only jumps through the standing wave. We get four additional equations by linking these unknowns with the left and right data $x_{k,L}$, $y_{k,L}$, and $x_{k,R}$, $y_{k,R}$. For example, since u_1 and π_1 are invariants of the $\{-a_2\tau_2\}$-wave, we have $\pi_1^- + a_1 u_1^- = \pi_{1,L}^* + a_1 u_{1,L}^*$. Moreover, $\pi_1 + a_1 u_1$ is a Riemann invariant of the $\{-a_1\tau_1\}$-wave which yields $\pi_1^- + a_1 u_1^- = \pi_{1,L}^* + a_1 u_{1,L}^* = \pi_{1,L} + a_1 u_{1,L}$. Now, knowing that $\alpha_1 = \alpha_{1,L}$ on the left side of the standing wave, we multiply this equation by $\alpha_{1,L}$ and we get $y_1^- + a_1 x_1^- = y_{1,L} + a_1 x_{1,L}$. By proceeding similarly, we get the three last equations of our system:

$$y_1^- + a_1 x_1^- = y_{1,L} + a_1 x_{1,L}, \tag{B.2.16}$$

$$y_2^- + a_2 x_2^- = y_{2,L} + a_2 x_{2,L}, \tag{B.2.17}$$

$$y_1^+ - a_1 x_1^+ = y_{1,R} - a_1 x_{1,R}, \tag{B.2.18}$$

$$y_2^+ - a_2 x_2^+ = y_{2,R} - a_2 x_{2,R}. \tag{B.2.19}$$

Then, we can prove (see the Appendix) that up to a nonzero multiplicative constant K, the determinant of this linear system is equal to

$$\text{Det} = K \frac{a_1}{a_2} \left(\frac{(1-\varphi)(1-\psi)}{(1+\varphi)(1+\psi)} \frac{a_1}{a_2} - 1 \right). \tag{B.2.20}$$

This determniant vanishes if and only if $\dfrac{(1-\varphi)(1-\psi)}{(1+\varphi)(1+\psi)} \dfrac{a_1}{a_2} - 1 = 0$, which is impossible since

$$\frac{(1-\varphi)(1-\psi)}{(1+\varphi)(1+\psi)} = -\frac{\alpha_1^+ + \alpha_1^-}{\alpha_2^+ + \alpha_2^-} (\alpha_1^+ - \alpha_1^-)^2 \leq 0.$$

Hence, the linear system is an invertible Cramer system which yields the existence and uniqueness of the solution. □

Numerical scheme

Let us now describe the numerical treatment of the first step resulting from the relaxation approximation of $(\mathscr{S}_1)$. Starting from the given data at time t^n: $\mathbb{U}_j^n$, the updated data at the fictive intermediate time $t^\sharp$: $\mathbb{U}_j^\sharp$ are computed as follows:

1. Define $\mathbb{W}_j^n$ by taking the additional variables $(\pi_k)_j^n$ equal to $p_k(\rho_{k,j}^n)$.
2. Apply the exact Godunov scheme to the relaxation system $(\mathscr{S}_1\mathscr{R})$ with the initial data $\mathbb{W}_j^n$. At this level, the numerical parameters a_k should be chosen, interface by interface, so as to satisfy Whitham's condition. In practice, Whitham's condition is replaced for simplicity by the following Whitham-like condition:

$$a_k^2 > \max\left(-\frac{\partial p_k}{\partial \tau_k}(\tau_{k,j}^n), -\frac{\partial p_k}{\partial \tau_k}(\tau_{k,j+1}^n) \right), \quad k = 1, 2. \tag{B.2.21}$$

   This condition is less restrictive than the classical Whitham condition stated in (B.2.6) but it appears that in practice, no instabilities pop up in the scheme. This step yields the updated value of $\mathbb{W}_j^\sharp$.

3. Drop the additional variable π_k by taking $\mathbb{U}_j^\sharp = \Big((\alpha_1)_j^\sharp, (\alpha_1\rho_1)_j^\sharp, (\alpha_1\rho_1 u_1)_j^\sharp, (\alpha_2\rho_2)_j^\sharp, (\alpha_2\rho_2 u_2)_j^\sharp\Big)$.

Points (1) to (3) provide the following finite volume scheme with non conservative numerical fluxes at the interfaces:

$$\alpha_{1,j}^\sharp = \alpha_{1,j}^n, \tag{B.2.22}$$

$$(\alpha_k\rho_k)_j^\sharp = (\alpha_k\rho_k)_j^n, \tag{B.2.23}$$

$$(\alpha_k\rho_k u_k)_j^\sharp = (\alpha_k\rho_k u_k)_j^n - \frac{\Delta t}{\Delta x}\left((\alpha_k\pi_k)_{j+\frac{1}{2}}^- - (\alpha_k\pi_k)_{j-\frac{1}{2}}^+\right), \tag{B.2.24}$$

where $(\alpha_k\pi_k)_{j+\frac{1}{2}}^-$ (resp. $(\alpha_k\pi_k)_{j+\frac{1}{2}}^+$) are the values of $(\alpha_k\pi_k)$ on the left (resp. on the right) of the standing wave in the Riemann problem defined by $\mathbb{W}_j^n$ and $\mathbb{W}_{j+1}^n$ (see Appendix the for their formulae). Or course, when applying Godunov's scheme to the relaxation system, one has to restrict the time step to a classical CFL condition which reads:

$$\frac{\Delta t}{\Delta x}\max_{j\in\mathbb{Z}}\max_{k\in\{1,2\}}|(a_k\tau_k)_j^n| < \frac{1}{2}. \tag{B.2.25}$$

We have the following proposition that summarizes the properties of the relaxation numerical scheme designed for $(\mathscr{S}_1)$:

Proposition B.2.4. *Under Whitham's condition (B.2.21) and the CFL restriction (B.2.25), equations (B.2.22)-(B.2.23)-(B.2.24) provide a numerical scheme for the first step $(\mathscr{S}_1)$ of the splitting method which has the following properties:*

(i) It preserves the maximum principle for the phase fractions : $0 < \alpha_k < 1$, on the time step $t^n \to t^\sharp$,

(ii) It preserves positive values of the densities $\rho_k > 0$, on the time step $t^n \to t^\sharp$,

(iii) The discretization of the partial masses $\alpha_k\rho_k$ is conservative,

(iv) The discretization of the total momentum $\alpha_1\rho_1u_1 + \alpha_2\rho_2u_2$ is conservative.

Proof. The only property which is not straightforward is the conservative discretization of the total momentum. Summing equations (B.2.24) over k yields:

$$(\alpha_1\rho_1u_1 + \alpha_2\rho_2u_2)_j^\sharp = (\alpha_1\rho_1u_1 + \alpha_1\rho_1u_2)_j^n - \frac{\Delta t}{\Delta x}\left((\alpha_1\pi_1 + \alpha_2\pi_2)_{j+\frac{1}{2}}^- - (\alpha_1\pi_1 + \alpha_2\pi_2)_{j-\frac{1}{2}}^+\right).$$

As $\alpha_1\pi_1 + \alpha_2\pi_2$ is a Riemann invariant of the standing wave for system $(\mathscr{S}_1\mathscr{R})$, we have $(\alpha_1\pi_1 + \alpha_2\pi_2)_{j+\frac{1}{2}}^- = (\alpha_1\pi_1 + \alpha_2\pi_2)_{j+\frac{1}{2}}^+$, which preserves the conservative form. □

B.2.3 Treatment of the second step

We now consider the numerical treatment of the time evolution corresponding to the second step. Starting from the output data of the first step, $\mathbb{U}_j^\sharp$, we want to compute the updated data at time t^{n+1}: $\mathbb{U}_j^{n+1}$.

$$(\mathscr{S}_2)\qquad \begin{aligned} &\partial_t \alpha_1 + u_2 \partial_x \alpha_1 = 0, && \text{(B.2.26)}\\ &\partial_t \alpha_k \rho_k + \partial_x \alpha_k \rho_k u_k = 0, && \text{(B.2.27)}\\ &\partial_t \alpha_k \rho_k u_k + \partial_x \alpha_k \rho_k u_k^2 = 0. && \text{(B.2.28)} \end{aligned}$$

Equations (B.2.27) and (B.2.28) can be written in the form of two decoupled systems, each one corresponding to the material convection of mass and momentum in one of the two phases:

$$\begin{aligned} &\partial_t \alpha_k \rho_k + \partial_x \alpha_k \rho_k u_k = 0,\\ &\partial_t \alpha_k \rho_k u_k + \partial_x \alpha_k \rho_k u_k^2 = 0, \end{aligned}$$

for $k = 1$ or 2. Each one of these two systems takes the following generic form:

$$\begin{aligned} &\partial_t \theta + \partial_x \theta v = 0,\\ &\partial_t \theta \Theta + \partial_x \theta \Theta v = 0, \end{aligned} \qquad \text{(B.2.29)}$$

where Θ is a vector of $\mathbb{R}^n, n \geq 1$ (here $\Theta = u_k \in \mathbb{R}$) and θ is a scalar unknown that is assumed to be positive (here $\theta = \alpha_k \rho_k$) and for which one has to provide a scheme which preserves its positivity. Finally, v is a velocity field that is assumed to depend only on the space variable: $v(x)$ (here $v(x) = u_k(t^\sharp, x)$). System (B.2.29) is only weakly hyperbolic, thus the numerical approximation of such a system is *a priori* not classical.

A positive scheme for (B.2.29)

In order to easily handle the lack of hyperbolicity, we discretize (B.2.29) with a two-step splitting operator method motivated by the following calculation:

$$\begin{aligned} &\partial_t \theta + \{\theta \partial_x v\} + \{v \partial_x \theta\} = 0,\\ &\{\partial_t \theta + \partial_x v \theta\}\, \Theta + \theta \{\partial_t \Theta + v \partial_x \Theta\} = 0. \end{aligned} \qquad \text{(B.2.30)}$$

The proposed splitting method consists in solving at first the ODE:

$$d_t \theta = -\theta \frac{d}{dx} v(x), \qquad \text{(B.2.31)}$$

followed by

$$\begin{aligned} &\partial_t \theta + v(x) \partial_x \theta = 0,\\ &\theta \{\partial_t \Theta + v(x) \partial_x \Theta\} = 0, \end{aligned} \qquad \text{(B.2.32)}$$

which can be re-written as $n + 1$ decoupled transport equations:

$$\begin{aligned} &\partial_t \theta + v(x) \partial_x \theta = 0,\\ &\partial_t \theta \Theta + v(x) \partial_x \theta \Theta = 0. \end{aligned} \qquad \text{(B.2.33)}$$

The objective here is to design a time explicit discretization of (B.2.31)-(B.2.33) which is conservative for both quantities θ and $\theta\Theta$ and which preserves the positivity of θ under some natural CFL restriction. The ODE (B.2.31) is discretized with an implicit scheme as follows:

$$\frac{\theta_j^{1/2}-\theta_j^\sharp}{\Delta t} = -\theta_j^{1/2}\frac{v_{j+\frac12}-v_{j-\frac12}}{\Delta x} \quad \Longleftrightarrow \quad \theta_j^{1/2} = \frac{\theta_j^\sharp}{1+\frac{\Delta t}{\Delta x}\left(v_{j+\frac12}-v_{j-\frac12}\right)}. \tag{B.2.34}$$

Hence, preserving the positivity of θ in this step amounts to imposing the following CFL-like condition:

$$1+\frac{\Delta t}{\Delta x}\left(v_{j+\frac12}-v_{j-\frac12}\right) > 0. \tag{B.2.35}$$

As for the second step (B.2.33), it is discretized using the classical first order upwind scheme:

$$\theta_j^{n+1} = \theta_j^{1/2} - \frac{\Delta t}{\Delta x}\left((v_{j+\frac12})^-\left(\theta_{j+1}^{1/2}-\theta_j^{1/2}\right)+(v_{j-\frac12})^+\left(\theta_j^{1/2}-\theta_{j-1}^{1/2}\right)\right), \tag{B.2.36}$$

$$(\theta\Theta)_j^{n+1} = \theta_j^{1/2}\Theta_j^\sharp - \frac{\Delta t}{\Delta x}\left((v_{j+\frac12})^-\left(\theta_{j+1}^{1/2}\Theta_{j+1}^\sharp-\theta_j^{1/2}\Theta_j^\sharp\right)+(v_{j-\frac12})^+\left(\theta_j^{1/2}\Theta_j^\sharp-\theta_{j-1}^{1/2}\Theta_{j-1}^\sharp\right)\right), \tag{B.2.37}$$

where for any real value X, we denoted $(X)^- = \min(0,X)$ and $(X)^+ = \max(0,X)$. Re-writing equation (B.2.36) as

$$\theta_j^{n+1} = -\frac{\Delta t}{\Delta x}(v_{j+\frac12})^-\theta_{j+1}^{1/2} + \left(1+\frac{\Delta t}{\Delta x}\left((v_{j+\frac12})^- - (v_{j-\frac12})^+\right)\right)\theta_j^{1/2} + \frac{\Delta t}{\Delta x}(v_{j-\frac12})^+\theta_{j-1}^{1/2}, \tag{B.2.38}$$

we can see that this second step also preserves positive values of θ provided the following CFL condition

$$1+\frac{\Delta t}{\Delta x}\left((v_{j+\frac12})^- - (v_{j-\frac12})^+\right) > 0. \tag{B.2.39}$$

Note that this last CFL condition may be more restrictive than (B.2.35).

We can now show that this two-step splitting operation provides a conservative discretization of (B.2.29). Injecting the result of the first step (B.2.34) in equation (B.2.36), one gets

$$\begin{aligned}\theta_j^{n+1} &= \theta_j^\sharp - \frac{\Delta t}{\Delta x}\theta_j^{1/2}\left(v_{j+\frac12}-v_{j-\frac12}\right) - \frac{\Delta t}{\Delta x}\left((v_{j+\frac12})^-\left(\theta_{j+1}^{1/2}-\theta_j^{1/2}\right)+(v_{j-\frac12})^+\left(\theta_j^{1/2}-\theta_{j-1}^{1/2}\right)\right)\\ &= \theta_j^\sharp - \frac{\Delta t}{\Delta x}\left((v_{j+\frac12})^+\theta_j^{1/2}+(v_{j+\frac12})^-\theta_{j+1}^{1/2}\right) + \frac{\Delta t}{\Delta x}\left((v_{j-\frac12})^+\theta_{j-1}^{1/2}+(v_{j-\frac12})^-\theta_j^{1/2}\right).\end{aligned}$$

This can be re-written in the following conservative form:

$$\theta_j^{n+1} = \theta_j^\sharp - \frac{\Delta t}{\Delta x}\left(v_{j+\frac12}\theta_{j+\frac12}^{1/2} - v_{j-\frac12}\theta_{j-\frac12}^{1/2}\right), \tag{B.2.40}$$

where for all j in $\mathbb{Z}$,

$$\theta_{j+\frac12}^{1/2} = \begin{cases}\theta_j^{1/2} & \text{if } v_{j+\frac12}\geq 0,\\ \theta_{j+1}^{1/2} & \text{otherwise.}\end{cases} \tag{B.2.41}$$

Similar calculations lead to

$$(\theta\Theta)_j^{n+1} = \theta_j^\sharp \Theta_j^\sharp - \frac{\Delta t}{\Delta x}\left(v_{j+\frac{1}{2}}\theta_{j+\frac{1}{2}}^{1/2}\Theta_{j+\frac{1}{2}}^\sharp - v_{j-\frac{1}{2}}\theta_{j-\frac{1}{2}}^{1/2}\Theta_{j-\frac{1}{2}}^\sharp\right), \tag{B.2.42}$$

where for all j in $\mathbb{Z}$,

$$\Theta_{j+\frac{1}{2}}^\sharp = \begin{cases} \Theta_j^\sharp & \text{if } v_{j+\frac{1}{2}} \geq 0, \\ \Theta_{j+1}^\sharp & \text{otherwise.} \end{cases} \tag{B.2.43}$$

Application to equations (B.2.27) and (B.2.28)

Now, in order to apply this positive scheme to equations (B.2.27) and (B.2.28), one has to define the values of the interface velocities at the initial time: $u_{k,j+\frac{1}{2}} := u_k(t^\sharp, x_{j+\frac{1}{2}})$. Concerning phase number 2, the velocity u_2 is a Riemann invariant of the standing wave in the first step $(\mathscr{S}_1)$. Thus, a natural choice for $u_{2,j+\frac{1}{2}}$ is $u_2^- = u_2^+$ the constant value of the velocity of phase 2 across the standing wave in $(\mathscr{S}_1)$. One could also take any other consistent choice for $u_{2,j+\frac{1}{2}}$ as for instance a convex combination of $u_{2,j}^\sharp$ and $u_{2,j+1}^\sharp$ at the end of the first step:

$$u_{2,j+\frac{1}{2}} = \beta u_{2,j}^\sharp + (1-\beta)u_{2,j+1}^\sharp, \ \beta \in [0,1]. \tag{B.2.44}$$

As for phase 1, whose velocity is not a Riemann invariant of the standing wave in $(\mathscr{S}_1)$, we decide to take:

$$u_{1,j+\frac{1}{2}} = \eta u_{1,j}^\sharp + (1-\eta)u_{1,j+1}^\sharp, \ \eta \in [0,1]. \tag{B.2.45}$$

In practice, we take $\beta = \eta = 1/2$.

Finally, with this definition of $u_{2,j+\frac{1}{2}}$, the advection equation on α_1 is discretized thanks to the first order upwind scheme:

$$\alpha_{1,j}^{n+1} = \alpha_{1,j}^\sharp - \frac{\Delta t}{\Delta x}\left((u_{2,j+\frac{1}{2}})^-\left(\alpha_{1,j+1}^\sharp - \alpha_{1,j}^\sharp\right) + (u_{2,j-\frac{1}{2}})^+\left(\alpha_{1,j}^\sharp - \alpha_{1,j-1}^\sharp\right)\right). \tag{B.2.46}$$

This discretization ensures the maximum principle on α_1 if the CFL condition (B.2.39) with $v = u_2$ is imposed.

We have the following proposition that summarizes the properties of the relaxation numerical scheme designed for $(\mathscr{S}_2)$:

Proposition B.2.5. *Under the CFL restriction (B.2.39), equations (B.2.34)-(B.2.36)-(B.2.37) applied to each one of the phasic systems (B.2.3) provide a numerical scheme for the second step $(\mathscr{S}_2)$ of the splitting method which has the following properties:*

(i) It preserves the maximum principle for the phase fractions : $0 < \alpha_k < 1$, on the time step $t^\sharp \to t^{n+1}$,

(ii) It preserves positive values of the densities $\rho_k > 0$, on the time step $t^\sharp \to t^{n+1}$,

(iii) The discretization of the partial masses $\alpha_k\rho_k$ is conservative,

(iv) The discretization of the total momentum $\alpha_1\rho_1 u_1 + \alpha_2\rho_2 u_2$ is conservative.

Proof. The proposition directly follows from the above discussion. □

B.3 Numerical experiments

In this section, we present two test cases in which we compare the approximate solution, computed with our fractional step numerical scheme, with the exact solution of a Riemann problem. In these two cases, the phasic equations of state are given by the following ideal gas pressure laws:

$$\begin{aligned} p_1(\rho_1) &= \kappa_1\rho_1^{\gamma_1}, \quad \text{with } \kappa_1 = 1 \text{ and } \gamma_1 = 3, \\ p_2(\rho_2) &= \kappa_2\rho_2^{\gamma_2}, \quad \text{with } \kappa_2 = 1 \text{ and } \gamma_2 = 1.5. \end{aligned} \tag{B.3.1}$$

The solutions are computed on the domain $[-0.5, 0.5]$ of the x-space. For both tests 1 and 2, a mesh refinement process is implemented in order to numerically check the convergence of the method. For this purpose, we compute the discrete L^1-error between the approximate solution and the exact one at the final time T, normalized by the discrete L^1-norm of the exact solution:

$$\text{error}(\Delta x) = \frac{\sum_{\text{cells}j} |\mathcal{U}_j^n - \mathcal{U}_{ex}(x_j, T)|\Delta x}{\sum_{\text{cells}j} |\mathcal{U}_{ex}(x_j, T)|\Delta x}, \tag{B.3.2}$$

where $\mathcal{U}$ denotes the state vector in **non conservative variables**:

$$\mathcal{U} = (\alpha_1, \rho_1, u_1, \rho_2, u_2).$$

The calculations have been implemented on several meshes. The coarser mesh is composed of 100 cells and the more refined one contains 200000 cells. The error error(Δx) is then plotted against Δx in a $log - log$ scale.

Notations:

- $\mathcal{R}_{\sigma_i}(\mathcal{U}^-, \mathcal{U}^+)$ stands for a σ_i-rarefaction wave, $i = 2, 3, 4, 5$, connecting the left-hand state $\mathcal{U}^-$ to the right-hand state $\mathcal{U}^+$.
- $\mathcal{S}_{\sigma_i}(\mathcal{U}^-, \mathcal{U}^+)$ stands for a σ_i-shock, $i = 2, 3, 4, 5$, connecting the left-hand state $\mathcal{U}^-$ to the right-hand state $\mathcal{U}^+$.
- $\mathcal{C}_{\sigma_1}(\mathcal{U}^-, \mathcal{U}^+)$ stands for a σ_1-contact discontinuity connecting the left-hand state $\mathcal{U}^-$ to the right-hand state $\mathcal{U}^+$.

Finally, a σ_i-wave connecting a state $\mathcal{U}_1$ to a state $\mathcal{U}_2$ followed by a σ_j-wave connecting $\mathcal{U}_2$ to $\mathcal{U}_3$ will be denoted $\mathcal{W}_{\sigma_i}(\mathcal{U}_1, \mathcal{U}_2) \longrightarrow \mathcal{W}_{\sigma_j}(\mathcal{U}_2, \mathcal{U}_3)$, $\mathcal{W} = \mathcal{R}, \mathcal{S}, \mathcal{C}$.

B.3.1 Test case 1: a contact discontinuity

The first test case is a Riemann problem with only a $\sigma_1 = u_2$ contact discontinuity. In the exact solution, all the physical quantities are transported with the constant velocity $u_2 = 0.1$, except u_2 which is constant. The initial data in non conservative variables is defined as

$$\begin{aligned} \mathcal{U}_L &= (0.3, 1., 0.2, 0.8, 0.1) && \text{for } x < 0, \\ \mathcal{U}_R &= (0.6, 1.0012502584, 0.1499375651, 0.6302289018, 0.1) && \text{for } x > 0. \end{aligned} \tag{B.3.3}$$

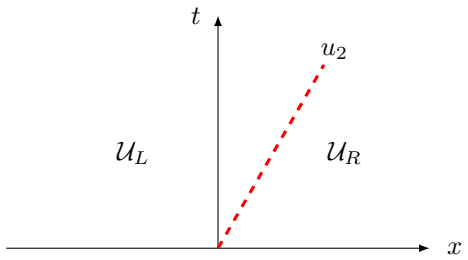

Wave structure of the exact Riemann solution

Figure B.1 shows that the moving contact is not exactly captured by our scheme. However, when the exact solution of a Riemann problem contains a contact discontinuity, the expected order of convergence in L^1-norm is $\Delta x^{1/2}$ for a first order scheme. In Figure B.1, we can see that our splitting method provides convergence towards the exact solution with the expected order of $\Delta x^{1/2}$. Note that, to our knowledge, there exists no solver that is able to capture exactly a moving contact discontinuity on coarse meshes, and our scheme compares rather well with other schemes (see [13]). Nevertheless, the method proposed in [16] exactly captures stationary contacts, *i.e.* contacts with $u_2 = 0$.
The strange behavior of the scheme on the density variable of phase 1 is due to the present choice of initial conditions on ρ_1 in which the left and right values are very close. This makes the jump more difficult to be captured on this variable, and it is all the more difficult for coarse meshes.
Finally, we would like the reader to be aware that the number of visible points in the figure for the 50000-cell mesh (especially in the contact wave) is not the real one since some points have been dropped for the clarity of the graph.

B.3.2 Test case 2: a complete case with all the waves

The second test case is a complete case with the contact discontinuity and all the acoustic waves. The initial data in non conservative variables is set to

$$\begin{aligned} \mathcal{U}_L &= (0.1, 0.85, 0.4609513139, 0.96, 0.0839315299) && \text{for } x < 0, \\ \mathcal{U}_R &= (0.6, 1.2520240113, 0.7170741165, 0.2505659851, -0.3764790609) && \text{for } x > 0. \end{aligned} \tag{B.3.4}$$

Observe that this is a hard case to run since the difference between the left and right values of the phase fraction α_1 is quite large. The intermediate states (also in non conservative variables) are

given by:

$$\mathcal{U}_1 = (0.1, 1., 0.2, 0.96, 0.0839315299),$$
$$\mathcal{U}_2 = (0.1, 1., 0.2, 0.8, 0.3),$$
$$\mathcal{U}_3 = (0.6, 1.0016192090, 0.2833602765, 0.5011319701, 0.3),$$
$$\mathcal{U}_4 = (0.6, 1.0016192090, 0.2833602765, 0.2505659851, -0.3764790609).$$

The Riemann solution is a $\{u_1 - c_1\}$-shock wave from $\mathcal{U}_L$ to $\mathcal{U}_1$, followed by a $\{u_2 - c_2\}$-rarefaction wave from $\mathcal{U}_1$ to $\mathcal{U}_2$, followed by a u_2-contact discontinuity from $\mathcal{U}_2$ to $\mathcal{U}_3$, followed by a $\{u_2 + c_2\}$-shock from $\mathcal{U}_3$ to $\mathcal{U}_4$ and finally followed by a $\{u_1 + c_1\}$-rarefaction wave from $\mathcal{U}_4$ to $\mathcal{U}_R$:

$$\mathcal{S}_{\sigma_2}(\mathcal{U}_L,\mathcal{U}_1) \longrightarrow \mathcal{R}_{\sigma_4}(\mathcal{U}_1,\mathcal{U}_2) \longrightarrow \mathcal{C}_{\sigma_1}(\mathcal{U}_2,\mathcal{U}_3) \longrightarrow \mathcal{S}_{\sigma_5}(\mathcal{U}_3,\mathcal{U}_4) \longrightarrow \mathcal{R}_{\sigma_3}(\mathcal{U}_4,\mathcal{U}_R).$$

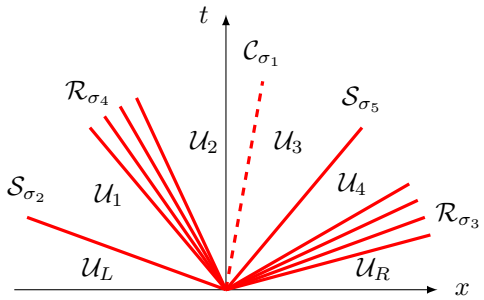

Wave structure of the exact Riemann solution

In Figure B.2, we can see that the intermediate states are correctly captured by the method even for a quite coarse mesh of 100 cells. Figure B.2 also shows that the approximate solution computed thanks to the splitting method converges towards the exact solution. Only the error on the phase fraction α_1 converges towards zero with the expected order of $\Delta x^{1/2}$, while the other variables seem to converge with a higher rate. However, the expected order of $\Delta x^{1/2}$ is only an asymptotic order of convergence, and in this particular case, one would have to implement the calculation on much more refined meshes in order to recover this expected order $\Delta x^{1/2}$.
Here again, we warn the reader that the number of visible points in the figure for the 50000-mesh (especially in the contact wave and in the shocks) is not the real one since some points have been dropped for the clarity of the graph.

B.4 Conclusion

The explicit scheme presented here provides convergent aproximations of discontinuous solutions of the barotropic Baer-Nunziato model, while preserving the maximum principle on the values of the statistical fractions α_k and positive values of the densities ρ_k. A sequel of this work consists in using the same fractional step strategy in order to derive an implicit version of the first step, and thus to get rid of a rather constraining CFL condition due to the propagation of fast acoustic waves.

Appendix: Proof of Proposition B.2.3 and formulae of the intermediate states $\mathbb{W}^-$ and $\mathbb{W}^+$

We prove here that the determinant of the system composed of equations (B.2.12) to (B.2.19) has the following expression

$$\text{Det} = K\frac{a_1}{a_2}\left(\frac{(1-\varphi)(1-\psi)}{(1+\varphi)(1+\psi)}\frac{a_1}{a_2} - 1\right), \tag{B.4.1}$$

for some constant $K \neq 0$. We first ease the notations by denoting the data in the right hand side part of equations (B.2.16) to (B.2.19) as follows:

$$A := y_{1,L} + a_1 x_{1,L}, \tag{B.4.2}$$
$$B := y_{2,L} + a_2 x_{2,L}, \tag{B.4.3}$$
$$C := y_{1,R} - a_1 x_{1,R}, \tag{B.4.4}$$
$$D := y_{2,R} - a_2 x_{2,R}. \tag{B.4.5}$$

We also denote $u = x_1^-$ and $v = x_1^+$. We express all the other unknowns in terms of u and v in order to bring this eight equation linear system to a system of two linear equations on u and v. We note that provided that $a_2 \neq 0$, equations (B.2.14), (B.2.15), (B.4.2), (B.4.3), (B.4.4) and (B.4.5) form an autonomous system that can be solved with respect to u and v and whose solution is

$$y_1^- = A - a_1 u, \tag{B.4.6}$$
$$y_1^+ = C + a_1 v, \tag{B.4.7}$$
$$y_2^- = \frac{a_1+a_2}{2}u + \frac{a_1-a_2}{2}v + \frac{B+C+D-A}{2}, \tag{B.4.8}$$
$$y_2^+ = \frac{a_2-a_1}{2}u - \frac{a_1+a_2}{2}v + \frac{A+B+D-C}{2}, \tag{B.4.9}$$
$$x_2^- = -\frac{1}{2}\left(1+\frac{a_1}{a_2}\right)u + \frac{1}{2}\left(1-\frac{a_1}{a_2}\right)v + \frac{A+B-C-D}{2a_2}, \tag{B.4.10}$$
$$x_2^+ = \frac{1}{2}\left(1-\frac{a_1}{a_2}\right)u - \frac{1}{2}\left(1+\frac{a_1}{a_2}\right)v + \frac{A+B-C-D}{2a_2}. \tag{B.4.11}$$

Denoting $X = a_1/a_2$ and injecting these expressions in equation (B.2.12) and (B.2.13), we get

$$\frac{A}{a_2} - Xu = \varphi\left(\frac{C}{a_2} + Xv\right) \Longleftrightarrow Xu + \varphi Xv = \frac{A-\varphi C}{a_2}, \tag{B.4.12}$$

and

$$\begin{aligned} &-(1+X)u + (1-X)v + \frac{A+B-C-D}{a_2} = \psi\left((1-X)u - (1+X)v + \frac{A+B-C-D}{a_2}\right) \\ &\Longleftrightarrow \left(\psi(1-X)+1+X\right)u + \left(X-1-\psi(1+X)\right)v = (1-\psi)\frac{A+B-C-D}{a_2}. \end{aligned} \tag{B.4.13}$$

Equations (B.4.12) and (B.4.13) form a 2×2 linear system whose determinant is

$$\begin{aligned} \text{Det} &= X(X - 1 - \psi(1 + X)) - \varphi X(\psi(1 - X) + 1 + X) \\ &= (1 - \varphi)(1 - \psi)X^2 - (1 + \varphi)(1 + \psi)X \\ &= (1 + \varphi)(1 + \psi)X \left(\frac{(1 - \varphi)(1 - \psi)}{(1 + \varphi)(1 + \psi)} X - 1 \right), \end{aligned} \tag{B.4.14}$$

which proves the expression of the determinant given in equation (B.2.20). Hence, using Cramer formulae, we deduce the expressions of u and v:

$$u = \frac{1}{\text{Det}} \left(\frac{A - \varphi C}{a_2} (X - 1 - \psi(1 + X)) - (1 - \psi) \frac{A + B - C - D}{a_2} \varphi X \right), \tag{B.4.15}$$

$$v = \frac{1}{\text{Det}} \left(X(1 - \psi) \frac{A + B - C - D}{a_2} - \frac{A - \varphi C}{a_2} (\psi(1 - X) + 1 + X) \right), \tag{B.4.16}$$

which yields $x_1^- = u$, $x_1^+ = v$. The formulae of y_1^-, y_1^+, y_2^-, y_2^+, x_2^- and x_2^+ are given in equations (B.4.6) to (B.4.11).

References

[1] A. Ambroso, C. Chalons, F. Coquel, and T. Galié. Relaxation and numerical approximation of a two-fluid two-pressure diphasic model. *M2AN Math. Model. Numer. Anal.*, 43(6):1063–1097, 2009.

[2] M.R. Baer and J.W. Nunziato. A two-phase mixture theory for the deflagration-to-detonation transition (DDT) in reactive granular materials. *International Journal of Multiphase Flow*, 12(6):861 – 889, 1986.

[3] R. Baraille. *Dévelopement de schémas numériques adaptés à l'hydrodynamique*. PhD thesis, Université Bordeaux I, 1991.

[4] D. Bresch, B. Desjardins, J. Ghidaglia, and E. Grenier. Global weak solutions to a generic two-fluid model. *Archive for Rational Mechanics and Analysis*, 196:599–629, 2010.

[5] C. Chalons, F. Coquel, S. Kokh, and N. Spillane. Large time-step numerical scheme for the seven-equation model of compressible two-phase flows. *Springer Proceedings in Mathematics, FVCA 6, 2011*, 4:225–233, 2011.

[6] F. Coquel, T. Gallouët, J-M. Hérard, and N. Seguin. Closure laws for a two-fluid two-pressure model. *C. R. Math. Acad. Sci. Paris*, 334(10):927–932, 2002.

[7] F. Coquel, E. Godlewski, and N. Seguin. Relaxation of fluid systems. *Math. Models Methods Appl. Sci.*, 22(8), 2012.

[8] P. Embid and M. Baer. Mathematical analysis of a two-phase continuum mixture theory. *Contin. Mech. Thermodyn.*, 4(4):279–312, 1992.

[9] S. Gavrilyuk and R. Saurel. Mathematical and numerical modeling of two-phase compressible flows with micro-inertia. *Journal of Computational Physics*, 175(1):326 – 360, 2002.

[10] J-M. Hérard and O. Hurisse. A fractional step method to compute a class of compressible gas-luiquid flows. *Computers & Fluids. An International Journal*, 55:57–69, 2012.

[11] A. K. Kapila, S. F. Son, J. B. Bdzil, R. Menikoff, and D. S. Stewart. Two-phase modeling of DDT: Structure of the velocity-relaxation zone. *Physics of Fluids*, 9(12):3885–3897, 1997.

[12] S. Karni and G. Hernàndez-Dueñas. A hybrid algorithm for the Baer-Nunziato model using the Riemann invariants. *Journal of Scientific Computing*, 45:382–403, 2010.

[13] Y. Liu. PhD thesis, Université Aix-Marseille, to appear in 2013.

[14] R. Saurel and R. Abgrall. A multiphase godunov method for compressible multifluid and multiphase flows. *Journal of Computational Physics*, 150(2):425 – 467, 1999.

[15] D.W. Schwendeman, C.W. Wahle, and A.K. Kapila. The Riemann problem and a high-resolution Godunov method for a model of compressible two-phase flow. *Journal of Computational Physics*, 212(2):490 – 526, 2006.

[16] M. D. Thanh, D. Kröner, and N. T. Nam. Numerical approximation for a Baer–Nunziato model of two-phase flows. *Applied Numerical Mathematics*, 61(5):702 – 721, 2011.

[17] S.A. Tokareva and E.F. Toro. HLLC-type Riemann solver for the Baer-Nunziato equations of compressible two-phase flow. *Journal of Computational Physics*, 229(10):3573 – 3604, 2010.

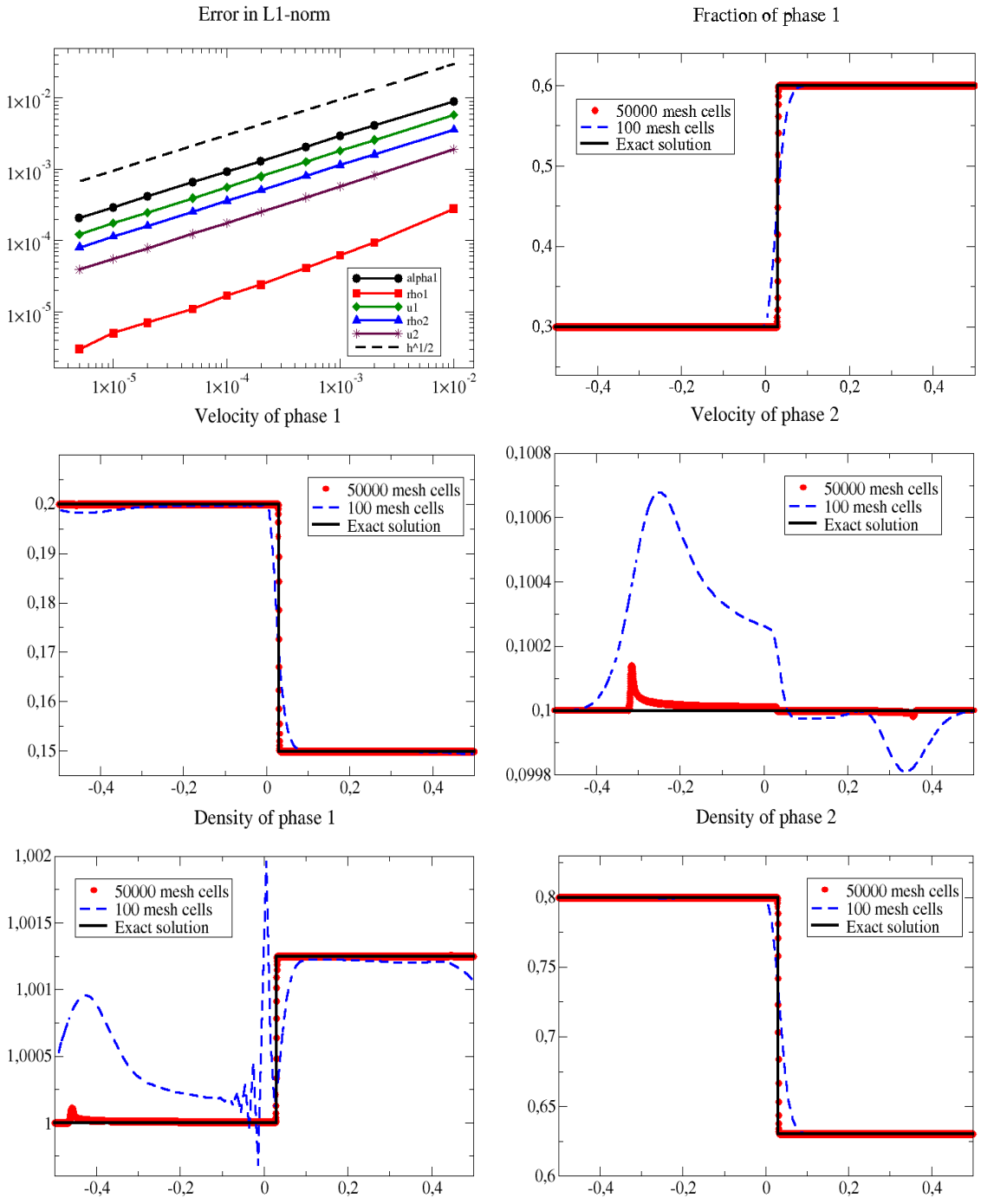

Figure B.1: Test 1: space variations of the physical variables at the final time $T = 0.3$, and L^1-norm of the error for several mesh sizes.

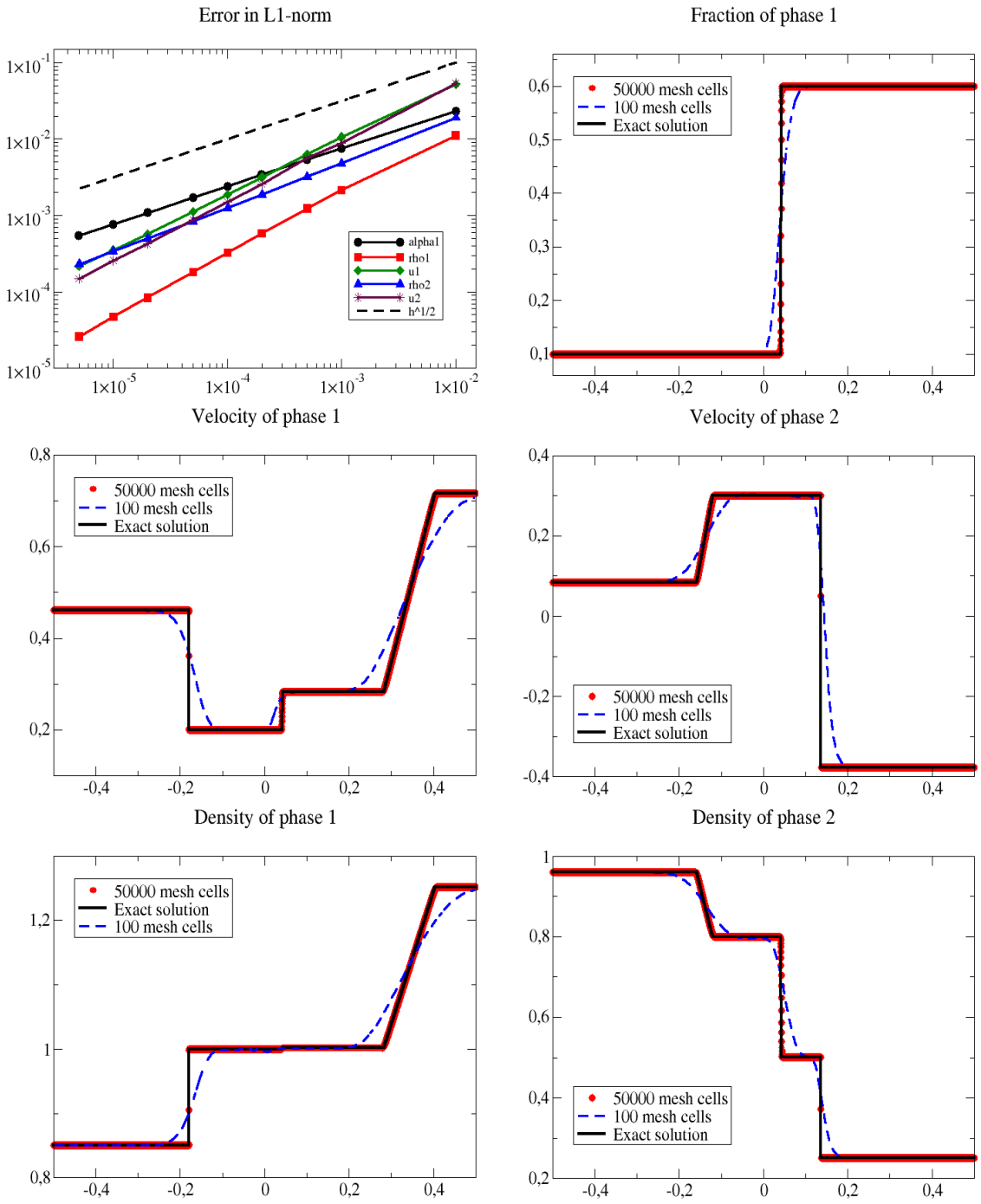

Figure B.2: Test 2: space variations of the physical variables at the final time $T = 0.14$, and L^1-norm of the error for several mesh sizes.

Appendix C

Un modèle de type Baer-Nunziato avec fermetures dynamiques des quantités interfaciales

A Class of Two-Fluid Two-Phase Flow Models[1]

Frédéric Coquel
Research Director in CNRS, CMAP, UMR 7671, Ecole Polytechnique, Route de Saclay, 91128, Palaiseau, France.
CMAP, Ecole Polytechnique, Route de Saclay, 91128, Palaiseau, France.

Jean-Marc Hérard
Senior engineer, EDF R&D, Fluid Dynamics, Power Generation and Environment, 6 quai Watier, 78400, Chatou, France.
EDF, R&D, 6 quai Watier, 78400, Chatou, France.

Khaled Saleh
PhD student, EDF, R&D, Fluid Dynamics, Power Generation and Environment, 6 quai Watier, 78400, Chatou, France, and: Laboratoire Jacques-Louis Lions, UMR 7598 , 4 place Jussieu, 75005, Paris, France.
EDF, R&D, 6 quai Watier, 78400, Chatou, France.

Nicolas Seguin
Associate Professor, Laboratoire Jacques-Louis Lions, Université Pierre et Marie Curie, UMR 7598, 4 place Jussieu, 75005, Paris, France.
LJLL, Université Pierre et Marie Curie, 4 place Jussieu, 75005, Paris, France.

Abstract

We introduce a class of two-fluid models that complies with a few theoretical requirements that include : (i) hyperbolicity of the convective subset, (ii) entropy inequality, (iii) uniqueness of jump conditions for non-viscous flows. These specifications are necessary in order to compute relevant approximations of unsteady flow patterns. It is shown that the Baer-Nunziato model belongs to this class of two-phase flow models, and the main properties of the model are given, before showing a few numerical experiments.

C.1 Introduction

The Baer-Nunziato model (called BN model afterwards) was introduced in the early eighties in order to provide a suitable representation of gas-particle granular flows, when compressible effects

[1] Cette annexe reprend un proceedings du congrès AIAA 2012 .

cannot be neglected, and more precisely in order to tackle deflagration to detonation transition. This model has been examined in detail since the early paper [4] ; we must at least mention Kapila and co-workers ([23, 5, 22]), Gavrilyuk and Saurel [12], but also Glimm and co-workers [15, 14, 21], among others (see [24, 25, 28] also). Many papers have been devoted to the numerical simulation of this model, among which we may point out those by Saurel and Abgrall [30], Gonthier and Powers [16], Toro [33], Andrianov and Warnecke [3], Lowe [27], Schwendemann et al [31], who proposed various approximate Riemann solvers, but also Coquel et al [1, 2], who suggested to use relaxation schemes as a keystone for such a purpose. Some recent computational results can be found in [32] and [19] for instance.

It was in fact shown in [6, 11] that the BN model is one among a few two-fluid models that benefit from several essential properties. Actually, noting as usual α_k (such that $\alpha_l + \alpha_v = 1$), U_k, ρ_k, $m_k = \alpha_k \rho_k$, E_k and P_k the statistical void fractions, velocities, densities, partial masses, total energies and pressures respectively (for $k = l, v$, where l and v subscripts respectively refer to the liquid and vapour phases), but also:

$$W = (\alpha_l, m_l, m_v, m_l U_l, m_v U_v, \alpha_l E_l, \alpha_v E_v)$$

and starting from the open set of PDEs, for $k = l, v$:

$$\left\{ \begin{array}{l} \partial_t (\alpha_k) + V_i(W) \partial_x (\alpha_k) = \varphi_k(W) \ ; \\ \partial_t (\alpha_k \rho_k) + \partial_x (\alpha_k \rho_k U_k) = 0 \ ; \\ \partial_t (\alpha_k \rho_k U_k) + \partial_x \left(\alpha_k \rho_k U_k^2 \right) + \alpha_k \partial_x (P_k) + (P_k - P_i(W)) \partial_x (\alpha_k) = D_k(W) \ ; \\ \partial_t (\alpha_k E_k) + \partial_x (\alpha_k U_k (E_k + P_k)) + P_i(W) \partial_t (\alpha_k) = \psi_k(W) + V_I D_k(W) \ . \end{array} \right. \tag{C.1.1}$$

where $D_k(W)$ and $\psi_k(W)$ enable to take drag effects and heat transfer into account, authors of the latter reference introduced three distinct couples $(P_i(W), V_i(W))$ which enable to achieve the following requirements:

- The two-fluid model is hyperbolic without any restriction on the space of physical states (other than those already existing for single-phase flow models);
- Smooth solutions of the whole set of partial differential equations are governed by a meaningful entropy inequality;
- Unique jump conditions can be exhibited within each isolated field;
- The model generates smooth solutions that comply with positivity constraints.

The first point is physically relevant, and it is indeed mandatory to compute solutions of a well-posed initial value problem, when tracking unsteady flow patterns. The second point is not only desirable from a physical point of view, but it also introduces a nice tool in order to control smooth but also shock solutions. The third one introduces an important difference with other classical two-fluid models, for instance those that assume a local instantaneous pressure equilibrium between phases: actually, this third property will also guarantee that (stable enough) schemes will converge towards the *same* solution when refining the mesh, which is of course implicitly assumed by users... We emphasize that these specifications have also been used in order to model granular flows and

flows in porous media (see [17, 10, 13]). The BN model is suitable for many water-vapour flows, for instance for standard computations in the primary circuit of nuclear power reactors, since the liquid flow is expected to contain a very small amount of vapour bubbles in standard conditions. It is also relevant for some applications where the vapour phase is dominant and when few liquid droplets are present in the field. In the first case, the closure laws for the couple $(P_i(W), V_i(W))$ should be (P_l, U_v), and in the second case one should use (P_v, U_l) reversely.

However, there are some applications where the BN model can hardly be used. This may happen in at least two distinct configurations:

- when the flow contains different regions in terms of topology at the beginning of the computation: this may happen in many practical cases;
- when some change occurs in the flow during the time interval which is of interest: this is the case for instance when heating a liquid flow through a wall boundary (this will correspond to the so-called boiling crisis in the nuclear safety framework).

These situations have led to the present proposition, which aims at providing a general framework which:

- complies with the four above-mentionned criteria;
- contains the BN model.

We present in the sequel this general framework [18]. Next we detail the main properties of the two-fluid model. We eventually discuss a few numerical experiments that illustrate the whole approach.

C.2 Governing set of equations of the two-fluid model

The new framework that is proposed in this paper introduces a *non-dimensional* scalar variable β that characterizes the flow regime. This variable is lying in the interval $[0, 1]$. Setting $m_k = \alpha_k \rho_k$, the governing set of equations reads:

$$\left\{ \begin{array}{l} \partial_t(\beta) + \mathcal{W}(W,\beta)\partial_x(\beta) = T_\beta(W,\beta) \ ; \\ \partial_t(\alpha_k) + V_i(W,\beta)\partial_x(\alpha_k) = \varphi_k(W) \ ; \\ \partial_t(m_k) + \partial_x(m_k U_k) = 0 \ ; \\ \partial_t(m_k U_k) + \partial_x\left(m_k U_k^2\right) + \alpha_k \partial_x(P_k) + (P_k - P_i(W,\beta))\partial_x(\alpha_k) = D_k(W) \ ; \\ \partial_t(\alpha_k E_k) + \partial_x(\alpha_k U_k (E_k + P_k)) + P_i(W,\beta)\partial_t(\alpha_k) = \psi_k(W) + \overline{V}_I(W) D_k(W) \ . \end{array} \right. \tag{C.2.1}$$

for $k = l, v$, noting $E_k = \rho_k(e_k(P_k, \rho_k) + U_k^2/2)$ the total energy within phase k, and assuming some relevant equation of state for $e_k(P_k, \rho_k)$. Terms on the right-hand side must follow the standard rule:

$$\sum_{k=l,v} \psi_k(W) = 0 \quad ; \quad \sum_{k=l,v} D_k(W) = 0 \quad ; \quad \sum_{k=l,v} \varphi_k(W) = 0 \ . \tag{C.2.2}$$

which means that these contributions account for interfacial transfer terms. The derivation of the governing open equation for α_k can be found in [18] ; the reader is also refered to [20] and [12] for that particular topic. Source terms $\varphi_k(W), D_k(W), \psi_k(W)$ will be detailed in the next section, and we note here:

$$\overline{V}_I(W) = (U_l + U_v)/2.$$

The so-called interface velocity $V_i(W, \beta)$ will be defined according to:

$$V_i(W, \beta) = \mu(W, \beta)U_l + (1 - \mu(W, \beta))U_v, \qquad \textit{with } \mu \in [0, 1]. \tag{C.2.3}$$

A straightforward consequence is that $U_1(x, t) = U_2(x, t) = U$ implies $V_i(x, t) = U$ locally. We will also assume that the following holds:

$$T_\beta(W, \beta = 0) = T_\beta(W, \beta = 1) = T_\beta(W, \beta = 1/2) = 0,$$

whatever W would be.

C.2.1 Closure laws for P_i and interfacial transfer terms

If we note c_k and S_k the sound velocity and the specific entropy within phase k, we may introduce the entropy-entropy flux couple (S, f_S) as follows :

$$S = m_l S_l + m_v S_v; \qquad f_S = m_l S_l U_l + m_v S_v U_v. \tag{C.2.4}$$

We also introduce temperatures T_k such that :

$$1/T_k = (\partial_{P_k}(S_k(P_k, \rho_k)))(\partial_{P_k}(e_k(P_k, \rho_k)))^{-1}, \tag{C.2.5}$$

for $k = l, v$.

Using these notations, we will assume that closure laws for φ_l, ψ_l, D_l comply with the conditions:

$$\left\{ \begin{array}{l} 0 \leq \psi_l(T_v - T_l) \ ; \\ 0 \leq \varphi_l(P_l - P_v) \ ; \\ 0 \leq D_l(U_v - U_l) \ . \end{array} \right. \tag{C.2.6}$$

We keep closure laws for ψ_l and D_l that are in agreement with those given in the standard literature [20], setting:

$$\left\{ \begin{array}{l} \psi_l = \frac{m_l m_v (C_v)_v (C_v)_l}{m_l (C_v)_l + m_v (C_v)_v}(T_v - T_l)/\tau_T \ ; \\ D_l = \frac{m_l m_v}{m_l + m_v}(U_v - U_l)/\tau_U \ . \end{array} \right. \tag{C.2.7}$$

where τ_U, τ_T respectively denote velocity and temperature relaxation time scales. The closure law for φ_l is assumed to be non zero when $P_v \neq P_l$. A possible choice is:

$$\varphi_l = \alpha_l \alpha_v (P_l - P_v)/\Pi_0/\tau_P,$$

where τ_P represents the pressure relaxation time scale (see [4, 12] for instance), and Π_0 is a pressure reference.

Turning then to the interfacial pressure $P_i(W,\beta)$, we introduce:

$$P_i(W,\beta) = ((1-\mu(W,\beta))P_l/T_l + \mu(W,\beta)P_v/T_v)/((1-\mu(W,\beta))/T_l + \mu(W,\beta)/T_v) \tag{C.2.8}$$

Actually, this closure law is mandatory in order to obtain a physically relevant entropy inequality. Hence the interface pressure is totally determined as soon as the interface velocity is prescribed. We recall that the same procedure applies when modelling three-phase flows (see [17]). Obviously, the local balance $P_v = P_l = P$ will imply $P_i = P$.

C.2.2 Closure laws for V_i and $\mathcal{W}$

We define : $\mathcal{W}(W,\beta) = \mathcal{W}_0$ or alternatively , $\mathcal{W}(W,\beta) = \mathcal{W}_1$ where:

$$\mathcal{W}_0 = 0 \qquad \textit{and:} \qquad \mathcal{W}_1 = (m_l U_l + m_v U_v)/(m_l + m_v), \tag{C.2.9}$$

and we introduce the interfacial velocity V_i such that μ in (C.2.3) reads:

$$\mu(\beta, W) = \frac{m_l \beta}{m_l \beta + m_v(1-\beta)}. \tag{C.2.10}$$

We note that the specific value $\beta = 0$ (respectively $\beta = 1$) corresponds to the BN model, since the associated values of the interface pressure and interface velocity become $P_i = P_l$ and $V_i = U_v$ (respectively $P_i = P_v$ and $V_i = U_l$), owing to (C.2.8). The BN model is appealing for many scientists, since it guarantees that the interface velocity corresponds to the velocity of the vanishing phase, and meanwhile it complies with the expected idea that the interface presssure should be driven by the most present phase. Moreover, the value $\beta = 1/2$ was already pointed out in [11]; in that very special case V_i and $\mathcal{W}_1$ identify. Obviously, when considering an initial condition such that $\beta(x, t=0) = 0$ (respectively $\beta(x, t=0) = 1$), an obvious solution of the first equation in (C.2.1) is simply : $\beta(x,t) = 0$ (respectively $\beta(x,t) = 1$). A similar remark holds for $\beta = 1/2$. Within our nuclear framework, a typical situation where the initial condition may involve two seperate regions Ω_A and Ω_B with distinct values of β, typically $\beta(x \in \Omega_A, 0) = 0$ on the one side and $\beta(x \in \Omega_B, 0) = 1$ on the other side, is the LOCA situation (Loss Of Coolant Accident). The governing set of equations is closed now, assuming that relaxation time scales τ_U, τ_P, τ_T and $T_\beta(W,\beta)$ are given.

C.3 Main properties of the two-fluid model

We provide now the main properties of the two-fluid model:

Proposition 1:

Smooth solutions of (C.2.1) *comply with the following entropy inequality:*

$$\partial_t (S) + \partial_x (f_S) = \Sigma_k(\psi_k + (\overline{V}_I - U_k)D_k - \varphi_k(P_i - P_k))/T_k \geq 0 \ . \tag{C.3.1}$$

The proof is straightforward (see [18]). This entropy inequality enables to select physically relevant shocks in the non-viscous case. We may now give the following main result:

Proposition 2:

- *System* (C.2.1) *is hyperbolic since it admits real eigenvalues:*
  $\lambda_1 = V_i$, $\lambda_2 = \mathcal{W}$, $\lambda_3 = U_l$, $\lambda_4 = U_l - c_l$, $\lambda_5 = U_l + c_l$, $\lambda_6 = U_v$, $\lambda_7 = U_v - c_v$, $\lambda_8 = U_v + c_v$.

  and associated right eigenvectors span the whole space $\mathcal{R}^8$ *if and only if:*

  $$|V_i - U_k| \neq c_k \quad \textit{and:} \quad |\mathcal{W} - U_k| \neq c_k$$

  for $k = l, v$. *Otherwise, the resonance phenomenon occurs in the solution.*

- *Waves associated with* $\lambda_1, \lambda_2, \lambda_3, \lambda_6$ *are linearly degenerate and those corresponding to* $\lambda_4, \lambda_5, \lambda_7, \lambda_8$ *are genuinely nonlinear.*

The most difficult part in the proof corresponds to the first claim in the second item (see [18]).

Proposition 3:

Field by field jump conditions are uniquely defined in system (C.2.1)*, unless resonance occurs (if a GNL field overlaps with a LD field).*

We note that for nuclear applications in pressurised water reactors, the resonance phenomenon is very unlikely to appear. However, even in that framework, we emphasize that shock waves may occur, due for instance to sudden high heating fluxes through wall boundaries, or due to modifications of inlet/outlet boundary conditions. Thus the third requirement is again relevant for these applications. Jump conditions actually coincide with single-phase jump conditions within each phase, on each side of the void fraction coupling wave associated with $\lambda = V_i$.

When focusing on solutions of the one-dimensional Riemann problem associated with the homogeneous part of (C.2.1), it appears that the contact discontinuity associated with V_i separates both regions $\Omega_L = \{(x,t)/x/t < V_i\}$ where $\alpha_l(x,t) = (\alpha_l)_L$, and $\Omega_R = \{(x,t)/x/t > V_i\}$ where $\alpha_l(x,t) = (\alpha_l)_R$. In each subdomain $\Omega_{L,R}$, the jump relations are:

$$\left\{ \begin{array}{l} -\sigma[\rho_k]_a^b + [\rho_k U_k]_a^b = 0 \\ -\sigma[\rho_k U_k]_a^b + [\rho_k U_k^2 + P_k]_a^b = 0 \\ -\sigma[E_k]_a^b + [U_k(E_k + P_k)]_a^b = 0 \end{array} \right. \tag{C.3.2}$$

if σ denotes the speed of the travelling shock wave separating states a and b, for $k = l, v$. Note also that the solution $\beta(x,t)$ in the Riemann problem is given by $\beta(x,t) = (\beta)_L$ in the subdomain $\omega_L = \{(x,t)/x/t < \mathcal{W}\}$, and : $\beta(x,t) = (\beta)_R$ in the subdomain $\omega_R = \{(x,t)/x/t > \mathcal{W}\}$. Eventually, noting $\mathcal{D}$ the whole physical domain, we get the next expected result:

Proposition 4:

Assuming positive inlet boundary conditions and initial conditions for $\alpha_{l,v}$ and $m_{l,v}$, then smooth solutions of system (C.2.1) are such that void fractions $\alpha_{l,v}$ and partial masses $m_{l,v}$ remain positive over $\mathcal{D} \times [0,T]$.

C.4 Numerical experiments

We provide here a numerical experiment that illustrates the behaviour of the two-fluid model. Numerical schemes are those that are used in [19]. We focus here on the particular choice $\mathcal{W}(W,\beta) = \mathcal{W}_0$, and $T_\beta(W,\beta) = -\beta(\beta^2 - 3\beta/2 + 1/2)/\tau_\beta(W)$ and we consider a very difficult test case, that is very unlikely to happen in our framework, since it includes the resonance phenomenon.

We consider a 1D computational domain $\mathcal{D} = [0,1]$, and set the initial discontinuity at the interface $x_0 = 0.5$. The initial values of the function β are: $\beta(x < x_0, t = 0) = 0$, and $\beta(x > x_0, t = 0) = 1$. Thus it means that we assume that the flow on the left side (or left code) $x < 0.5$ is modeled with the BN model corresponding to $(P_i, U_i) = (P_l, U_v)$, and that we have retained the couple $(P_i, U_i) = (P_v, U_l)$ on its right-hand side. The initial conditions are the following:

	Initial left state L	Initial right state R
β	0	1
α_l	0.98	0.02
α_v	0.02	0.98
ρ_l	1	0.125
ρ_v	4	0.5
U_l	0.	
U_v	0.	
P_l	10^5	10^4
P_v	4×10^5	4×10^4

Initial condition in test case.

Perfect gas EOS have been considered within each phase: $P_{l,v} = (\gamma_{l,v} - 1)\rho_{l,v} e_{l,v}$, with $\gamma_v = 1.2$ and $\gamma_l = 1.2$. The flow is at rest at the beginning of the computation and time scales τ_U, τ_P, τ_T have been set to 1, thus the solution is very close to the solution of a Riemann problem corresponding to : $\tau_U = \tau_P = \tau_T = +\infty$, since the final time of the computation is $T = 10^{-3}$. We use two regular meshes with 10^4 and 4×10^4 cells respectively. Two shock waves (one within each phase) are created

and move to the right side of the interface. The liquid (resp. vapour) rarefaction wave is subsonic (resp. supersonic, see figure 1).

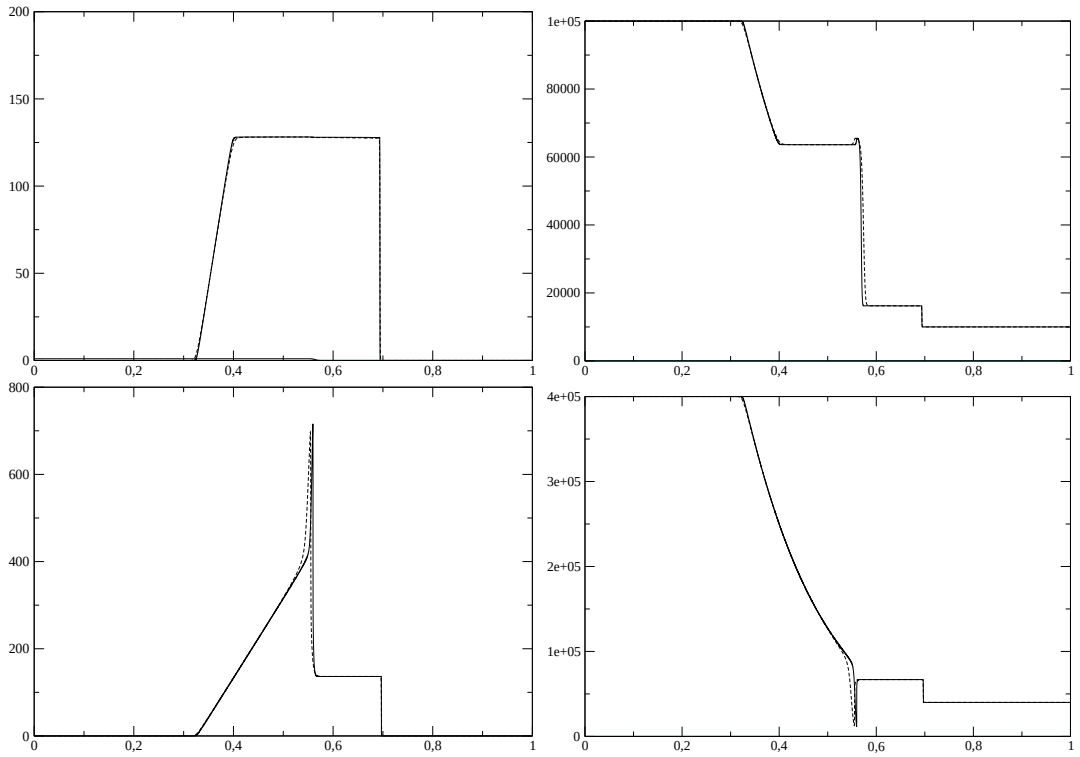

Figure C.1: Velocity (left) and pressure (right) profiles for the vapour phase (down) and liquid phase (top) respectively. The two regular meshes contain 10000 (dashed line) and 40000 (plain line) cells.

Conclusion

The general class of two-fluid models that has been introduced herein may in fact be viewed as a symetrized dynamical version of the BN model. It contains a scalar function β which specifies the flow regime. The main properties of the two-fluid model have been given, and more details can be found in the reference [18]; some first numerical experiments have been achieved, but there is now of course a need for an extensive investigation and validation that requires a great amount of work. Among others, the fractional step method introduced in [7] may be used for computational purposes, and we refer to this reference which gives numerical rates of convergence obtained while focusing on some particular Riemann problems. This method takes advantage of the LD structure of the 1 and 2-waves, and it enables to retrieve expected rates of convergence.

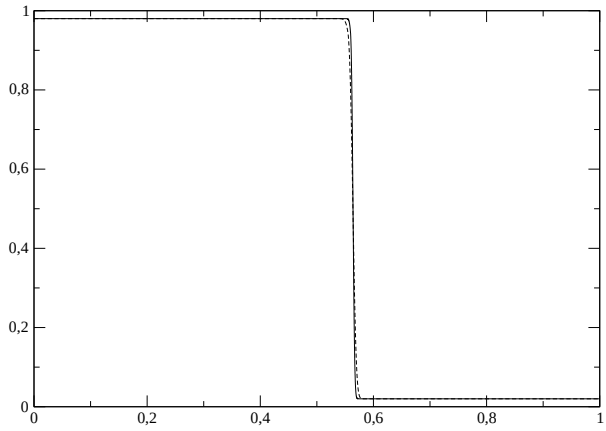

Figure C.2: Void fraction profiles.

We expect the model to be able to handle such flows as those encountered in the boiling crisis and in some other specific situations occuring in the framework of nuclear safety analysis. We also refer to the paper [19] , that presents some preliminary results of the flow along a heated wall, which have been obtained in a 2D framework with the BN model.

Acknowledgments:

The third author receives some financial support by ANRT under grant CIFRE/EDF 2009/529.

References

[1] Ambroso, A., Chalons, C., Coquel, F., and Galié, T., "Relaxation and numerical approximation of a two-fluid two-pressure diphasic model " *Math. Model. and Numer. Anal.*, vol. 43(6), 2009, pp. 1063–1098.

[2] Ambroso, A., Chalons, C., and Raviart, P.A., "A Godunov-type method for the seven-equation model of compressible two-phase flow " *Computers and Fluids*, vol.54 , 2012, pp. 67-91 .

[3] Andrianov, N., and Warnecke, G., " The Riemann problem for the Baer-Nunziato two-phase flow model", *J. Comp. Physics.*, vol. 195, 2004, pp. 434-464 .

[4] Baer, M.R., and Nunziato, J.W., "A two-phase mixture theory for the deflagration to detonation transition (DDT) in reactive granular materials", *Int. J. Multiphase Flow*, vol. 12(6), 1986, pp. 861–889.

[5] Bdzil, J.B., Menikoff, R., Son, S.F., Kapila, A.K., and Stewart, D.S., "Two-phase modeling of a DDT in granular materials: a critical examination of modeling issues", *Phys. of Fluids*, vol. 11, 1999, pp. 378-402.

[6] Coquel, F., Gallouët, T., Hérard, J.M., and Seguin, N., "Closure laws for a two-fluid two-pressure model", *C. R. Acad. Sci. Paris*, vol. I-332, 2002, pp. 927–932.

[7] Crouzet, F., Daude, F., Galon, P., Helluy, P., Hérard, J.-M., and Liu, Y., "On the computation of the Baer-Nunziato model", *contribution to the 42th AIAA FD conference*, 2012.

[8] Drew, D.A, and Passman, M., "Theory of multicomponent fluids", *Applied Mathematical Sciences*, vol. 135, Springer, 1999.

[9] Embid, P., and Baer, M., "Mathematical analysis of a two-phase continuum mixture theory", *Contin. Mech. Thermodyn.*, vol. 4, 1992, pp. 279–312.

[10] Gallouët, T., Helluy, P., Hérard, J.-M., and Nussbaum J., "Hyperbolic relaxation models for granular flows", *Math. Model. and Numer. Anal.*, vol.44(2), 2010, pp.371-400.

[11] Gallouët, T., Hérard, J.-M., and Seguin, N., "Numerical modelling of two phase flows using the two-fluid two-pressure approach", *Math. Mod. Meth. in Appl. Sci.*, vol. 14(5), 2004, pp. 663-700.

[12] Gavrilyuk, S., and Saurel, R., "Mathematical and numerical modelling of two phase compressible flows with inertia", *J. Comp. Physics.*, vol. 175, 2002, pp. 326-360.

[13] Girault, L., and Hérard, J.-M., "A two-fluid hyperbolic model in a porous medium", *Math. Model. and Numer. Anal.*, vol. 44(6), 2010, pp. 1319-1348.

[14] Glimm, J., Saltz, D., and Sharp, D.H., "Renomalization group solution of two-phase flow equations for Rayleigh Taylor mixing", *Phys. Lett.*, vol. A222, 1996, pp. 171-1763.

[15] Glimm, J., Saltz, D., and Sharp, D.H., "Two phase flow modelling of a fluid mixing layer", *J. Fluid Mechanics*, vol. 378, 1999, pp. 119-143.

[16] Gonthier, K.A., and Powers, J.M., "A high resolution method for a two-phase flow model of deflagration to detonation transition ", *J. Comp. Physics.*, vol. 163 , 2000, pp.376-433.

[17] Hérard, J.-M., "A three-phase flow model", *Mathematical Computer Modelling*, vol. 45, 2007, pp. 432-455.

[18] Hérard, J.-M., "Une classe de modèles diphasiques bi-fluides avec changement de régime", *internal EDF report H-I81-2010-0486-FR*, in French, 2010.

[19] Hérard, J.-M., and Hurisse, O., "Computing two-fluid models of compressible water-vapour flows with mass transfer", *contribution to the 42th AIAA FD conference*, 2012.

[20] Ishii, M., "Thermofluid dynamic theory of two-phase flow", *Collection de la Direction des Etudes et Recherches d'Electricité de France* , Collection Eyrolles, 1975.

[21] Jin, H., and Glimm, J., "Weakly compressible two-pressure two-phase flow", *Acta Mathematica Scienta*, vol. 29, 2009, pp. 1497-1540.

[22] Kapila, A.K., Menikoff, R., Bdzil, J.B., Son, S.F., and Stewart, D.S., "Two-phase modeling of a DDT in granular materials: reduced equations", *Phys. of Fluids*, vol. 13, 2001, pp. 3002-3024.

[23] Kapila, A.K., Son, S.F., Bdzil, J.B., Menikoff, R., and Stewart, D.S., "Two-phase modeling of a DDT: structure of the velocity relaxation zone", *Phys. of Fluids*, vol. 9(12), 1997, pp. 3885–3897.

[24] Lhuillier, D., "A mean field description of two-phase flows with phase changes", *Int. J. of Multiphase Flow*,, vol. 29, 2003, pp. 511-525.

[25] Lhuillier, D., "Evolution of the volumetric interfacial area in two-phase mixtures", *C. R. Mécanique*, vol. 332, 2004, pp. 103-108.

[26] Liu, Y., *PhD thesis*, Université Aix-Marseille I, Marseille, France, in preparation, 2013.

[27] Lowe, C.A., " Two-phase shock-tube problems and numerical methods of solution", *J. Comp. Physics.*, vol. 204, 2005, pp. 598-632.

[28] Papin, M., and Abgrall, R., "Fermetures entropiques pour les systèmes bifluides à sept équations", *C. R. Mécanique*, vol. 333, 2005, pp. 838-842.

[29] Saleh, K., *PhD thesis*, Université Pierre et Marie Curie, Paris, France, in preparation, 2012.

[30] Saurel, R., and Abgrall, R., " A Multiphase Godunov Method for Compressible Multifluid and Multiphase Flows ", *J. Comp. Physics.*, vol. 150, 1999, pp. 425-467.

[31] Schwendeman, D.W., Wahle, C.W., and Kapila, A.K., " The Riemann problem and a high-resolution Godunov method for a model of compressible two-phase flow ", *J. Comp. Physics.*, vol. 212, 2006, pp. 490-526.

[32] Schwendeman, D.W., Kapila, A.K., and Henshaw, W.D., " A study of detonation diffraction and failure for a model of compressible two-phase reactive flow ", *Combustion Theory and Modelling*, vol. 14, 2010, pp. 331-366.

[33] Tokareva, S.A., and Toro, E.F., " HLLC type Riemann solver for the Baer-Nunziato equations of compressible two-phase flow", *J. Comp. Physics.*, vol. 229, 2010, pp. 3573-3604.